**NASA Reference Publication 1201**

March 1988

# The 1987 Airborne Antarctic Ozone Experiment

## *The Nimbus-7 TOMS Data Atlas*

Arlin J. Krueger,
Philip E. Ardanuy,
Frank S. Sechrist,
Lanning M. Penn,
David E. Larko,
Scott D. Doiron,
and Reginald N. Galimore



NASA

1Front RP1201

NASA
Reference
Publication
1201

1988

# The 1987 Airborne Antarctic Ozone Experiment

## *The Nimbus-7 TOMS Data Atlas*

Arlin J. Krueger
*Goddard Space Flight Center*
*Greenbelt, Maryland*

Philip E. Ardanuy,
Frank S. Sechrist,
Lanning M. Penn,
and David E. Larko
*Research and Data Systems Corporation*
*Lanham, Maryland*

Scott D. Doiron
and Reginald N. Galimore
*Science Applications Research Corporation*
*Lanham, Maryland*

NASA
National Aeronautics
and Space Administration

Scientific and Technical
Information Division

/Ber

# THE 1987 AIRBORNE ANTARCTIC OZONE EXPERIMENT:
# THE NIMBUS-7 TOMS DATA ATLAS

Table of Contents



PRECEDING PAGE BLANK NOT FILMED

PAGE ii INTENTIONALLY BLANK

# 1. INTRODUCTION

Both ground-based (Farman et al., 1985) and satellite (Stolarski et al., 1986; Schoeberl and Krueger, 1986; Krueger et al., 1987) observations have documented a startling downward trend in the total column ozone amounts over Antarctica. This decrease, which occurs seasonally during September and October, has resulted in a depletion in the column ozone amounts by as much as 50%. The Antarctic ozone minimum, termed "the ozone hole," reached the lowest values ever observed in 1987. Several theories have been advanced to explain the loss of the ozone over Antarctica and the formation of the ozone hole. These include the effects on the total column ozone abundance due to climatic variability and changes in the stratospheric circulation patterns (Newman and Schoeberl, 1986; Chandra and McPeters, 1986), interactions with the 11-year solar sunspot cycle (Callis and Natarajan, 1986), and chemical reactions with enhanced levels of chlorine monoxide (possibly caused by the introduction of chlorofluorocarbons into the atmosphere) (Farman et al., 1985). Observations from the Satellite Aerosol Measurement (SAM II) instrument (McCormick and Trepte, 1986) and the Limb Infrared Monitor of the Stratosphere (LIMS) instrument (Austin et al., 1986) on board the Nimbus-7 spacecraft have revealed the presence of Antarctic Polar Stratospheric Clouds (PSC's). These PSC's are present in the Antarctic lower stratosphere with cloud tops of from 15 to over 20 km throughout September. It has been suggested that heterogeneous reactions on the surface of the cloud particles may be related to the formation of the ozone hole (Toon et al., 1986; Crutzen et al., 1986).

## 1.1 The 1987 Airborne Antarctic Ozone Experiment

The goal of the 1987 Airborne Antarctic Ozone Experiment was to improve the understanding of the mechanisms involved in the formation of the Antarctic ozone hole. The campaign was conducted during the period between August 8, when the mission go/no-go criteria were satisfied, and September 29, when the last Antarctic flight was conducted. This duration permitted a sampling of the preconditions to the formation of the ozone hole, as well as the opportunity to directly observe the onset and intensification of the ozone hole as it evolved during the field experiment. During the experiment, two specially instrumented NASA research aircraft were based in Punta Arenas, Chile. These aircraft flew into and below the ozone hole to make in situ and remotely sensed observations of the atmospheric chemistry and thermodynamic structure. Excluding the transfer flights to and from Punta Arenas, the ER-2 aircraft made 12 flights from Punta Arenas along the Palmer Peninsula at altitudes of from 12 to 19 km, while the DC-8 made 13 long-range flights at lower altitudes of 13 kilometers and below.

The Nimbus-7 Total Ozone Mapping Spectrometer (TOMS) played a central role in the experiment by supplying timely maps of the total ozone distribution over the southern hemisphere. These data were made available to the experiment in a near-real time mode and thus were useful in directing the aircraft by providing the locations of the ozone hole boundary, and in project planning activities in general. TOMS data coverage over several orbital segments centered about the Palmer Peninsula was supplied within several hours of real time, and TOMS data coverage over the entire southern hemisphere was supplied within a day of real time.

## 1.2 The Nimbus-7 TOMS Experiment

On October 24, 1978, the Nimbus-7 spacecraft was launched into a local-noon, sun-synchronous, near-polar orbit. The satellite has provided a measuring platform for eight different experiments and instruments which have observed the Earth's surface, atmosphere, and oceans, and the Sun, in the ultraviolet, visible, near-infrared, infrared, and microwave regions of the spectrum. The TOMS experiment on board Nimbus-7 continues to take high quality data at this time, after more than 9 years of operation.

The TOMS has a 3° by 3° instantaneous field of view (IFOV), with a ground resolution of 50 km at the subsatellite point. The TOMS radiances are sampled in 3° steps ±51° from nadir across the ground track, yielding a total of 35 samples every 8 seconds (Heath et al., 1978). With the 104-minute orbital period of the Nimbus-7, the 8-second scan cycle means that successive scan lines are displaced a little less than 0.5°, or about 50 km, along the orbital track. Due to the Earth's rotation, each orbit of data taken by the Nimbus-7 satellite is located approximately 26° of longitude west of the preceding orbits. At the 51° extreme scan position, the field of view extends to slightly over 13° of the Earth central angle from nadir. Thus, there is no data void between orbits, even at the equator, and true global total ozone mapping is assured.

The TOMS is a single Ebert-Fastie spectrometer, and measures reflected shortwave radiation at six wavelengths ranging from 0.312 μm to 0.380 μm for each sample. The total ozone retrieval algorithm is based on a technique measuring the backscattered ultraviolet radiation (Dave and Mateer, 1967), and closely follows the Nimbus-4 BUV total ozone algorithm (Mateer et al., 1971; Klenk et al., 1982). The measured intensities at the satellite are the sum of both the atmospheric backscattered radiation and the surface-reflected direct and diffuse contributions. The term involving the surface-reflected ultraviolet component is dependent on the atmospheric transmission, itself a function of the ozone optical depth along the slant path of the radiometer's field of view. The two longest wavelengths, which are outside the ozone absorption band and have centers at 0.360 μm and 0.380 μm, are used to determine the surface reflectance. Given the surface reflectance, the total column amount of ozone is computed from radiances observed with the four shortest wavelengths (0.313 μm, 0.318 μm, 0.331 μm, and 0.340 μm) through a table lookup and interpolation procedure (Fleig et al., 1982).

The backscattered ultraviolet radiances are inverted to yield total ozone up to a solar zenith angle of 88°. No nighttime total ozone observations are taken. Thus, the only areas of the Earth for which total ozone measurements are not recovered are in the winter polar regions during 24-hour night.

# 2. TOMS DATA PREPARATION AND TRANSFER

The near-real-time processing and transfer of TOMS ozone data commenced on August 8, 1987 and concluded on September 29, 1987. The processing involved two data sets: (1) complete southern hemispheric data for the 24 hours ending at midnight of the day prior to transmission and (2) orbital swath data for the region including and adjacent to Punta Arenas, Chile, and the Palmer Peninsula of Antarctica processed the same day it was observed.

## 2.1 Data Available to Punta Arenas

The orbital swath data consisted of 2 to 3 orbits daily, which were processed and transferred to Punta Arenas as they were received. Selection of the particular orbits was effected well in advance through the use of predictive ephemeris to generate tables of the orbital ascending-node times and longitudes and plots of the orbital subsatellite tracks (Figure 1). The real-time data flow and transfer is illustrated in Figure 2. Telemetry from the Nimbus-7 spacecraft was downlinked to one of NASA's network of spaceflight tracking stations, such as at Wallops Island, Goldstone, or Santiago, and then transmitted over the NASA Deep-Space Network to the Goddard Space Flight Center (GSFC). The raw TOMS data from each orbit were received at the Mission Operations Control Center (MOCC) in Building 3 at the GSFC and placed onto magnetic tape. This tape was then manually transferred to the NASA Space and Earth Sciences Computing Center (NSESCC) in Building 1 at the GSFC where the raw data were processed into total ozone and reflectivity data on an IBM 3081 computer in Ozone-T standard tape format.

The ozone data were copied to the dedicated TOMS MicroVAX II computer in Building 21 at the GSFC via a fiber optics Ethernet connection. At this point, the orbital swath data were processed prior to release to Punta Arenas. This processing included the gridding of the calibrated Ozone-T data to create an image file, with further processing to display the image file. Once the image was viewed and deemed acceptable, the Ozone-T data files, one for each of up to three orbital swaths, were then transferred via DECnet and two Racal-Milgo 9632 forward error-checking modems at 9.6 kilobits/second (kbps) to a second MicroVAX II located in Punta Arenas. The orbital-swath processing required approximately 30 minutes. The total elapsed time between the actual Nimbus-7 pass over the orbital area and the receipt of total ozone data in Punta Arenas varied between 3 and 4 hours. Once received at Punta Arenas (and at GSFC as well), the data were plotted both in contour form using GEMPAK, as shown here, and in color using a Tektronix 4692 plotter and 4208 color graphics terminal and a standardized color look-up table. The color plots facilitated comparison and permitted rapid interpretation of day-to-day changes in the ozone pattern.

The hemispheric data were processed in a similar fashion, but the elapsed time was greater. A full duration of 24 hours is required for the Nimbus-7 TOMS to obtain global (or southern hemispheric) coverage. The hemispheric data set, containing total ozone data from a complete day of Nimbus-7 orbits, was available to the TOMS MicroVAX by approximately noon of the following day, or 12 hours after Nimbus-7 completed its last orbit of the day. This data set was gridded on the IBM 3081 in Grid-T format and required minimal further processing prior to transfer. The hemispheric ozone data were also transferred to the Punta Arenas MicroVAX II via a DECnet link.

## 2.2 The Near-Real Time Telecommunications Network

To support the voice, facsimile, and digital data telecommunications requirements of the 1987 Antarctic Airborne Ozone experiment, a tri-continental network of dedicated lines and associated signal processing equipment was designed, installed, and operated during the experiment by Research and Data Systems (RDS) Corporation. The network design is illustrated in Figure 3. The telecommunications network configuration permitted meteorological forecast and analysis

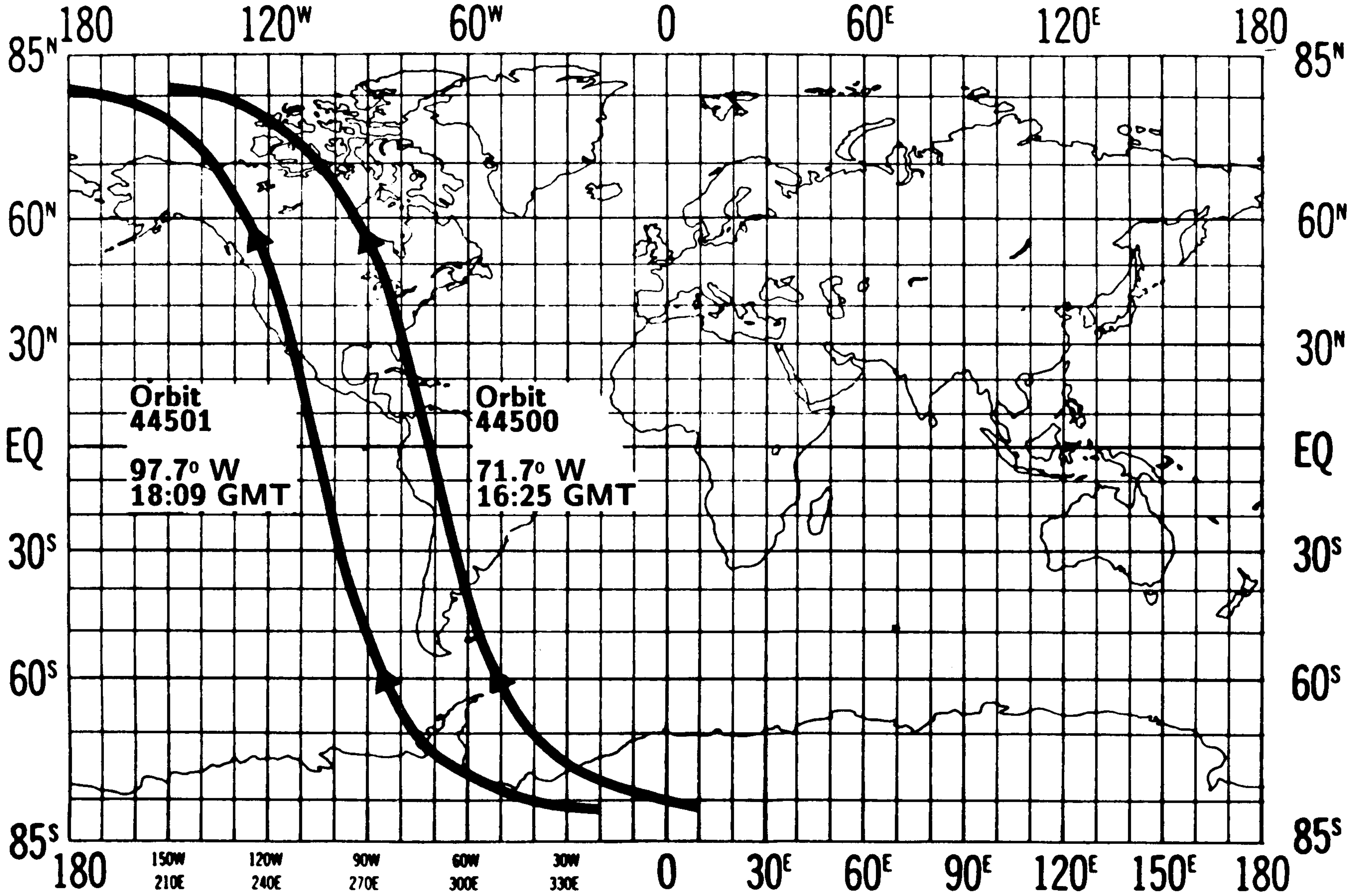


Figure 1. Subsatellite Tracks Produced from Predictive Ephemeris for Orbits 44500-1 on August 17, 1987.

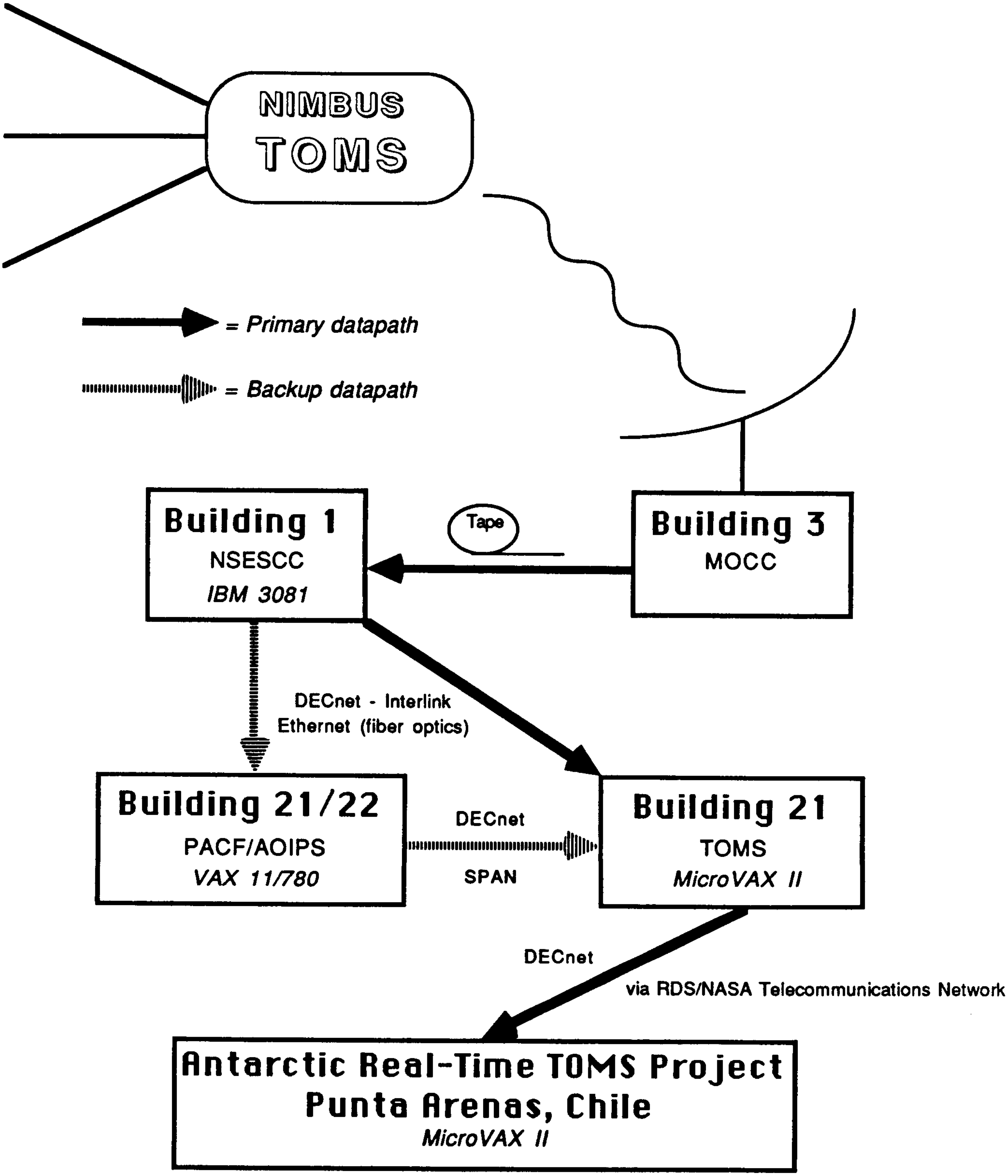


Figure 2. Real-Time TOMS Data Flow and Transfer During the 1987 Airborne Antarctic Ozone Experiment.

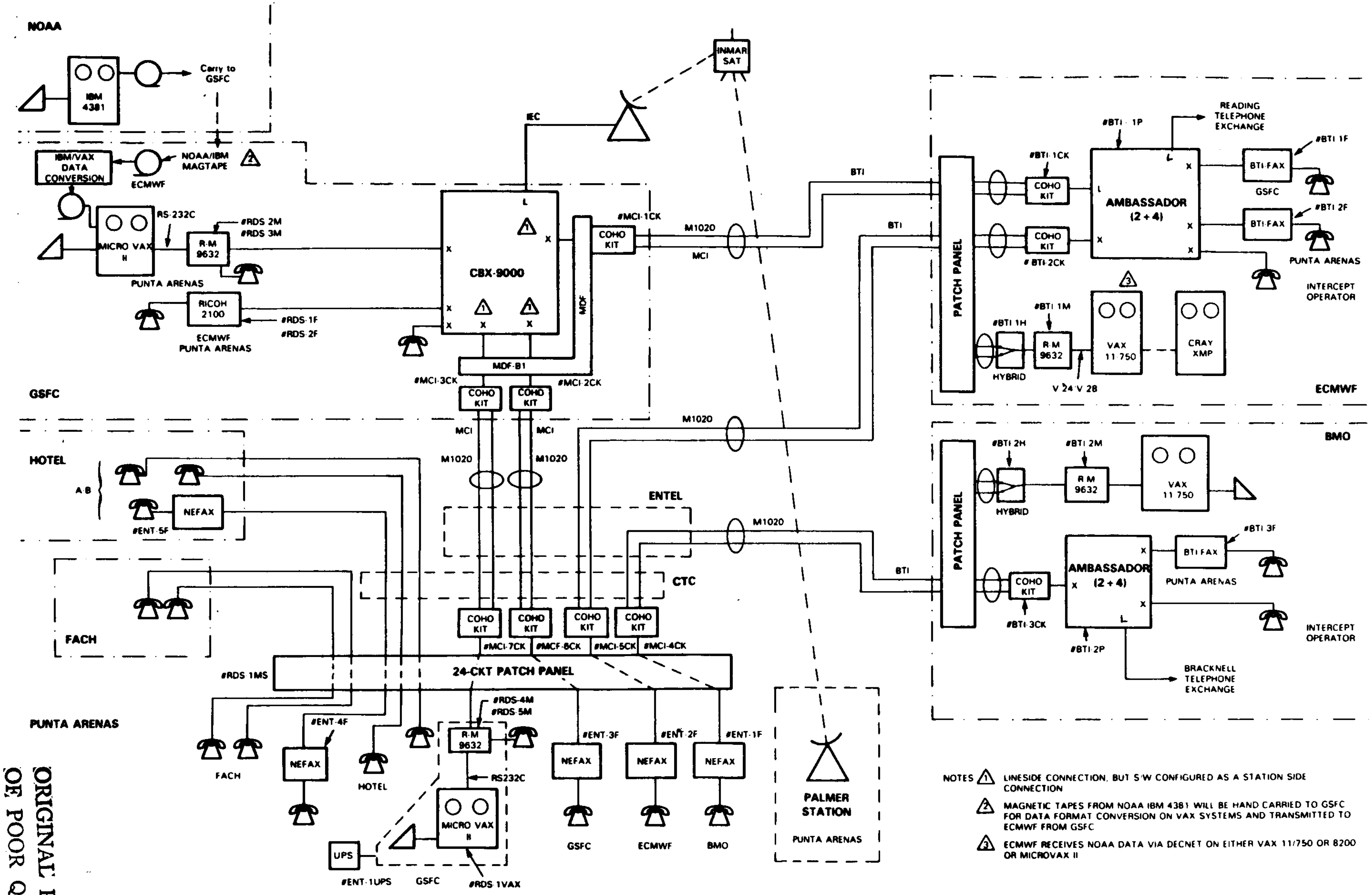




Figure 3. Design of the Telecommunications Network Used to Support the Voice, Facsimile, and Digital Data Requirements of the 1987 Airborne Antarctic Ozone Experiment.

facsimile maps to be supplied to the operations centers at the NASA/GSFC and in Punta Arenas, Chile. Both the European Centre for Medium-Range Weather Forecasting (ECMWF) and the United Kingdom Meteorological Office (UKMO) supplied meteorological products in support of the experiment. The network also permitted general voice and facsimile communications between the Punta Arenas Communications Center, Europe (via the ECMWF and UKMO exchanges), and the United States (via the GSCF CBX-9000 exchange), and voice-only communications to Palmer Station in Antarctica (via the INMARSAT gateway). A more complete discussion of the telecommunications network may be found in Ardanuy et al. (1987).

As shown in Figure 2, the TOMS total ozone data sets were transferred to the MicroVAX II in Punta Arenas via the above-stated network using the DECnet protocol. Because of the dedicated nature of the lines, the high data rate (9.6 kbps), the 24-hour manning of the communications center in Punta Arenas, and the extremely reliable operation of the network as a whole, the TOMS data sets were routinely transferred to the investigators in Punta Arenas in an extremely timely manner. The near-real time orbital total ozone data and delayed hemispheric data were thus of the highest utility in directing the ER-2 and DC-8 aircraft by providing the locations of the ozone hole boundary and navigational information for the mission. The data sets also were used to support the project planning activities in general.

The ability of the network to provide numerical weather prediction charts to the mission forecaster and to provide TOMS total ozone data to the operations center in Punta Arenas were critical to the success of the compaign and were designated go/no-go criteria for the release of the research aircraft from the NASA/Ames Research Center. In view of the desired August 17 beginning of the experimental flight period, the project's go/no-go decision date was set at August 8. The mission criteria were satisfied on August 8 as required, and the DC-8 and ER-2 aircraft left NASA/Ames to fly to Punta Arenas.

## 2.3 Data Analysis and Presentation

Raw TOMS data are converted into total ozone estimates and Earth-located, after which the ungridded TOMS measurements are archived on the Ozone-T tape product. When gridded, the TOMS total ozone observations are stored on the GRIDTOMS archival tape product. During the experiment, the Ozone-T processing was conducted as soon as each orbit within the domain of interest was received at GSFC, while the GRIDTOMS processing was performed once per day on the most recent 24 hours of data. Thus, the orbital swath data were derived from the Ozone-T data sets, while the hemispheric charts were based on data from the GRIDTOMS data sets. During the experiment, the near-real-time processing was accomplished by accessing the respective data sets, which resided in disk storage on the IBM 3081 in "virtual magnetic tape" format.

Data on the GRIDTOMS tapes (Nimbus, 1986) are organized into one-degree latitude zones. The latitude zones are subdivided into cells, each of which contain total ozone values and related parameters and cover the entire globe. As the poles are approached and the distance around the globe along a latitude circle diminishes, the orbits overlap. The number of cells in a zone, in turn, will vary from 288 at the equator to 72 at the poles. The longitudinal resolution of the cellular total ozone values thus varies from 1.25° between 50°N and 50°S latitude, to 10° poleward of the 80° latitudes. The cells contain total ozone estimates which are taken from that satellite orbit closest to the center of each cell. These estimates correspond to the samples nearest the 18th (nadir) scan position. In the latitude zones poleward of 50° the tape also contains, depending on the latitude, up to seven additional total ozone estimates which are obtained from the next closest orbits. Of course, these alternative estimates possess local times which are separated by 104-minute orbital period increments from the total ozone estimate taken at the closest approach. Only the total ozone measurements from the closest satellite overpass are considered here. This selection is performed for two reasons: first, the most vertical glimpse and the smallest footprint is obtained, and second, time-averaging of the ozone field is avoided. After extraction from tape, poleward of the 50° latitudes, the TOMS data are initially repeated at the globally uniform longitudinal resolution of 1.25°. The data are next reduced to a global array with a uniform resolution of 5° of longitude by 2° of latitude. This is accomplished by producing a weighted average of the larger array for each element, i.e., two by four observations. The averaging scheme uses the following set of weights:

$$\begin{bmatrix} 1/16 & 3/16 & 3/16 & 1/16 \\ 1/16 & 3/16 & 3/16 & 1/16 \end{bmatrix}$$

The weighting is adjusted if values are missing from the 2 by 4 element box. If five or more values are missing, then the weighted value is also recorded as missing. The total ozone values at the poles are computed by averaging all the cells between 89° and 90°. The hemispheric plots presented in this atlas consist of a subset of this 91 by 72 element array located between 10° and 90° south latitude. The plots were produced using an interactive data analysis and graphics package, termed GEMPAK (desJardins and Petersen, 1985). GEMPAK requires input dat to be gridded onto a uniform latitude/longitude grid. Since these data are now in such a format, no further processing is required prior to plotting. The advantages of using the reduced resolution data set are that all small data gaps are eliminated and the synoptic and planetary-scale features are clearly displayed. The disadvantage is that any mesoscale features present in the unfiltered TOMS data are eliminated.

The orbital total ozone data, tagged by the latitude and longitude of the IFOV center point, along with several other products, were extracted from the Ozone-T data set (Fleig et al., 1982) for the southern-hemisphere analysis domain and processed using GEMPAK. Because of storage limitations imposed by GEMPAK, measurements from every third scan line, and every third observation in that scan line, were extracted from the orbital swath data. The selected observations for each day were objectively analyzed within GEMPAK using two passes through a Barnes objective analysis routine. The grid spacing produced was 2° in latitude and 1.5° in longitude. Because of the excellent signal-to-noise characteristics of the TOMS total ozone data, the numerical convergence parameter (Koch et al., 1983) was set at 0.3, yielding a minimum of additional smoothing and the greatest detail in the final analysis. Figure 4 depicts a small portion of a single orbital swath from August 17, 1987 displaying digitally the ozone values prior to objective analysis. This orbit (number 44500) is the first of two orbits of Earth-located total ozone observations used to compose the objectively analyzed near-real-time ozone field for the day. The satellite track is from the bottom to the top of the figure, with each cross-track scan sweeping from right to left across the track. The data are unevenly distributed, with the greatest density of observations occurring near nadir (right), and the least out towards the Earth's limb (left). Figure 5 depicts the same area after the data have been objectively analyzed onto a uniform grid as described above. A more uniform density of total ozone values has been achieved. A minimum of 172 DU is achieved midway up the eastern coast of the Antarctic Peninsula, with a strong gradient to the west, north, and south. Comparing the analysis to the original data, we find good agreement. At the eastern base of the peninsula, an analyzed value of 235 DU compares well to the pre-analysis magnitude of 237 DU. At the tip of the peninsula, an analyzed magnitude of 230 DU is in good agreement with the 231 DU observation. However, slight differences are apparent. For example, the minimum value of the ungridded data from orbit 44500 is 161 DU at about 70°S, compared to 172 DU in the analysis. There are three reasons for this sort of discrepancy: (1) two orbits of data (44500-1) are used in the final analysis and, due in part to temporal variability, overlapping data from neighboring orbits are not perfectly in agreement; (2) a subset of the complete set of measurements are used, though in the objective analysis routine a measurement as low as 162 DU is retained from orbit 44501 (not shown); and (3) the Barnes scheme filters all high frequency modes with wavelengths close to and smaller than twice the average separation between nearest observations. Clearly, the final analysis of the total ozone distribution (see the August 17 map of Section 3.4) is faithful to the structure and magnitude of the original set of observations (Figure 4).

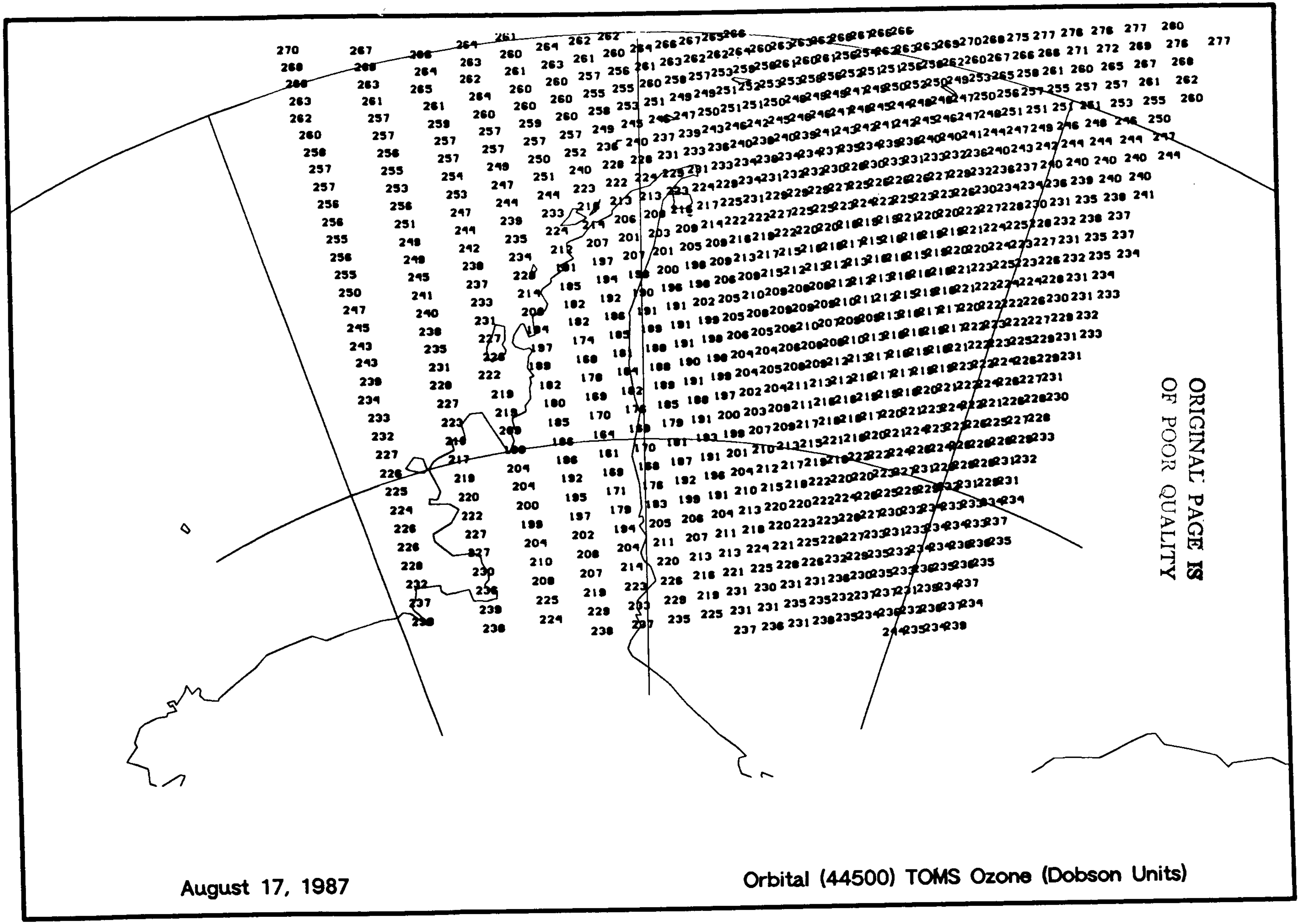




Figure 4. A Sample of TOMS Total Ozone Observations from Portions of 36 Scan Lines During Orbit 44500 of August 17,1987.

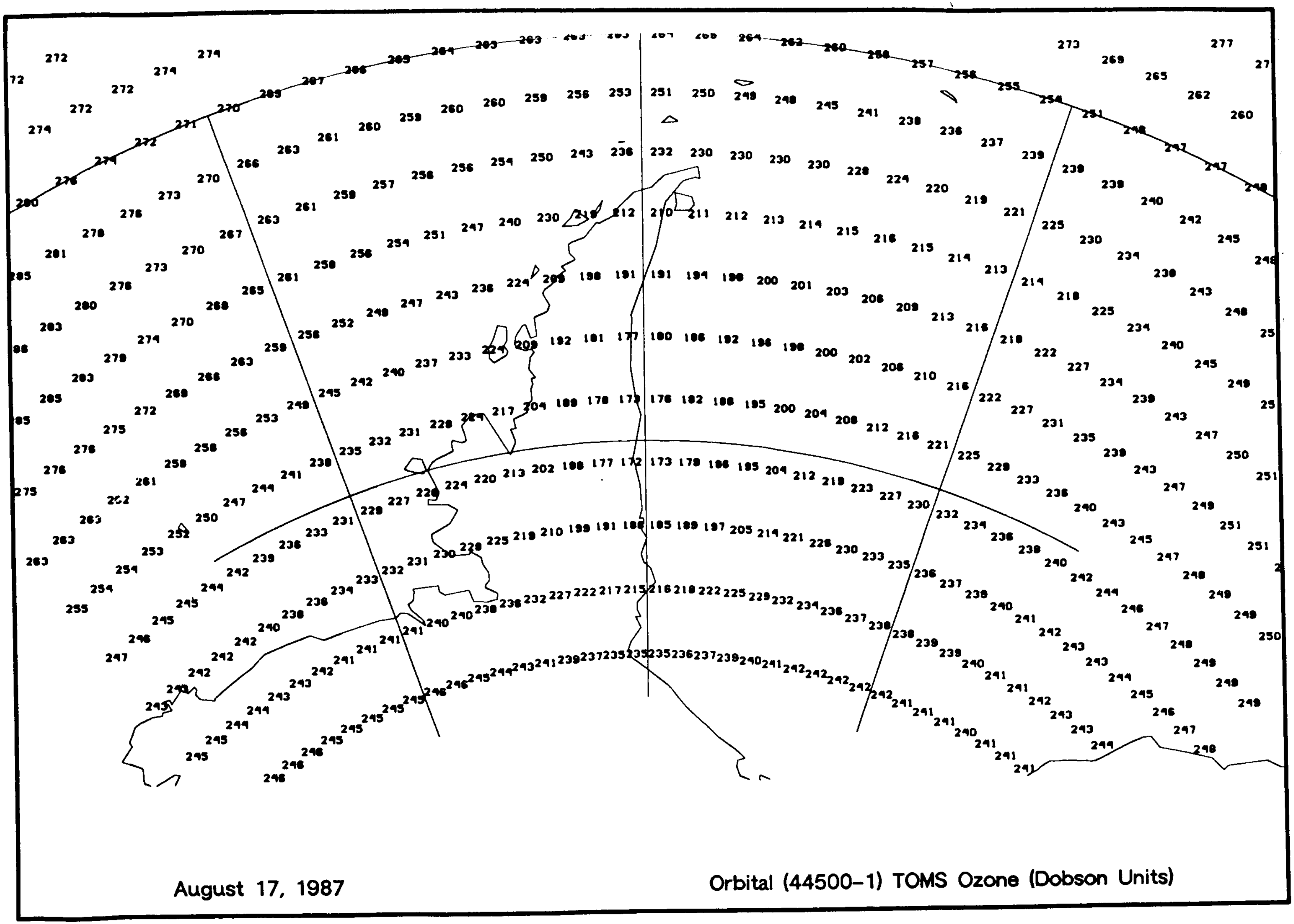


Figure 5. Objectively Analyzed TOMS Total Ozone Data Obtained from Measurements Taken During Orbits 44500-1



ORIGINAL PAGE IS OF POOR QUALITY

The daily orbital swath data consist of from two to three orbital segments located in the latitude range extending from 20°S through the southern terminator (near 75°S in mid-August through 90°S in late September), centered at approximately 70°W longitude, and covering Punta Arenas and the Palmer Peninsula of Antarctica. The precise domain differs from day to day due to the longitudinal differences in the subsatellite tracks. The orbital swaths displayed in this atlas are precisely those produced in near real time in support of the experiment.

2Front RP1201

# 3. TOMS TOTAL OZONE DATA

## 3.1 Chronology of the Experiment

To facilitate the use of the TOMS total ozone data displayed in this atlas, in particular the sets of orbital and hemispheric maps displayed in Sections 3.4 and 3.5, a chronology of relevant events during the experiment has been prepared. We do not consider every day during the period of TOMS coverage, but instead emphasize here the salient points in the data set. In addition, all flights of the ER-2 and DC-8 research aircraft are noted explicitly.

AUGUST 2, 1987
This is the first day for which a TOMS hemispheric image is obtained in near-real-time. The lowest ozone values are present west of the Antarctic Peninsula off the Getz ice shelf. Minimum values of between 200 and 225 Dobson units (DU) are observed.

AUGUST 3, 1987
A large mid-latitude total ozone maximum propagates eastward to between western Australia and Antarctica. Values in excess of 425 DU are recorded.

AUGUST 6, 1987
A small area of minimum total ozone values, less than 250 DU, appears just east of Cape Horn, while the maximum south of Australia exceeds 475 DU.

AUGUST 8, 1987
The go/no-go mission criteria are satisfied as the real-time TOMS system and the associated communications network become fully operational. Near-real-time TOMS total ozone from GSFC and numerical weather prediction forecast charts from UKMO and ECMWF are received in Punta Arenas. The ER-2 and DC-8 aircraft are released for deployment in Punta Arenas. The large maximum formed on August 3rd drifts slowly eastward and merges with a second maximum off Cape Adare.

AUGUST 10, 1987
The small minimum formed on August 6th drifts south and east toward the coast just east of Halley Bay and expands in size.

AUGUST 12, 1987
ER-2 Flight (i) from NASA/AMES to Panama. Observations were made, but these are not officially part of the experiment. The previous total ozone minimum washes out and another area of low total ozone amount appears at the base of the Antarctic peninsula, with total ozone values less than 225 DU. This region expands slightly in size on August 13th and then vanishes on August 14th.

AUGUST 14, 1987
ER-2 Flight (ii) from Panama to Puerto Montt, Chile, with observations. A dominant wavenumber-5 pattern has formed at 50°S, with maxima centered over Chile, southwest of Cape Hope, southeast of Madagascar, south of Australia, and in the central Pacific Ocean.

AUGUST 15, 1987
ER-2 Flight (iii) from Puerto Montt to Punta Arenas, Chile. A new minimum area develops, again at the base of the Antarctic peninsula, and is accompanied by a secondary minimum near the Mawson coast. Both minima have values below 225 DU.

AUGUST 16, 1987
Minimum values in the peninsular "mini-hole" drop below 200 DU for the first time. Orbital imagery suggests the possibility of a lee wave type of pattern in the ozone distribution over the western Weddell Sea.

AUGUST 17, 1987
ER-2 Flight #1. The first official flight of the experiment. The mini-hole persists just east of the peninsula, with a slight increase in area, and with central values of less than 175 DU.

AUGUST 18, 1987
ER-2 Flight #2.

AUGUST 19, 1987
DC-8 Flight (i) makes observations on flight from NASA/AMES to Costa Rica.

AUGUST 22, 1987
DC-8 Flight (ii) from Costa Rica to Punta Arenas. The August 15 minimum near the Weddell Sea has begun to propagate eastward at about 30° longitude per day.

AUGUST 23, 1987
ER-2 Flight #3. During the past week, several minima areas of total ozone wax and wane along the edges of the continent with values in the vicinity of 200 to 225 DU.

AUGUST 28, 1987
ER-2 Flight #4. DC-8 Flight #1. In the last day or two, a quasi-stationary expanding area of low total ozone values develops over the base of the peninsula.

AUGUST 30, 1987
ER-2 Flight #5. DC-8 Flight #2. The end of August finds the area of minimum total ozone in the vicinity of the Weddell Sea and the Antarctic peninsula.

SEPTEMBER 1, 1987
The month begins with one prominent total ozone minimum centered over the base of the Antarctic peninsula. The total ozone values are less than 225 DU over a small area near the center.

SEPTEMBER 2, 1987
ER-2 Flight #6. DC-8 Flight #3. There is a dramatic appearance of a secondary minimum of total ozone on the opposite side of the Antarctic continent and centered between Vostok and the Shackleton Ice Shelf.

SEPTEMBER 4, 1987
ER-2 Flight #7. There are some areas of merged minima surrounding the western half of the Antarctic continent. No values below 200 DU presently exist.

SEPTEMBER 5, 1987
DC-8 Flight #4. A sudden drop in minimum total ozone value near the eastern base of the Antarctic peninsula occurs. Values are now noted below 175 DU. Half of Antarctica is now covered with total ozone magnitudes of less than 225 DU. This is now purported to be the authentic beginning of the 1987 Antarctic ozone hole.

SEPTEMBER 8, 1987
DC-8 Flight #5.

2 Barn

SEPTEMBER 9, 1987
ER-2 Flight #8. The region of lowest total ozone abundances has drifted away from the peninsula, across portions of the Weddell Sea and onto the continent in the vicinity of the Greenwich meridian and latitude 85°S. The lowest total ozone values in the hole are now below 175 DU.

SEPTEMBER 11, 1987
DC-8 Flight #6. Pronounced total ozone maxima in excess of 425 DU circle the hole at 50°S.

SEPTEMBER 14, 1987
DC-8 Flight #7. By now, practically the entire Antarctic continent is covered with total ozone magnitudes of less than 225 DU, with half of the continent experiencing values below 200 DU. Persistent regions with less than 175 DU are present.

SEPTEMBER 16, 1987
ER-2 Flight #9. DC-8 Flight #8. The hole has continued to expand considerably and become more zonally symmetric during the past week. The lowest values over the continent continue to be in the range of 150 to 175 DU. The mid-latitude ozone gradient at 60°S has intensified markedly around three-quarters of the southern hemisphere.

SEPTEMBER 18, 1987
The ozone hole is now very zonally symmetric and is centered almost directly over the south pole. No values below 150 DU have been noted as yet.

SEPTEMBER 19, 1987
DC-8 Flight #9.

SEPTEMBER 20, 1987
ER-2 Flight #10. The hole becomes more organized over the eastern half of the Antarctic continent.

SEPTEMBER 21, 1987
ER-2 Flight #11. DC-8 Flight #10. Polar night ends.

SEPTEMBER 22, 1987
ER-2 Flight #12 is the last flight for this aircraft for this experiment. The ozone hole has shifted its orientation and, for the first time this year, values of total ozone below 150 DU were recorded by TOMS.

SEPTEMBER 24, 1987
DC-8 Flight #11.

SEPTEMBER 26, 1987
DC-8 Flight #12.

SEPTEMBER 29, 1987
DC-8 Flight #13. Both aircraft leave Punta Arenas. The ER-2 flies to Puerto Montt and the DC-8 overflies Antarctica on its way to Christ Church, New Zealand. A significant portion of Antarctica is covered with total ozone amounts of less than 150 DU.

SEPTEMBER 30, 1987
The ozone hole at the end of the month is symmetric and centered near the south pole. Values between 125 and 150 DU continue to be recorded.

OCTOBER 1, 1987
The ER-2 departs Puerto Montt for Panama. The month begins with a slightly egg-shaped ozone hole with a long axis oriented along a line from Rio de Janeiro to Melbourne. The minimum values remain below 150 DU and cover an increasingly larger domain. By this day, all latitudes south of 80°S possess total ozone amounts of less than 150 DU.

OCTOBER 2, 1987
The DC-8 departs Christ Church for Hawaii.

OCTOBER 3, 1987
The ER-2 returns to NASA/AMES from Panama.

OCTOBER 4, 1987
The DC-8 returns to NASA/AMES from Hawaii.

OCTOBER 5, 1987
On this day, the total ozone amount reached its all-time lowest recorded value of 109 DU. The orientation of the ozone hole shifted in such a way that its long axis now lies along the Greenwich meridian. The hole remains very symmetrical, and its center is near 87 degrees south. The mid-latitude gradient of total ozone is extremely steep and quite uniform around the entire Antarctic continent.

OCTOBER 10, 1987
The axis of the ozone hole continues to rotate in a clockwise manner around the hemisphere. The minimum values at this time are everywhere above 125 DU.

OCTOBER 15, 1987
The total ozone imagery on this date shows a very well developed horn-shaped maximum in mid-latitudes between Australia and Antarctica. Values of total ozone in this maximum exceed 450 DU. Meanwhile, there has been very little rotation of the hole's axis during the past five days.

OCTOBER 16, 1987
In the center of the ozone hole, near the South Pole, minimum values below 125 DU again appear. These persist only until October 18.

OCTOBER 23, 1987
The long axis of the egg-shaped ozone hole is oriented along the 90th meridian and the large maximum values of just a few days before have relaxed considerably. The total ozone pattern on this date just begins to erode.

OCTOBER 24, 1987
There now appears to be a definite intrusion of higher latitude air into the ozone hole on its western flank. The intrusion resembles the tongues of dry air which spiral into the center of mid-latitude cyclones.

OCTOBER 26, 1987
The ozone hole continues to erode slowly away. Meanwhile, the total ozone maxima on either side of the hole begin again to rotate from west to east around the central vortex. These maxima were previously relatively stationary.

OCTOBER 31, 1987
The central portion of the ozone hole has shrunk to its smallest area so far this month. Values of total ozone less than 150 DU occur in a very small area between the Ross ice shelf and the South Pole.

NOVEMBER 1, 1987
The area of total ozone values less than 150 DU breaks up into five much smaller areas.

NOVEMBER 9, 1987
The ozone hole, during the past week, remains unusually stable. Areas of maximum total ozone continued to rotate east to west around the hole and the strong ozone gradients persist in mid-latitudes.

NOVEMBER 13, 1987
Almost two weeks into the month of November, the ozone hole essentially maintains its shape and size. Only the minimum values have increased slowly. For the first time during the past month, minimum values exceeded 150 DU. In previous years the ozone hole was not nearly so persistent and had usually shown a good deal of dissipation by this time.

NOVEMBER 18, 1987
The ozone hole begins to dramatically elongate along the axis of the Greenwich meridian and the date line. At the same time, it begins to rotate clockwise at the rate of about 30° longitude per day.

NOVEMBER 25, 1987
For the first time since its incipient stages, the center of the hole moves off the south pole. No ozone values below 175 DU now exist. The ozone ridge extending along the date line toward the pole is probably a result of the rotation of the elongated hole. Twenty-four hours separate data on either side of the date line, during which the ozone trough has apparently crossed the date line.

NOVEMBER 30, 1987
The center of the ozone hole is located along the Antarctic coast at 30°E, while the south pole is centered in a steep ozone gradient. Only a very small area contains ozone values less than 200 DU. The hole itself is now strongly elongated into a pronounced wavenumber one pattern.

## 3.2 Latitudinal Cross-Sections

Figures 6a-d are cross-sections across the south pole and illustrate the development of the ozone hole in the southern hemisphere during the 1987 Airborne Antarctic Ozone Experiment. The abscissa of these plots represents a cross-section (along the 70°W and 110°E longitudes), beginning at 20°S, 70°W, through the south pole, to 20°S, 110°E. Figure 6a presents four curves, each an average for eight days in August. Figures 6b and 6c present a similar display for September and October. Figure 6d is a cross-section for a single day, October 5, 1987, during which the lowest ozone values were observed for this season.

From Figure 6a it can be seen that ozone levels reach a maximum at mid-latitudes, dropping off toward the pole and the equator. Since the immediate polar region is still in 24-hour darkness, no TOMS total ozone measurement is obtained. Although the poleward minima appear to be slightly lower than those at the equator, no pronounced "hole" is yet apparent. The mid-latitude maxima appear to increase somewhat over time, although the trend is inconsistent. No discernible trend exists in the polar minima for this month.

Progressing through September (Figure 6b), one is able to see the hole in the total ozone field develop. The trend, especially at 80°S 110°E, refutes any suggestion that the ozone hole was present all along, only becoming observable as the pole was illuminated. The total ozone gradient, especially near 60°S 110°E, becomes pronounced. There does not appear to be any trend in the mid-latitude maxima worthy of note.

In October (Figure 6c), much of the longitudinal symmetry observed in August and September is perturbed. While the minimum total ozone values exhibit little change, there is a pronounced shifting of the center of the hole southward along 70°W and northward along 110°E. In a two-dimensional view (see Section 3.5), this corresponds to a shifting of the major axis of the then elliptically shaped ozone hole. In addition, along 110°E, the maxima are persistently higher and the gradient steeper than along 70°W. This feature is also evident in the individual polar charts for the period. The maxima along 110°E seem to diminish over time, due in part to a rotation in the major axis of the pattern. Figure 6d shows the pattern as it appeared on October 5, 1987, the amplitude when the total ozone hole was most pronounced, and the lowest total ozone measurements for the year were recorded by TOMS.

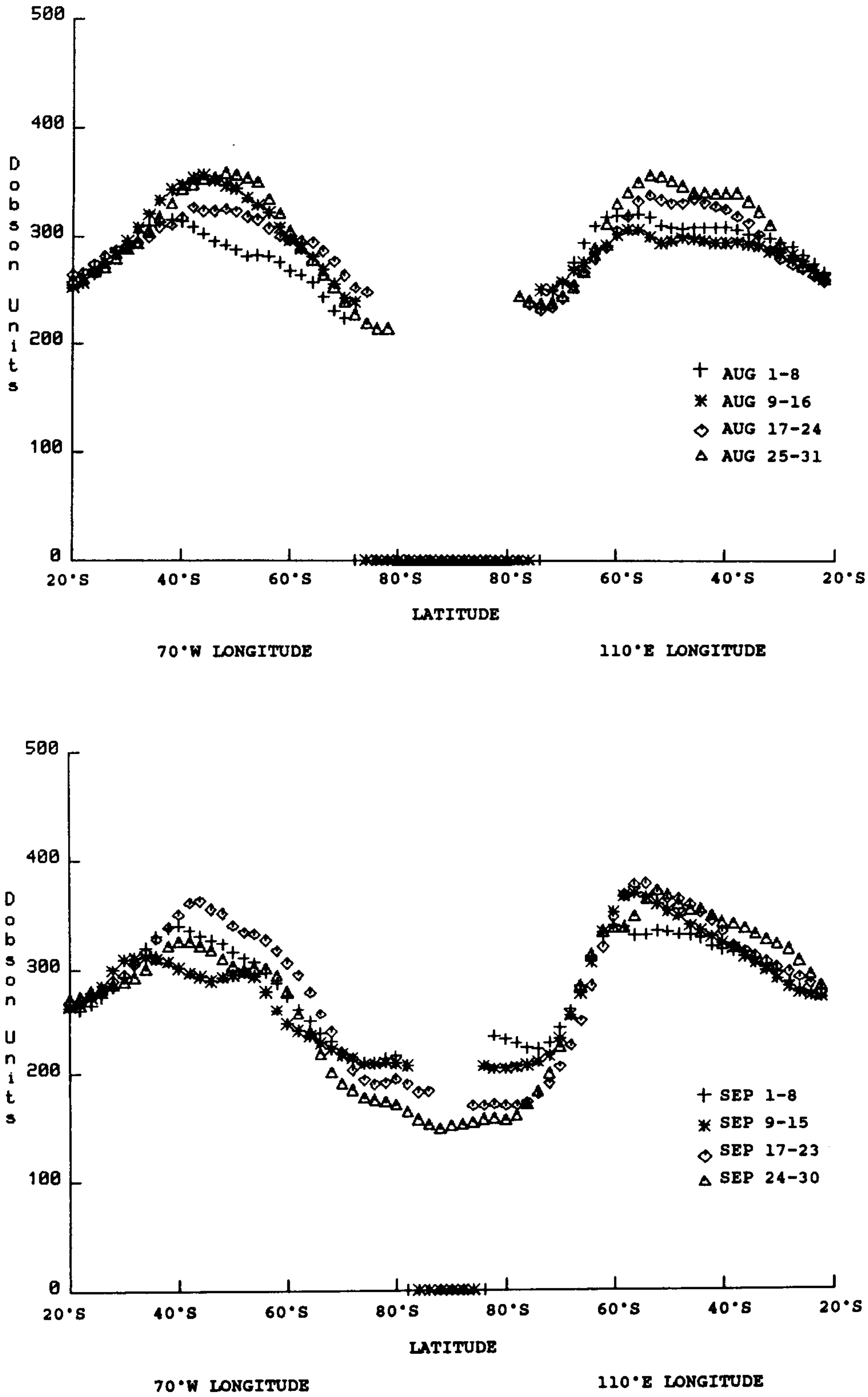


Figure 6a-b. Cross-sections of TOMS total ozone measurements along the 70°W and 110°E longitudes across the south pole for four periods during (a) August 1987 and (b) September 1987.

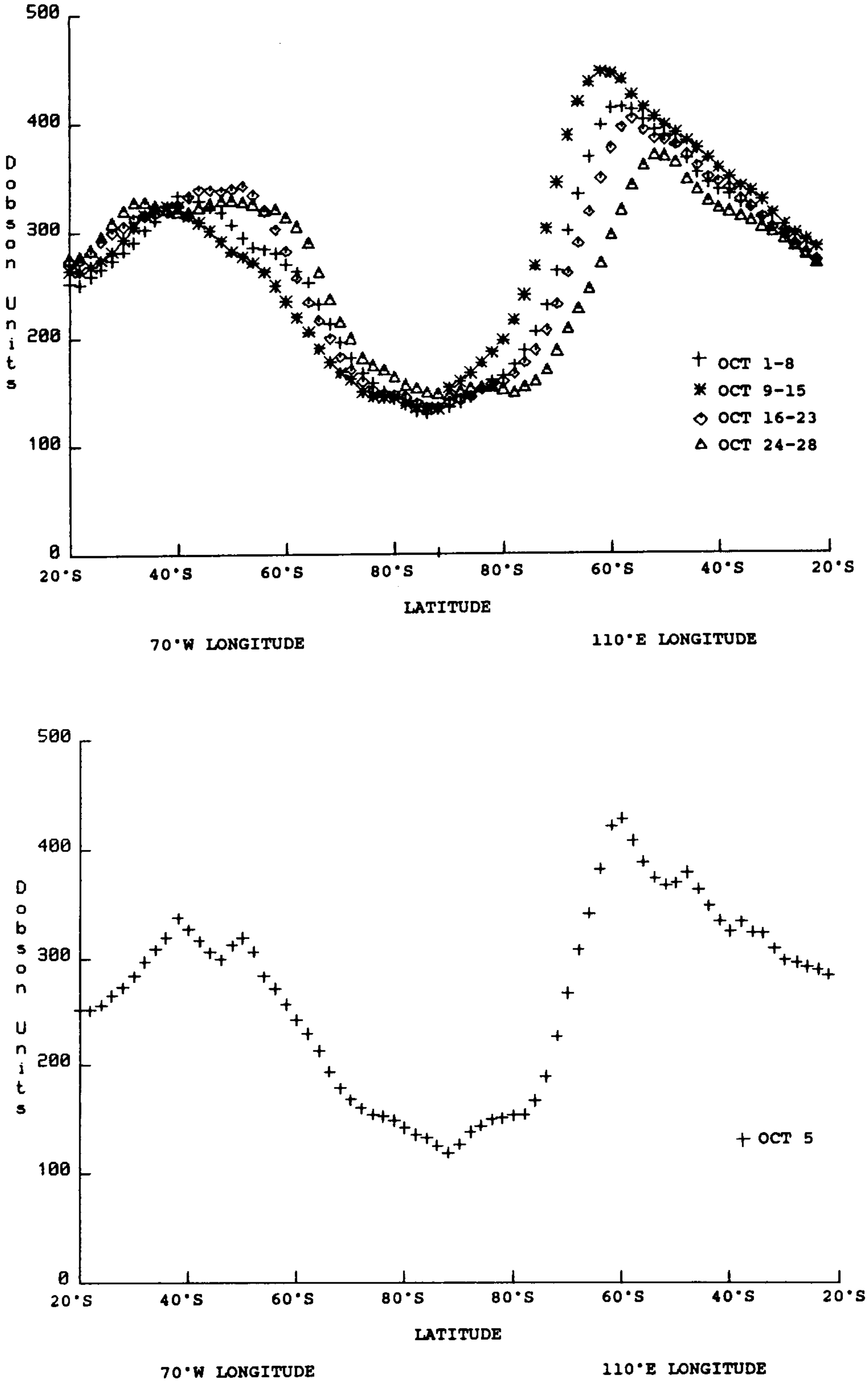


Figure 6c-d. Cross-sections of TOMS total ozone measurements along the 70°W and 110°E longitudes across the south pole for (c) four periods during October 1987 and (d) October 5, 1987.

## 3.3 Time Series at Locations of Interest

Time series of TOMS total ozone estimates have been constructed for a set of eleven locations in Antarctica. A similar time series for the experiment's base of operations in Punta Arenas was also produced. A list of the selected locations, and their coordinates, is provided in Table 1. The time series incorporate daily gridded measurements from the southern-hemispheric grids (Section 2.3), and are extracted from that 2° (latitude) by 5° (longitude) grid element within which each station resides. At the mean latitude of 70°S, this corresponds to spatial average over an area of 222 km by 189 km. Table 2 presents the time series for the period August 1 through November 15, 1987. Note that Palmer Station and Faraday Station, located some 50 km apart, fall within the same grid element and are assigned the same total column ozone values. Of course, a number of the stations are located south of the Antarctic circle and experience 24-hour night during a portion of the experiment. During these periods, the TOMS total ozone estimates at these stations, which include Amundsen-Scott, Halley Bay, McMurdo Sound, and Vostok, are not available. The zero values denote missing data.

**Punta Arenas**

Punta Arenas, Chile, located near Cape Horn in extreme southern Chile at 53°S, lies outside the boundary of the ozone hole throughout the 1987 experiment. The daily TOMS total ozone estimates fluctuate between 240 DU and 393 DU (Figure 7a). The minimum of 240 DU on August 19 occurs as a result of an in-phase relationship between two total ozone minima: one quasi-stationary minimum over the Antarctic Peninsula, and a second component related to an eastward propagating wave. Interestingly, a value approaching the maximum value for the period occurs only two days later as a strong eastward-propagating center moves over southern Chile.

**B.A. Vice Comodoro Marambio**

The Marambio station is located at 64°S, just off the tip of the Antarctic Peninsula. The daily TOMS total-column ozone amounts at Marambio range from 168 to 399 DU (Figure 7b). The time series exhibits some very interesting fluctuations. Consider the minimum of August 16-19 (days 228-231). Referring to the corresponding maps, the short-lived minimum is caused by the presence of a "mini-hole" over the peninsula, a situation which recurs on about September 5 (day 248), as another relatively small minimum moves over the station. The minima of September 23-26 (days 266-269) and October 8-12 (days 281-285), however, are caused by the growth of the ozone hole boundary beyond the tip of the peninsula, so that Marambio is located to the south of the steep total-ozone gradient. Similarly, the periodic maxima such as during the period of September 16-22 (days 259-265) are caused by a local southward movement of the hole's boundary, such that the station is located within (or to the north of) the total ozone gradient. Abruptly, on October 28 (day 301), the total ozone measurements over the location reached their highest values for the period. The month of November brings large oscillations in ozone amount as the station falls alternately within and outside of the hole.

**Palmer Station/Faraday Station**

The Palmer and Faraday stations, located at 65°S, lie within the same grid element and are considered jointly. The total ozone data for this location (Figure 7c) are closely correlated with, though independent of, the TOMS measurements taken over Marambio.

Table 1

Selected Locations for TOMS Total Ozone Time Series

| Location | Abbreviation | Latitude | Longitude |
|---|---|---|---|
| Amundsen-Scott | SPO | 90°00'S | 00°00'W |
| B.A. Vice Comodoro Marambio | MAR | 64°14'S | 56°43'W |
| Davis | DAV | 68°36'S | 78°00'E |
| Dumont D'Urville | DUD | 66°42'S | 140°00'E |
| Faraday Station, Argentine Islands | FAR | 65°15'S | 64°16'W |
| Halley Bay | HAL | 75°30'S | 26°39'W |
| McMurdo | MCM | 77°51'S | 166°40'E |
| Molodeznaja | MOL | 67°42'S | 45°54'E |
| Palmer Station | PAL | 64°46'S | 64°04'W |
| Punta Arenas | PUN | 53°02'S | 70°51'W |
| Syowa | SYO | 69°00'S | 39°36'E |
| Vostok | VOS | 78°30'S | 106°54'E |

Table 2

Time Series of Daily Total Ozone Values (DU)

| DAY | DATE | SPO | FAR | HAL | MAR | MCM | PAL | PUN | DAV | SYO | VOS | MOL | DUM |
|---|---|---|---|---|---|---|---|---|---|---|---|---|---|
| 213 | AUG 01 | 0 | 240 | 0 | 261 | 0 | 240 | 273 | 288 | 246 | 0 | 252 | 270 |
| 214 | AUG 02 | 0 | 237 | 0 | 252 | 0 | 237 | 312 | 258 | 237 | 0 | 240 | 318 |
| 215 | AUG 03 | 0 | 249 | 0 | 261 | 0 | 249 | 330 | 246 | 237 | 0 | 237 | 330 |
| 216 | AUG 04 | 0 | 240 | 0 | 255 | 0 | 240 | 261 | 237 | 243 | 0 | 243 | 303 |
| 217 | AUG 05 | 0 | 243 | 0 | 255 | 0 | 243 | 276 | 243 | 243 | 0 | 246 | 318 |
| 218 | AUG 06 | 0 | 234 | 0 | 255 | 0 | 234 | 255 | 249 | 249 | 0 | 261 | 303 |
| 219 | AUG 07 | 0 | 0 | 0 | 231 | 0 | 0 | 0 | 255 | 237 | 0 | 240 | 297 |
| 220 | AUG 08 | 0 | 252 | 0 | 249 | 0 | 252 | 327 | 249 | 246 | 0 | 249 | 276 |
| 221 | AUG 09 | 0 | 264 | 0 | 264 | 0 | 264 | 363 | 240 | 258 | 0 | 255 | 279 |
| 222 | AUG 10 | 0 | 270 | 0 | 288 | 0 | 270 | 327 | 252 | 255 | 0 | 249 | 276 |
| 223 | AUG 11 | 0 | 291 | 0 | 282 | 0 | 291 | 360 | 258 | 252 | 0 | 252 | 249 |
| 224 | AUG 12 | 0 | 270 | 0 | 288 | 0 | 270 | 372 | 255 | 246 | 0 | 252 | 273 |
| 225 | AUG 13 | 0 | 249 | 0 | 261 | 0 | 249 | 315 | 267 | 234 | 0 | 237 | 261 |
| 226 | AUG 14 | 0 | 261 | 0 | 255 | 0 | 261 | 306 | 252 | 243 | 0 | 243 | 270 |
| 227 | AUG 15 | 0 | 243 | 0 | 258 | 0 | 243 | 327 | 237 | 231 | 0 | 225 | 261 |
| 228 | AUG 16 | 0 | 219 | 0 | 246 | 0 | 219 | 300 | 231 | 240 | 0 | 243 | 261 |
| 229 | AUG 17 | 0 | 201 | 0 | 222 | 0 | 201 | 282 | 255 | 237 | 0 | 231 | 273 |
| 230 | AUG 18 | 0 | 234 | 0 | 237 | 0 | 234 | 279 | 228 | 240 | 0 | 237 | 255 |
| 231 | AUG 19 | 0 | 216 | 0 | 222 | 0 | 216 | 240 | 243 | 237 | 0 | 243 | 261 |
| 232 | AUG 20 | 0 | 285 | 264 | 276 | 0 | 285 | 291 | 219 | 228 | 0 | 234 | 237 |
| 233 | AUG 21 | 0 | 309 | 258 | 300 | 0 | 309 | 393 | 243 | 258 | 0 | 258 | 249 |
| 234 | AUG 22 | 0 | 339 | 264 | 351 | 0 | 339 | 330 | 255 | 252 | 0 | 252 | 270 |
| 235 | AUG 23 | 0 | 324 | 258 | 354 | 0 | 324 | 348 | 258 | 231 | 0 | 240 | 255 |
| 236 | AUG 24 | 0 | 303 | 267 | 321 | 0 | 303 | 351 | 243 | 234 | 0 | 237 | 243 |
| 237 | AUG 25 | 0 | 291 | 264 | 312 | 0 | 291 | 372 | 240 | 219 | 0 | 216 | 279 |
| 238 | AUG 26 | 0 | 273 | 261 | 291 | 237 | 273 | 357 | 240 | 231 | 243 | 240 | 282 |
| 239 | AUG 27 | 0 | 276 | 240 | 291 | 237 | 276 | 342 | 243 | 240 | 246 | 231 | 258 |
| 240 | AUG 28 | 0 | 276 | 237 | 291 | 237 | 276 | 345 | 237 | 249 | 255 | 255 | 255 |
| 241 | AUG 29 | 0 | 279 | 213 | 297 | 264 | 279 | 348 | 264 | 255 | 237 | 261 | 249 |
| 242 | AUG 30 | 0 | 243 | 222 | 267 | 240 | 243 | 333 | 252 | 249 | 240 | 252 | 285 |
| 243 | AUG 31 | 0 | 231 | 219 | 246 | 240 | 231 | 339 | 246 | 246 | 246 | 255 | 273 |
| 244 | SEP 01 | 0 | 240 | 219 | 267 | 258 | 240 | 282 | 246 | 249 | 252 | 243 | 264 |
| 245 | SEP 02 | 0 | 255 | 228 | 276 | 255 | 255 | 321 | 231 | 237 | 216 | 234 | 261 |
| 246 | SEP 03 | 0 | 255 | 222 | 264 | 231 | 255 | 306 | 228 | 240 | 207 | 231 | 252 |
| 247 | SEP 04 | 0 | 237 | 216 | 267 | 210 | 237 | 309 | 237 | 234 | 234 | 231 | 234 |
| 248 | SEP 05 | 0 | 204 | 222 | 225 | 216 | 204 | 288 | 243 | 240 | 246 | 237 | 249 |
| 249 | SEP 06 | 0 | 213 | 183 | 222 | 240 | 213 | 306 | 237 | 258 | 228 | 234 | 243 |
| 250 | SEP 07 | 0 | 249 | 192 | 267 | 225 | 249 | 309 | 231 | 243 | 228 | 252 | 282 |
| 251 | SEP 08 | 0 | 240 | 192 | 255 | 228 | 240 | 306 | 249 | 228 | 225 | 240 | 288 |
| 252 | SEP 09 | 0 | 225 | 207 | 225 | 234 | 225 | 297 | 261 | 222 | 219 | 222 | 294 |
| 253 | SEP 10 | 0 | 225 | 192 | 228 | 240 | 225 | 282 | 237 | 222 | 237 | 231 | 285 |
| 254 | SEP 11 | 0 | 225 | 180 | 231 | 240 | 225 | 270 | 225 | 219 | 219 | 228 | 276 |
| 255 | SEP 12 | 0 | 216 | 177 | 225 | 231 | 216 | 282 | 219 | 225 | 213 | 225 | 324 |
| 256 | SEP 13 | 0 | 219 | 189 | 222 | 219 | 219 | 330 | 219 | 213 | 192 | 225 | 303 |
| 257 | SEP 14 | 0 | 234 | 192 | 240 | 204 | 234 | 309 | 207 | 213 | 180 | 222 | 267 |
| 258 | SEP 15 | 0 | 228 | 189 | 228 | 192 | 228 | 270 | 213 | 225 | 162 | 228 | 246 |
| 259 | SEP 16 | 0 | 264 | 207 | 279 | 180 | 264 | 321 | 237 | 219 | 171 | 231 | 234 |

Table 2 (continued)

Time Series of Daily Total Ozone Values (DU)

| DAY | DATE | SPO | FAR | HAL | MAR | MCM | PAL | PUN | DAV | SYO | VOS | MOL | DUM |
|---|---|---|---|---|---|---|---|---|---|---|---|---|---|
| 260 | SEP 17 | 0 | 252 | 180 | 267 | 180 | 252 | 387 | 216 | 204 | 189 | 207 | 240 |
| 261 | SEP 18 | 0 | 243 | 186 | 261 | 198 | 243 | 390 | 204 | 198 | 183 | 204 | 252 |
| 262 | SEP 19 | 0 | 246 | 198 | 258 | 183 | 246 | 354 | 219 | 183 | 177 | 189 | 267 |
| 263 | SEP 20 | 0 | 255 | 180 | 261 | 186 | 255 | 312 | 201 | 177 | 165 | 180 | 249 |
| 264 | SEP 21 | 0 | 282 | 192 | 285 | 186 | 282 | 282 | 198 | 198 | 147 | 189 | 255 |
| 265 | SEP 22 | 0 | 240 | 189 | 282 | 180 | 240 | 294 | 201 | 198 | 147 | 210 | 252 |
| 266 | SEP 23 | 0 | 210 | 177 | 231 | 174 | 210 | 294 | 225 | 216 | 168 | 249 | 237 |
| 267 | SEP 24 | 0 | 201 | 168 | 204 | 165 | 201 | 276 | 258 | 210 | 165 | 261 | 273 |
| 268 | SEP 25 | 0 | 183 | 177 | 189 | 177 | 183 | 285 | 261 | 195 | 153 | 231 | 270 |
| 269 | SEP 26 | 153 | 192 | 177 | 192 | 162 | 192 | 273 | 249 | 186 | 168 | 207 | 237 |
| 270 | SEP 27 | 147 | 204 | 174 | 219 | 177 | 204 | 270 | 201 | 192 | 162 | 210 | 252 |
| 271 | SEP 28 | 141 | 219 | 165 | 216 | 174 | 219 | 327 | 213 | 219 | 147 | 258 | 240 |
| 272 | SEP 29 | 132 | 234 | 165 | 249 | 162 | 234 | 339 | 261 | 198 | 144 | 255 | 180 |
| 273 | SEP 30 | 117 | 219 | 168 | 231 | 162 | 219 | 312 | 249 | 183 | 147 | 216 | 234 |
| 274 | OCT 01 | 123 | 210 | 153 | 219 | 144 | 210 | 303 | 237 | 177 | 159 | 204 | 273 |
| 275 | OCT 02 | 132 | 225 | 153 | 198 | 153 | 225 | 309 | 225 | 201 | 153 | 237 | 267 |
| 276 | OCT 03 | 135 | 255 | 147 | 258 | 141 | 255 | 318 | 243 | 207 | 150 | 255 | 231 |
| 277 | OCT 04 | 135 | 237 | 156 | 264 | 150 | 237 | 297 | 276 | 174 | 147 | 195 | 252 |
| 278 | OCT 05 | 117 | 183 | 150 | 183 | 144 | 183 | 285 | 270 | 177 | 153 | 186 | 225 |
| 279 | OCT 06 | 120 | 258 | 135 | 240 | 156 | 258 | 261 | 264 | 156 | 192 | 159 | 234 |
| 280 | OCT 07 | 138 | 237 | 138 | 246 | 180 | 237 | 246 | 204 | 165 | 192 | 168 | 369 |
| 281 | OCT 08 | 144 | 177 | 138 | 195 | 225 | 177 | 288 | 201 | 153 | 168 | 165 | 405 |
| 282 | OCT 09 | 132 | 162 | 138 | 168 | 210 | 162 | 285 | 228 | 186 | 177 | 201 | 387 |
| 283 | OCT 10 | 144 | 174 | 141 | 186 | 234 | 174 | 273 | 291 | 183 | 204 | 204 | 390 |
| 284 | OCT 11 | 156 | 180 | 138 | 195 | 249 | 180 | 264 | 261 | 177 | 225 | 210 | 444 |
| 285 | OCT 12 | 147 | 174 | 144 | 189 | 255 | 174 | 270 | 270 | 174 | 183 | 195 | 444 |
| 286 | OCT 13 | 141 | 201 | 135 | 183 | 189 | 201 | 264 | 273 | 186 | 189 | 216 | 360 |
| 287 | OCT 14 | 138 | 198 | 141 | 198 | 195 | 198 | 255 | 285 | 198 | 192 | 216 | 384 |
| 288 | OCT 15 | 141 | 201 | 150 | 228 | 207 | 201 | 297 | 252 | 177 | 195 | 195 | 429 |
| 289 | OCT 16 | 141 | 189 | 150 | 189 | 228 | 189 | 276 | 192 | 198 | 183 | 234 | 426 |
| 290 | OCT 17 | 138 | 189 | 150 | 198 | 246 | 189 | 321 | 198 | 198 | 171 | 228 | 417 |
| 291 | OCT 18 | 135 | 177 | 153 | 183 | 213 | 177 | 327 | 234 | 198 | 159 | 246 | 351 |
| 292 | OCT 19 | 141 | 210 | 141 | 219 | 195 | 210 | 336 | 258 | 183 | 153 | 207 | 354 |
| 293 | OCT 20 | 138 | 189 | 153 | 198 | 177 | 189 | 363 | 204 | 165 | 162 | 183 | 342 |
| 294 | OCT 21 | 132 | 234 | 159 | 240 | 180 | 234 | 333 | 180 | 207 | 156 | 204 | 345 |
| 295 | OCT 22 | 129 | 267 | 153 | 297 | 186 | 267 | 366 | 186 | 216 | 138 | 237 | 315 |
| 296 | OCT 23 | 126 | 249 | 150 | 276 | 195 | 249 | 342 | 195 | 171 | 135 | 180 | 294 |
| 297 | OCT 24 | 147 | 216 | 162 | 237 | 186 | 216 | 327 | 171 | 177 | 144 | 192 | 261 |
| 298 | OCT 25 | 150 | 210 | 174 | 225 | 177 | 210 | 291 | 171 | 231 | 159 | 234 | 255 |
| 299 | OCT 26 | 144 | 189 | 183 | 207 | 162 | 189 | 306 | 219 | 243 | 144 | 282 | 255 |
| 300 | OCT 27 | 141 | 315 | 165 | 327 | 150 | 315 | 348 | 243 | 240 | 153 | 291 | 237 |
| 301 | OCT 28 | 144 | 396 | 177 | 399 | 162 | 396 | 348 | 240 | 219 | 147 | 264 | 207 |
| 302 | OCT 29 | 141 | 393 | 180 | 372 | 168 | 393 | 354 | 261 | 228 | 159 | 255 | 213 |
| 303 | OCT 30 | 144 | 381 | 210 | 363 | 165 | 381 | 369 | 282 | 201 | 168 | 207 | 213 |
| 304 | OCT 31 | 147 | 408 | 270 | 393 | 165 | 408 | 384 | 231 | 198 | 153 | 192 | 255 |

Table 2 (continued)

Time Series of Daily Total Ozone Values (DU)

| DAY | DATE | SPO | FAR | HAL | MAR | MCM | PAL | PUN | DAV | SYO | VOS | MOL | DUM |
|---|---|---|---|---|---|---|---|---|---|---|---|---|---|
| 305 | NOV 01 | 153 | 309 | 246 | 345 | 171 | 309 | 390 | 210 | 204 | 150 | 198 | 270 |
| 306 | NOV 02 | 153 | 351 | 201 | 345 | 159 | 351 | 360 | 210 | 234 | 159 | 237 | 207 |
| 307 | NOV 03 | 153 | 348 | 207 | 384 | 156 | 348 | 372 | 216 | 234 | 162 | 258 | 216 |
| 308 | NOV 04 | 159 | 237 | 198 | 294 | 159 | 237 | 342 | 246 | 213 | 162 | 264 | 234 |
| 309 | NOV 05 | 159 | 198 | 171 | 216 | 165 | 198 | 0 | 282 | 201 | 162 | 225 | 237 |
| 310 | NOV 06 | 150 | 204 | 168 | 207 | 168 | 204 | 303 | 261 | 210 | 174 | 240 | 315 |
| 311 | NOV 07 | 150 | 222 | 168 | 240 | 180 | 222 | 360 | 270 | 225 | 189 | 249 | 318 |
| 312 | NOV 08 | 156 | 258 | 174 | 276 | 192 | 258 | 375 | 300 | 213 | 204 | 249 | 351 |
| 313 | NOV 09 | 153 | 264 | 168 | 309 | 207 | 264 | 318 | 300 | 204 | 192 | 249 | 402 |
| 314 | NOV 10 | 150 | 225 | 225 | 246 | 198 | 225 | 294 | 255 | 222 | 183 | 222 | 366 |
| 315 | NOV 11 | 153 | 204 | 195 | 216 | 192 | 204 | 285 | 219 | 315 | 180 | 294 | 357 |
| 316 | NOV 12 | 165 | 222 | 186 | 267 | 192 | 222 | 336 | 243 | 309 | 171 | 354 | 324 |
| 317 | NOV 13 | 168 | 210 | 168 | 234 | 192 | 210 | 330 | 243 | 264 | 174 | 288 | 252 |
| 318 | NOV 14 | 162 | 255 | 165 | 252 | 180 | 255 | 336 | 249 | 219 | 177 | 252 | 234 |
| 319 | NOV 15 | 174 | 267 | 168 | 276 | 183 | 267 | 369 | 216 | 213 | 174 | 228 | 282 |
| 320 | NOV 16 | 177 | 261 | 174 | 285 | 198 | 261 | 384 | 228 | 216 | 159 | 249 | 282 |
| 321 | NOV 17 | 168 | 336 | 195 | 324 | 177 | 336 | 348 | 321 | 210 | 165 | 279 | 285 |
| 322 | NOV 18 | 168 | 321 | 222 | 369 | 180 | 321 | 372 | 381 | 231 | 189 | 300 | 255 |
| 323 | NOV 19 | 177 | 291 | 195 | 333 | 189 | 291 | 354 | 369 | 222 | 276 | 264 | 369 |
| 324 | NOV 20 | 183 | 363 | 195 | 372 | 234 | 363 | 339 | 318 | 228 | 261 | 231 | 369 |
| 325 | NOV 21 | 186 | 300 | 210 | 345 | 237 | 300 | 330 | 240 | 207 | 222 | 222 | 354 |
| 326 | NOV 22 | 180 | 258 | 216 | 288 | 243 | 258 | 312 | 228 | 267 | 216 | 270 | 372 |
| 327 | NOV 23 | 177 | 213 | 216 | 213 | 255 | 213 | 288 | 258 | 336 | 189 | 339 | 372 |
| 328 | NOV 24 | 183 | 213 | 213 | 222 | 219 | 213 | 291 | 336 | 354 | 195 | 369 | 300 |
| 329 | NOV 25 | 192 | 207 | 207 | 216 | 207 | 207 | 282 | 369 | 354 | 255 | 393 | 243 |
| 330 | NOV 26 | 207 | 213 | 195 | 237 | 240 | 213 | 321 | 372 | 330 | 315 | 348 | 339 |
| 331 | NOV 27 | 276 | 210 | 192 | 225 | 303 | 210 | 336 | 372 | 312 | 363 | 333 | 378 |
| 332 | NOV 28 | 303 | 222 | 195 | 240 | 375 | 222 | 312 | 378 | 279 | 372 | 306 | 381 |
| 333 | NOV 29 | 285 | 234 | 210 | 267 | 396 | 234 | 336 | 381 | 243 | 360 | 264 | 381 |
| 334 | NOV 30 | 279 | 246 | 198 | 276 | 393 | 246 | 288 | 357 | 231 | 363 | 234 | 402 |

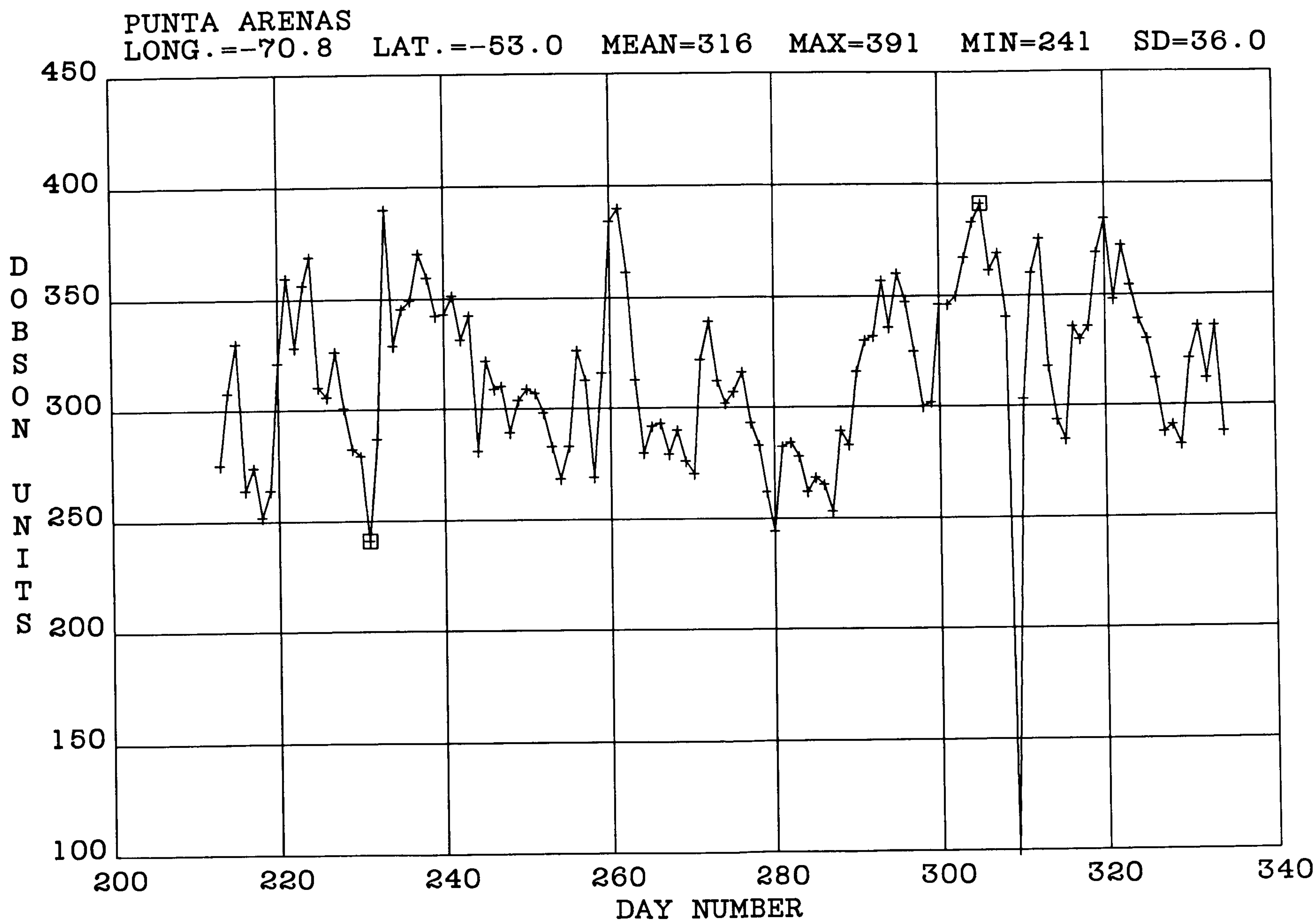


Figure 7a. Daily TOMS Total Ozone Values over Punta Arenas (DU).

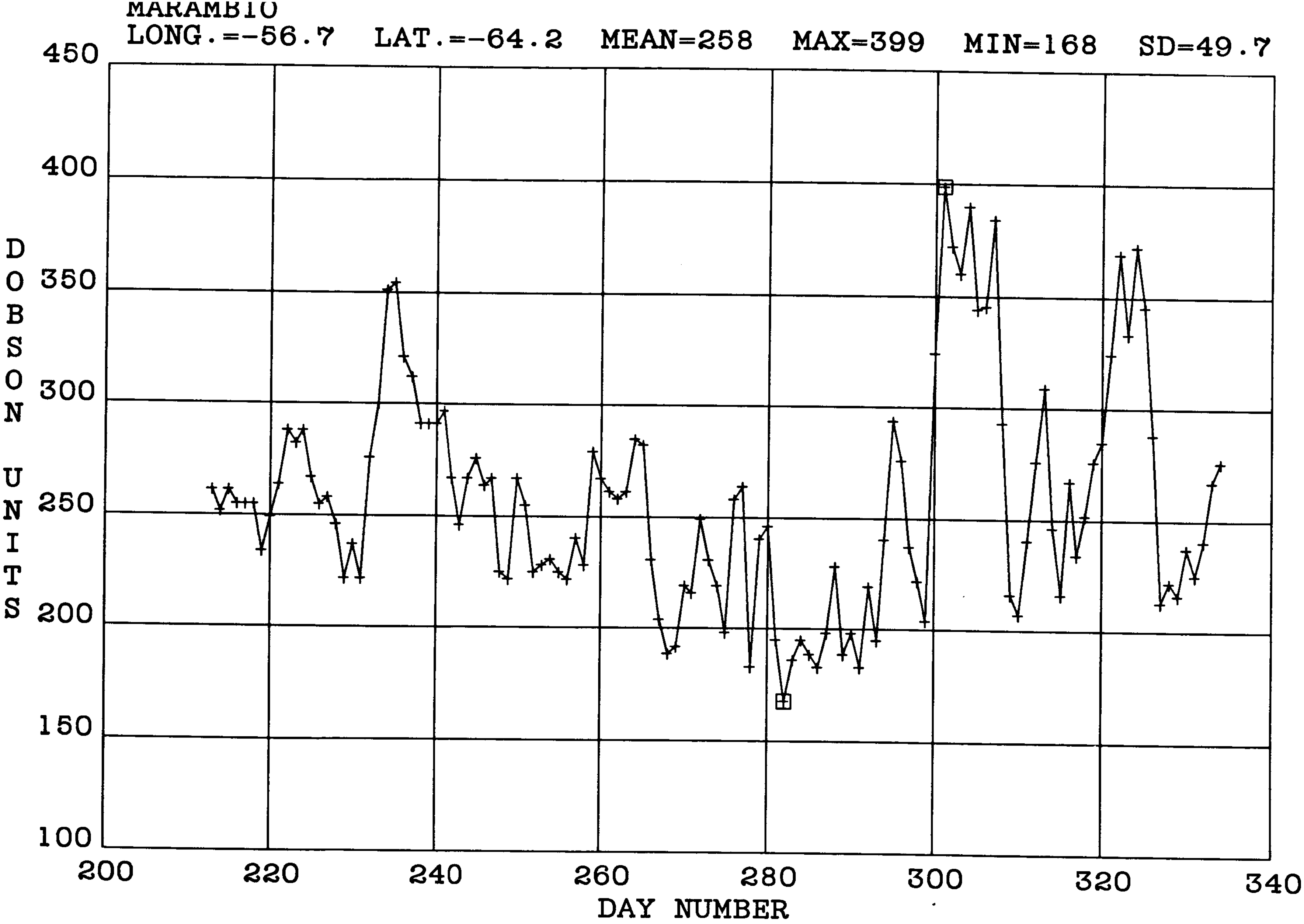


Figure 7b. Daily TOMS Total Ozone Values over Marambio (DU).

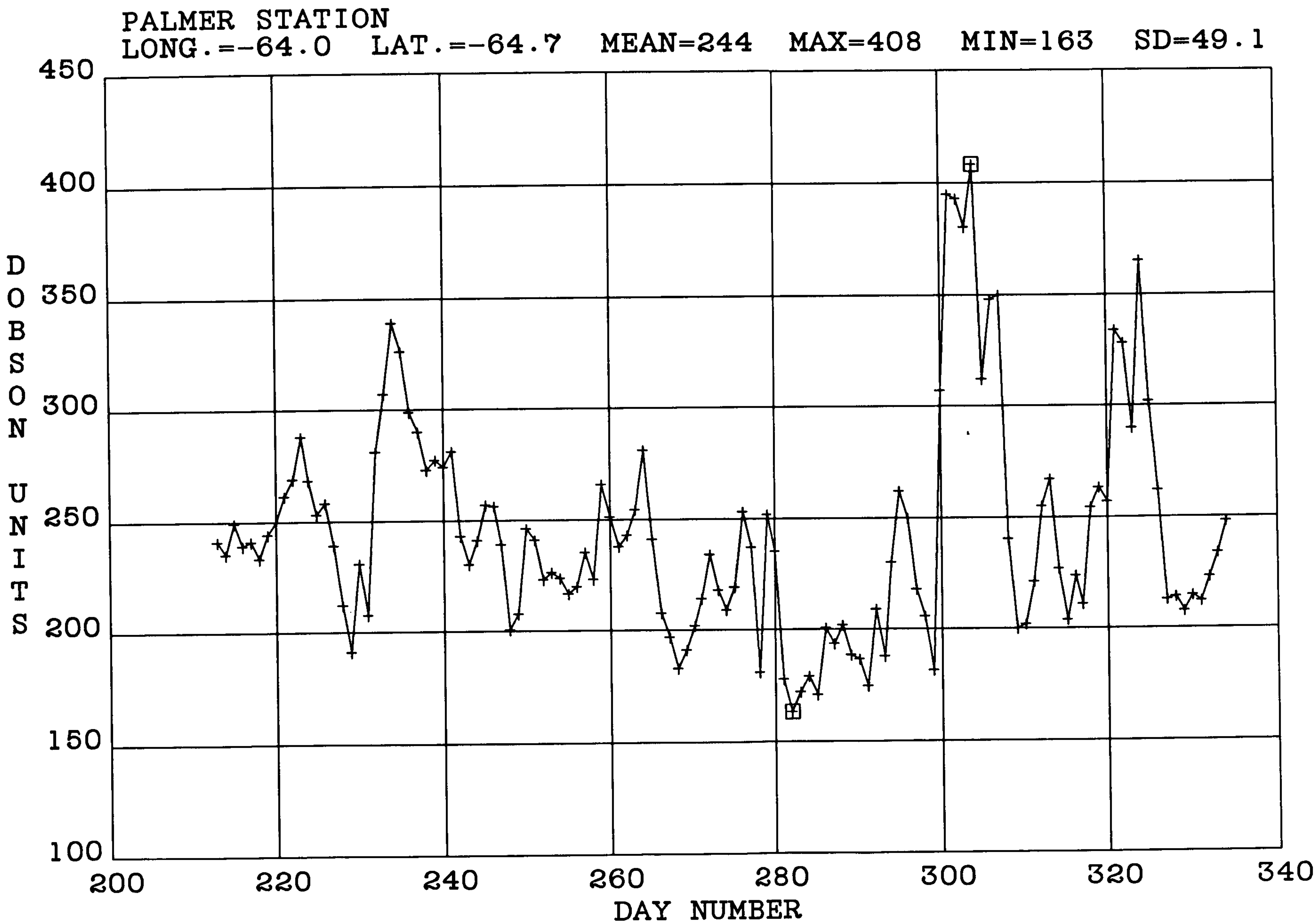


Figure 7c. Daily TOMS Total Ozone Values over Palmer Station (DU).

**Dumont D'Urville Station**

The Dumont D'Urville station is located at 67°S on the edge of Antarctica almost 180° in longitude away from the Antarctic Peninsula. During the experiment, the station can be observed to lie within the steep gradient associated with the boundary of the ozone hole. As such, the day-to-day fluctuations in total ozone encountered (Figure 7d) are caused by slight adjustments in the position of the ozone-hole boundary. However, on about October 7 (day 280), a 90° rotation in the major axis of the (by then) elliptical ozone hole, coupled with a 10° latitudinal shift in the hole's center causes the total ozone measurements for this location to alter dramatically. By the end of October, another change in the orientation of the ozone-hole boundary causes the station's readings to decrease once again. This continues in November, with rapid shifts in ozone amount, as the boundary of the hole passes the station.

**Molodeznaya Station**

Molodeznaya is located in coastal Antarctica at 68°S. The total-ozone time series for this station exhibits a decidedly nonstationary character during the period of the experiment (Figure 7e). Prior to mid-September (day 258) the TOMS measurements drop smoothly and almost monotonically from near 250 DU to near 220 DU as the hole forms. However, in late September and throughout October the total ozone abundances fluctuate widely by as much as 50 to 100 DU, with a periodicity of about five days. This oscillation continues in November, but with an increased ozone variation which approaches 175 DU.

**Syowa Station**

Syowa is located at 69°S, and is quite close to Molodeznaya. As such, the two time series (Figure 7f) are highly correlated, though the amplitude of the 5-day mode noted at the former station is markedly reduced.

**Davis Station**

Davis is located on the coast of Antarctica at 69°S, about 30° of longitude away from Molodeznaya. Not surprisingly, the time series for the two locations are quite similar. Substantial differences do occur in the first half of October (Figure 7g), however, when the shape of the ozone hole alters such that Davis, which is about 1° poleward from Molodeznaya, actually lies farther outside the hole.

**Halley Bay**

The total ozone measurements at Halley Bay at 76°S first become available on August 20. From late August through early October, the total ozone readings drop at an average rate of about 2 to 3 DU per day (Figure 7h), and reach their lowest value of 135 DU on October 6. From the middle to the end of October, the total ozone measurements increase, reaching values of 200 to 300 DU by the end of the month. However, the station remains in the hole throughout November.

**McMurdo Station**

The McMurdo station is located at 78°S on the McMurdo Sound near the dateline. The TOMS total ozone measurements first become available on McMurdo on August 26 (day 238) and decrease in magnitude throughout September, from about 250 DU down to a minimum value of 141 on October 3 (Figure 7i). During October, several oscillations of the total-column ozone occur, with a period of approximately 6 days. Referring to the hemispheric charts for the month it is clear that this behavior is caused by the morphology of the ozone hole itself. The

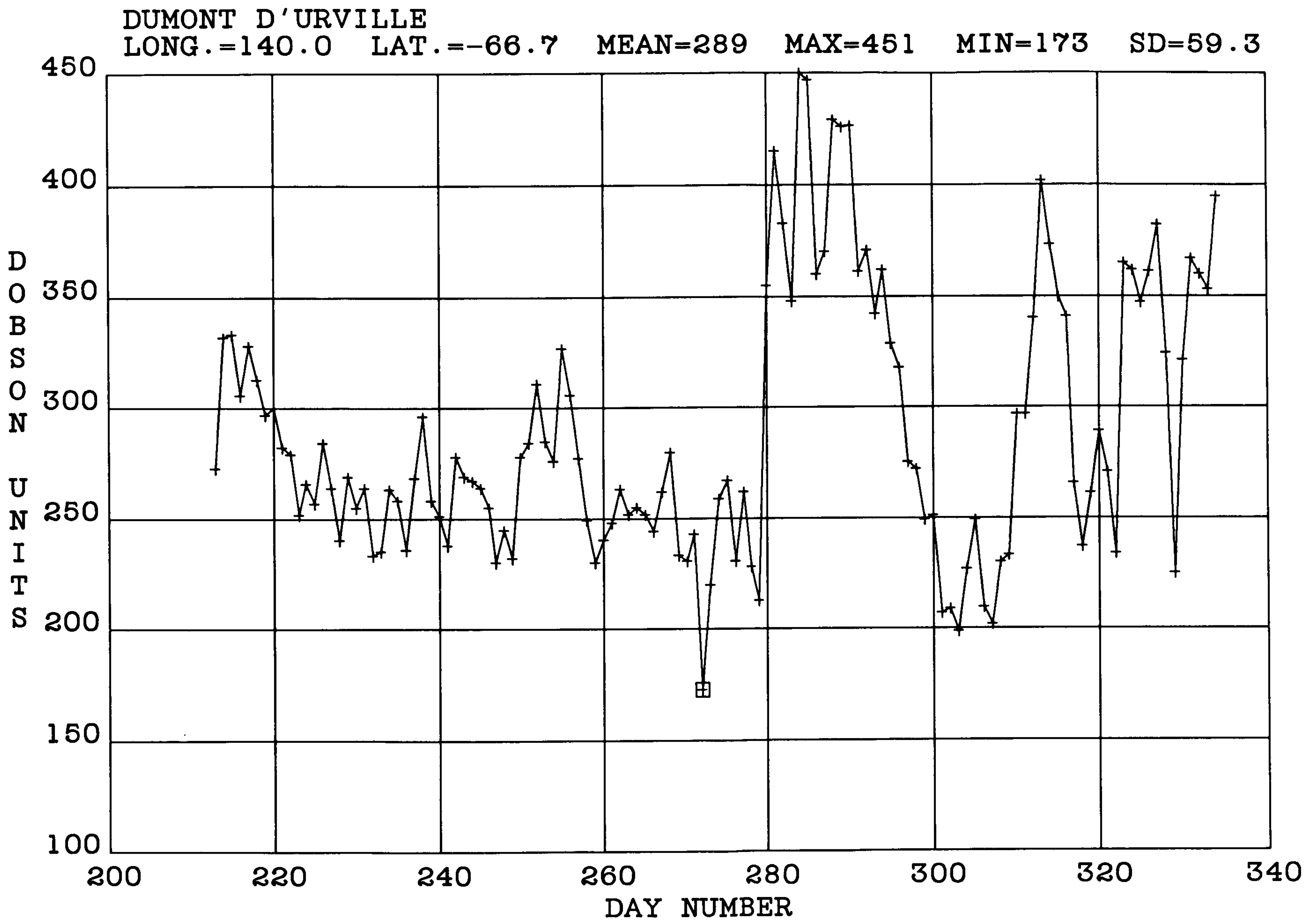


Figure 7d. Daily TOMS Total Ozone Values over Dumont D'Urville (DU).

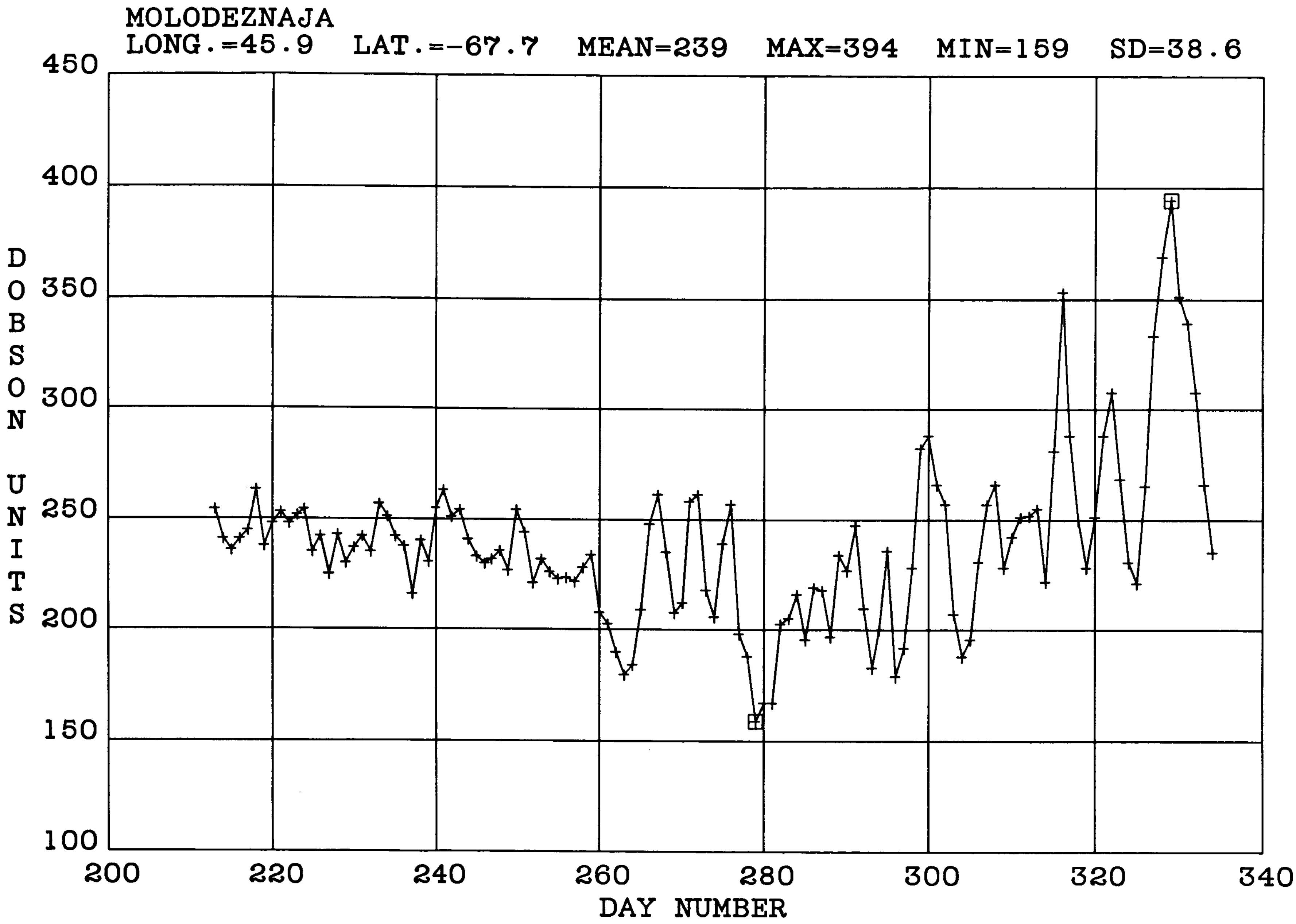


Figure 7e. Daily TOMS Total Ozone Values over Molodeznaya (DU).

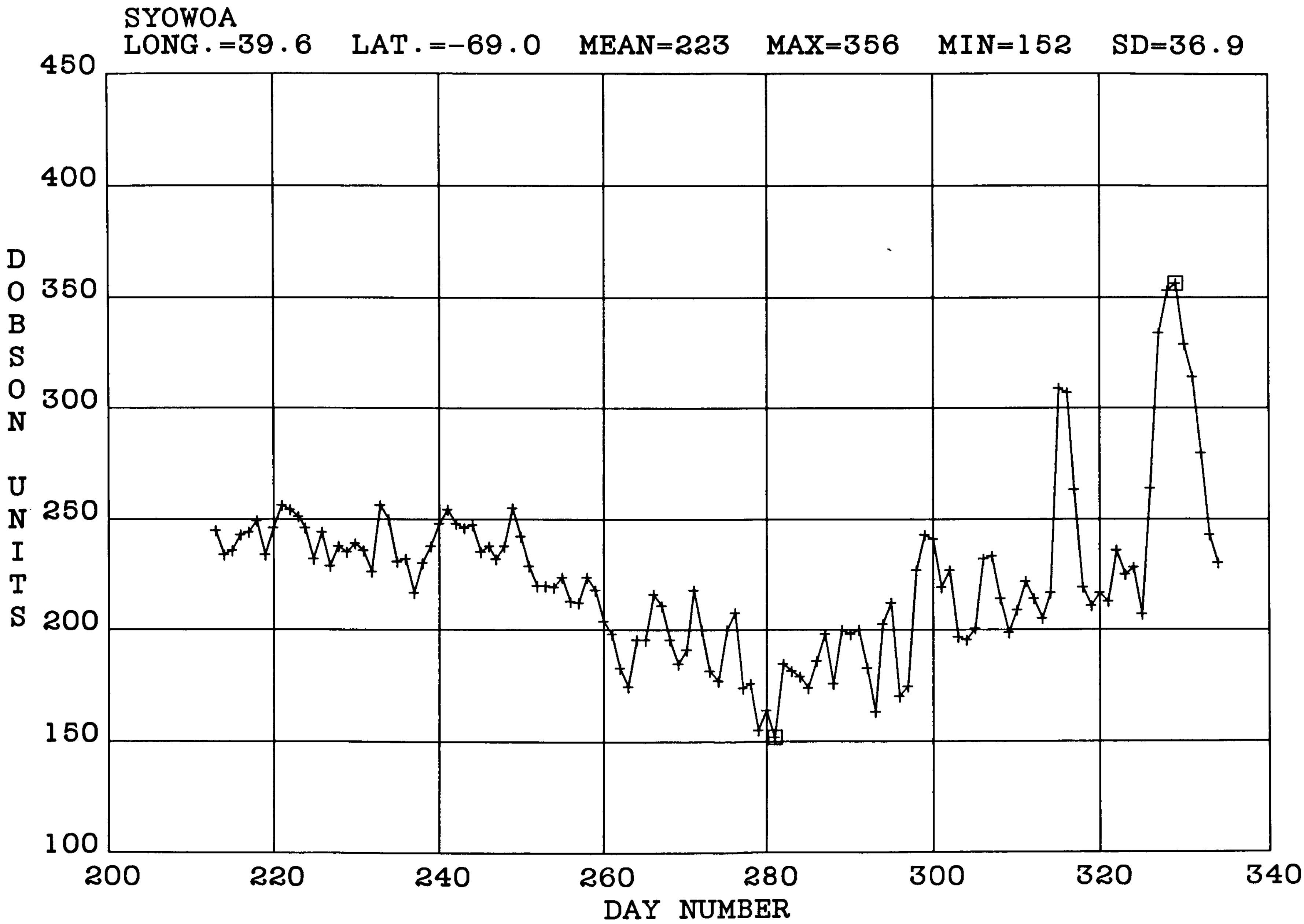


Figure 7f. Daily TOMS Total Ozone Values over Syowa (DU).

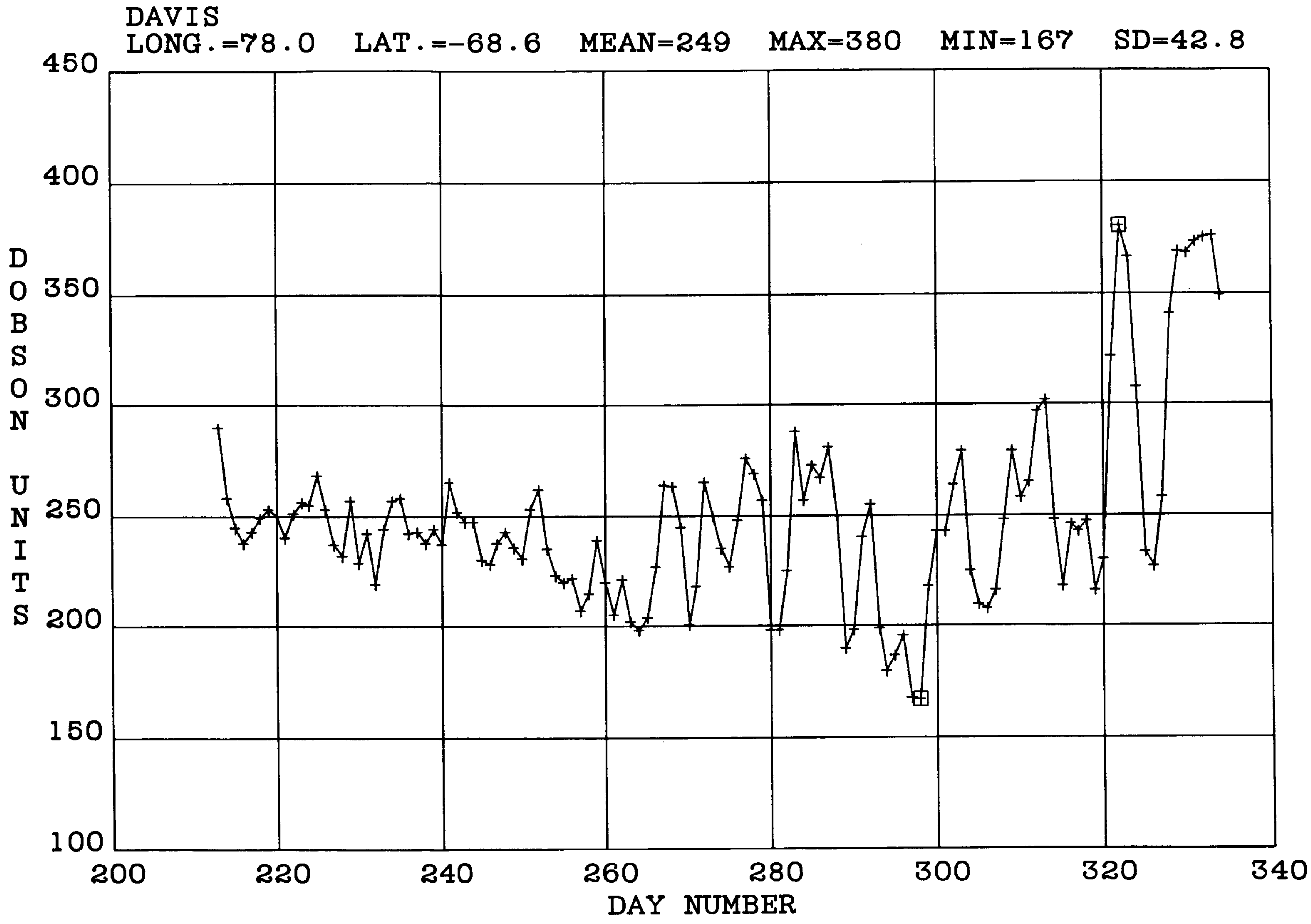


Figure 7g. Daily TOMS Total Ozone Values over Davis (DU).

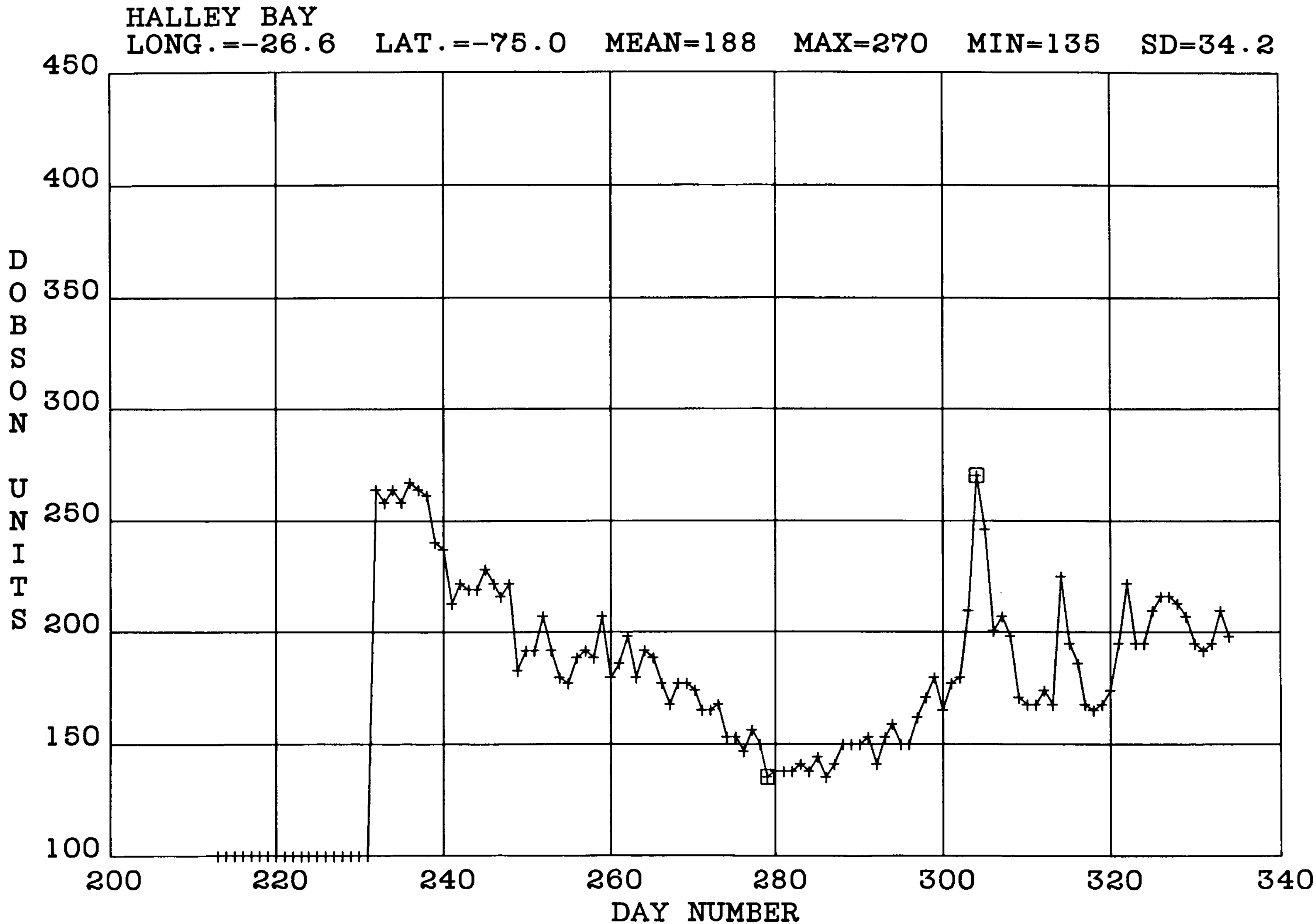


Figure 7h. Daily TOMS Total Ozone Values over Halley Bay (DU).

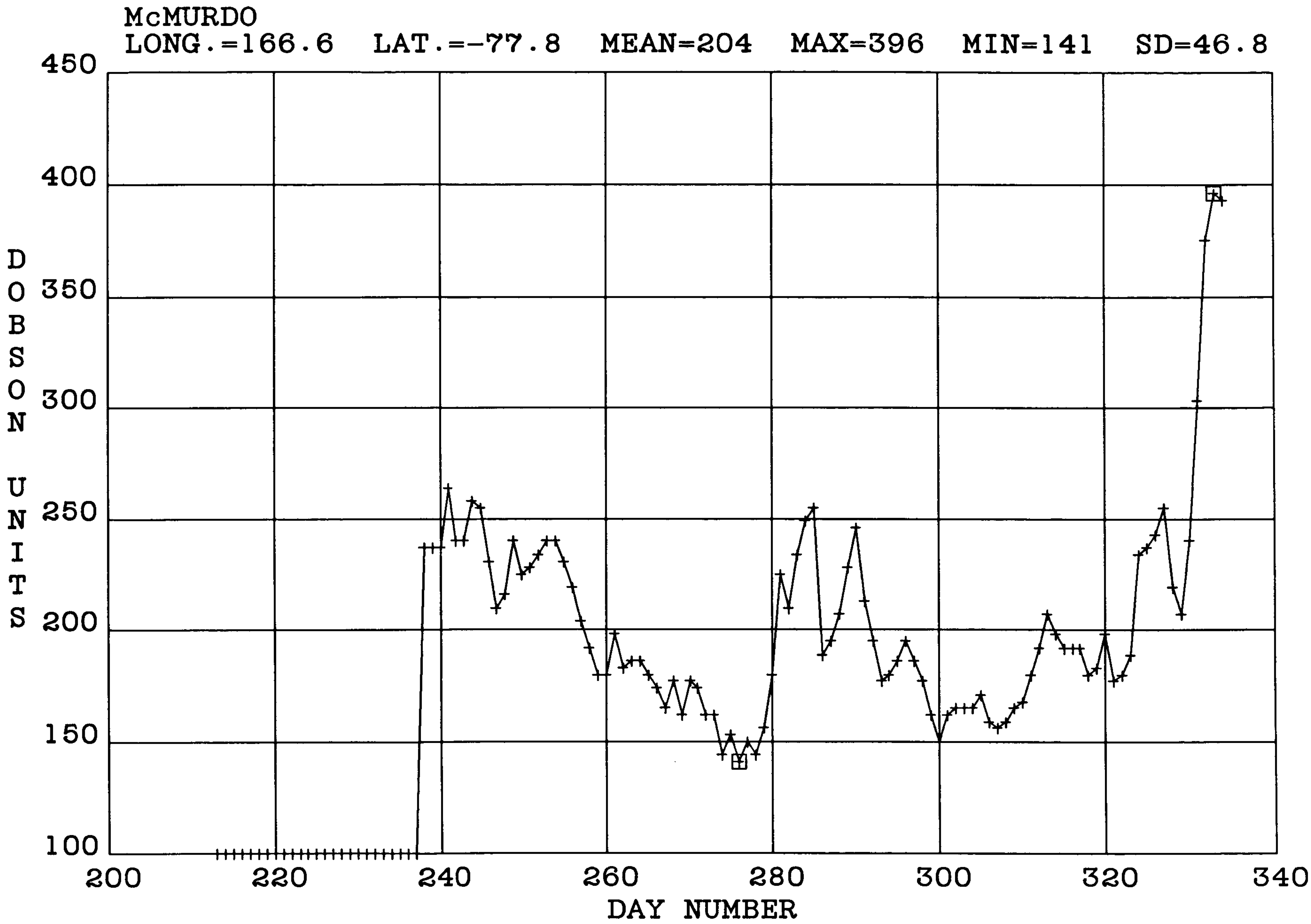


Figure 7i. Daily TOMS Total Ozone Values over McMurdo (DU).

maximum values during the period of October 8-12 (days 281-285) are caused by a shift in the center of the ozone hole away from the South Pole, such that the McMurdo Station becomes located within the hole's boundary. The termination of the large total ozone measurements after October 17 (day 290) is clearly caused by the propagation of an extension of the hole over the station. The rotation of the hole and its movement off the pole result in the station leaving the hole completely in late November, with ozone amounts approaching 400 DU.

**Vostok Station**

The Vostok Station is located deep within continental Antarctica at 78°S. As with McMurdo, total ozone measurements are first obtained on August 26 (Figure 7j) and also exhibit a general downward trend throughout September and into the beginning of October, reaching a minimum value of 144 DU on September 29. Slightly elevated abundances are recorded during most of October, before dropping once again to a new minimum of 135 DU on October 23. Because of the proximity of Vostok to McMurdo, it is clear that the total ozone readings at the two locations are responding in a similar manner to fluctuations in the structure of the ozone hole.

**Amundsen-Scott Station**

The Amundsen-Scott Station is located at 90°S on the South Pole. At this extreme location, total ozone observations from TOMS do not become available until September 26 (day 269), shortly after the autumnal equinox (Figure 7k). Referring to the TOMS measurement time series, we note that the values remain between 153 DU and 117 DU for the period, without any noticable trend until late November. Then the movement of the hole off the pole results in a rapid increase in ozone amount to 275 to 300 DU. The implication is that, for this location, the ozone hole had formed prior to the beginning of the polar day.

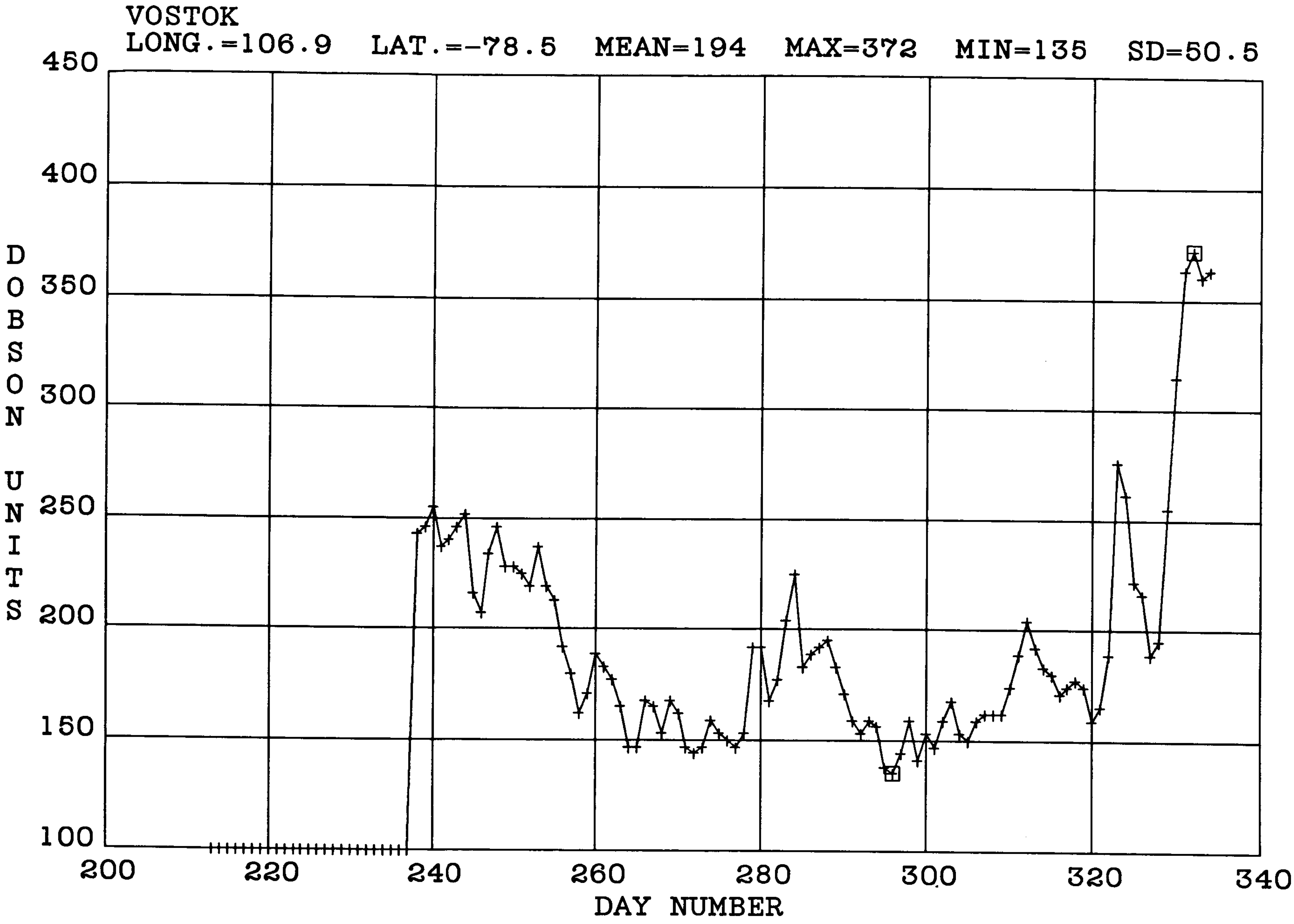


Figure 7j. Daily TOMS Total Ozone Values over Vostok (DU).

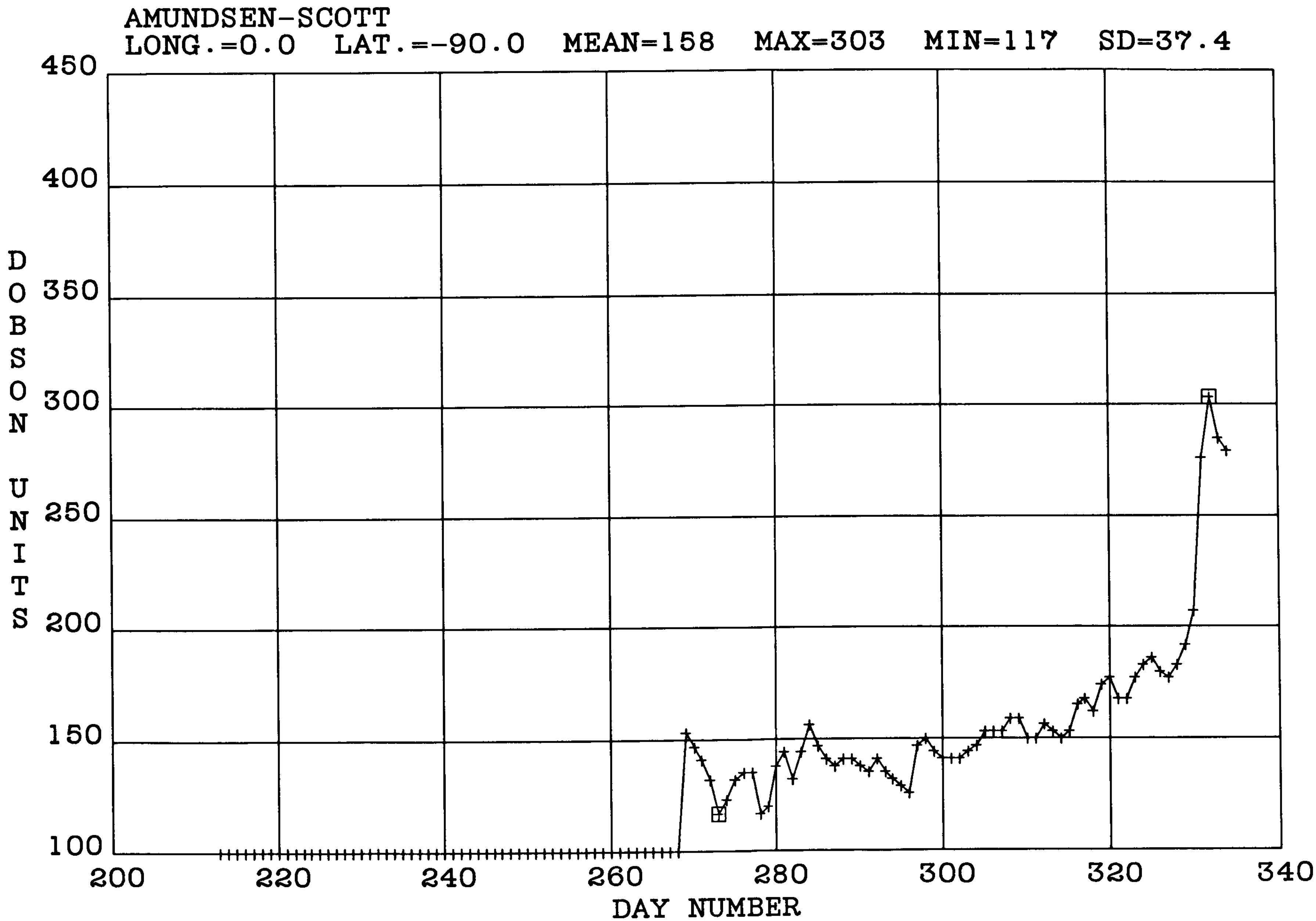


Figure 7b. Daily TOMS Total Ozone Values over Amundsen-Scott (DU)

## 3.4 Near-Real-Time Orbital Charts

A set of orbital TOMS total ozone estimates for a southern hemisphere domain covering portions of South America and Antarctica, and adjacent areas of the Atlantic and Pacific Oceans are presented here. The daily data, over the period August 8 through September 29, 1987, are resolved on the uniform 2° latitude by 1.5° longitude grid for each day, and include those orbits incorporating measurements which were of interest to the experiment for near real time mission-planning purposes.

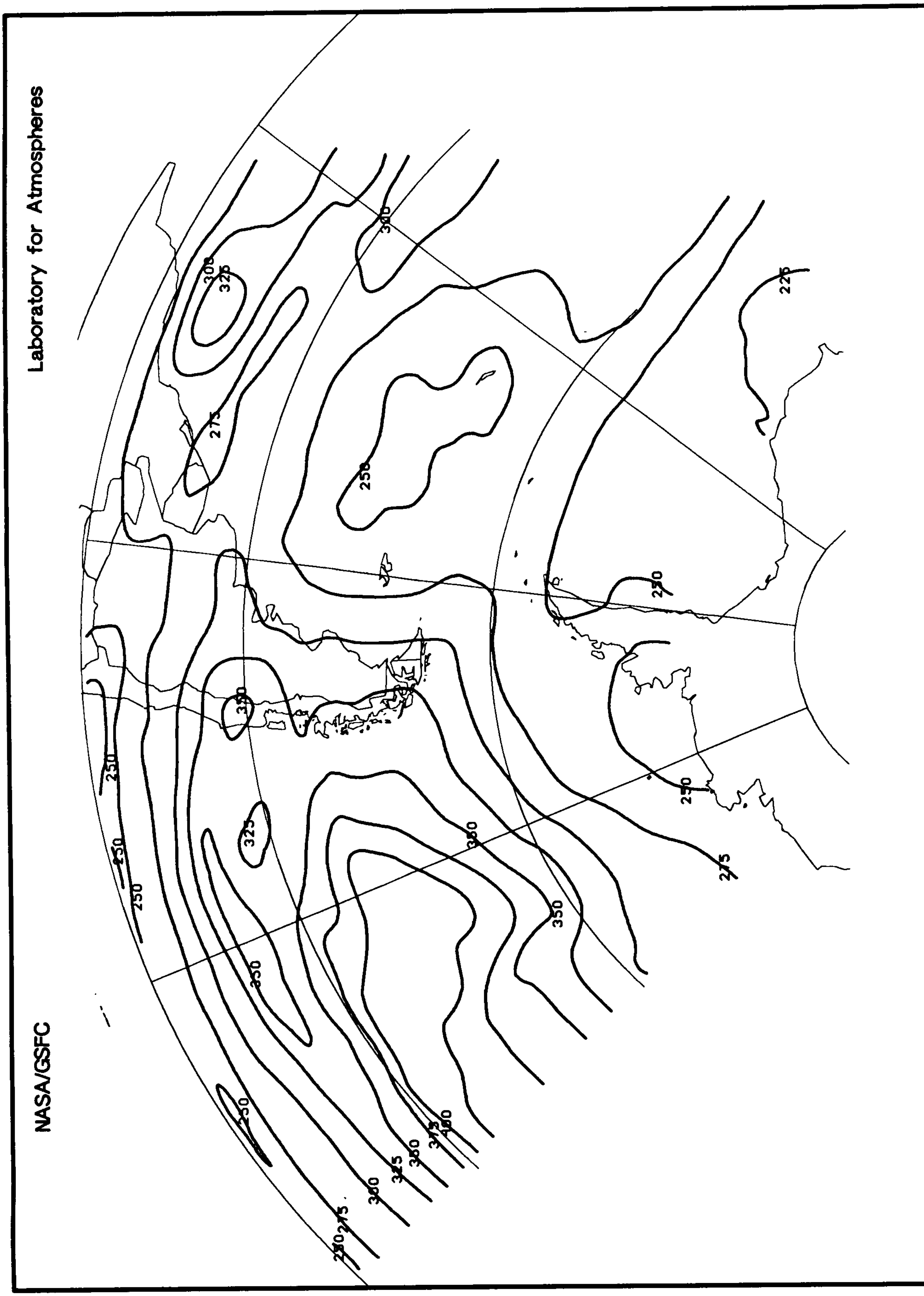


August 8, 1987 Orbital (44375-7) TOMS Ozone (Dobson Units)

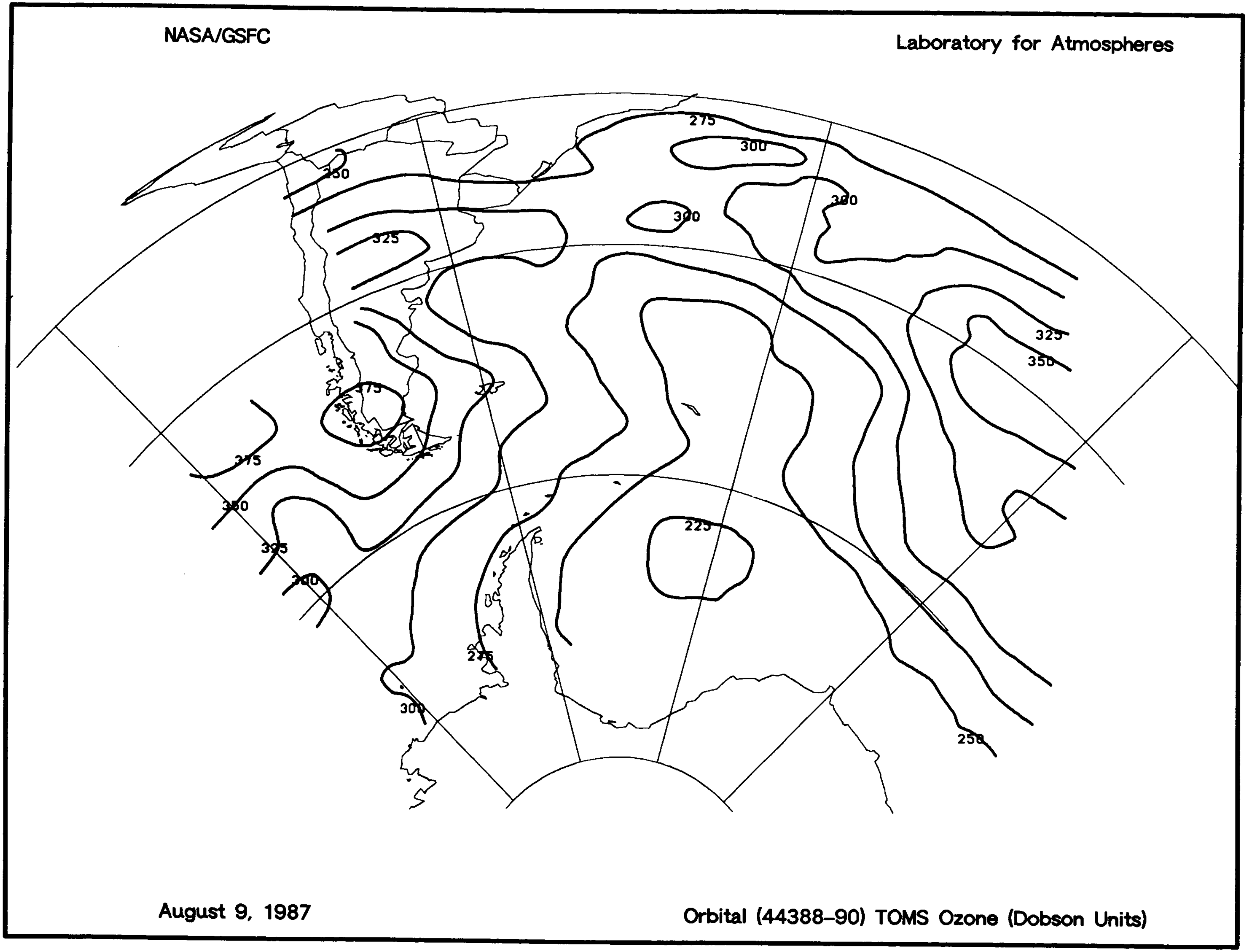
NASA/GSFC
Laboratory for Atmospheres
275
300
300
300
350
325
325
350
375
375
350
325
300
275
300
225
250
August 9, 1987
Orbital (44388-90) TOMS Ozone (Dobson Units)

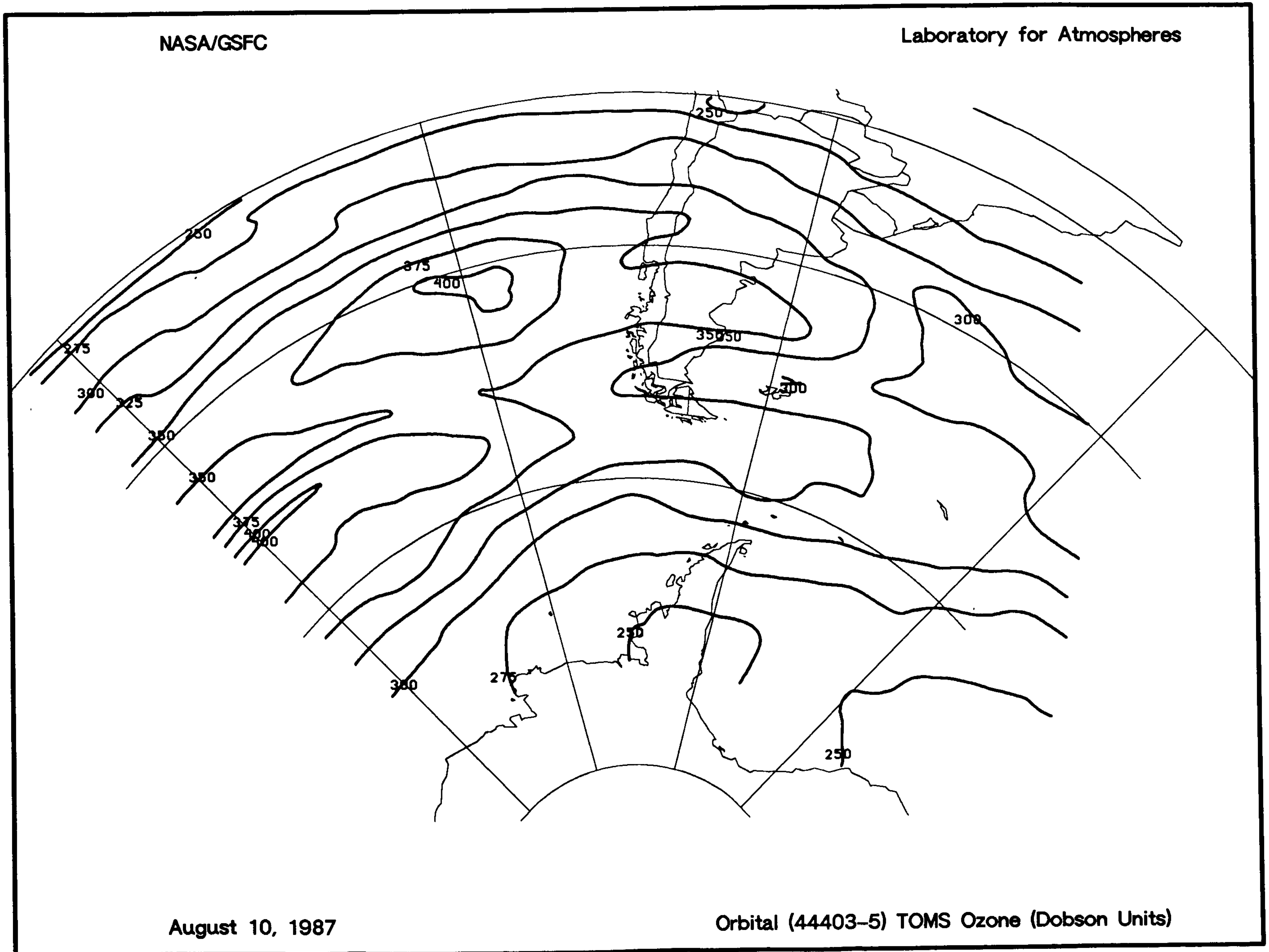
NASA/GSFC
Laboratory for Atmospheres
August 10, 1987
Orbital (44403-5) TOMS Ozone (Dobson Units)

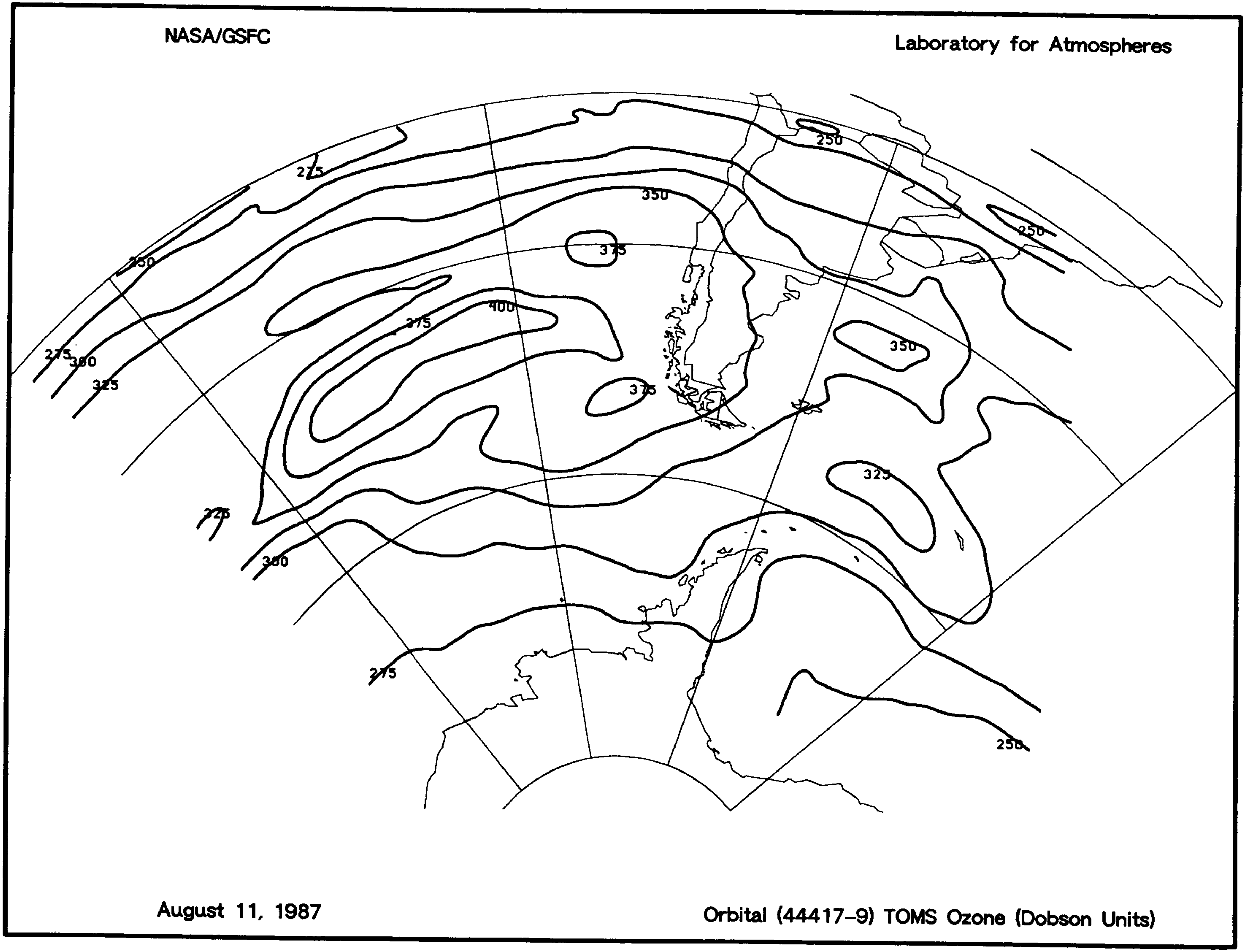
NASA/GSFC
Laboratory for Atmospheres
250
275
350
375
400
325
300
August 11, 1987
Orbital (44417-9) TOMS Ozone (Dobson Units)

NASA/GSFC

Laboratory for Atmospheres

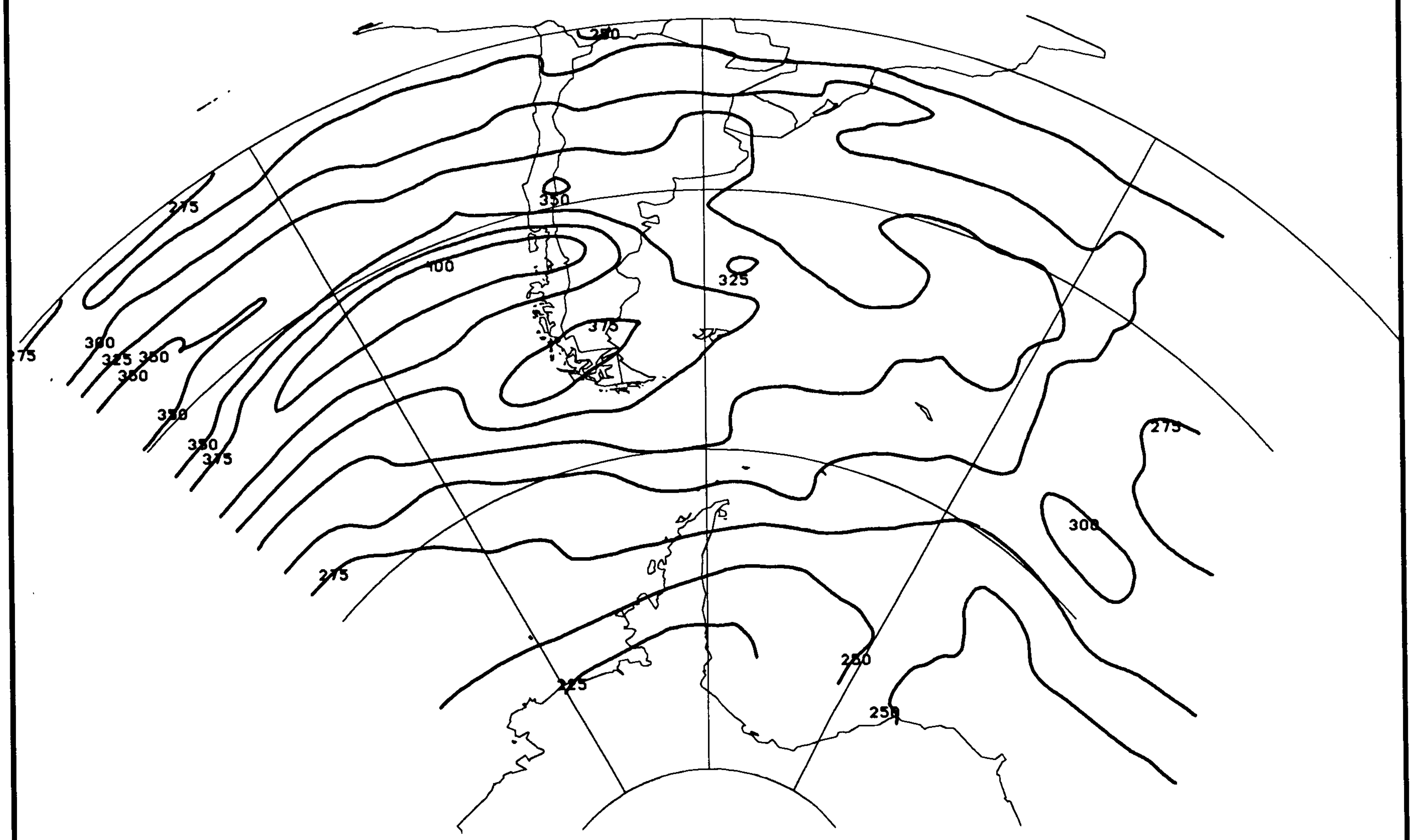


August 12, 1987

Orbital (44430-2) TOMS Ozone (Dobson Units)

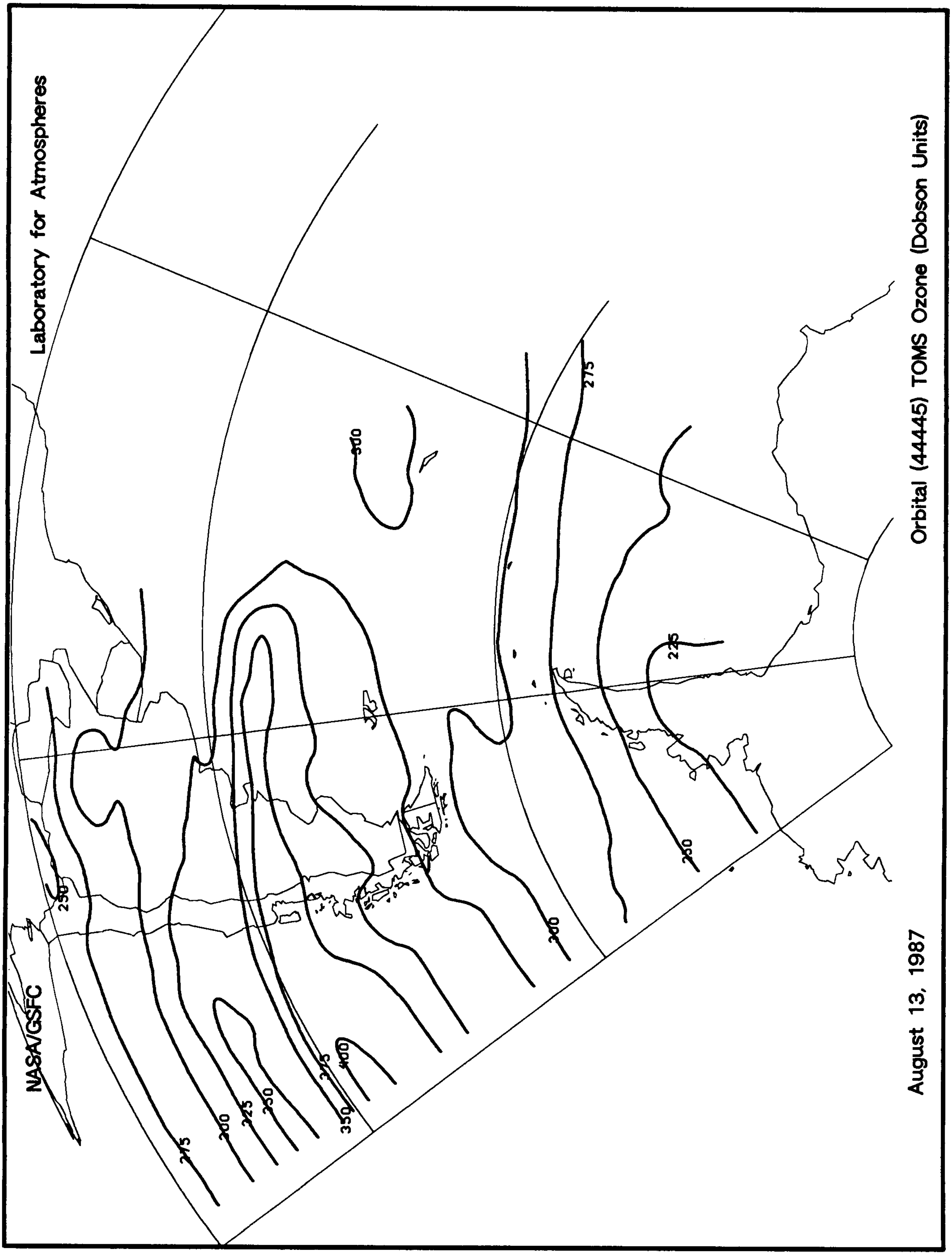
Laboratory for Atmospheres
NASA/GSFC
August 13, 1987
Orbital (44445) TOMS Ozone (Dobson Units)
275
300
325
350
375
400
350
250
300
275
250
225
300

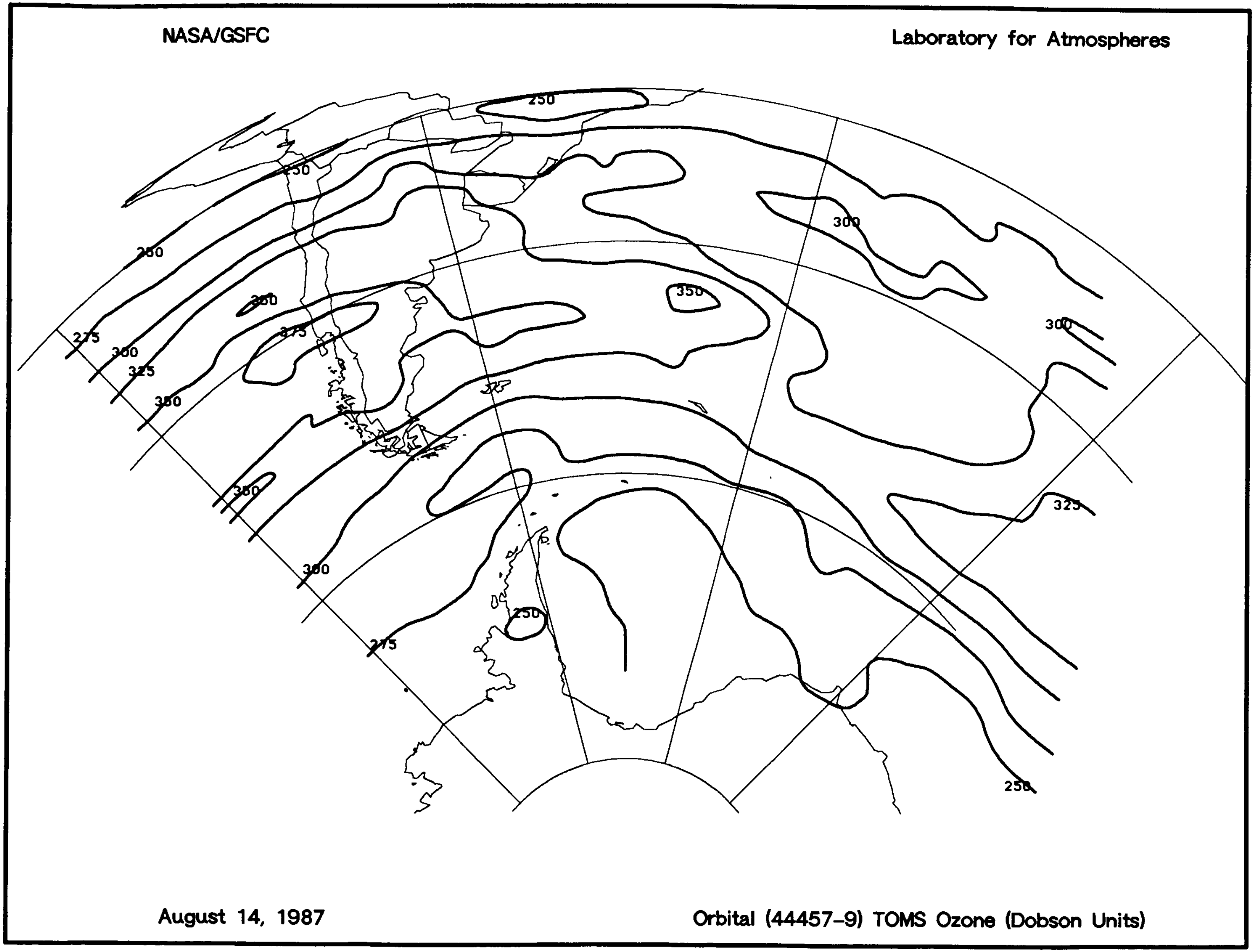
NASA/GSFC
Laboratory for Atmospheres
250
300
350
275
325
August 14, 1987
Orbital (44457-9) TOMS Ozone (Dobson Units)

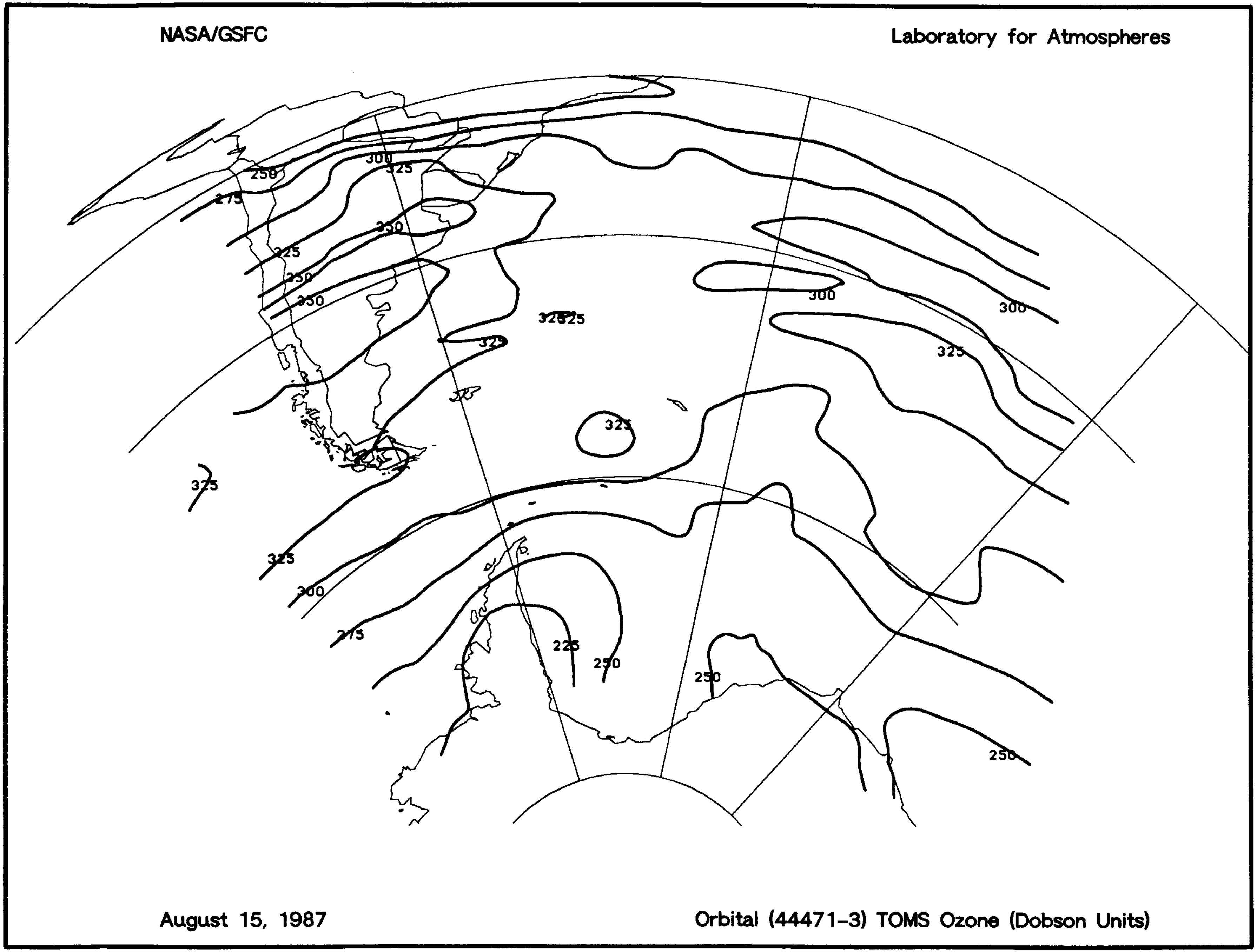
NASA/GSFC
Laboratory for Atmospheres
250
275
300
325
325
350
350
350
325
325
300
300
325
325
325
325
300
275
225
250
250
250
August 15, 1987
Orbital (44471-3) TOMS Ozone (Dobson Units)

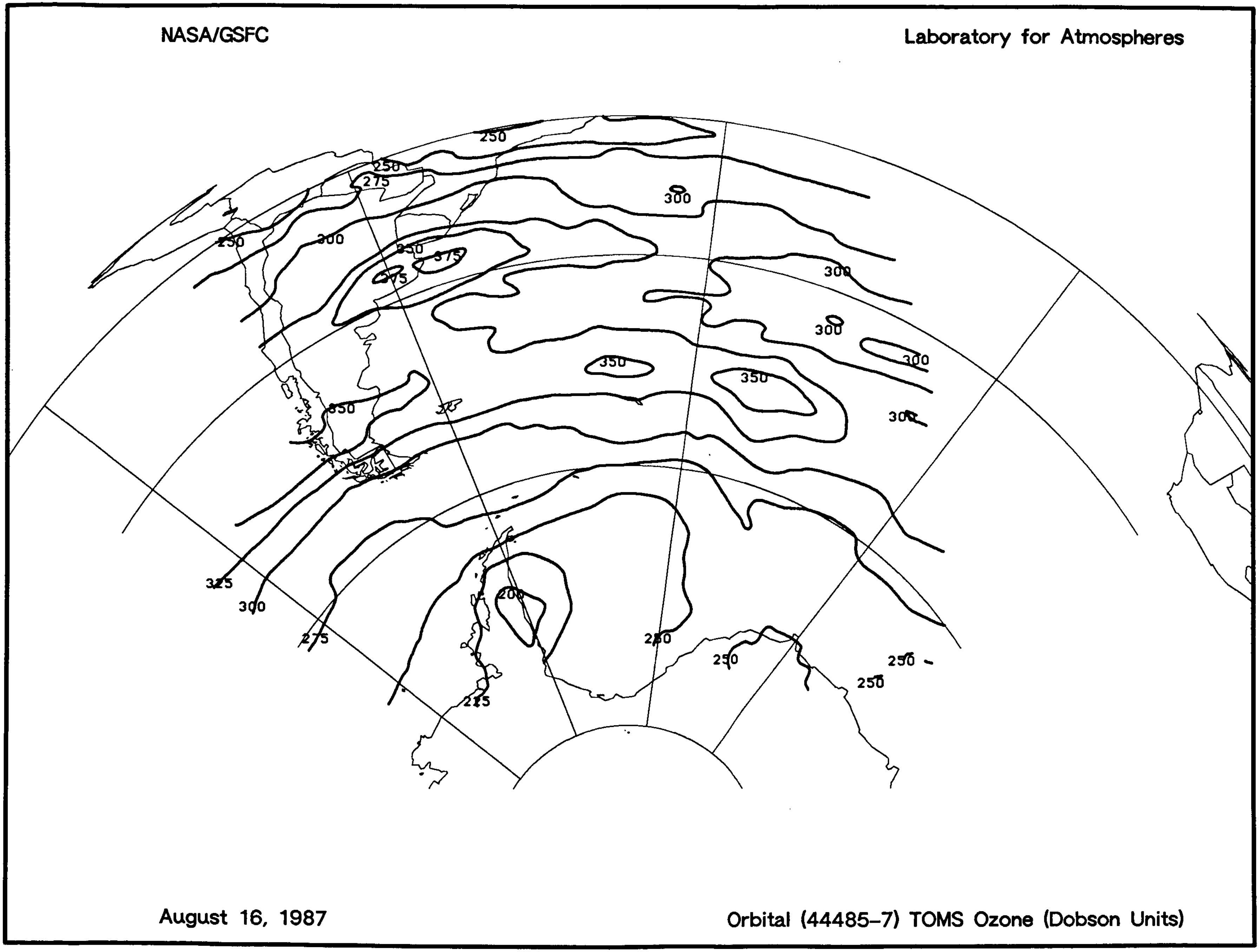
NASA/GSFC
Laboratory for Atmospheres
250
275
300
350
375
200
225
325
August 16, 1987
Orbital (44485-7) TOMS Ozone (Dobson Units)

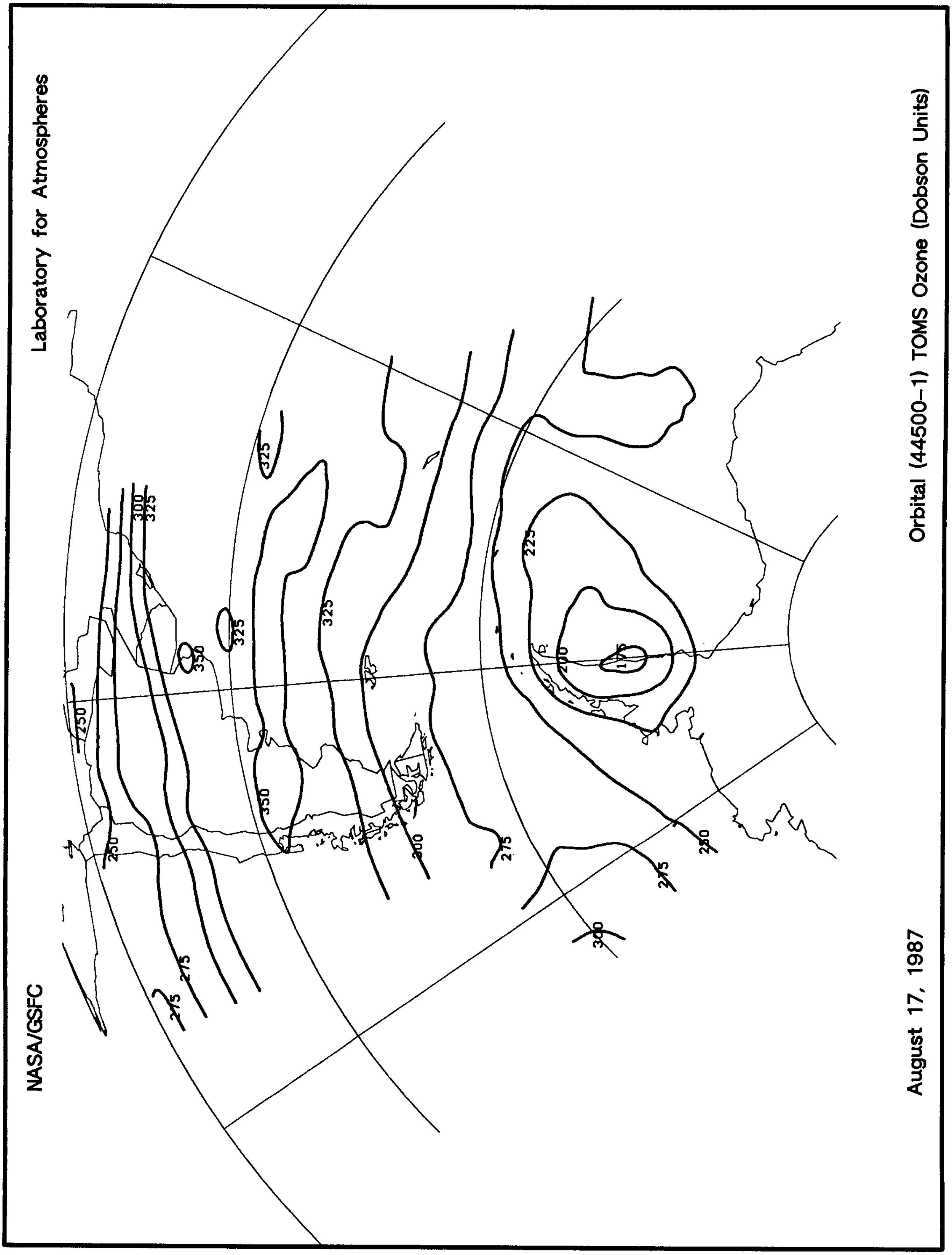
Laboratory for Atmospheres
NASA/GSFC
Orbital (44500-1) TOMS Ozone (Dobson Units)
August 17, 1987

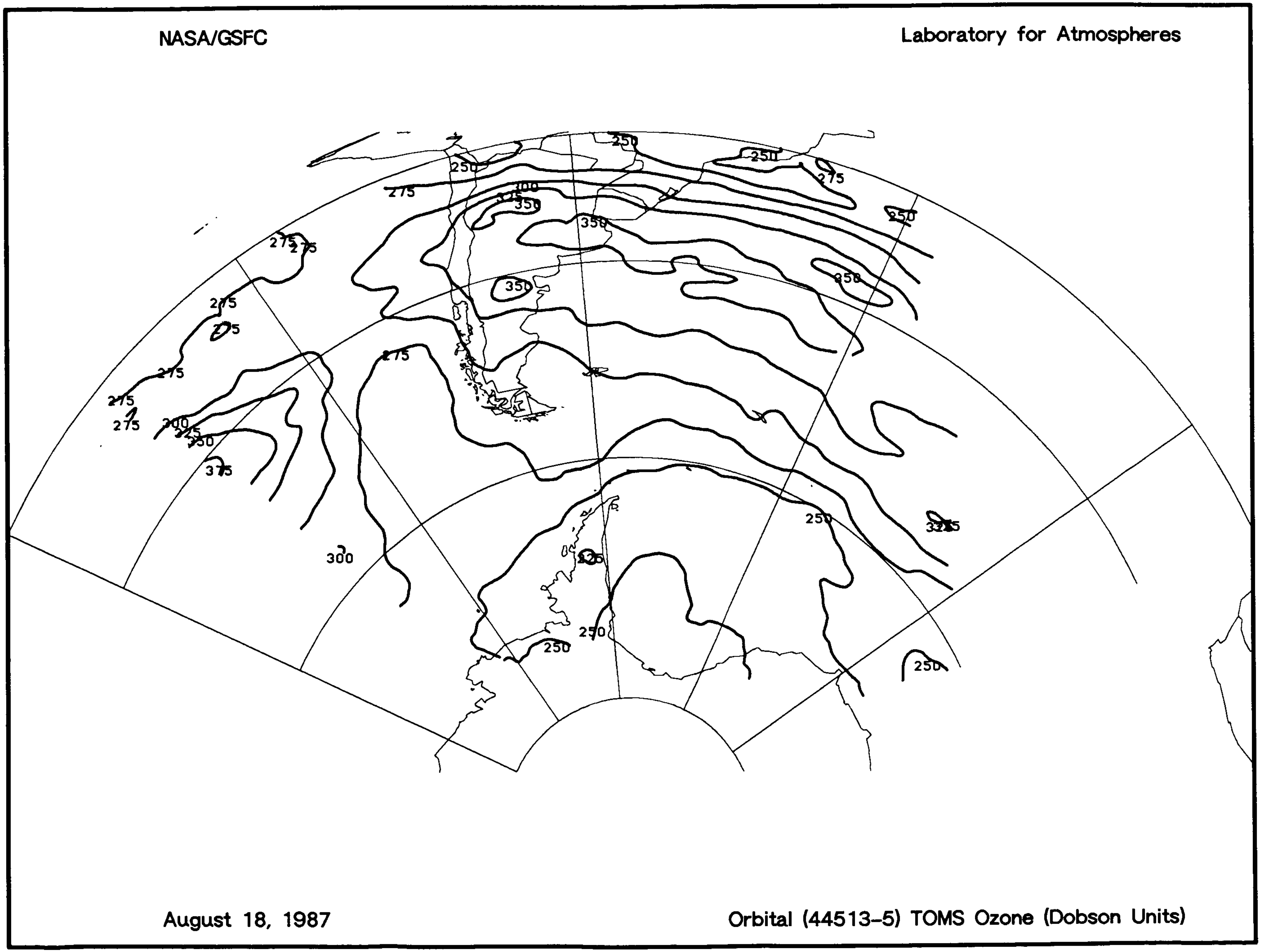
NASA/GSFC
Laboratory for Atmospheres
August 18, 1987
Orbital (44513-5) TOMS Ozone (Dobson Units)

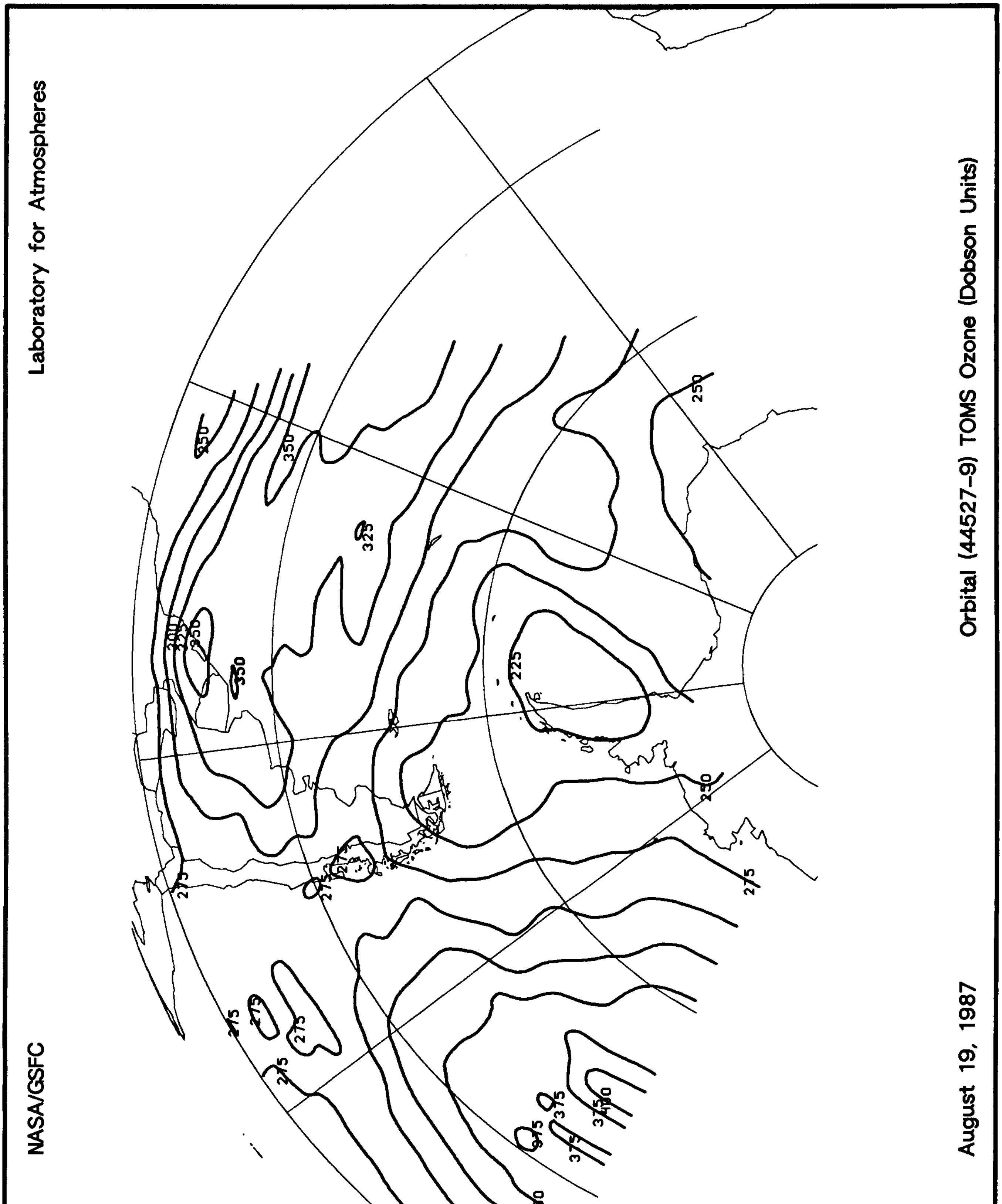
NASA/GSFC
Laboratory for Atmospheres
August 19, 1987
Orbital (44527-9) TOMS Ozone (Dobson Units)

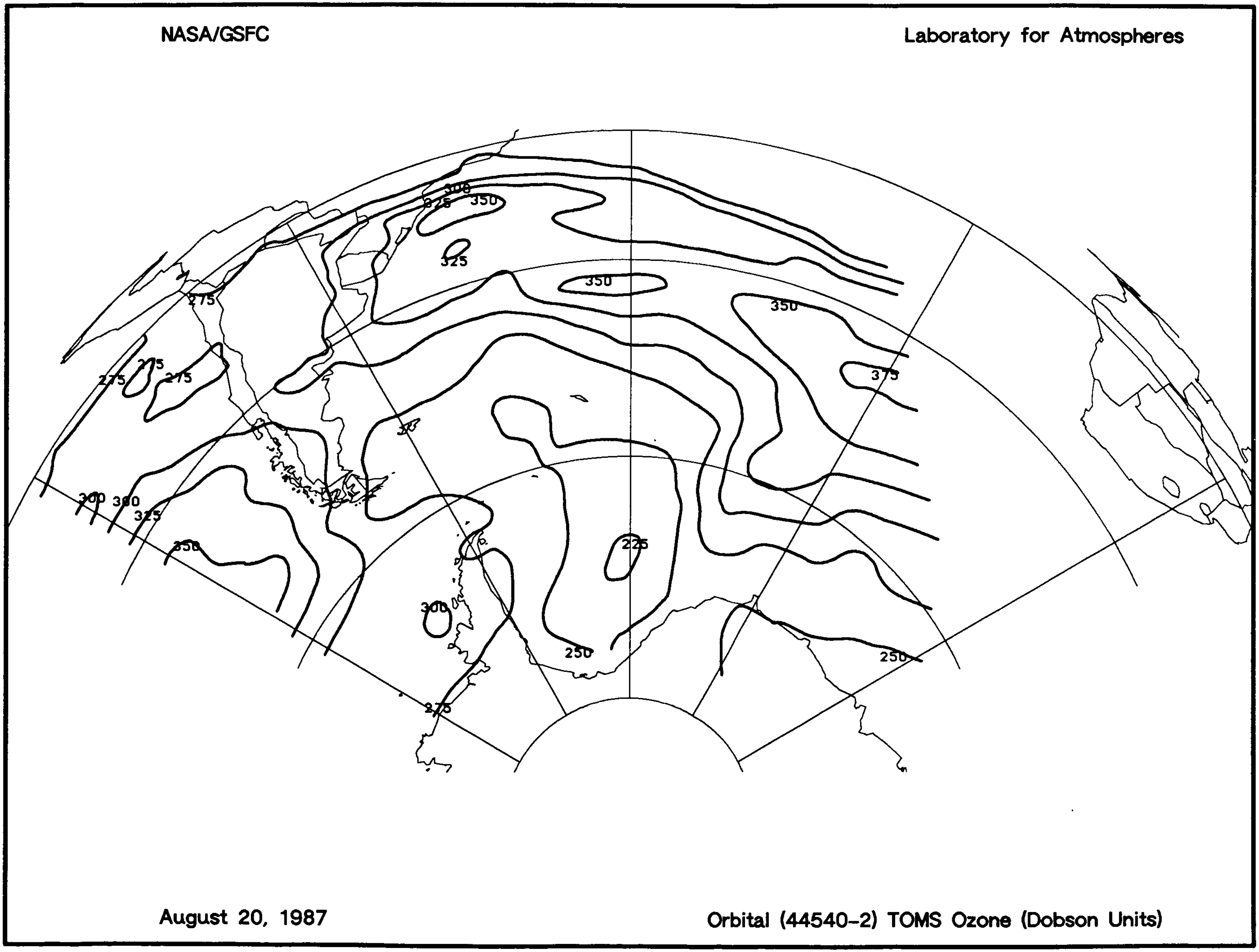
NASA/GSFC
Laboratory for Atmospheres
August 20, 1987
Orbital (44540-2) TOMS Ozone (Dobson Units)
300
325
350
275
375
225
250

NASA/GSFC

Laboratory for Atmospheres

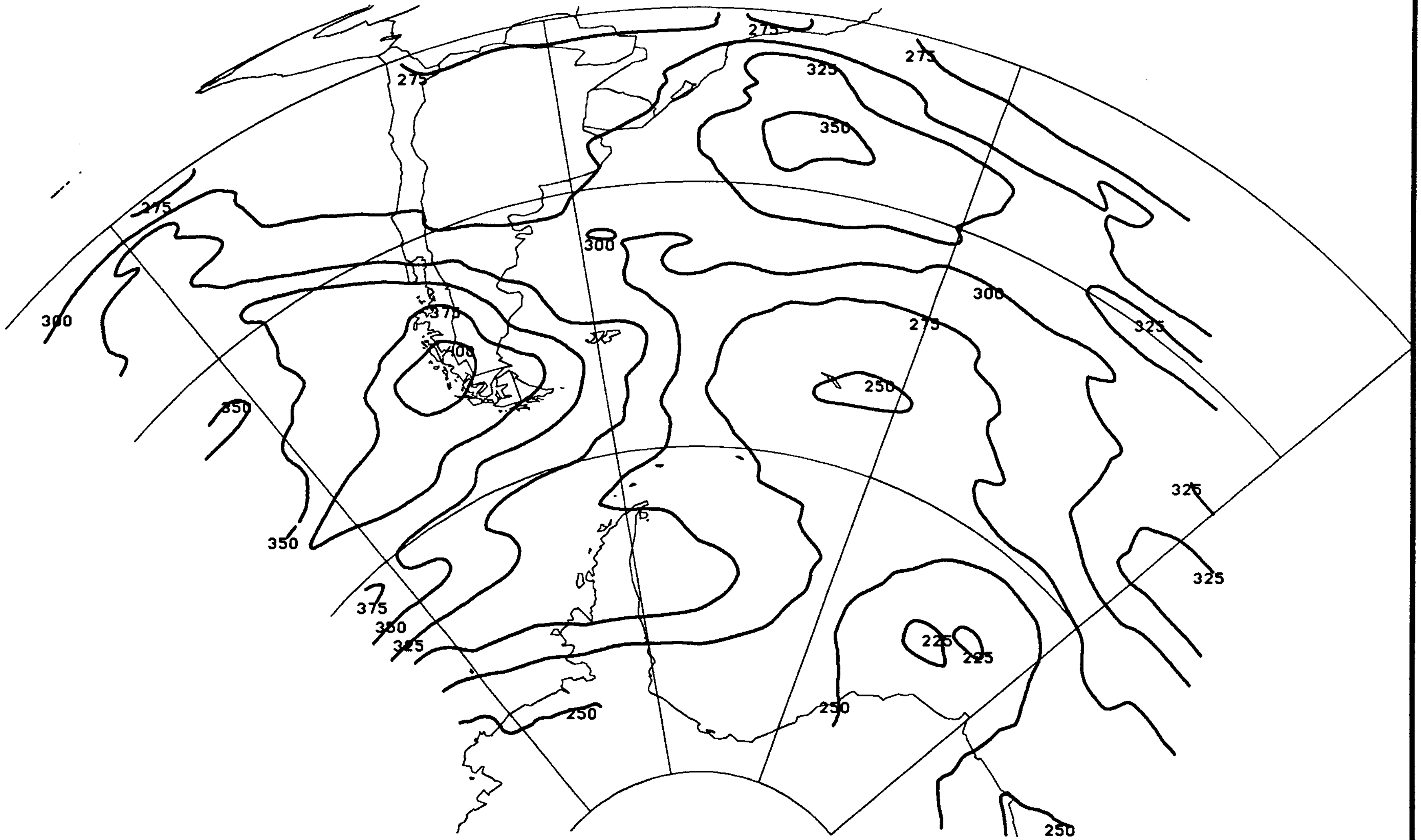


August 21, 1987

Orbital (44554–6) TOMS Ozone (Dobson Units)

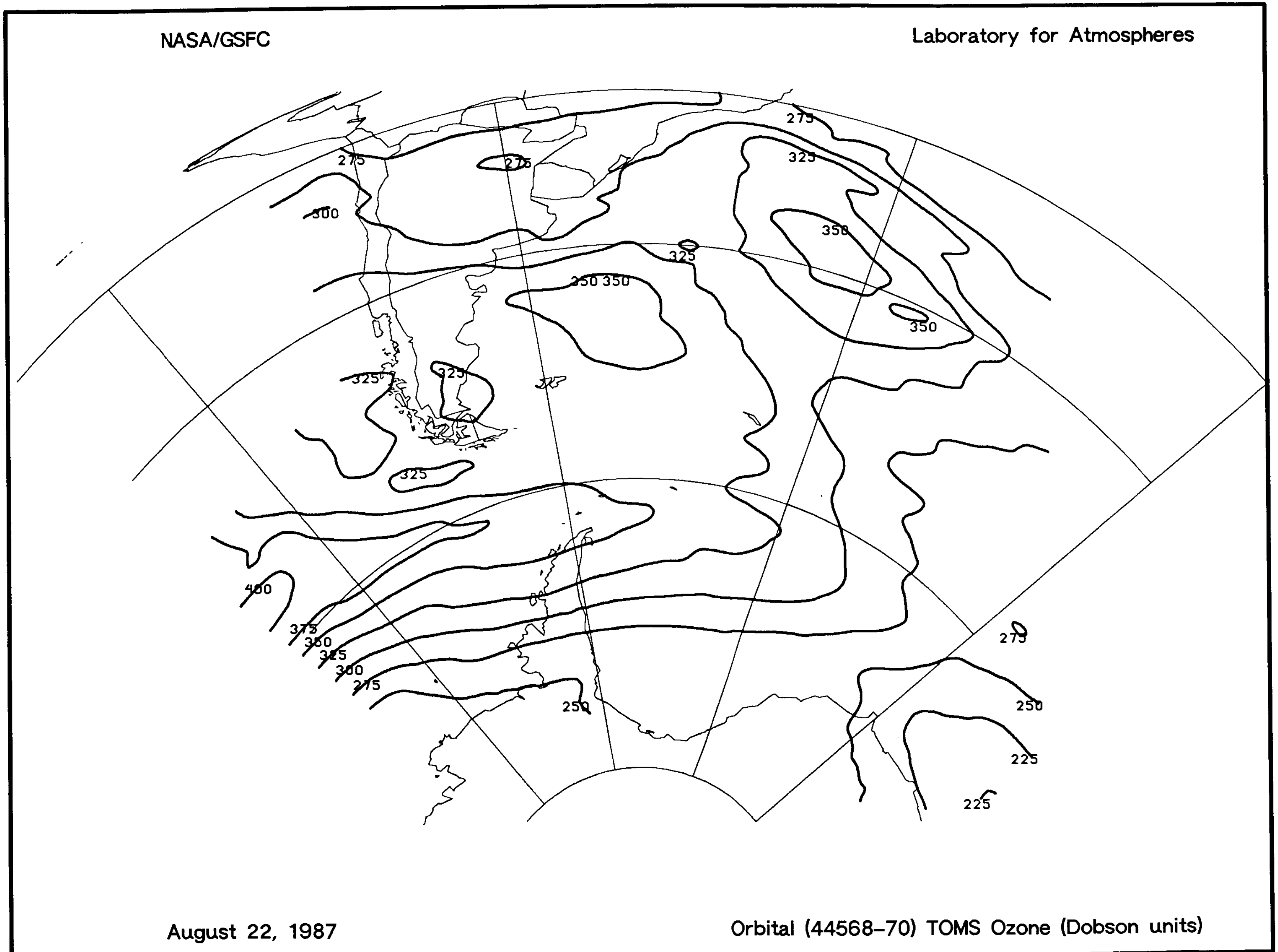
NASA/GSFC
Laboratory for Atmospheres
275
275
300
275
325
350
325
350 350
350
325
325
325
400
375
350
325
300
275
250
275
250
225
225
August 22, 1987
Orbital (44568-70) TOMS Ozone (Dobson units)

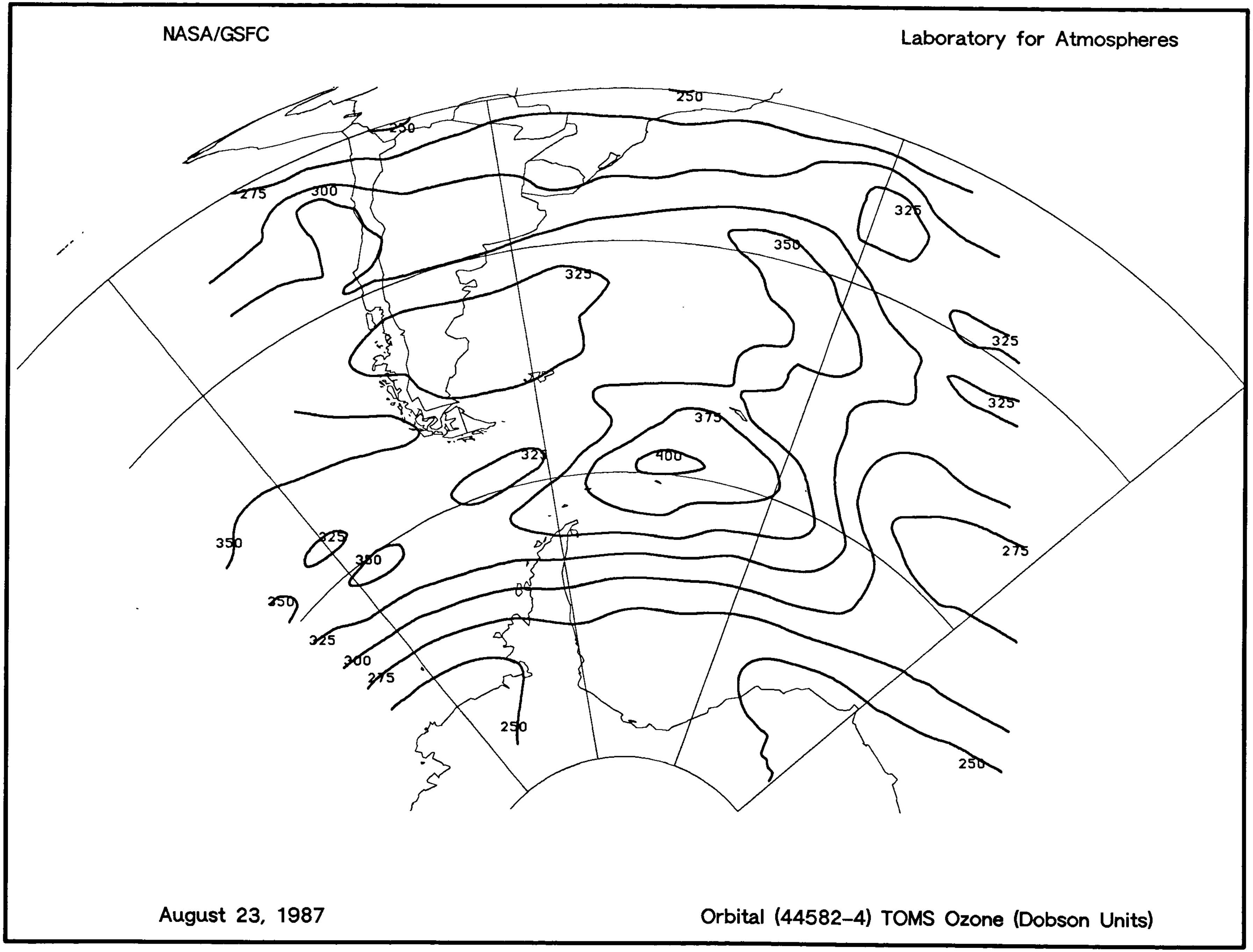
NASA/GSFC
Laboratory for Atmospheres
250
275
300
325
350
375
400
August 23, 1987
Orbital (44582-4) TOMS Ozone (Dobson Units)

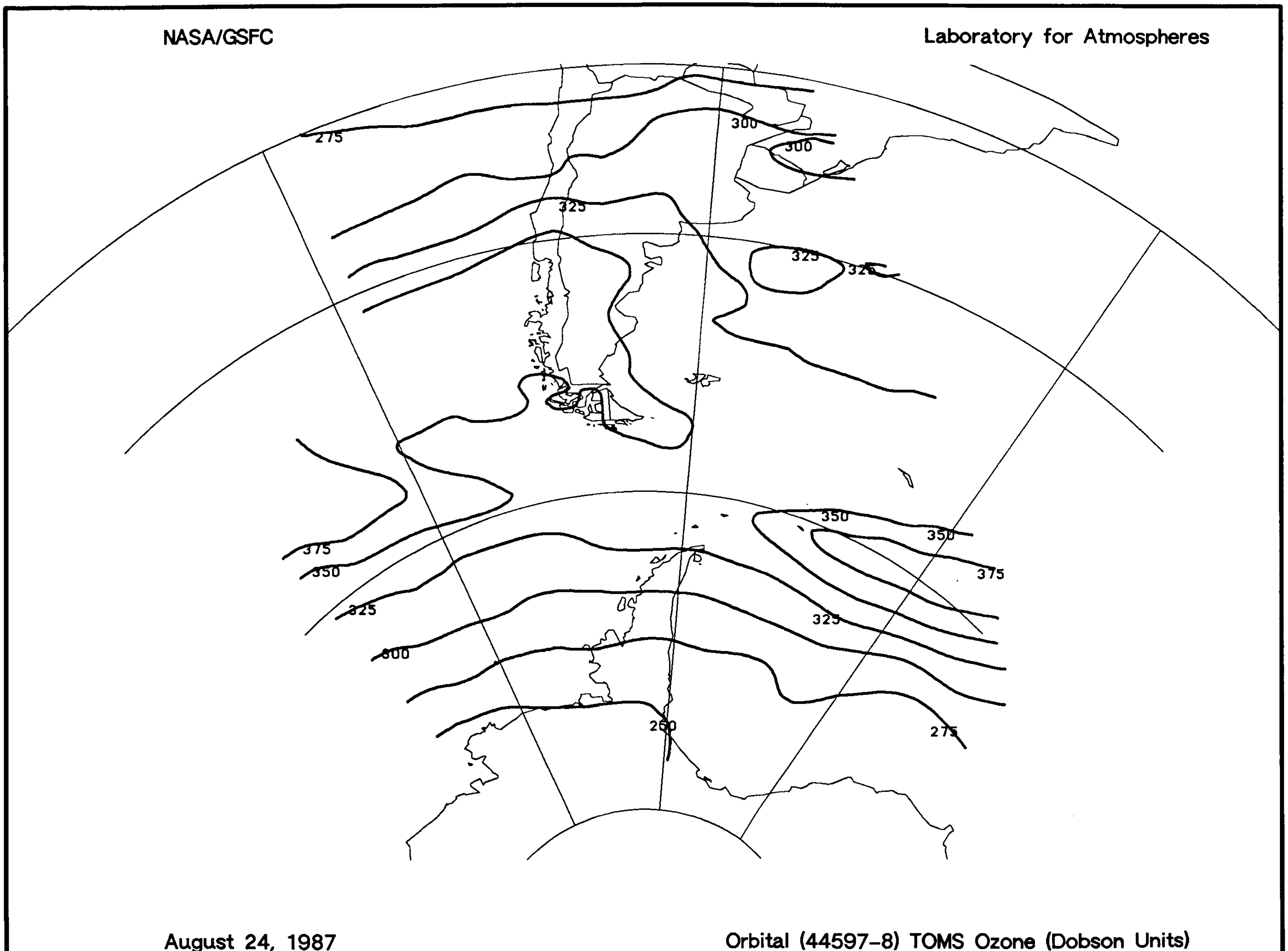
NASA/GSFC
Laboratory for Atmospheres
275
300
300
325
325
325
350
350
375
350
375
325
325
300
250
275
August 24, 1987
Orbital (44597-8) TOMS Ozone (Dobson Units)

NASA/GSFC

Laboratory for Atmospheres

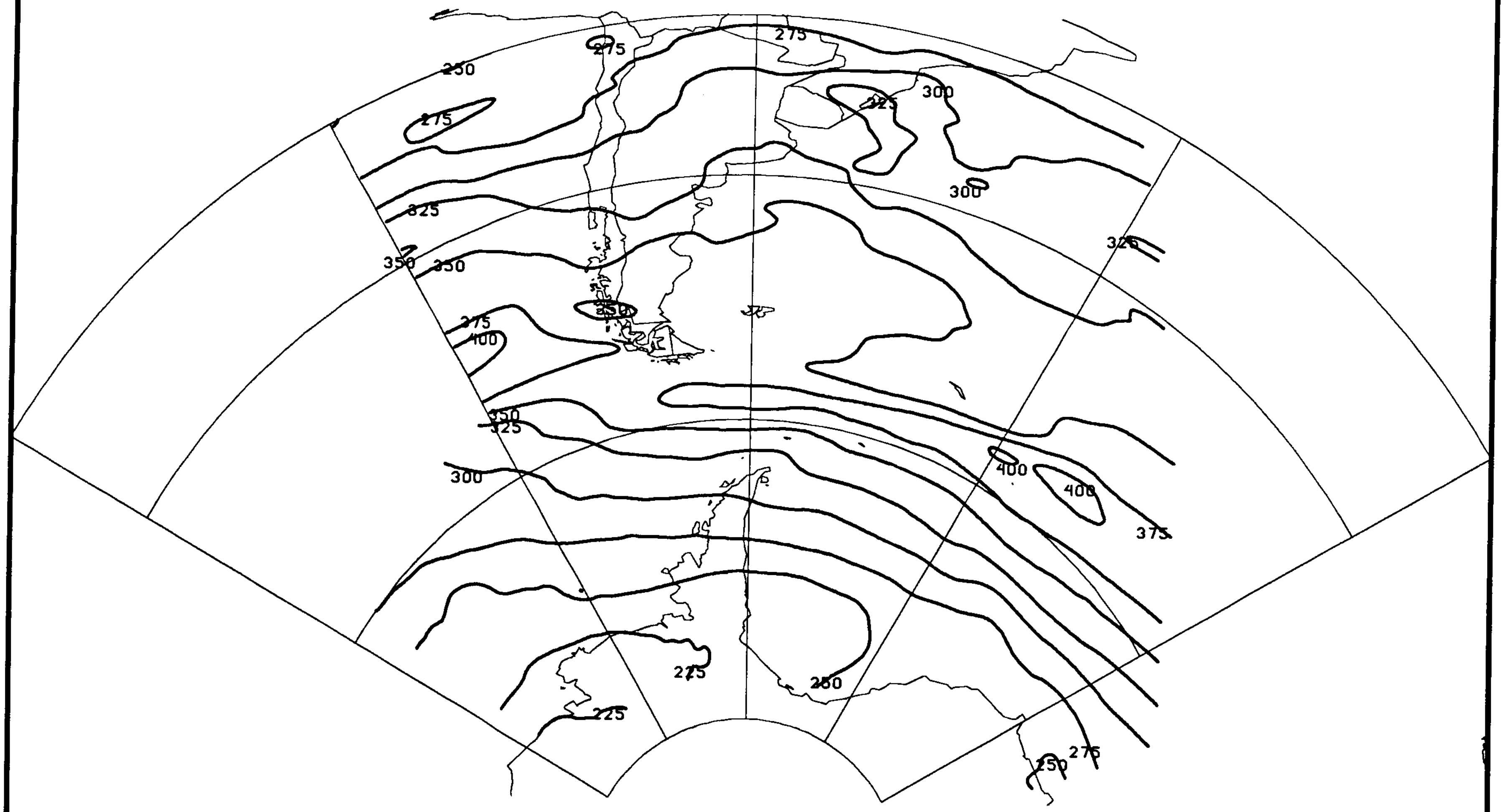


August 25, 1987

Orbital (44610-2) TOMS Ozone (Dobson Units)

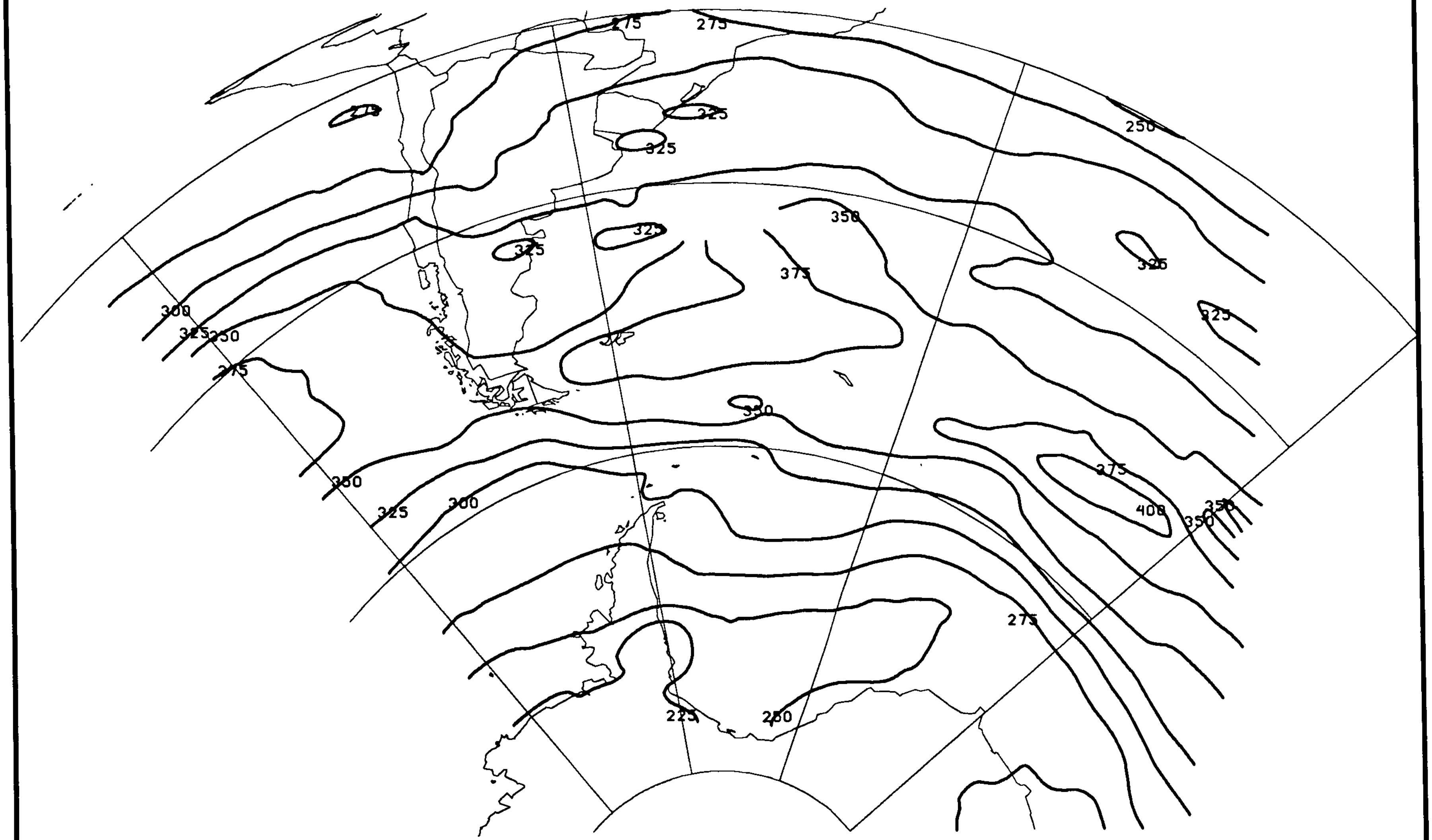
NASA/GSFC
Laboratory for Atmospheres
August 26, 1987
Orbital (44623-5) TOMS Ozone (Dobson Units)

NASA/GSFC

Laboratory for Atmospheres

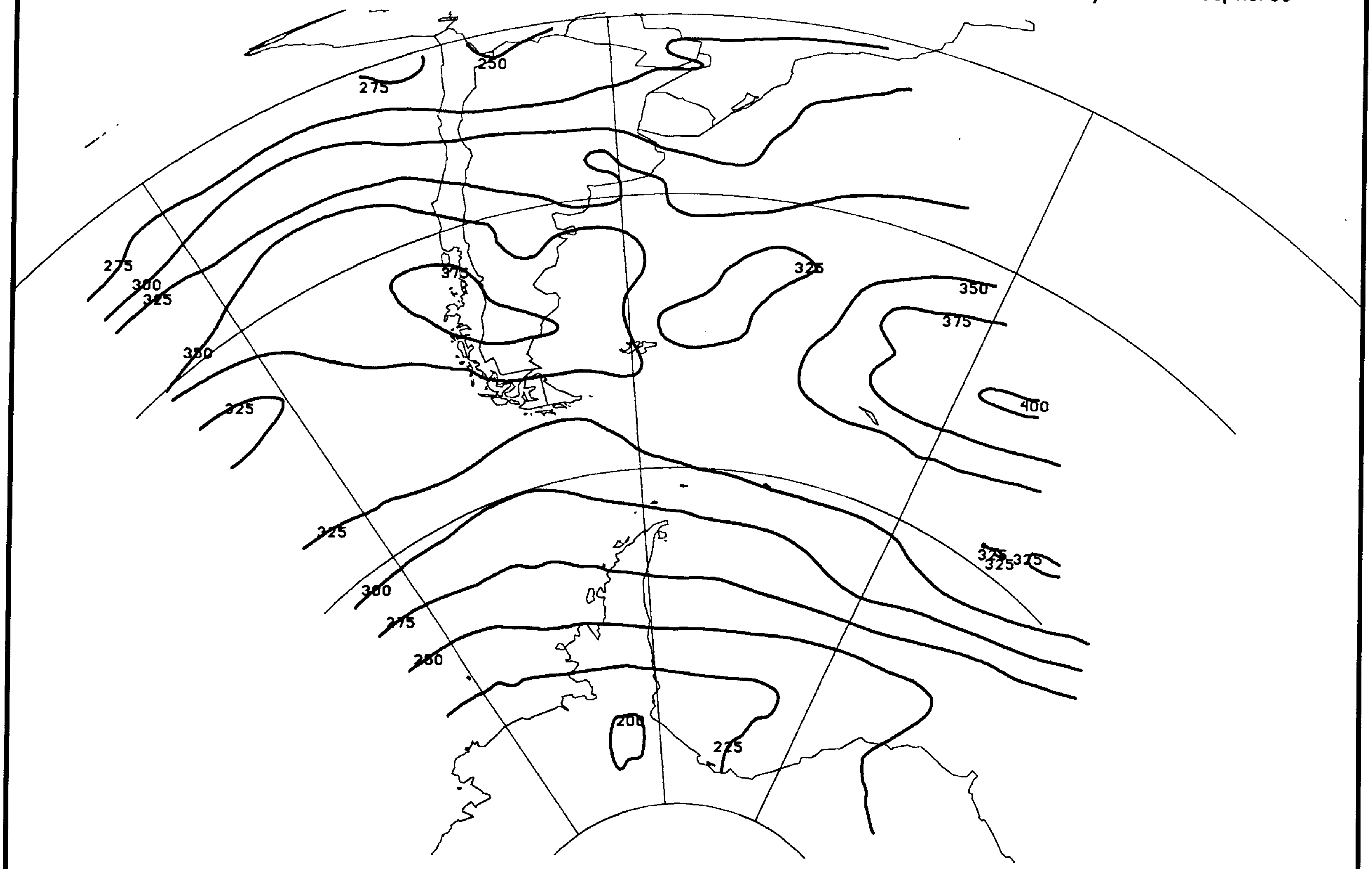


August 27, 1987

Orbital (44638-9) TOMS Ozone (Dobson Units)

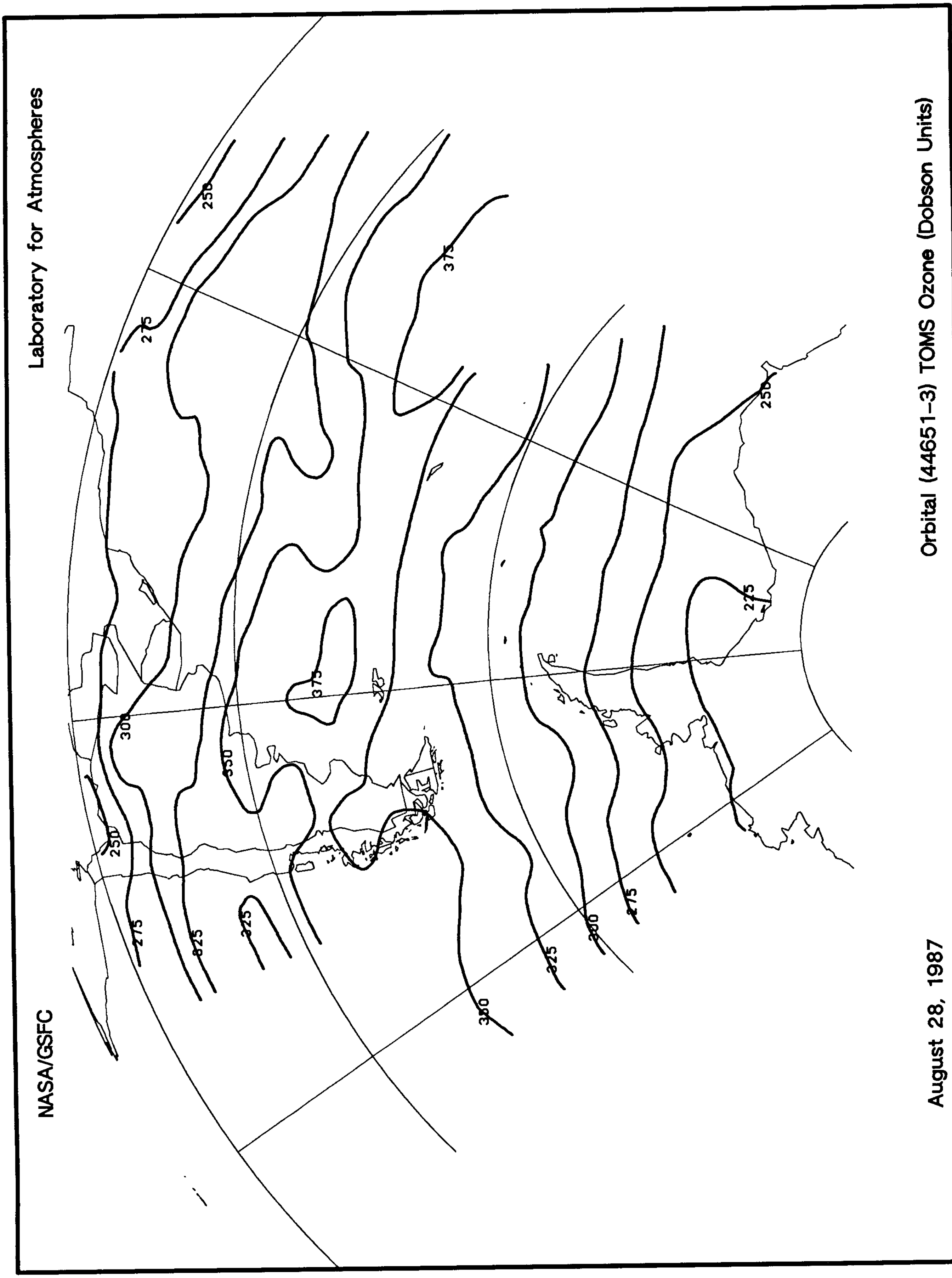
NASA/GSFC
Laboratory for Atmospheres
August 28, 1987
Orbital (44651-3) TOMS Ozone (Dobson Units)

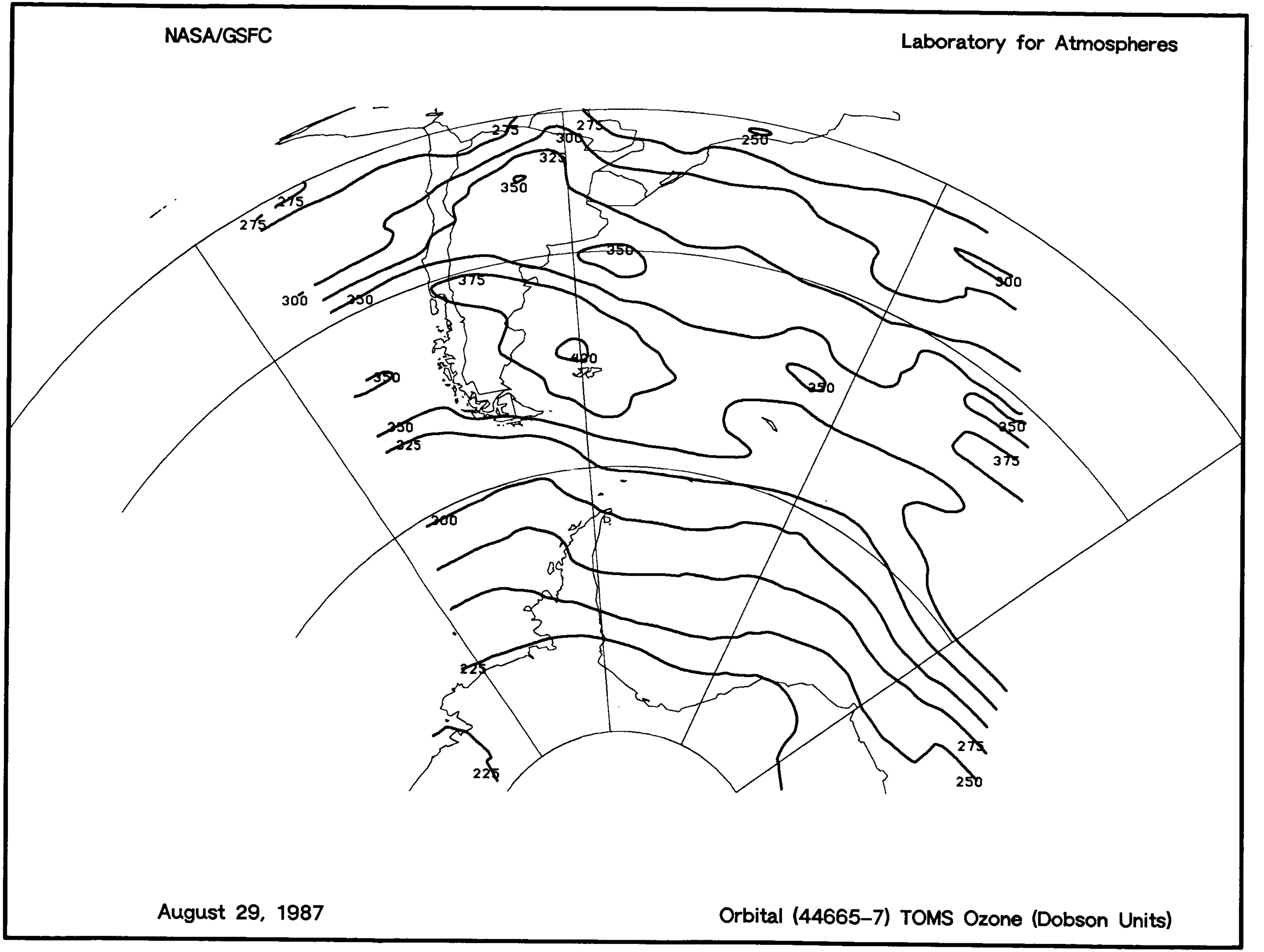
NASA/GSFC
Laboratory for Atmospheres
275
300
325
350
375
400
250
225
August 29, 1987
Orbital (44665-7) TOMS Ozone (Dobson Units)

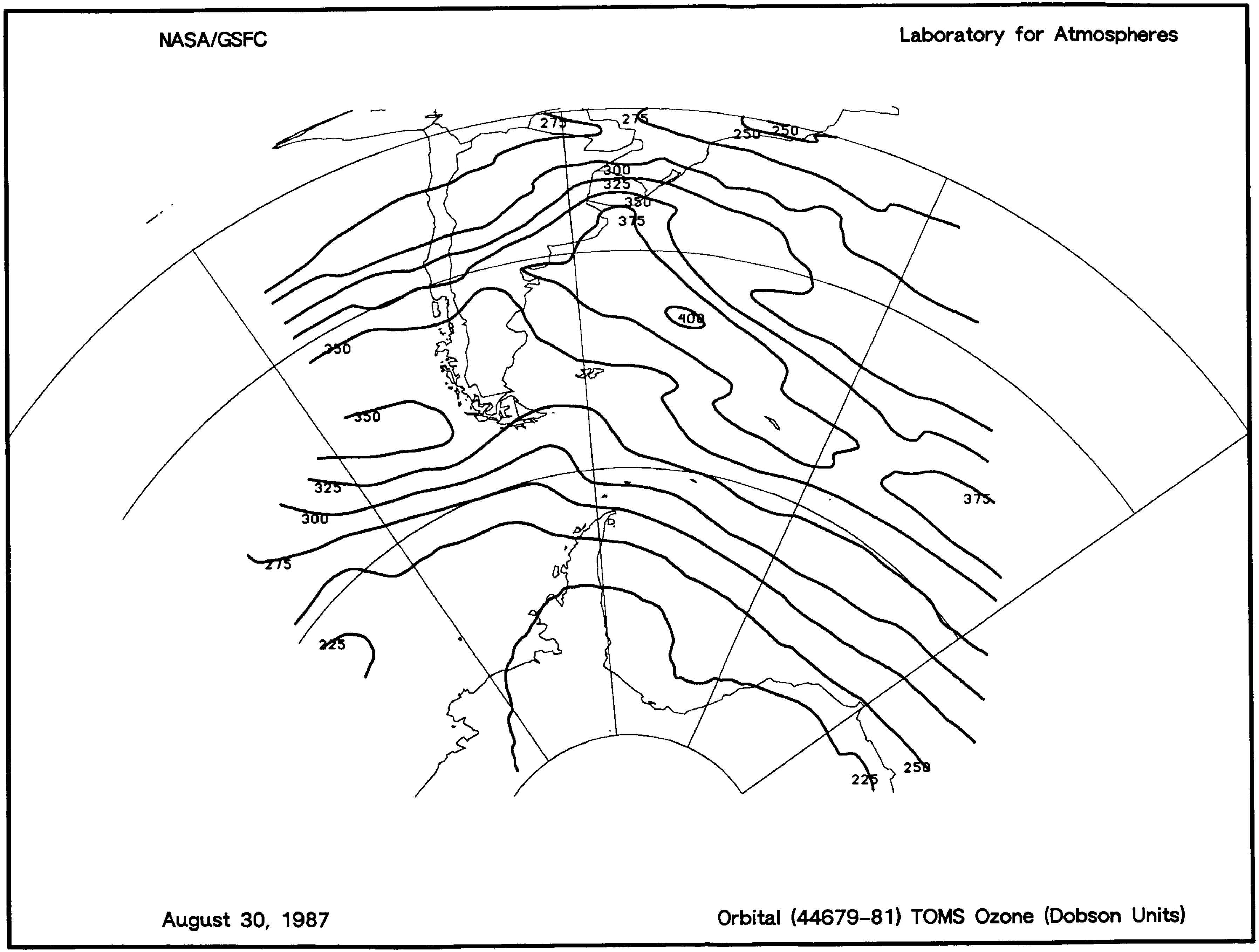
NASA/GSFC
Laboratory for Atmospheres
275
275
250
250
300
325
350
375
400
350
350
325
300
275
225
375
225
250
August 30, 1987
Orbital (44679-81) TOMS Ozone (Dobson Units)

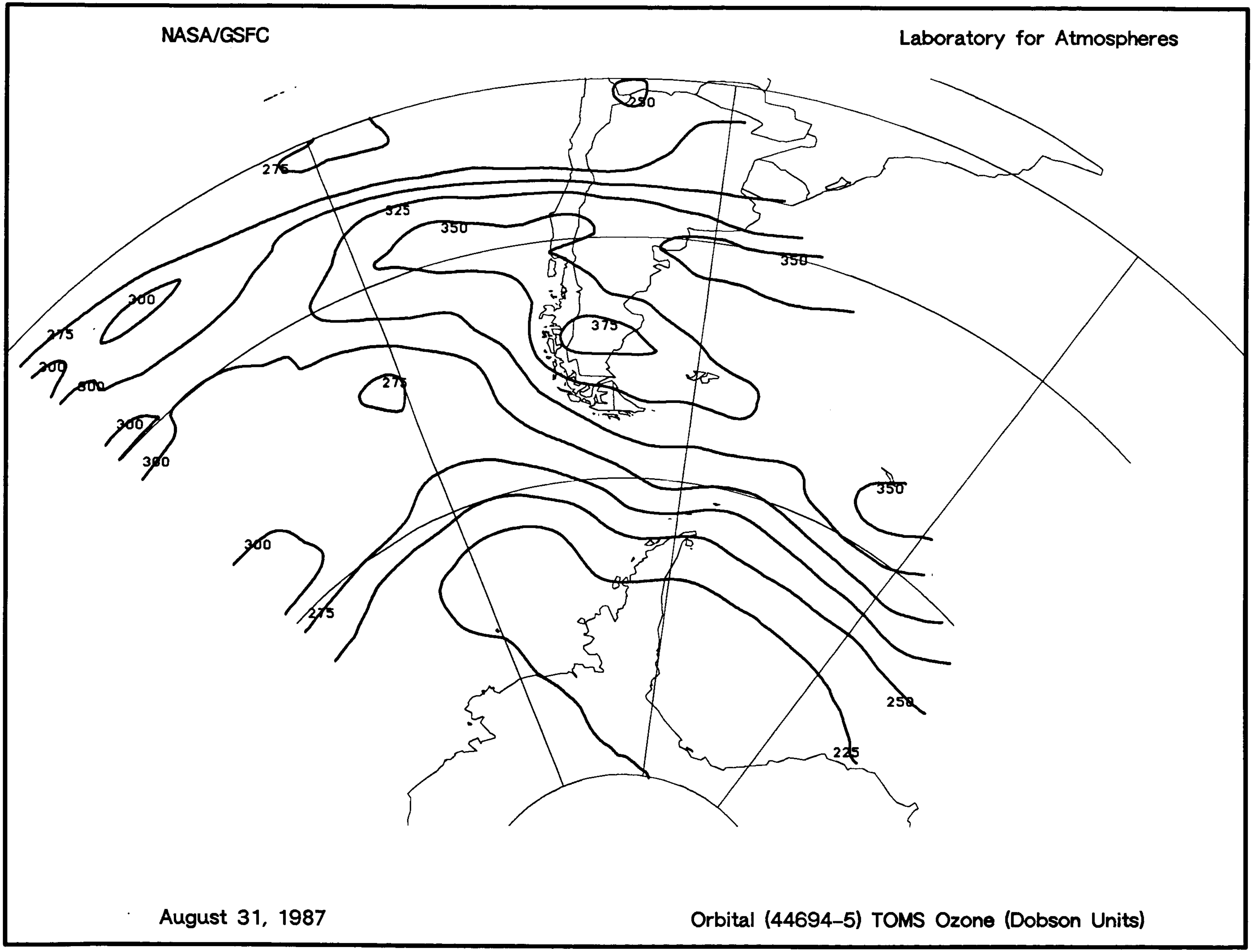
NASA/GSFC
Laboratory for Atmospheres
275
325
350
300
375
250
225
August 31, 1987
Orbital (44694-5) TOMS Ozone (Dobson Units)

NASA/GSFC

Laboratory for Atmospheres

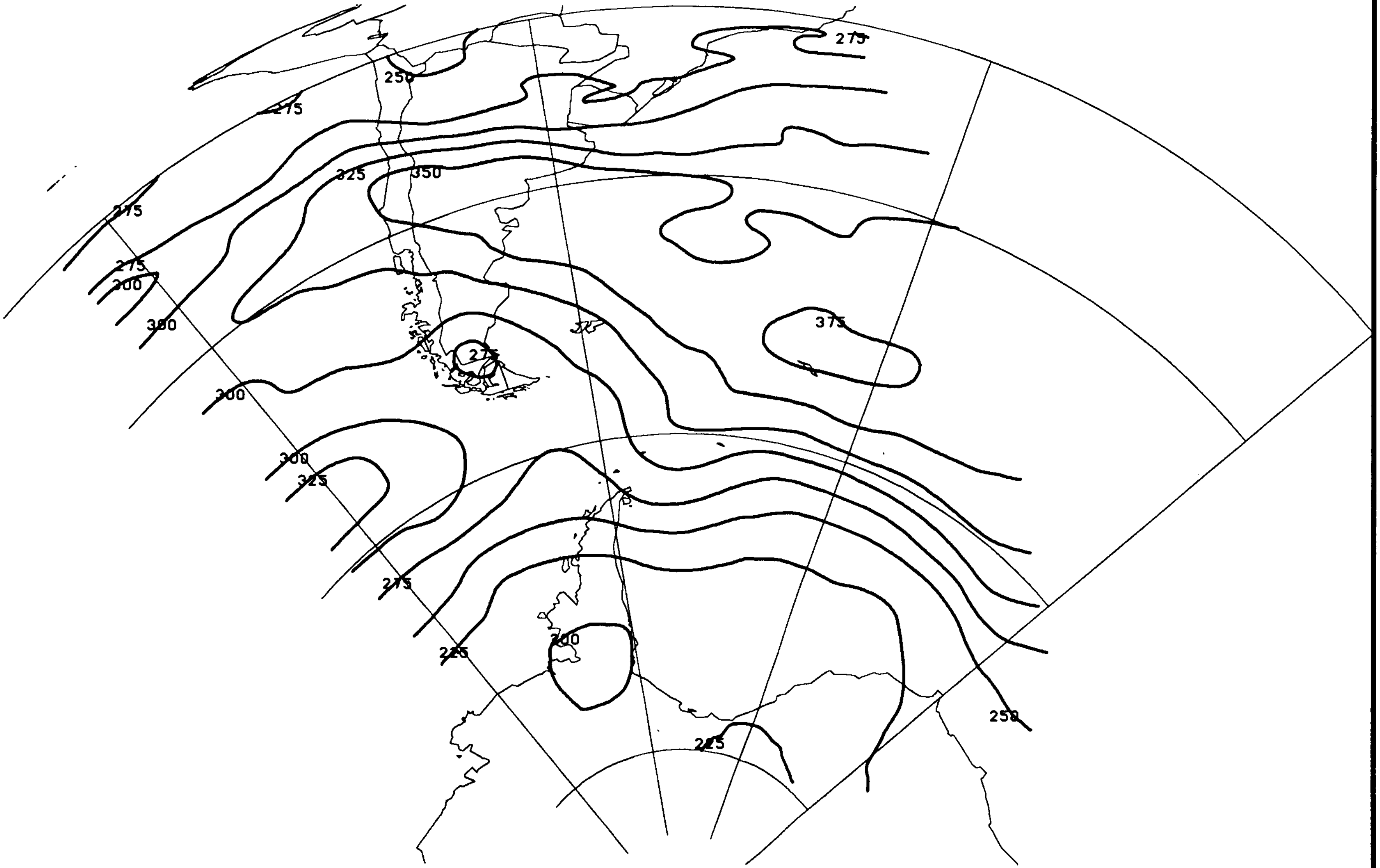


September 1, 1987

Orbital (44707-8) TOMS Ozone (Dobson Units)

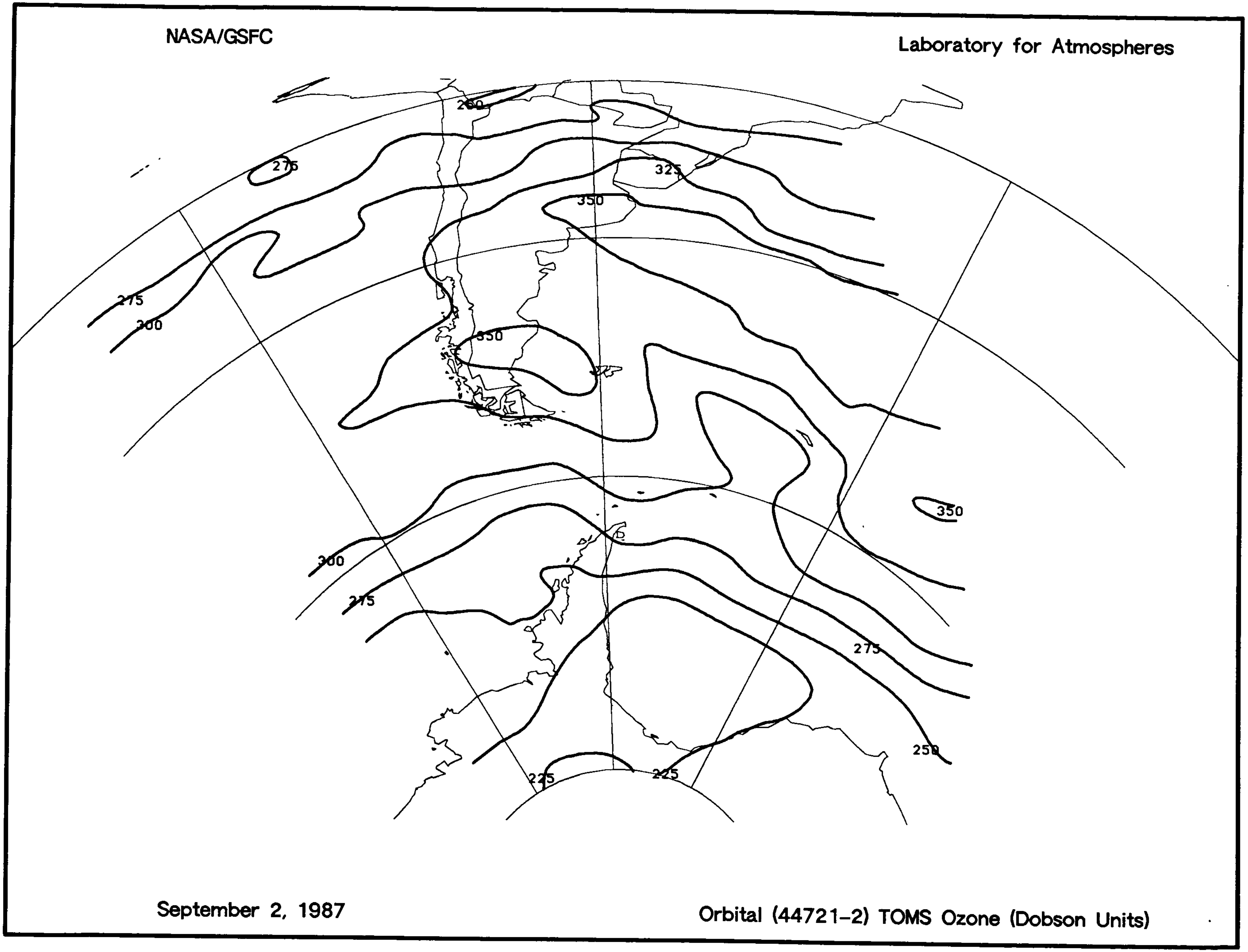
NASA/GSFC
Laboratory for Atmospheres
260
275
325
350
275
300
350
350
300
275
275
250
225
225
September 2, 1987
Orbital (44721-2) TOMS Ozone (Dobson Units)

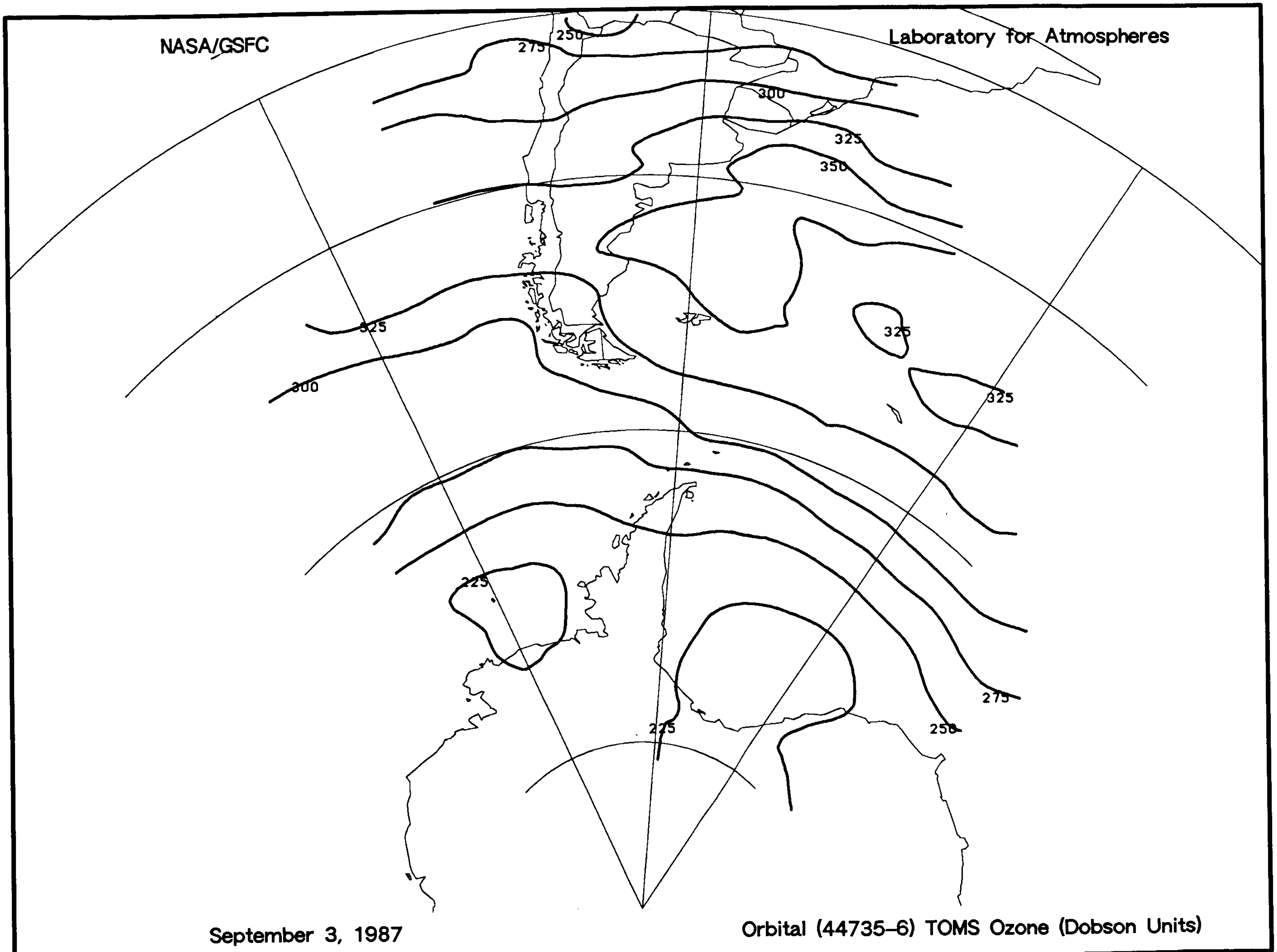
NASA/GSFC
Laboratory for Atmospheres
250
275
300
325
350
325
325
325
300
225
275
250
275
September 3, 1987
Orbital (44735-6) TOMS Ozone (Dobson Units)

NASA/GSFC

Laboratory for Atmospheres

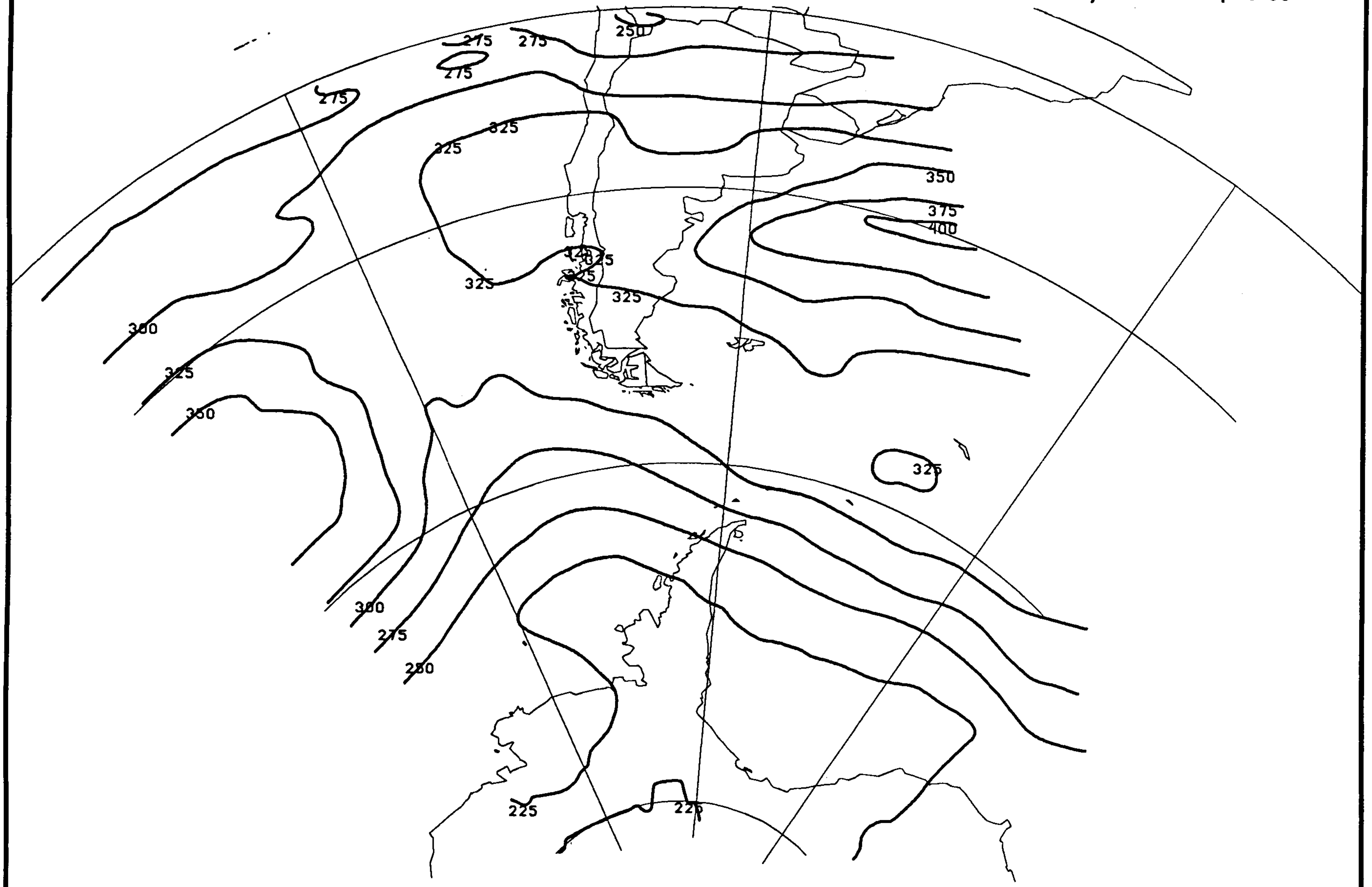


September 4, 1987

Orbital (44749-50) TOMS Ozone (Dobson Units)

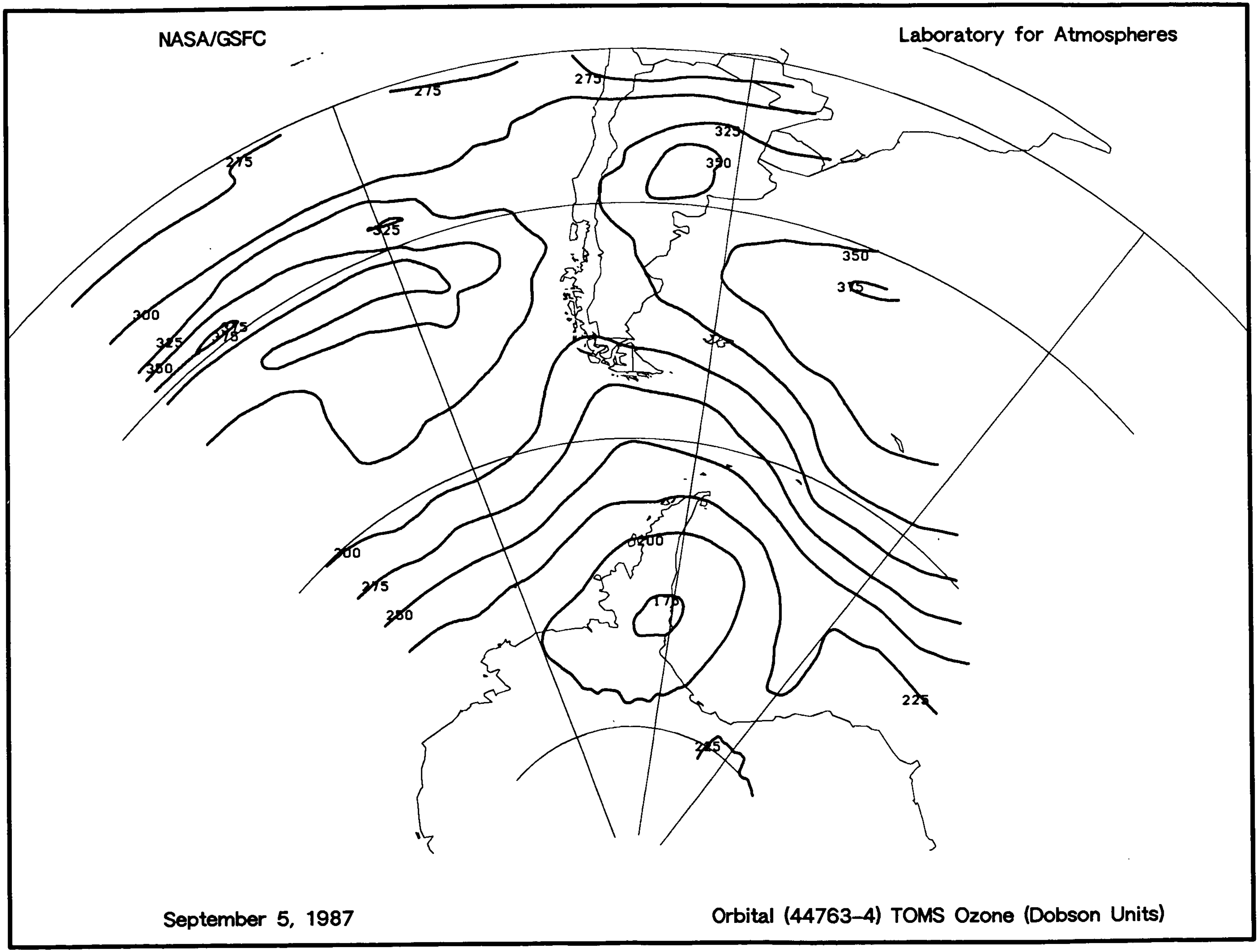
NASA/GSFC
Laboratory for Atmospheres
275
275
275
325
350
325
390
350
325
300
325
350
200
300
275
250
175
225
225
September 5, 1987
Orbital (44763-4) TOMS Ozone (Dobson Units)

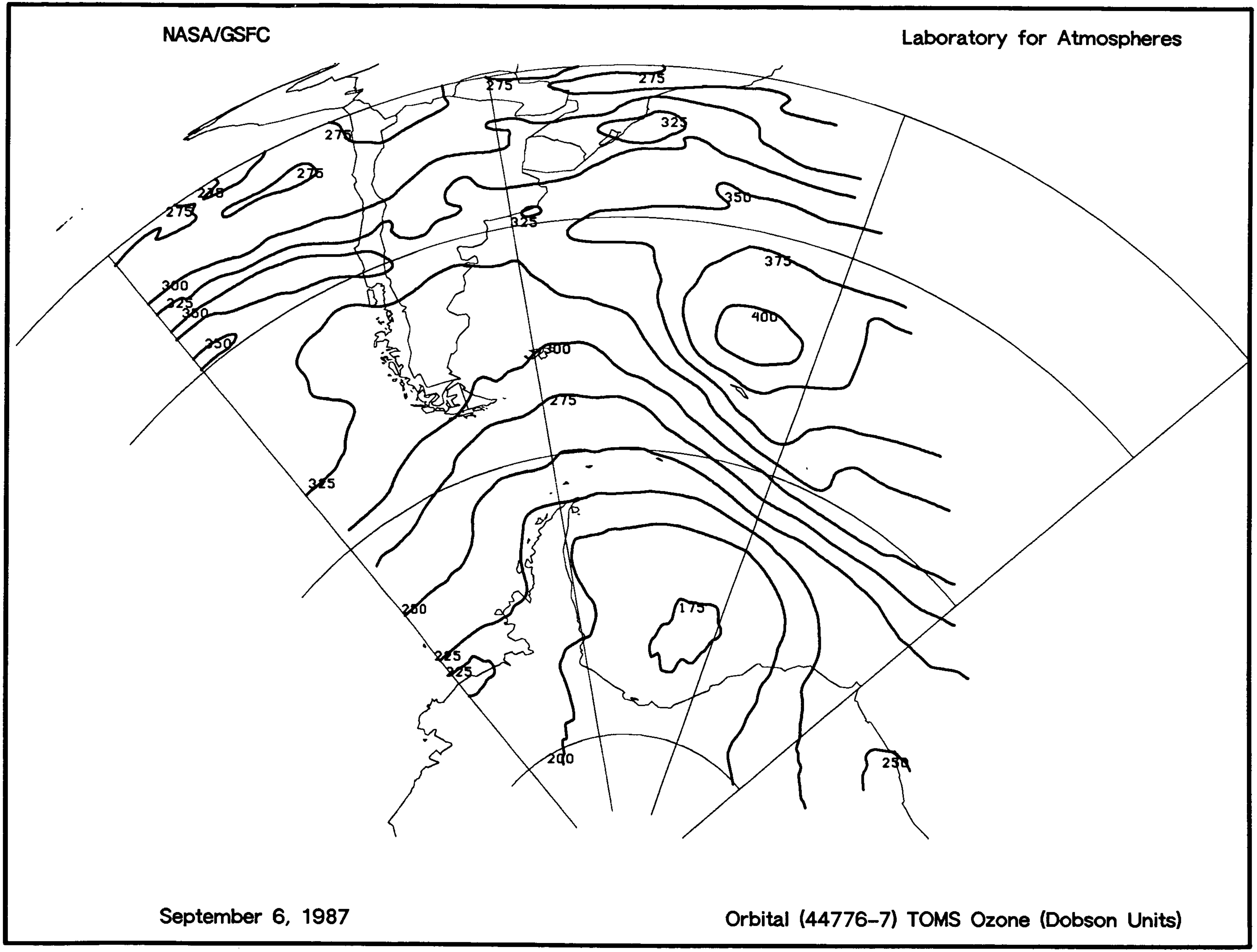
NASA/GSFC
Laboratory for Atmospheres
275
275
325
275
275
275
350
325
375
400
300
325
300
350
300
275
325
250
225
225
175
200
250
September 6, 1987
Orbital (44776-7) TOMS Ozone (Dobson Units)

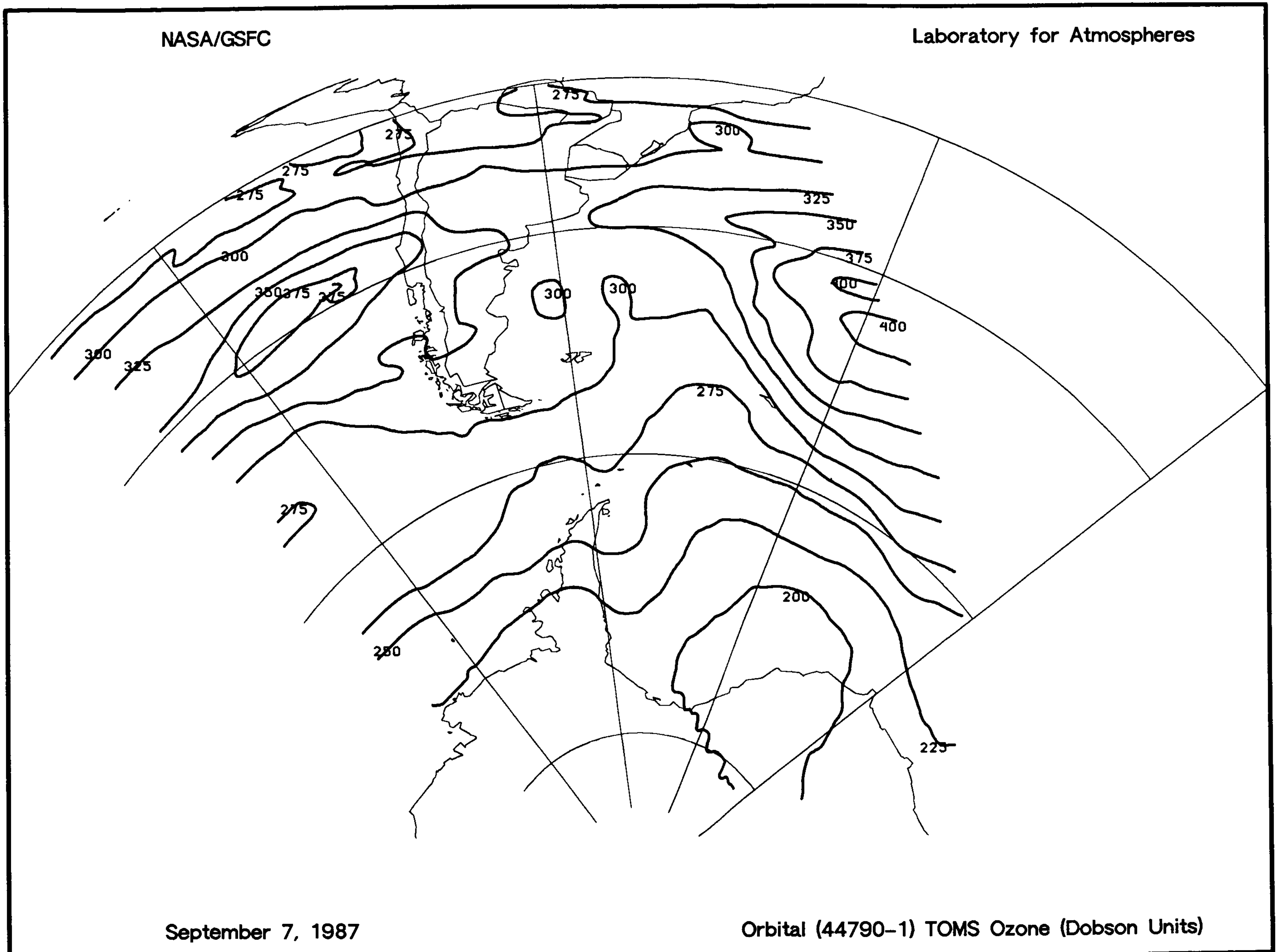
NASA/GSFC
Laboratory for Atmospheres
275
300
325
350
375
400
300
275
250
200
225
September 7, 1987
Orbital (44790-1) TOMS Ozone (Dobson Units)

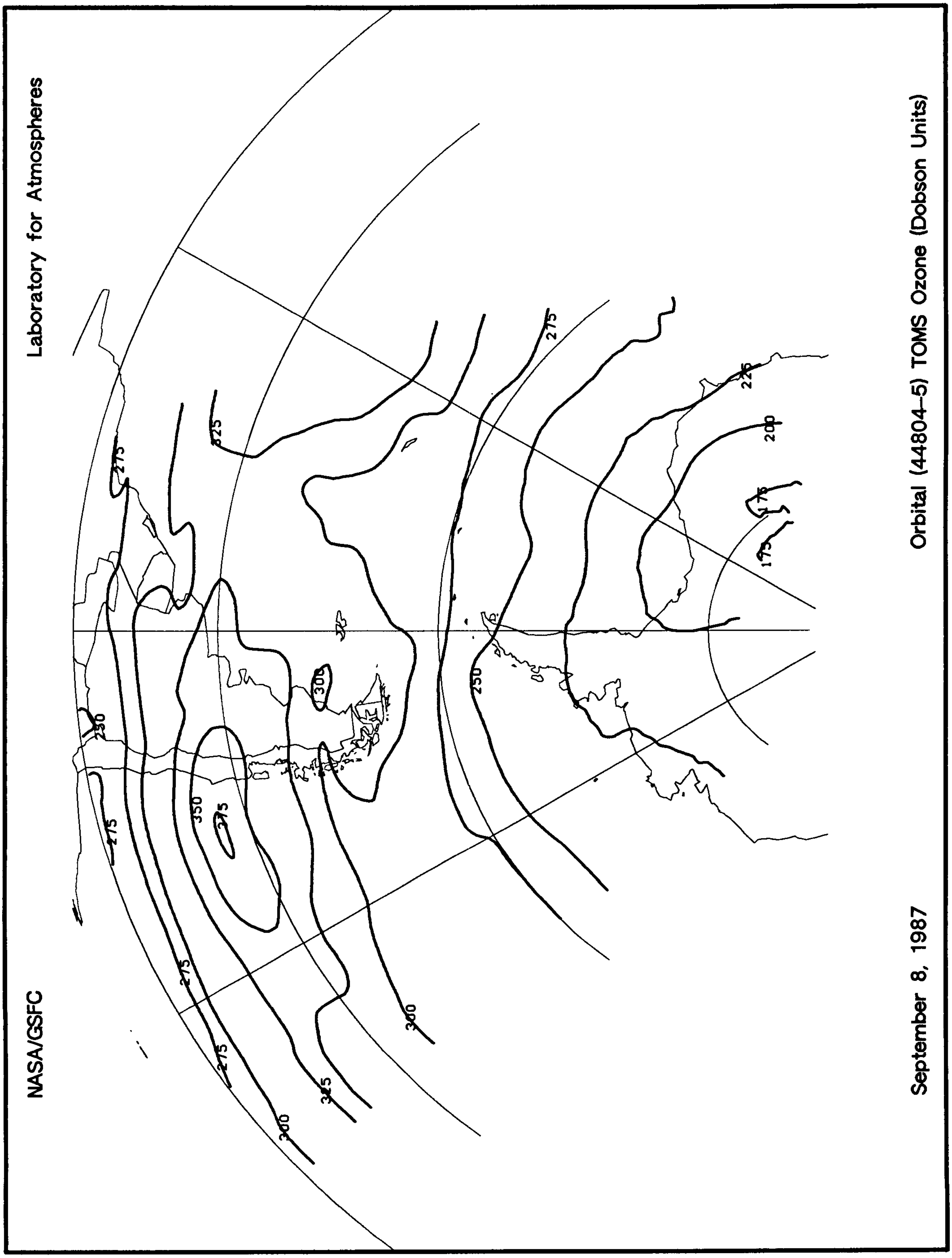
NASA/GSFC
Laboratory for Atmospheres
September 8, 1987
Orbital (44804–5) TOMS Ozone (Dobson Units)

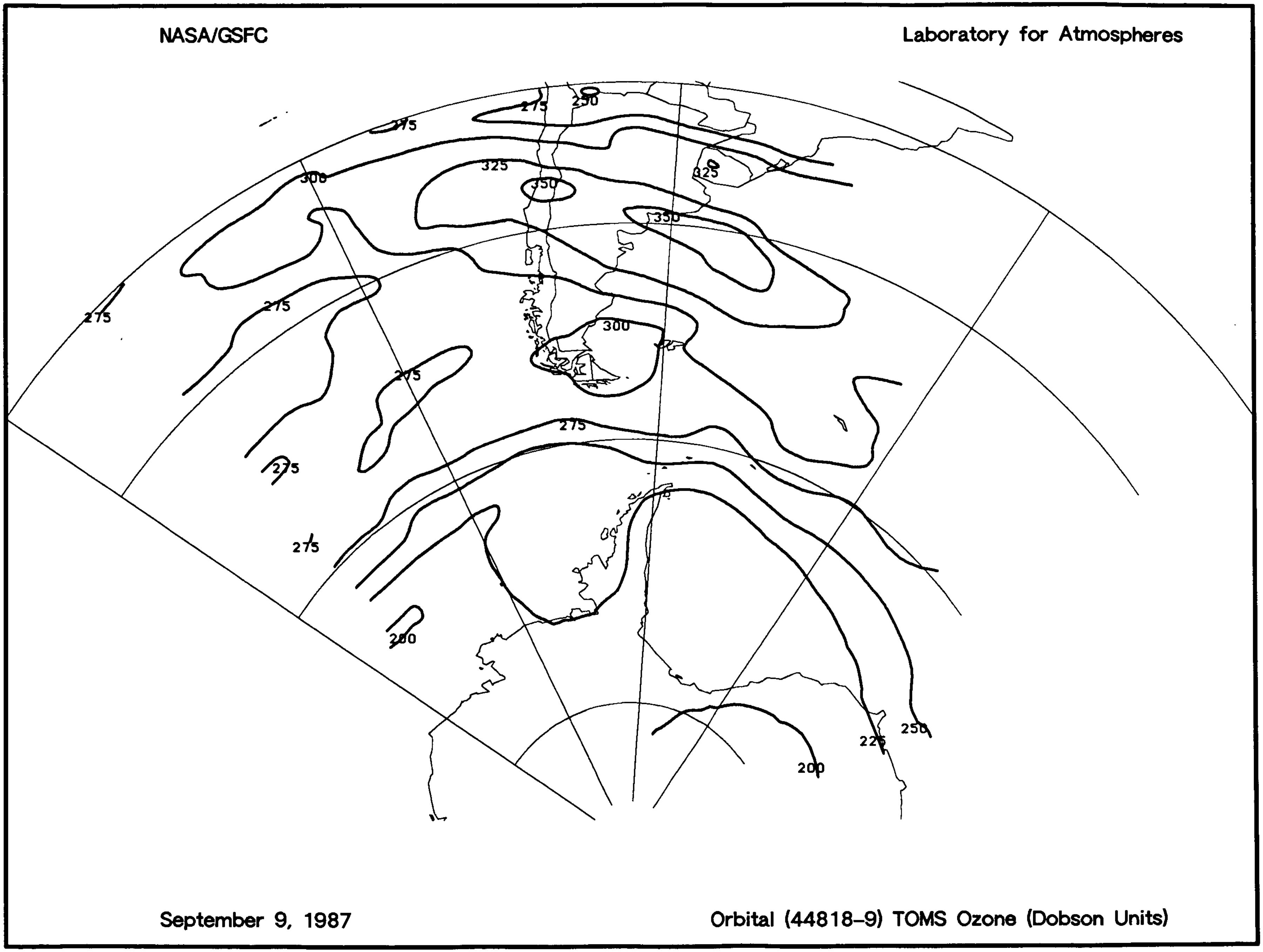
NASA/GSFC
Laboratory for Atmospheres
275
250
275
300
325
350
325
350
275
275
300
275
275
275
275
200
225
250
200
September 9, 1987
Orbital (44818-9) TOMS Ozone (Dobson Units)

NASA/GSFC

Laboratory for Atmospheres

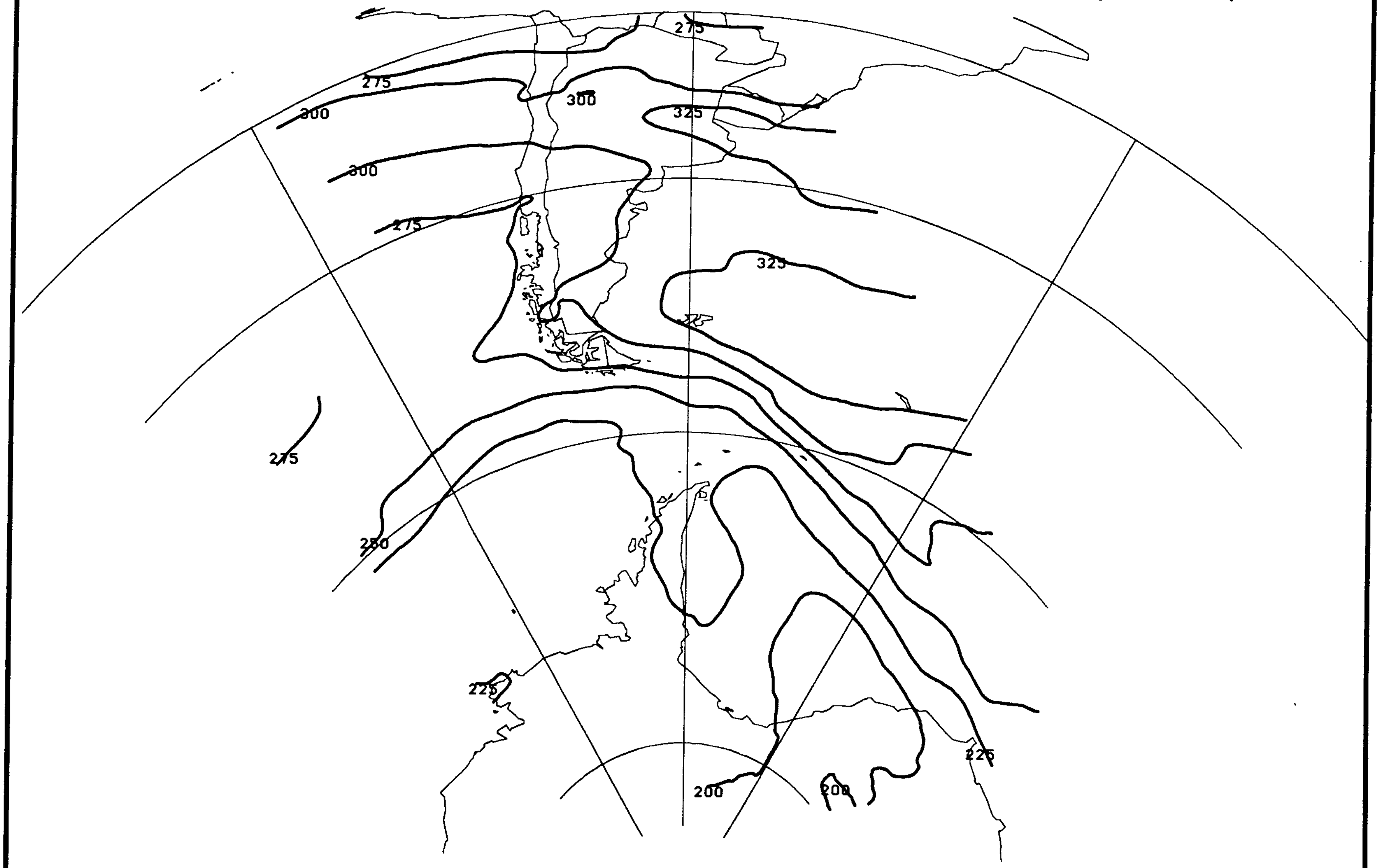


September 10, 1987

Orbital (44832-3) TOMS Ozone (Dobson Units)

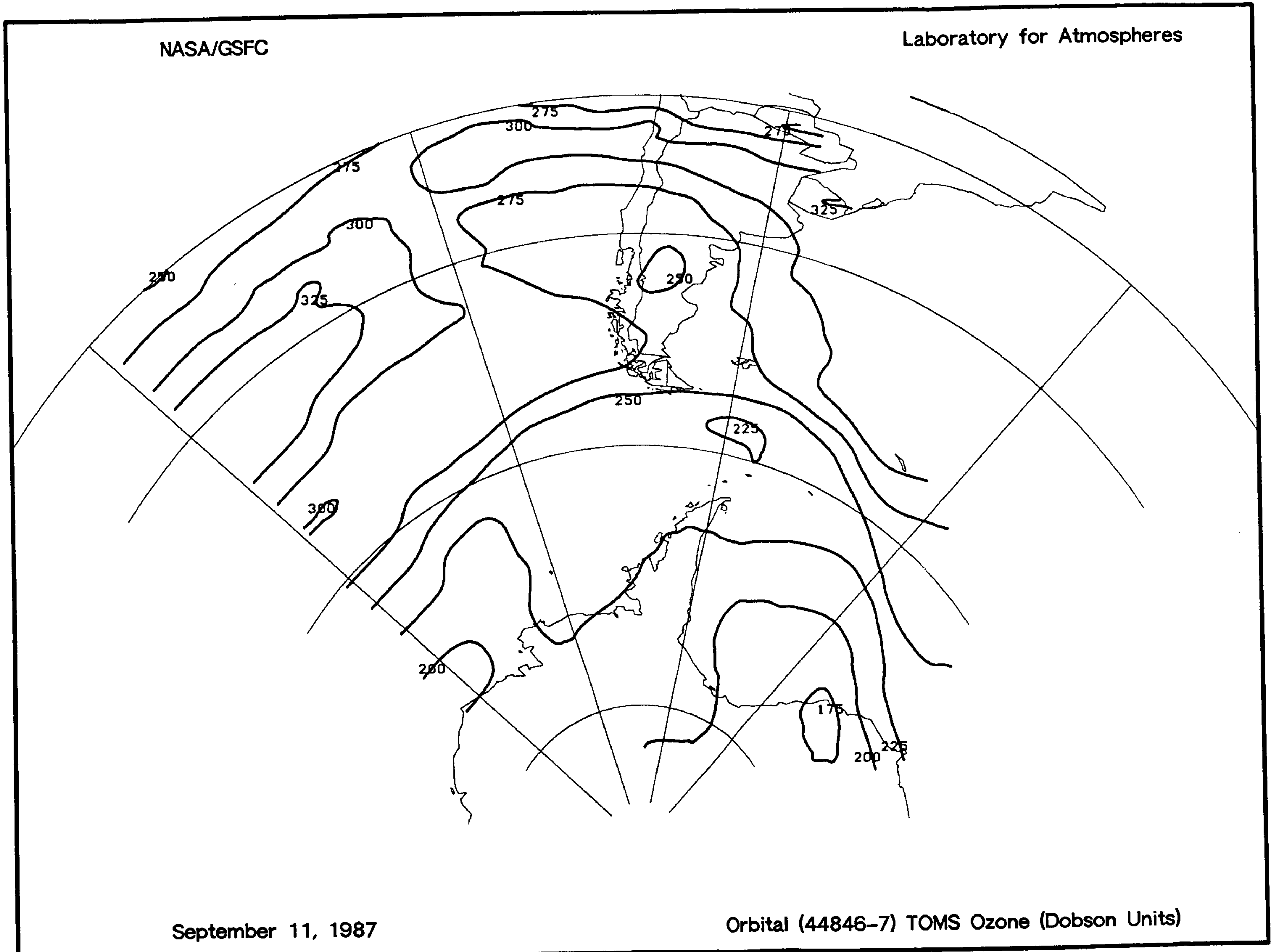
NASA/GSFC
Laboratory for Atmospheres
275
300
275
275
325
300
275
250
250
325
250
225
300
200
175
200
225
September 11, 1987
Orbital (44846-7) TOMS Ozone (Dobson Units)

NASA/GSFC

Laboratory for Atmospheres

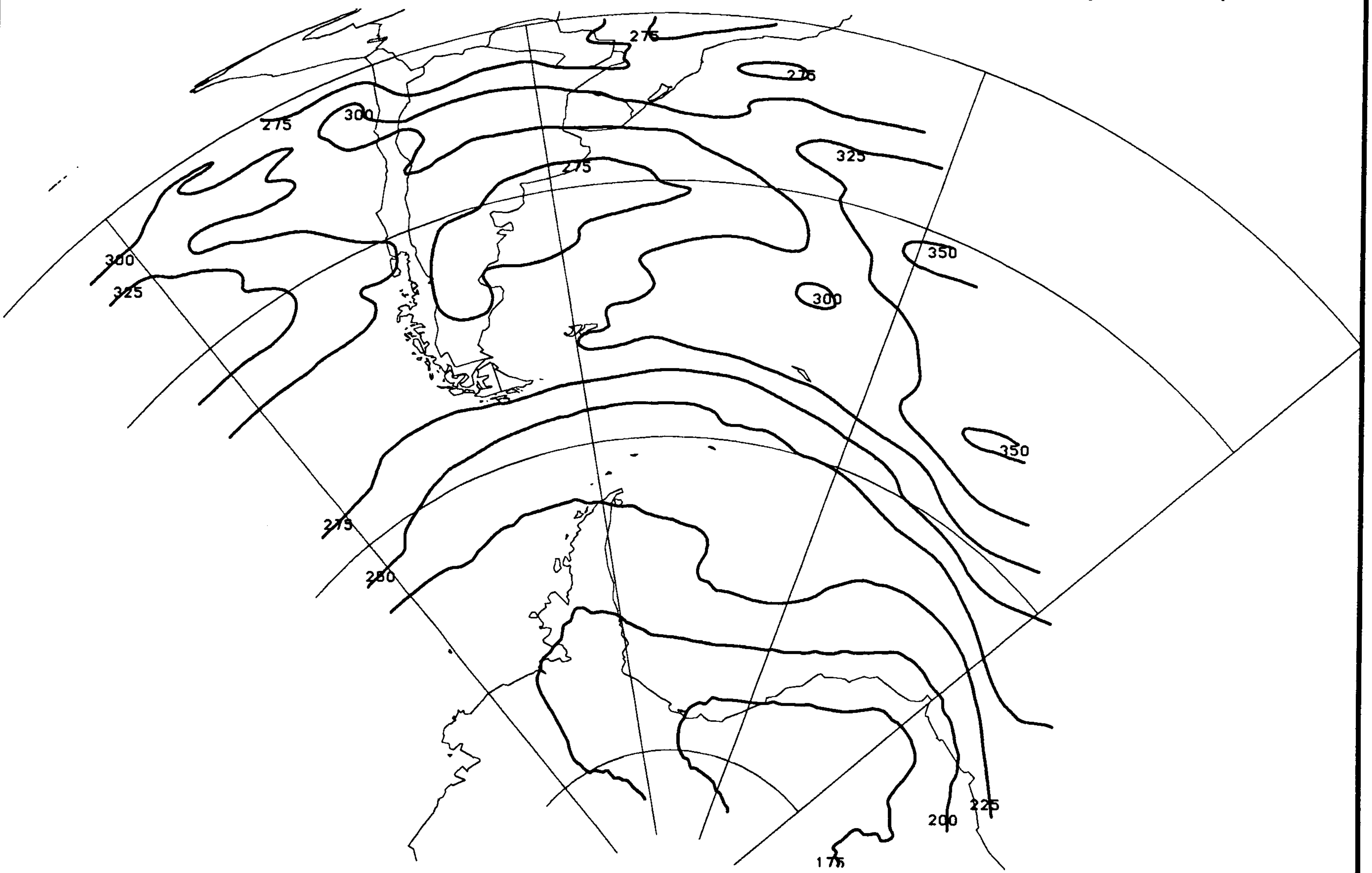


September 12, 1987

Orbital (44859-60) TOMS Ozone (Dobson Units)

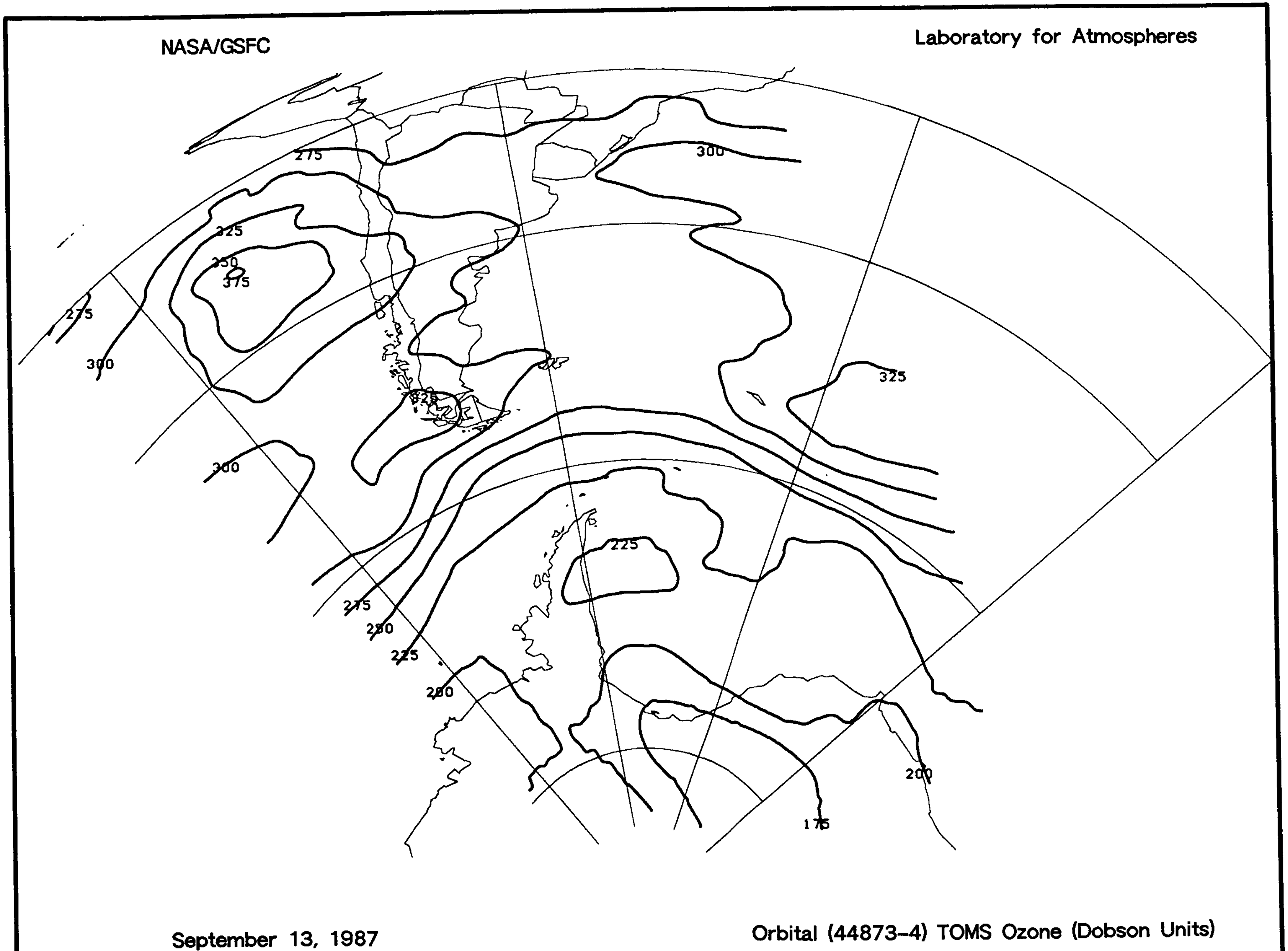
NASA/GSFC
Laboratory for Atmospheres
275
300
325
350
375
225
250
200
175
September 13, 1987
Orbital (44873-4) TOMS Ozone (Dobson Units)

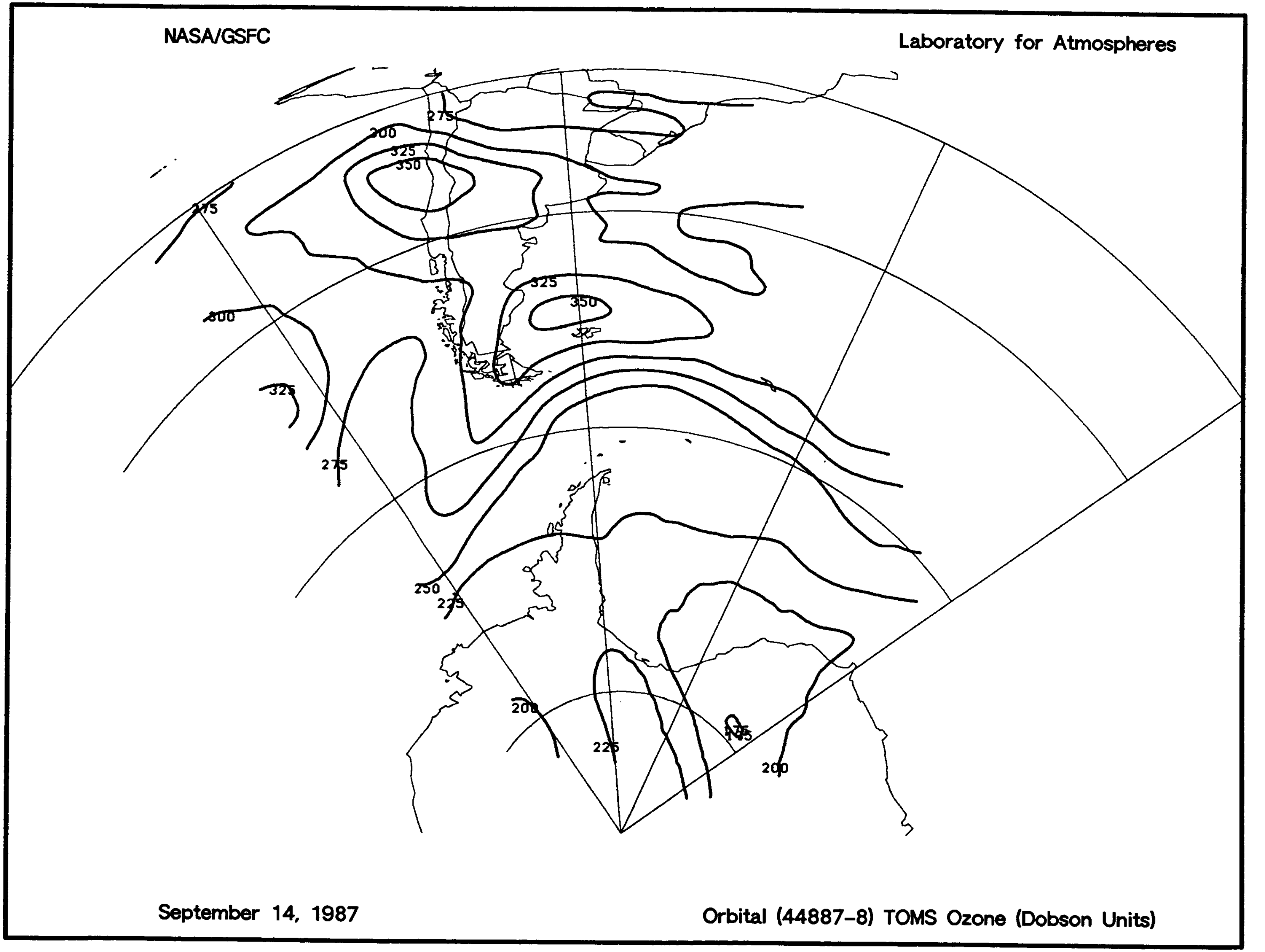
NASA/GSFC
Laboratory for Atmospheres
275
300
325
350
325
350
275
300
325
275
250
225
200
225
175
200
September 14, 1987
Orbital (44887-8) TOMS Ozone (Dobson Units)

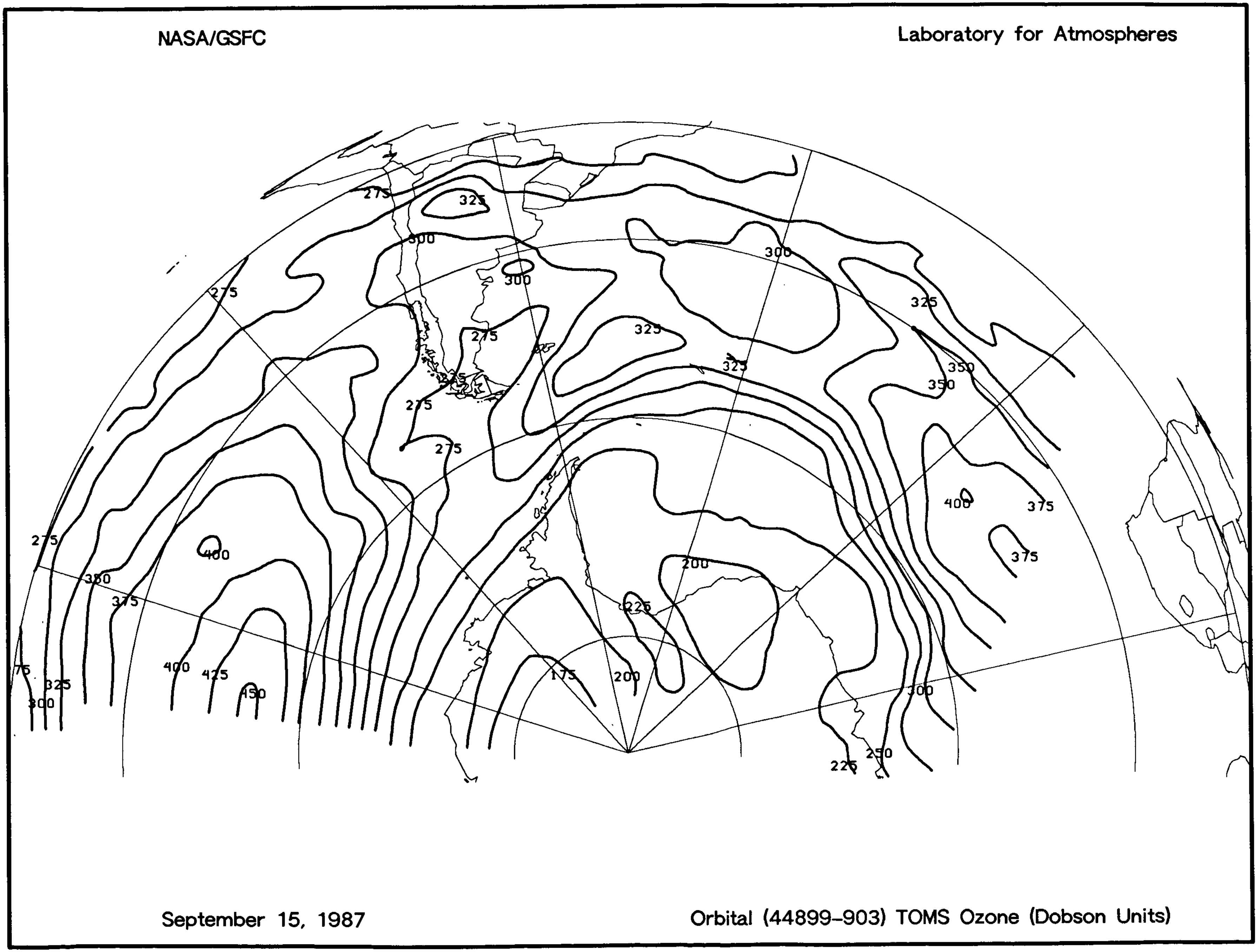
NASA/GSFC
Laboratory for Atmospheres
275
325
300
300
275
275
325
325
300
325
350
350
275
275
275
400
375
375
400
200
225
275
350
375
400
425
450
75
325
300
175
200
300
250
225
September 15, 1987
Orbital (44899-903) TOMS Ozone (Dobson Units)

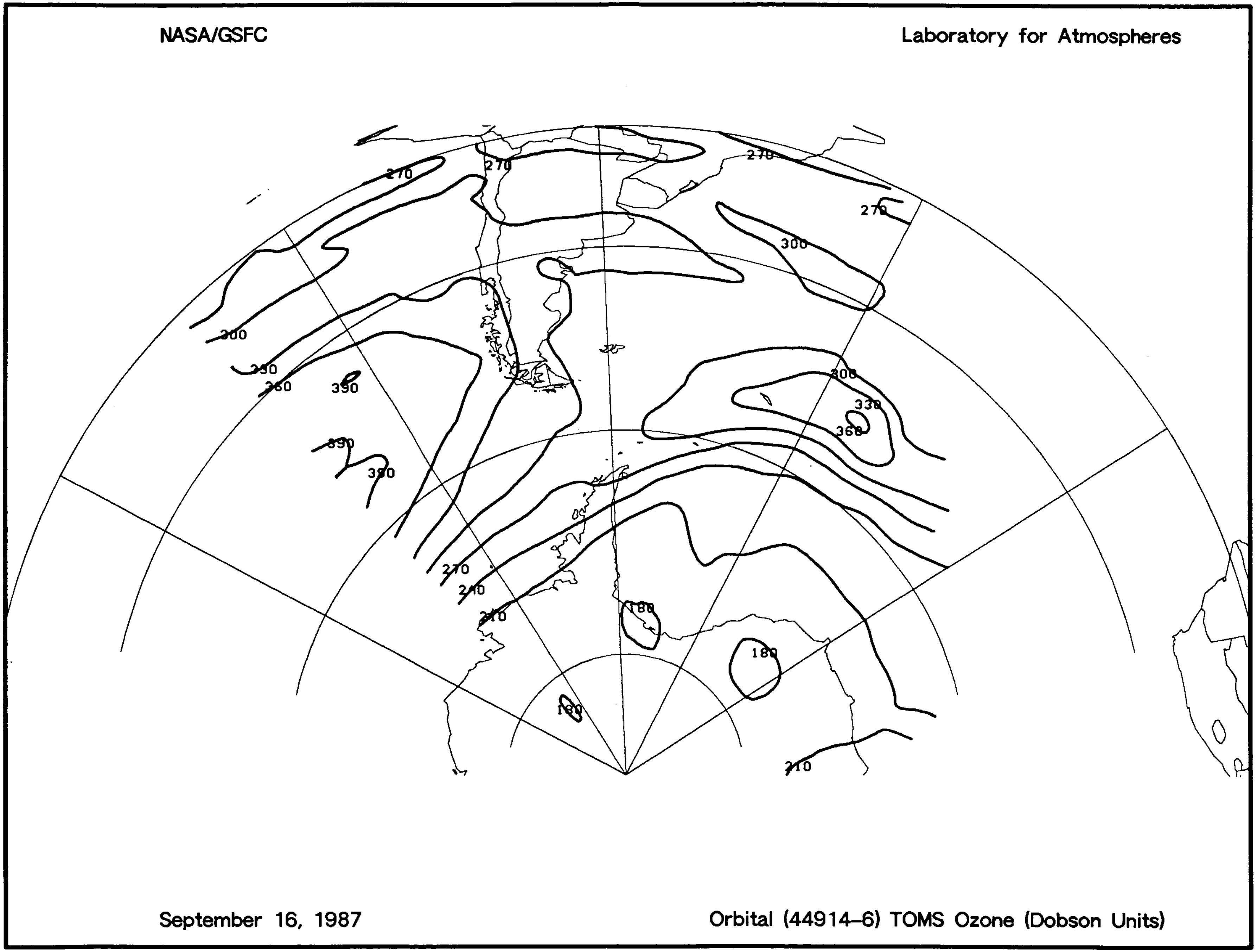
NASA/GSFC
Laboratory for Atmospheres
September 16, 1987
Orbital (44914-6) TOMS Ozone (Dobson Units)

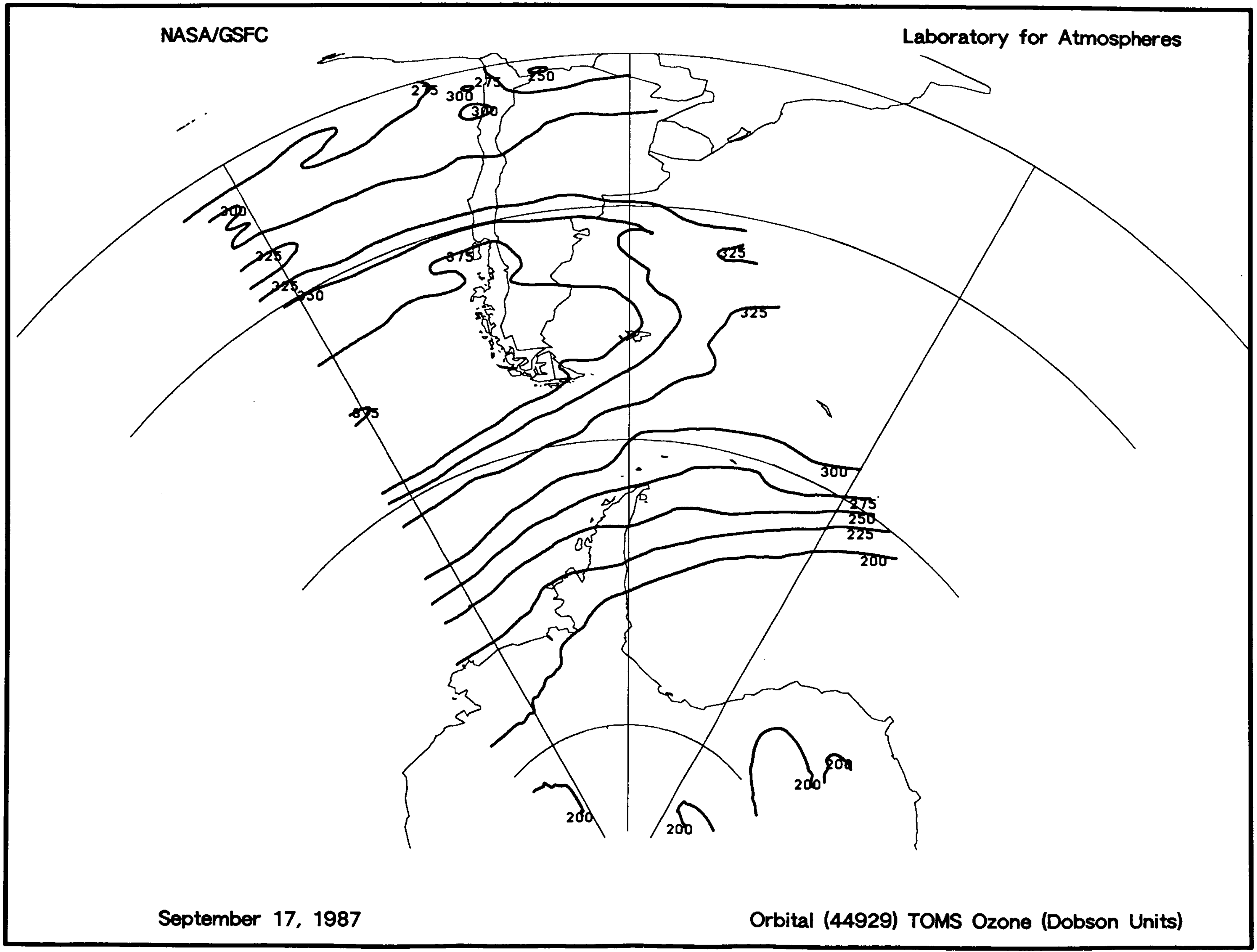
NASA/GSFC
Laboratory for Atmospheres
September 17, 1987
Orbital (44929) TOMS Ozone (Dobson Units)

NASA/GSFC

Laboratory for Atmospheres

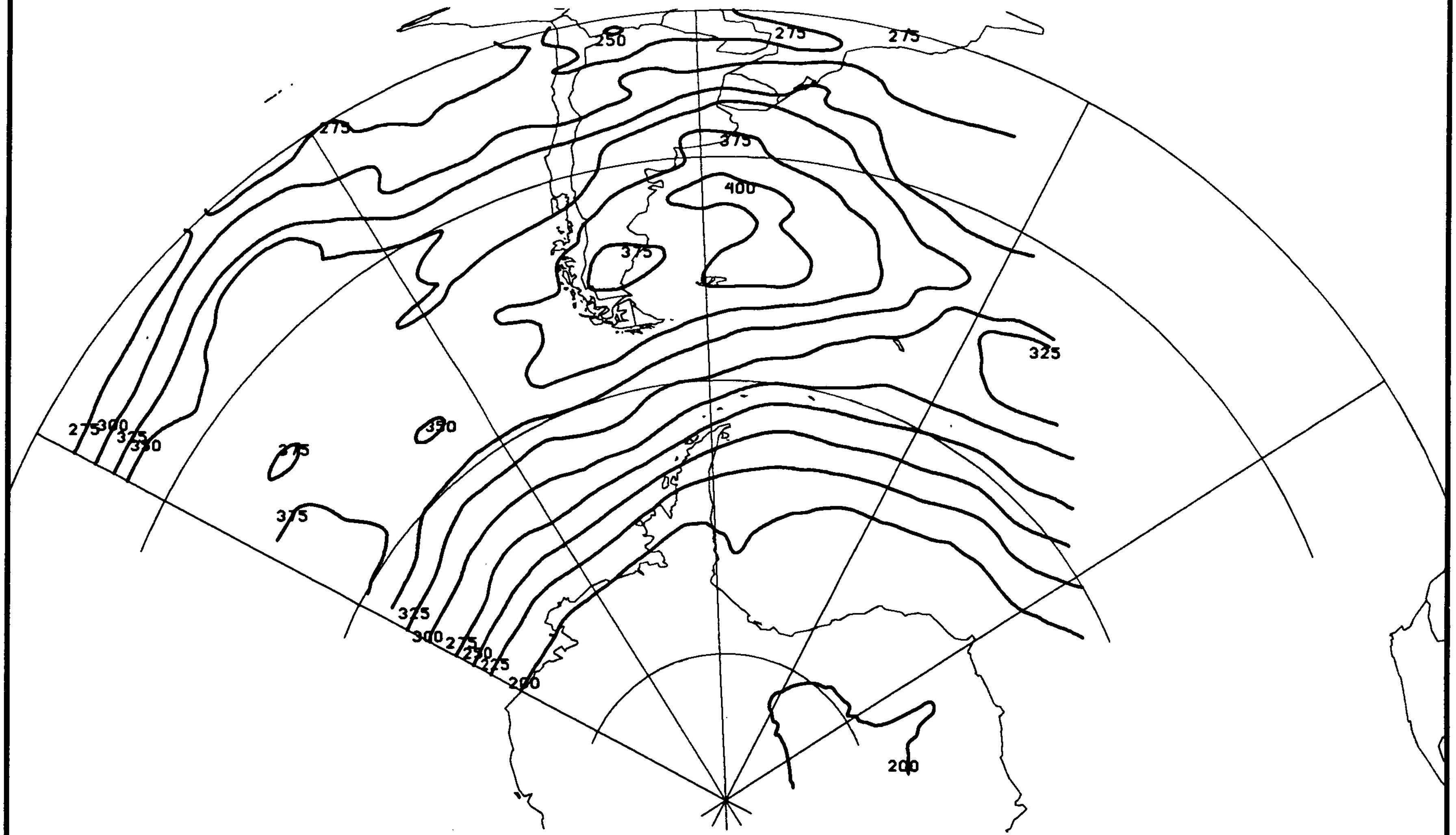


September 18, 1987

Orbital (44942–4) TOMS Ozone (Dobson Units)

NASA/GSFC

Laboratory for Atmospheres

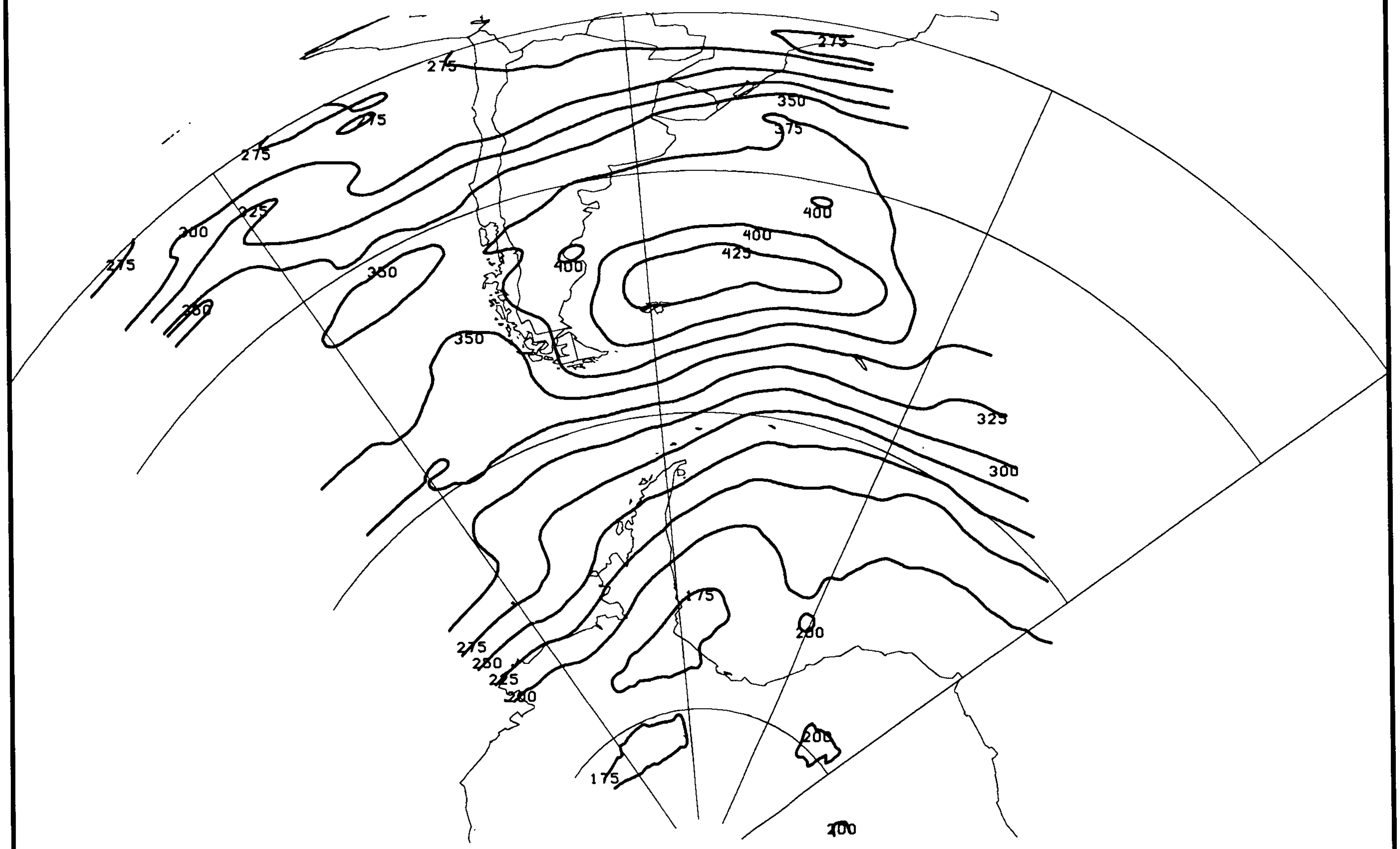


September 19, 1987

Orbital (44956-7) TOMS Ozone (Dobson Units)

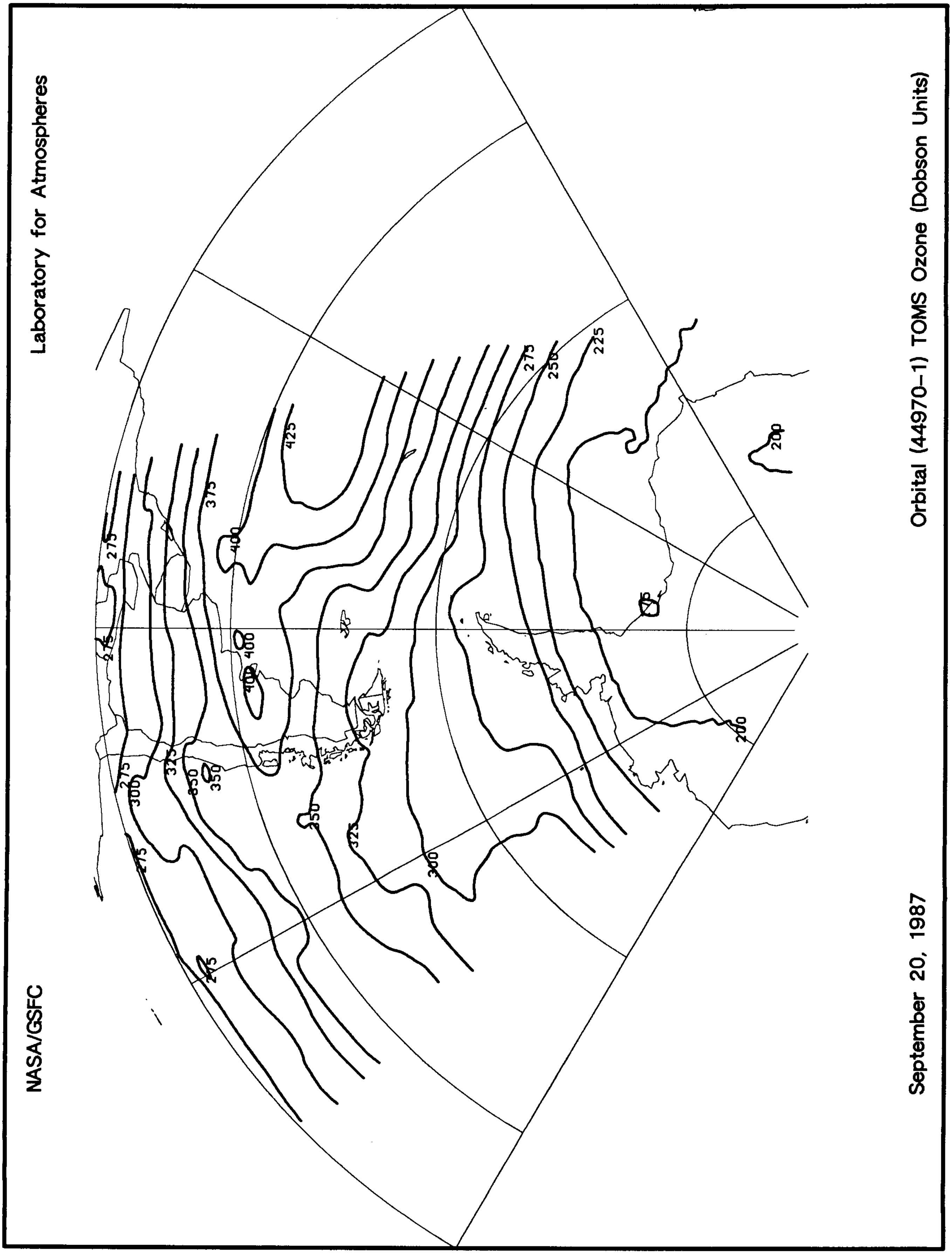
Laboratory for Atmospheres
NASA/GSFC
Orbital (44970-1) TOMS Ozone (Dobson Units)
September 20, 1987

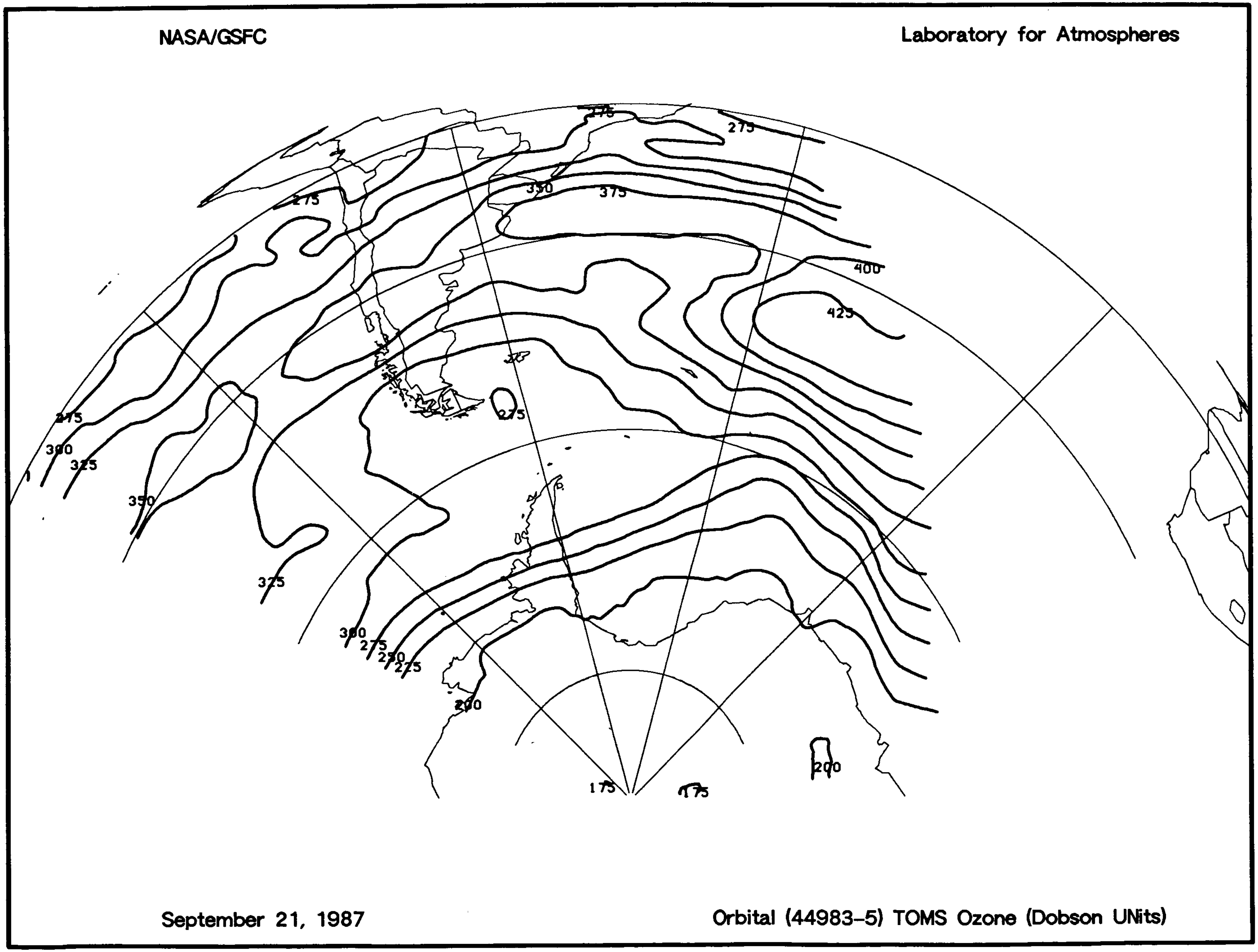
NASA/GSFC
Laboratory for Atmospheres
275
375
350
400
425
300
325
275
250
225
200
175
September 21, 1987
Orbital (44983-5) TOMS Ozone (Dobson UNits)

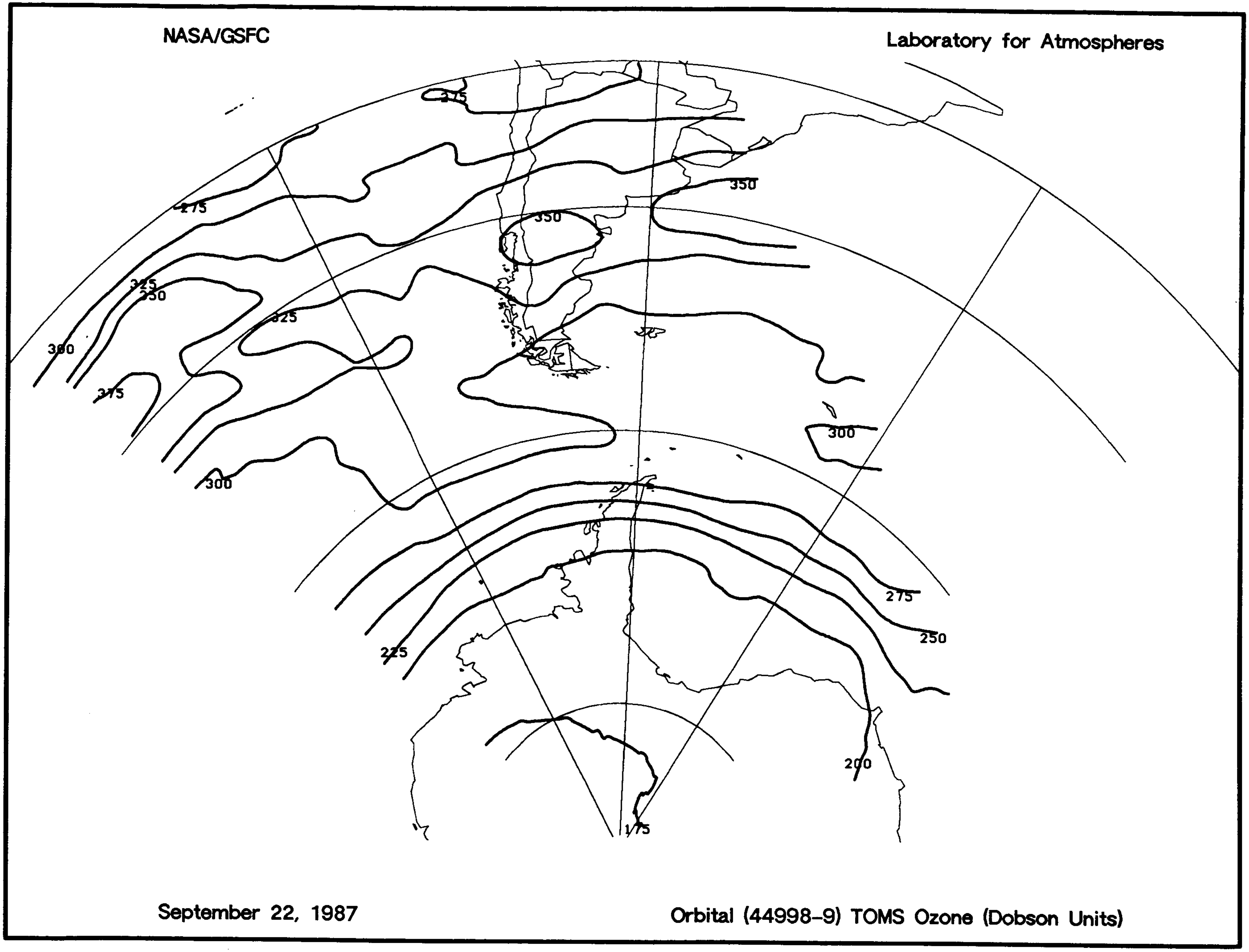
NASA/GSFC
Laboratory for Atmospheres
375
275
350
350
325
250
325
300
375
300
300
275
250
225
200
175
September 22, 1987
Orbital (44998-9) TOMS Ozone (Dobson Units)

NASA/GSFC

Laboratory for Atmospheres

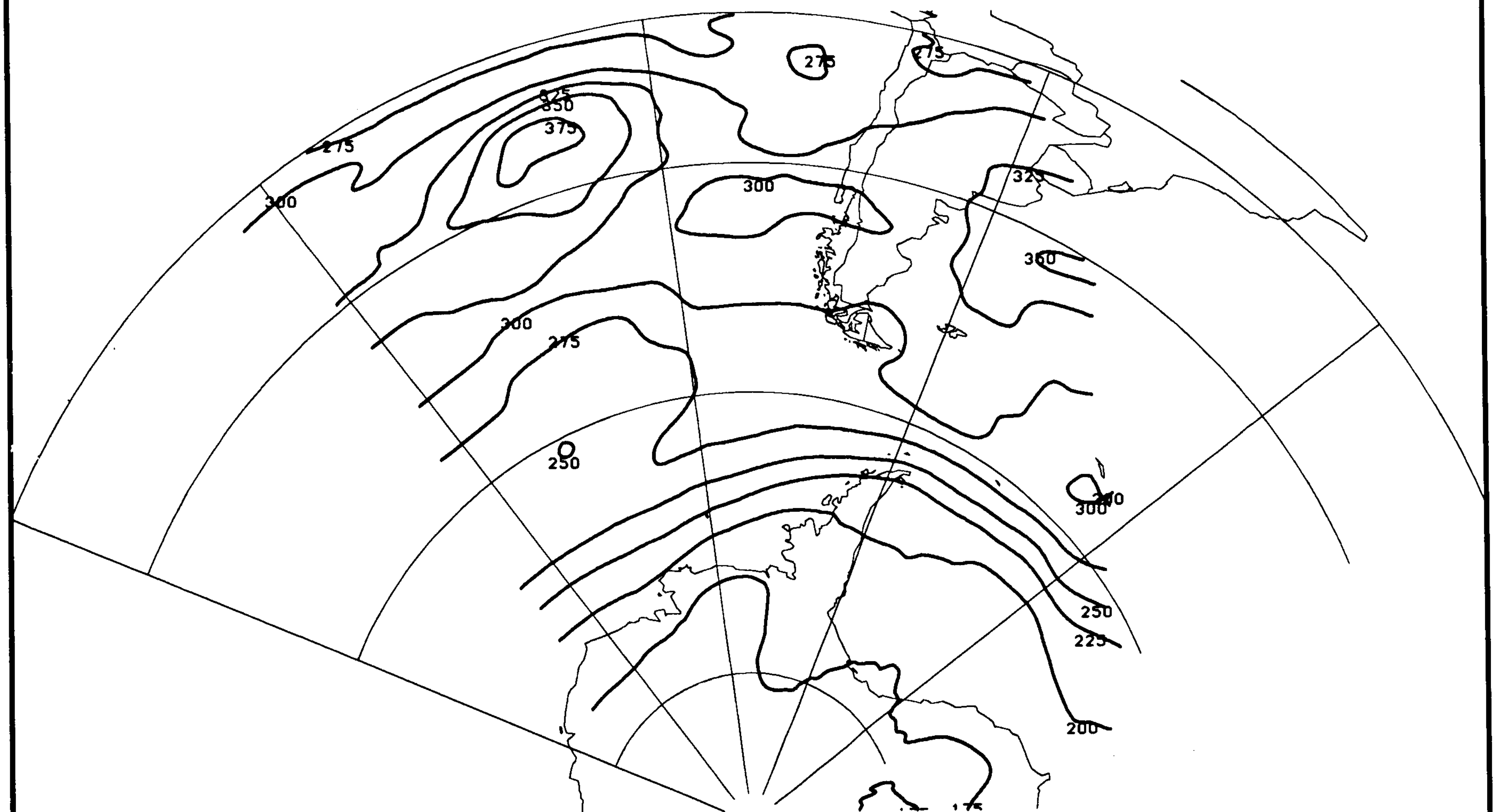


September 23, 1987

Orbital (45012-3) TOMS Ozone (Dobson Units)

NASA/GSFC

Laboratory for Atmospheres

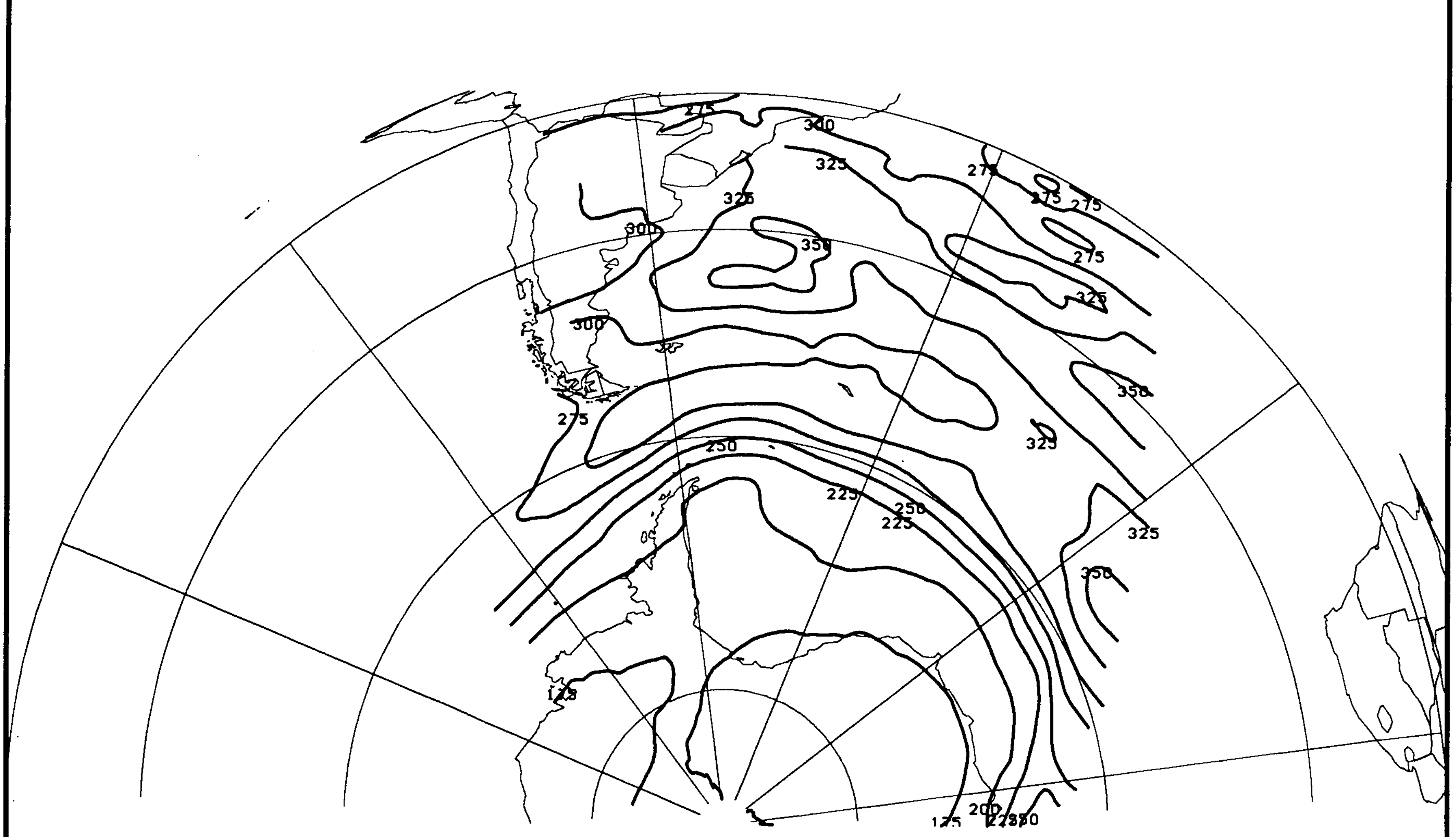


September 24, 1987

Orbital (45024-6) TOMS Ozone (Dobson UNits)

NASA/GSFC

Laboratory for Atmospheres

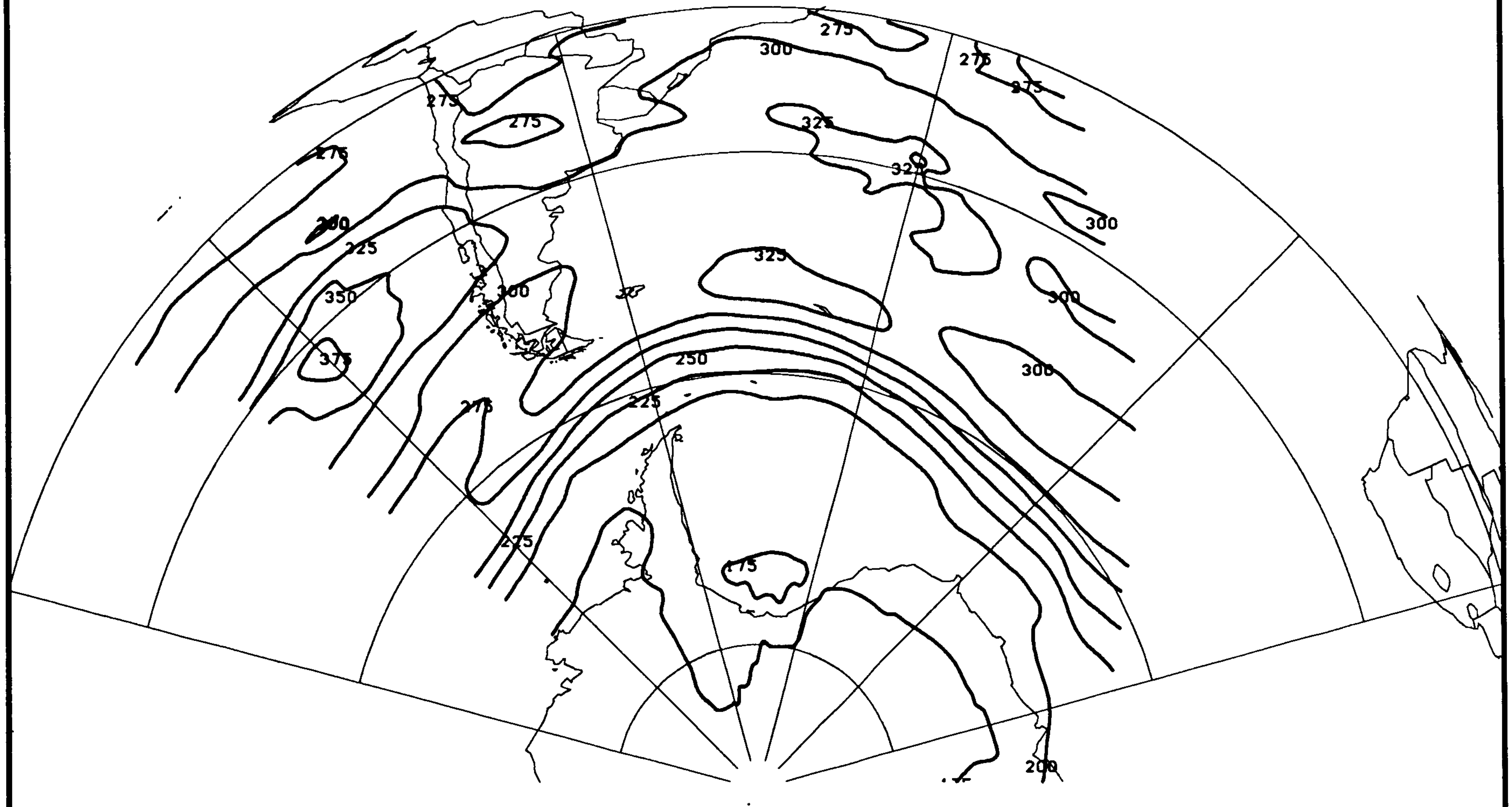


September 25, 1987

Orbital (45038-40) TOMS Ozone (Dobson Units)

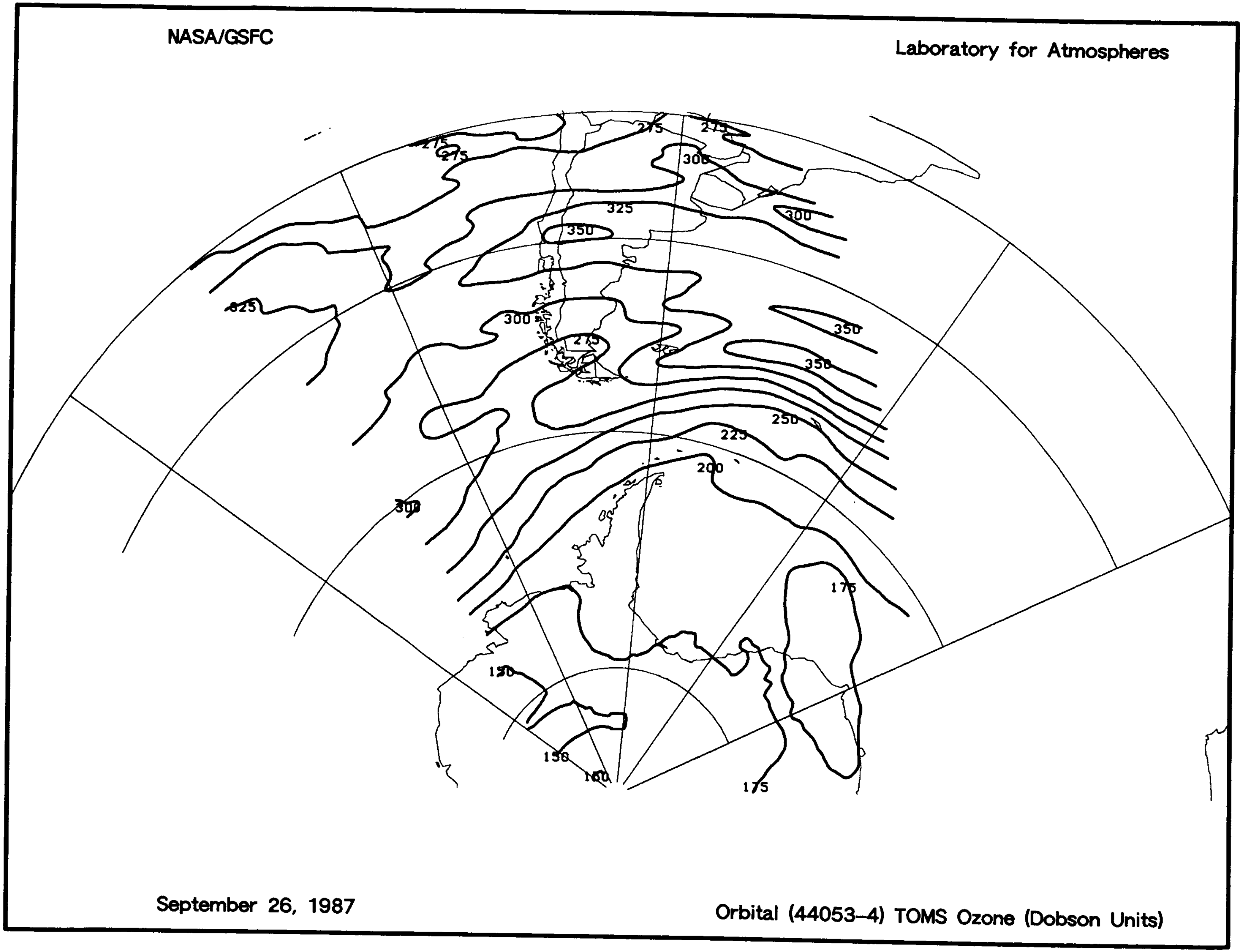
NASA/GSFC
Laboratory for Atmospheres
275
300
325
350
250
225
200
175
150
September 26, 1987
Orbital (44053-4) TOMS Ozone (Dobson Units)

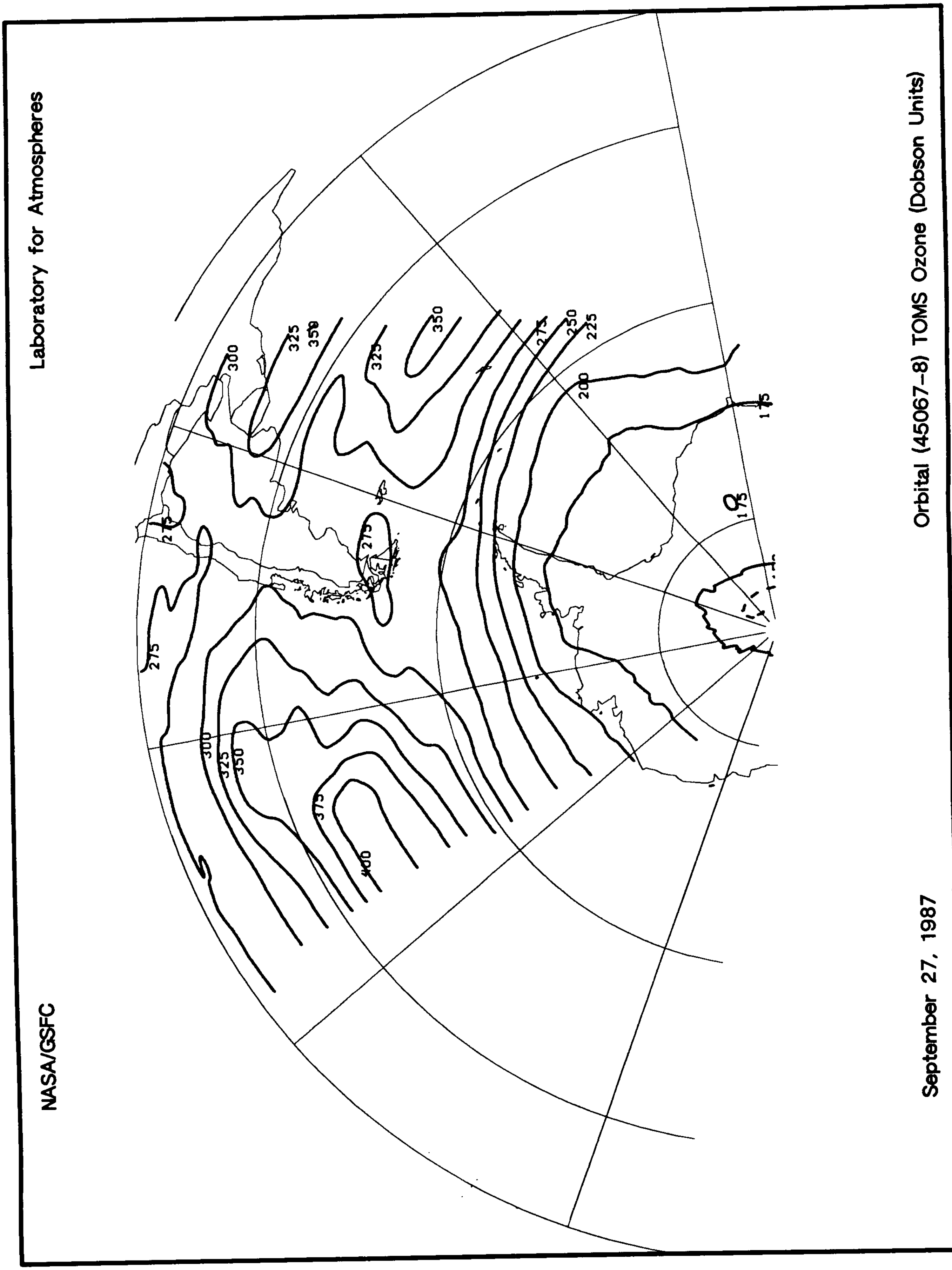

Laboratory for Atmospheres
NASA/GSFC
September 27, 1987
Orbital (45067-8) TOMS Ozone (Dobson Units)

NASA/GSFC

Laboratory for Atmospheres

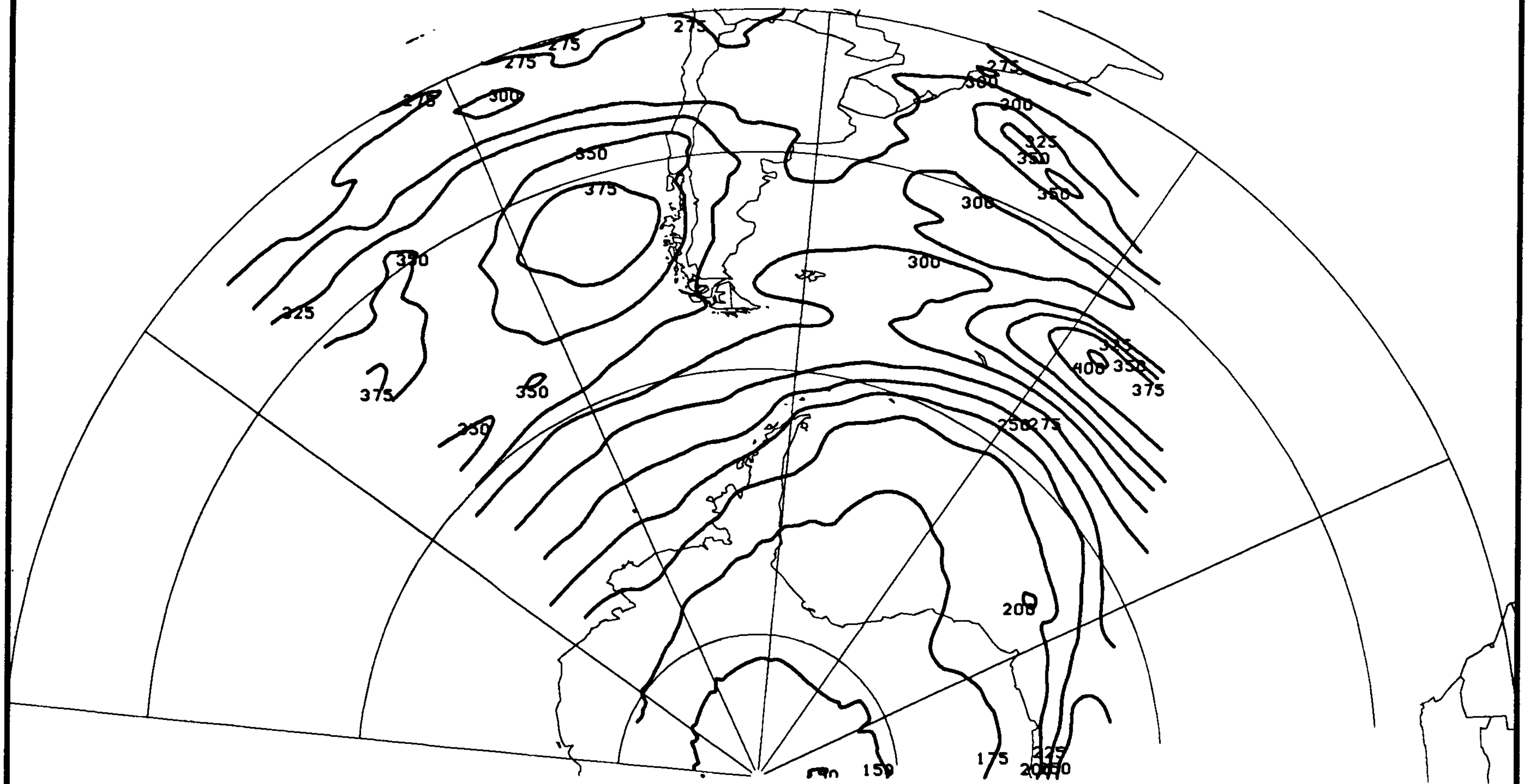


September 28, 1987

Orbital (45080-2) TOMS Ozone (Dobson Units)

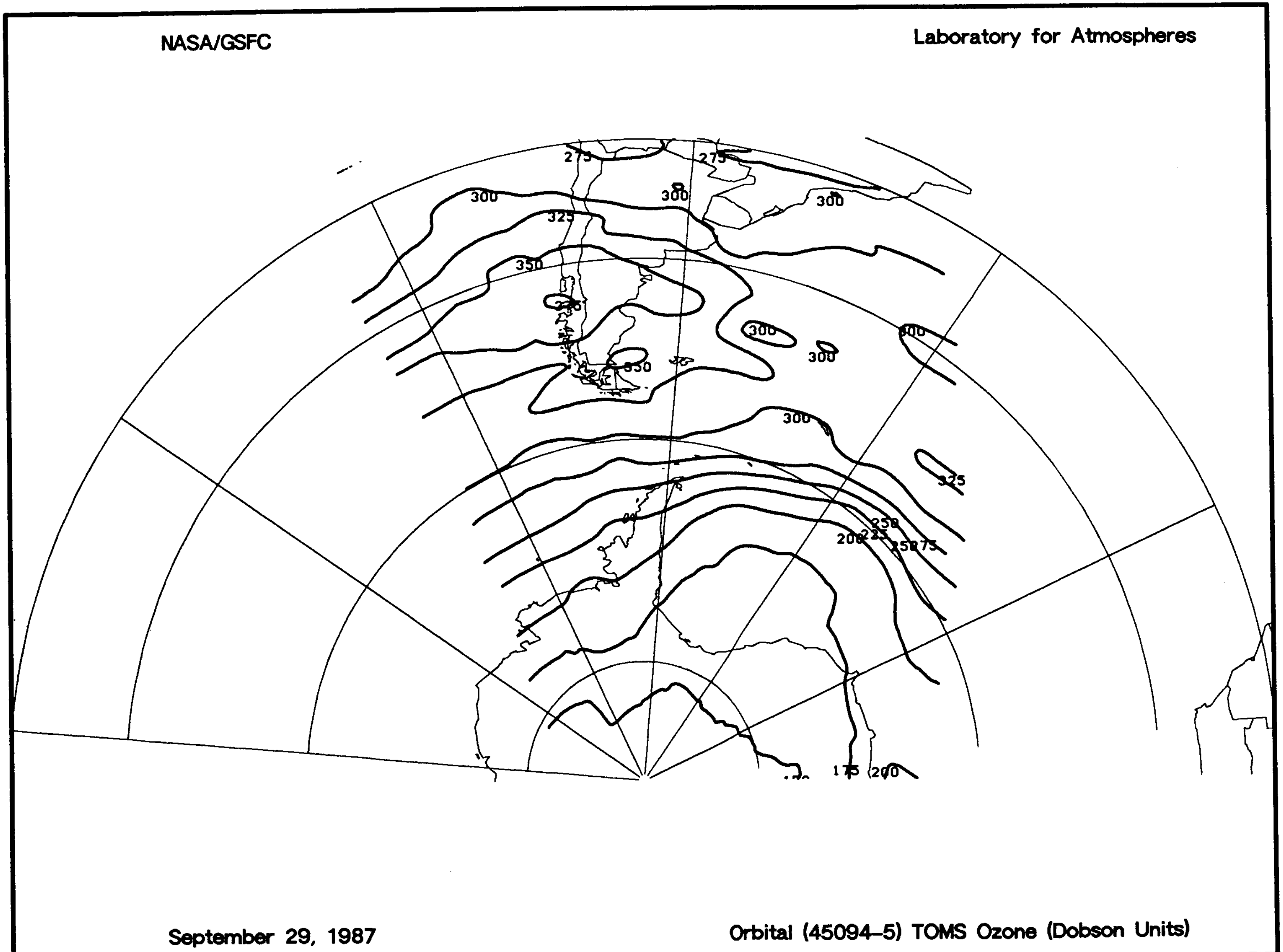
NASA/GSFC
Laboratory for Atmospheres
275
300
325
350
200
225
250
175
September 29, 1987
Orbital (45094-5) TOMS Ozone (Dobson Units)

## 3.5 Southern Hemispheric Polar Charts

A set of daily TOMS total ozone estimates for the southern hemisphere, over the period August 1 through November 30, 1987, are presented here. The daily data are resolved on a uniform 2° latitude by 5° longitude grid for each day, and displayed using a south-polar orthographic projection. The advantage of this projection is that emphasis is placed over precisely those high-latitude regions of interest to the Antarctic experiment.

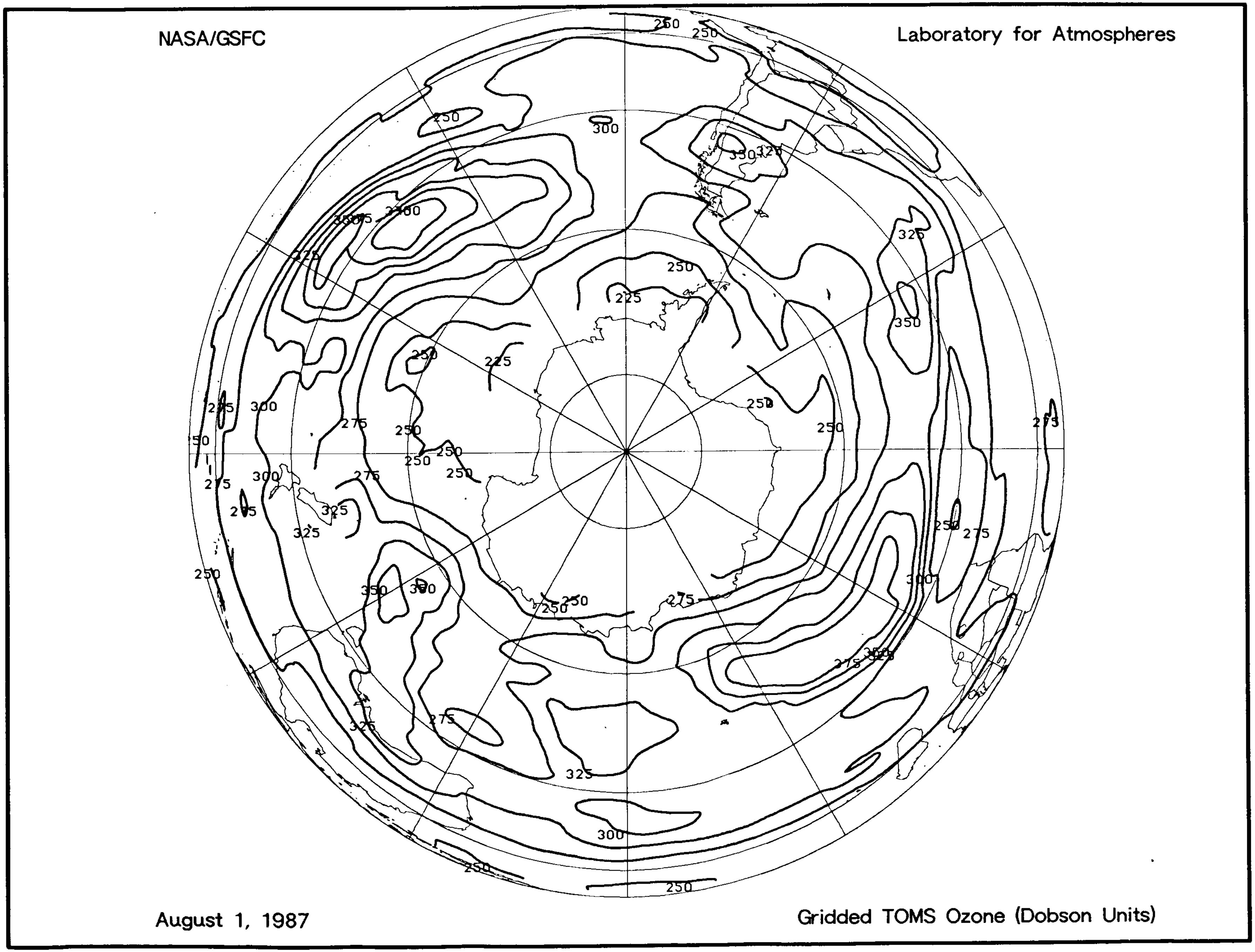
NASA/GSFC
Laboratory for Atmospheres
August 1, 1987
Gridded TOMS Ozone (Dobson Units)

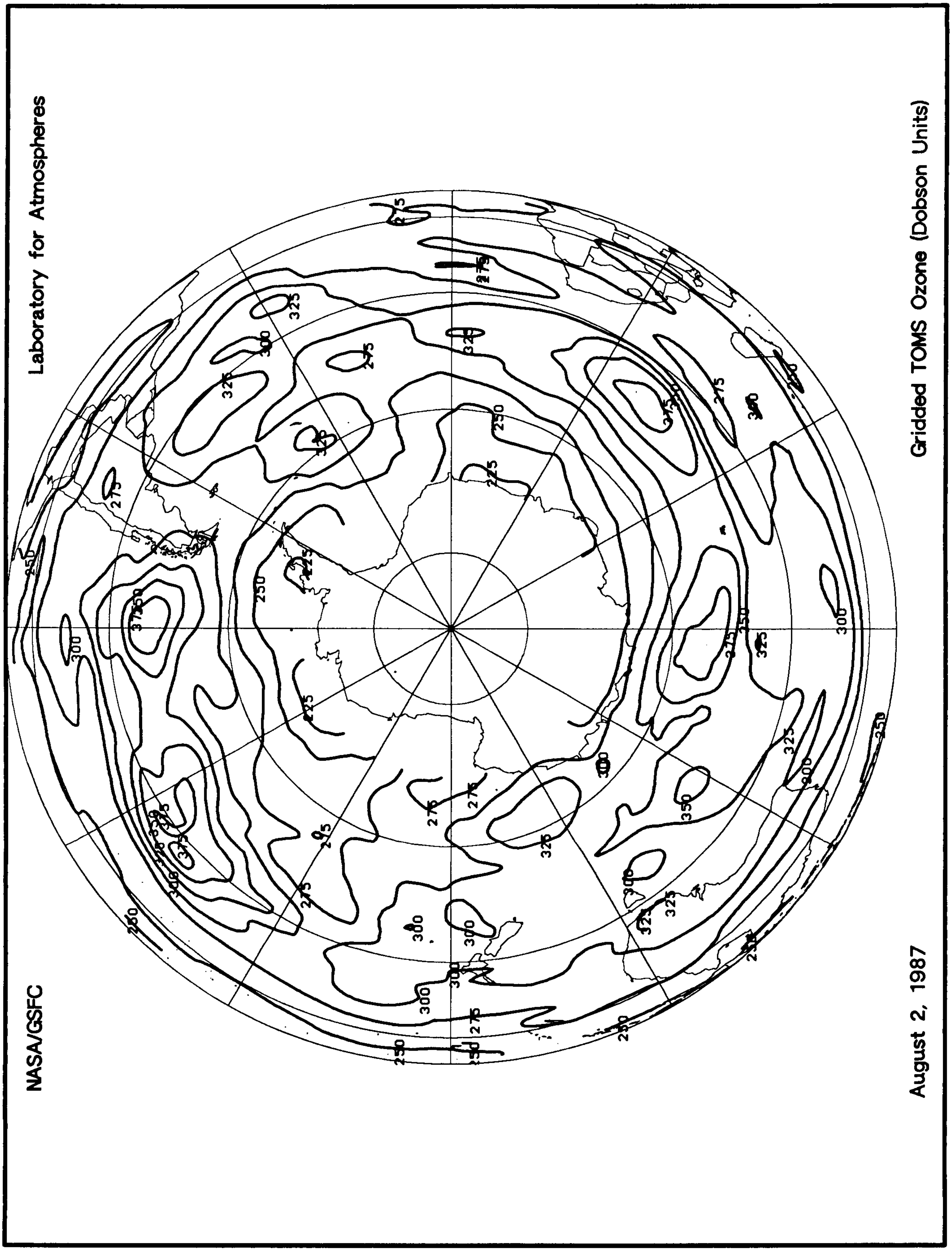
Laboratory for Atmospheres
NASA/GSFC
Gridded TOMS Ozone (Dobson Units)
August 2, 1987

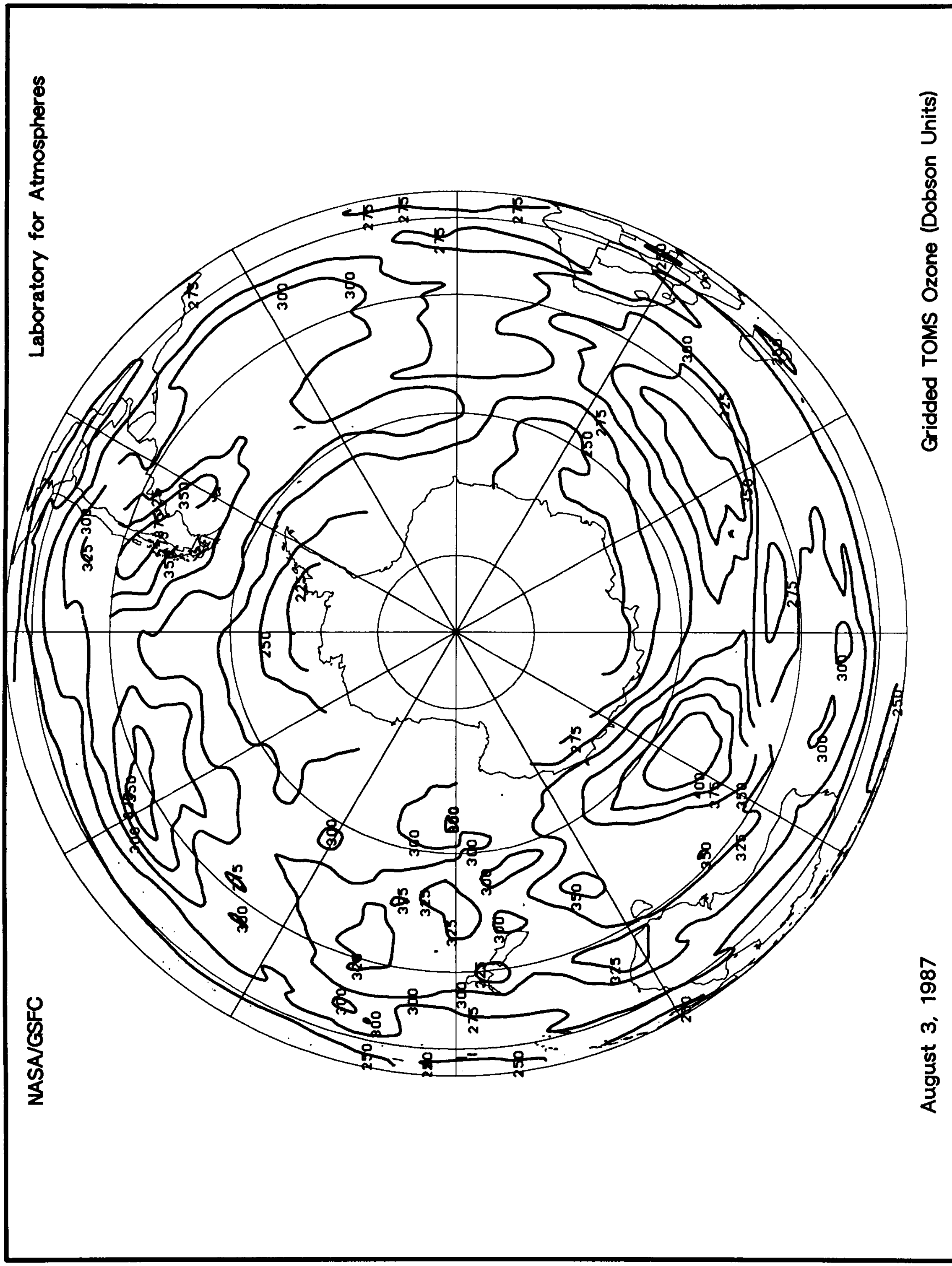
Laboratory for Atmospheres
NASA/GSFC
Gridded TOMS Ozone (Dobson Units)
August 3, 1987



C-2

NASA/GSFC

Laboratory for Atmospheres

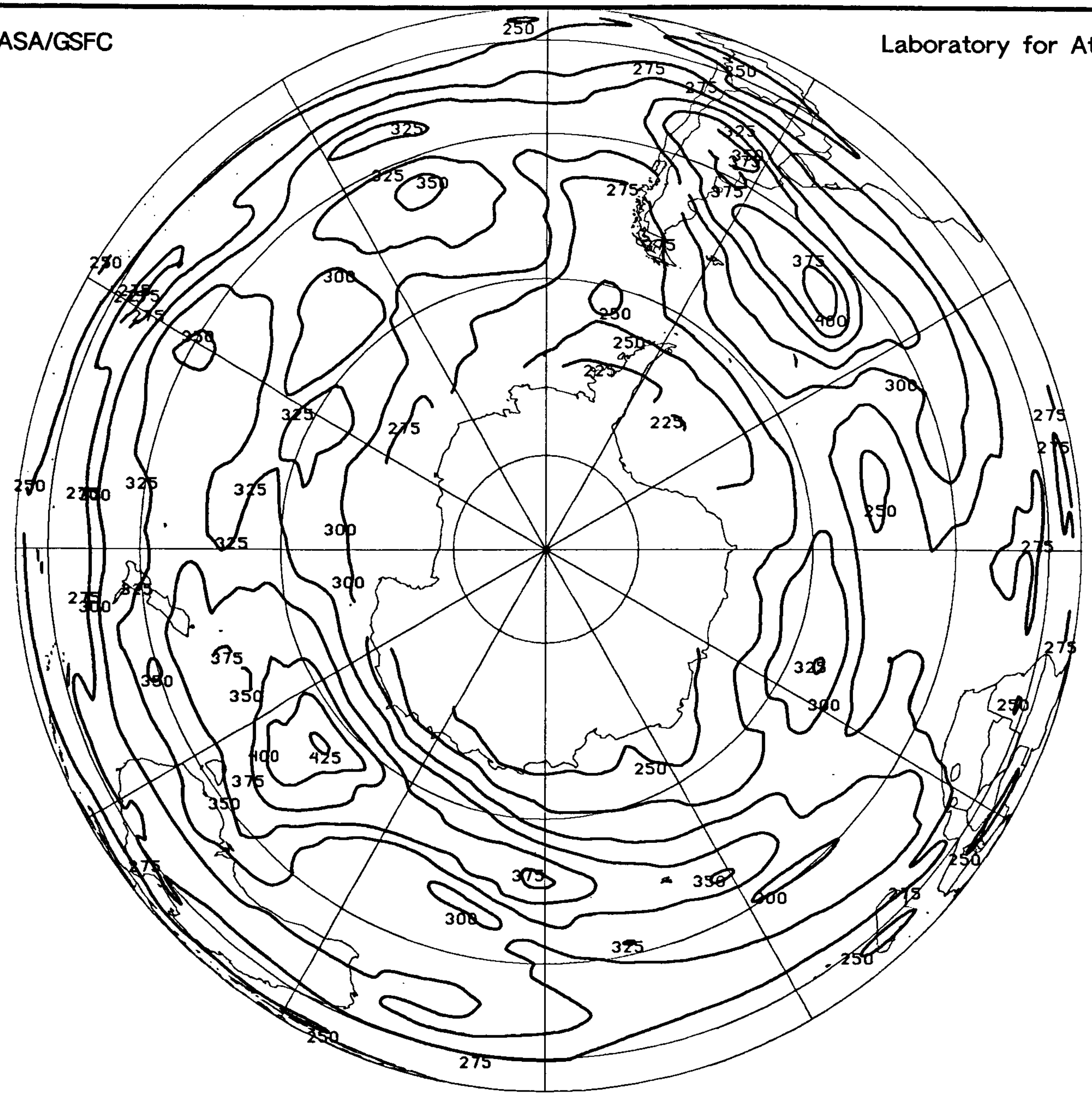

August 4, 1987

Gridded TOMS Ozone (Dobson Units)

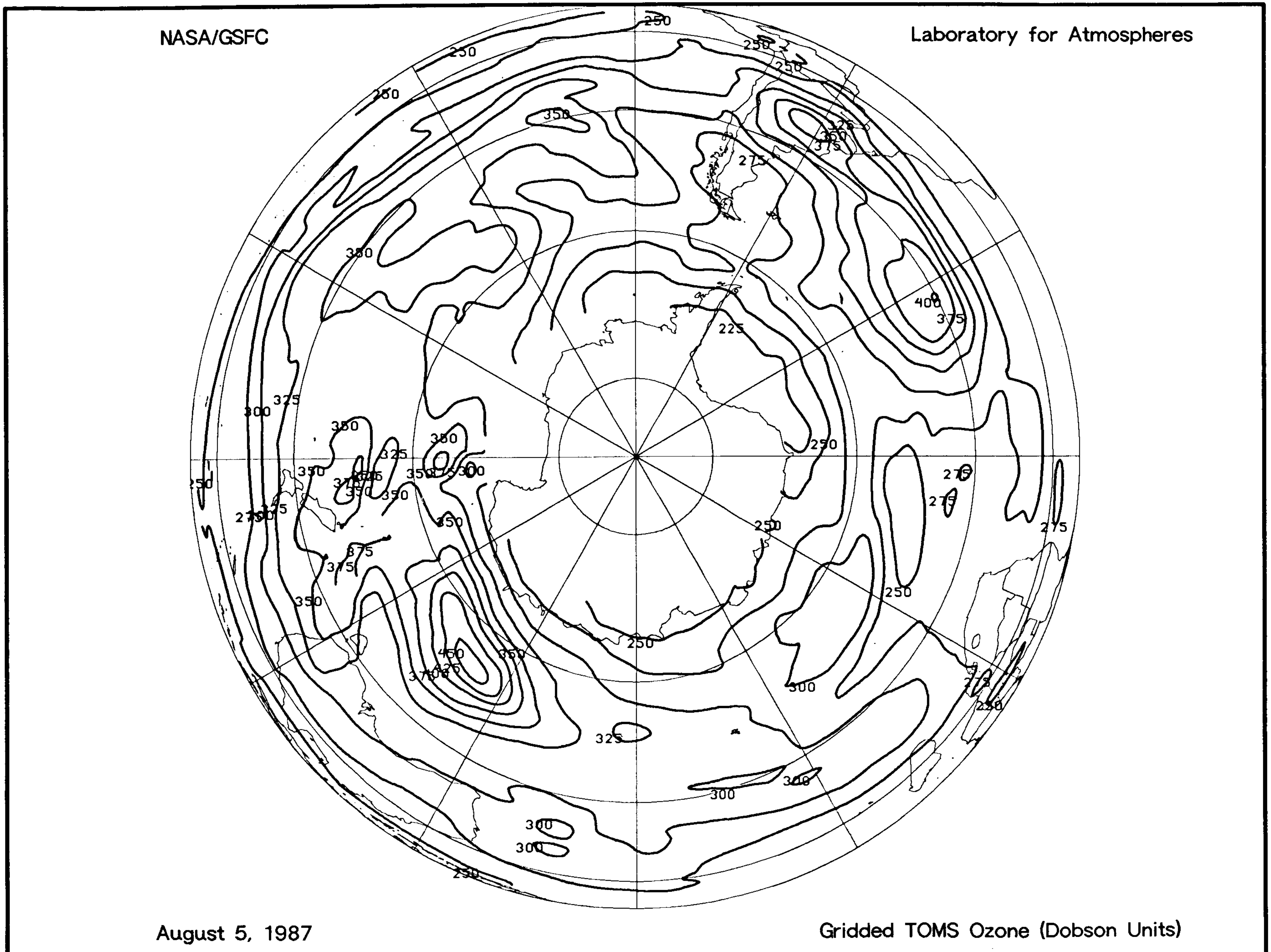
NASA/GSFC
Laboratory for Atmospheres
August 5, 1987
Gridded TOMS Ozone (Dobson Units)

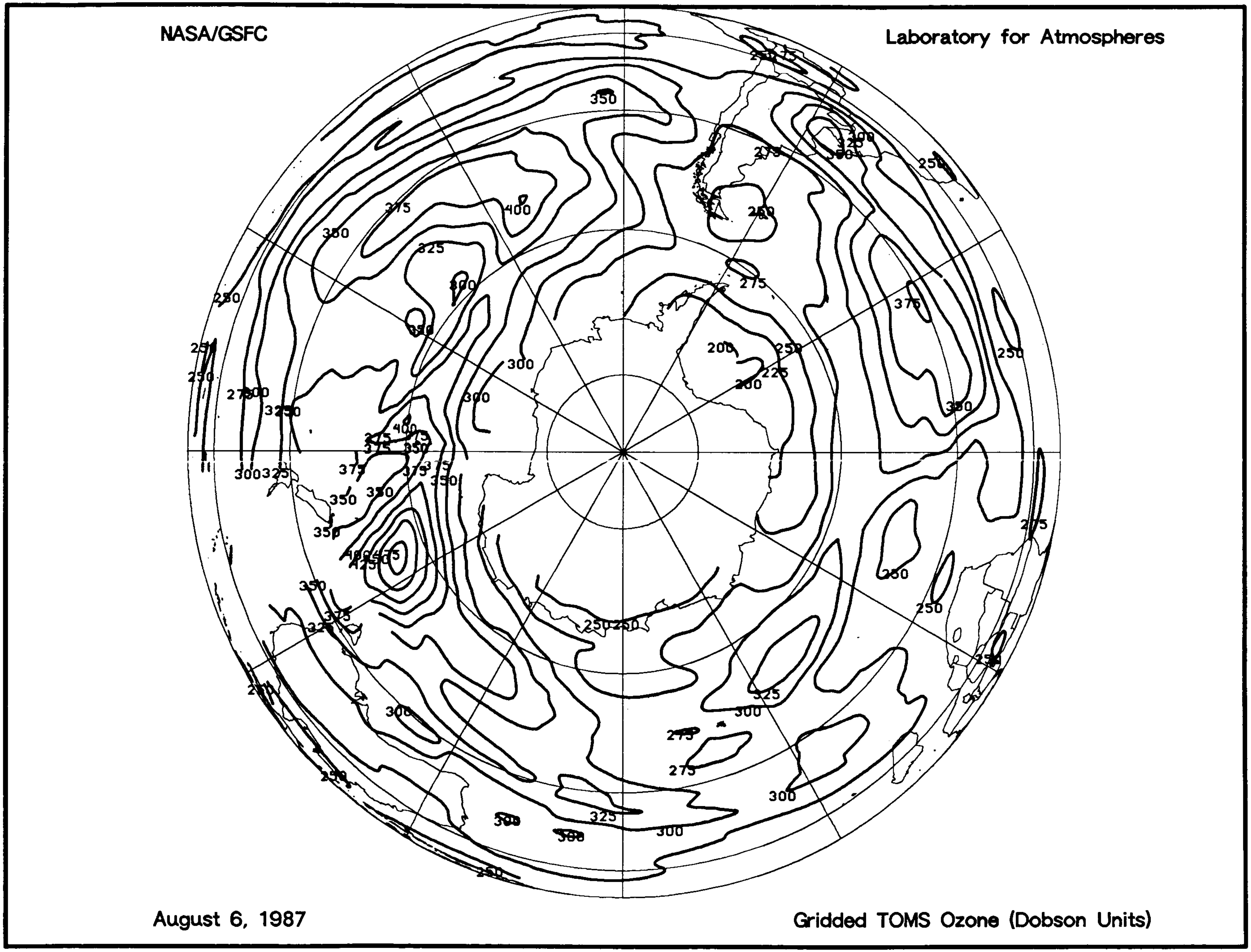
NASA/GSFC
Laboratory for Atmospheres
August 6, 1987
Gridded TOMS Ozone (Dobson Units)

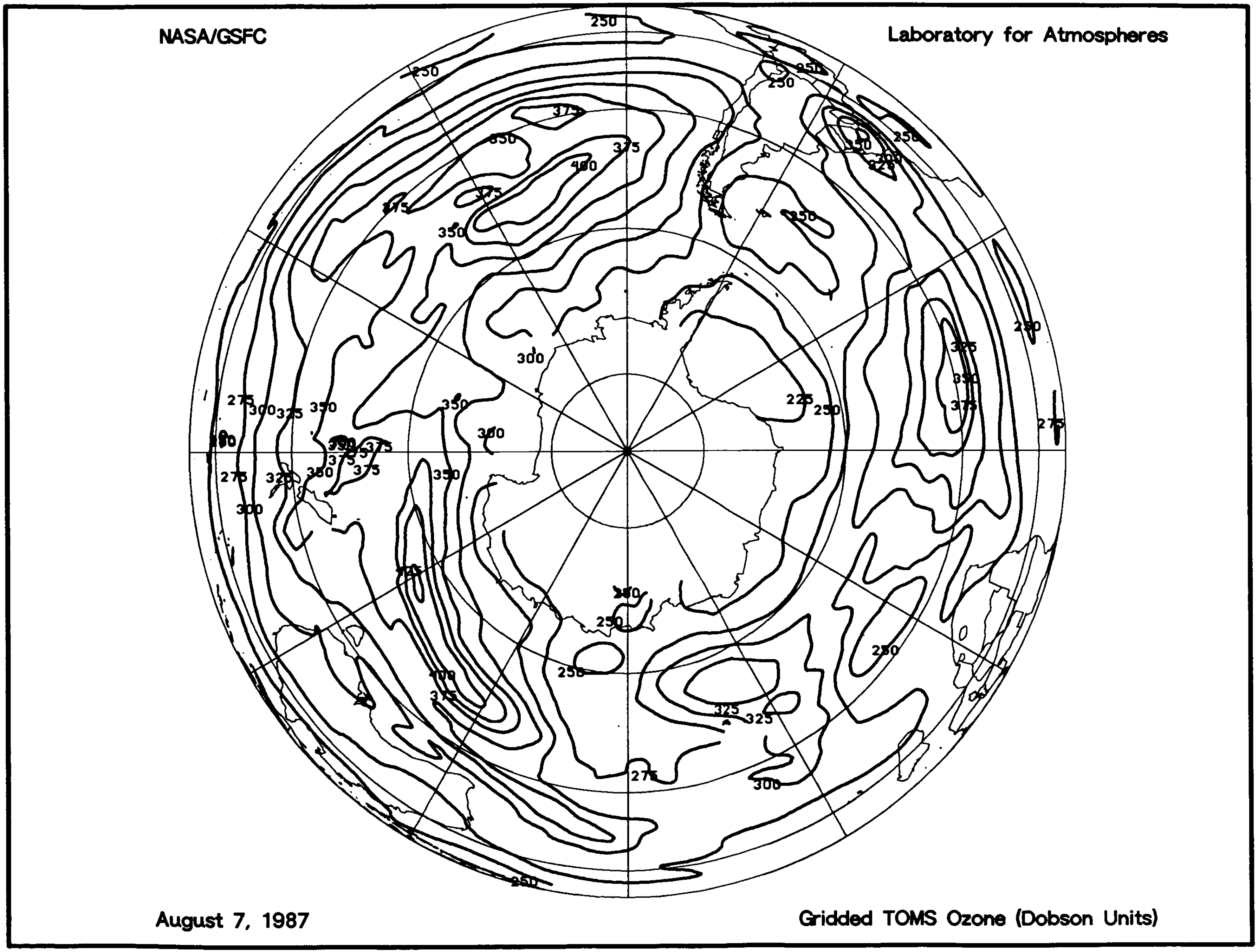
NASA/GSFC
Laboratory for Atmospheres
August 7, 1987
Gridded TOMS Ozone (Dobson Units)

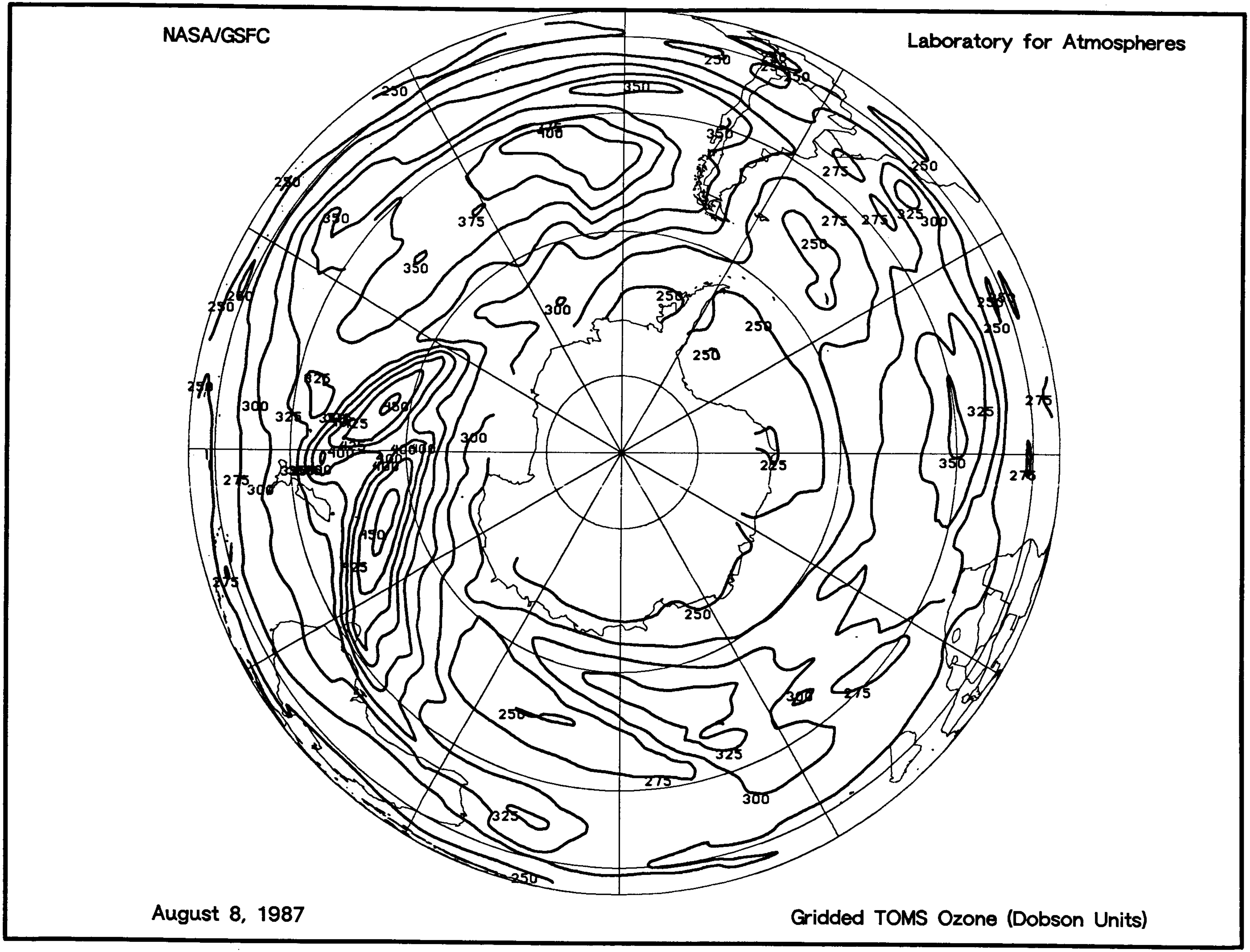
NASA/GSFC
Laboratory for Atmospheres
August 8, 1987
Gridded TOMS Ozone (Dobson Units)

NASA/GSFC

Laboratory for Atmospheres

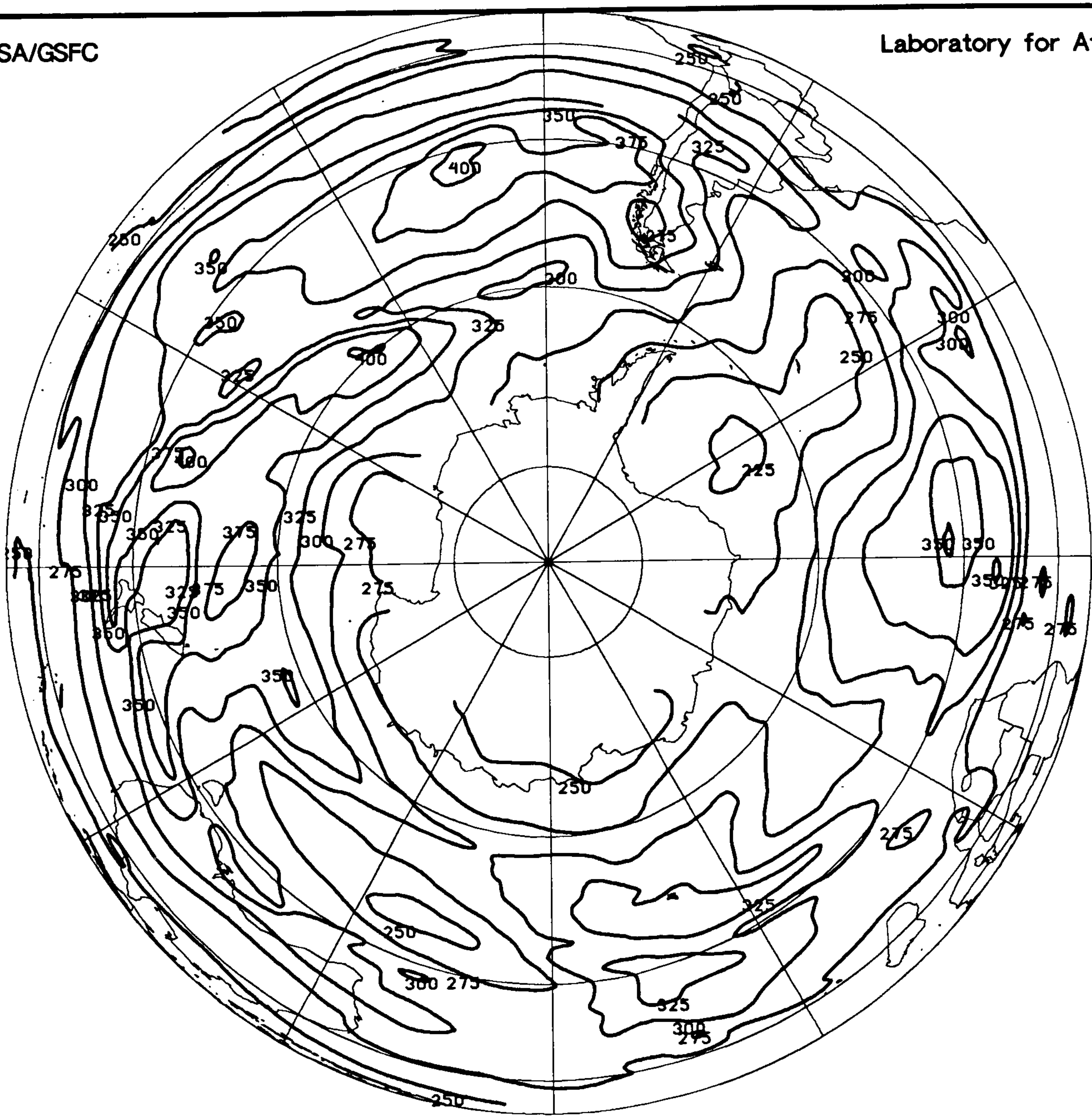


August 9, 1987

Gridded TOMS Ozone (Dobson Units)

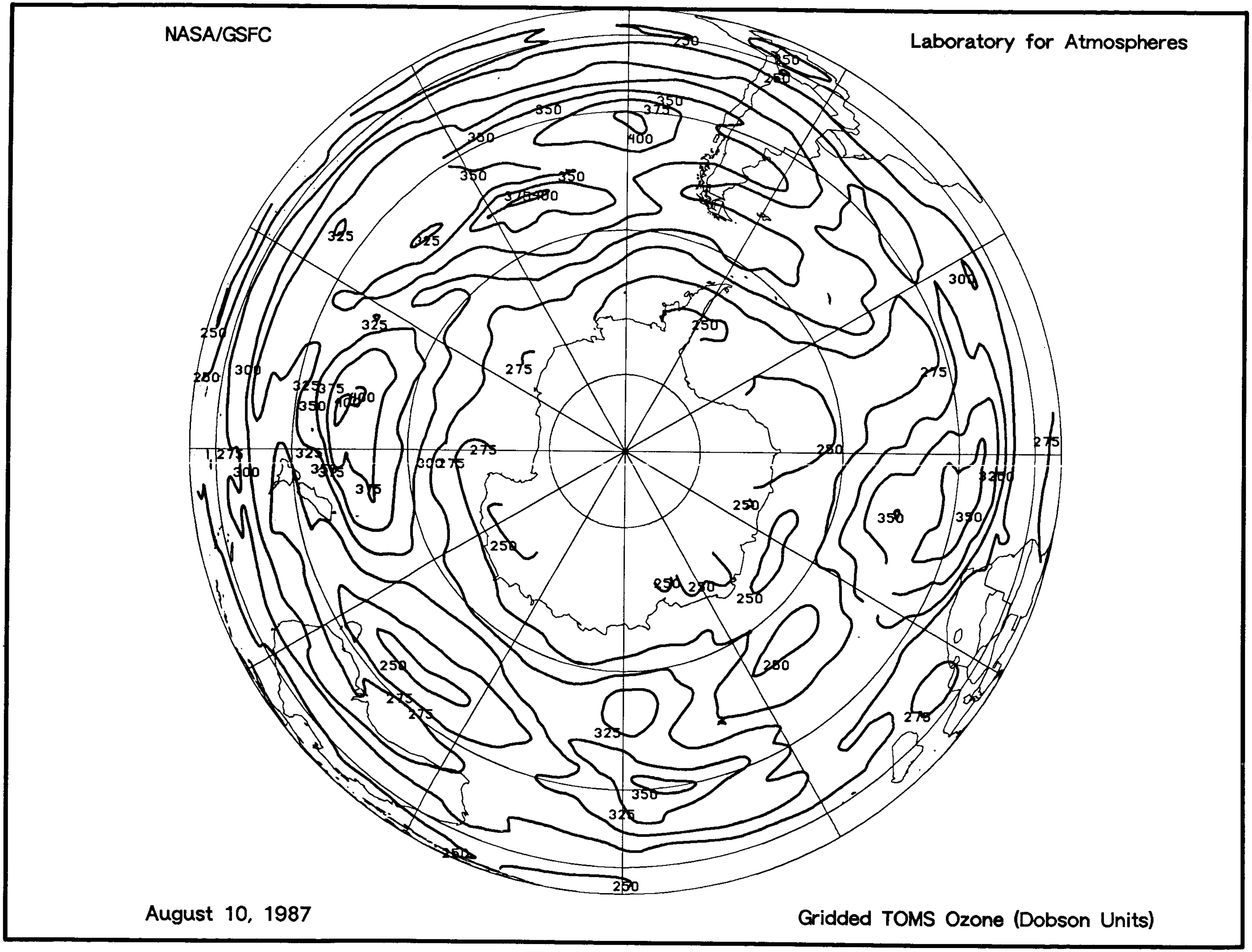
NASA/GSFC
Laboratory for Atmospheres
August 10, 1987
Gridded TOMS Ozone (Dobson Units)

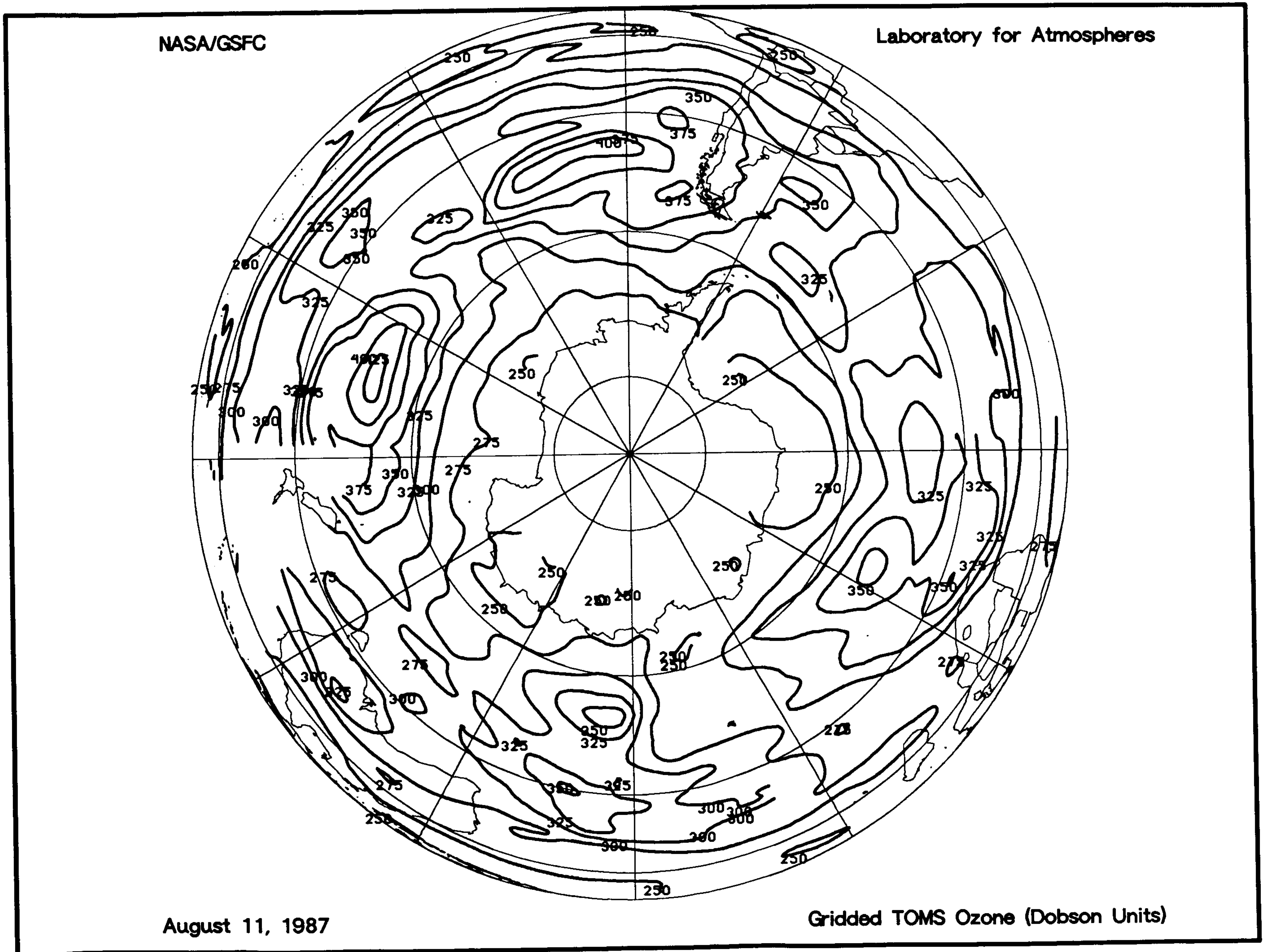
NASA/GSFC
Laboratory for Atmospheres
August 11, 1987
Gridded TOMS Ozone (Dobson Units)

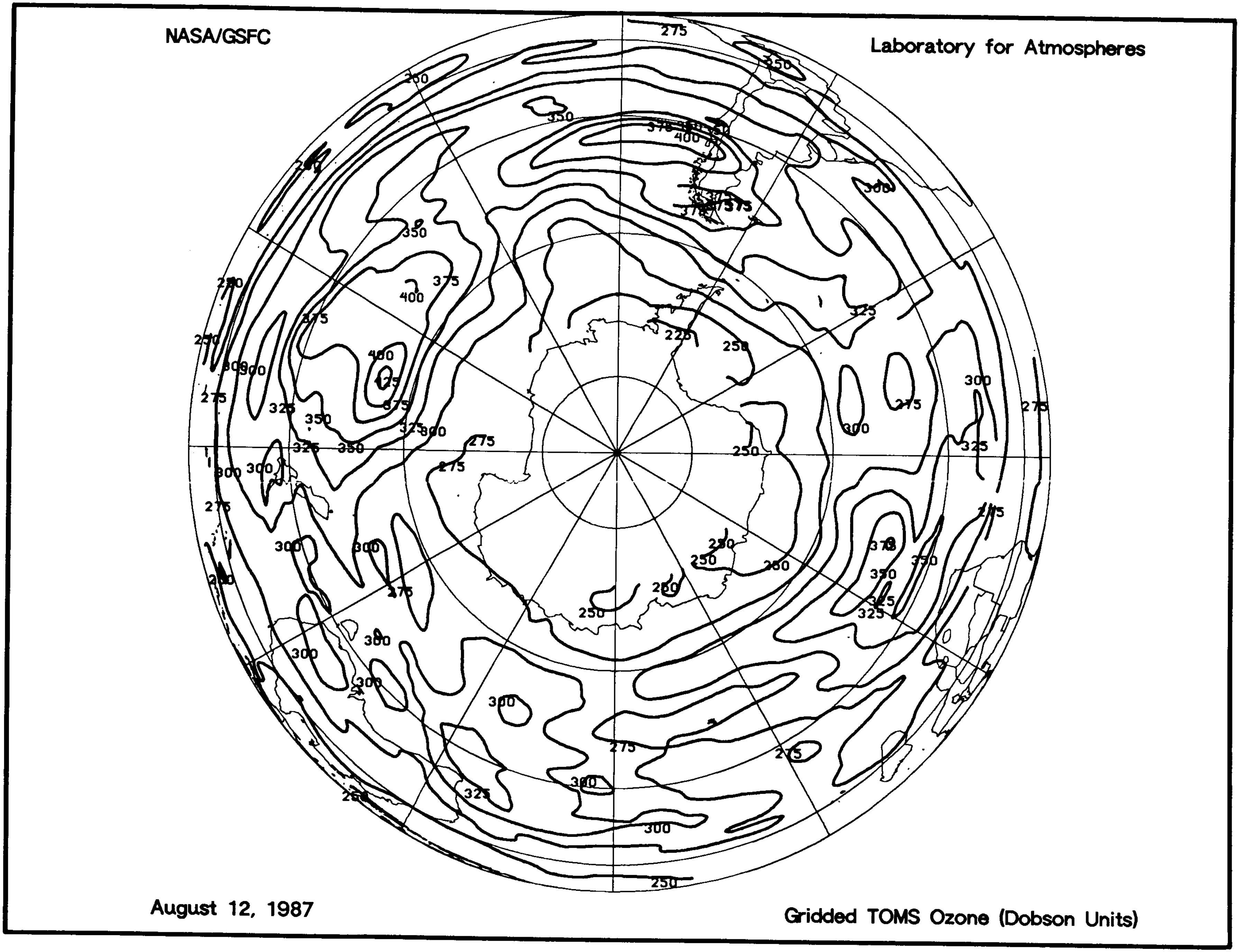
NASA/GSFC
Laboratory for Atmospheres
August 12, 1987
Gridded TOMS Ozone (Dobson Units)

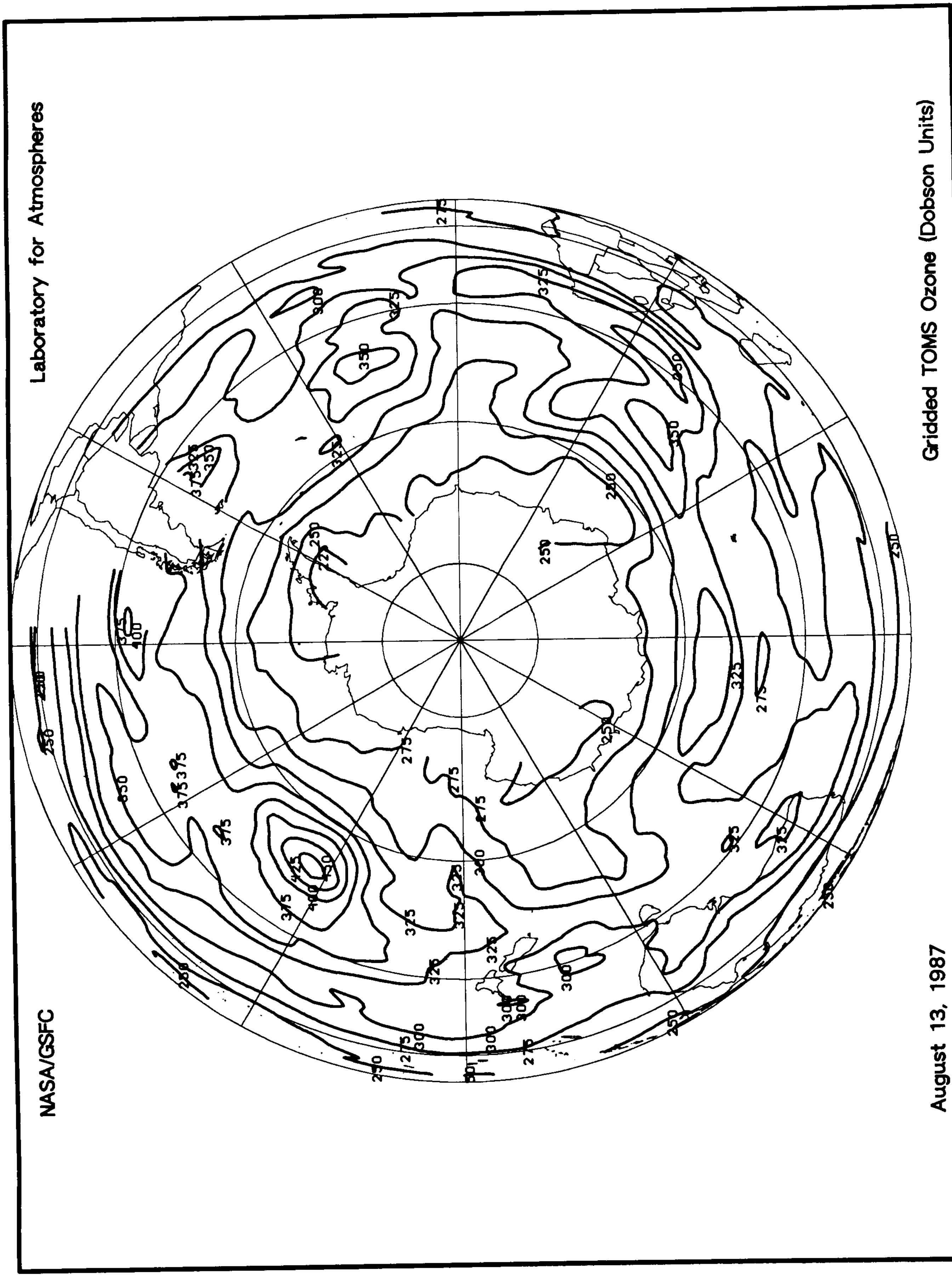
Laboratory for Atmospheres
Gridded TOMS Ozone (Dobson Units)
NASA/GSFC
August 13, 1987

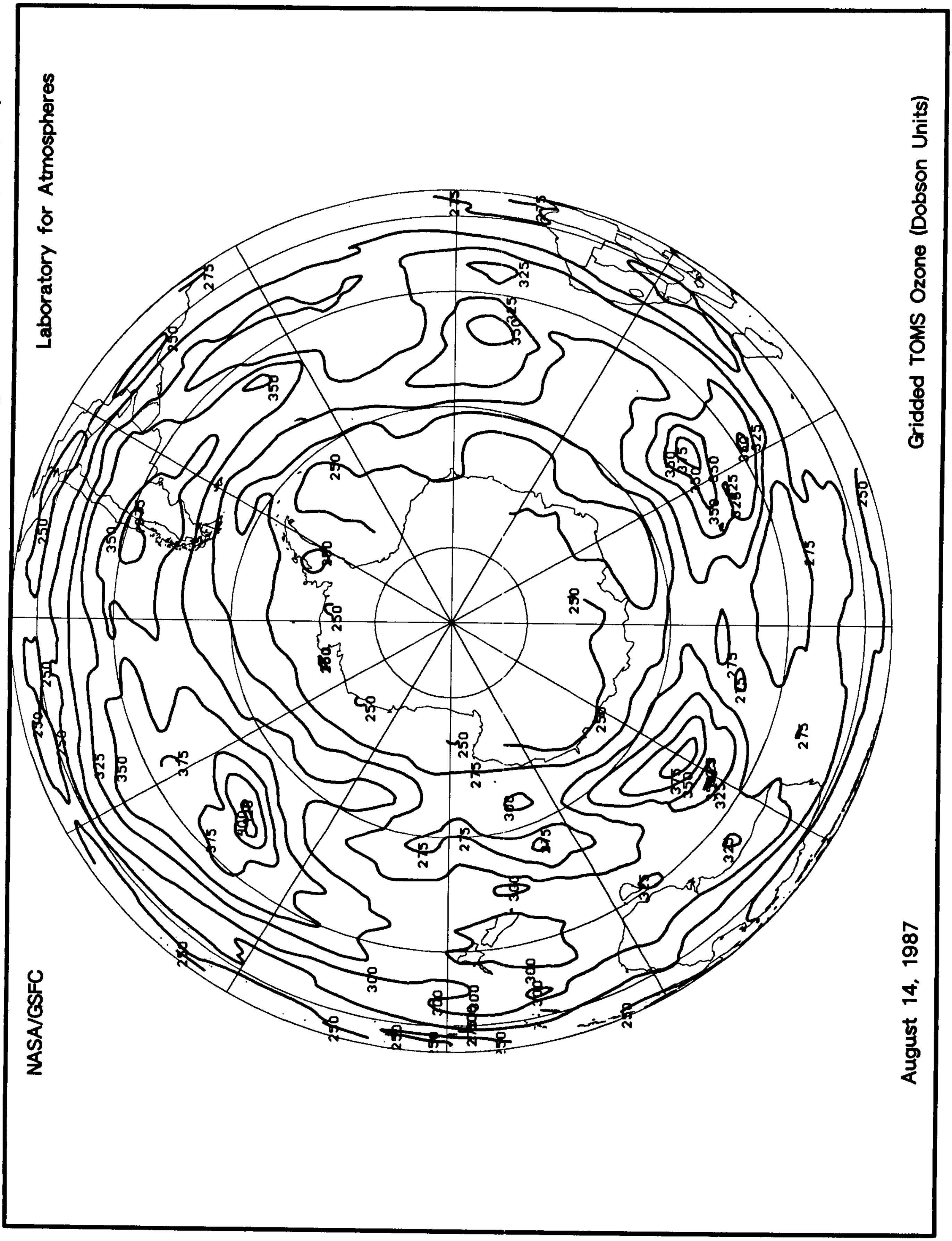
Laboratory for Atmospheres
NASA/GSFC
August 14, 1987
Gridded TOMS Ozone (Dobson Units)

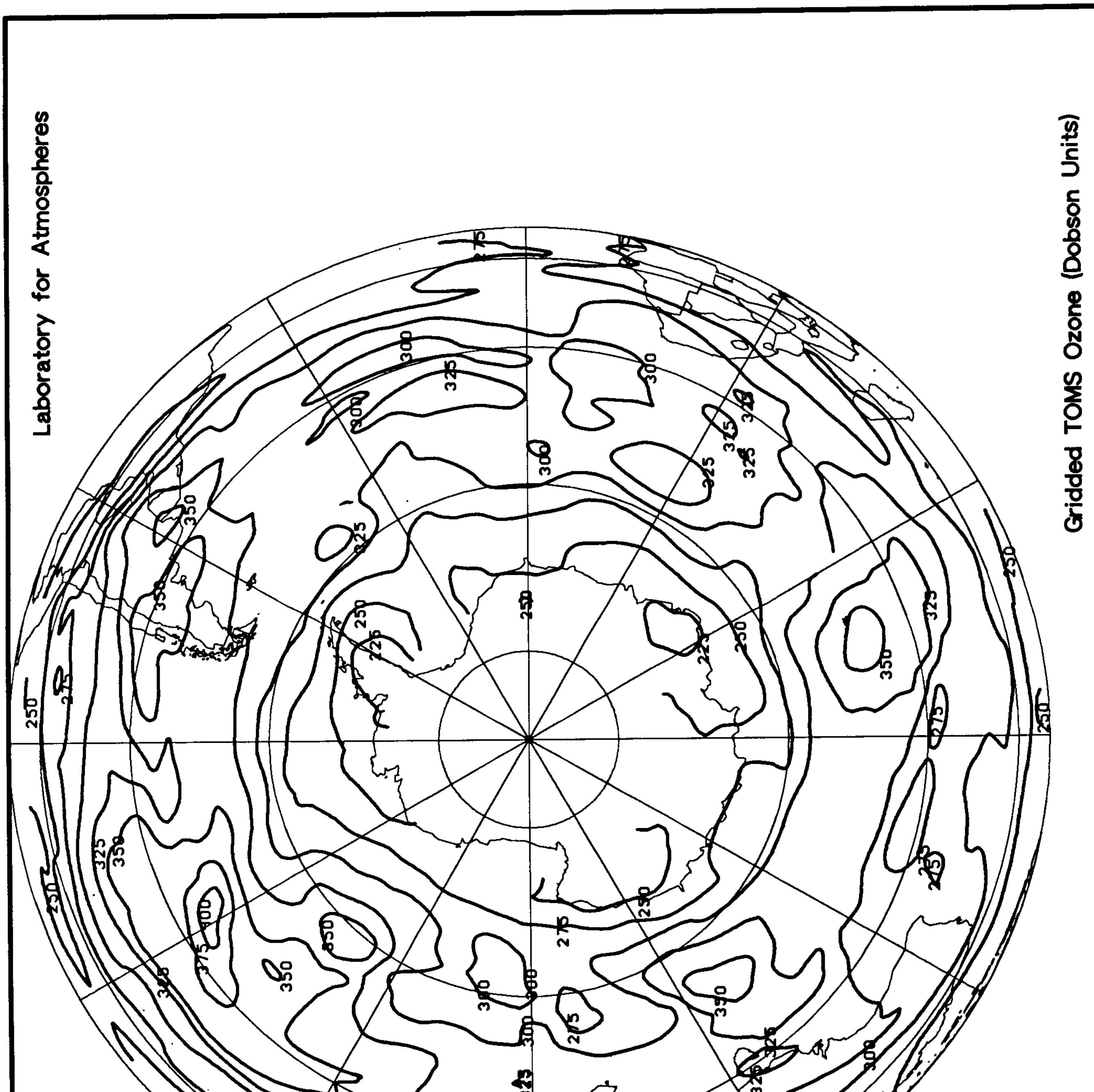
NASA/GSFC
Laboratory for Atmospheres
August 15, 1987
Gridded TOMS Ozone (Dobson Units)

NASA/GSFC

Laboratory for Atmospheres

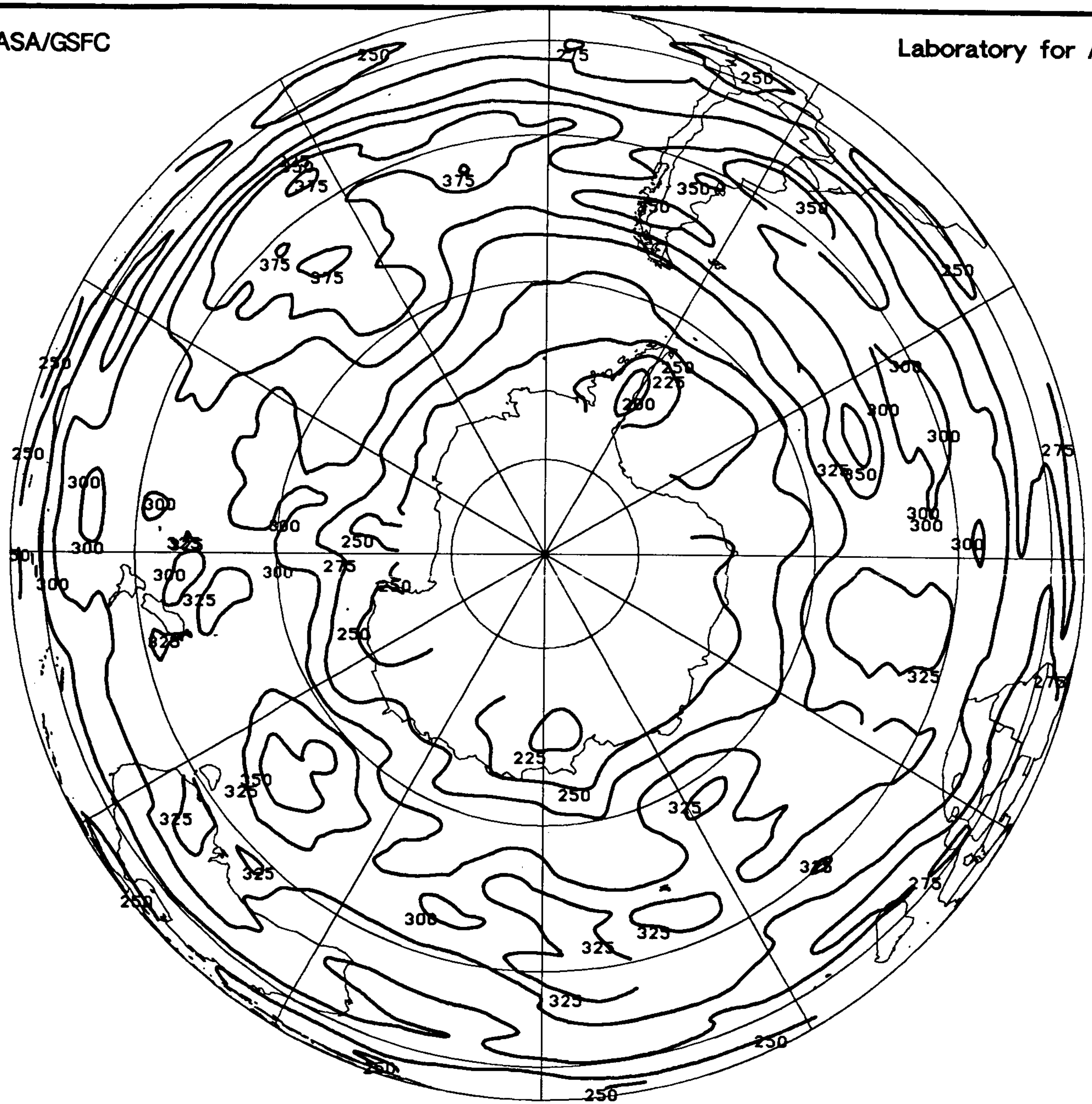


August 16, 1987

Gridded TOMS Ozone (Dobson Units)

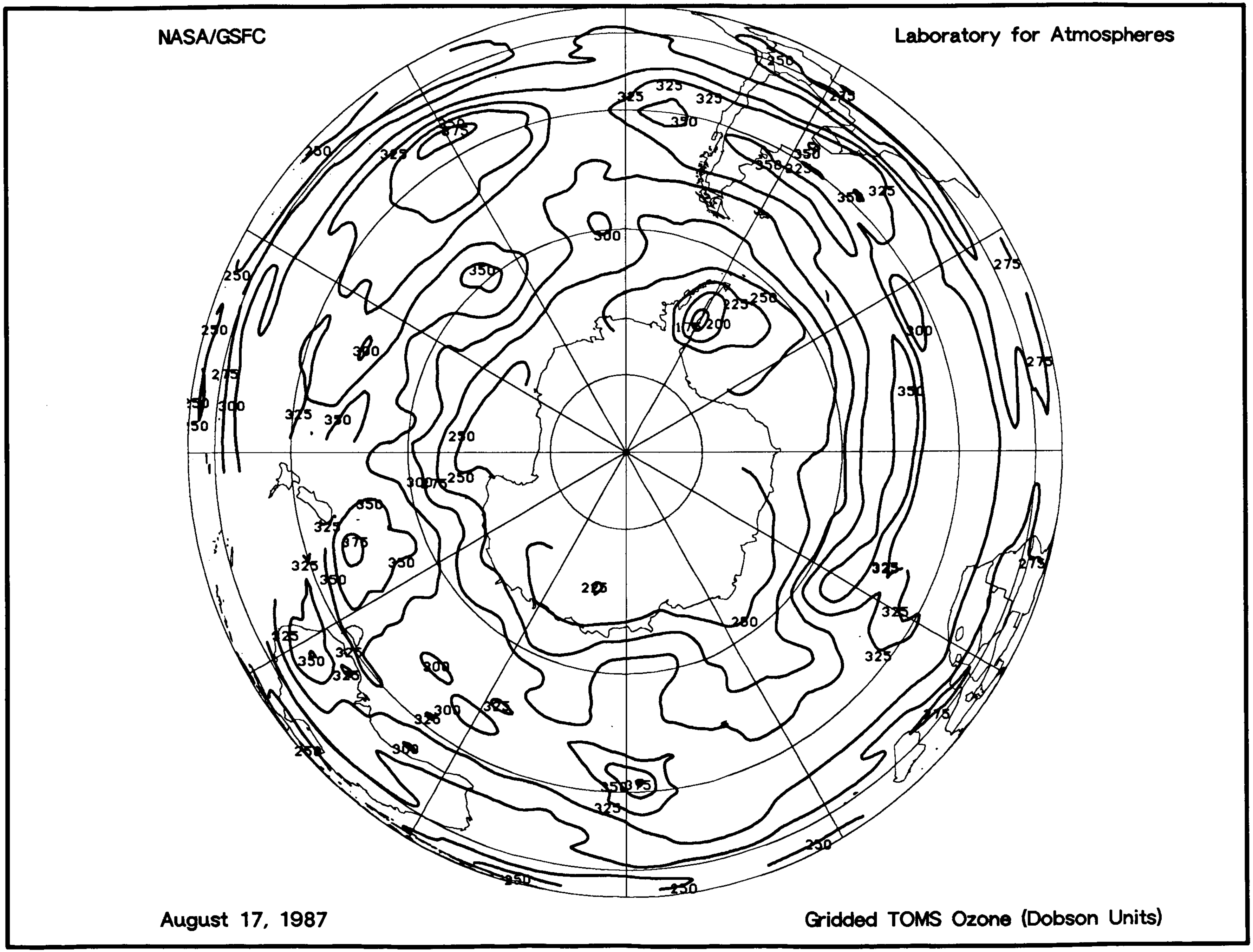
NASA/GSFC
Laboratory for Atmospheres
August 17, 1987
Gridded TOMS Ozone (Dobson Units)

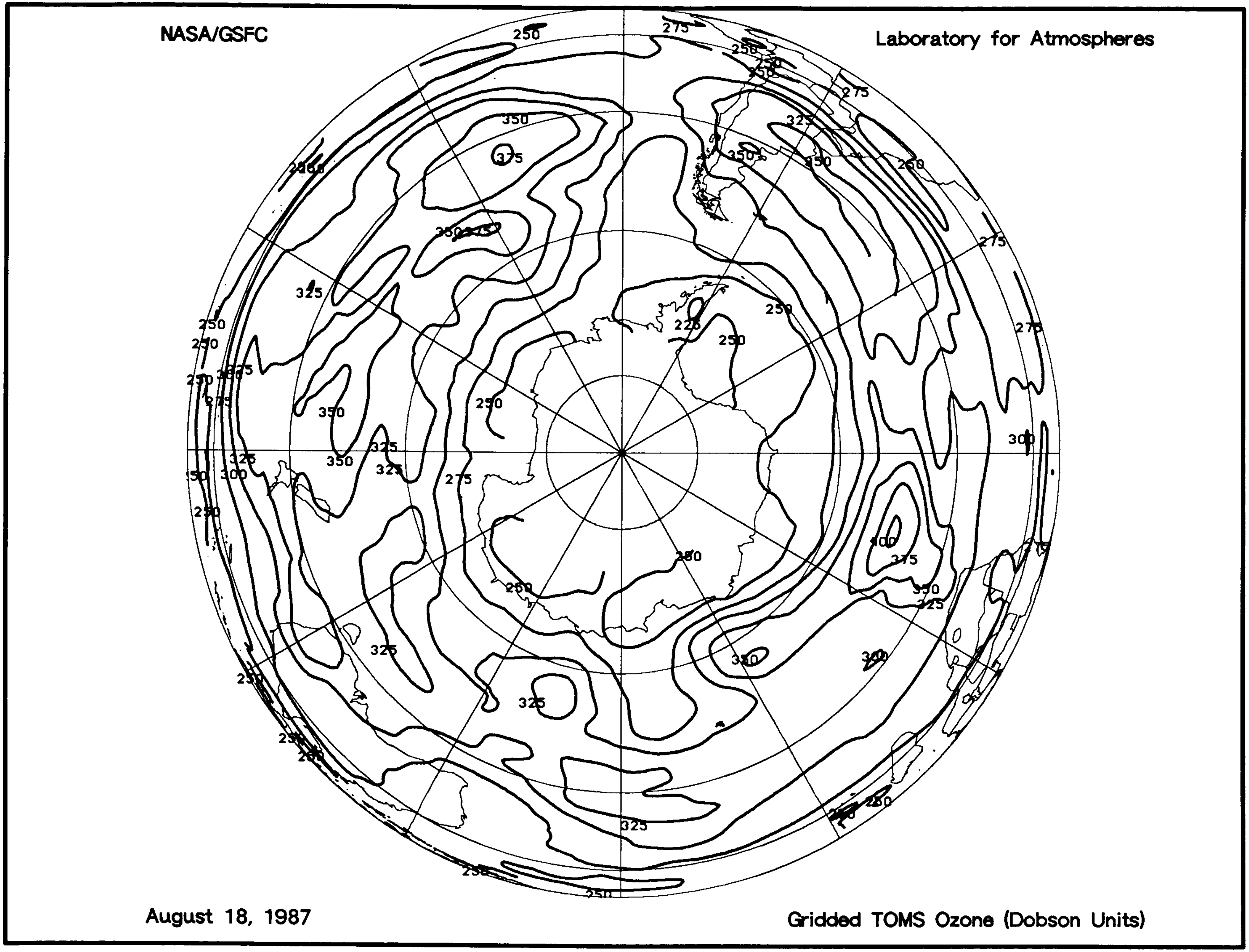
NASA/GSFC
Laboratory for Atmospheres
August 18, 1987
Gridded TOMS Ozone (Dobson Units)

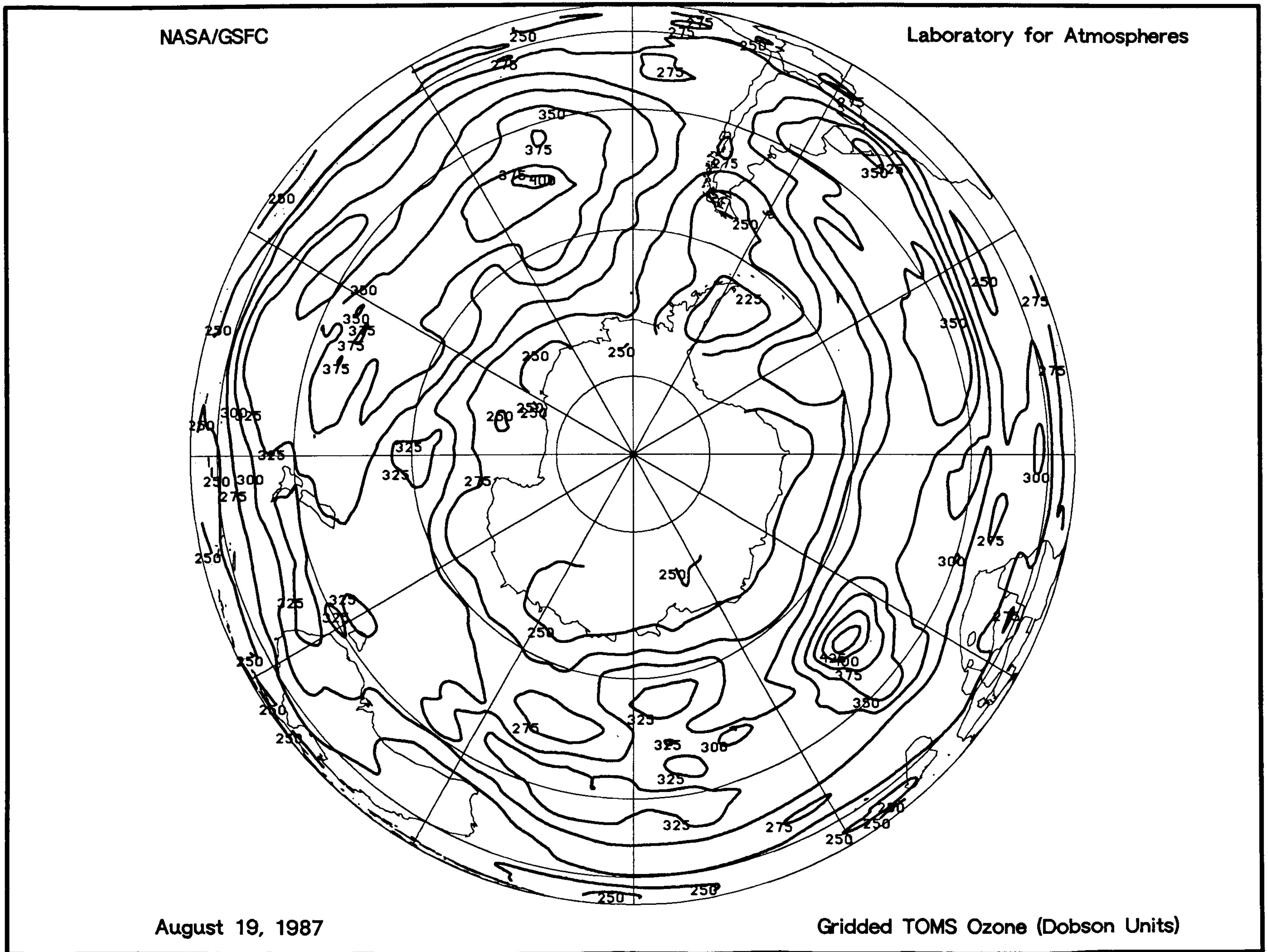
NASA/GSFC
Laboratory for Atmospheres
August 19, 1987
Gridded TOMS Ozone (Dobson Units)

NASA/GSFC

Laboratory for Atmospheres

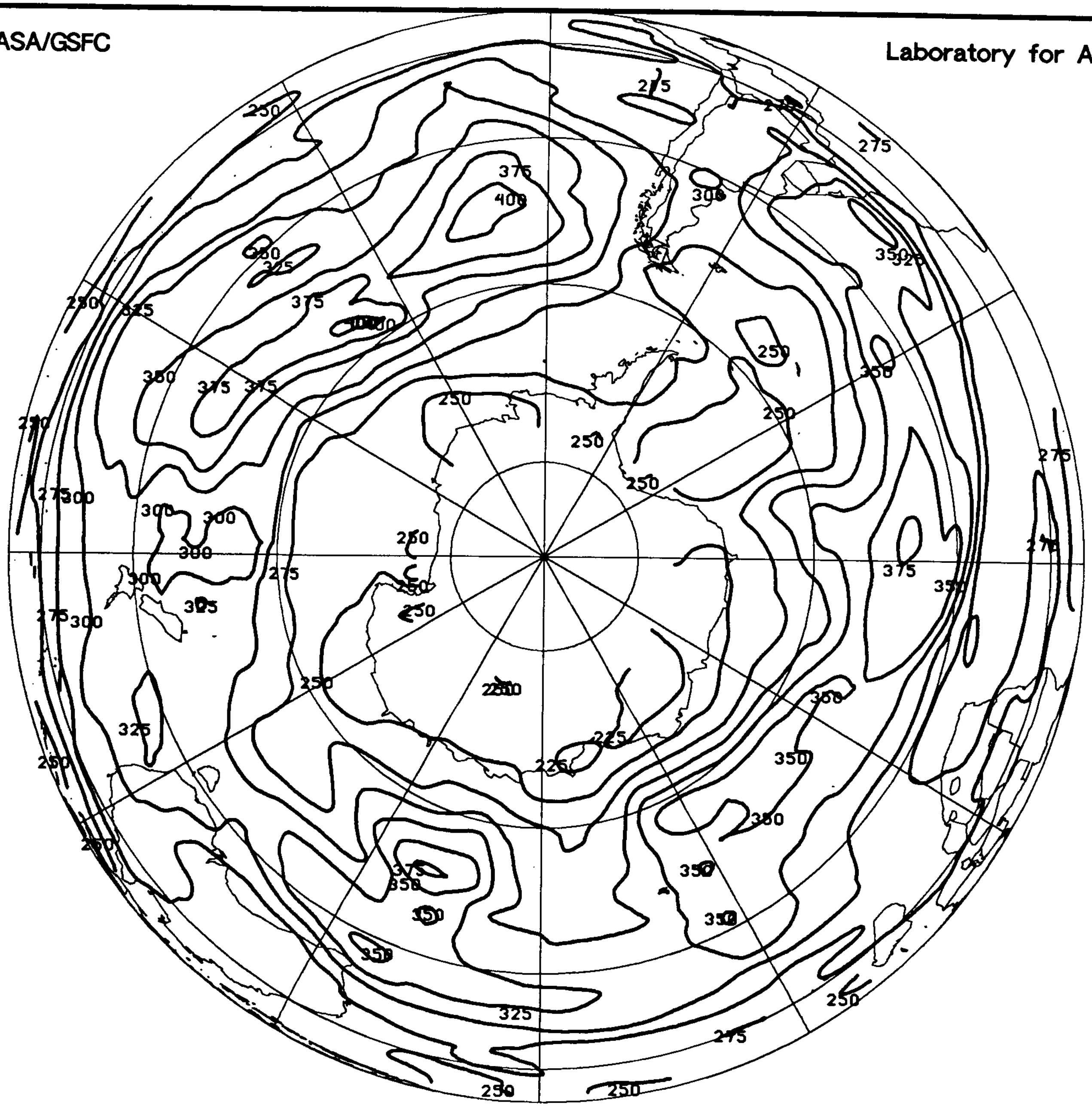

August 20, 1987

Gridded TOMS Ozone (Dobson Units)

NASA/GSFC

Laboratory for Atmospheres

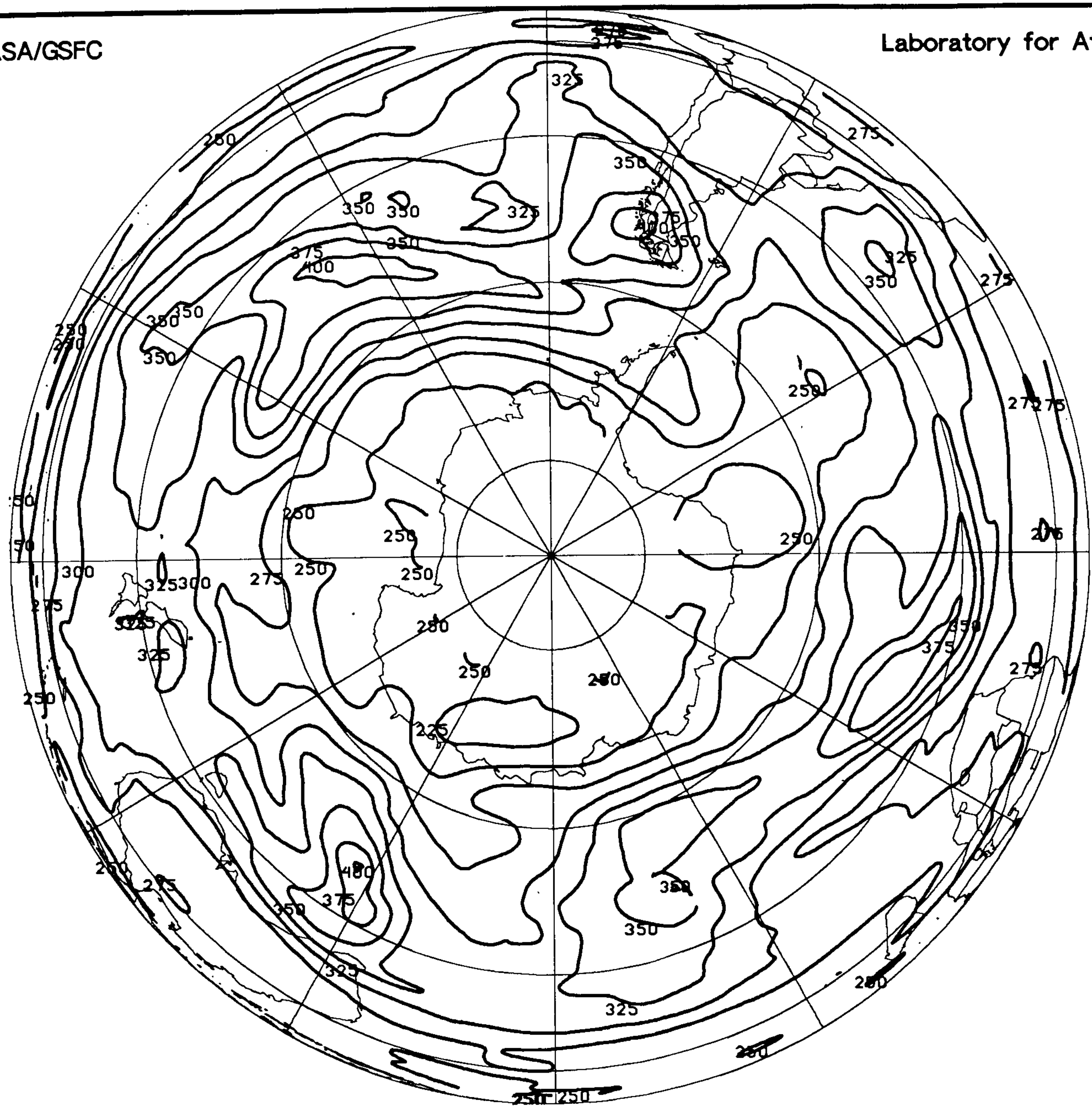

August 21, 1987

Gridded TOMS Ozone (Dobson Units)

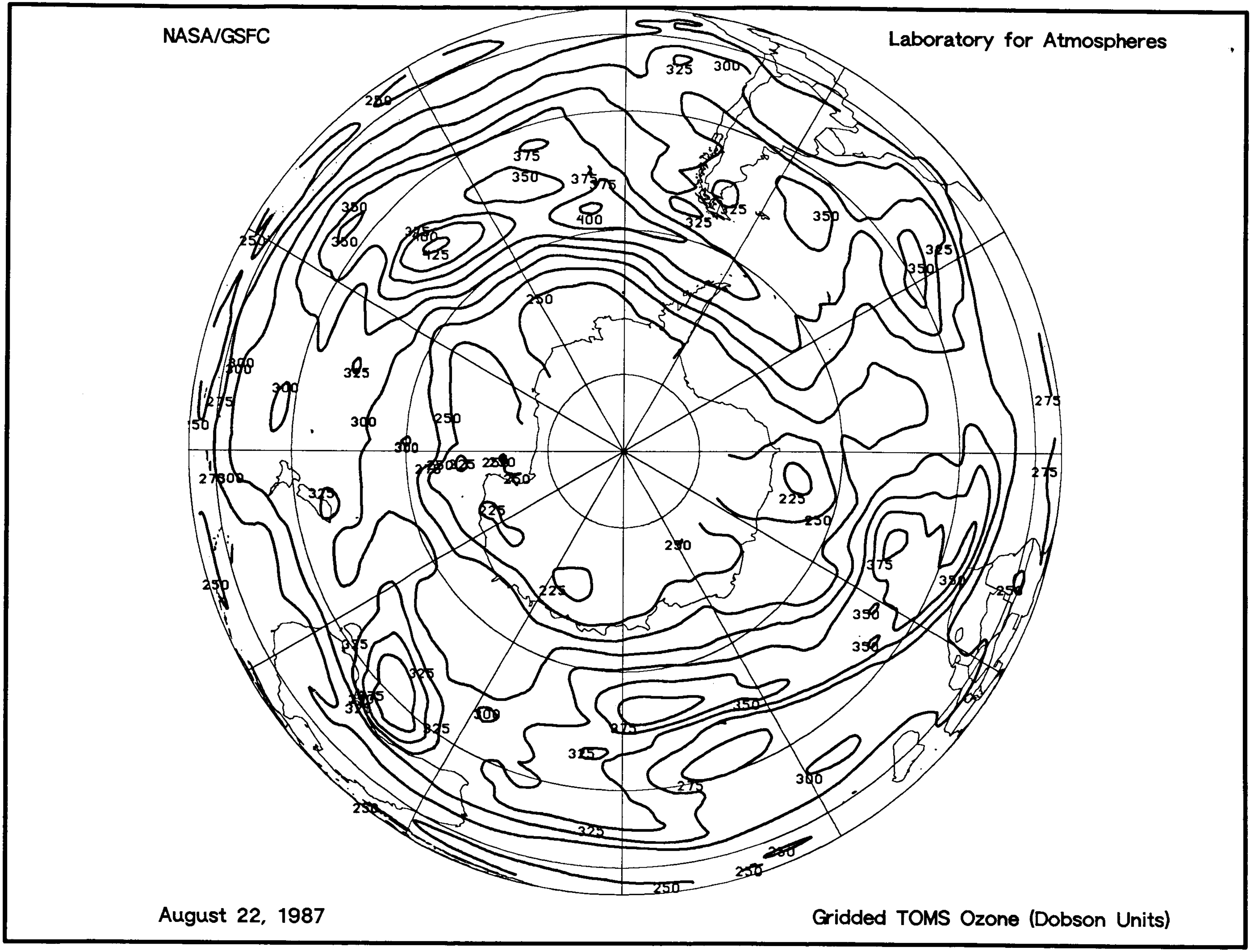
NASA/GSFC
Laboratory for Atmospheres
August 22, 1987
Gridded TOMS Ozone (Dobson Units)

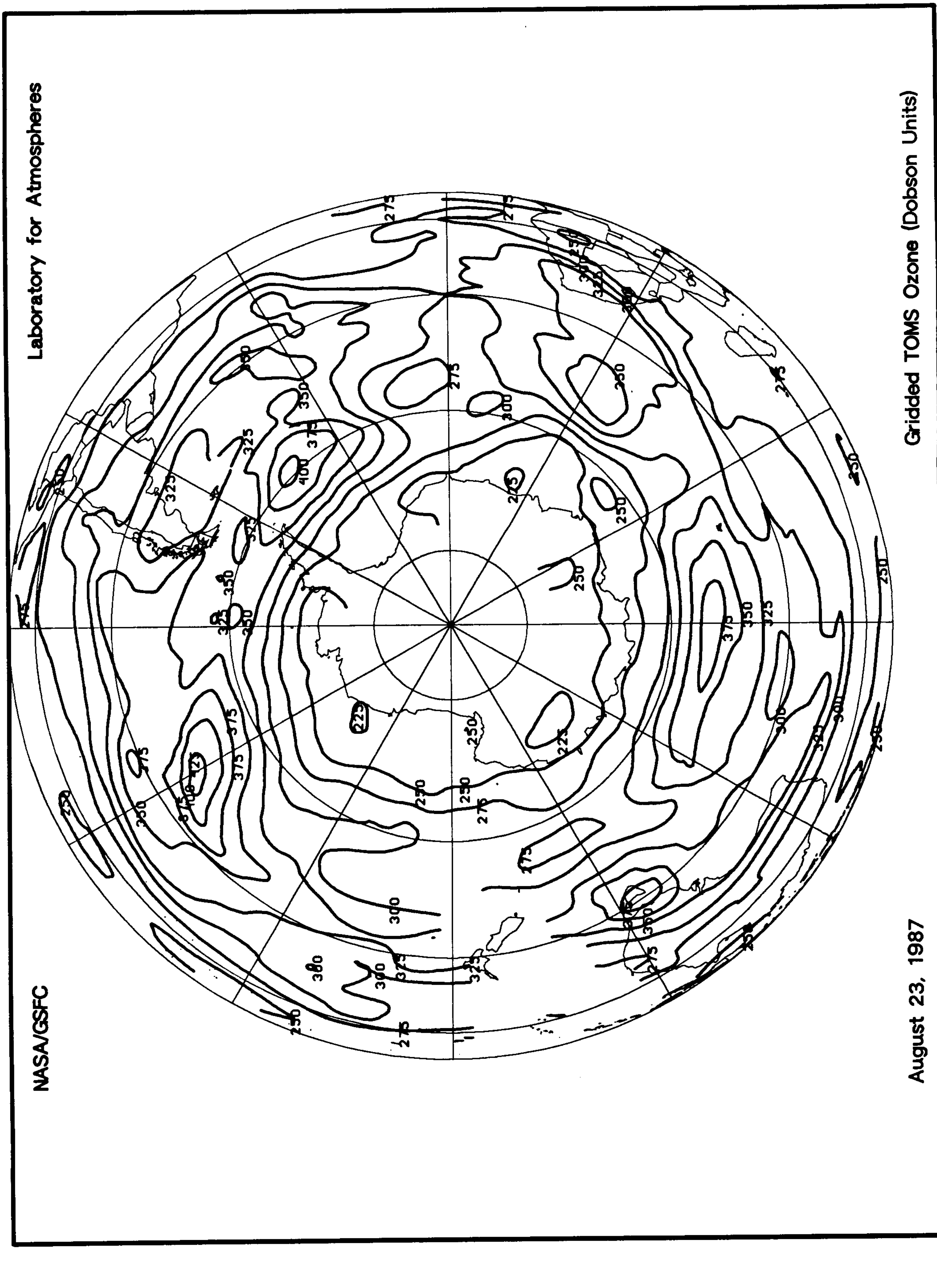

Laboratory for Atmospheres
NASA/GSFC
Gridded TOMS Ozone (Dobson Units)
August 23, 1987

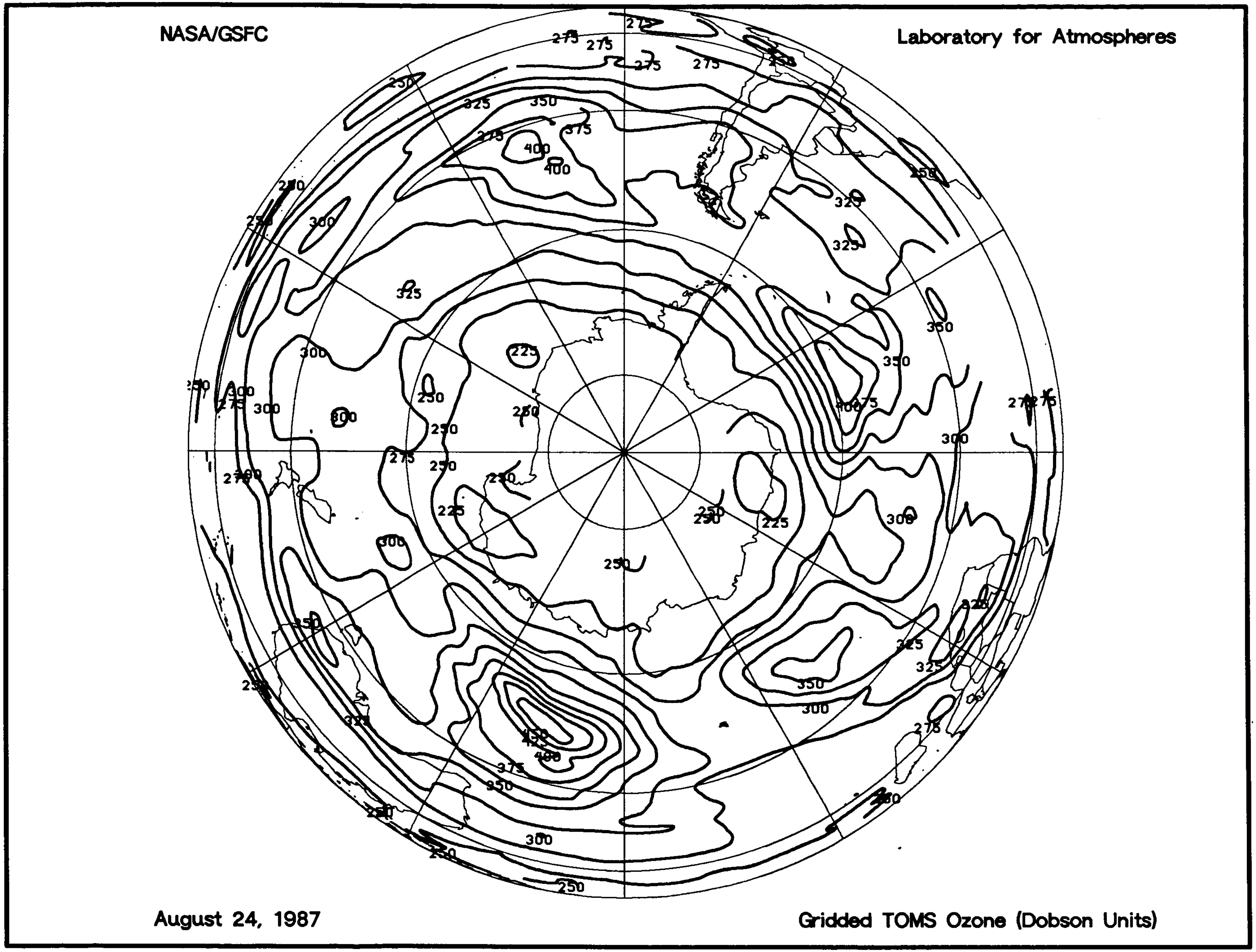
NASA/GSFC
Laboratory for Atmospheres
August 24, 1987
Gridded TOMS Ozone (Dobson Units)

NASA/GSFC

Laboratory for Atmospheres

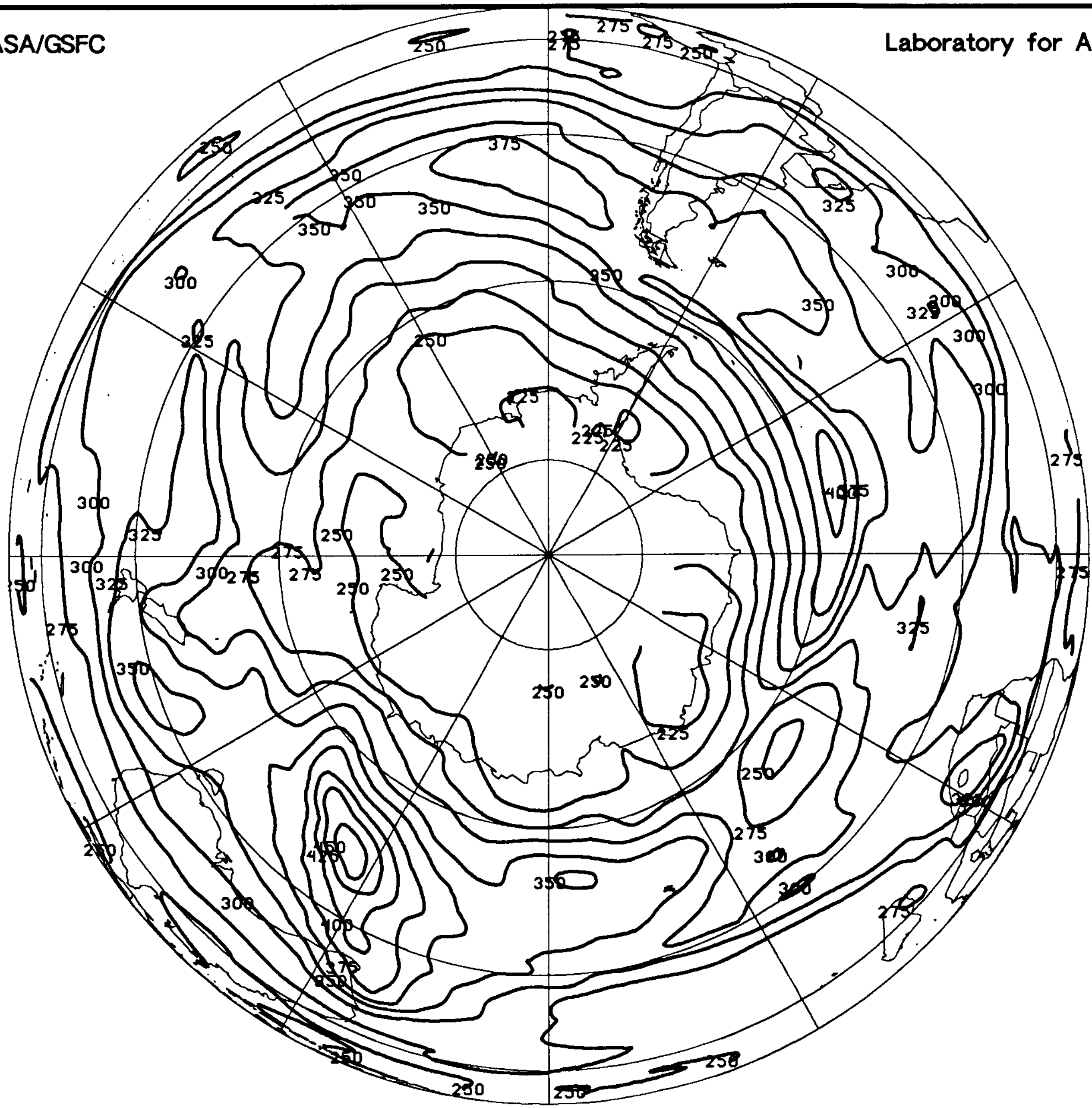

August 25, 1987

Gridded TOMS Ozone (Dobson Units)

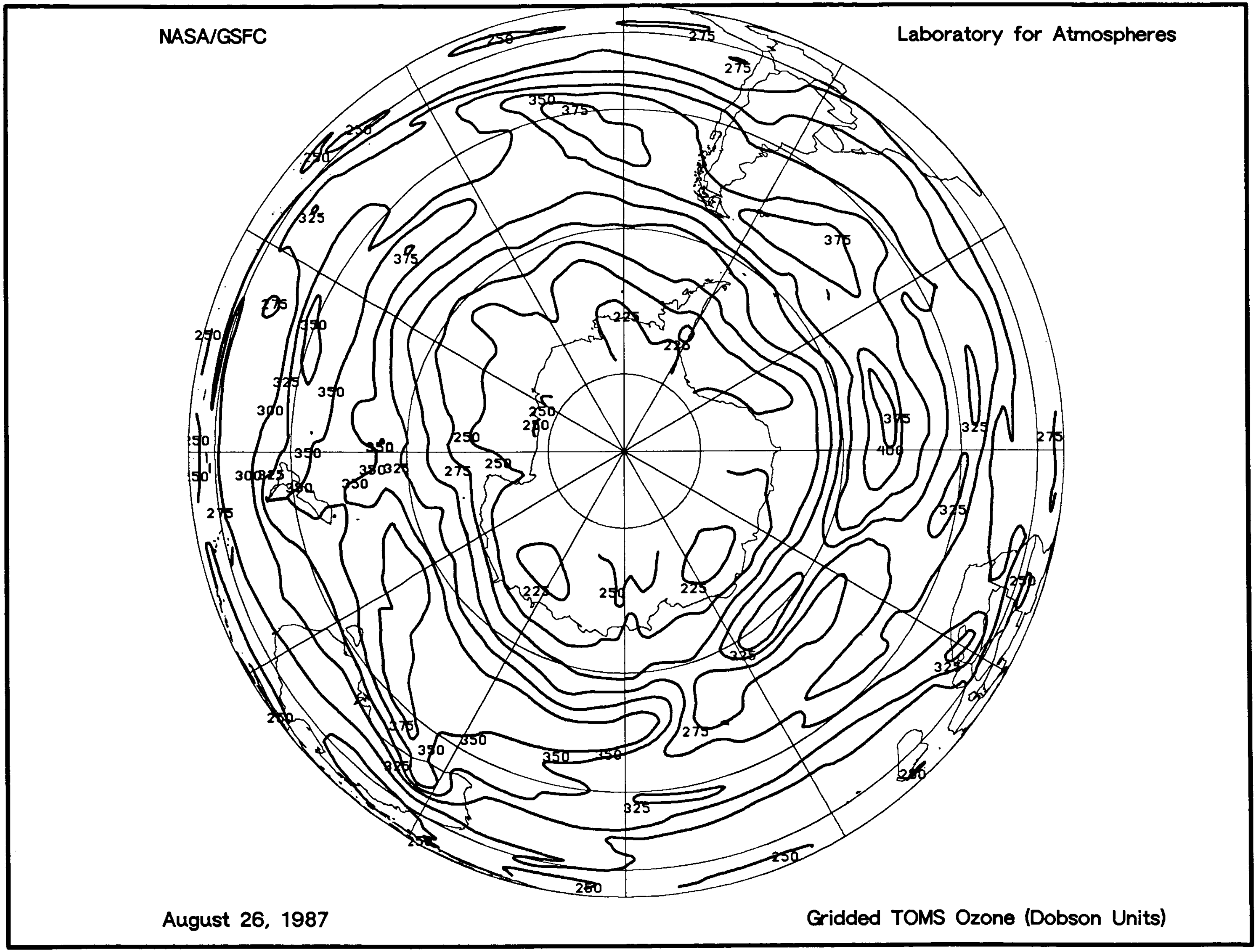
NASA/GSFC
Laboratory for Atmospheres
August 26, 1987
Gridded TOMS Ozone (Dobson Units)

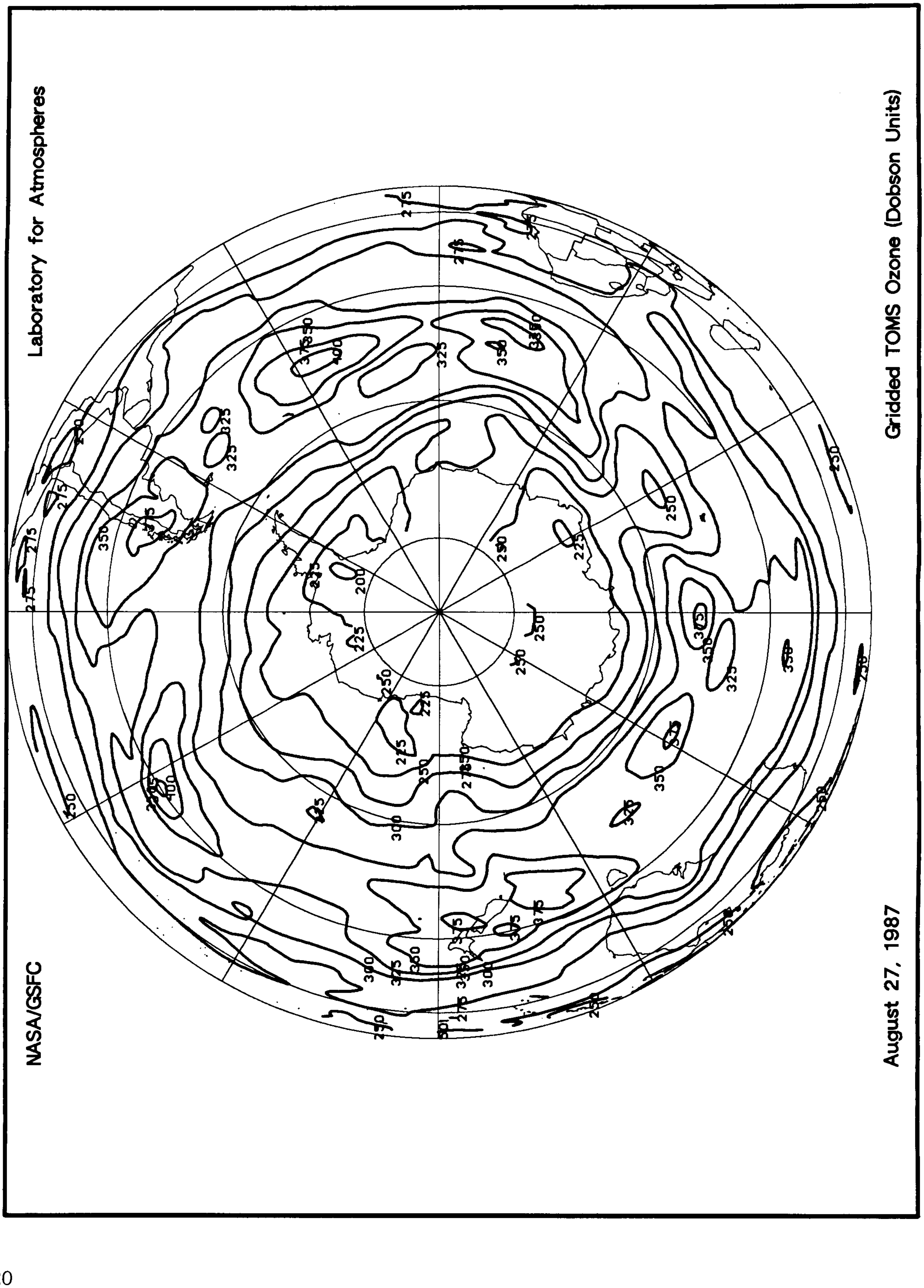
NASA/GSFC
Laboratory for Atmospheres
August 27, 1987
Gridded TOMS Ozone (Dobson Units)

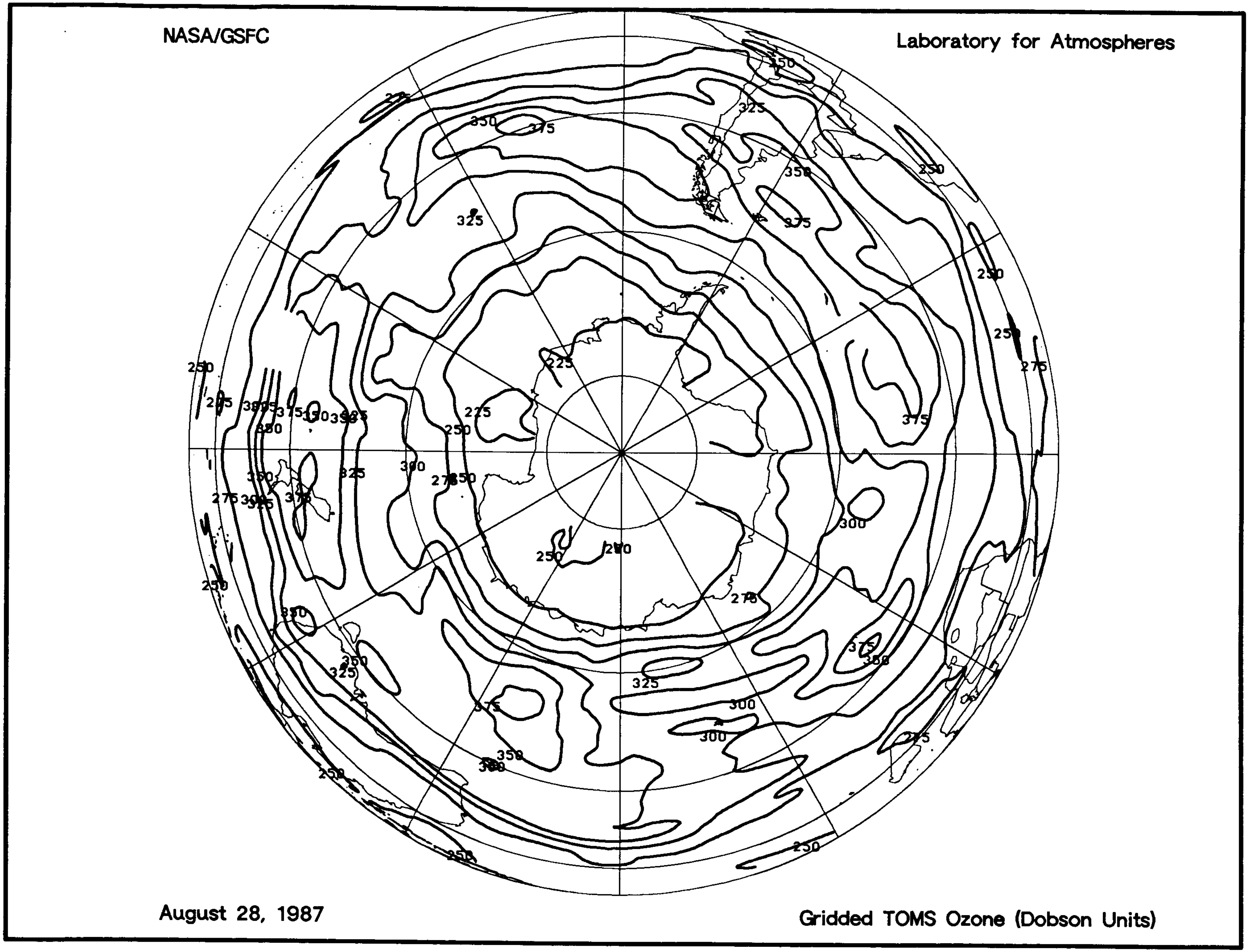
NASA/GSFC
Laboratory for Atmospheres
August 28, 1987
Gridded TOMS Ozone (Dobson Units)

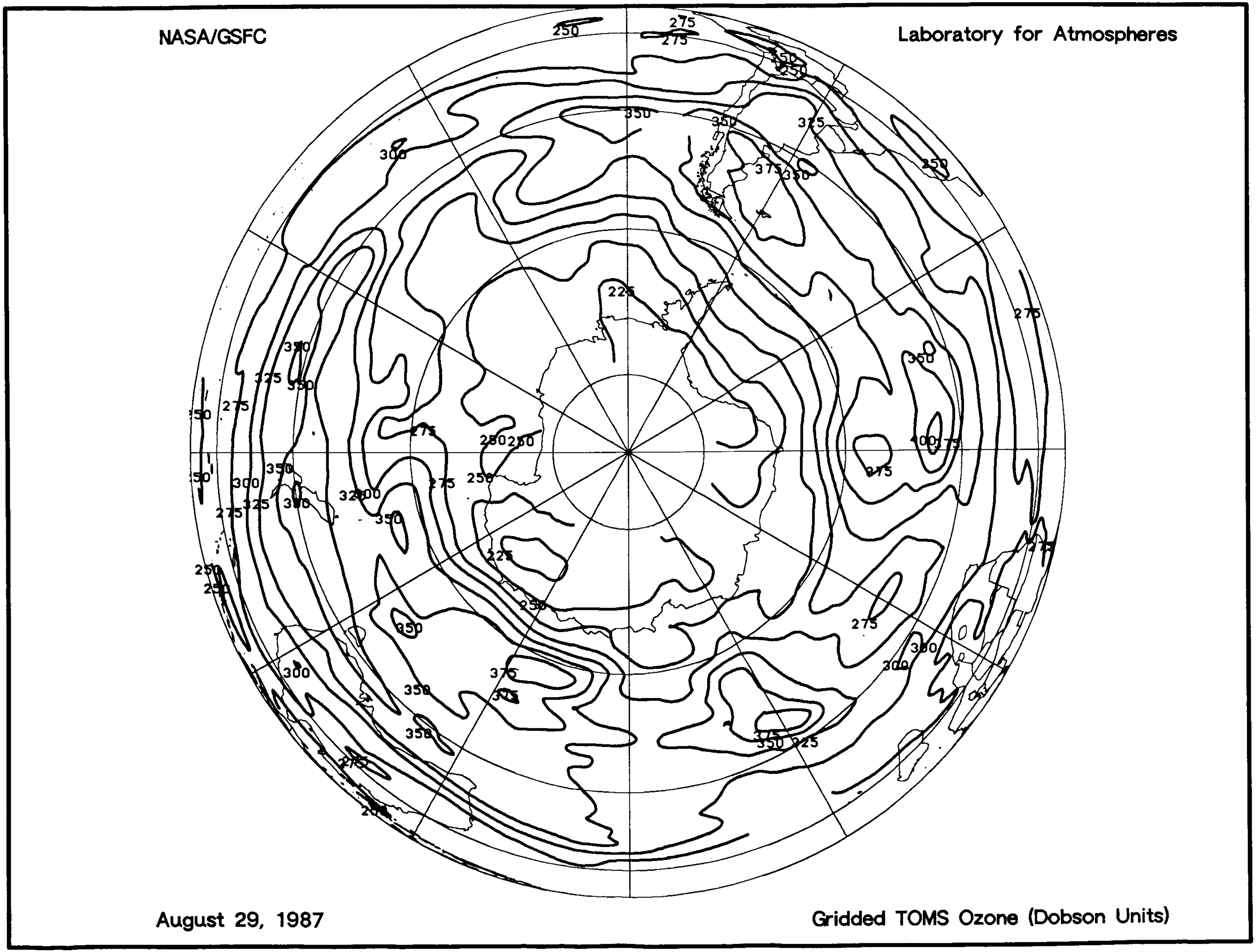
NASA/GSFC
Laboratory for Atmospheres
August 29, 1987
Gridded TOMS Ozone (Dobson Units)

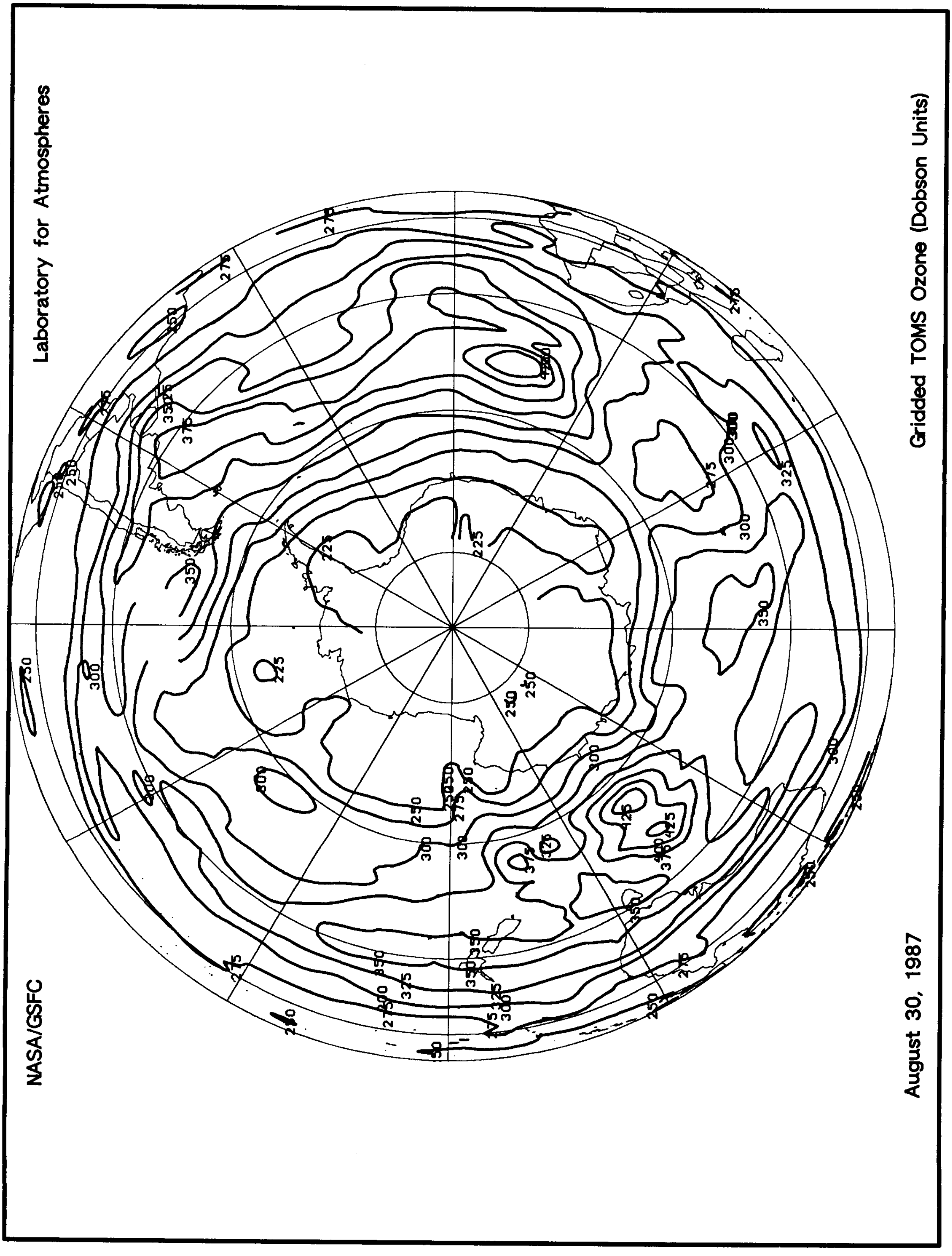
Laboratory for Atmospheres
NASA/GSFC
August 30, 1987
Gridded TOMS Ozone (Dobson Units)

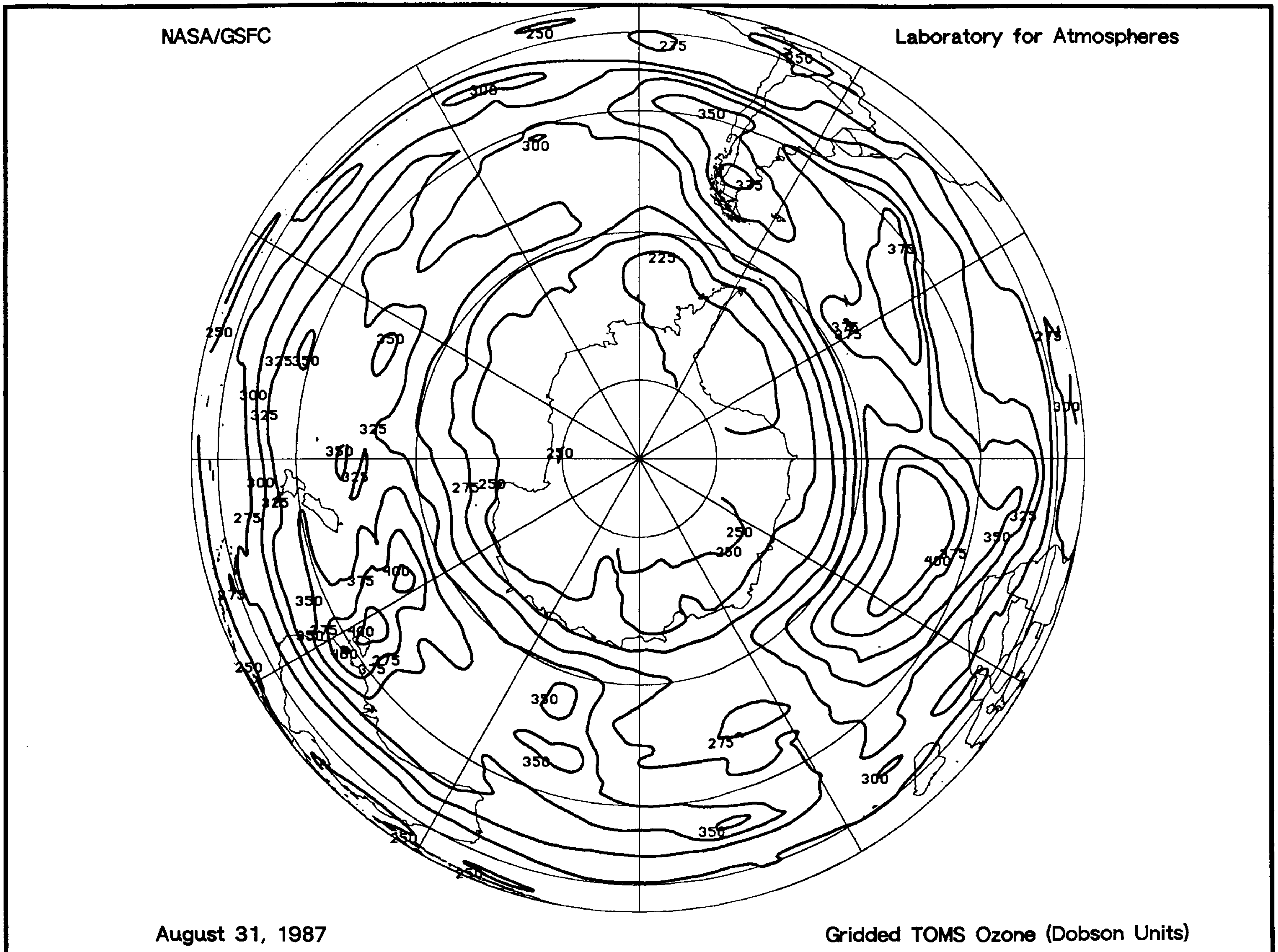
NASA/GSFC
Laboratory for Atmospheres
August 31, 1987
Gridded TOMS Ozone (Dobson Units)

NASA/GSFC

Laboratory for Atmospheres

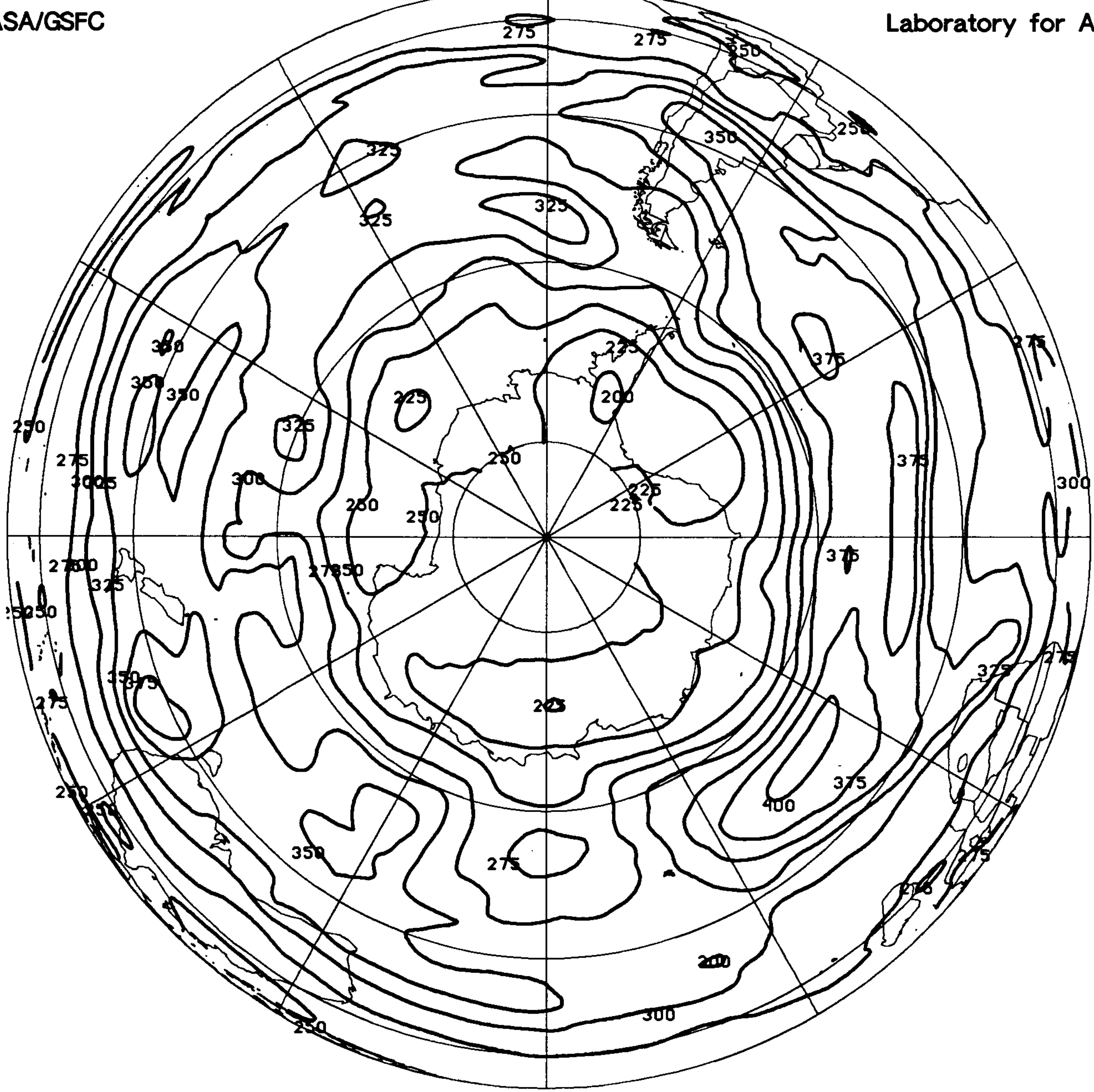

September 1, 1987

Gridded TOMS Ozone (Dobson Units)

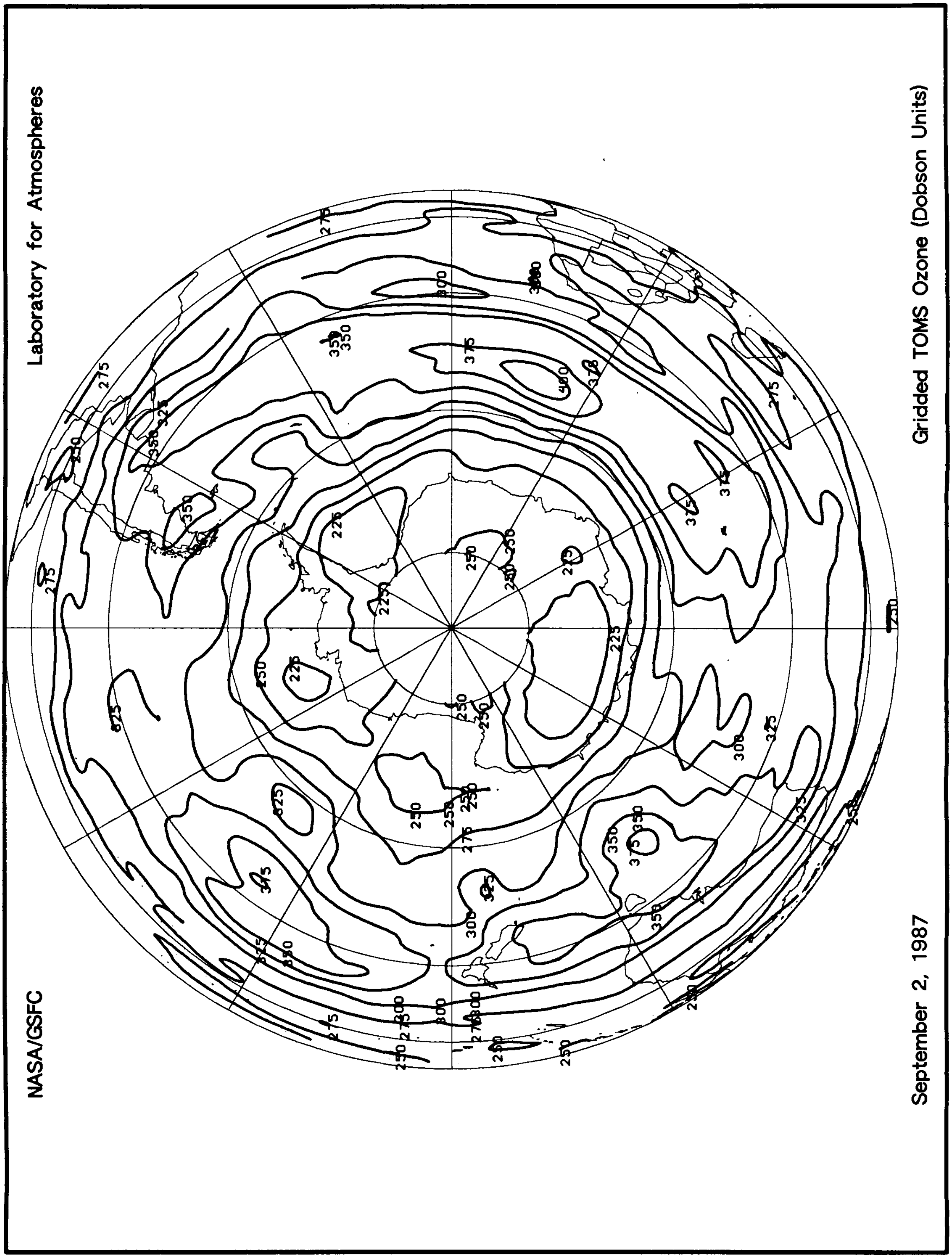
NASA/GSFC
Laboratory for Atmospheres
September 2, 1987
Gridded TOMS Ozone (Dobson Units)

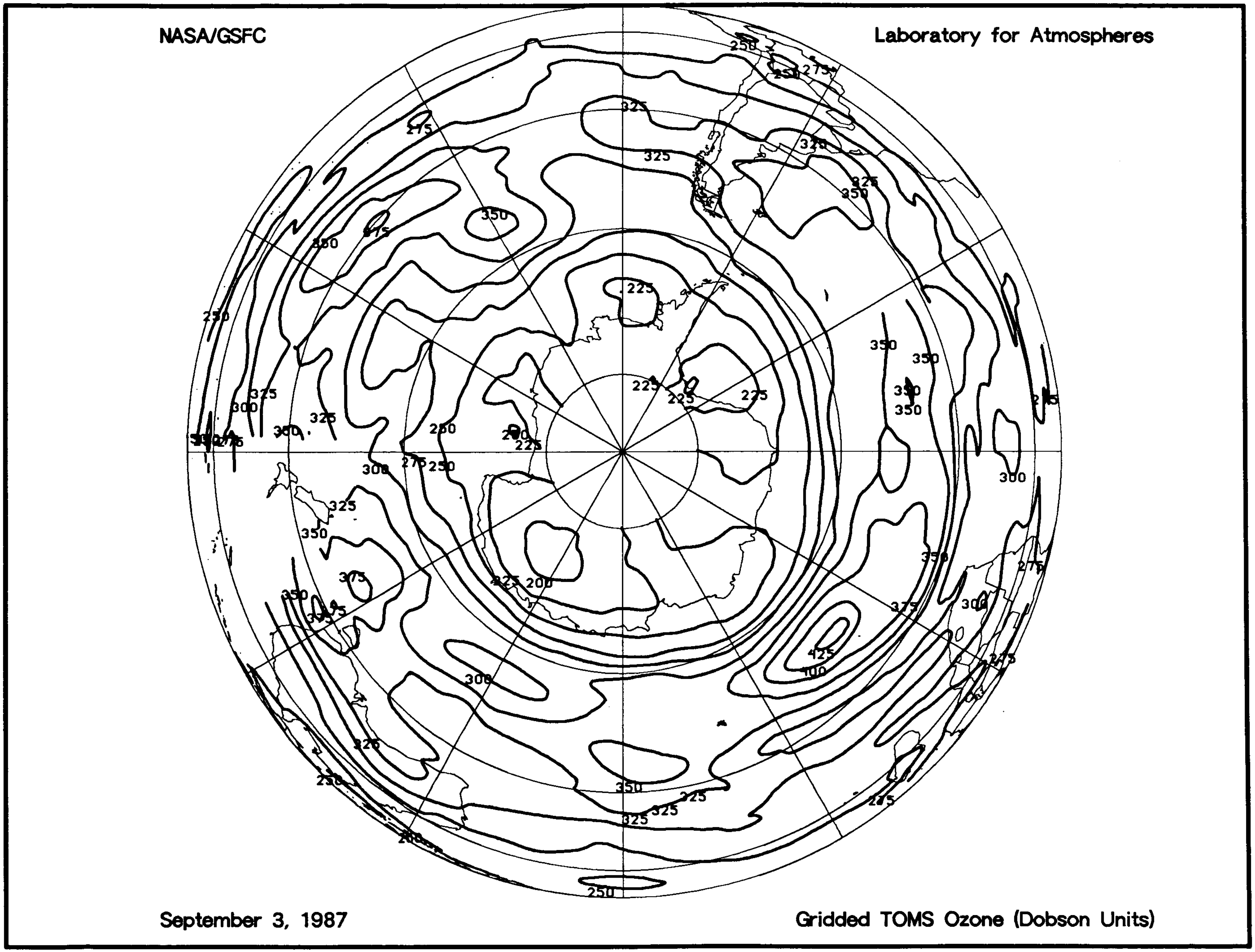
NASA/GSFC
Laboratory for Atmospheres
September 3, 1987
Gridded TOMS Ozone (Dobson Units)

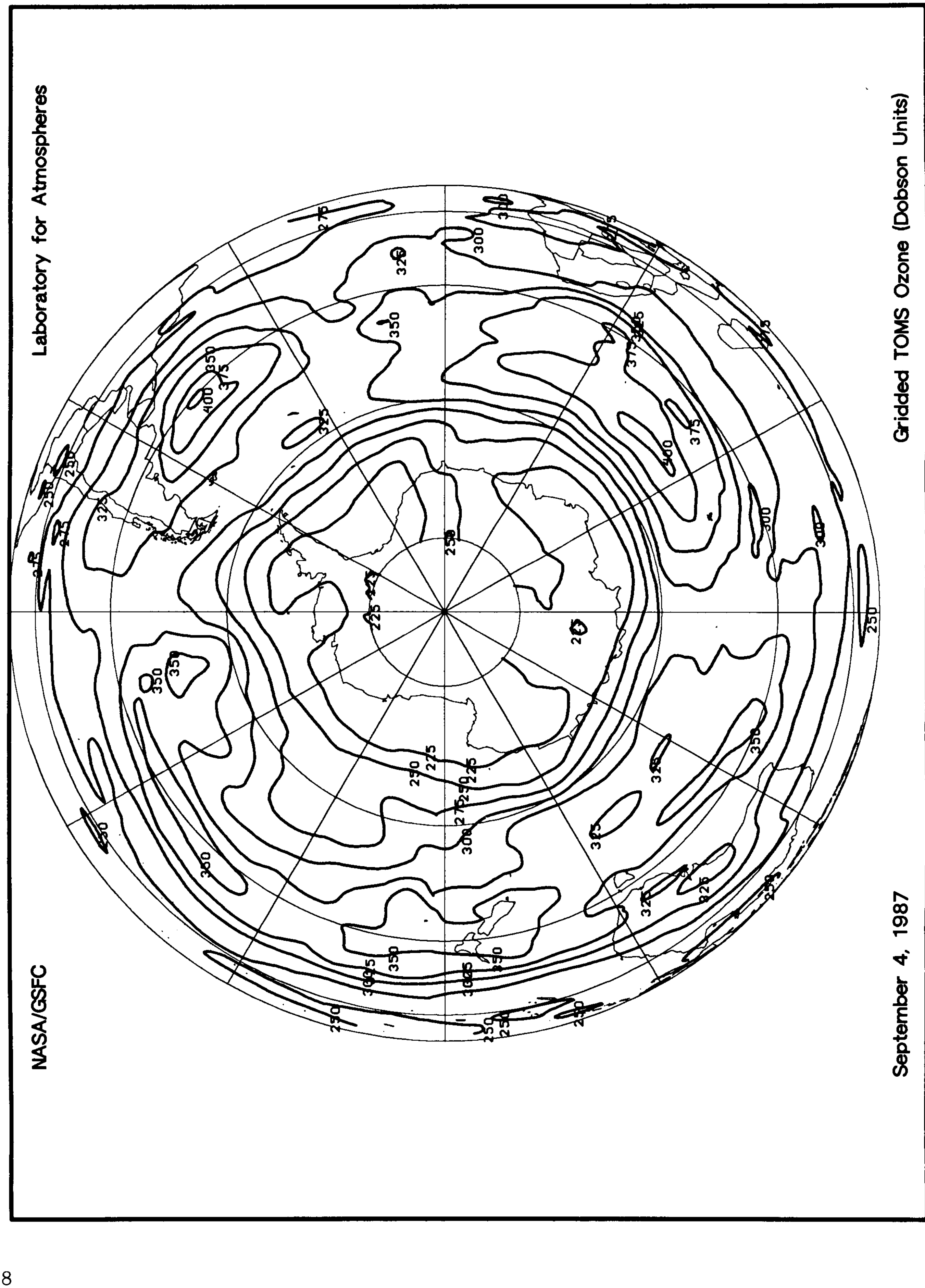
NASA/GSFC
Laboratory for Atmospheres
September 4, 1987
Gridded TOMS Ozone (Dobson Units)

NASA/GSFC

Laboratory for Atmospheres

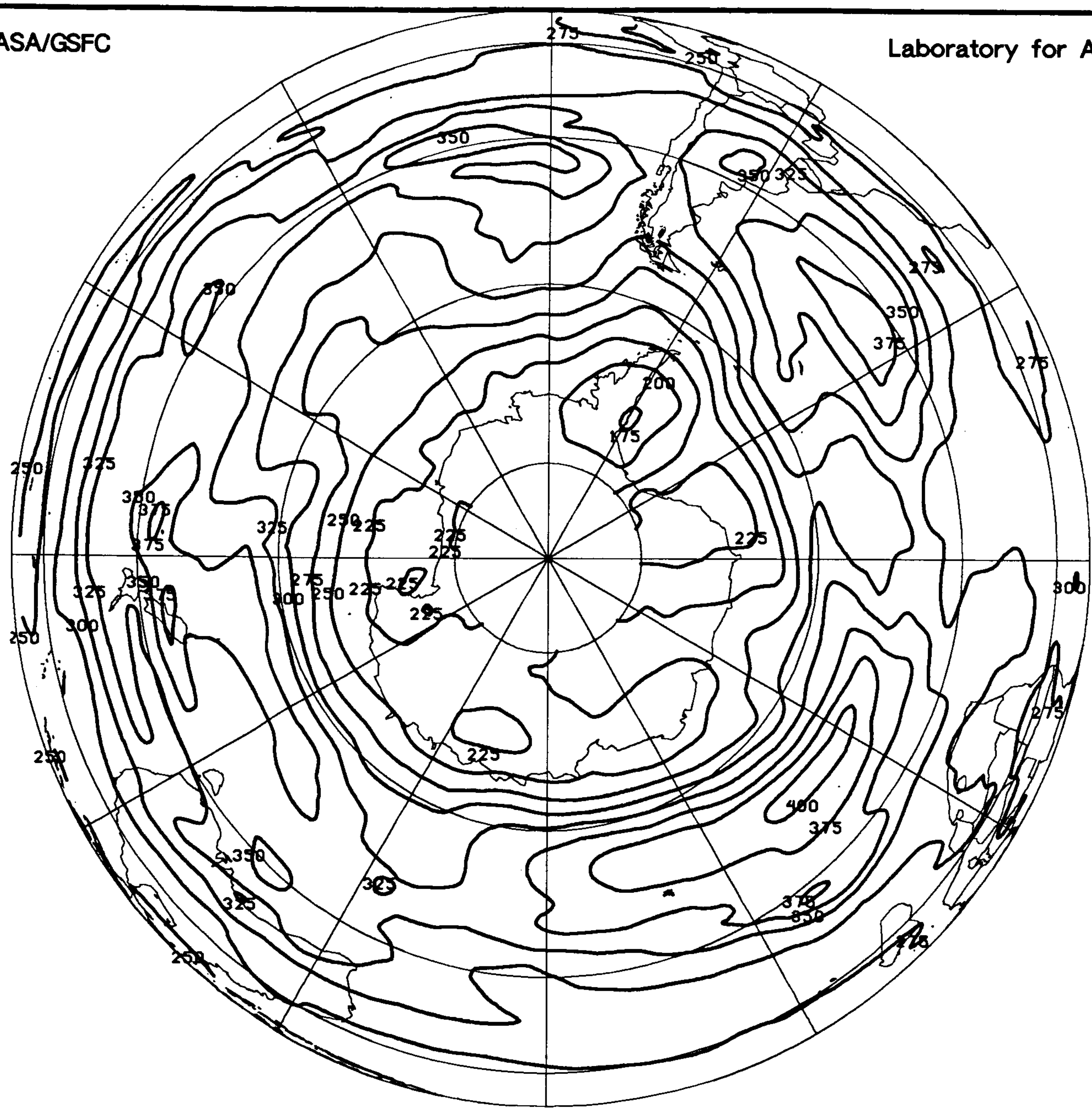

September 5, 1987

Gridded TOMS Ozone (Dobson Units)

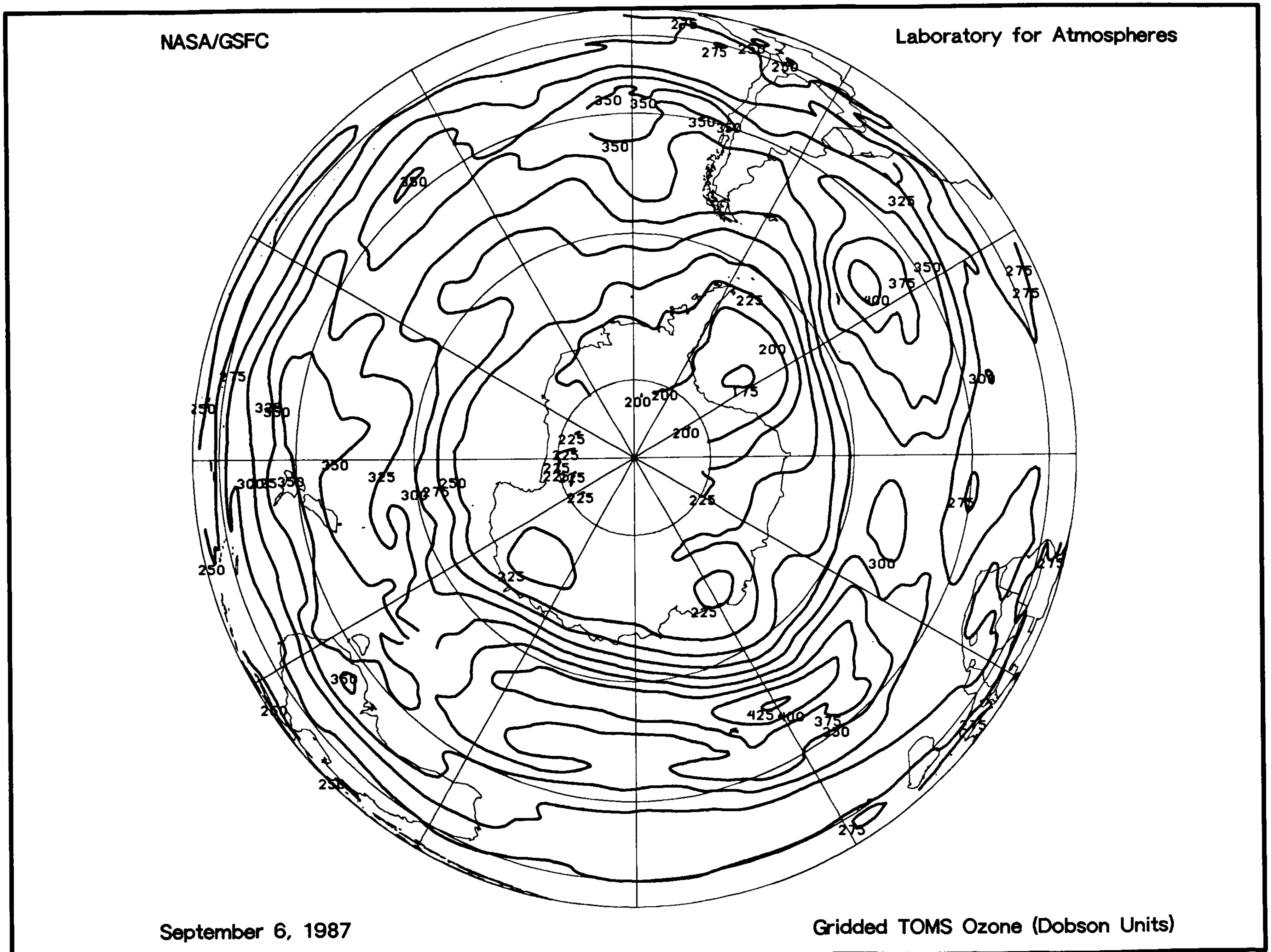
NASA/GSFC
Laboratory for Atmospheres
September 6, 1987
Gridded TOMS Ozone (Dobson Units)

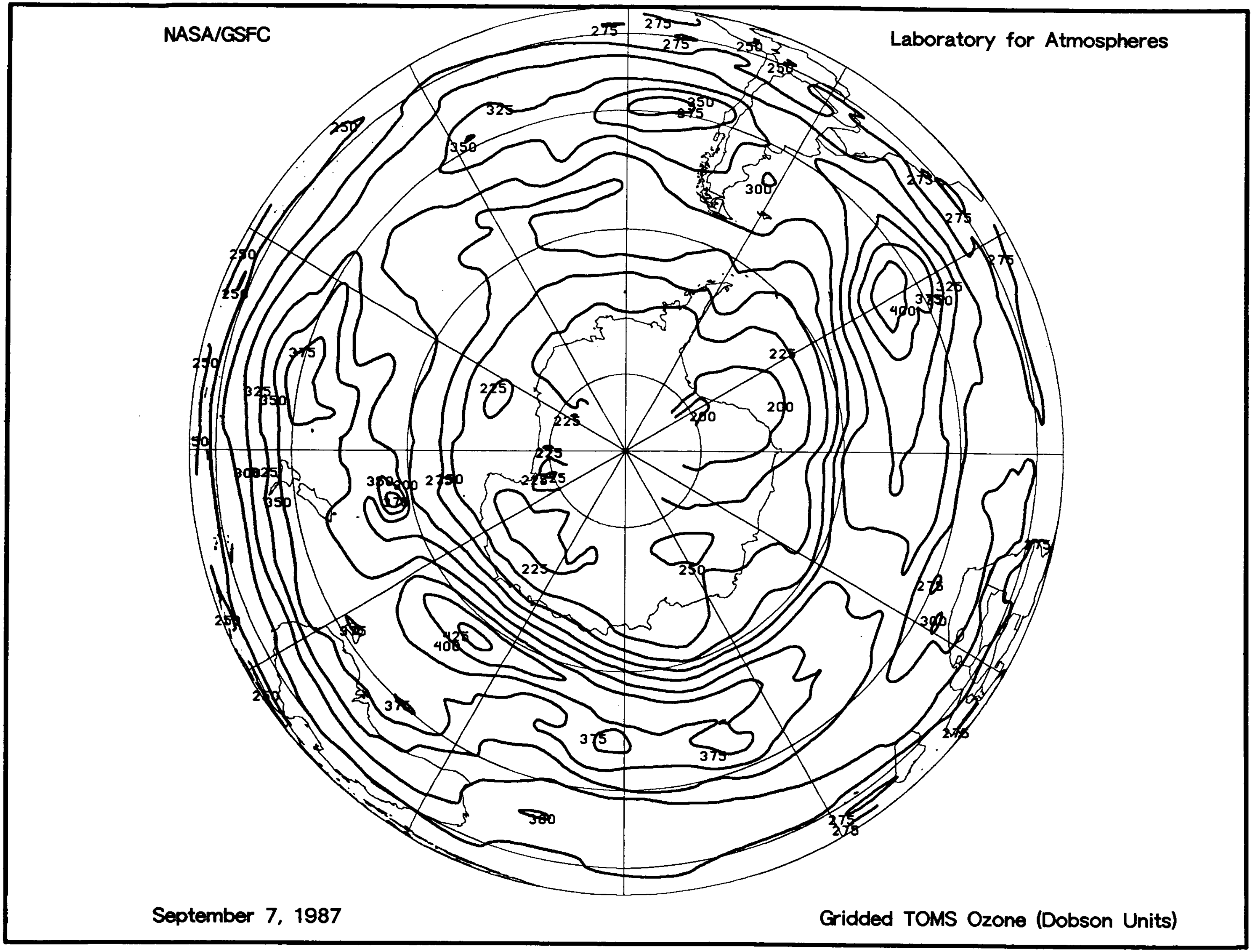
NASA/GSFC
Laboratory for Atmospheres
September 7, 1987
Gridded TOMS Ozone (Dobson Units)

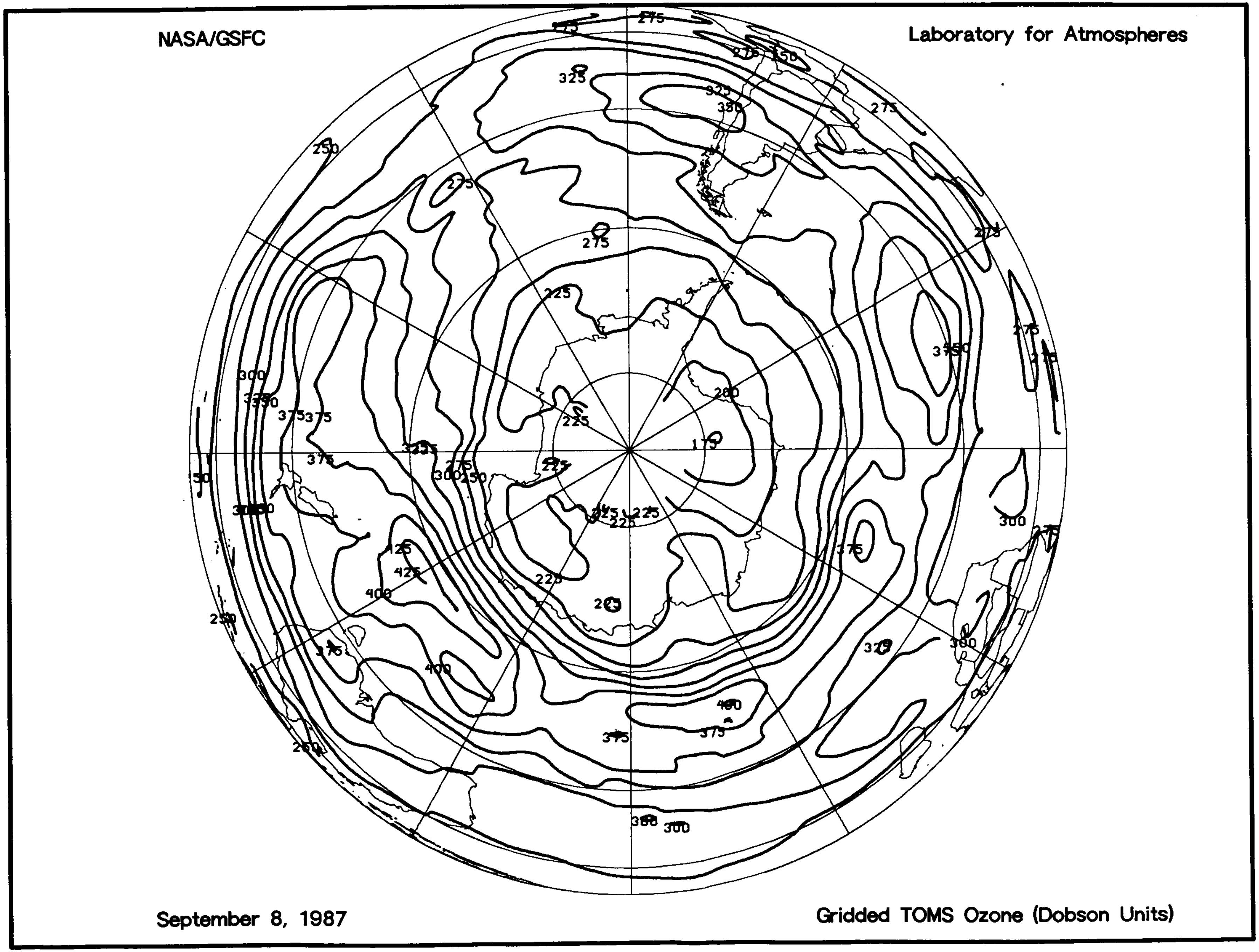
NASA/GSFC
Laboratory for Atmospheres
September 8, 1987
Gridded TOMS Ozone (Dobson Units)

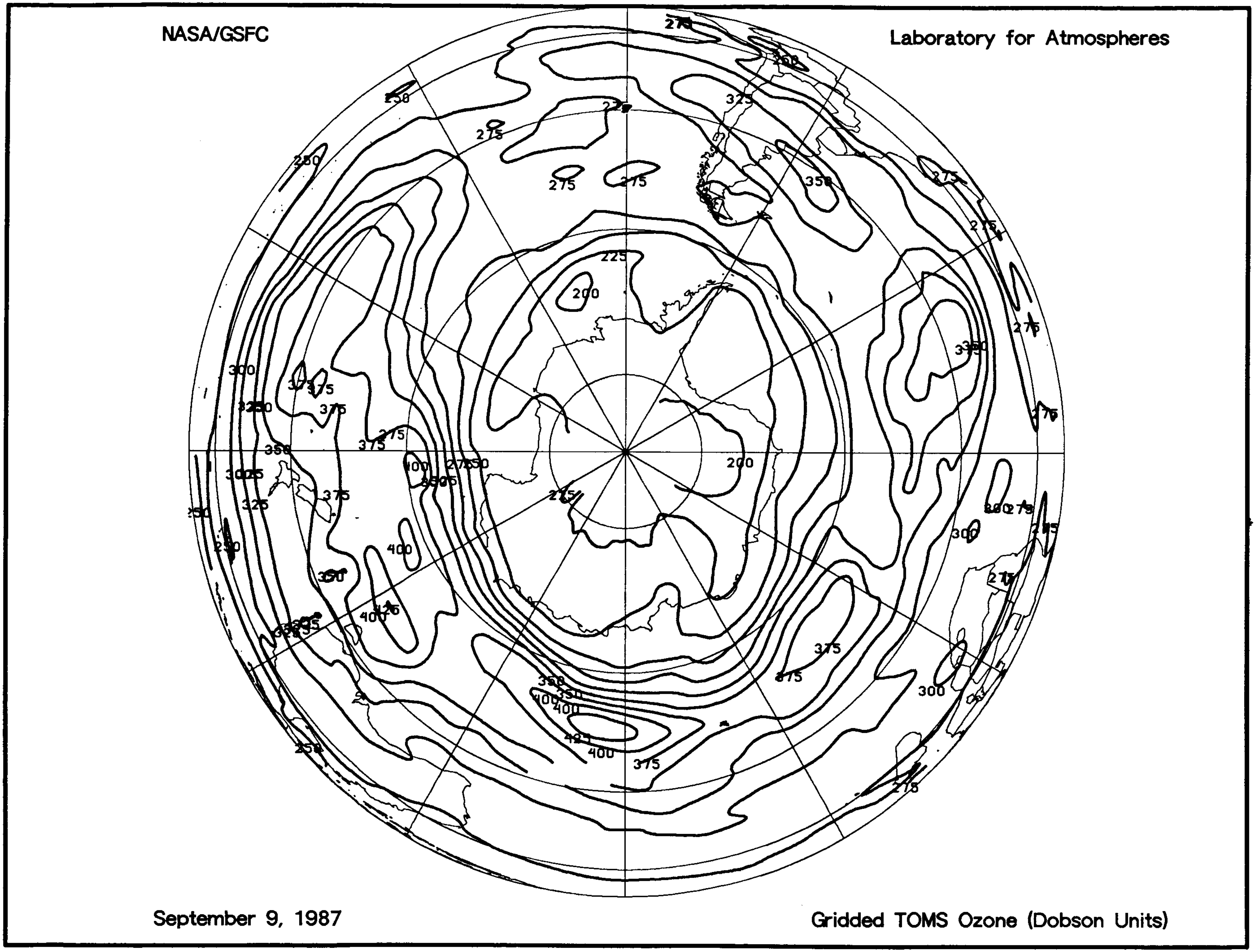
NASA/GSFC
Laboratory for Atmospheres
September 9, 1987
Gridded TOMS Ozone (Dobson Units)

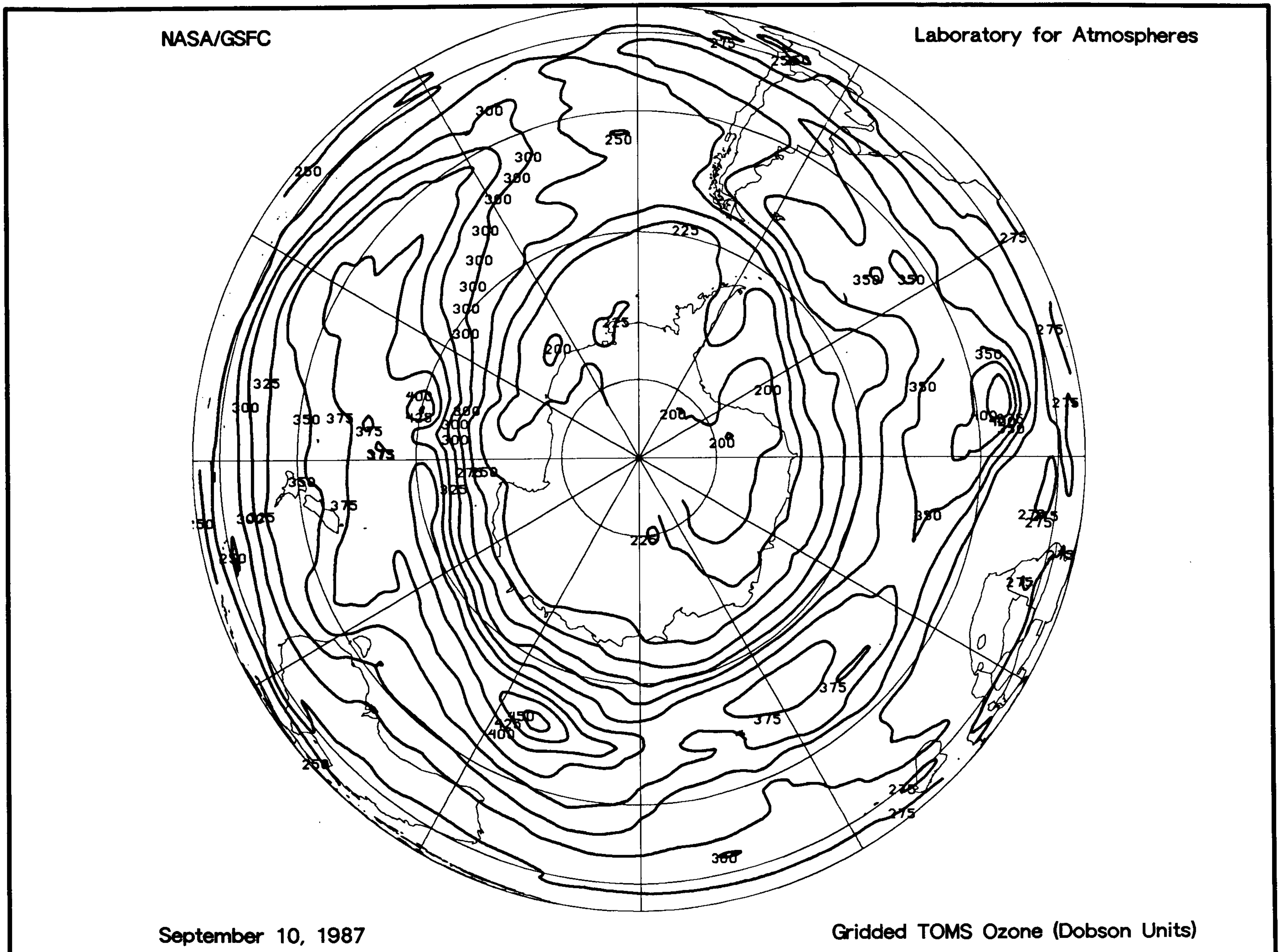
NASA/GSFC
Laboratory for Atmospheres
September 10, 1987
Gridded TOMS Ozone (Dobson Units)

NASA/GSFC

Laboratory for Atmospheres

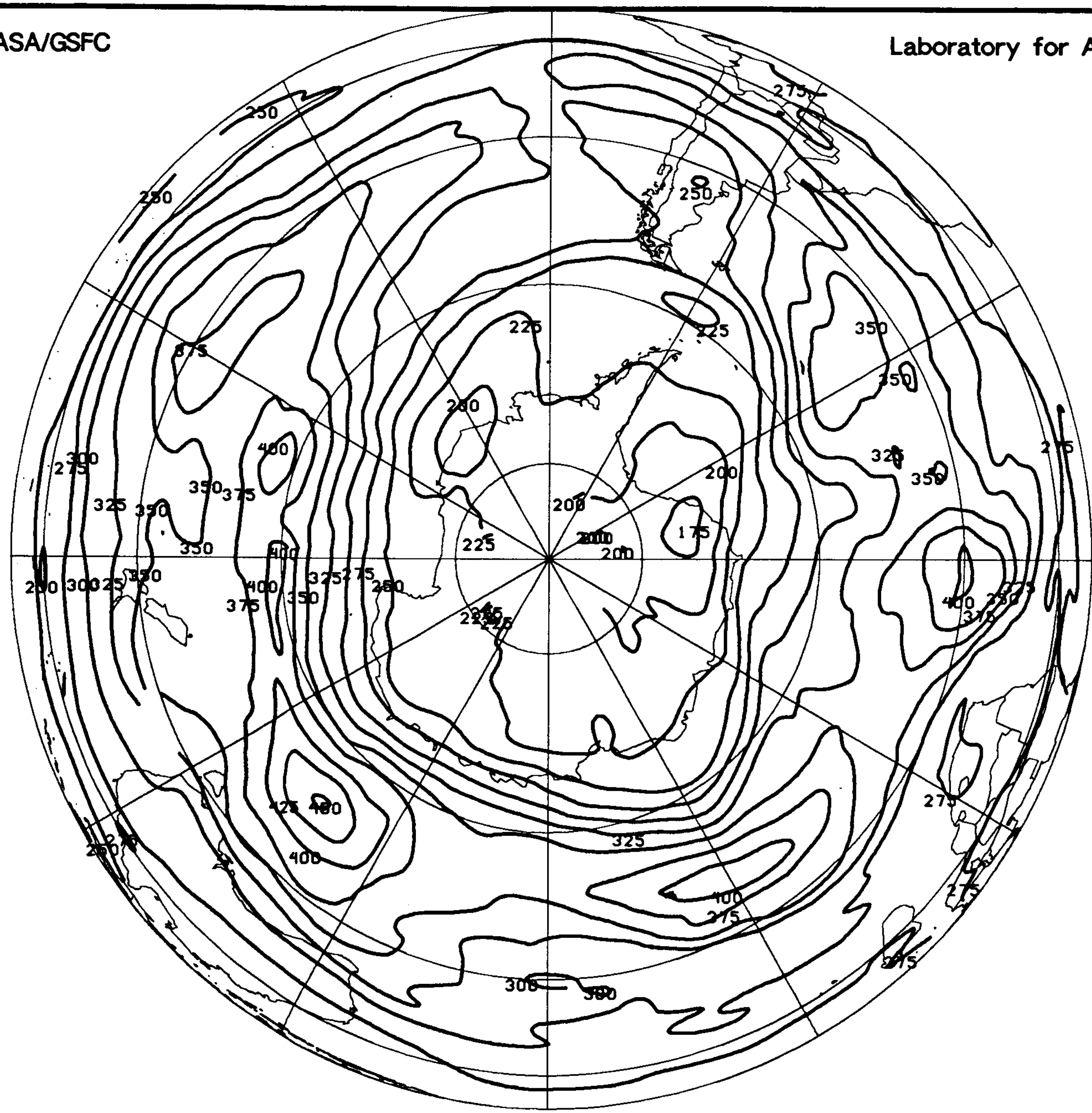

September 11, 1987

Gridded TOMS Ozone (Dobson Units)

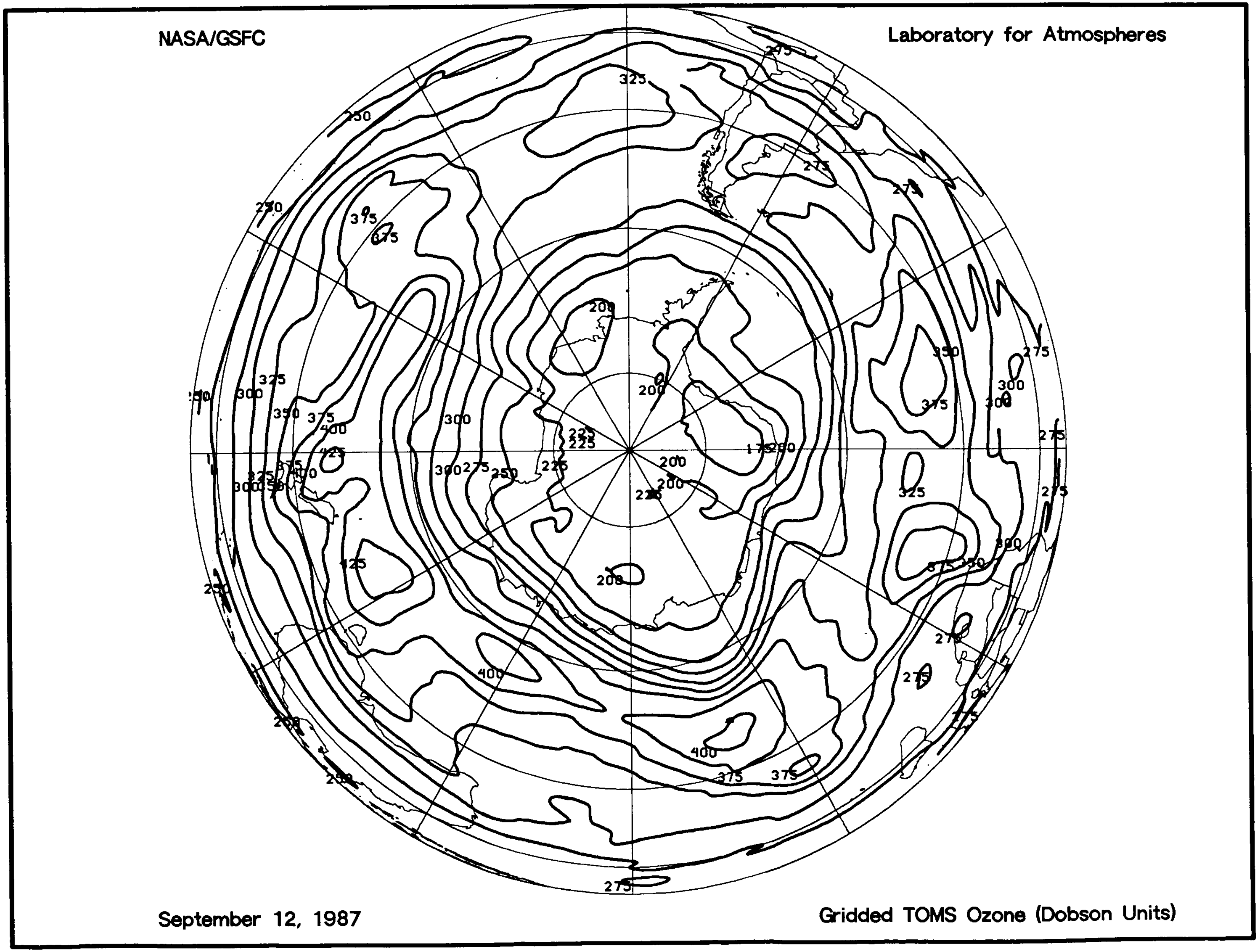
NASA/GSFC
Laboratory for Atmospheres
September 12, 1987
Gridded TOMS Ozone (Dobson Units)

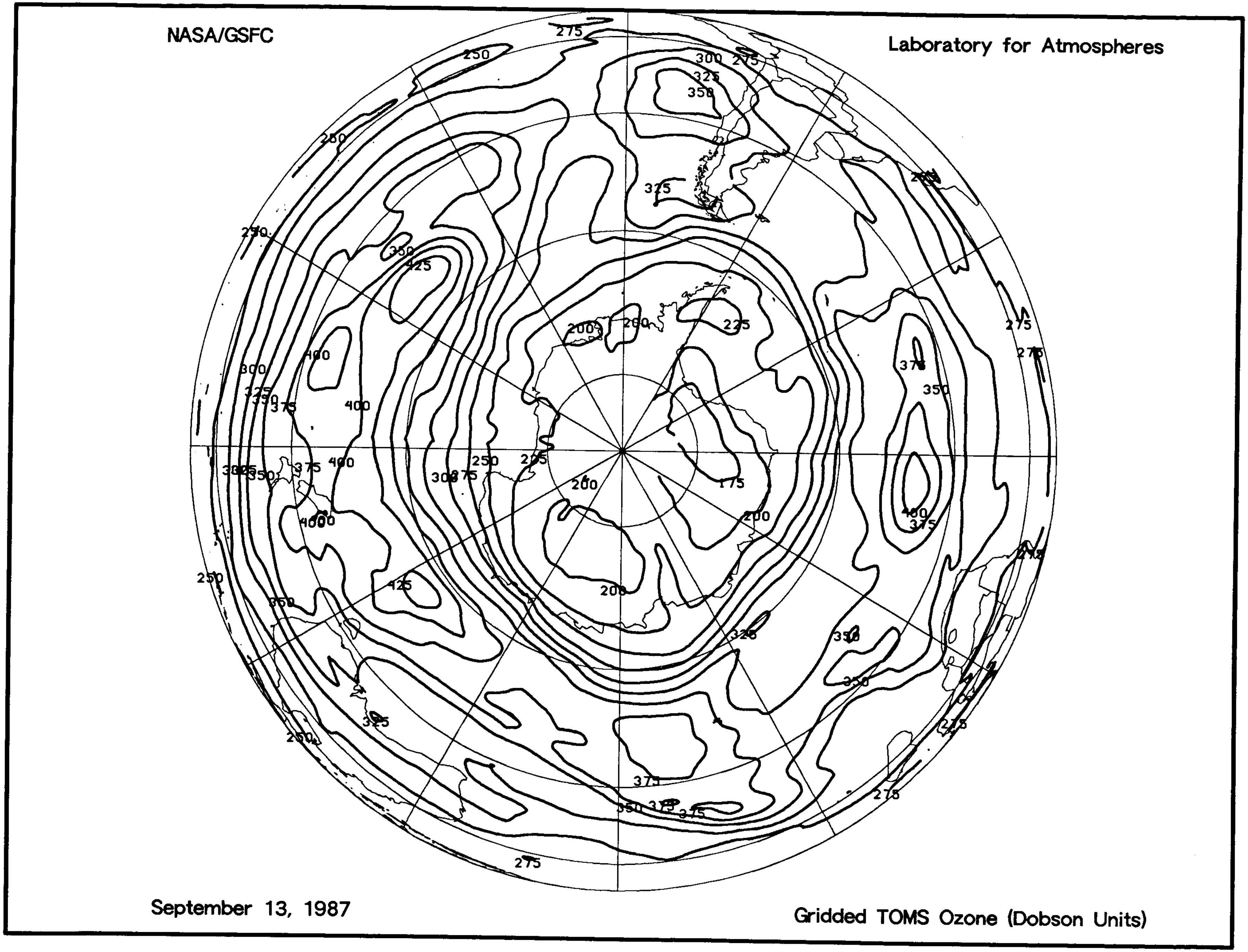
NASA/GSFC
Laboratory for Atmospheres
September 13, 1987
Gridded TOMS Ozone (Dobson Units)

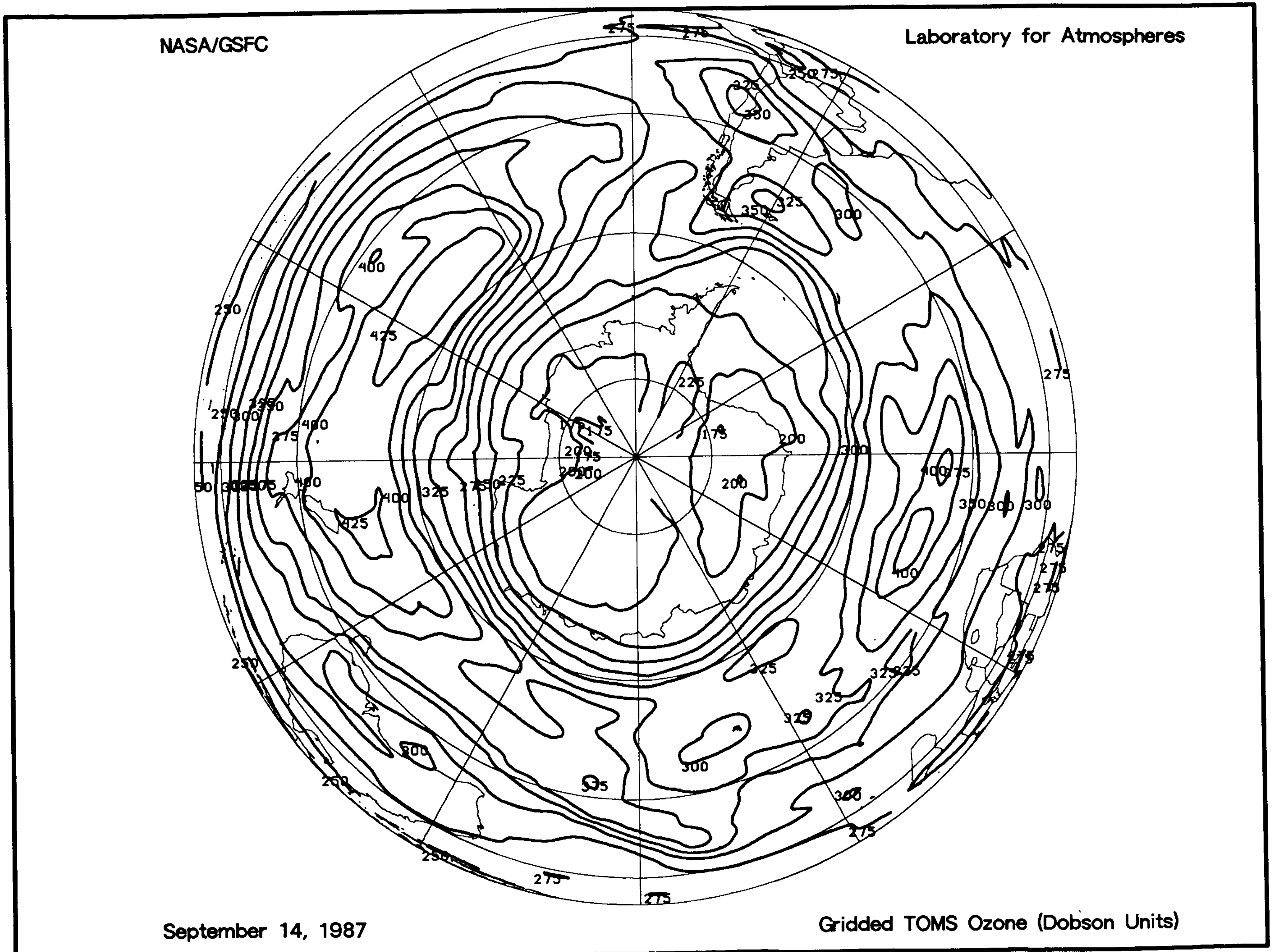
NASA/GSFC
Laboratory for Atmospheres
September 14, 1987
Gridded TOMS Ozone (Dobson Units)

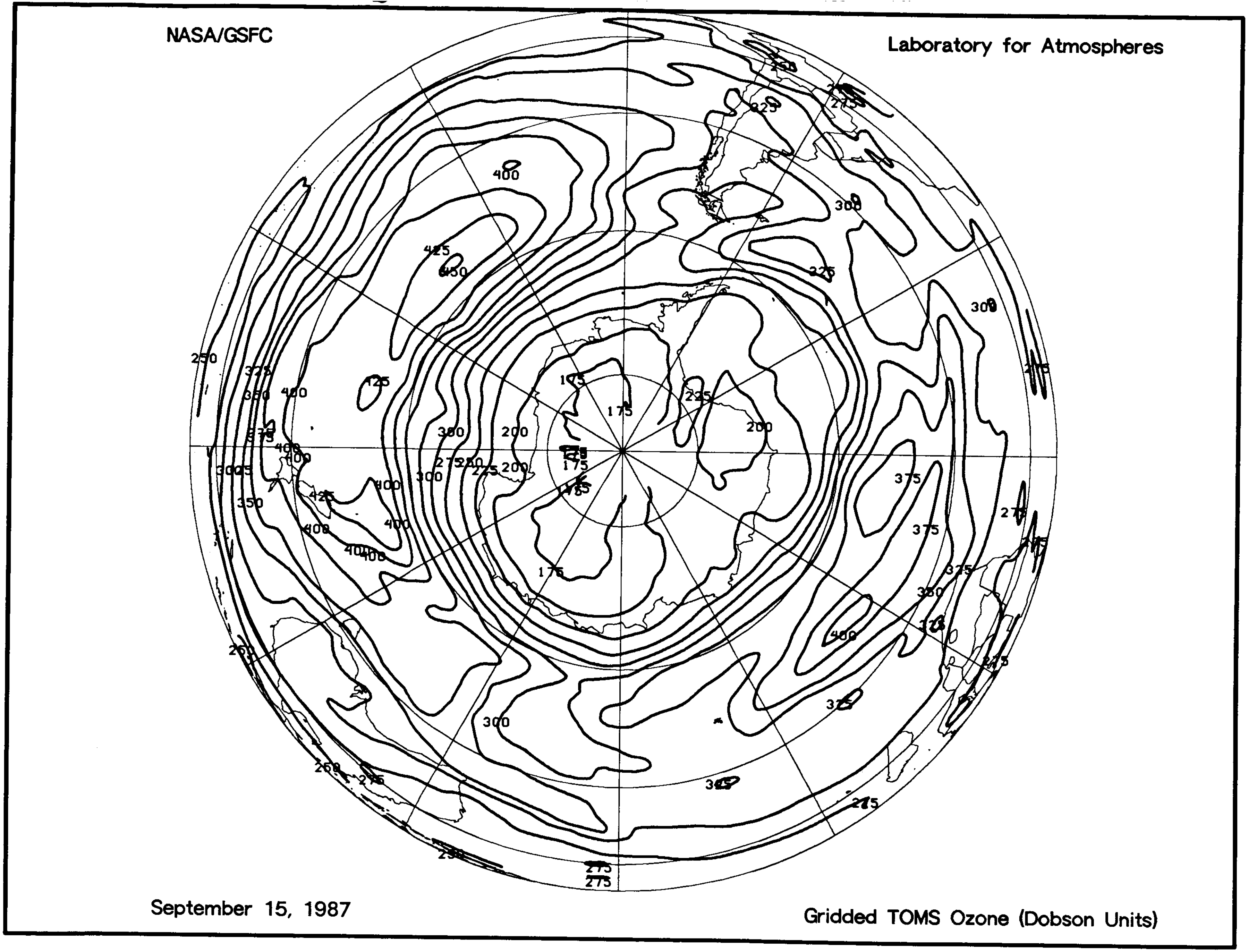
NASA/GSFC
Laboratory for Atmospheres
September 15, 1987
Gridded TOMS Ozone (Dobson Units)

NASA/GSFC

Laboratory for Atmospheres

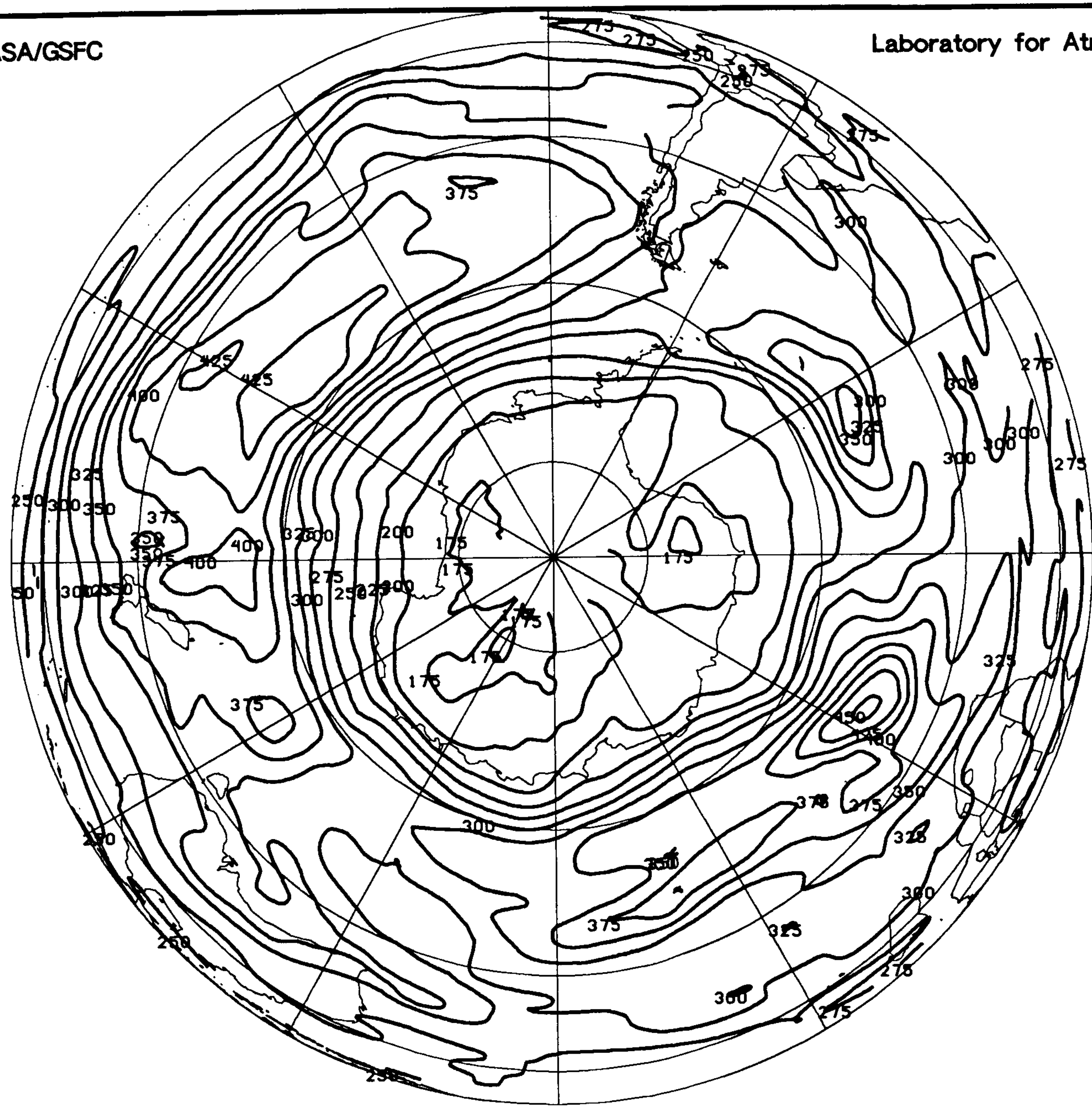

September 16, 1987

Gridded TOMS Ozone (Dobson Units)

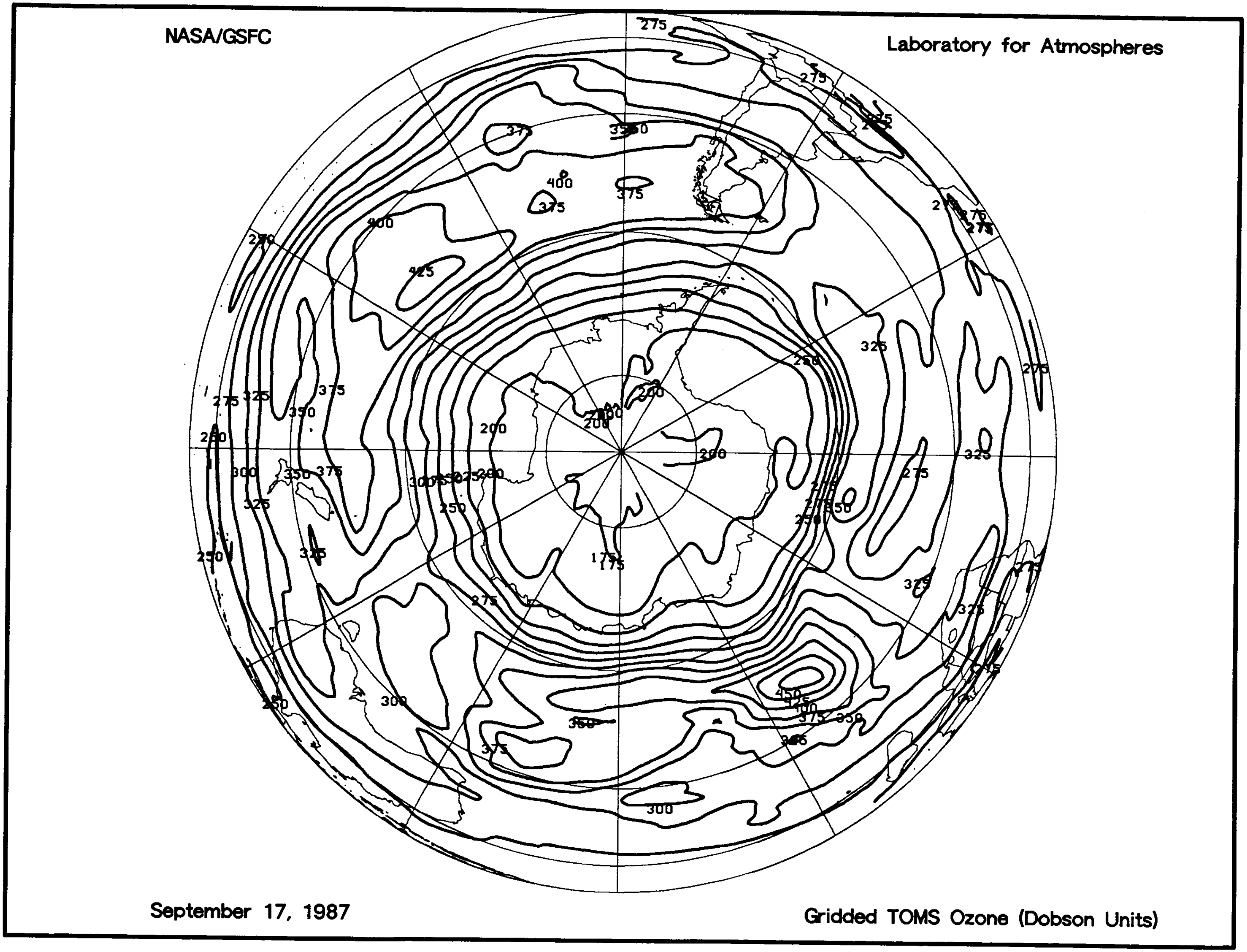
NASA/GSFC
Laboratory for Atmospheres
September 17, 1987
Gridded TOMS Ozone (Dobson Units)

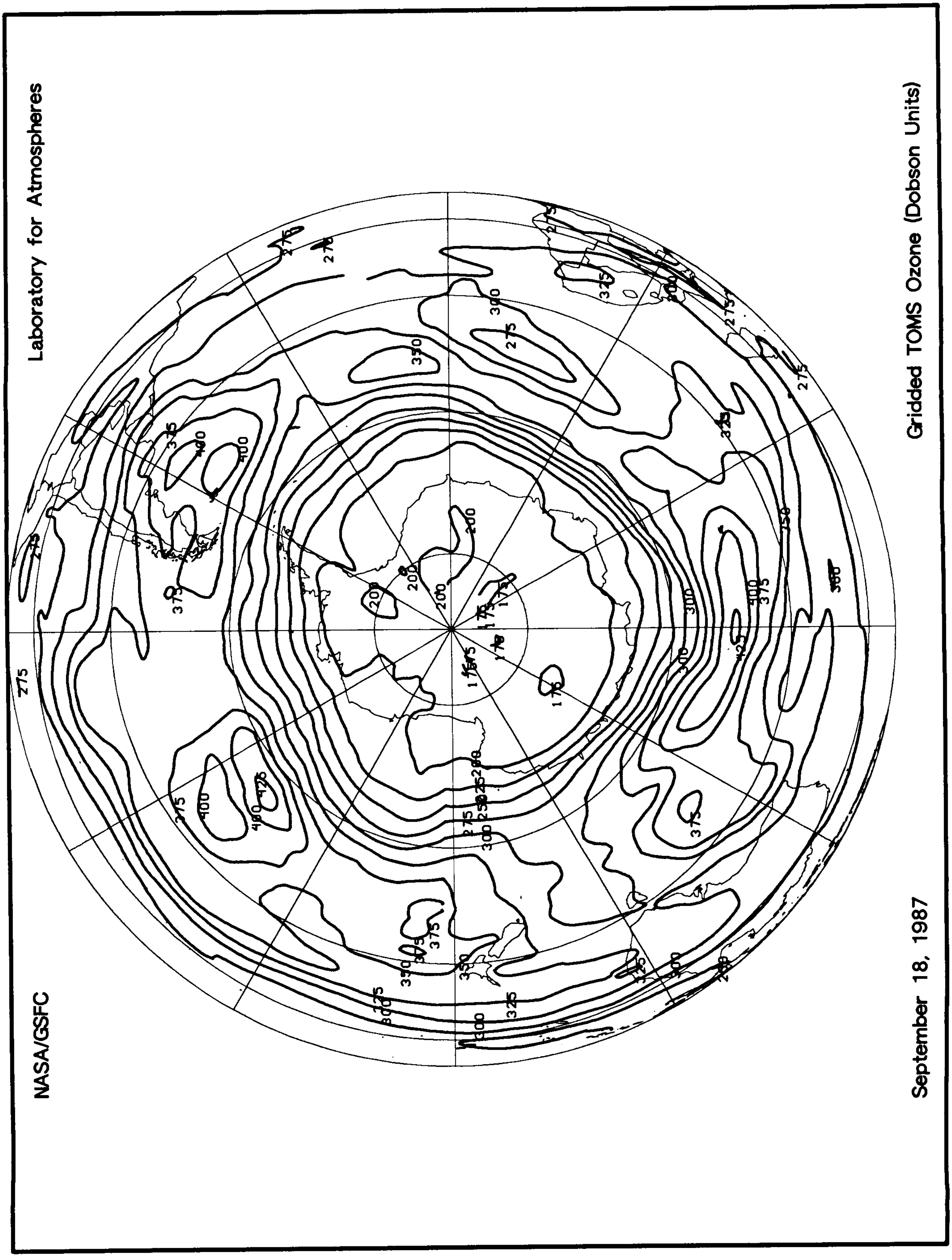
Laboratory for Atmospheres
NASA/GSFC
Gridded TOMS Ozone (Dobson Units)
September 18, 1987

NASA/GSFC

Laboratory for Atmospheres

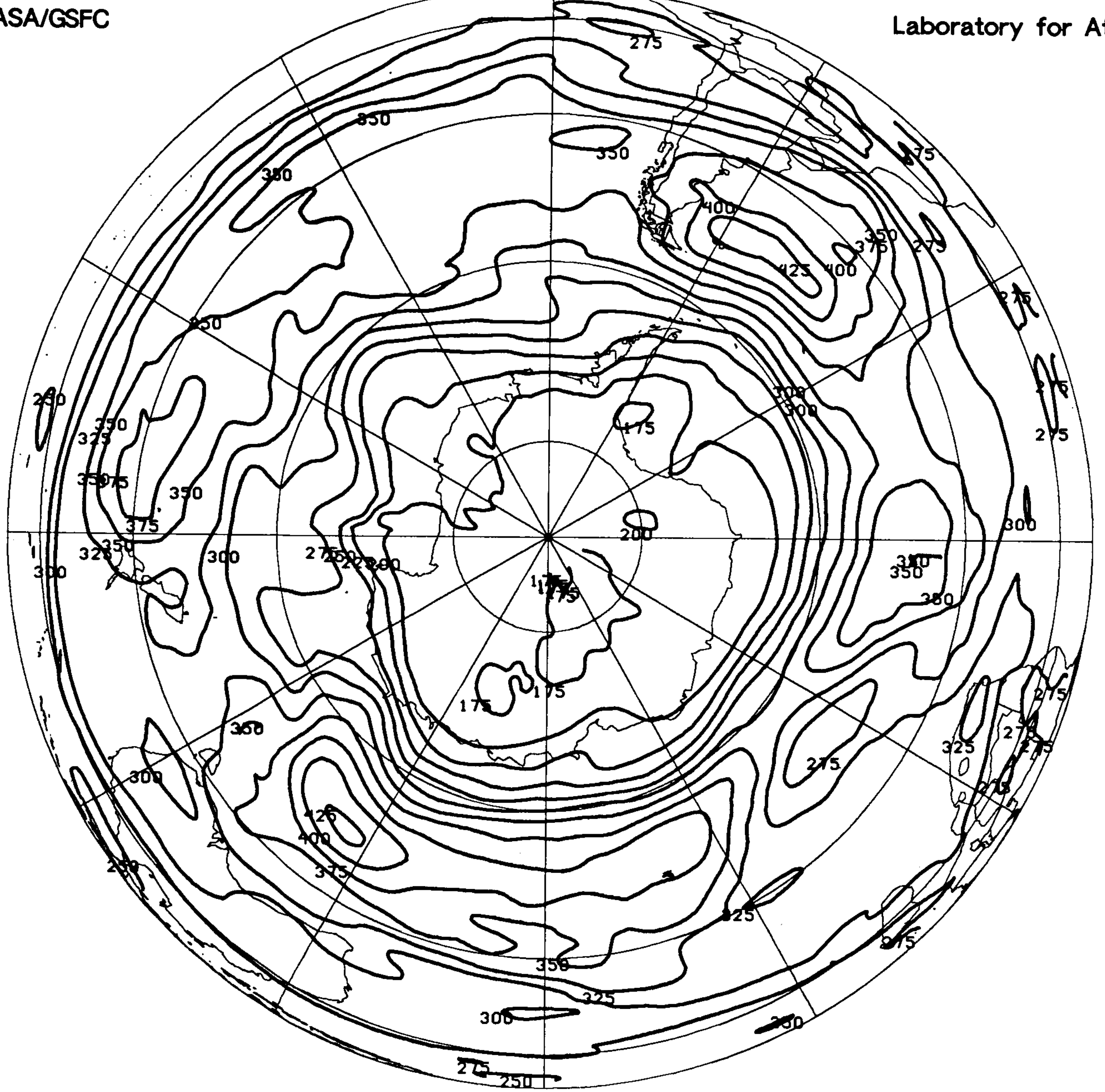

September 19, 1987

Gridded TOMS Ozone (Dobson Units)

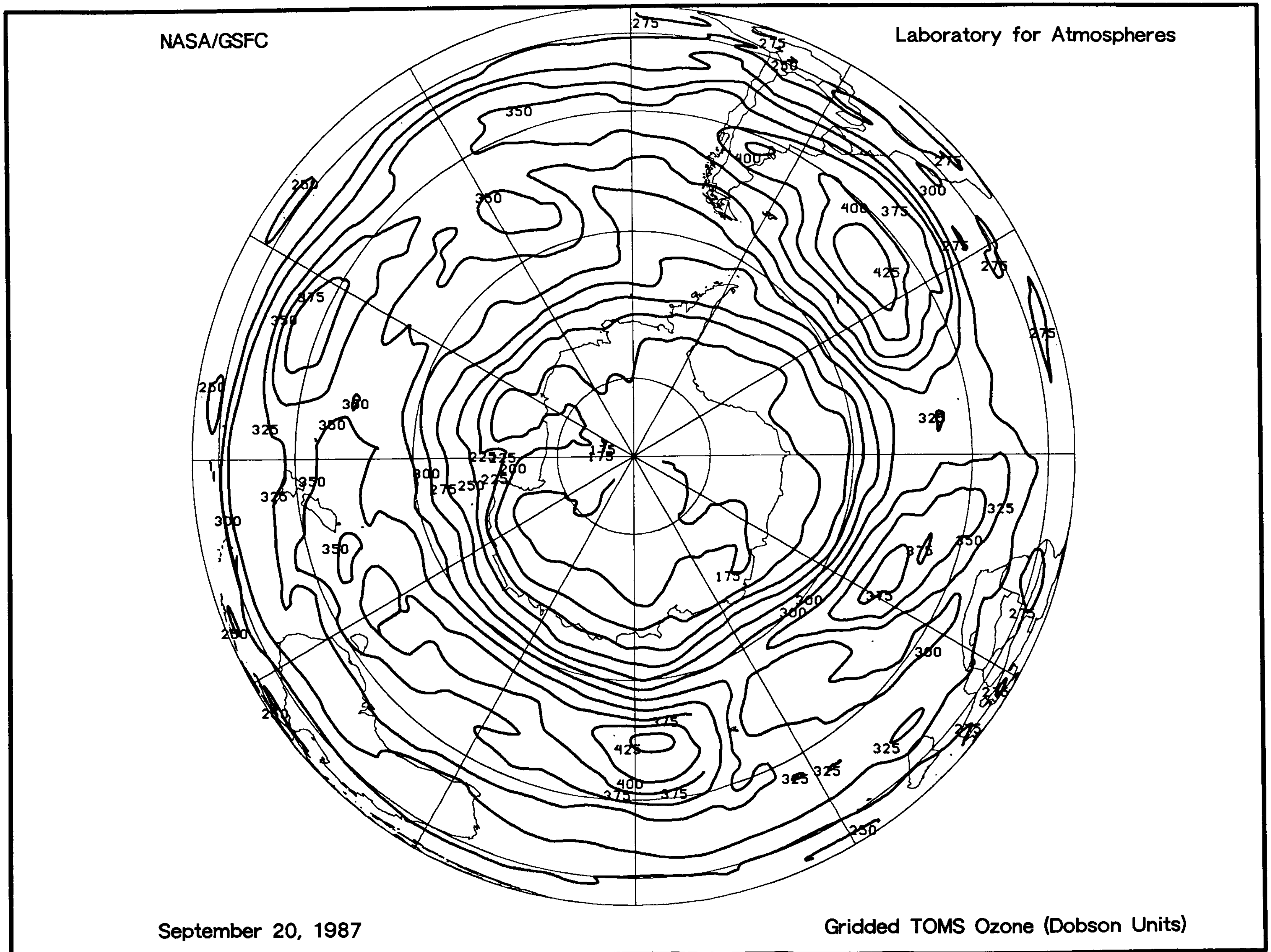
NASA/GSFC
Laboratory for Atmospheres
September 20, 1987
Gridded TOMS Ozone (Dobson Units)

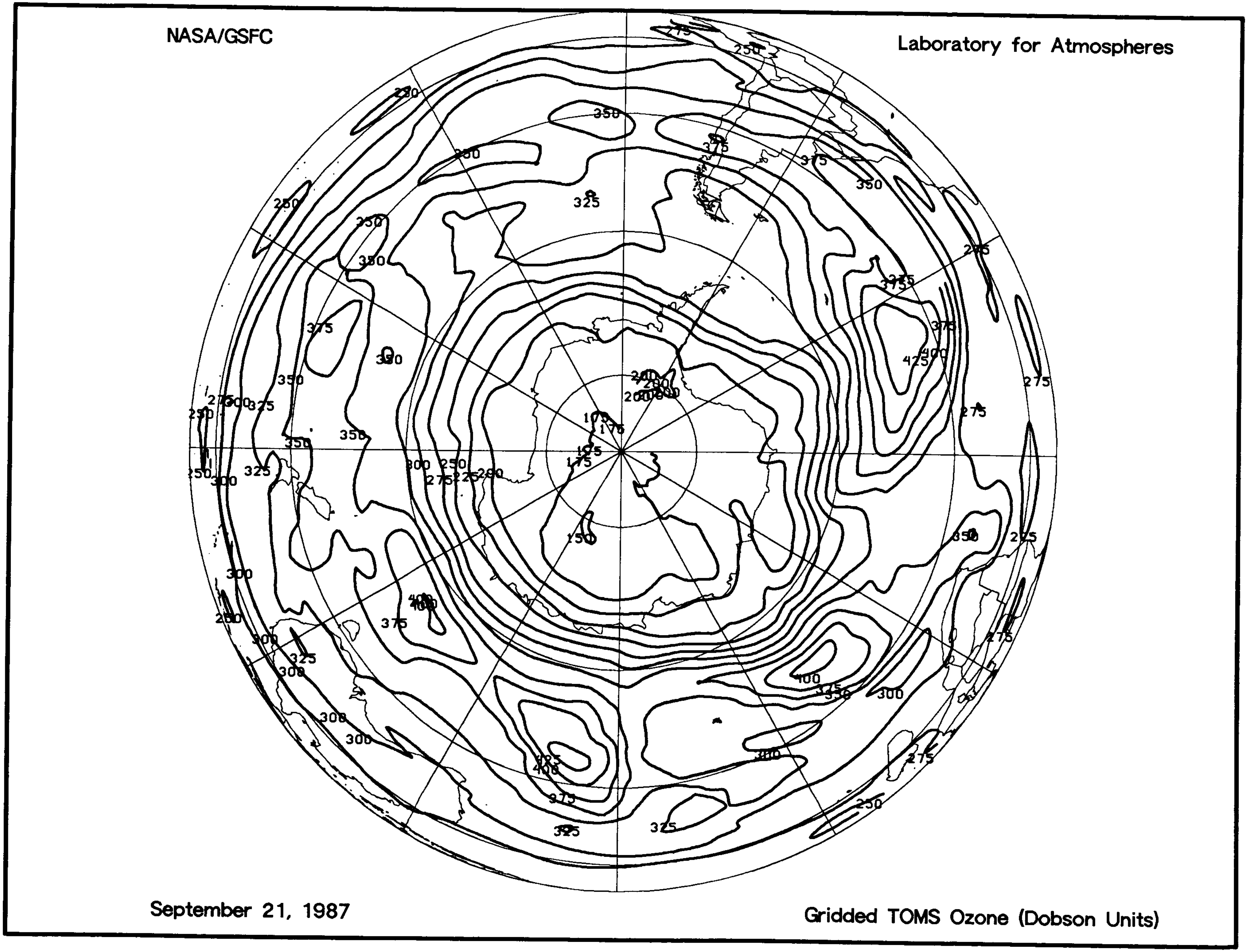
NASA/GSFC
Laboratory for Atmospheres
September 21, 1987
Gridded TOMS Ozone (Dobson Units)

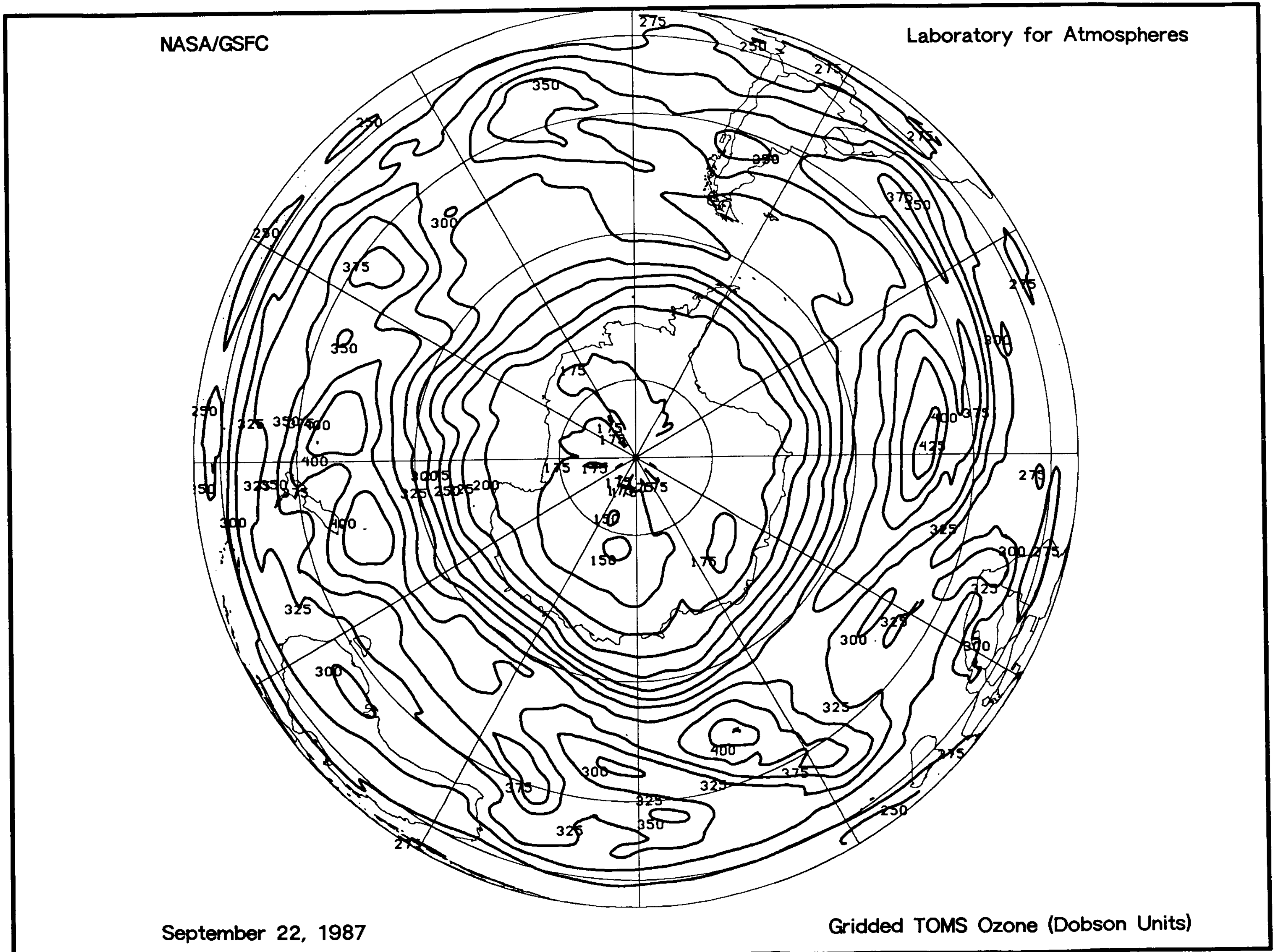
NASA/GSFC
Laboratory for Atmospheres
September 22, 1987
Gridded TOMS Ozone (Dobson Units)

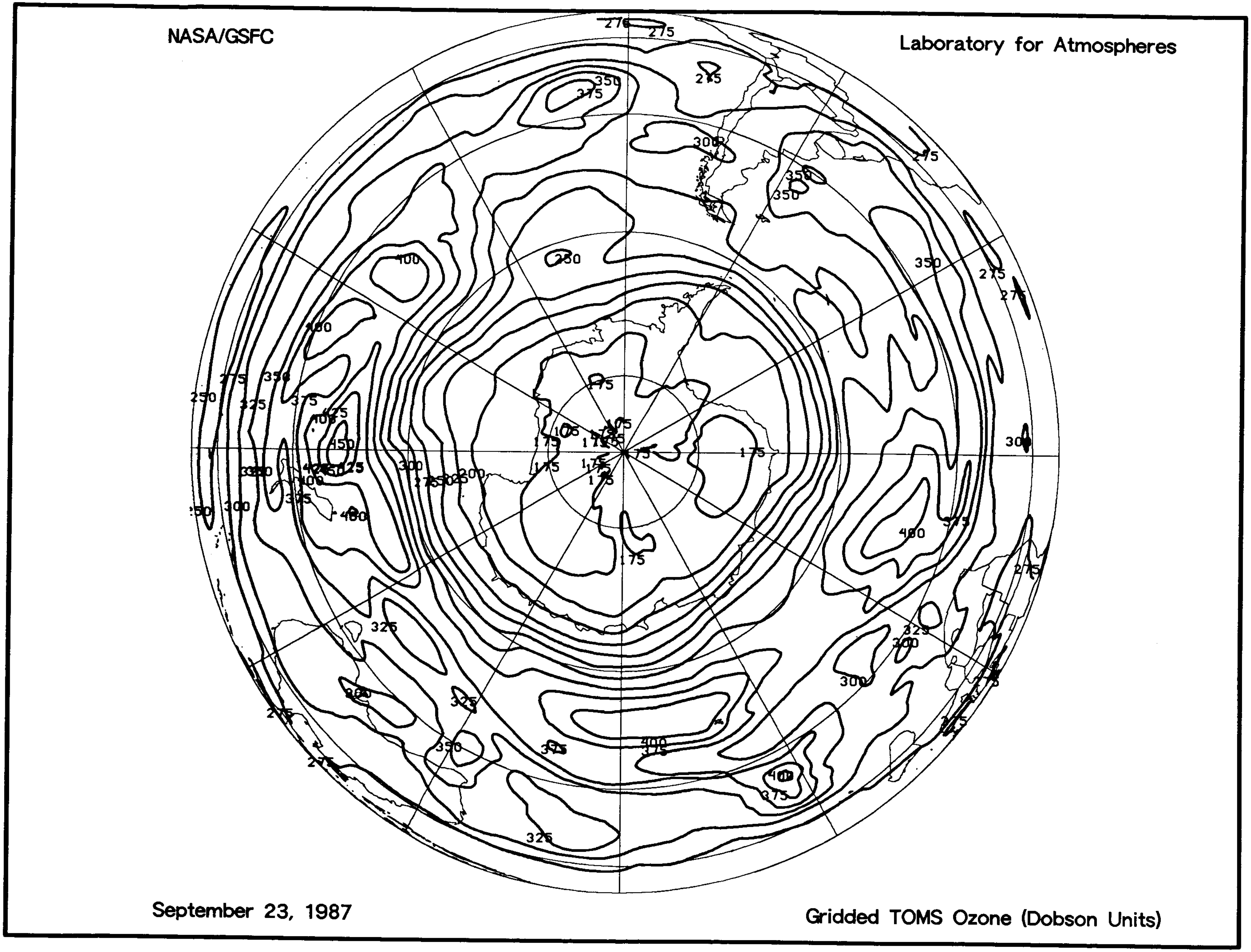

NASA/GSFC
Laboratory for Atmospheres
September 23, 1987
Gridded TOMS Ozone (Dobson Units)

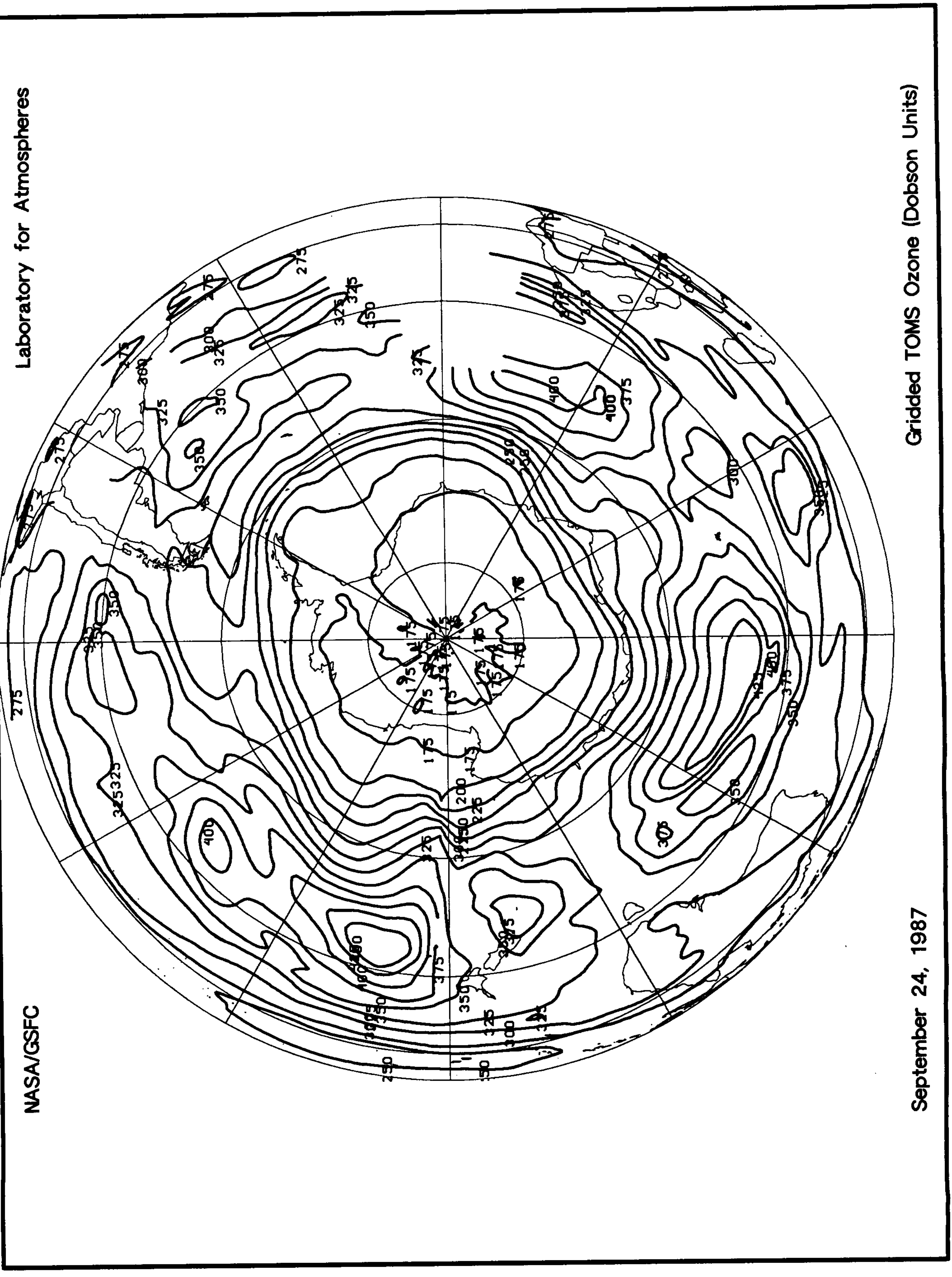
Laboratory for Atmospheres
Gridded TOMS Ozone (Dobson Units)
NASA/GSFC
September 24, 1987

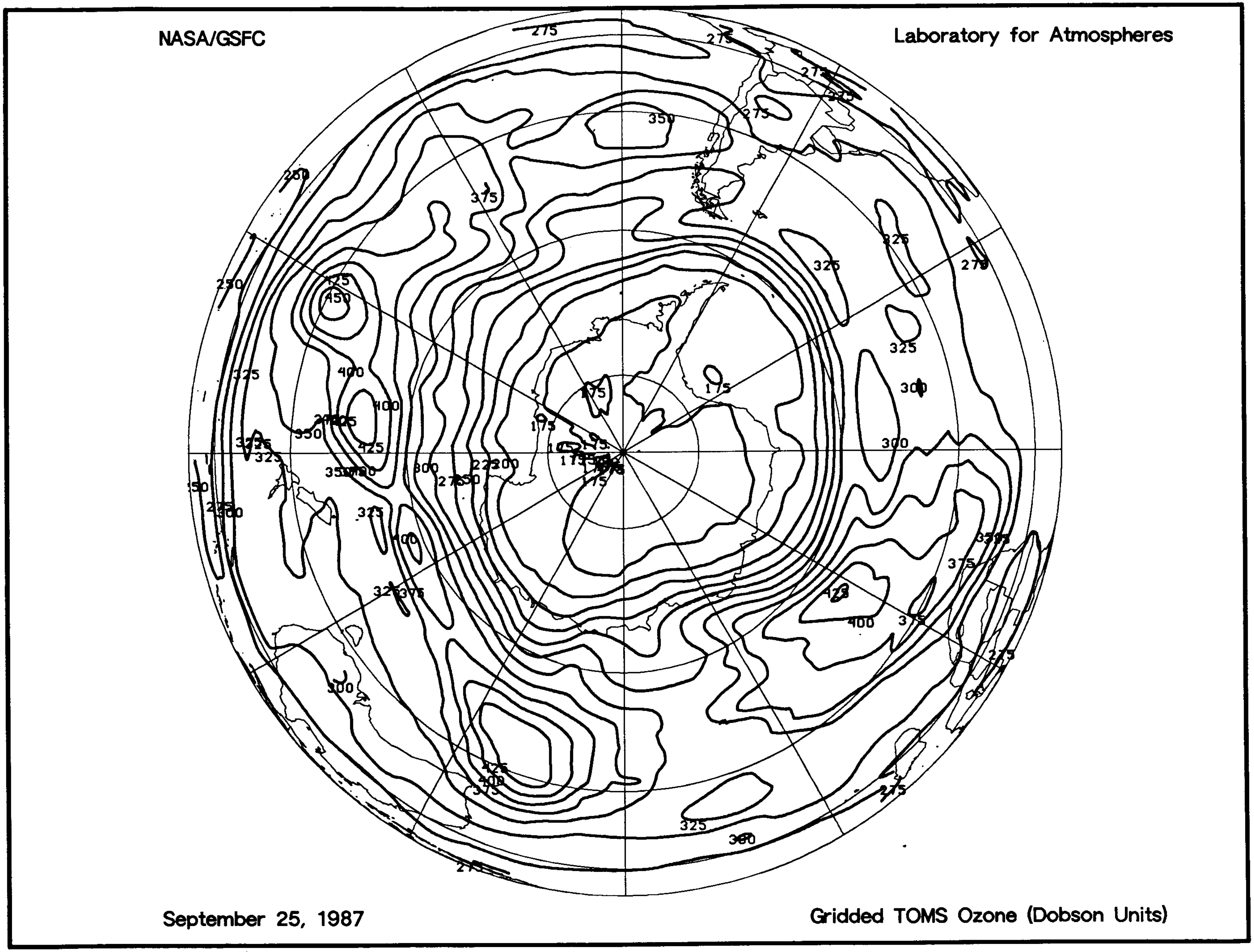
NASA/GSFC
Laboratory for Atmospheres
September 25, 1987
Gridded TOMS Ozone (Dobson Units)

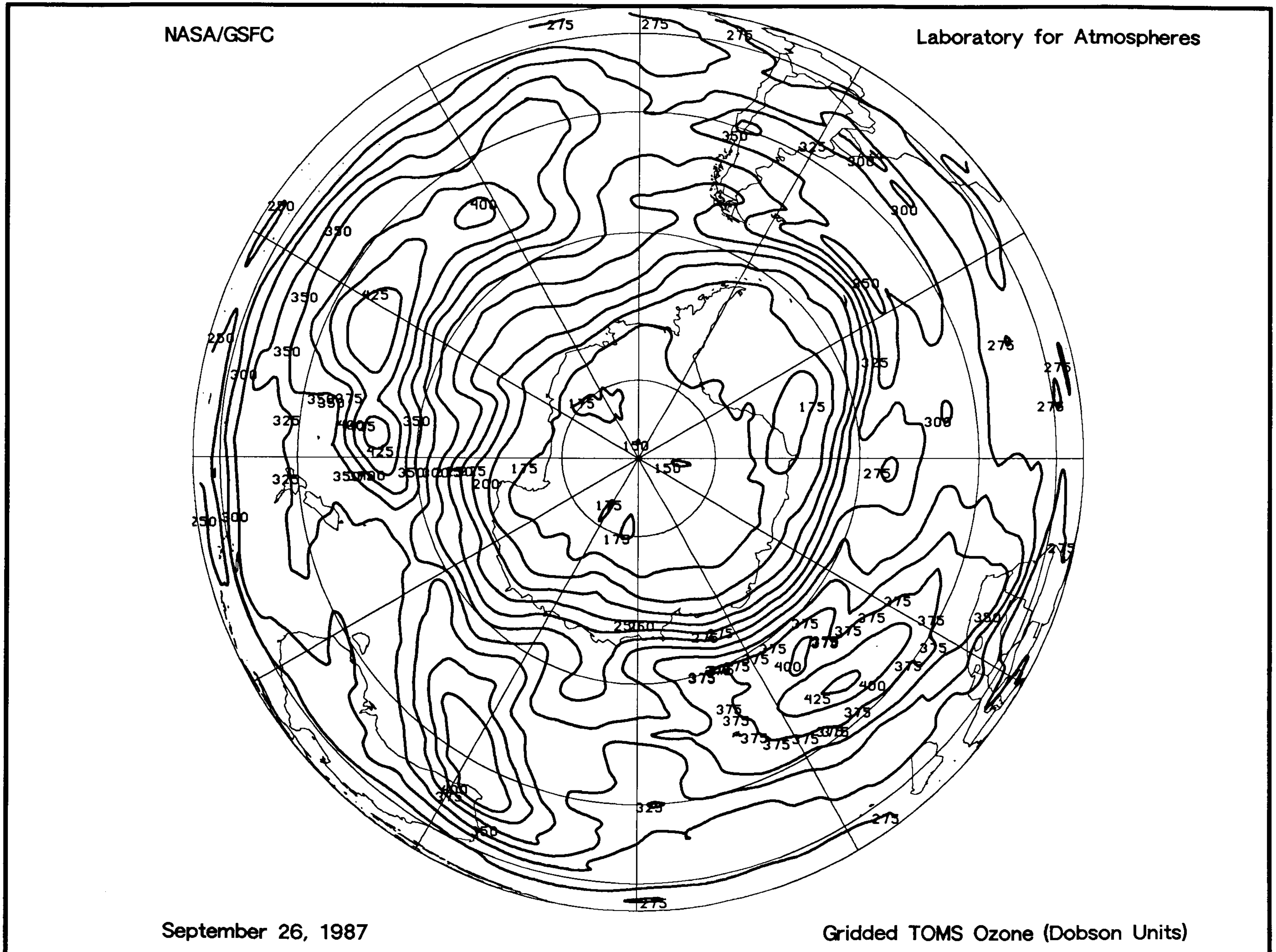
NASA/GSFC
Laboratory for Atmospheres
September 26, 1987
Gridded TOMS Ozone (Dobson Units)

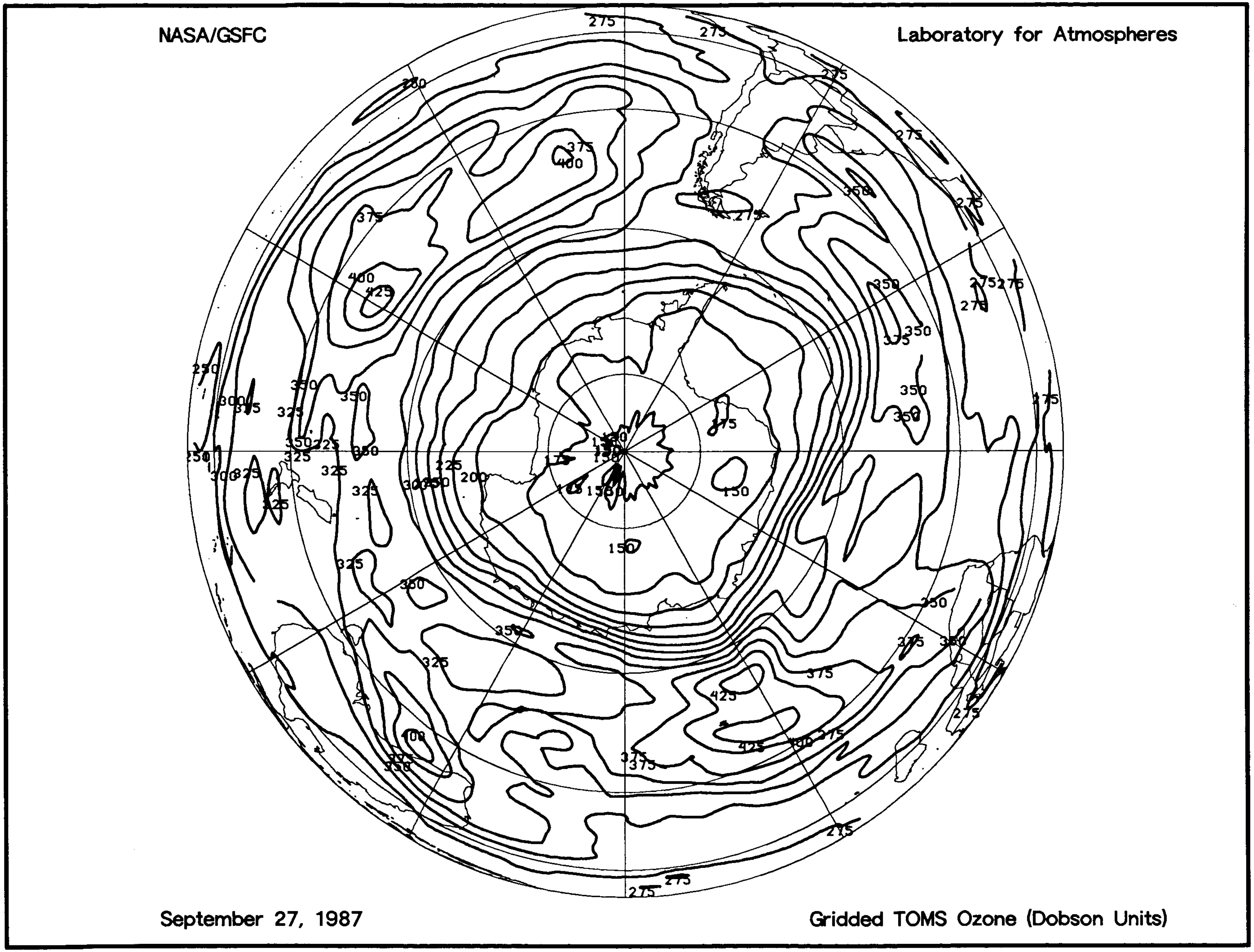
NASA/GSFC
Laboratory for Atmospheres
September 27, 1987
Gridded TOMS Ozone (Dobson Units)

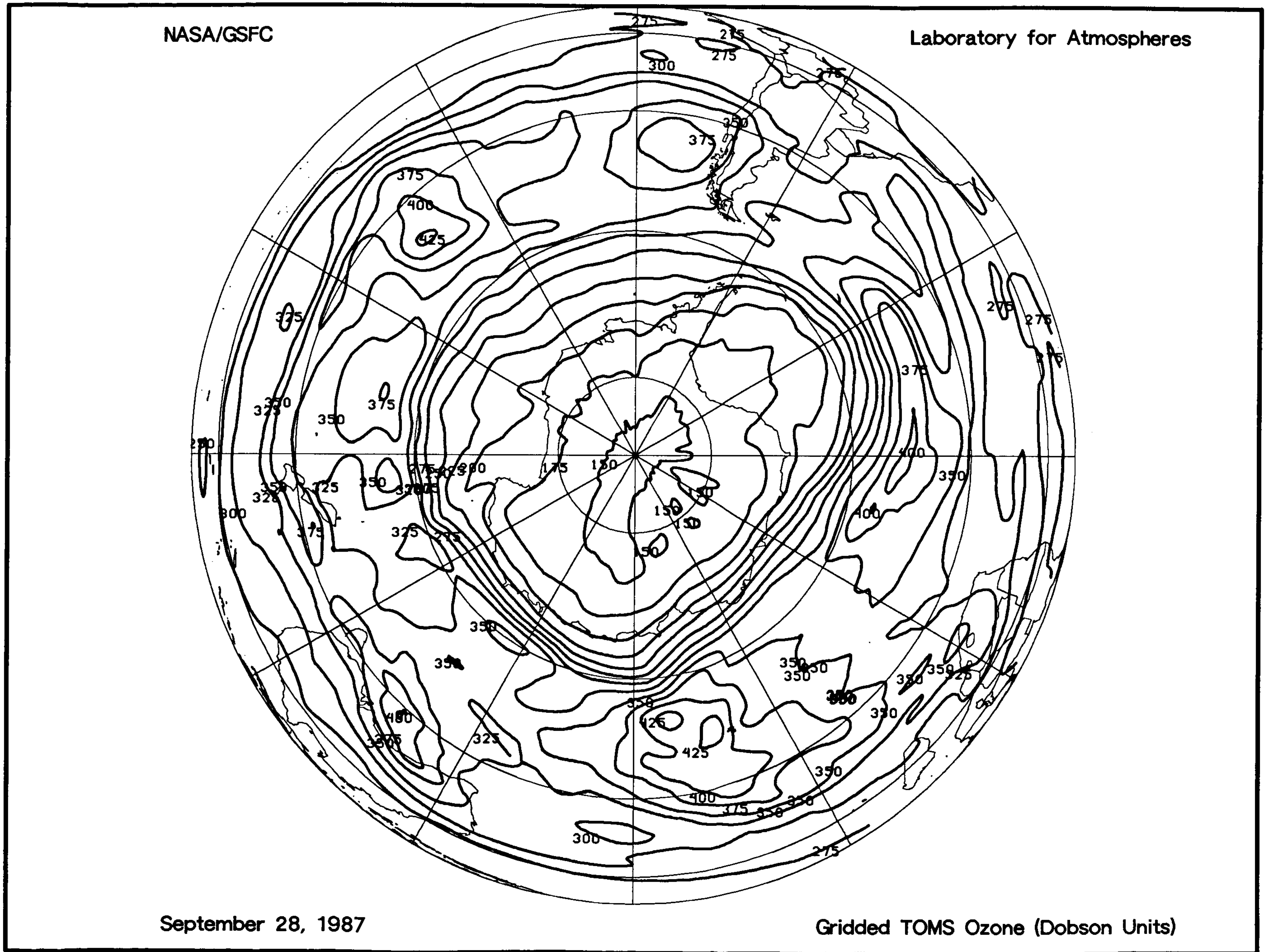
NASA/GSFC
Laboratory for Atmospheres
September 28, 1987
Gridded TOMS Ozone (Dobson Units)

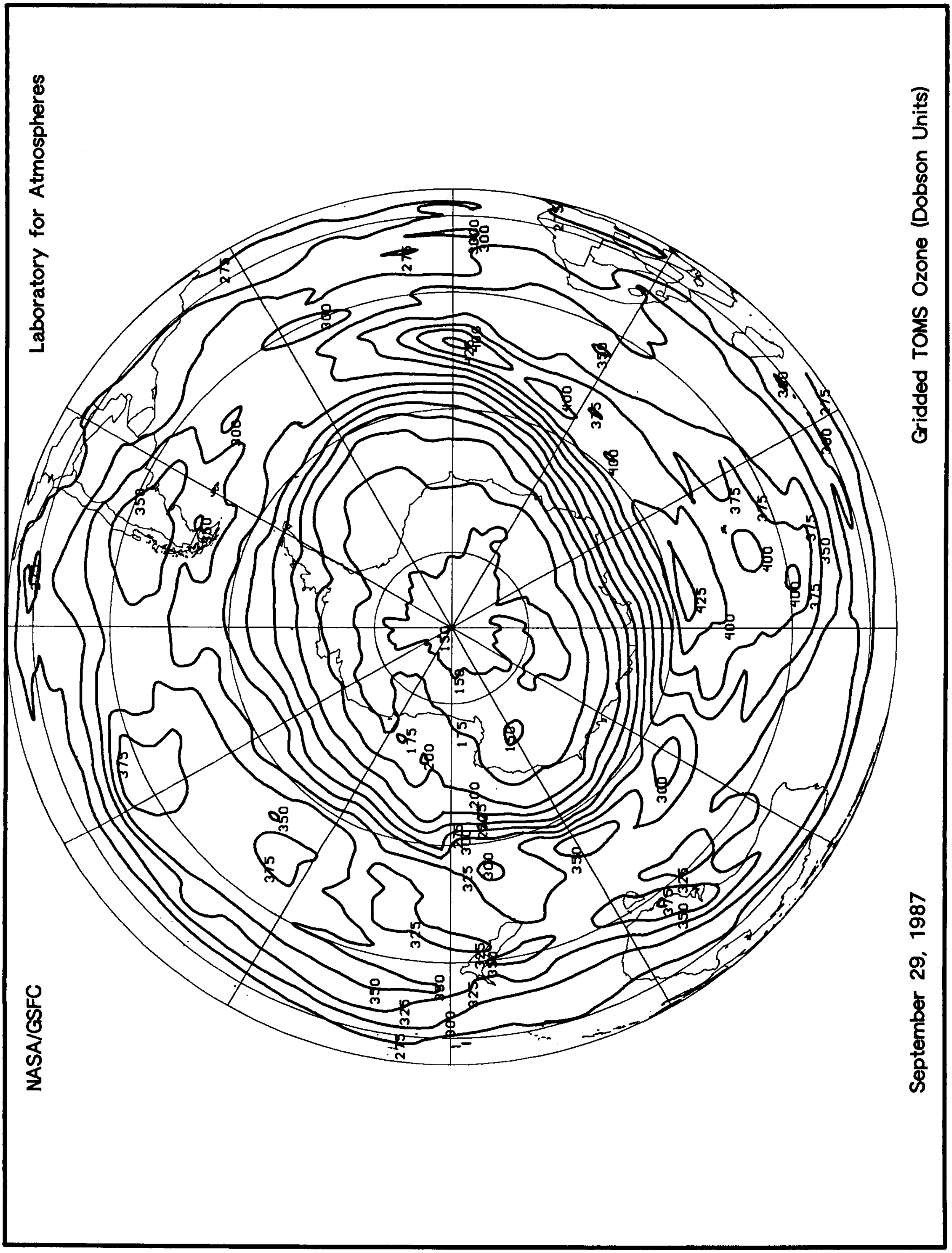
Laboratory for Atmospheres
NASA/GSFC
September 29, 1987
Gridded TOMS Ozone (Dobson Units)

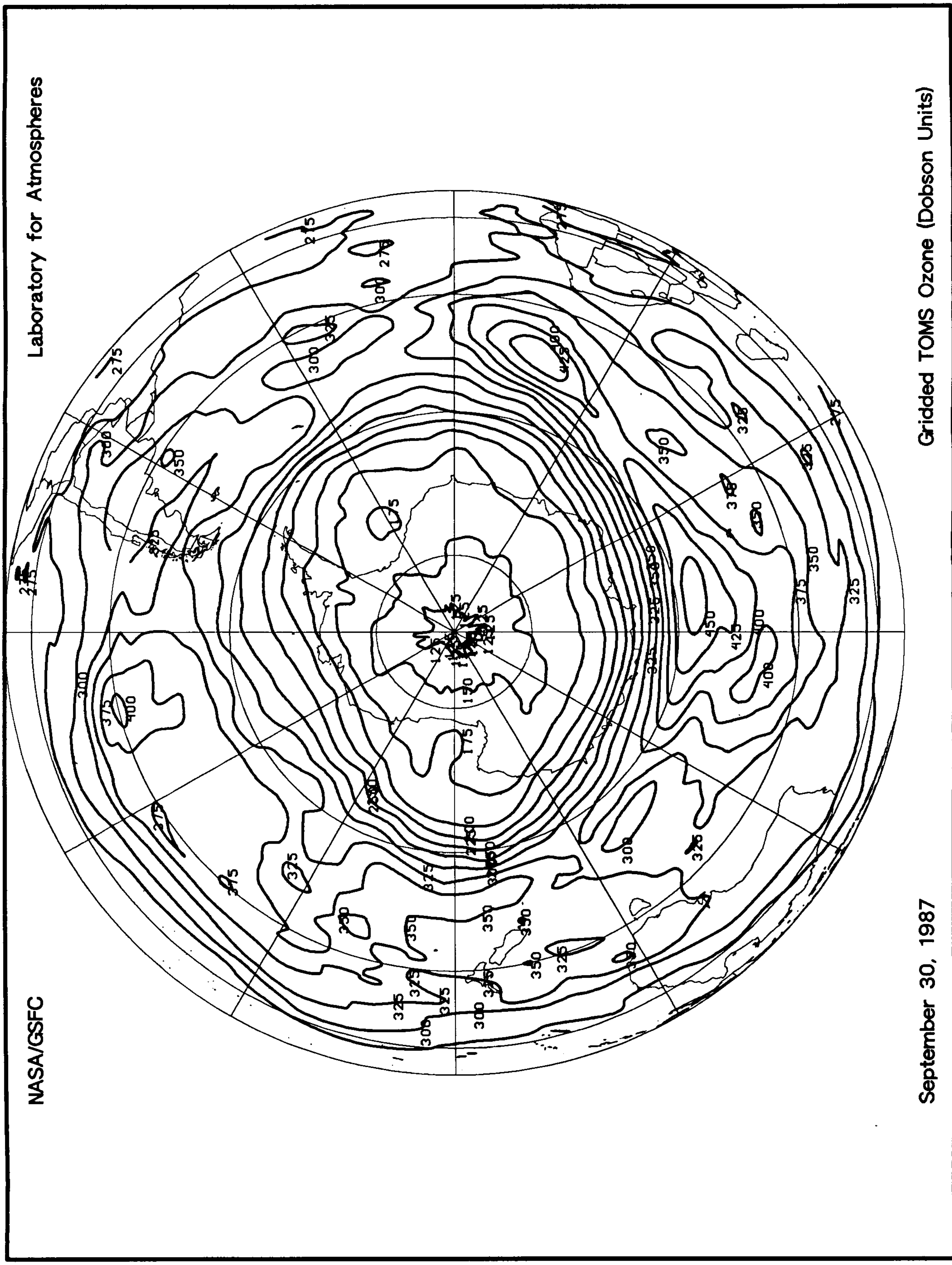
NASA/GSFC
Laboratory for Atmospheres
September 30, 1987
Gridded TOMS Ozone (Dobson Units)

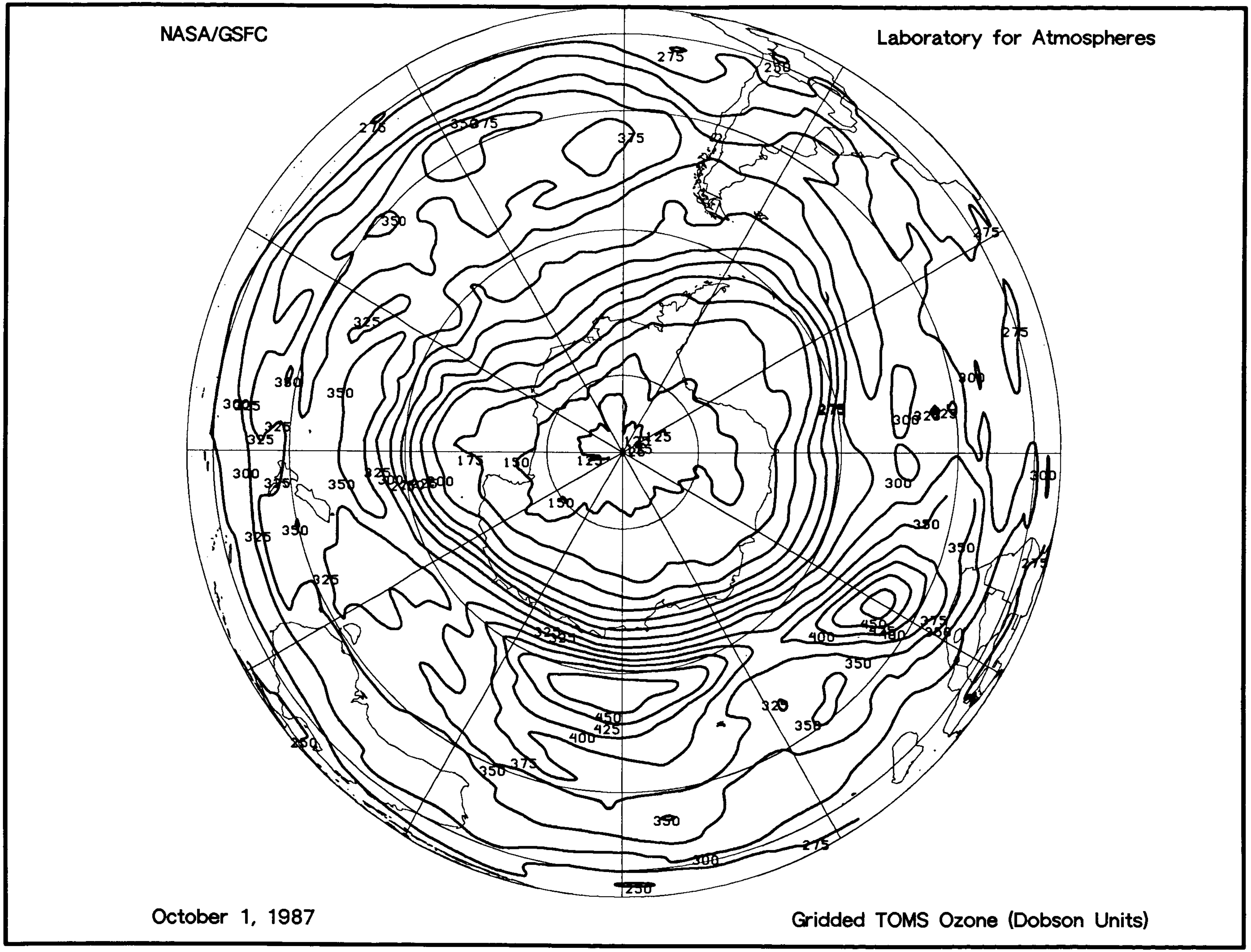
NASA/GSFC
Laboratory for Atmospheres
October 1, 1987
Gridded TOMS Ozone (Dobson Units)

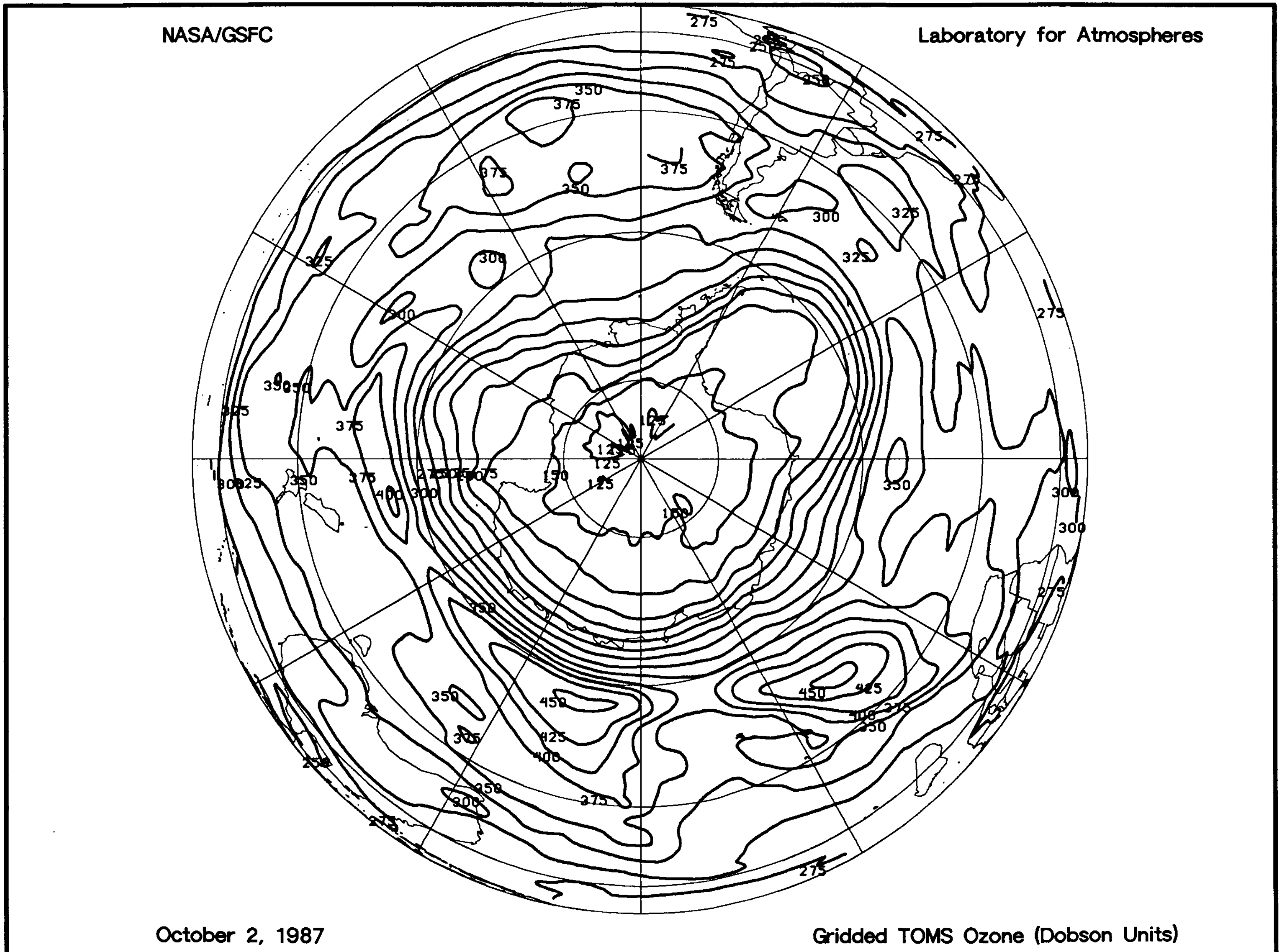
NASA/GSFC
Laboratory for Atmospheres
October 2, 1987
Gridded TOMS Ozone (Dobson Units)

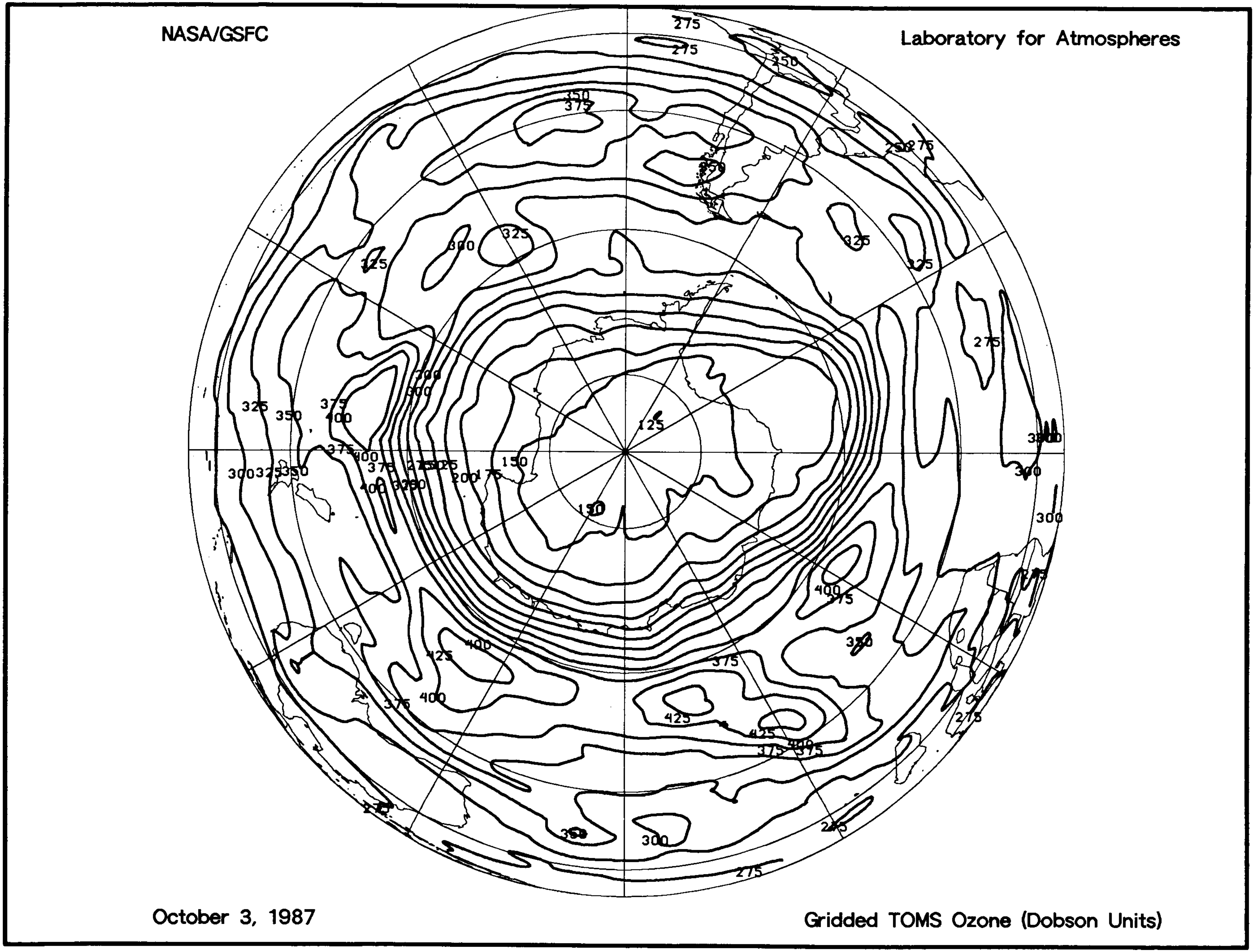
NASA/GSFC
Laboratory for Atmospheres
October 3, 1987
Gridded TOMS Ozone (Dobson Units)

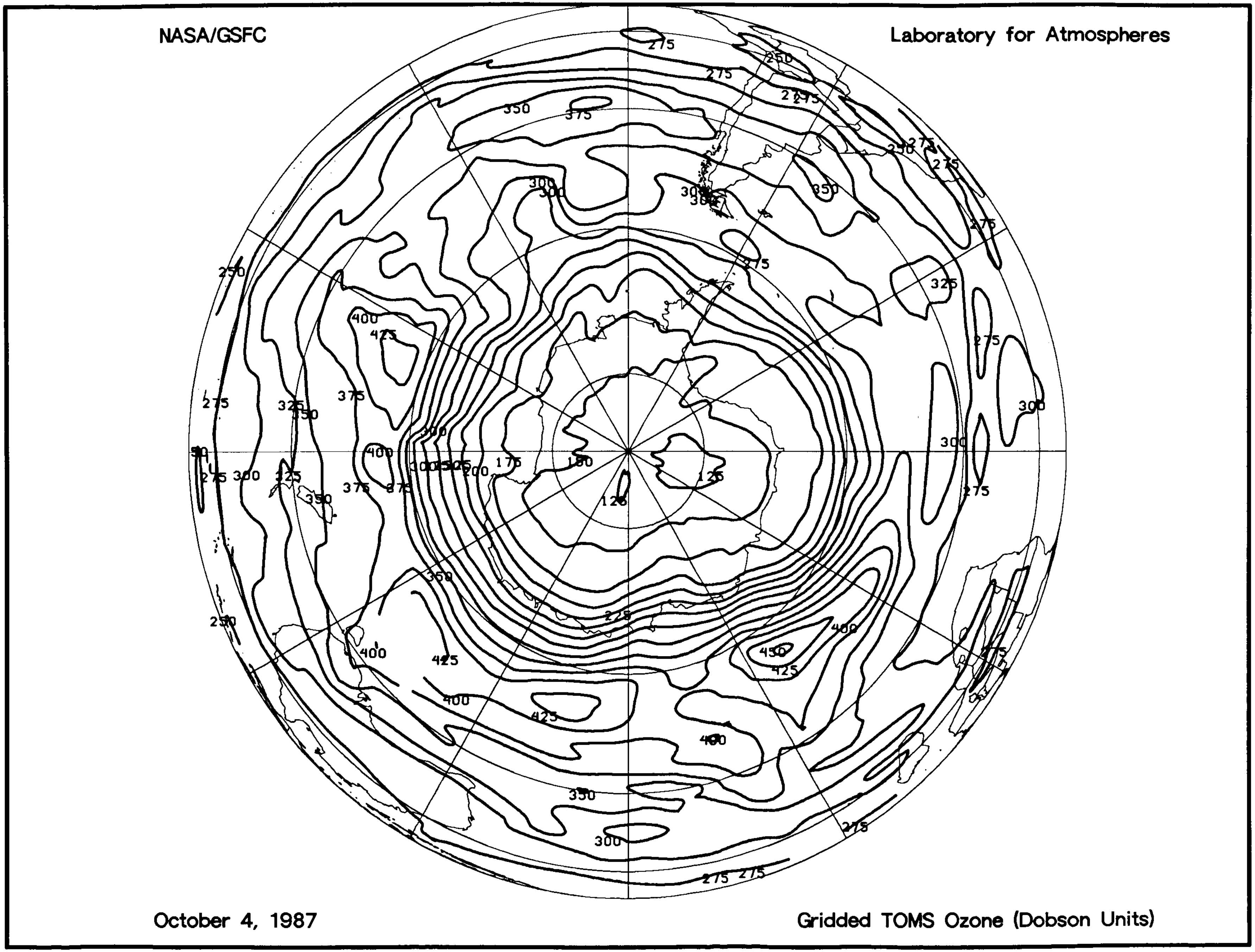

NASA/GSFC
Laboratory for Atmospheres
October 4, 1987
Gridded TOMS Ozone (Dobson Units)

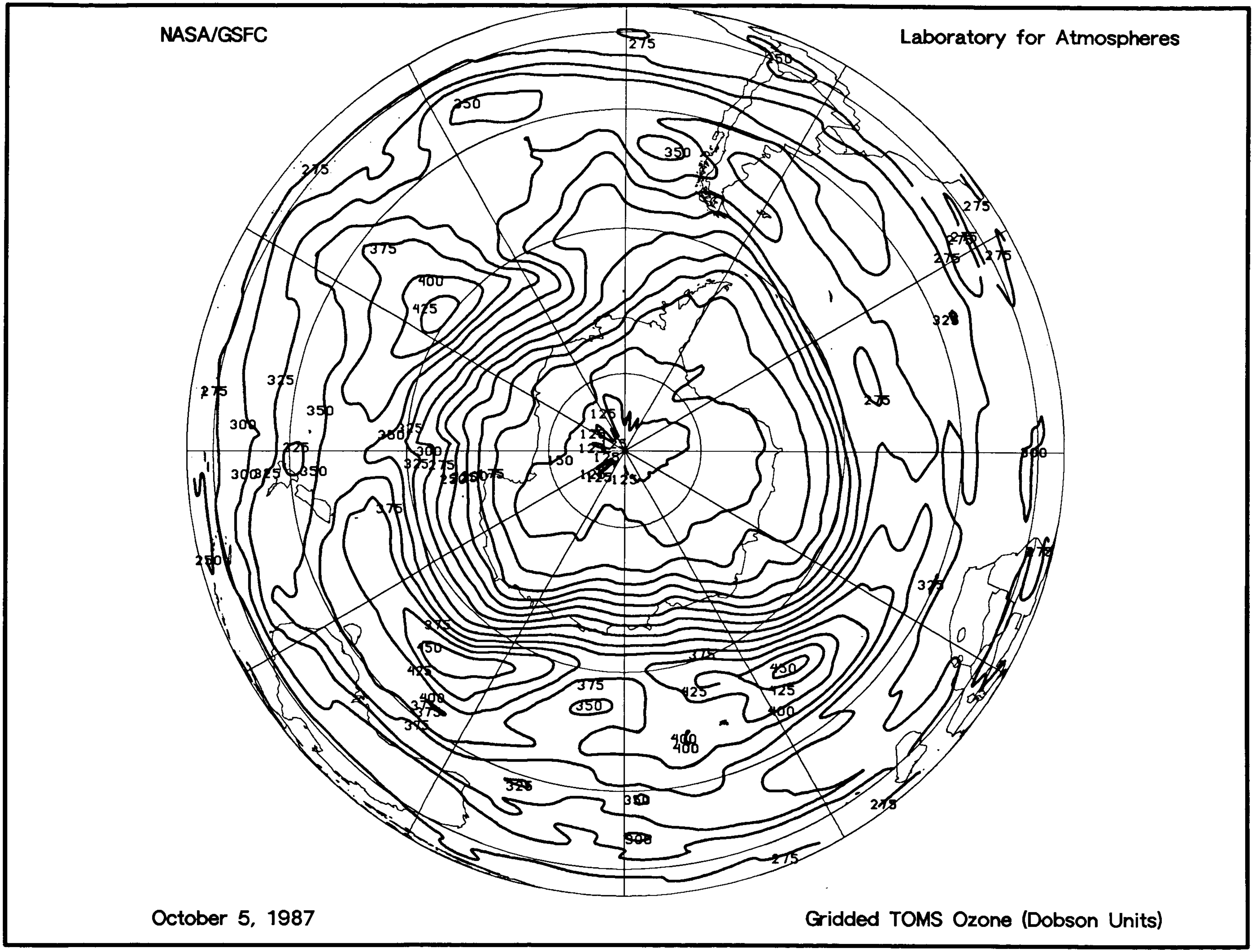
NASA/GSFC
Laboratory for Atmospheres
October 5, 1987
Gridded TOMS Ozone (Dobson Units)
275
350
375
400
425
450
300
325
250
125
150

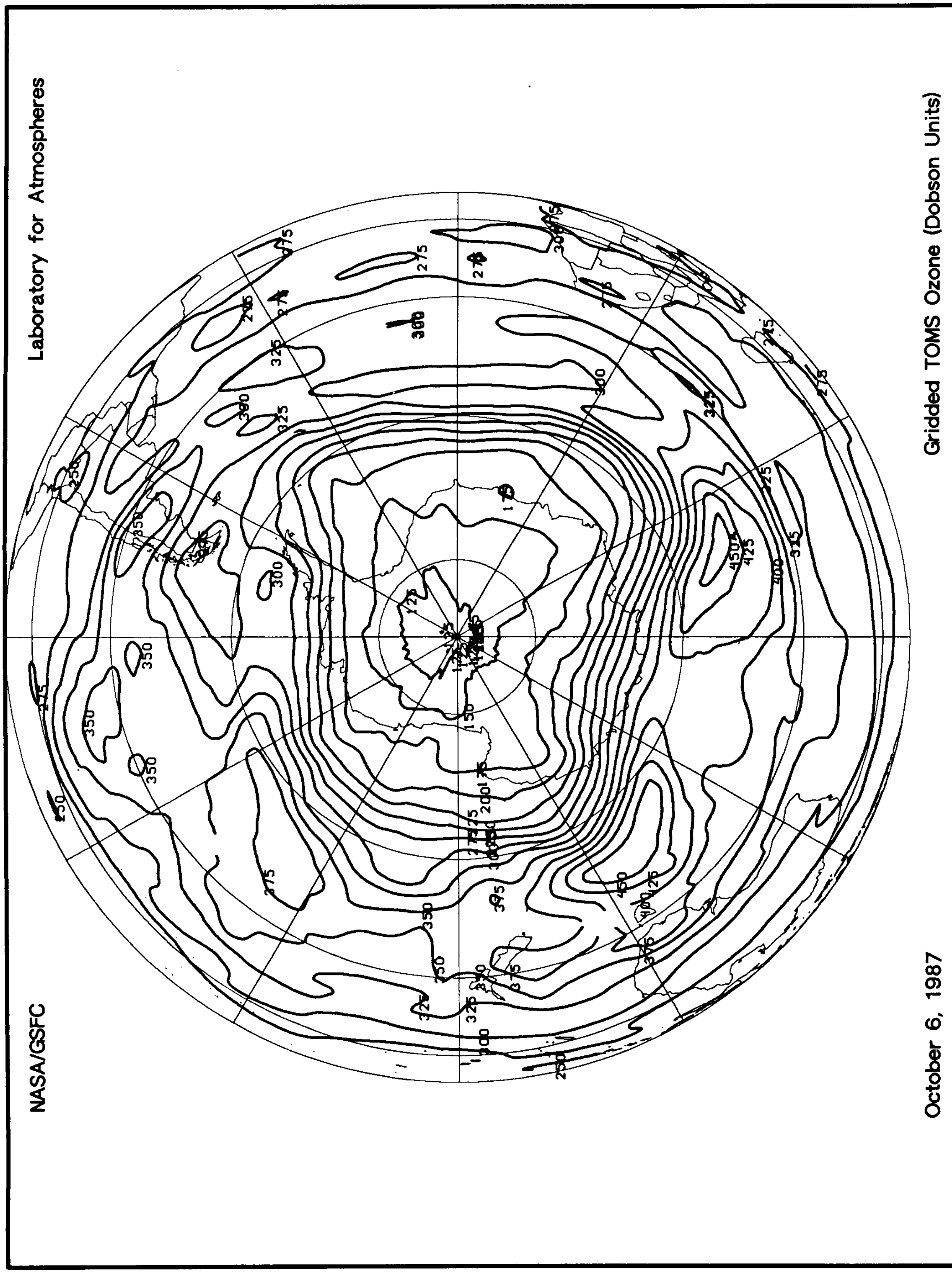

Laboratory for Atmospheres
NASA/GSFC
Gridded TOMS Ozone (Dobson Units)
October 6, 1987

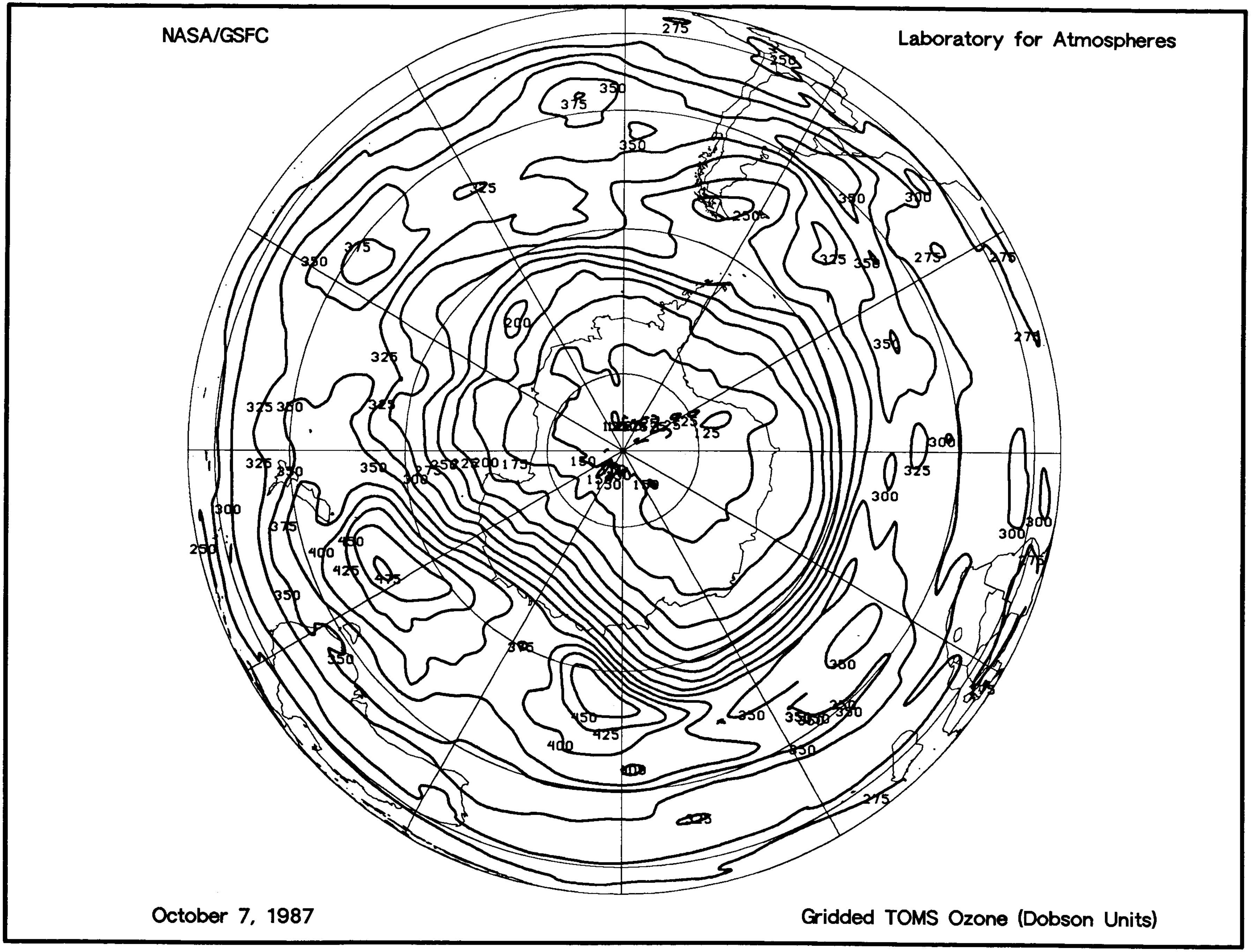
NASA/GSFC
Laboratory for Atmospheres
October 7, 1987
Gridded TOMS Ozone (Dobson Units)

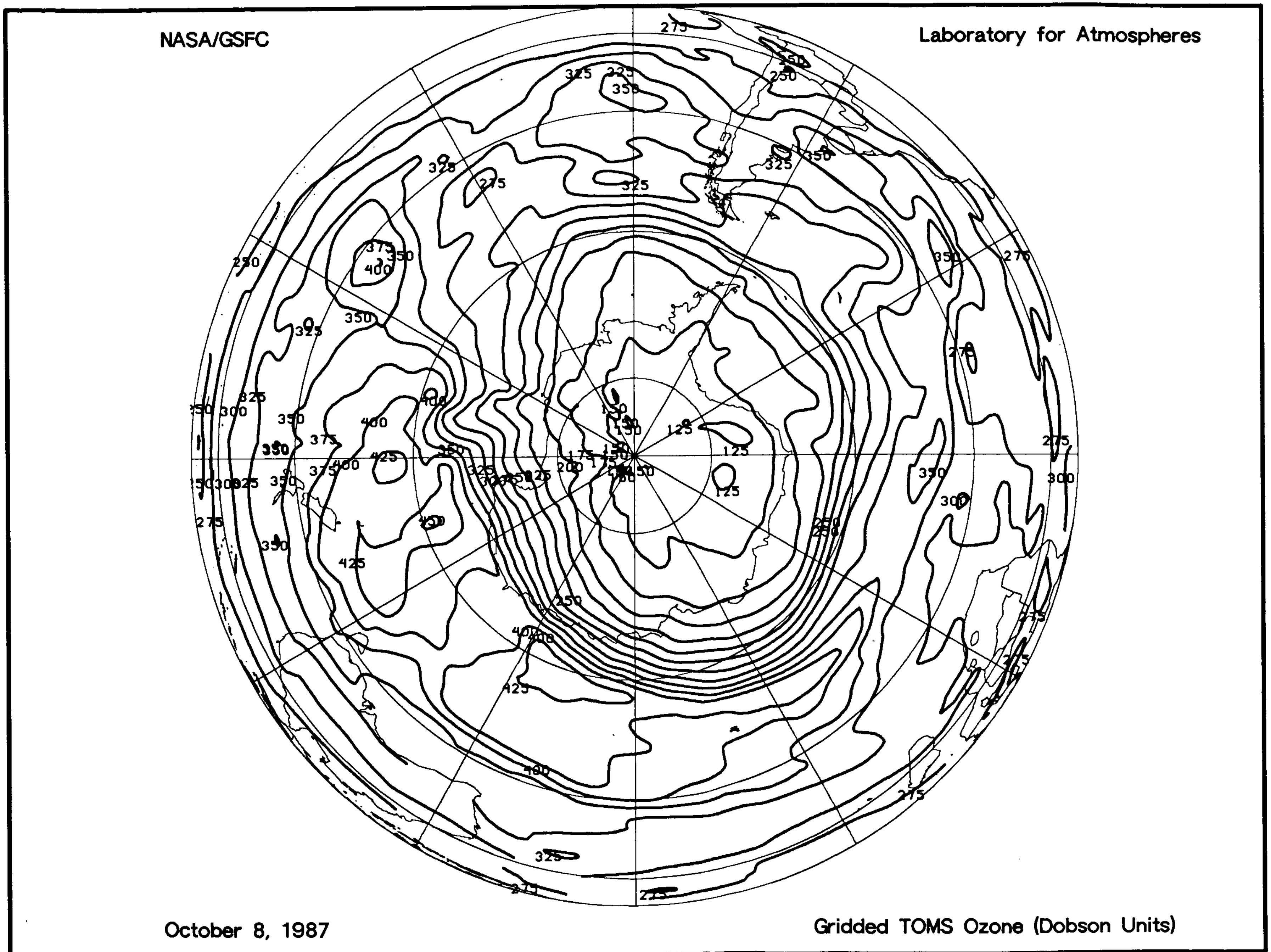
NASA/GSFC
Laboratory for Atmospheres
October 8, 1987
Gridded TOMS Ozone (Dobson Units)

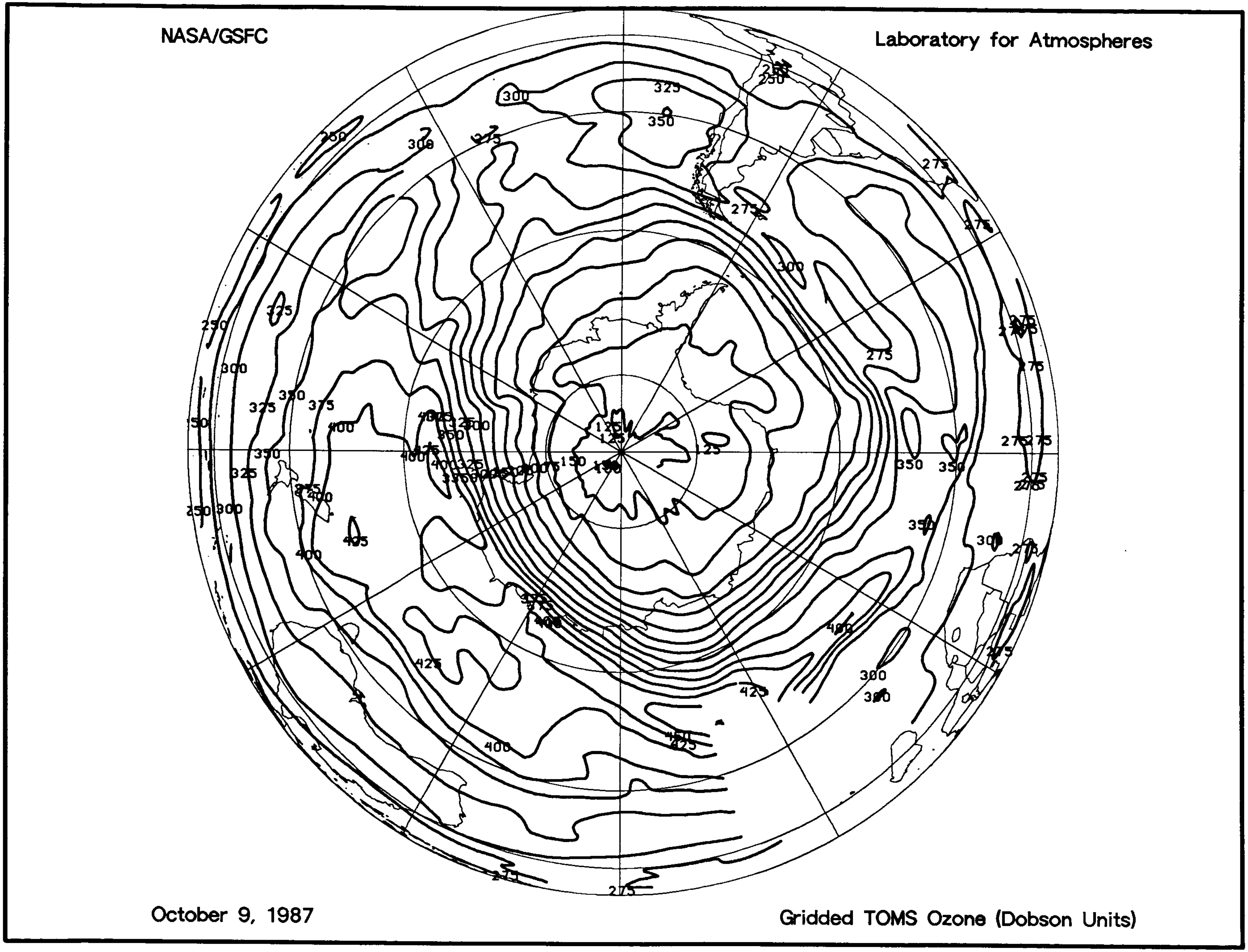
NASA/GSFC
Laboratory for Atmospheres
October 9, 1987
Gridded TOMS Ozone (Dobson Units)

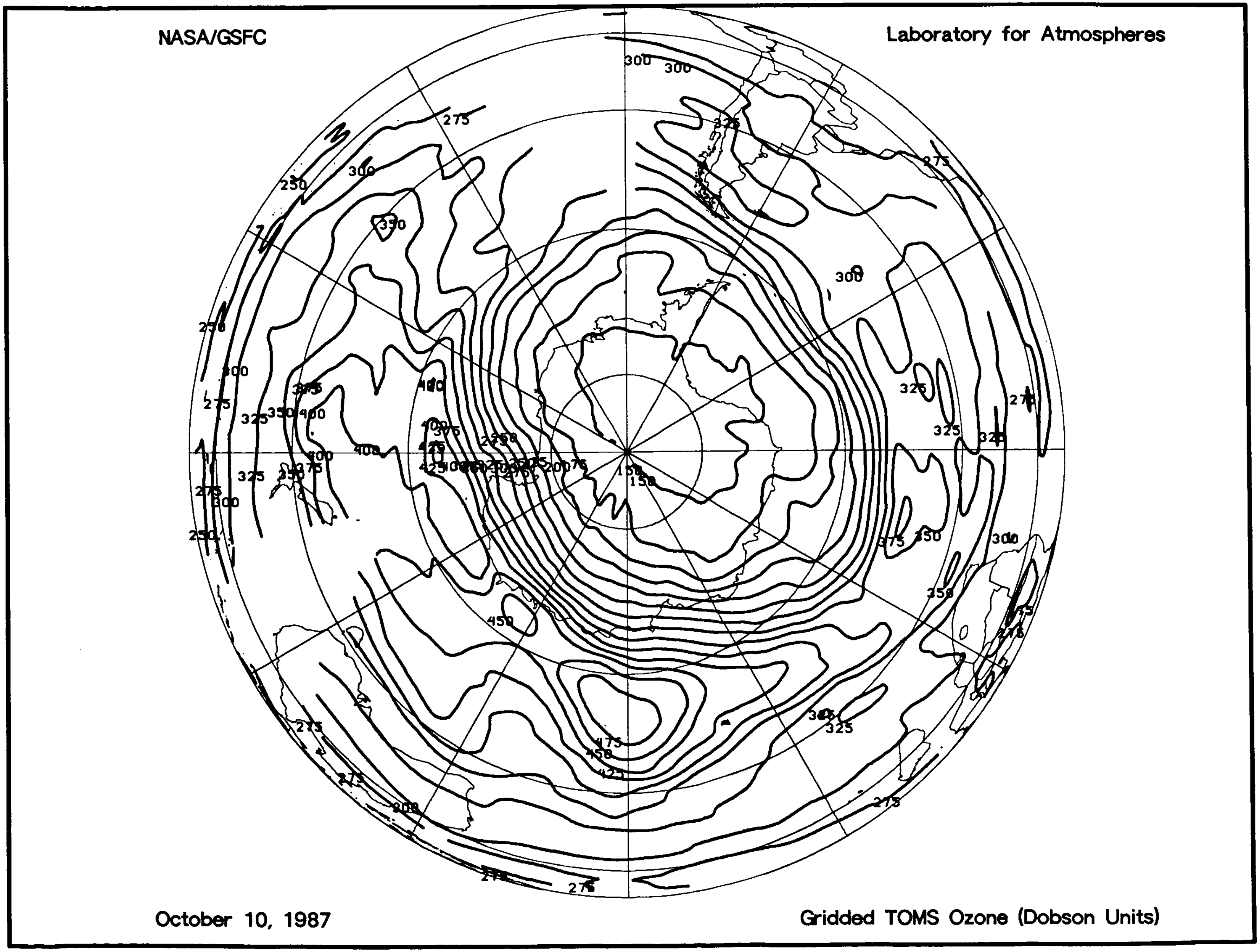
NASA/GSFC
Laboratory for Atmospheres
October 10, 1987
Gridded TOMS Ozone (Dobson Units)

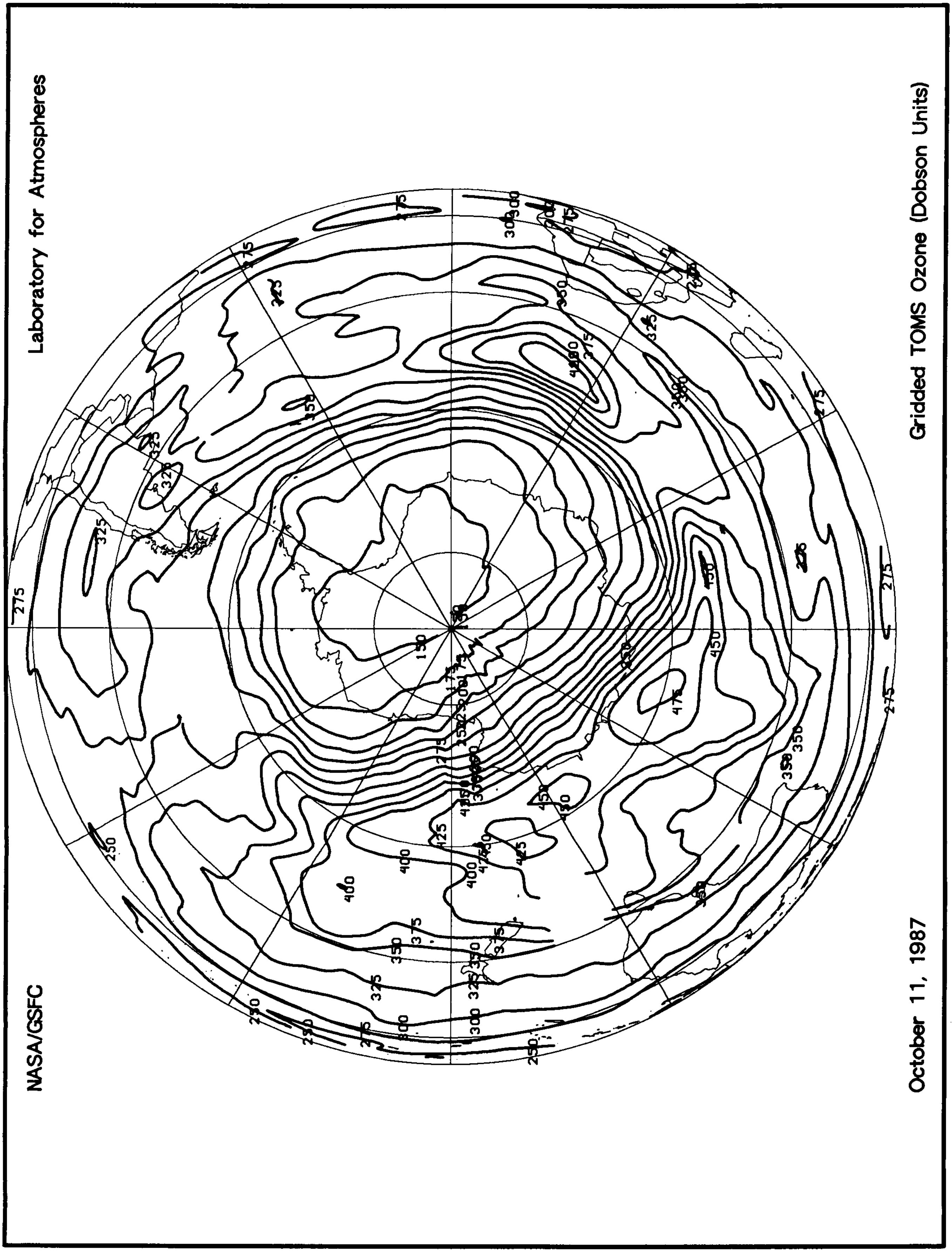
NASA/GSFC
Laboratory for Atmospheres
October 11, 1987
Gridded TOMS Ozone (Dobson Units)

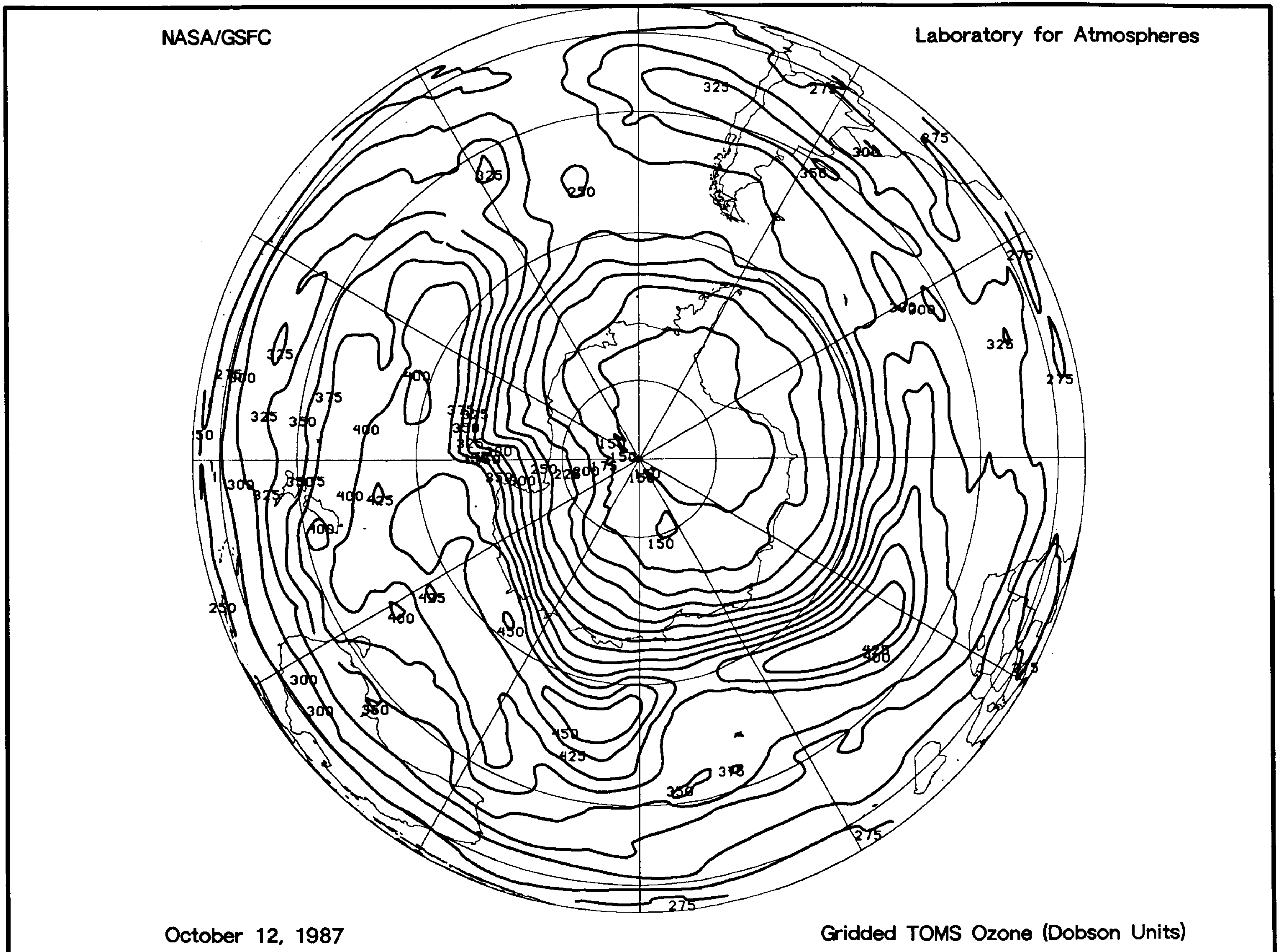
NASA/GSFC
Laboratory for Atmospheres
October 12, 1987
Gridded TOMS Ozone (Dobson Units)

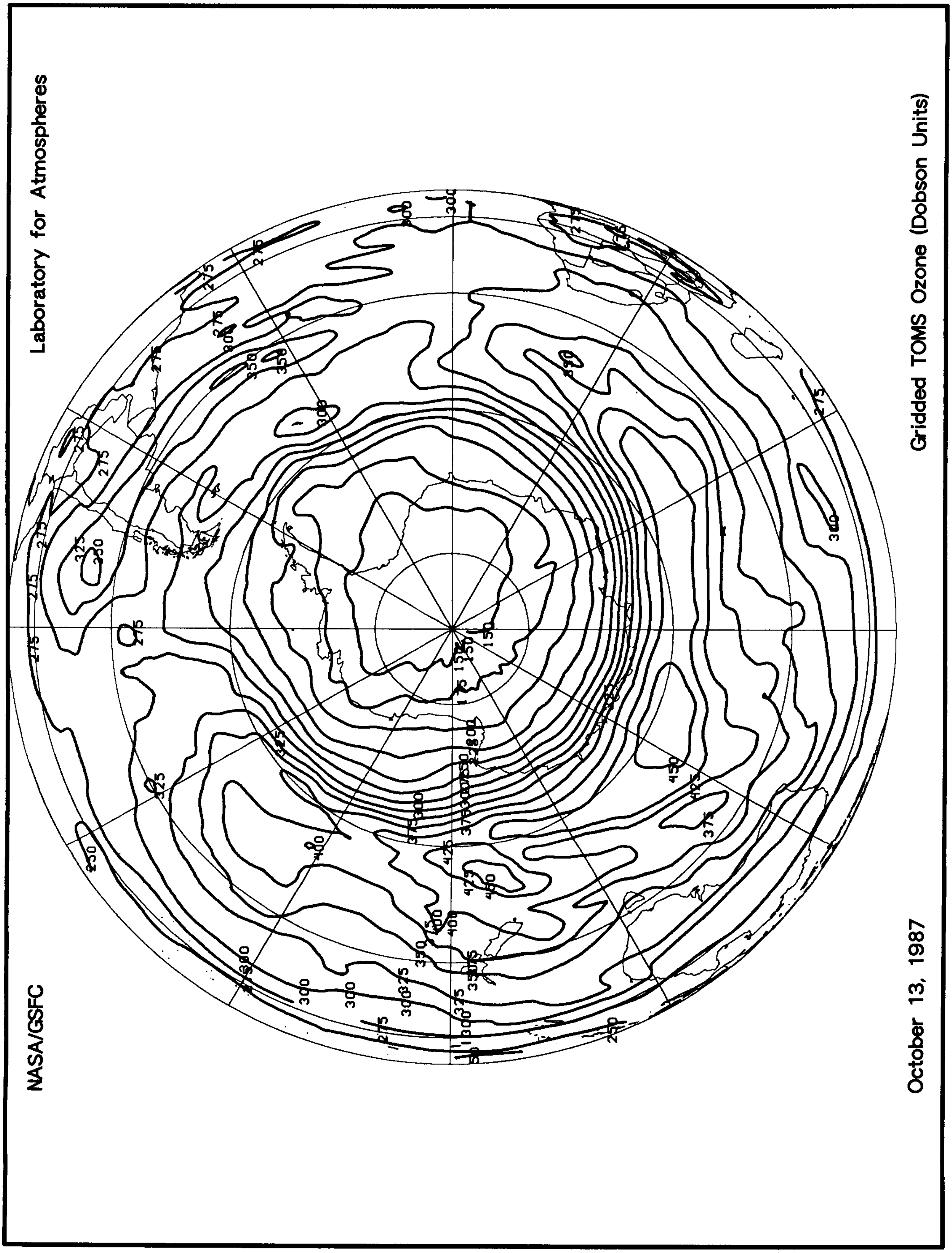
Laboratory for Atmospheres
NASA/GSFC
October 13, 1987
Gridded TOMS Ozone (Dobson Units)

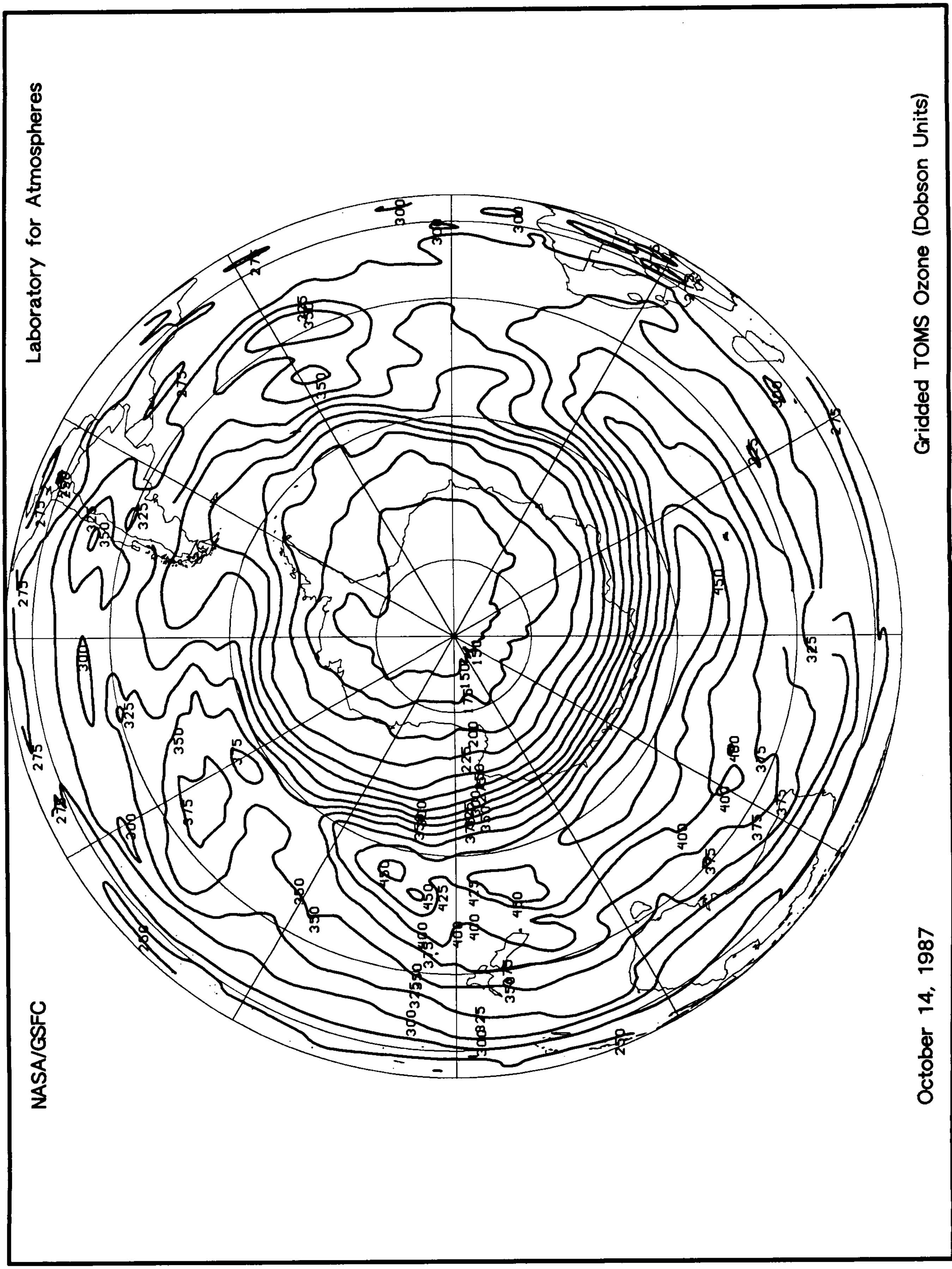
Laboratory for Atmospheres
Gridded TOMS Ozone (Dobson Units)
NASA/GSFC
October 14, 1987

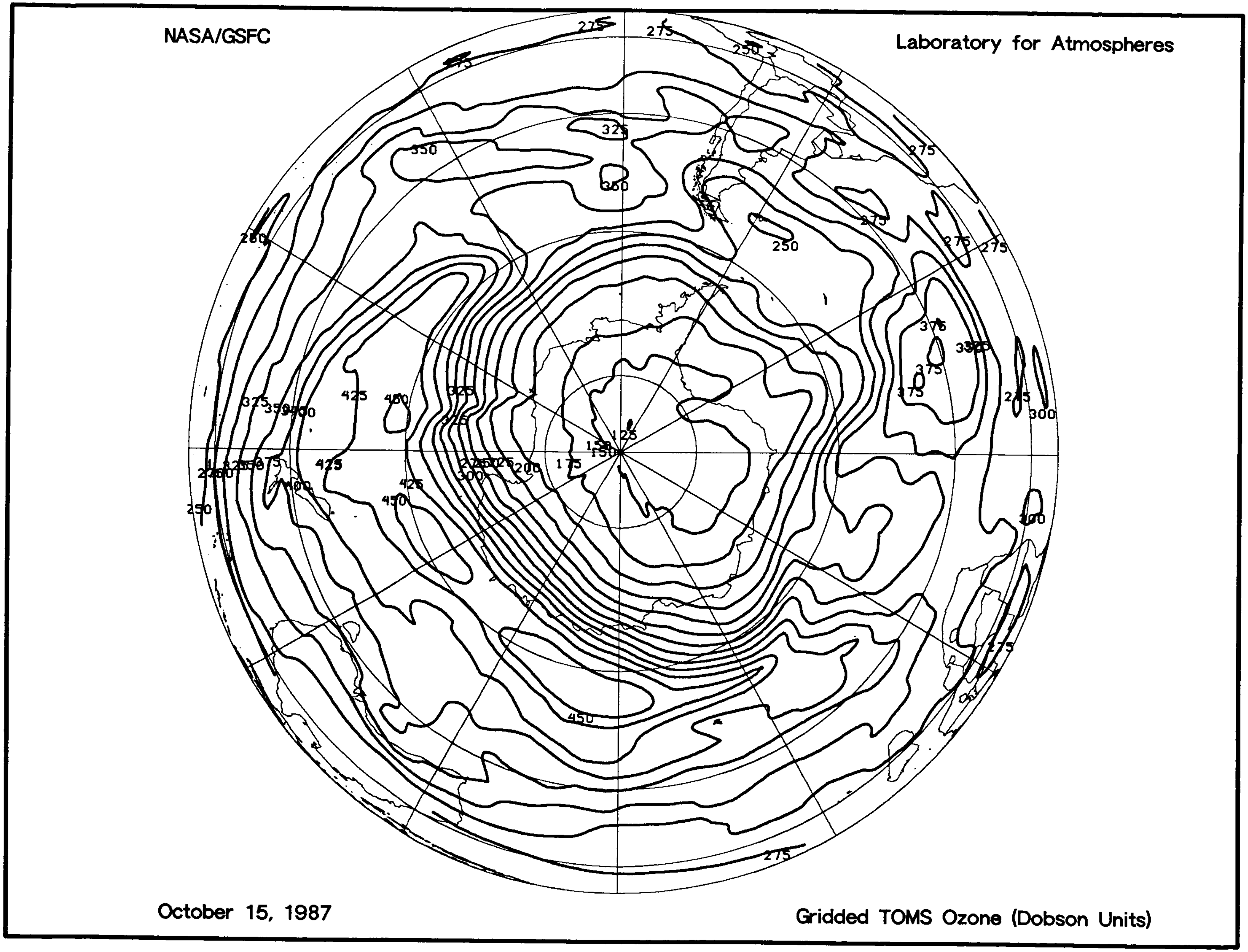
NASA/GSFC
Laboratory for Atmospheres
October 15, 1987
Gridded TOMS Ozone (Dobson Units)

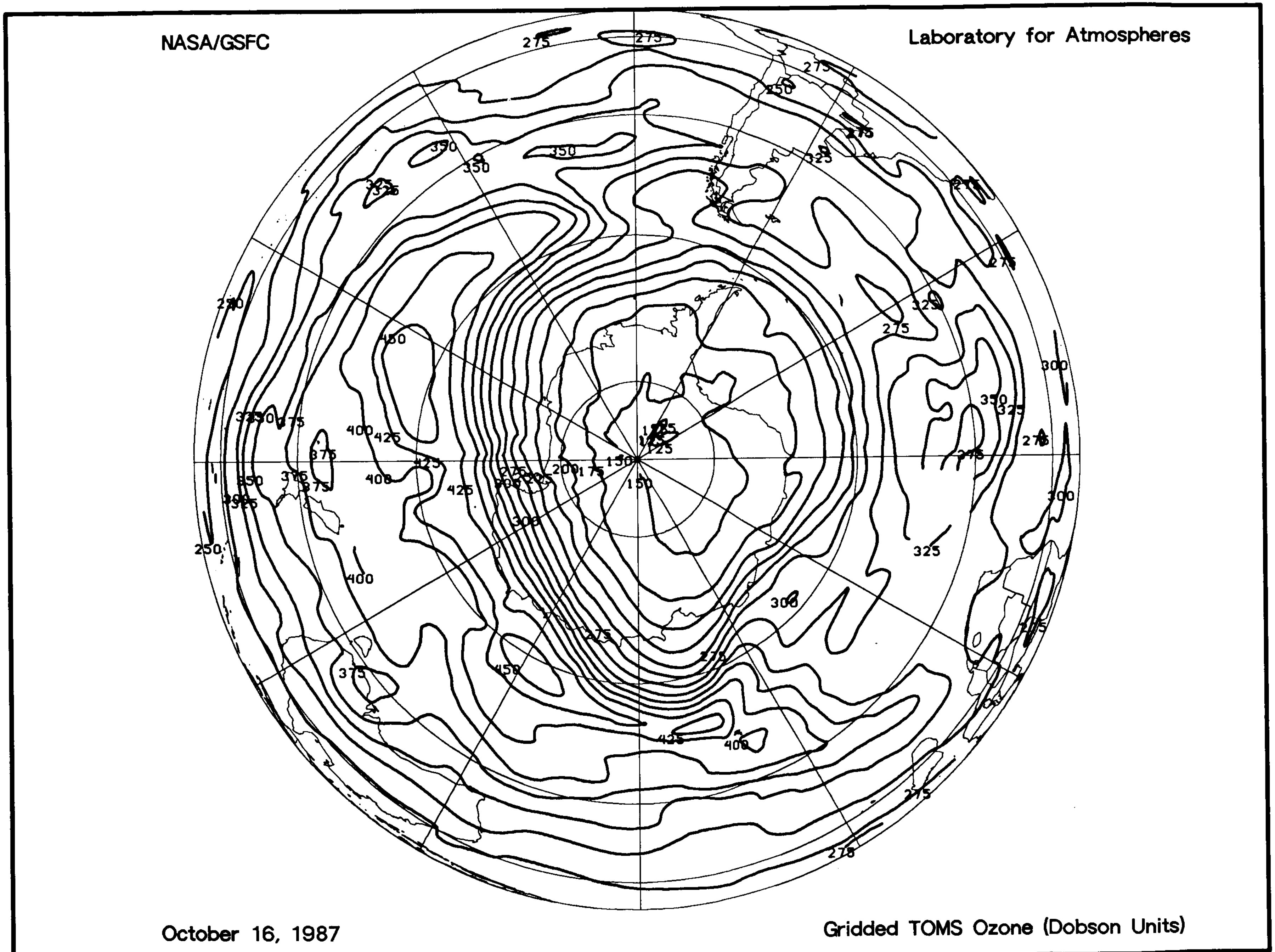
NASA/GSFC
Laboratory for Atmospheres
October 16, 1987
Gridded TOMS Ozone (Dobson Units)

NASA/GSFC

Laboratory for Atmospheres

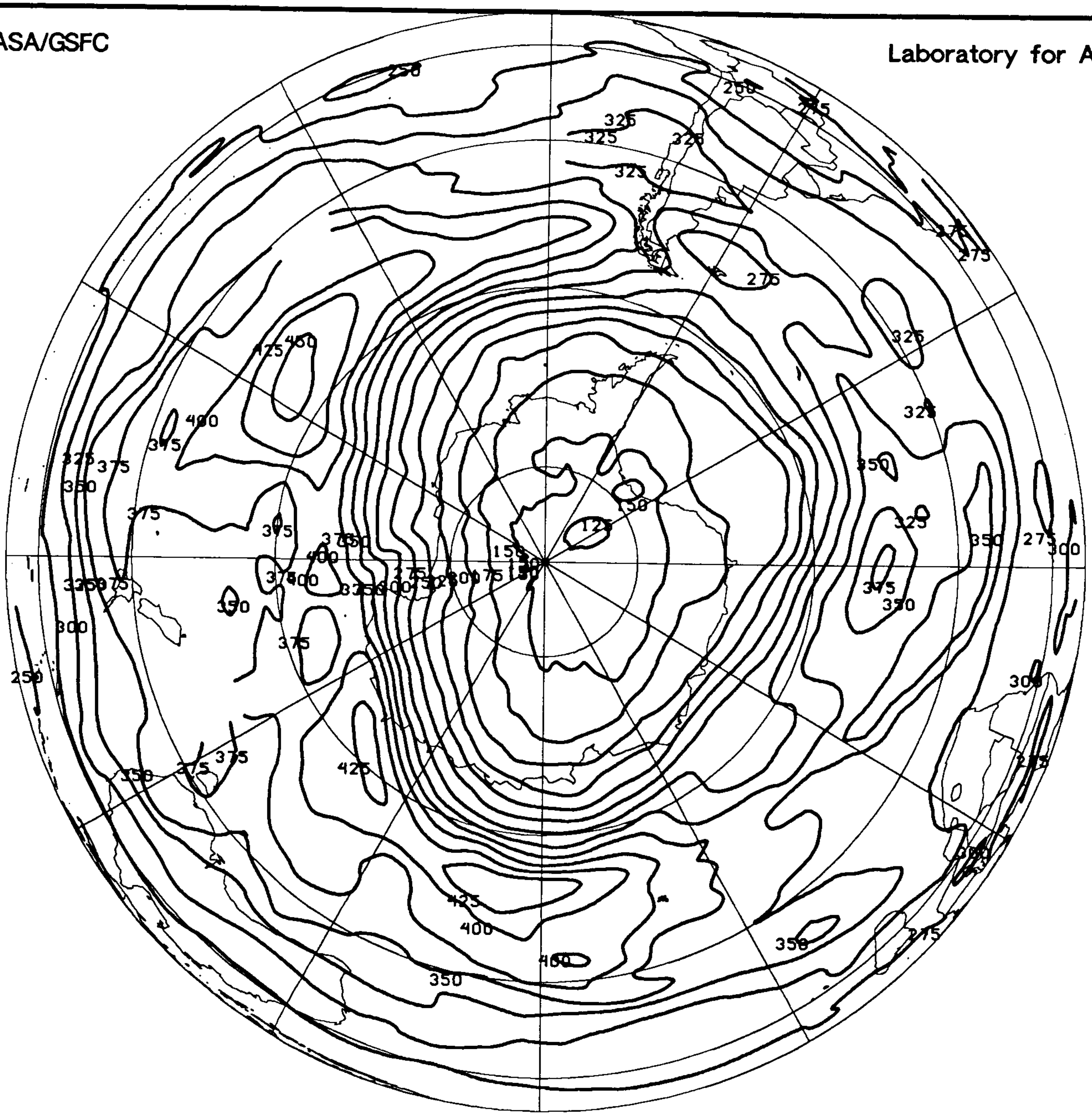


October 17, 1987

Gridded TOMS Ozone (Dobson Units)

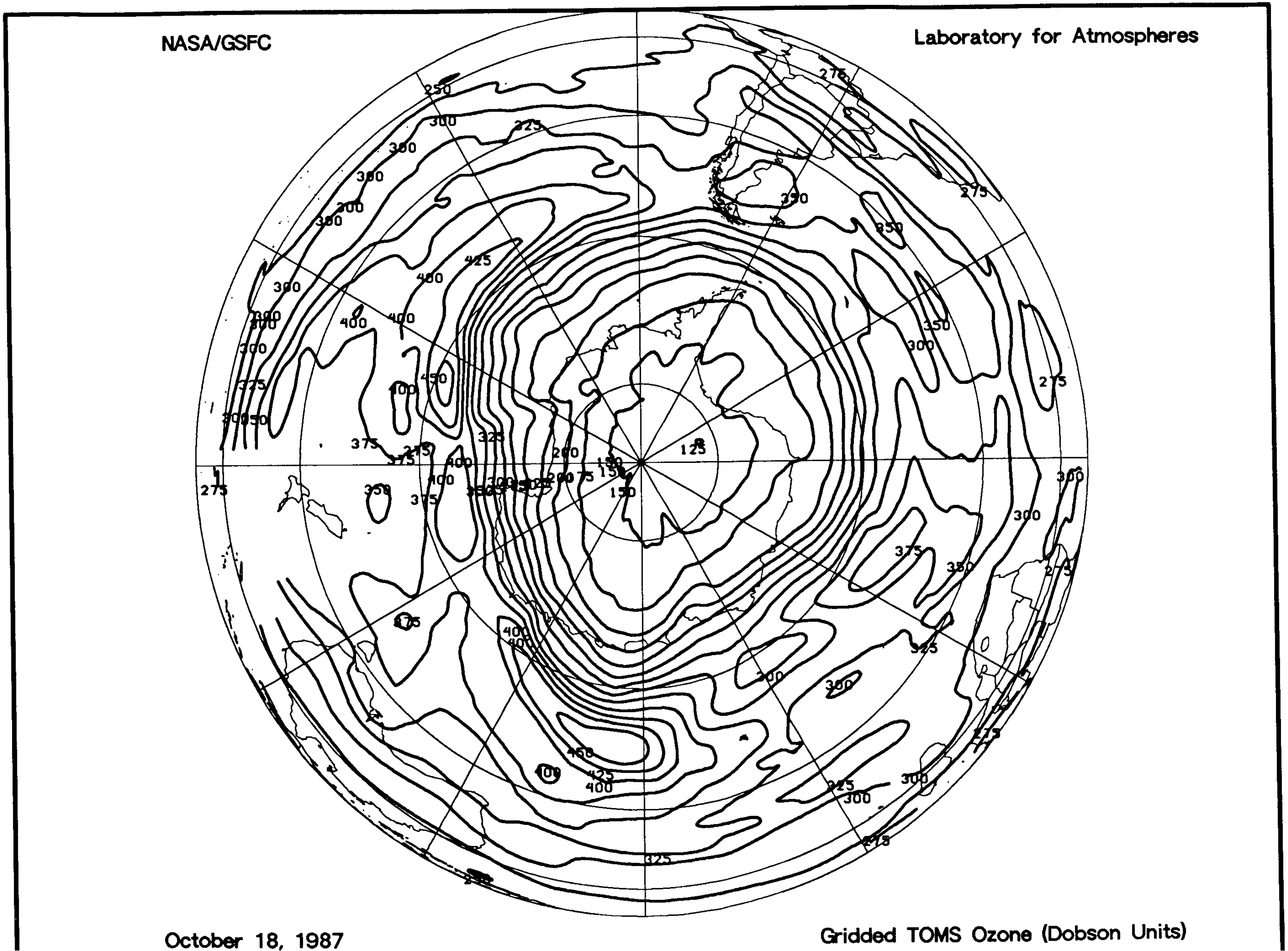
NASA/GSFC
Laboratory for Atmospheres
October 18, 1987
Gridded TOMS Ozone (Dobson Units)

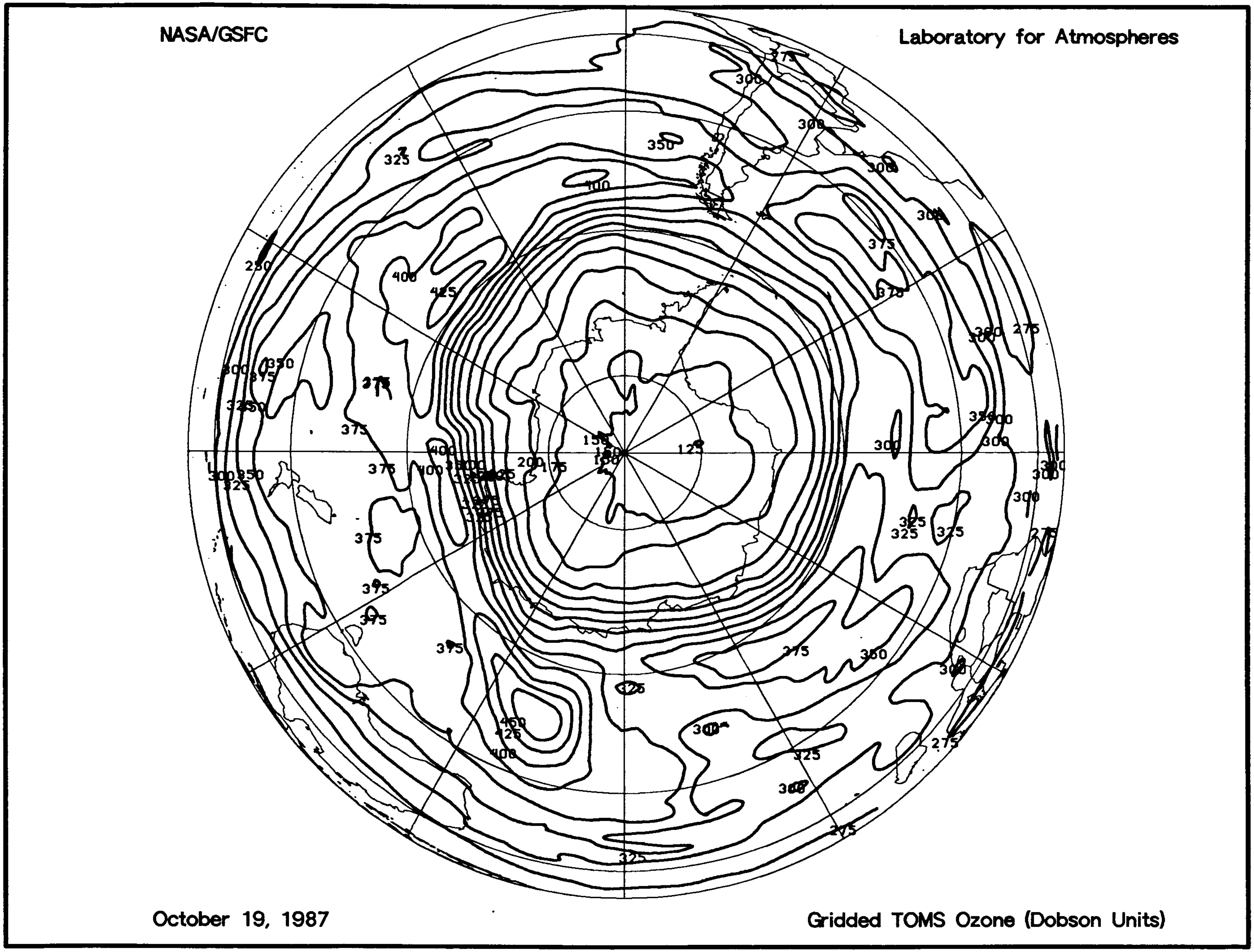
NASA/GSFC
Laboratory for Atmospheres
October 19, 1987
Gridded TOMS Ozone (Dobson Units)

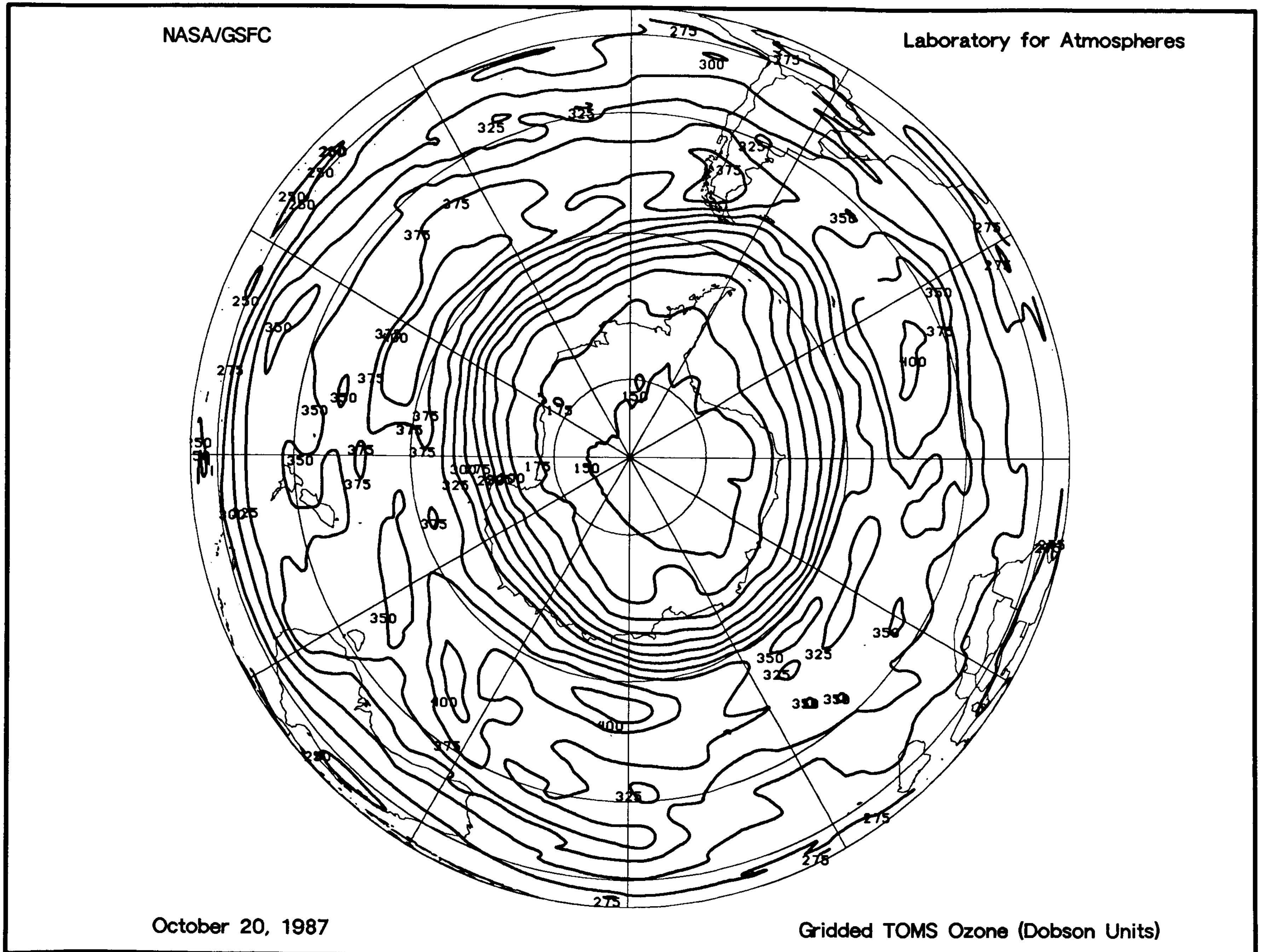
NASA/GSFC
Laboratory for Atmospheres
October 20, 1987
Gridded TOMS Ozone (Dobson Units)

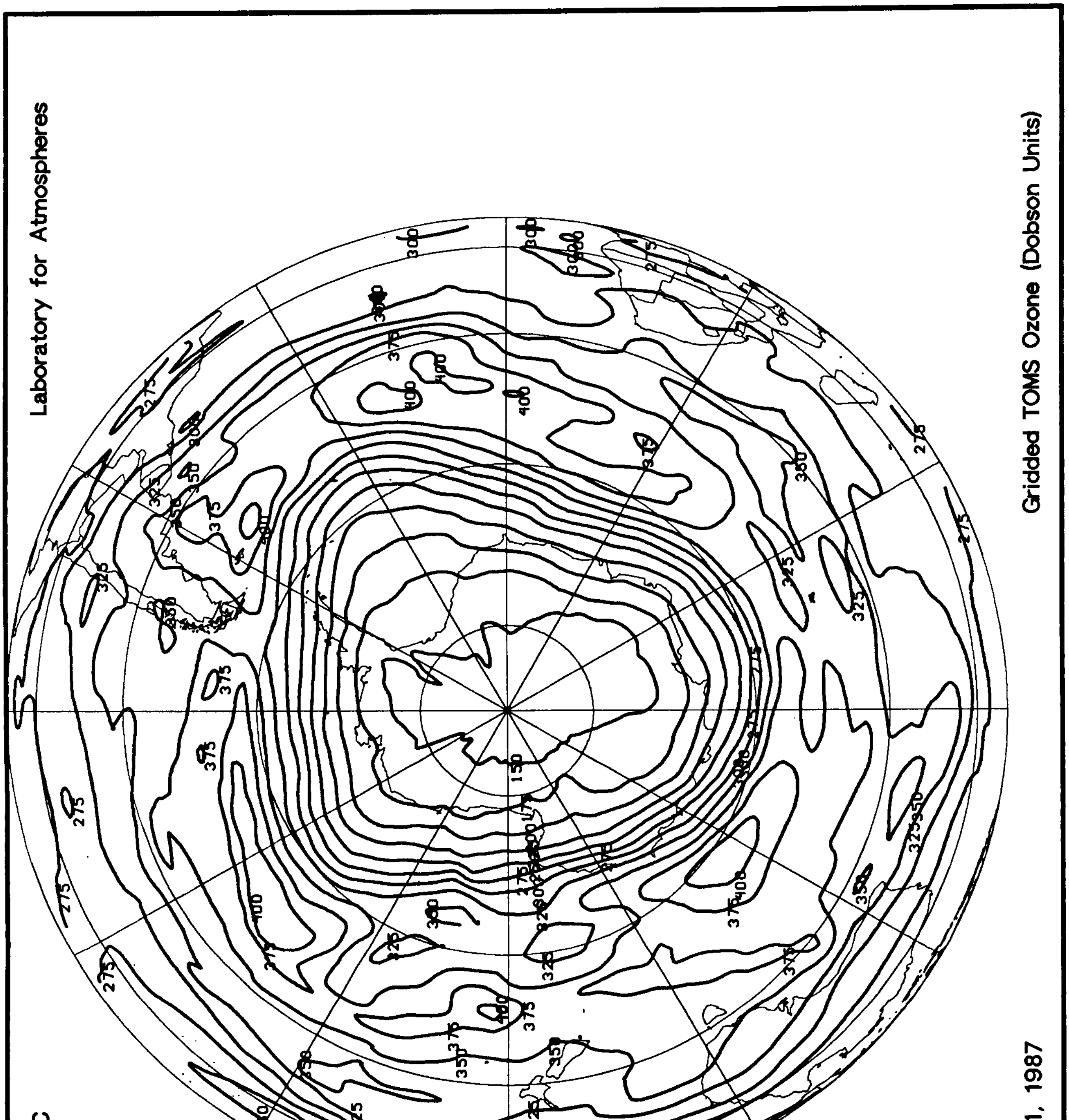

Laboratory for Atmospheres
NASA/GSFC
October 21, 1987
Gridded TOMS Ozone (Dobson Units)

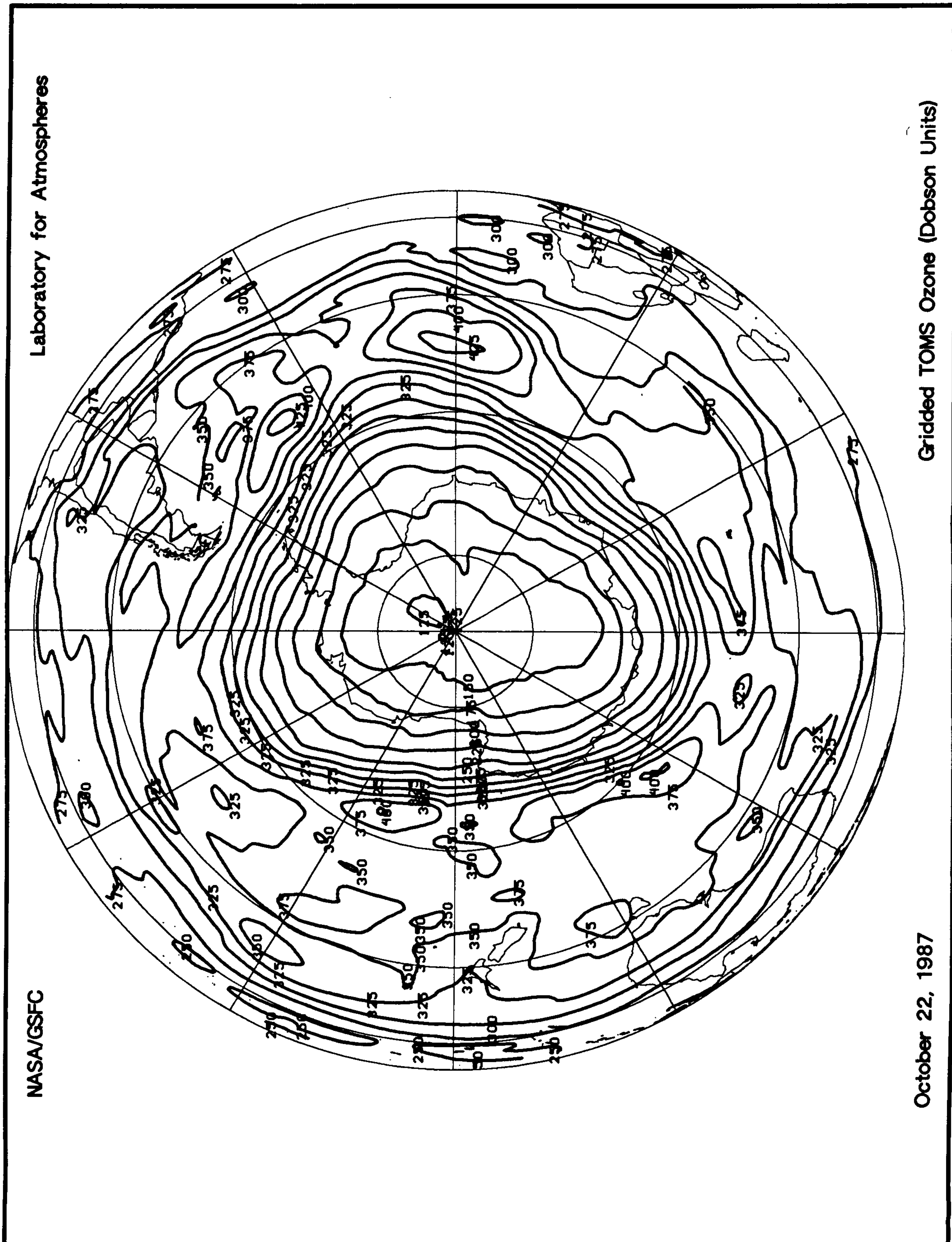
NASA/GSFC
Laboratory for Atmospheres
October 22, 1987
Gridded TOMS Ozone (Dobson Units)

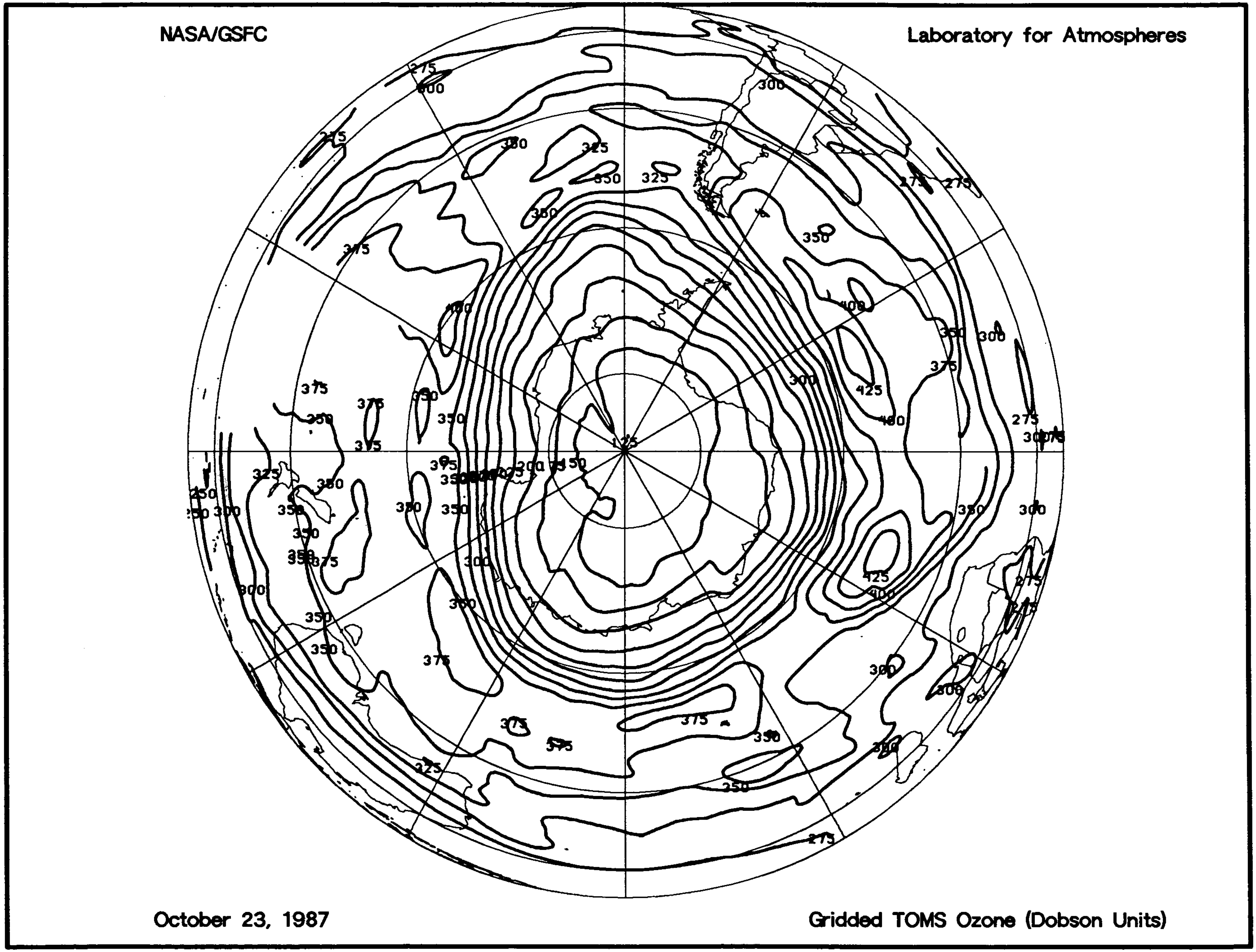
NASA/GSFC
Laboratory for Atmospheres
October 23, 1987
Gridded TOMS Ozone (Dobson Units)

NASA/GSFC

Laboratory for Atmospheres

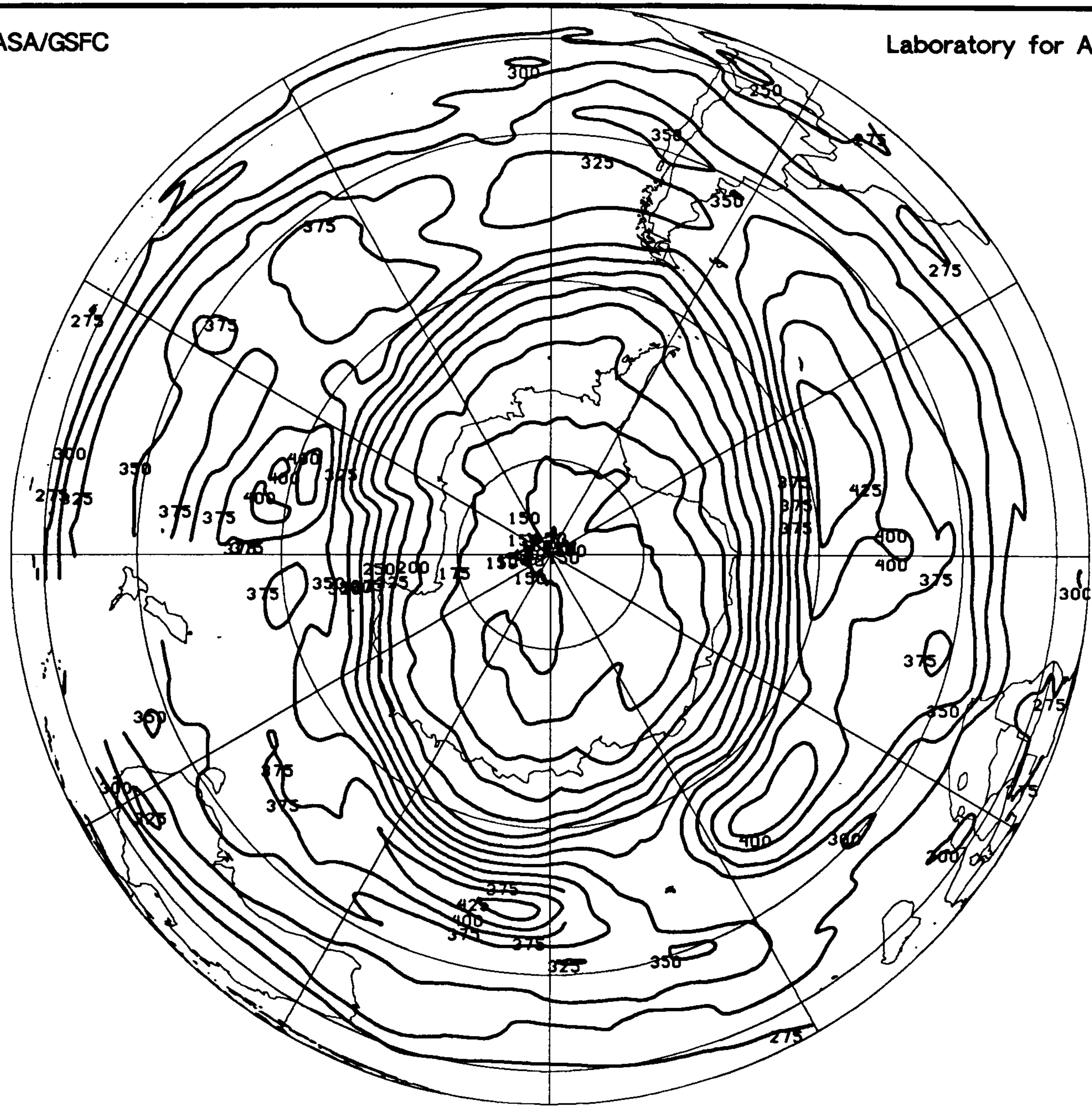


October 24, 1987

Gridded TOMS Ozone (Dobson Units)

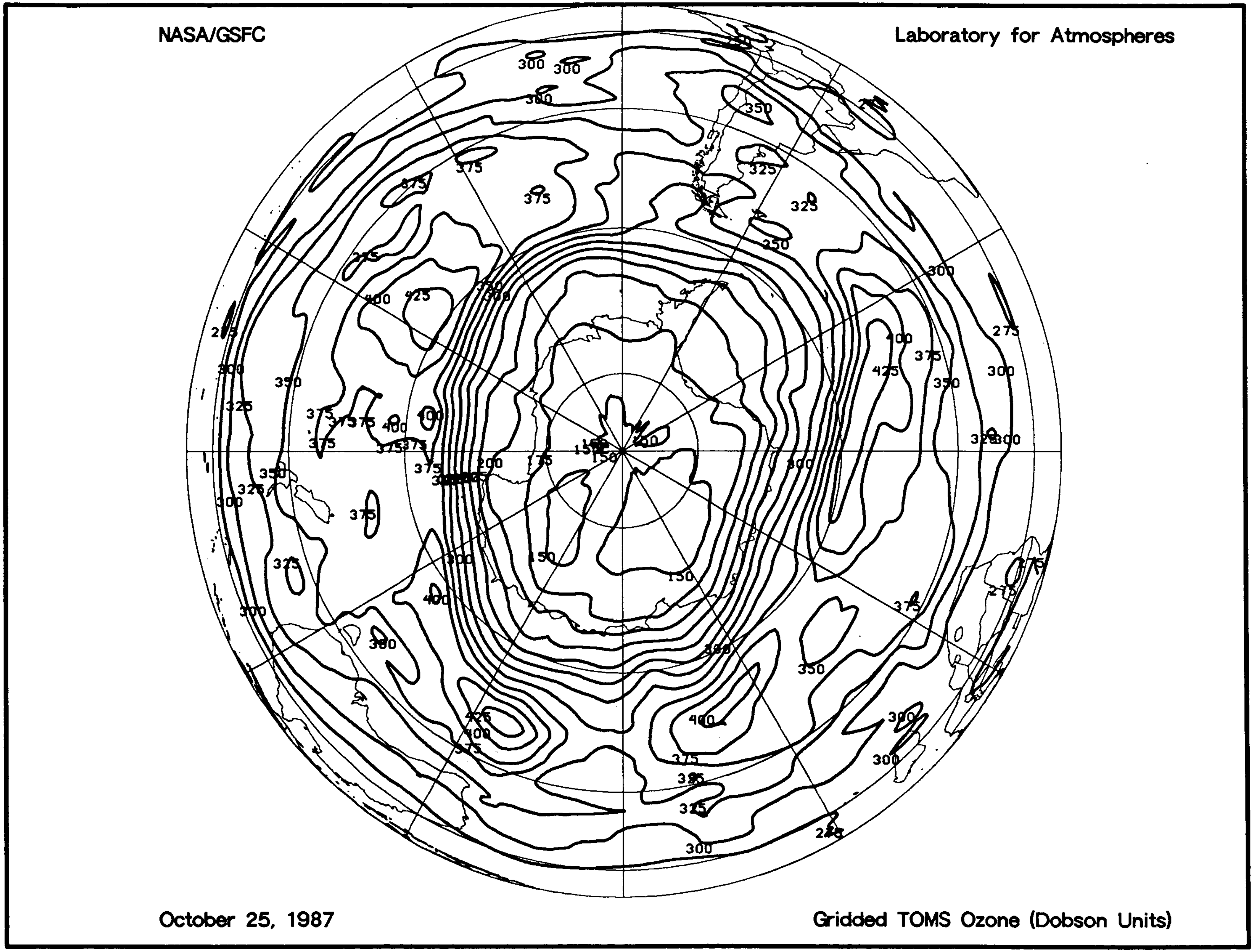
NASA/GSFC
Laboratory for Atmospheres
October 25, 1987
Gridded TOMS Ozone (Dobson Units)

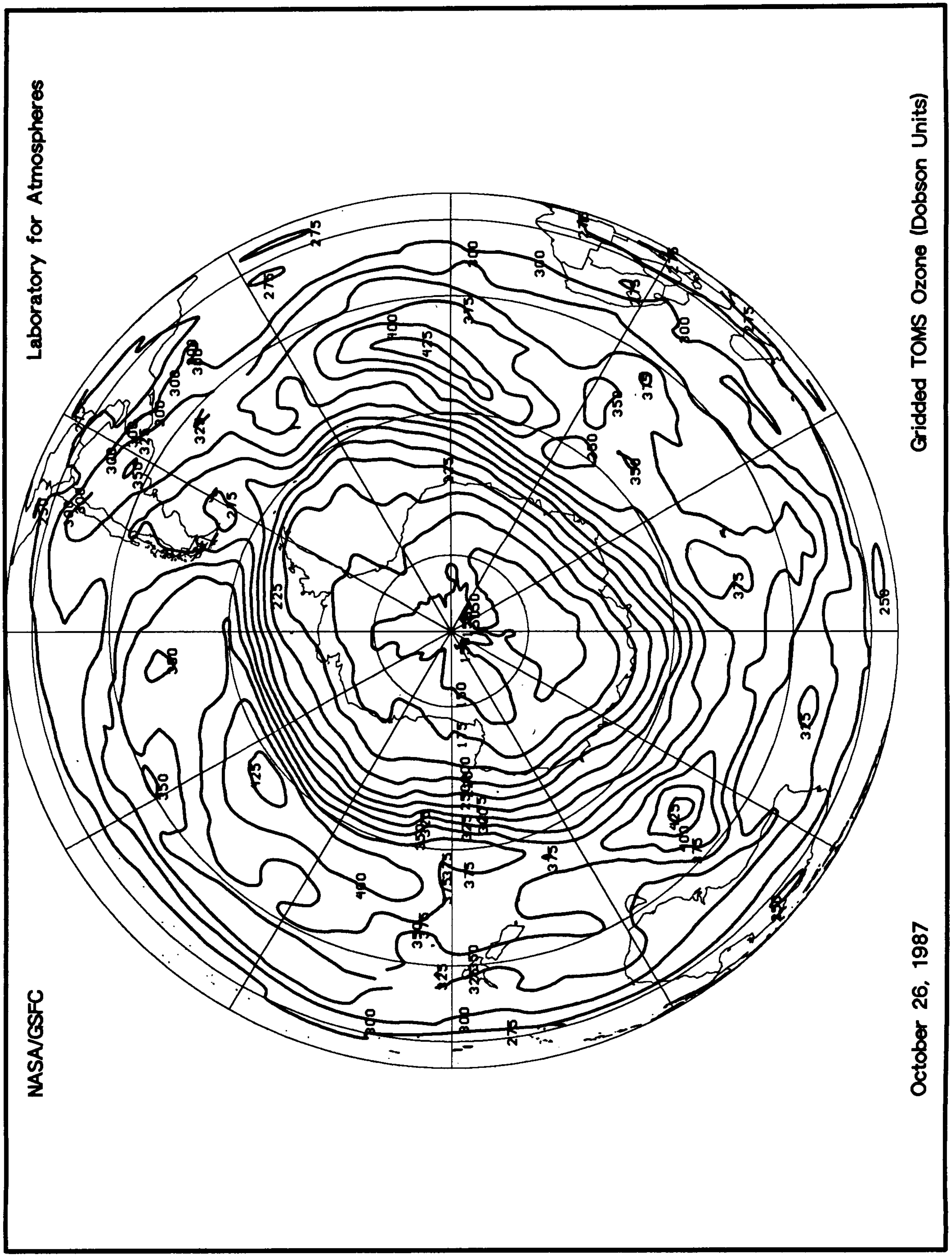
Laboratory for Atmospheres
NASA/GSFC
Gridded TOMS Ozone (Dobson Units)
October 26, 1987

NASA/GSFC

Laboratory for Atmospheres

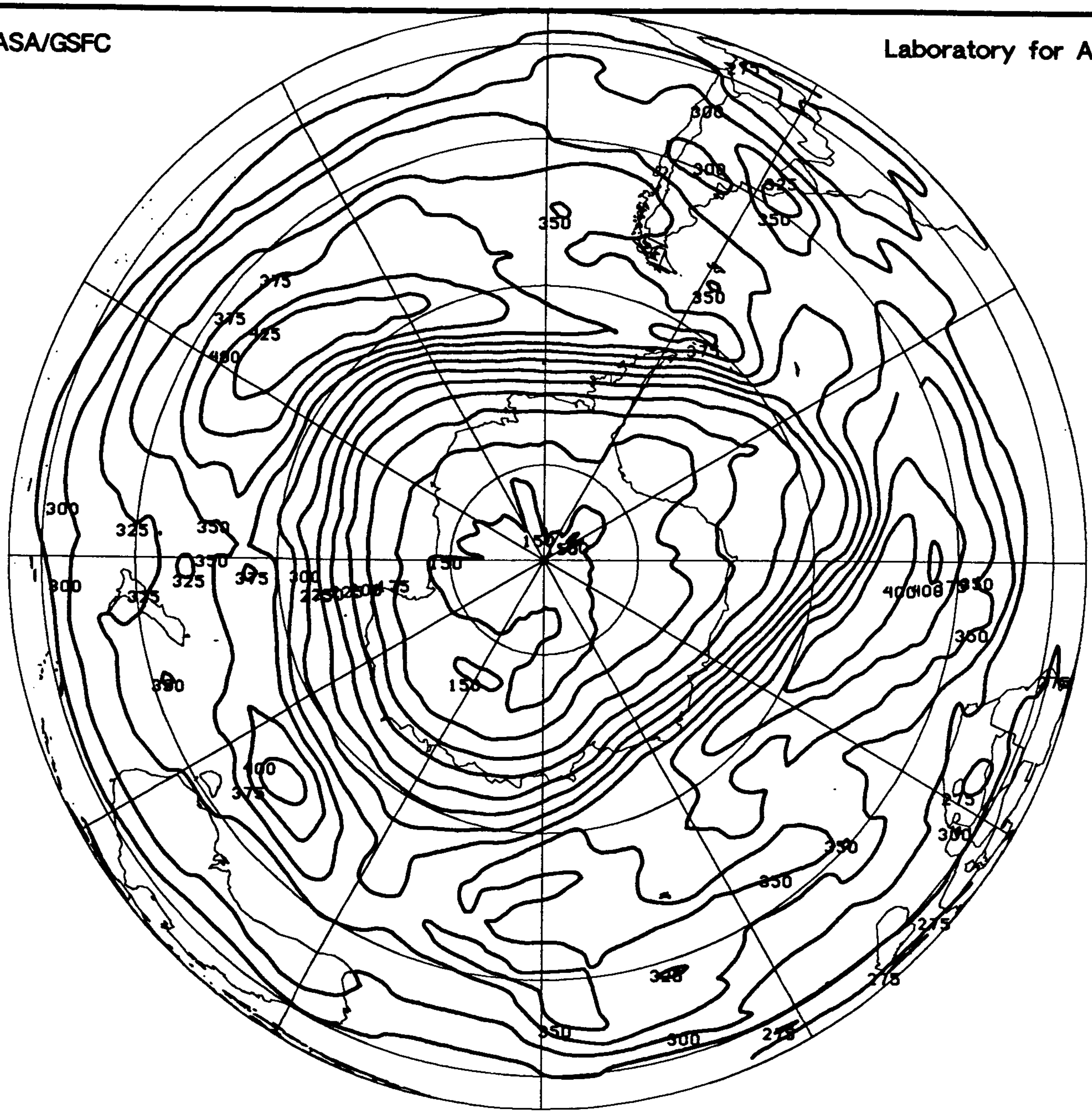


October 27, 1987

Gridded TOMS Ozone (Dobson Units)

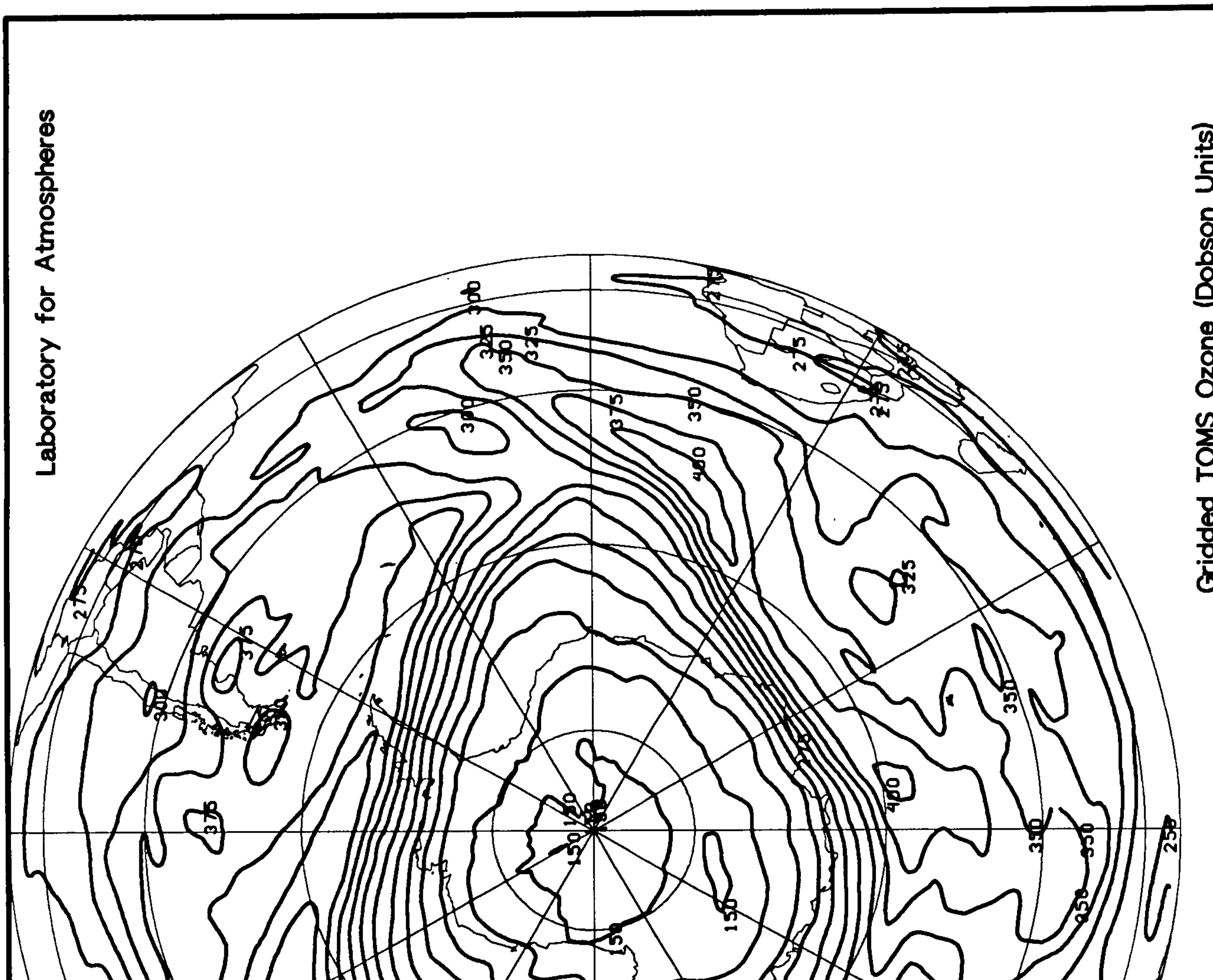

Laboratory for Atmospheres
NASA/GSFC
October 28, 1987
Gridded TOMS Ozone (Dobson Units)

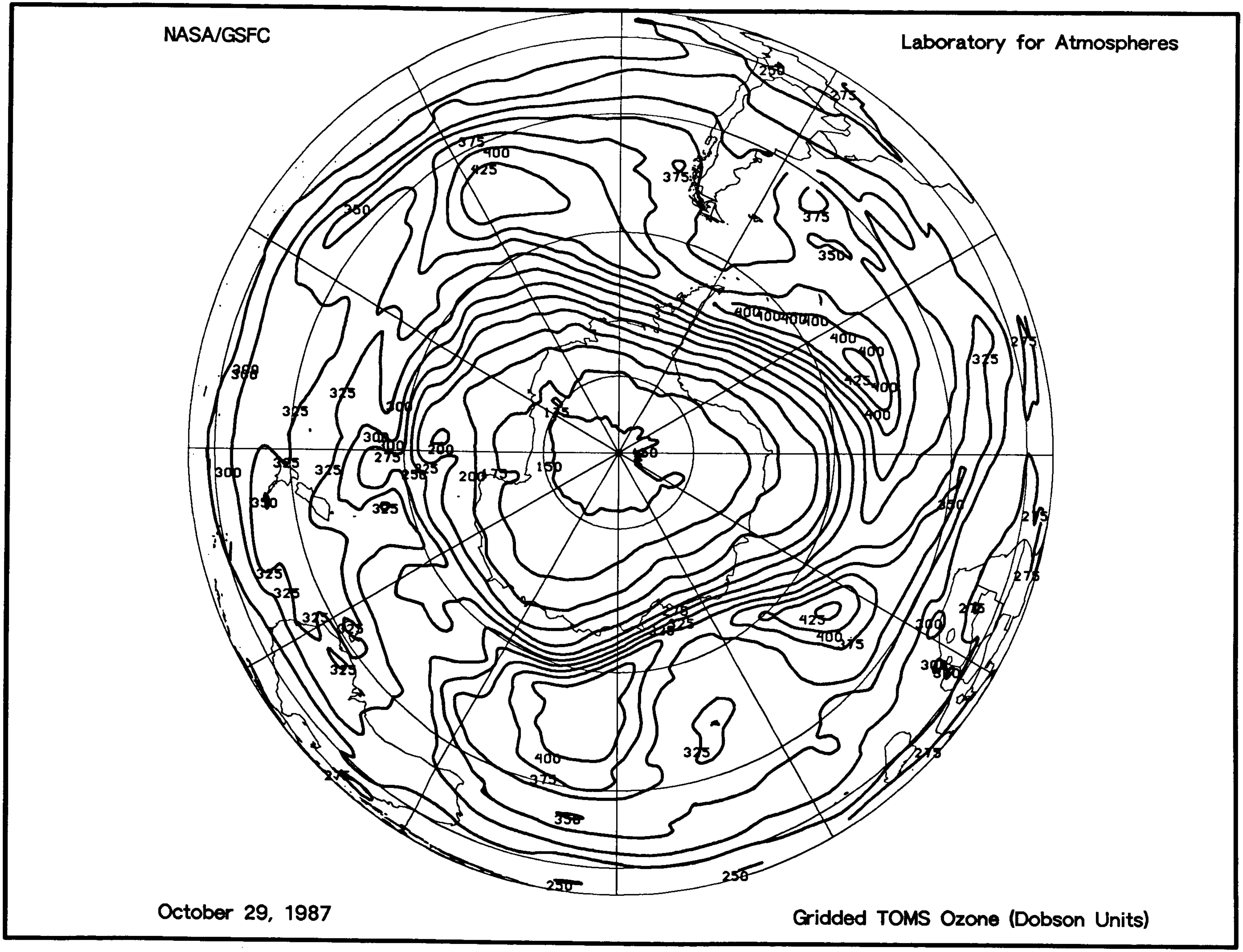
NASA/GSFC
Laboratory for Atmospheres
October 29, 1987
Gridded TOMS Ozone (Dobson Units)

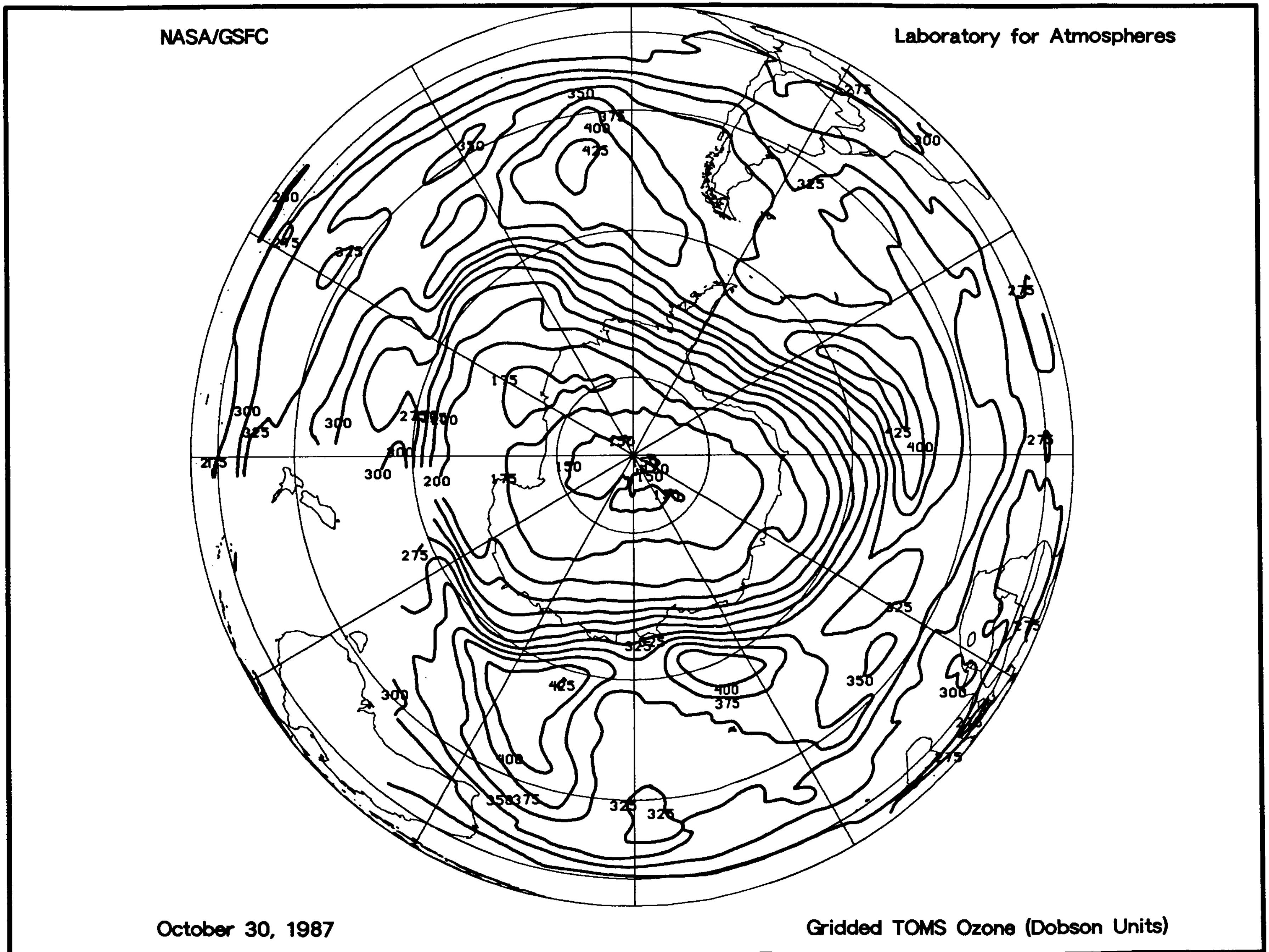

NASA/GSFC
Laboratory for Atmospheres
October 30, 1987
Gridded TOMS Ozone (Dobson Units)

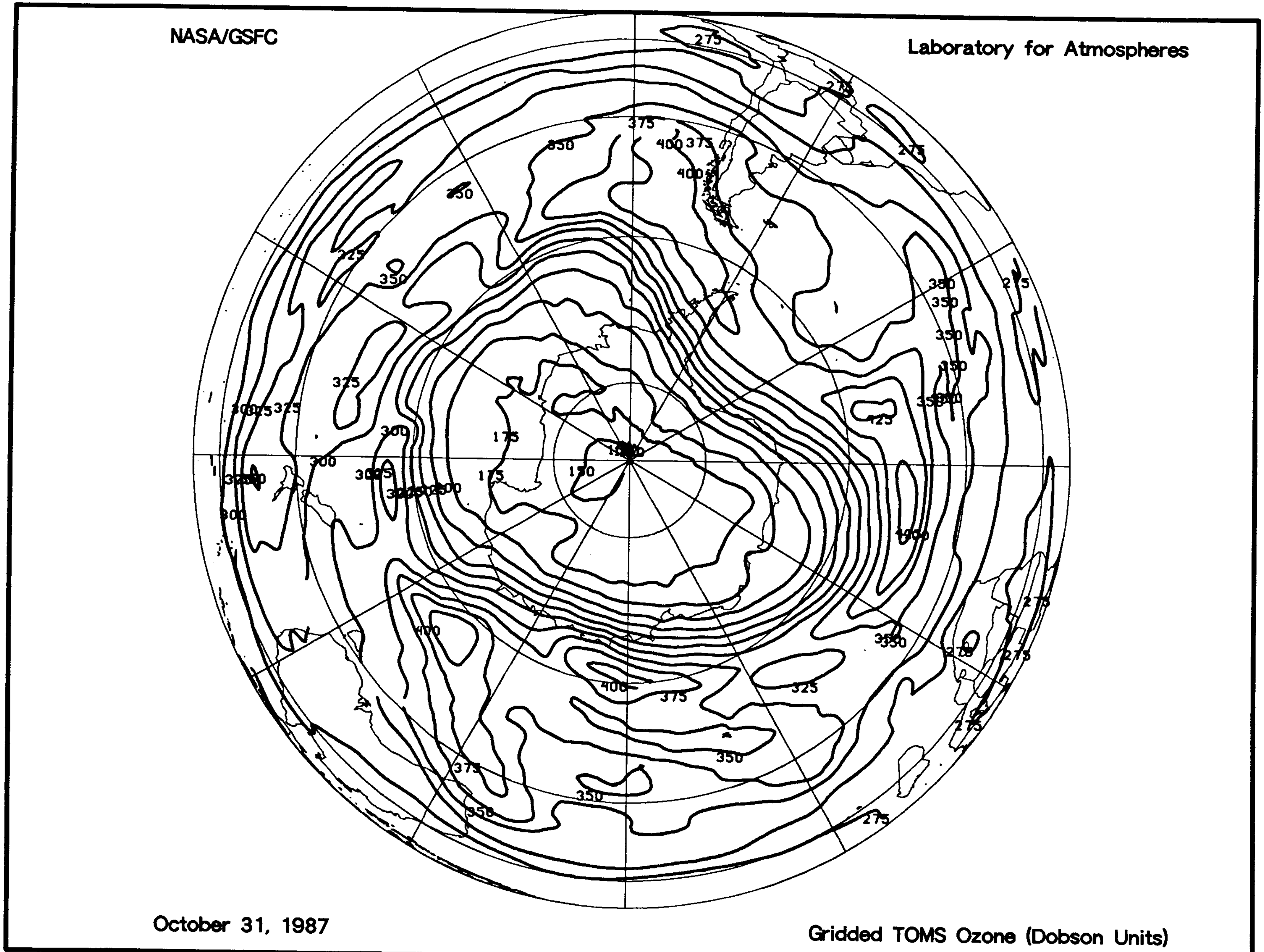
NASA/GSFC
Laboratory for Atmospheres
October 31, 1987
Gridded TOMS Ozone (Dobson Units)

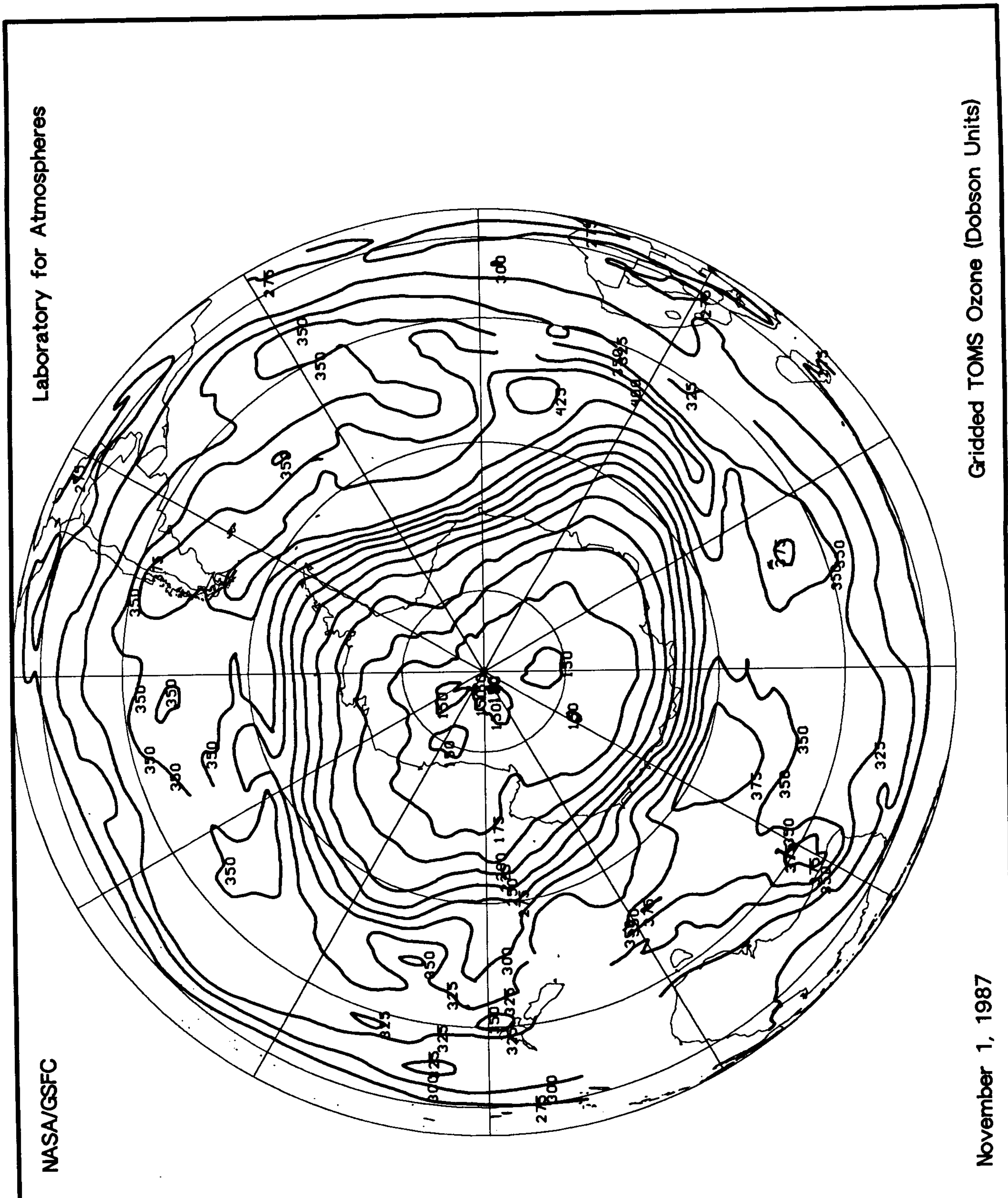
Laboratory for Atmospheres
NASA/GSFC
November 1, 1987
Gridded TOMS Ozone (Dobson Units)

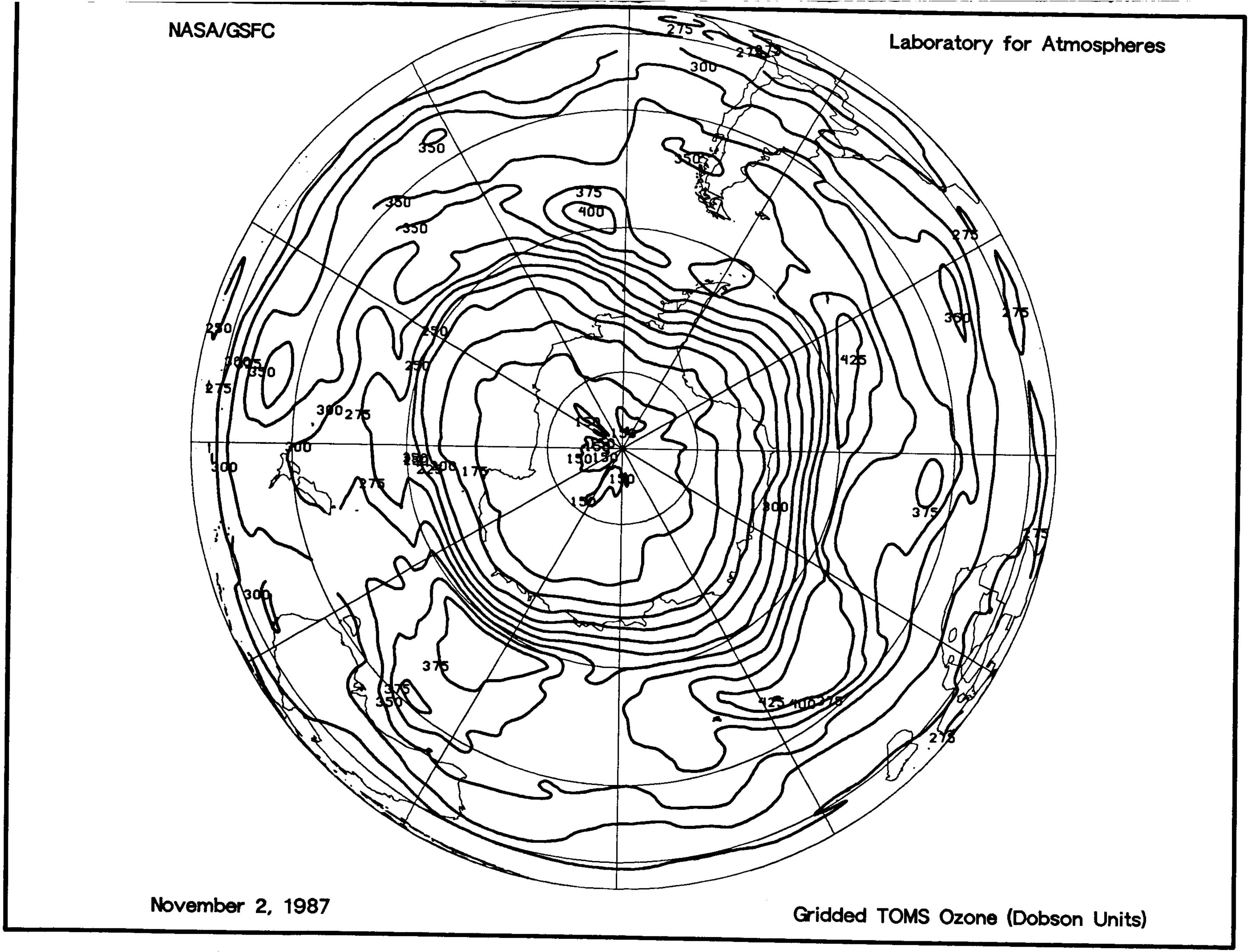
NASA/GSFC
Laboratory for Atmospheres
November 2, 1987
Gridded TOMS Ozone (Dobson Units)

NASA/GSFC

Laboratory for Atmospheres

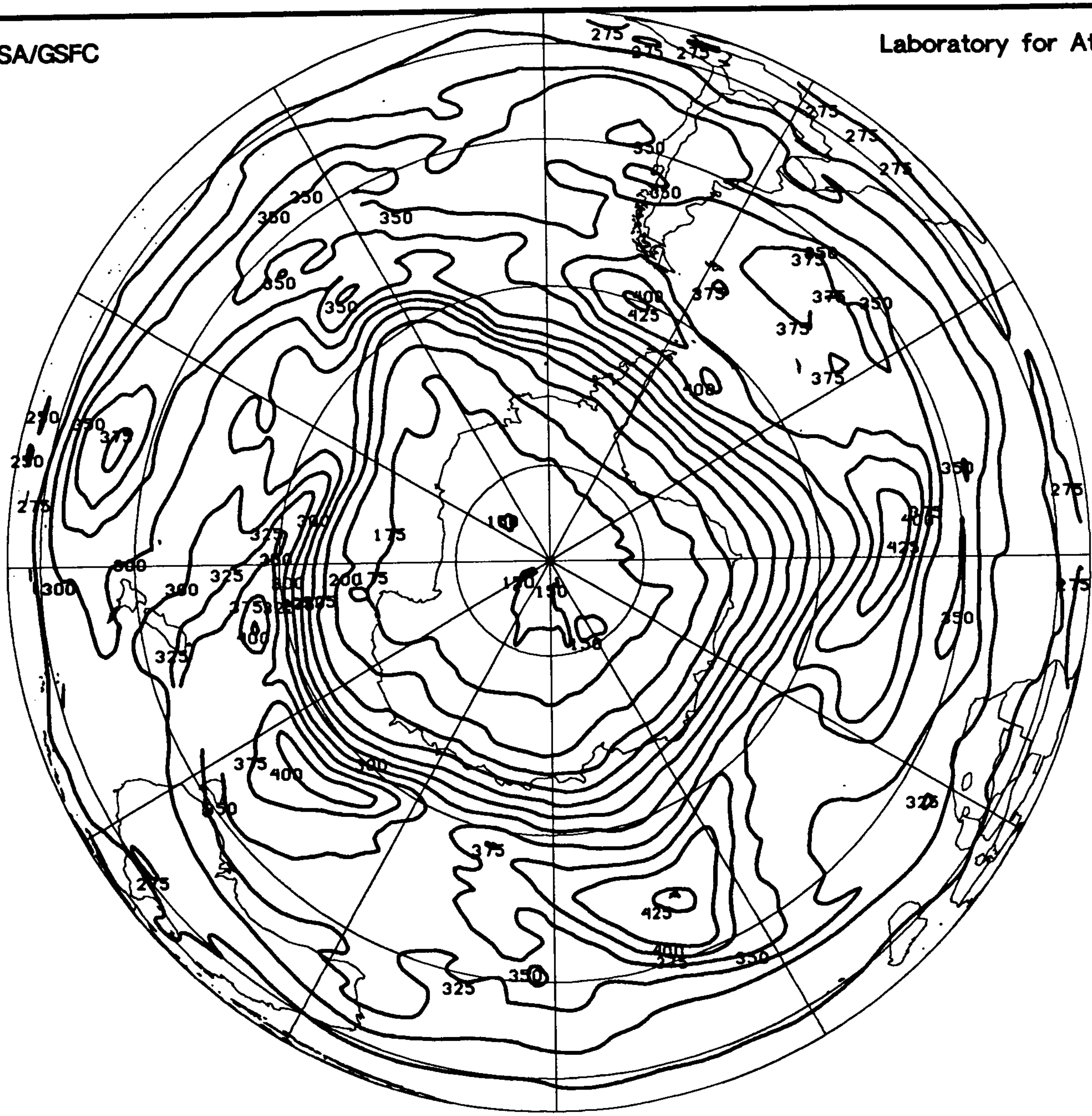

November 3, 1987

Gridded TOMS Ozone (Dobson Units)

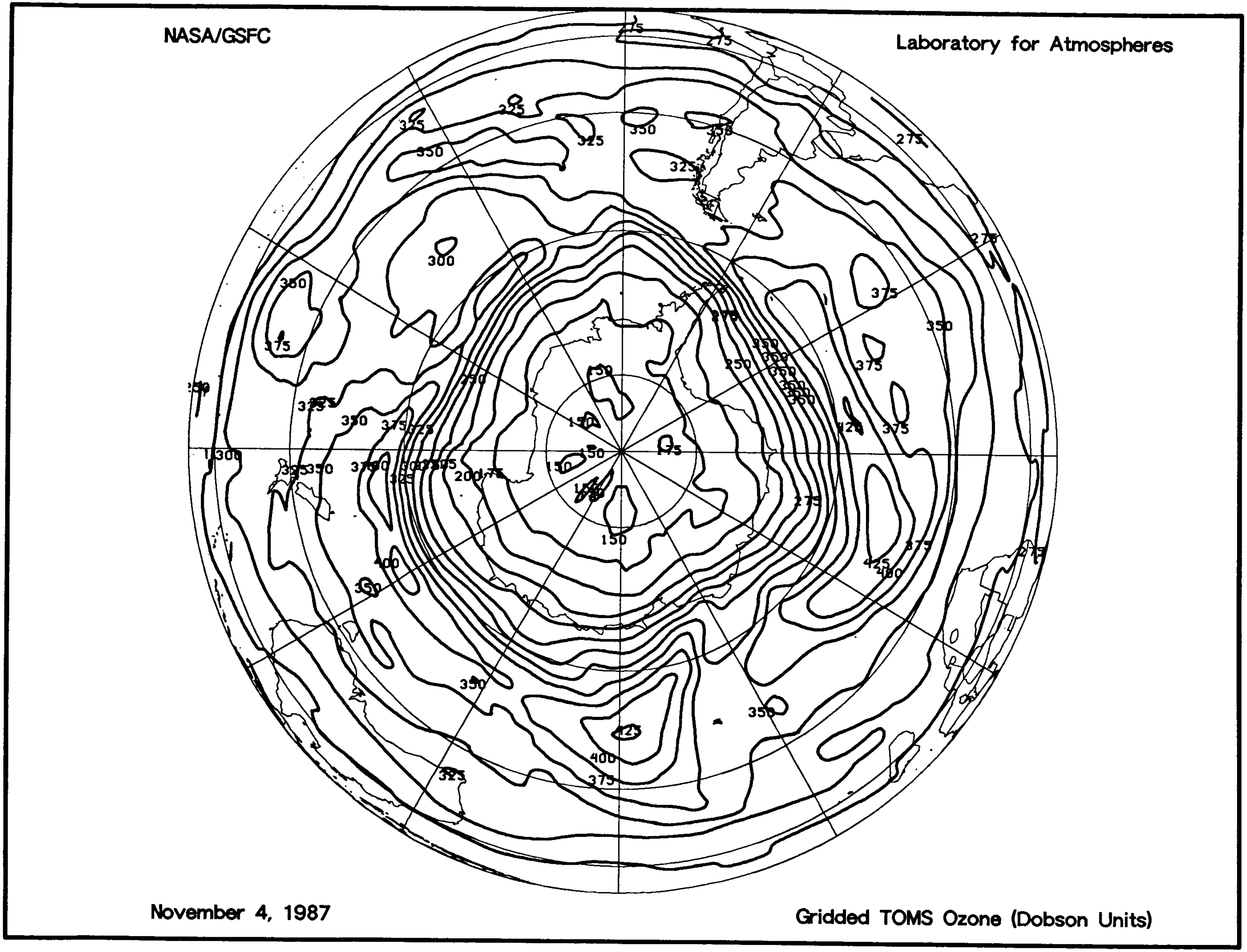
NASA/GSFC
Laboratory for Atmospheres
November 4, 1987
Gridded TOMS Ozone (Dobson Units)

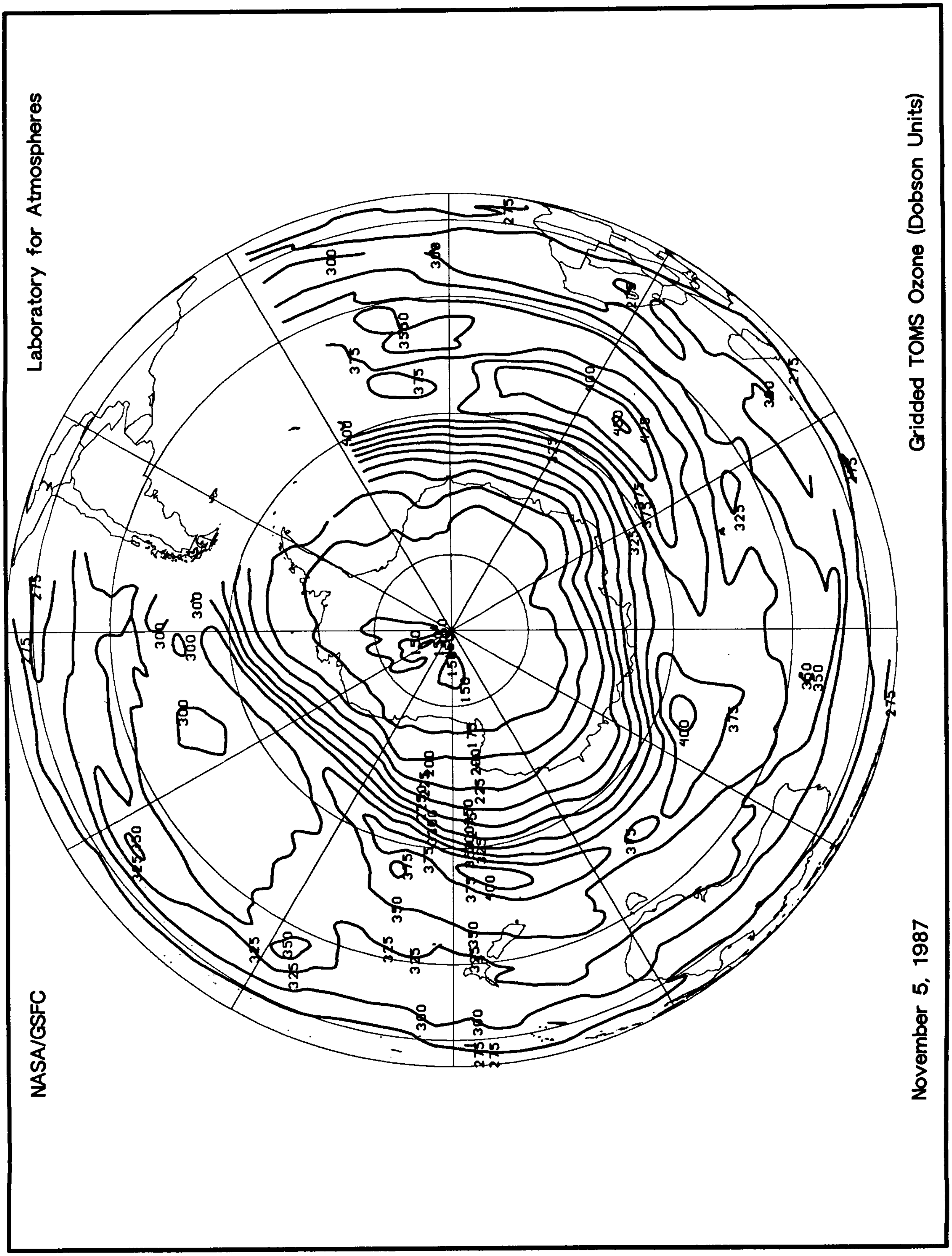

Laboratory for Atmospheres
Gridded TOMS Ozone (Dobson Units)
NASA/GSFC
November 5, 1987

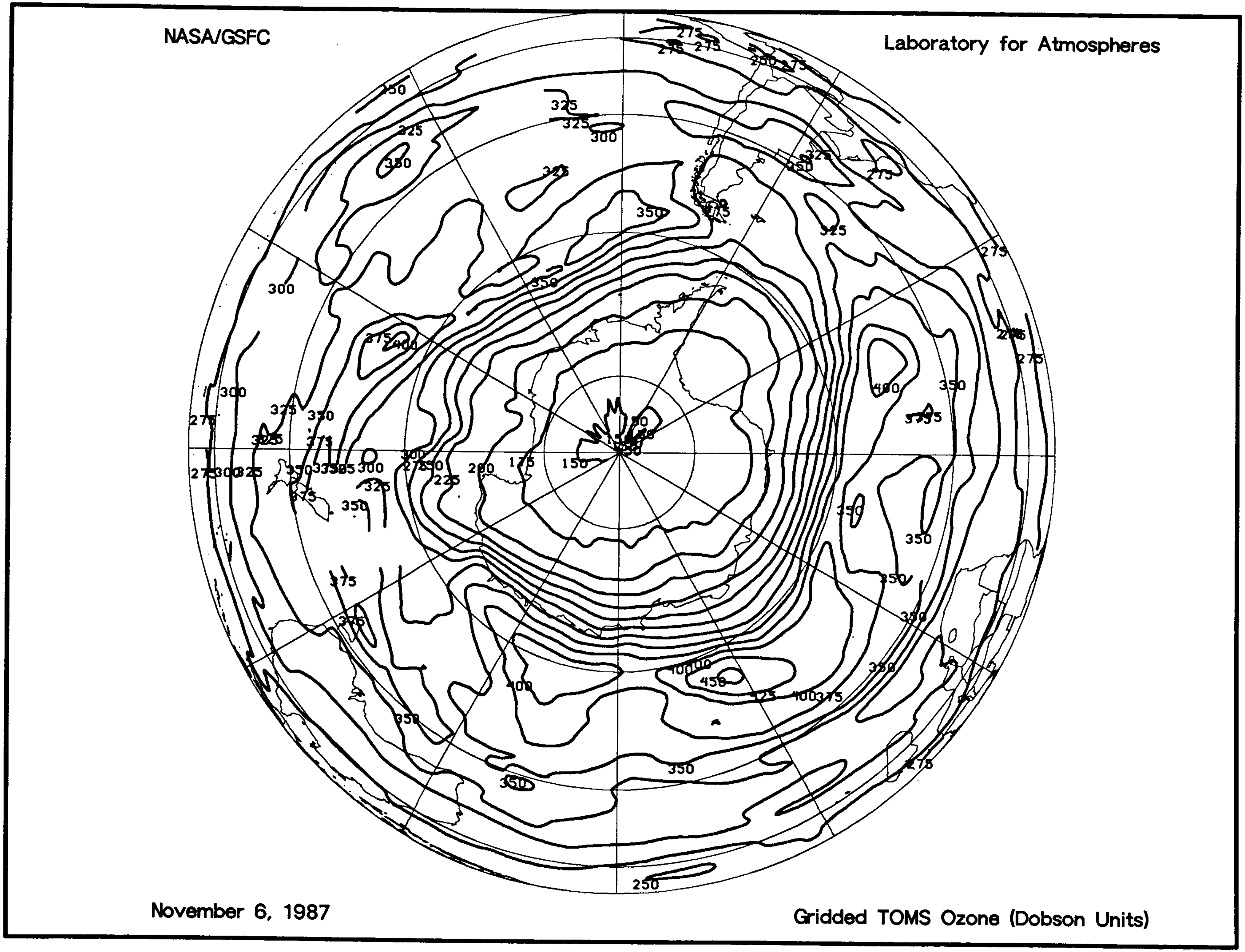
NASA/GSFC
Laboratory for Atmospheres
November 6, 1987
Gridded TOMS Ozone (Dobson Units)

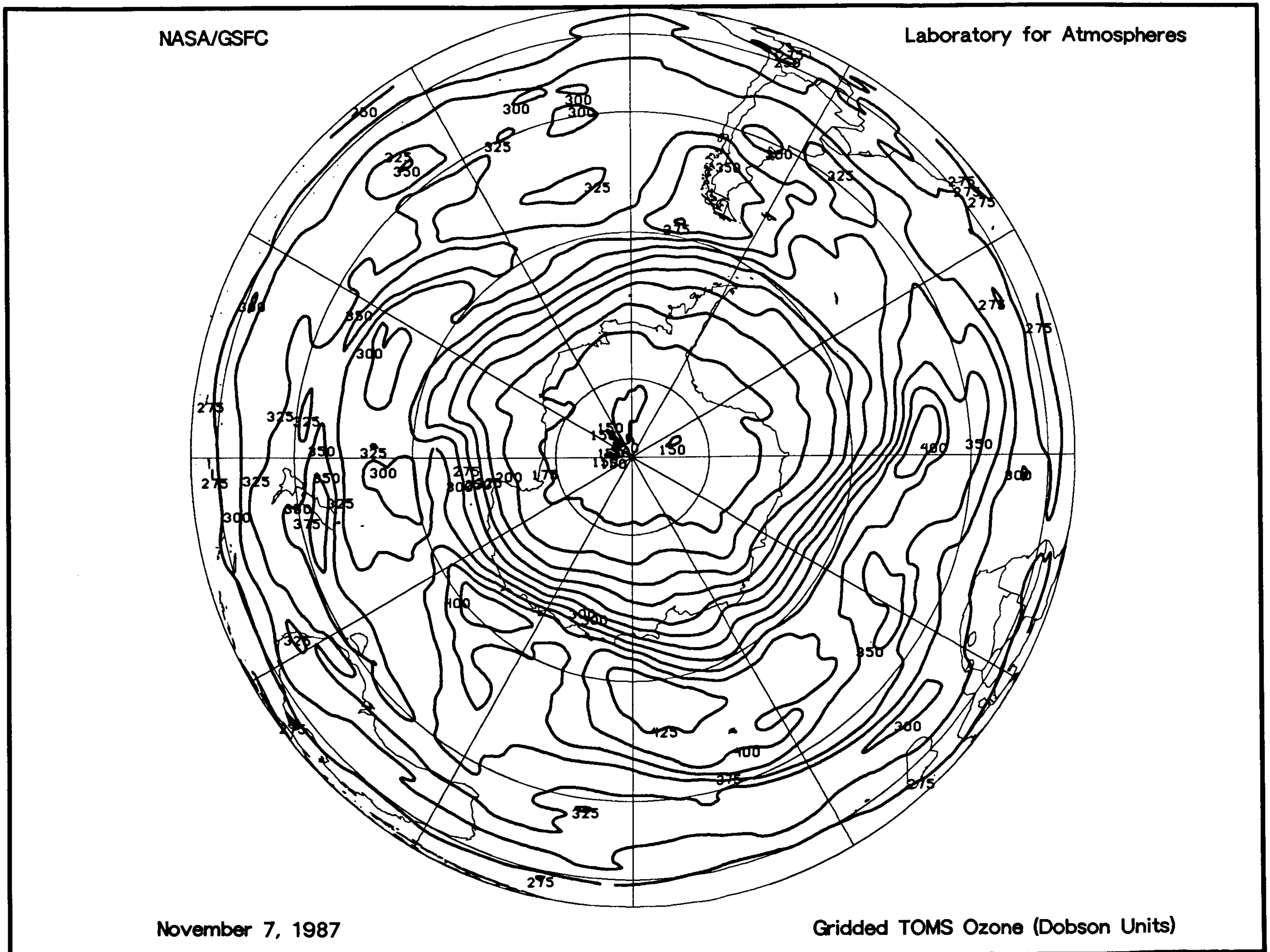
NASA/GSFC
Laboratory for Atmospheres
November 7, 1987
Gridded TOMS Ozone (Dobson Units)

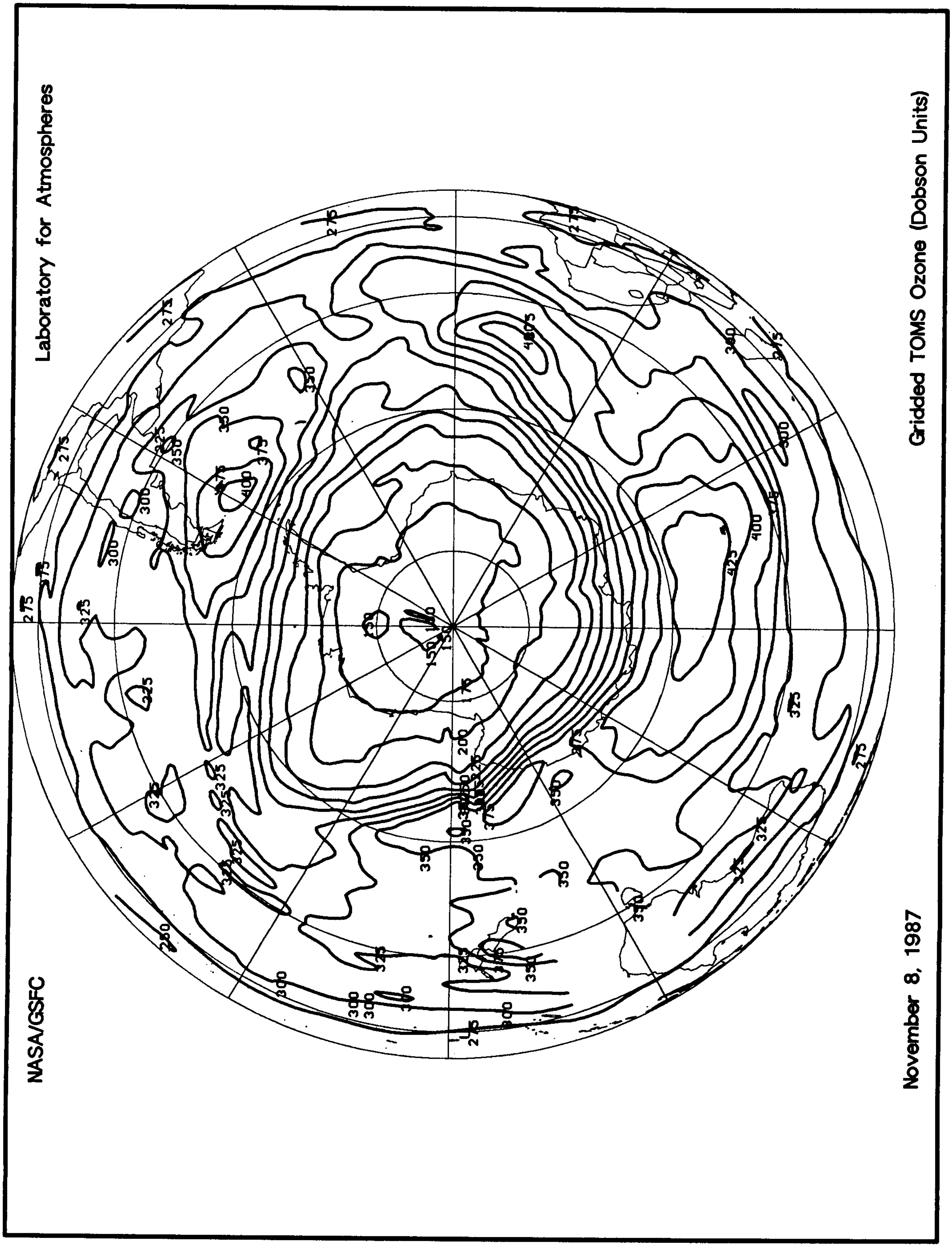
Laboratory for Atmospheres
Gridded TOMS Ozone (Dobson Units)
NASA/GSFC
November 8, 1987

C-3

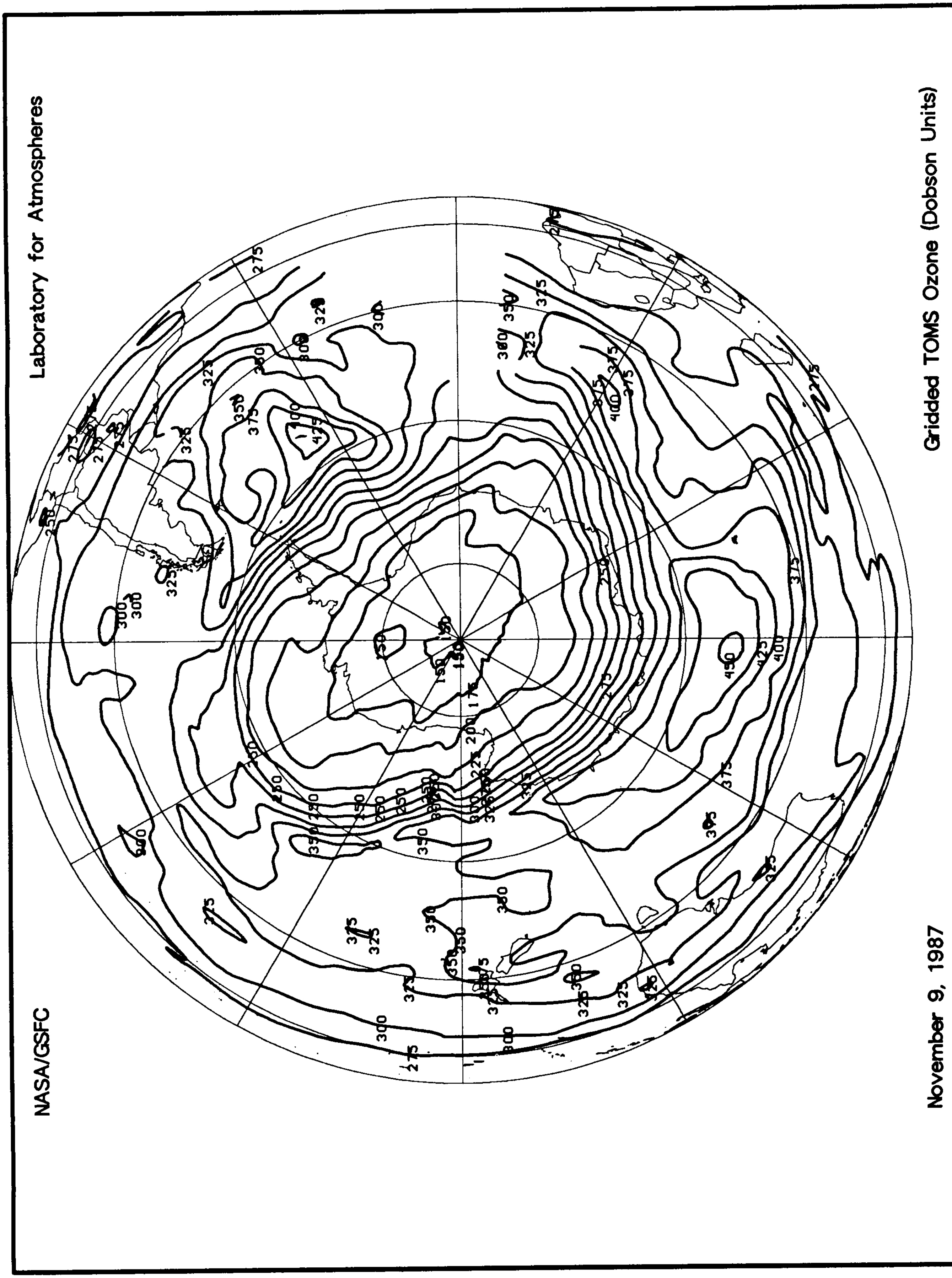
Laboratory for Atmospheres
NASA/GSFC
Gridded TOMS Ozone (Dobson Units)
November 9, 1987

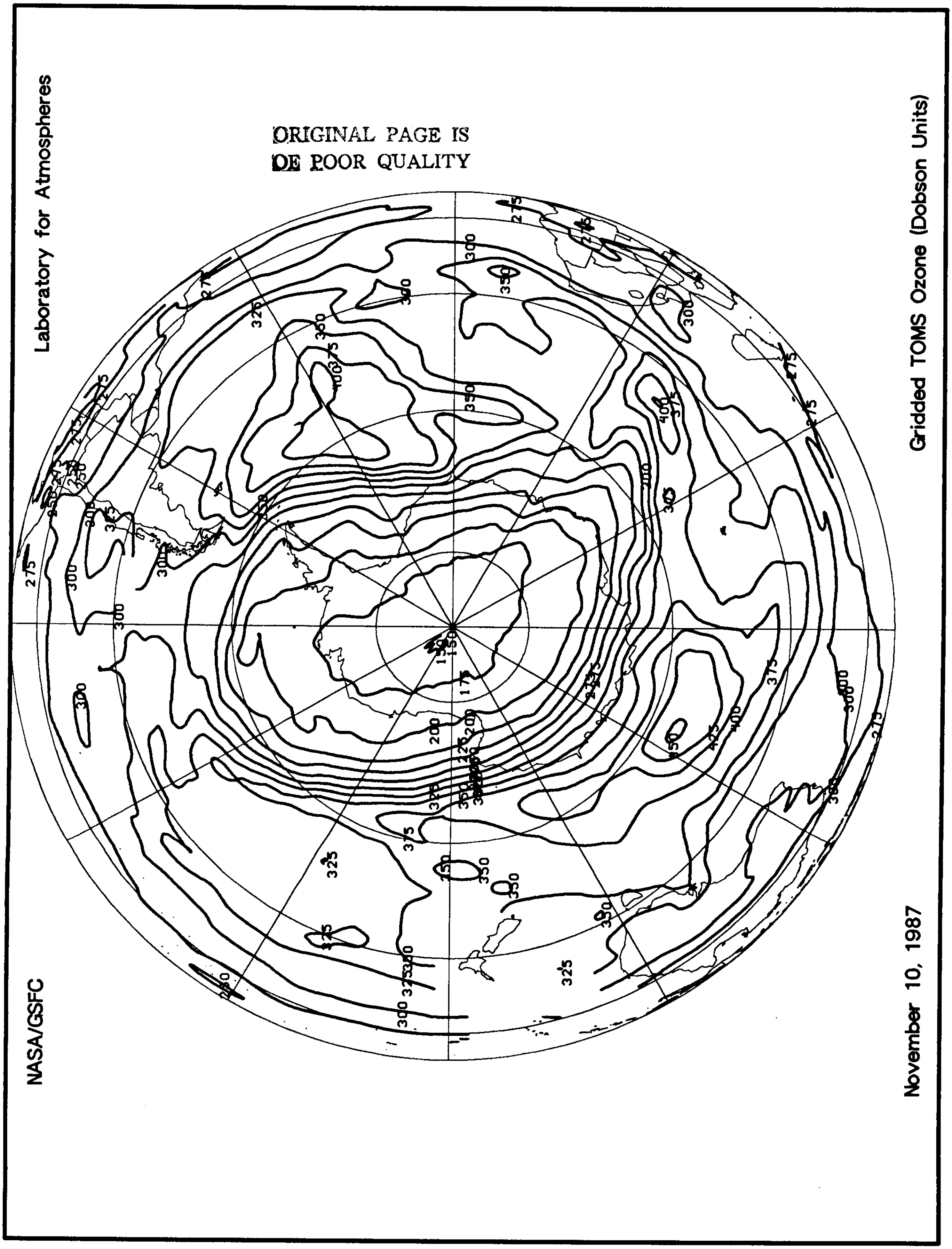
Laboratory for Atmospheres
NASA/GSFC
Gridded TOMS Ozone (Dobson Units)
November 10, 1987

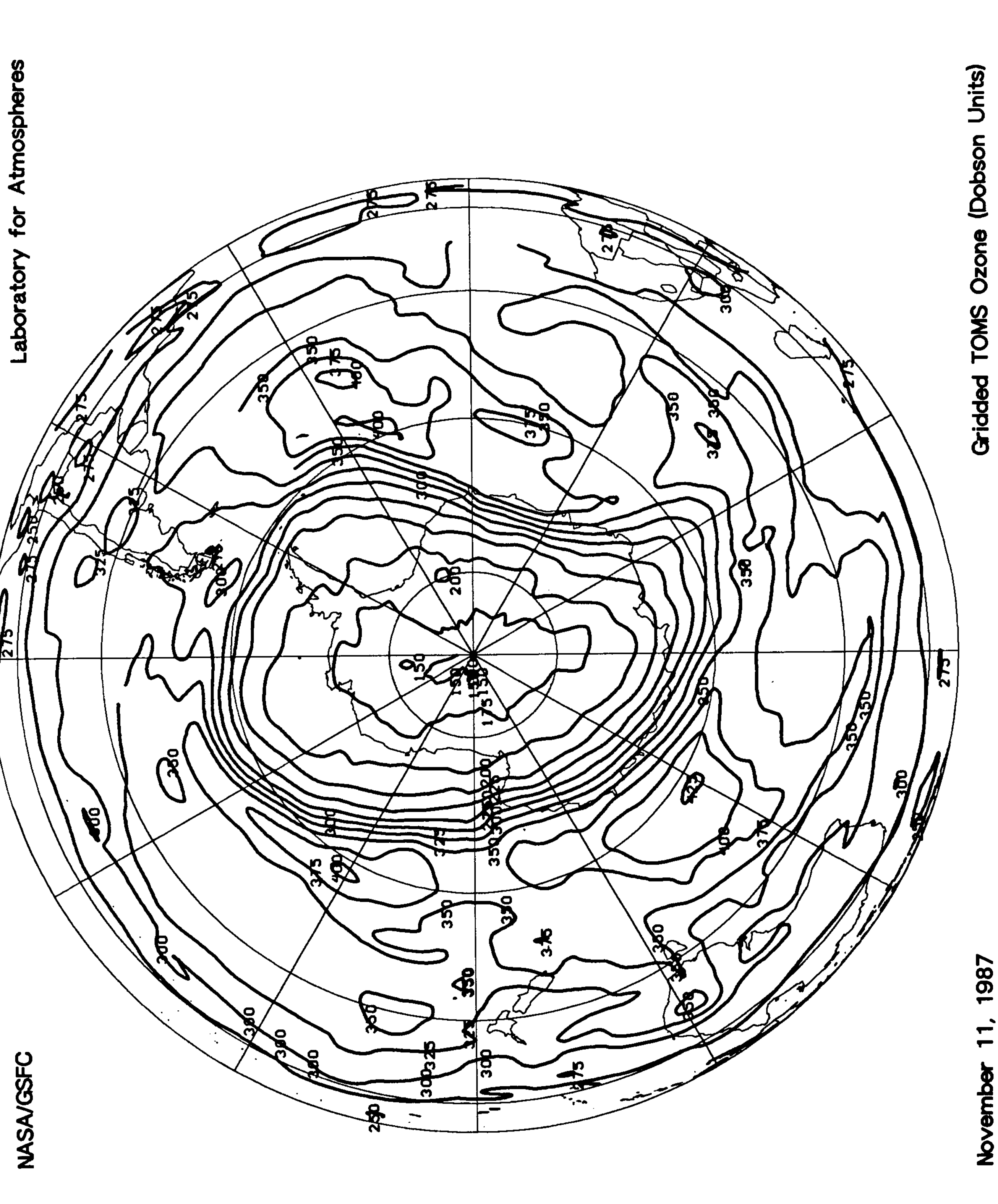


ORIGINAL PAGE IS
OF POOR QUALITY

NASA/GSFC

Laboratory for Atmospheres

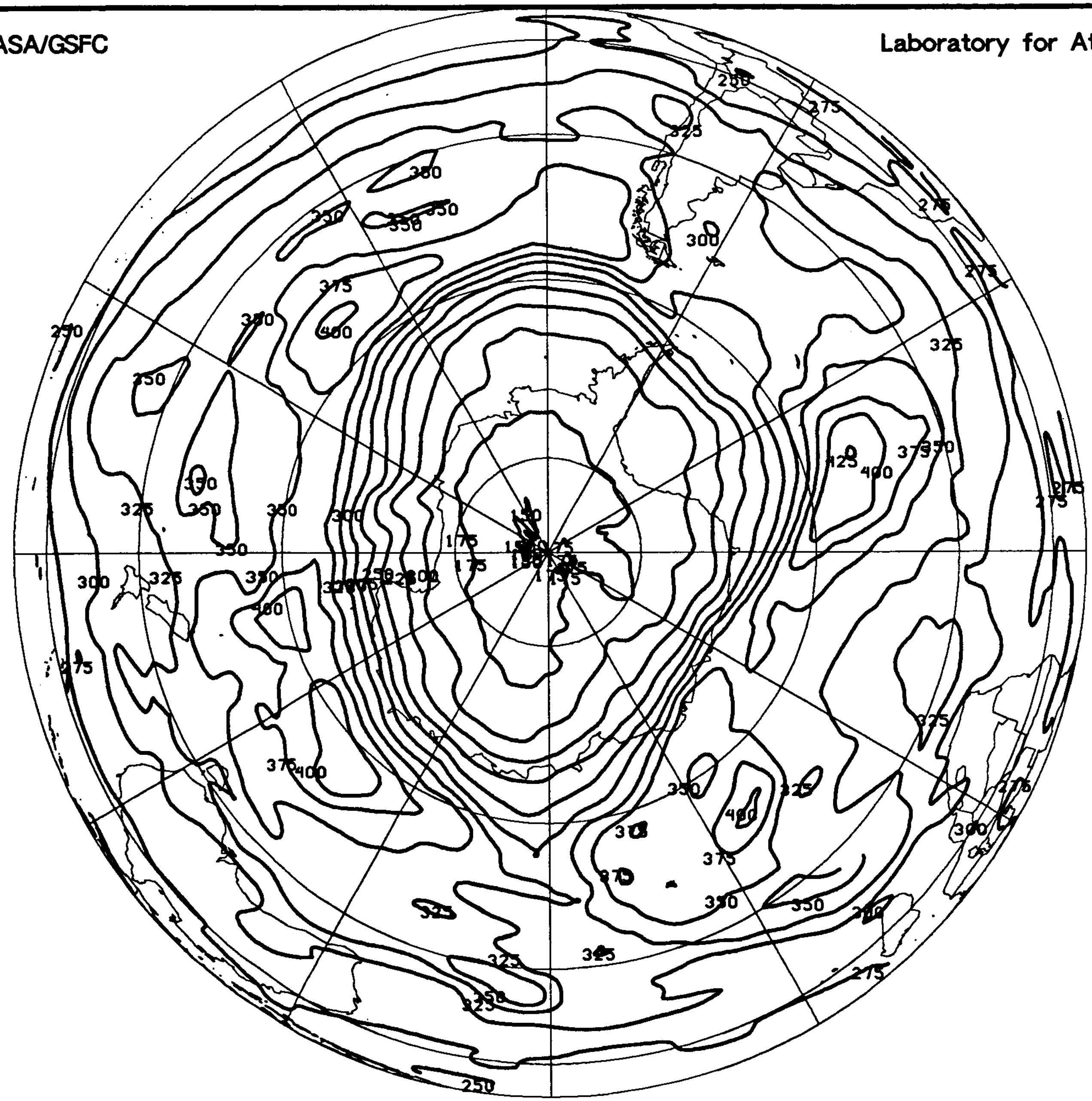

November 12, 1987

Gridded TOMS Ozone (Dobson Units)

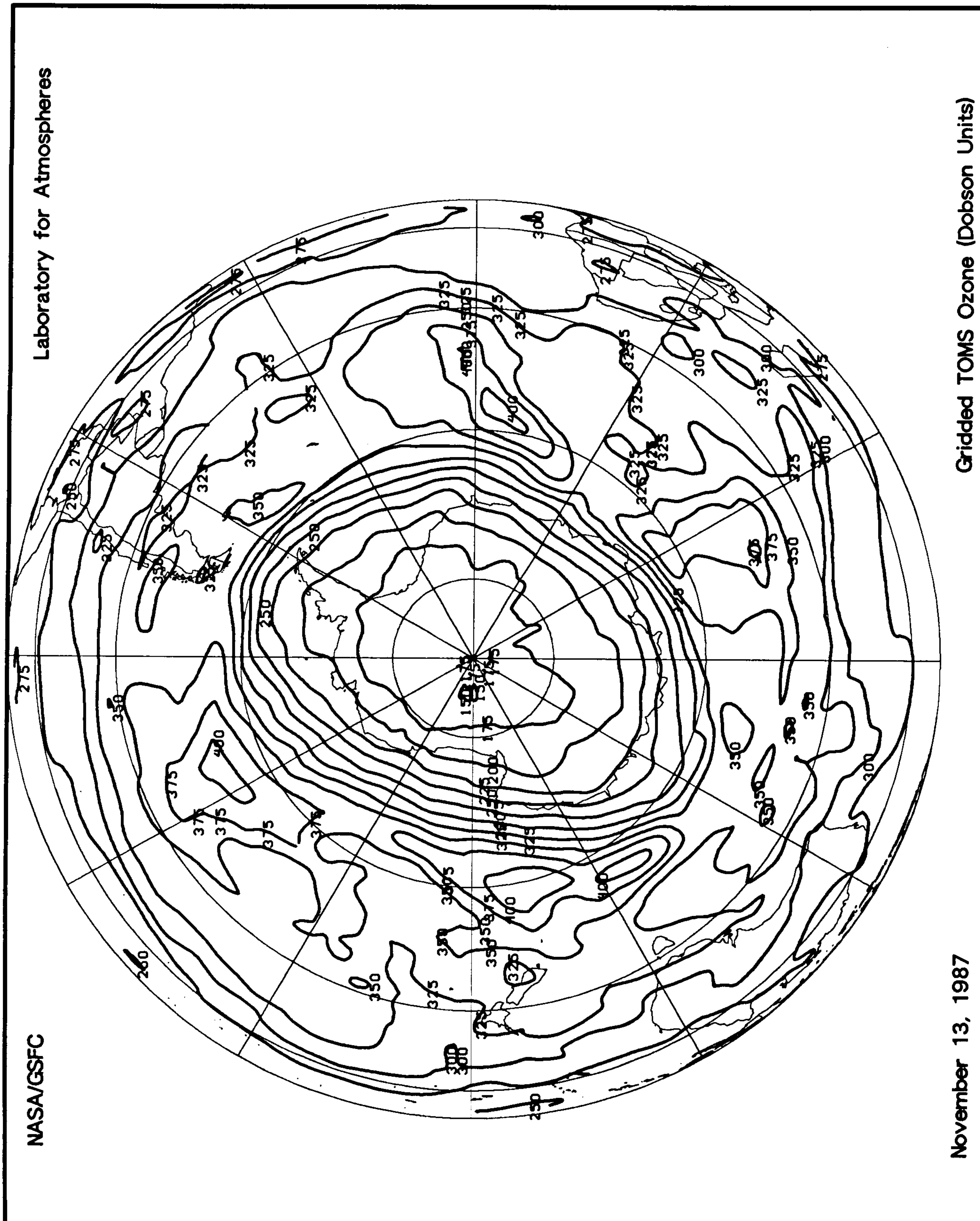


ORIGINAL PAGE IS
OF POOR QUALITY

NASA/GSFC

Laboratory for Atmospheres

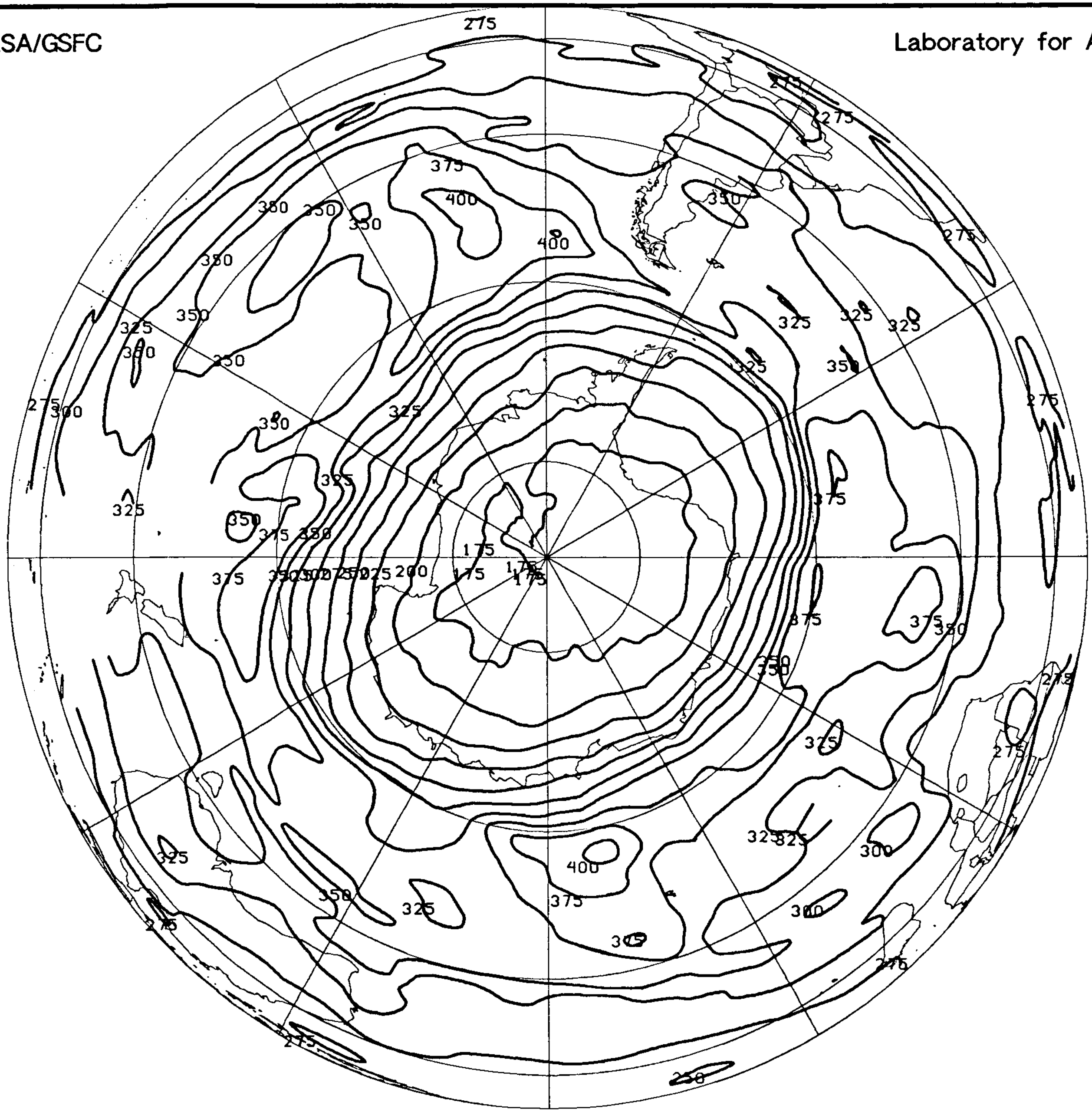

November 14, 1987

Gridded TOMS Ozone (Dobson Units)

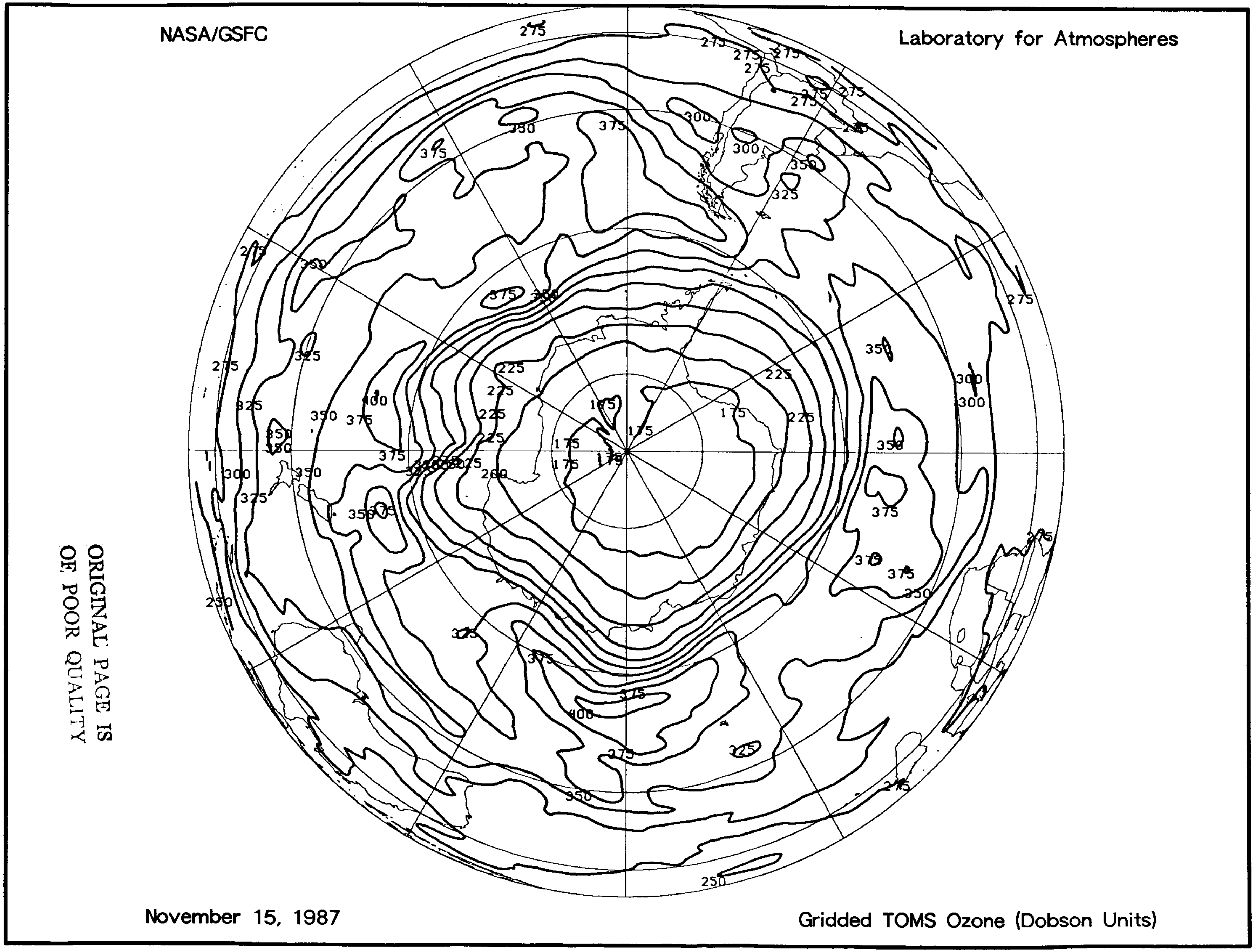


ORIGINAL PAGE IS
OF POOR QUALITY

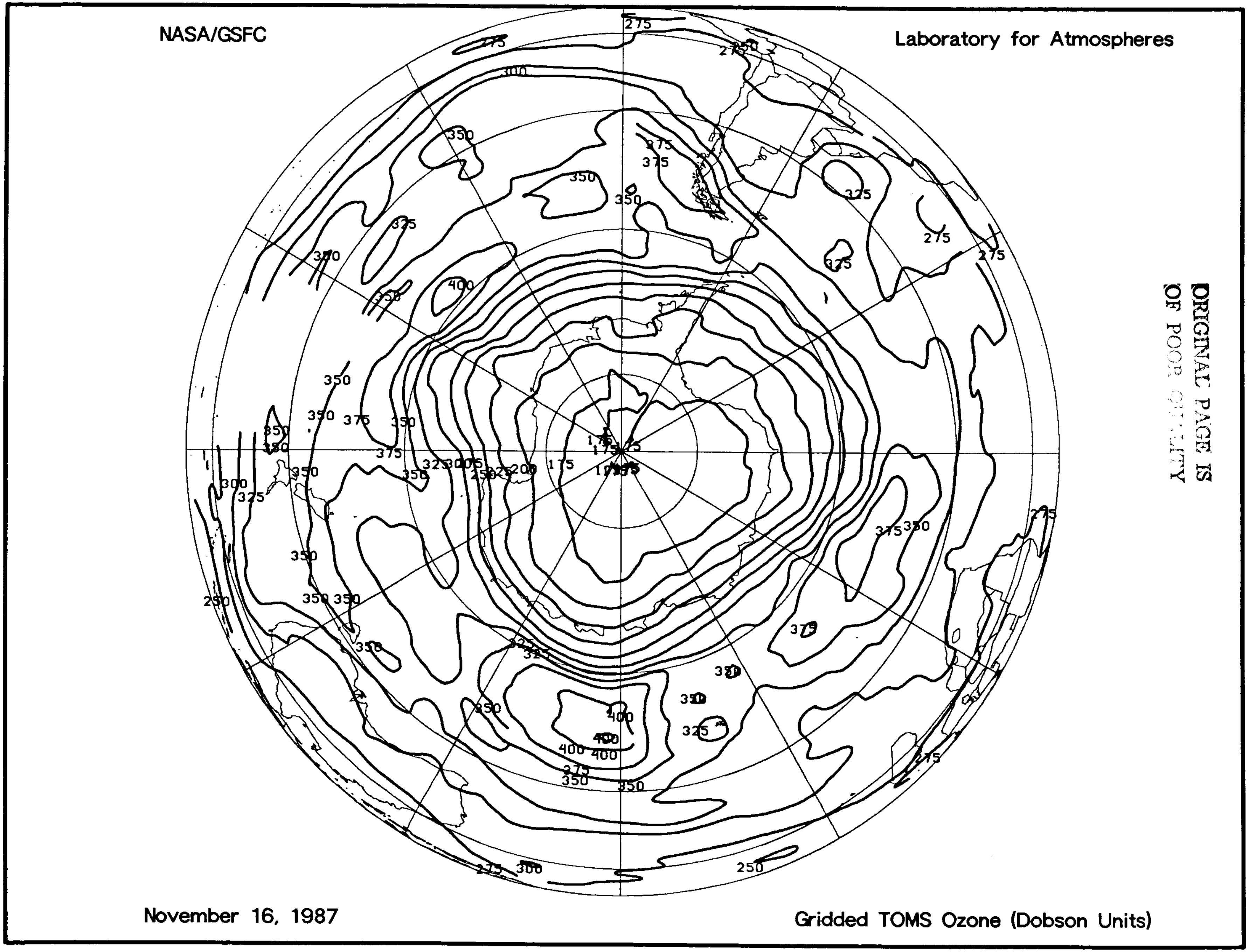
NASA/GSFC
Laboratory for Atmospheres
November 16, 1987
Gridded TOMS Ozone (Dobson Units)

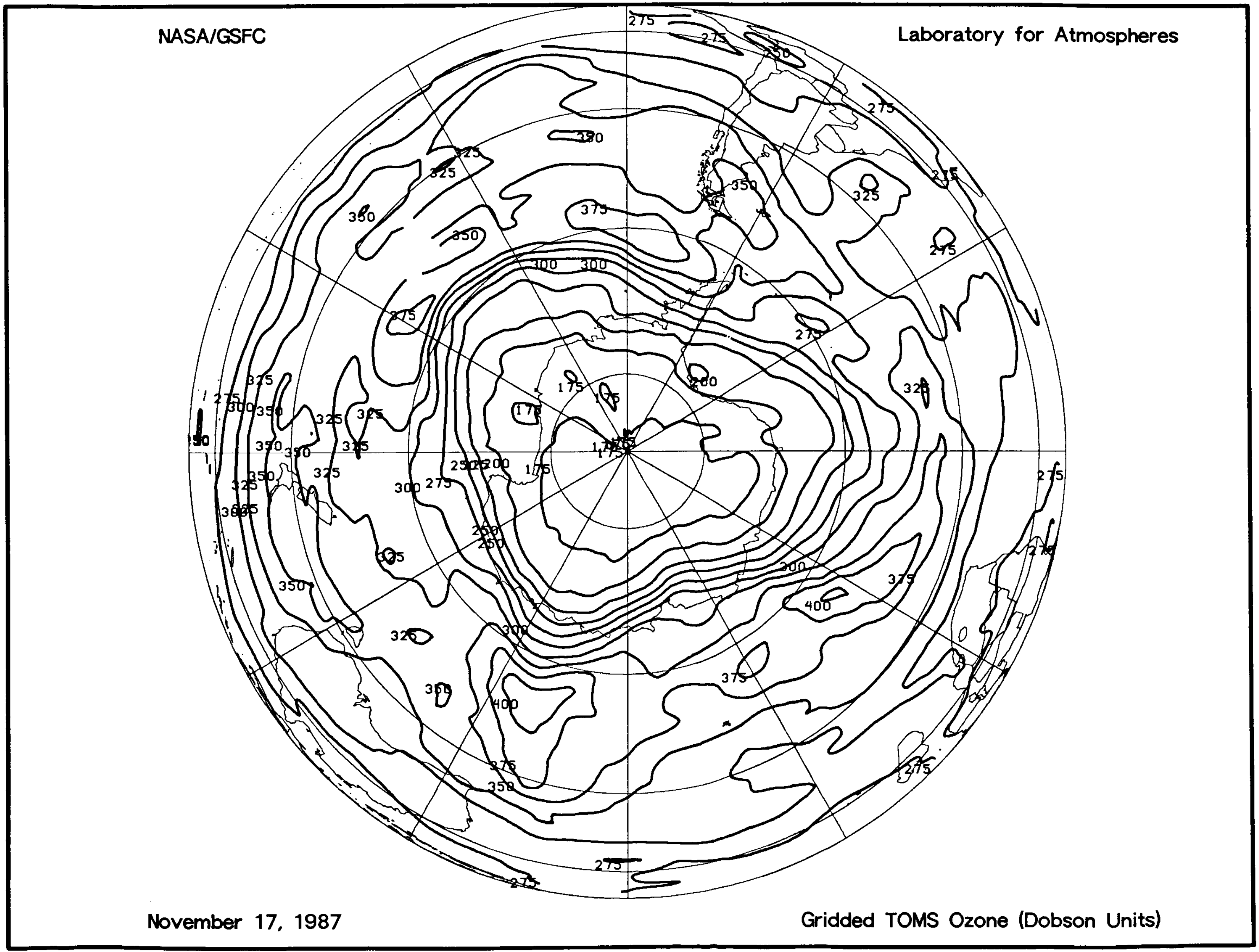
NASA/GSFC
Laboratory for Atmospheres
November 17, 1987
Gridded TOMS Ozone (Dobson Units)

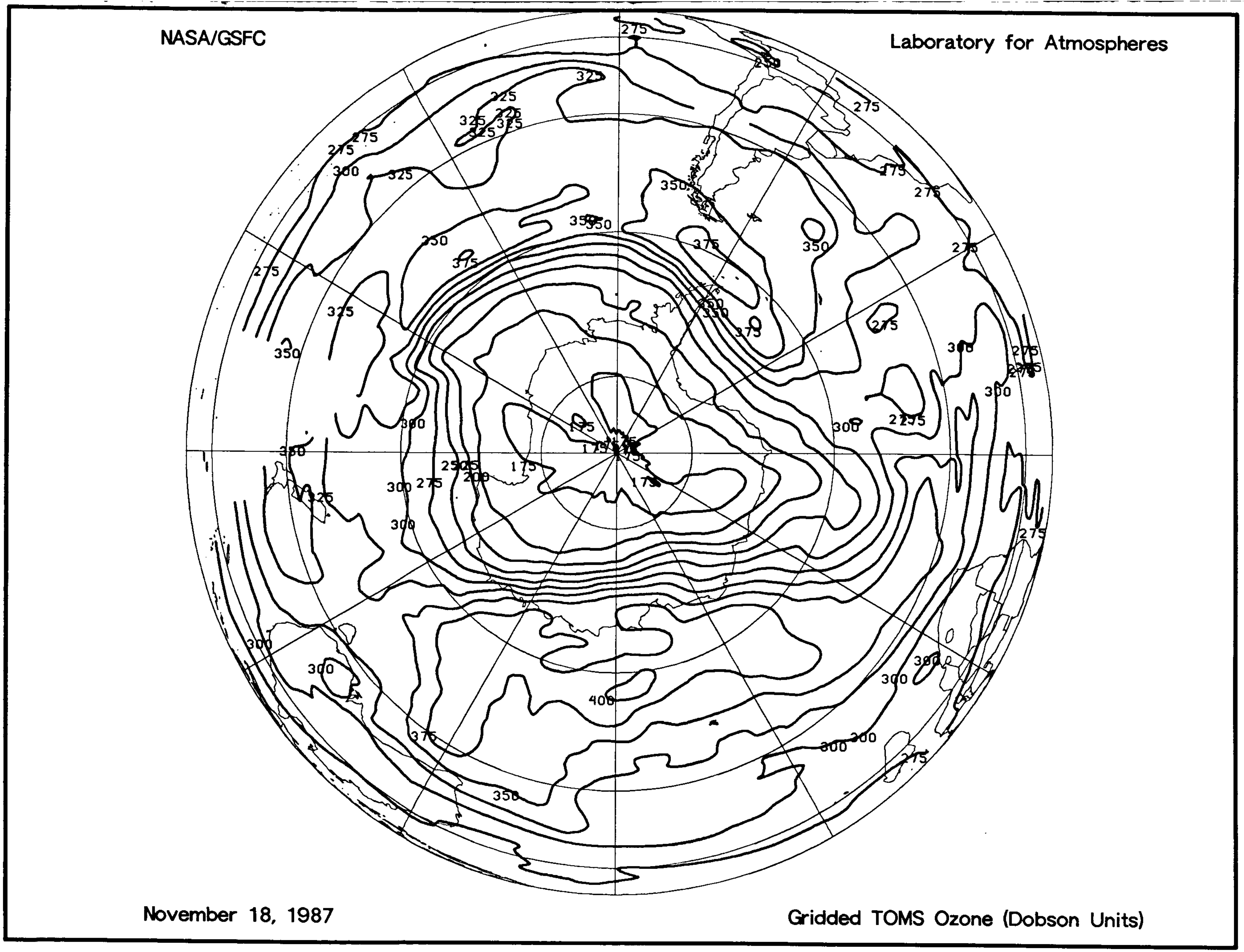
NASA/GSFC
Laboratory for Atmospheres
November 18, 1987
Gridded TOMS Ozone (Dobson Units)

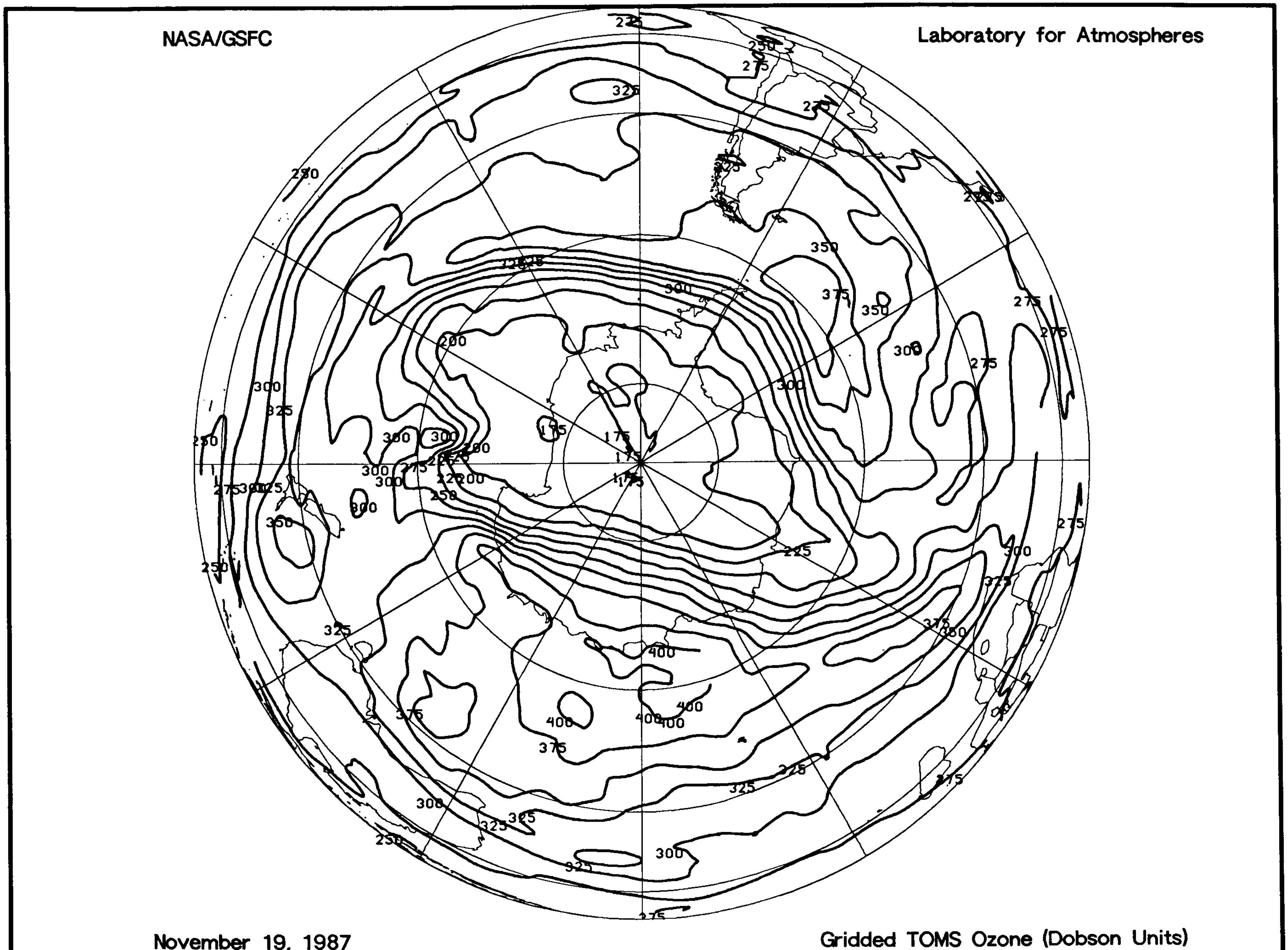
NASA/GSFC
Laboratory for Atmospheres
November 19, 1987
Gridded TOMS Ozone (Dobson Units)

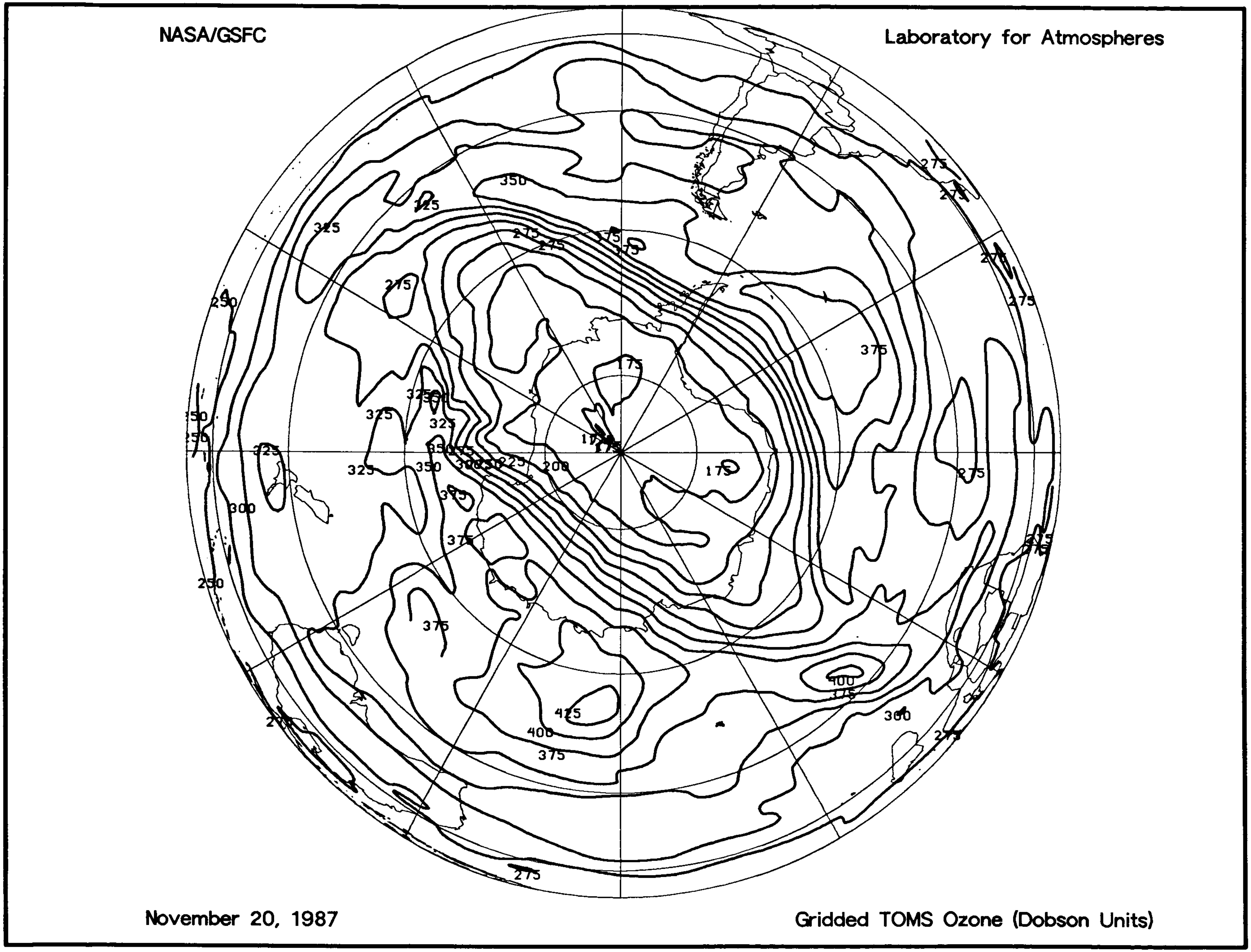
NASA/GSFC
Laboratory for Atmospheres
November 20, 1987
Gridded TOMS Ozone (Dobson Units)

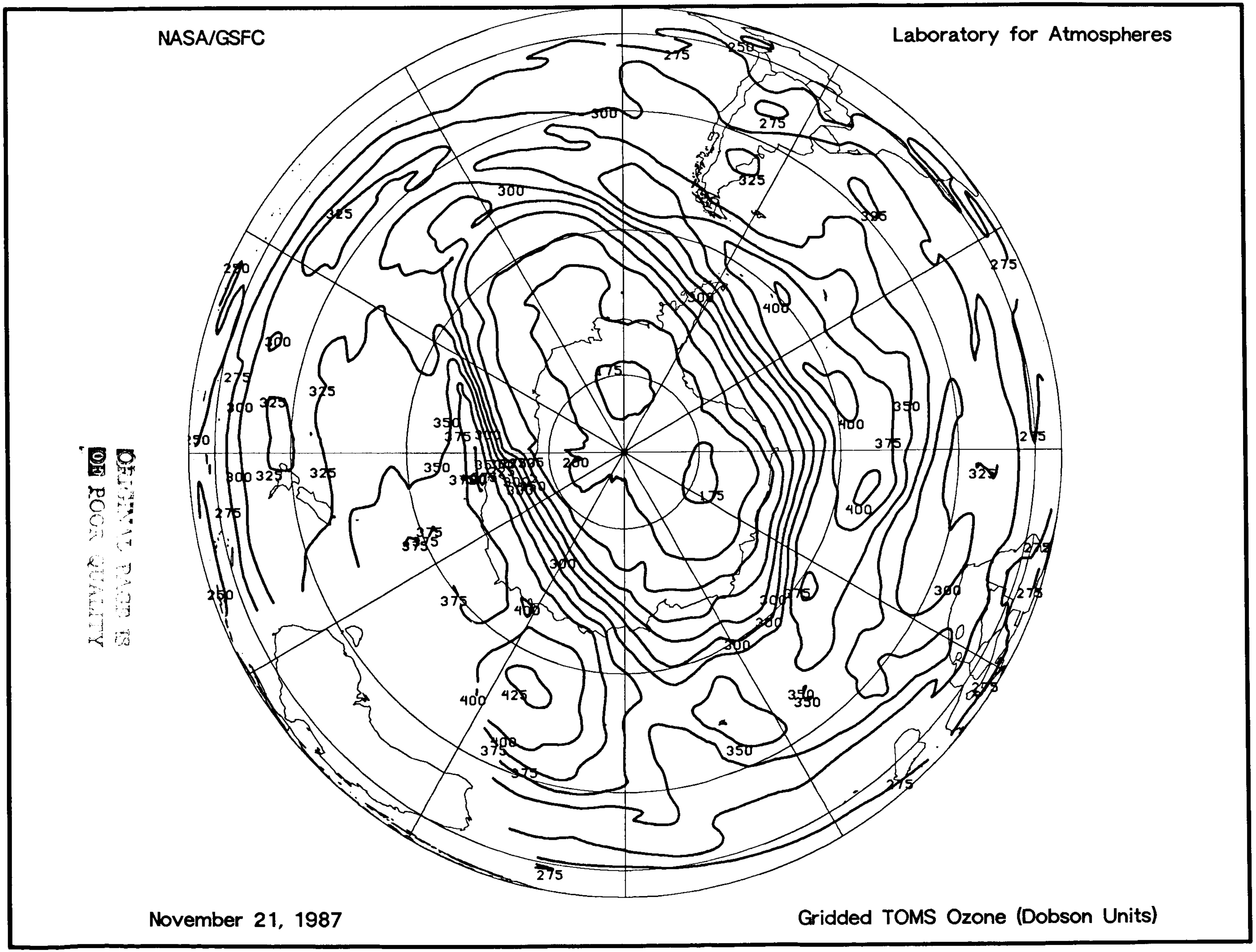
NASA/GSFC
Laboratory for Atmospheres
November 21, 1987
Gridded TOMS Ozone (Dobson Units)

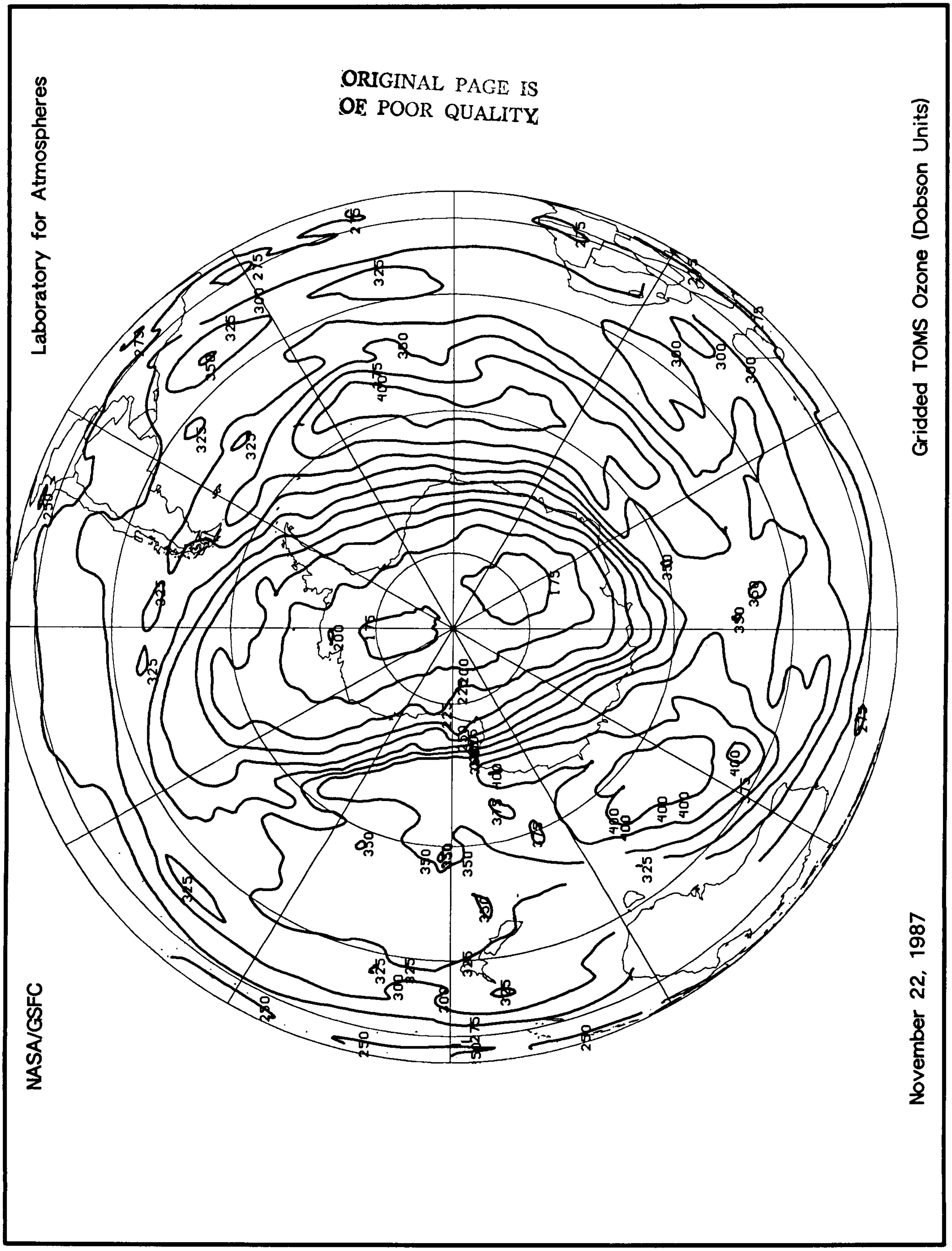
Laboratory for Atmospheres
NASA/GSFC
Gridded TOMS Ozone (Dobson Units)
November 22, 1987

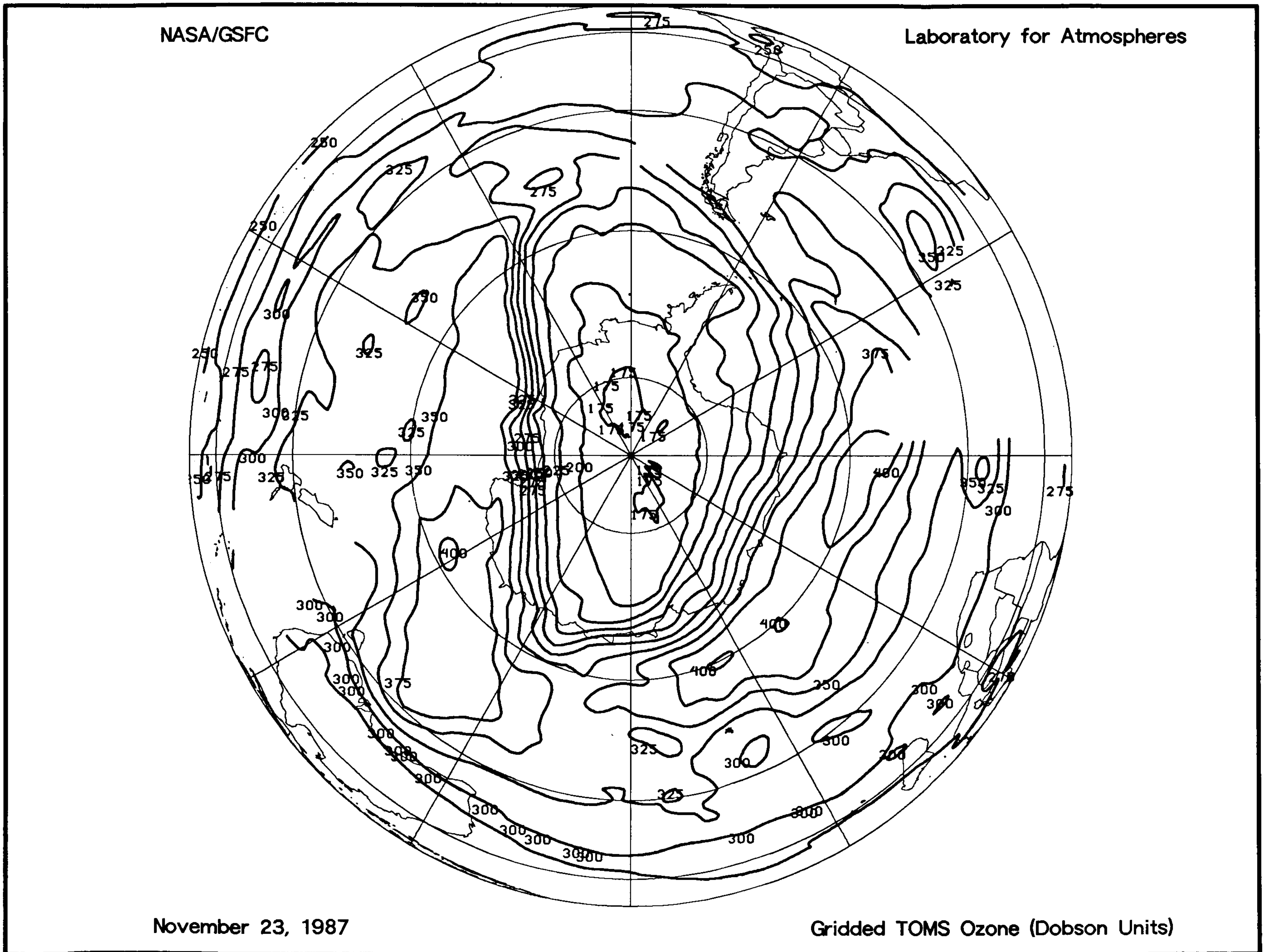
NASA/GSFC
Laboratory for Atmospheres
November 23, 1987
Gridded TOMS Ozone (Dobson Units)

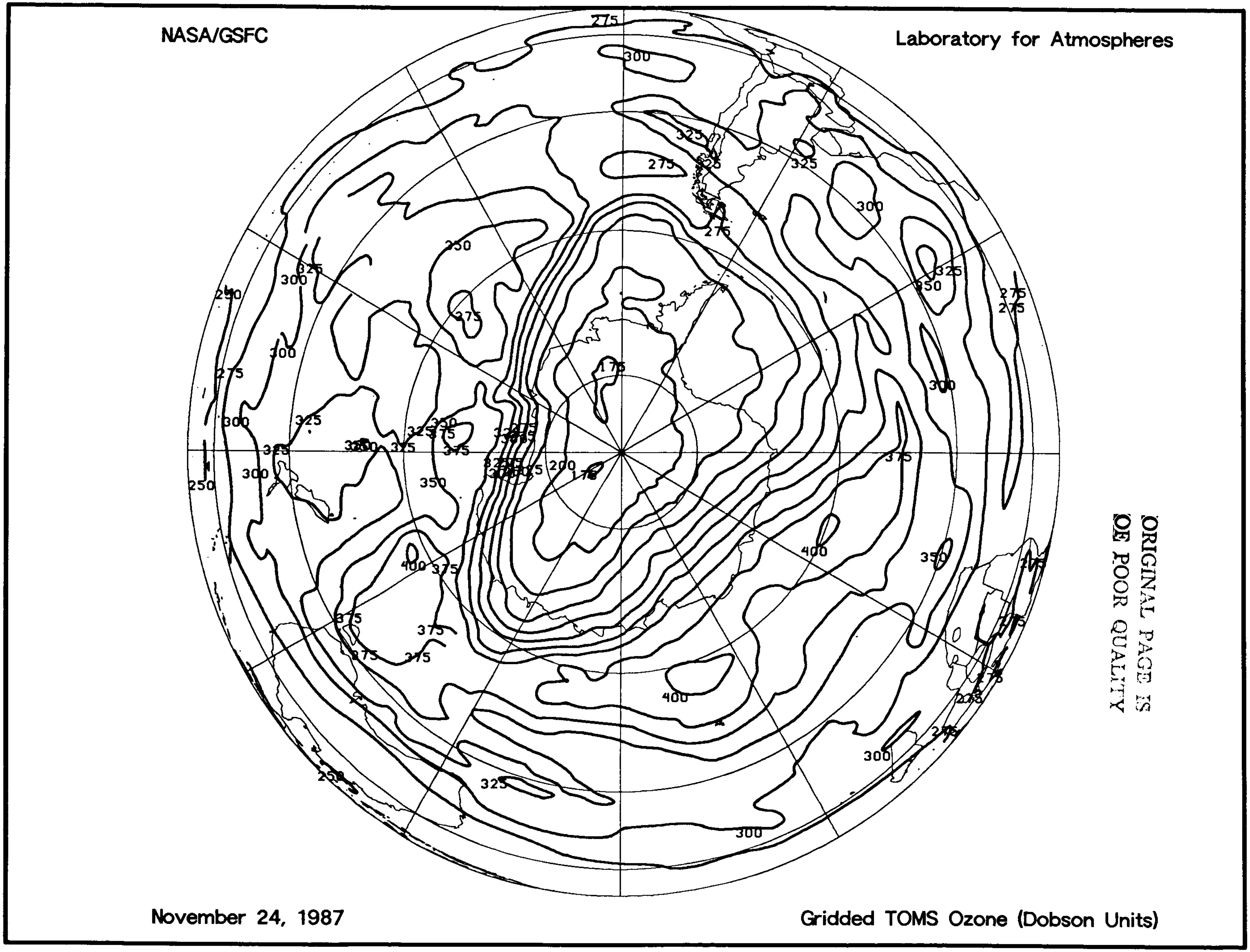
NASA/GSFC
Laboratory for Atmospheres
November 24, 1987
Gridded TOMS Ozone (Dobson Units)

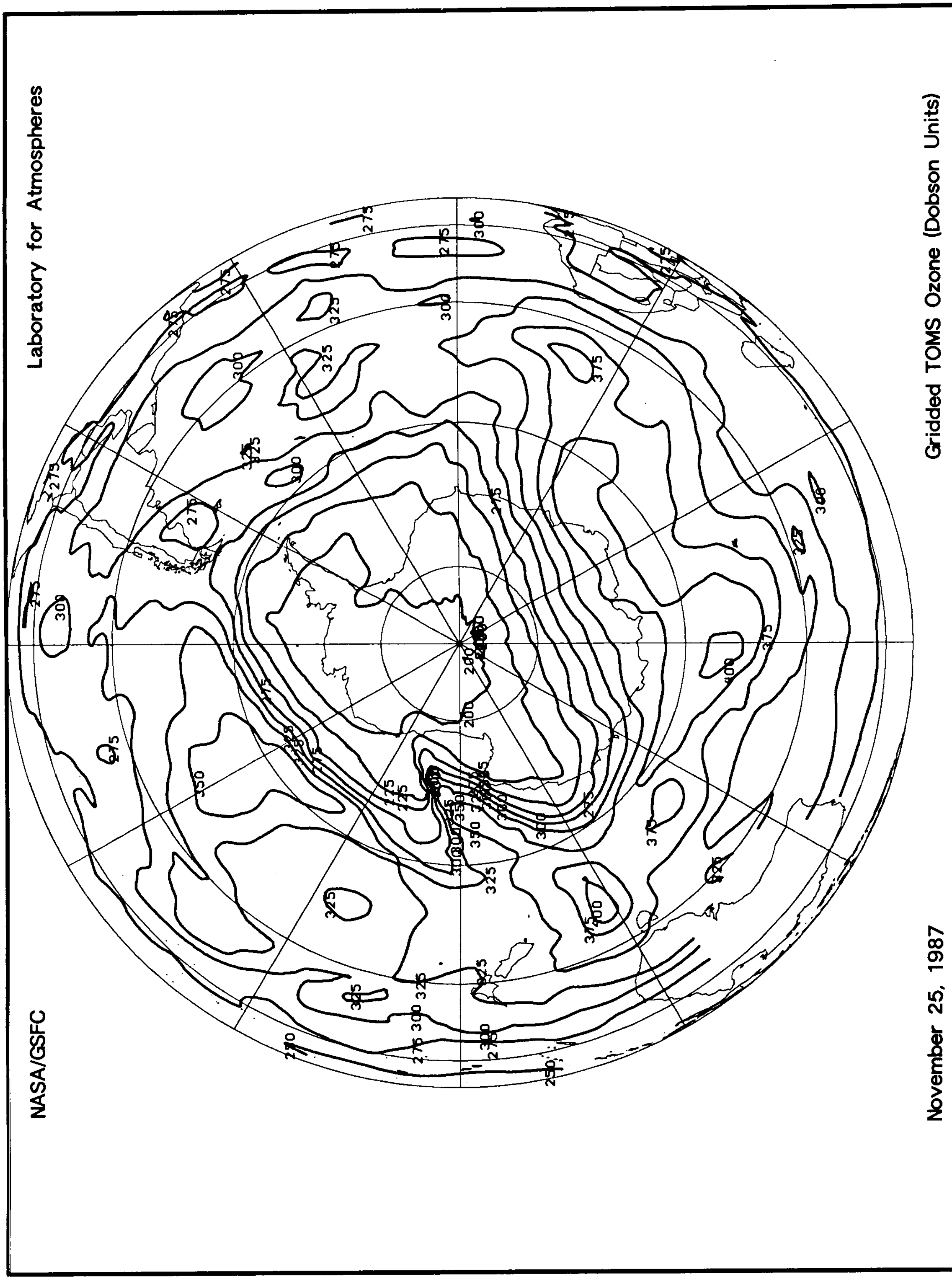
Laboratory for Atmospheres
NASA/GSFC
Gridded TOMS Ozone (Dobson Units)
November 25, 1987

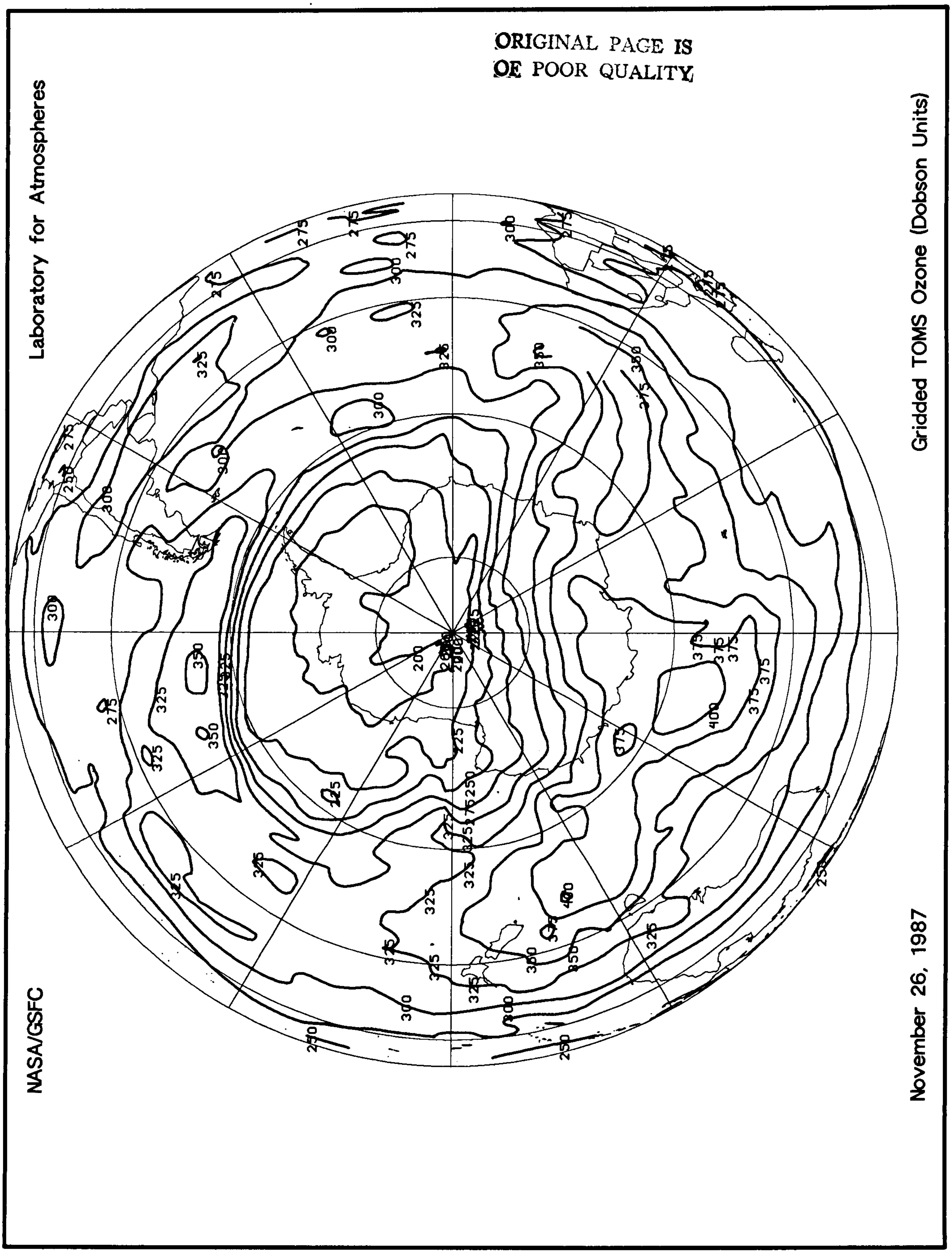
Laboratory for Atmospheres
NASA/GSFC
Gridded TOMS Ozone (Dobson Units)
November 26, 1987

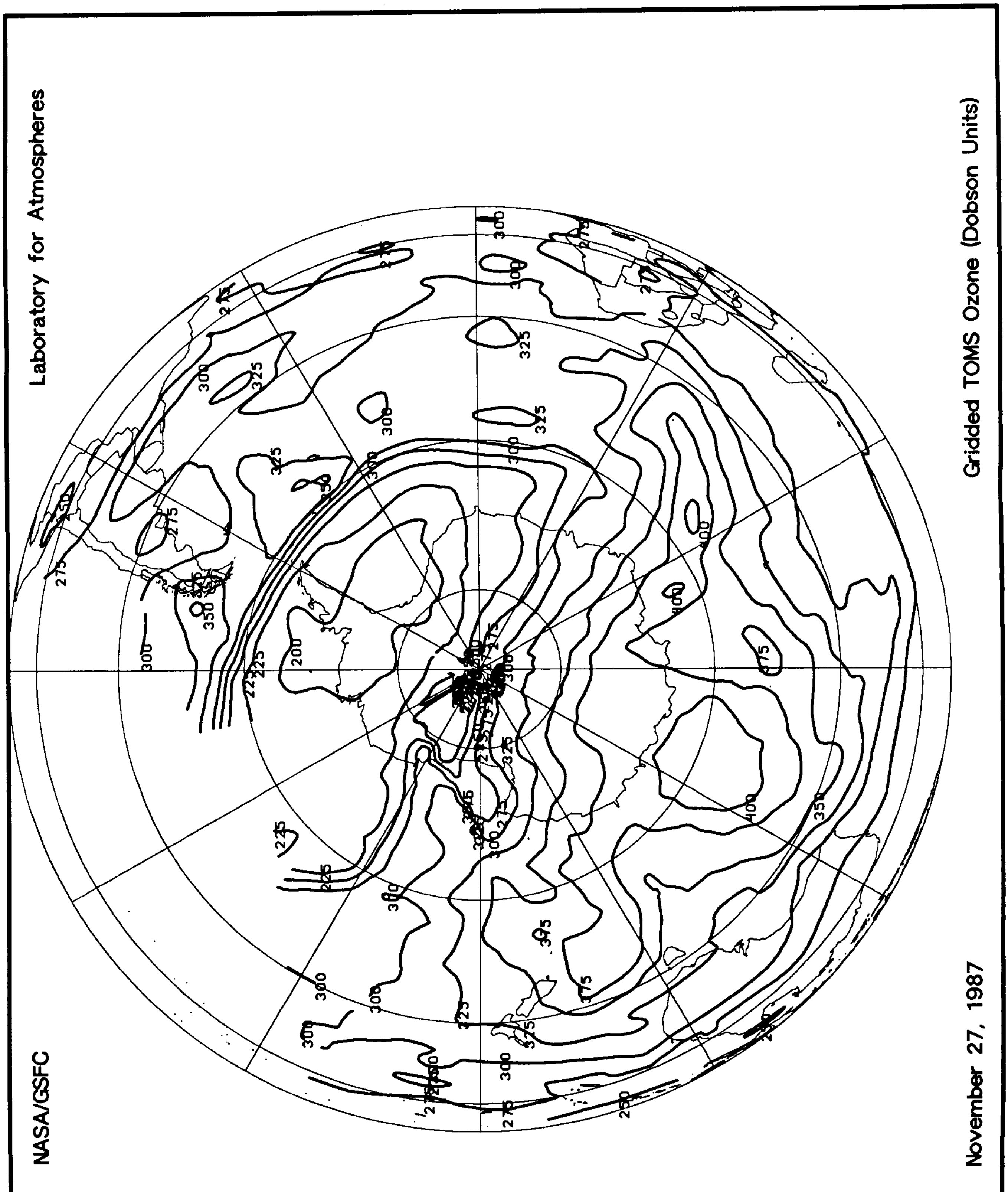

Laboratory for Atmospheres
Gridded TOMS Ozone (Dobson Units)
NASA/GSFC
November 27, 1987

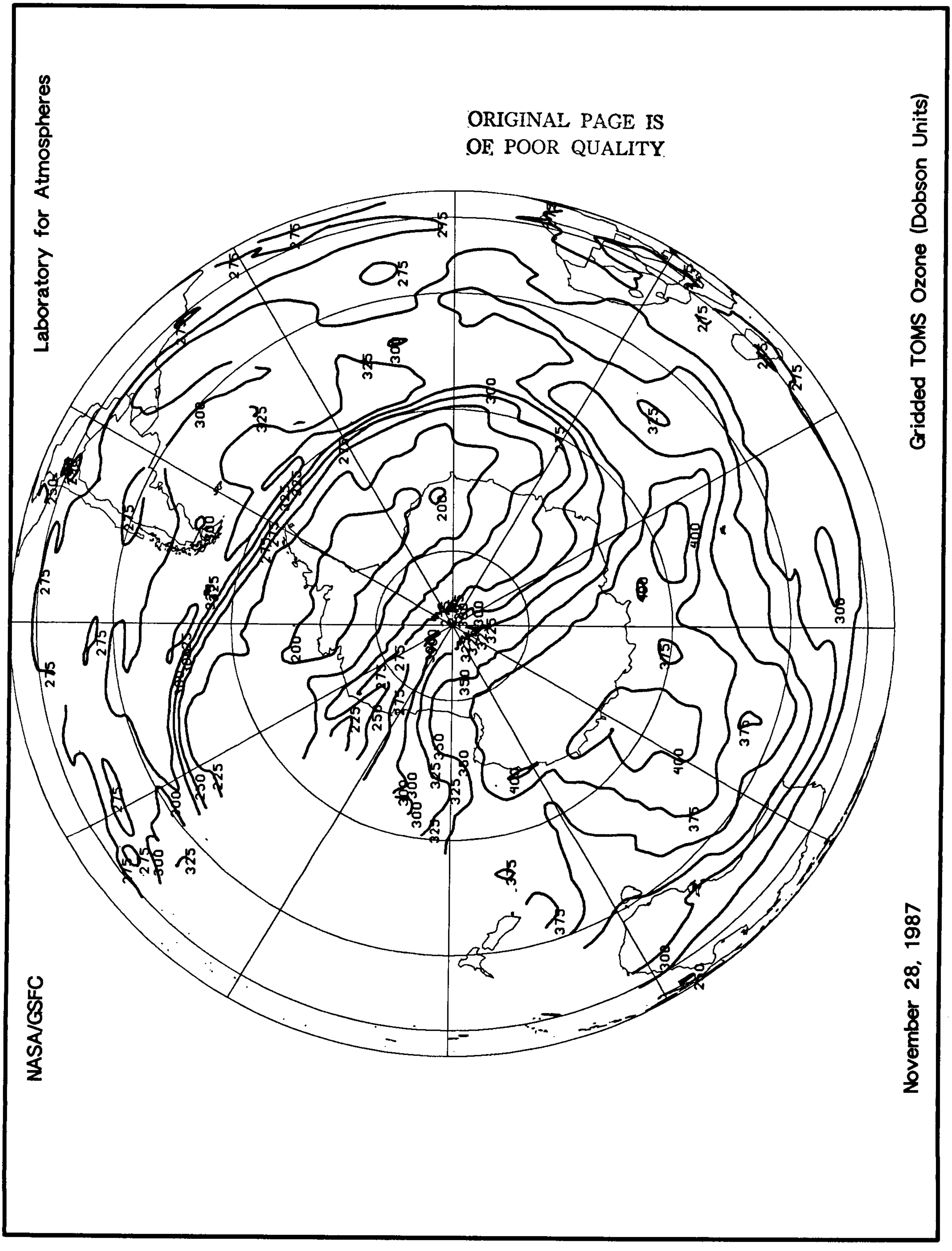
Laboratory for Atmospheres
Gridded TOMS Ozone (Dobson Units)
NASA/GSFC
November 28, 1987

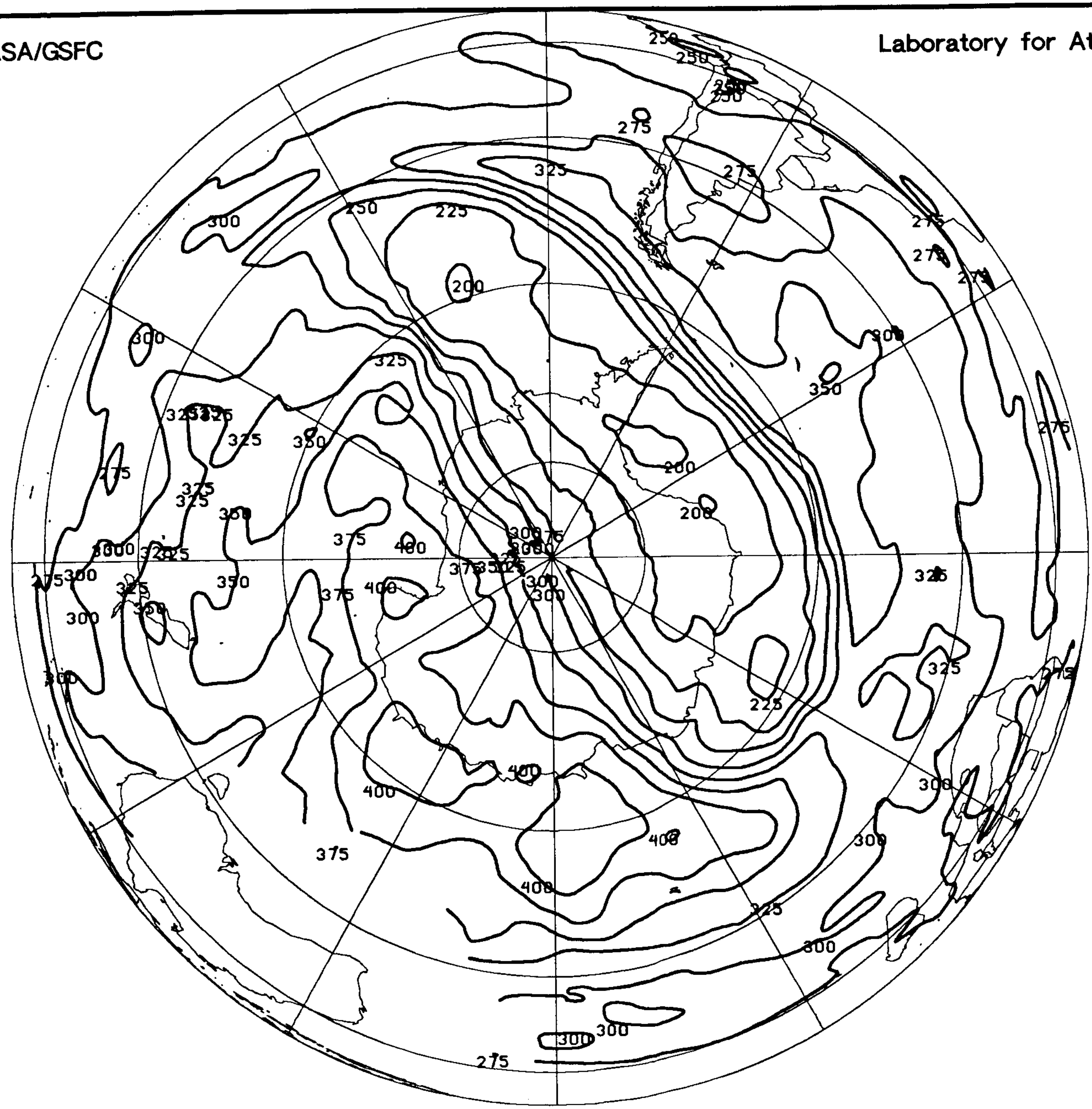
NASA/GSFC
Laboratory for Atmospheres
November 29, 1987
Gridded TOMS Ozone (Dobson Units)

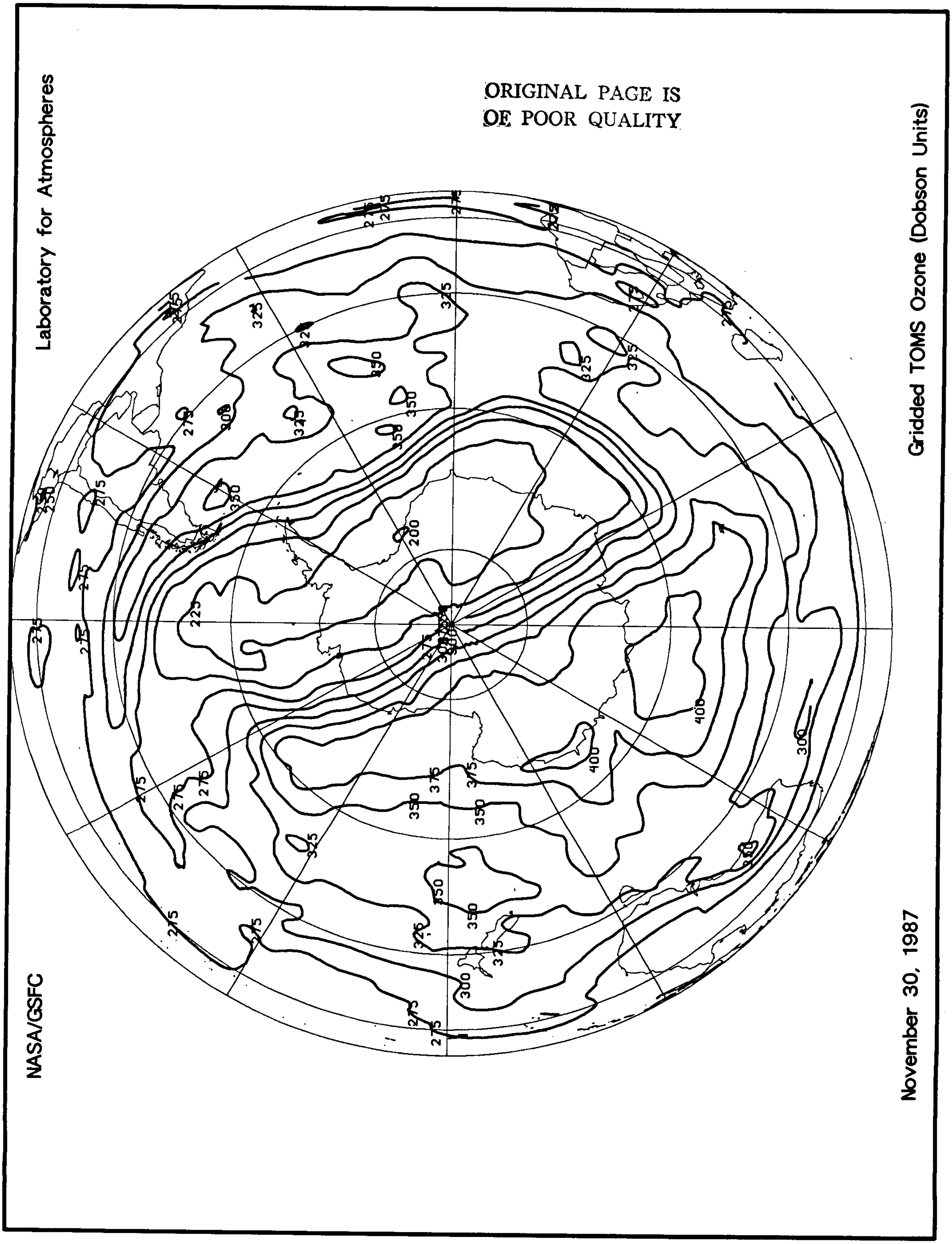
Laboratory for Atmospheres
Gridded TOMS Ozone (Dobson Units)
NASA/GSFC
November 30, 1987

## 3.6 Mapping Onto Aircraft Flight Paths

In this section, we relate the distribution of the TOMS total-ozone to the flight paths of the NASA ER-2 and DC-8 research aircraft for their missions during the 1987 Airborne Antarctic Ozone Experiment. The flights were previously tabulated in the chronology. In each figure, the upper panel gives the reader an idea of the flight path of each aircraft mission as projected onto a polar plot, while the bottom panel evaluates the TOMS total-ozone estimates along each flight track. While the abscissa of the bottom panel is time, the reader should be cautioned that the TOMS instrument is carried on board the Nimbus-7 satellite which is sun-synchronous. As such, there is no temporal evolution of the TOMS ozone values during the course of the mission. However, these maps clearly indicate the position of the ozone hole and its boundary relative to each research flight.

Though the NASA ER-2 left Ames Research Center on August 12, it did not fly its first mission out of Punta Arenas, Chile for the experiment until August 17. Here we do not consider the three transfer flights (i, ii, and iii) and just illustrate data for the twelve ER-2 missions between the period August 17 and September 22 (Figure 8a-8l). Similarly, we do not consider the two DC-8 flights between NASA Ames and Punta Arenas between the period August 19 and August 22 Data for the thirteen DC-8 missions during the experiment is illustrated in Figure 9a-9m, and includes the final flight between Punta Arenas, Chile and Christchurch, New Zealand.

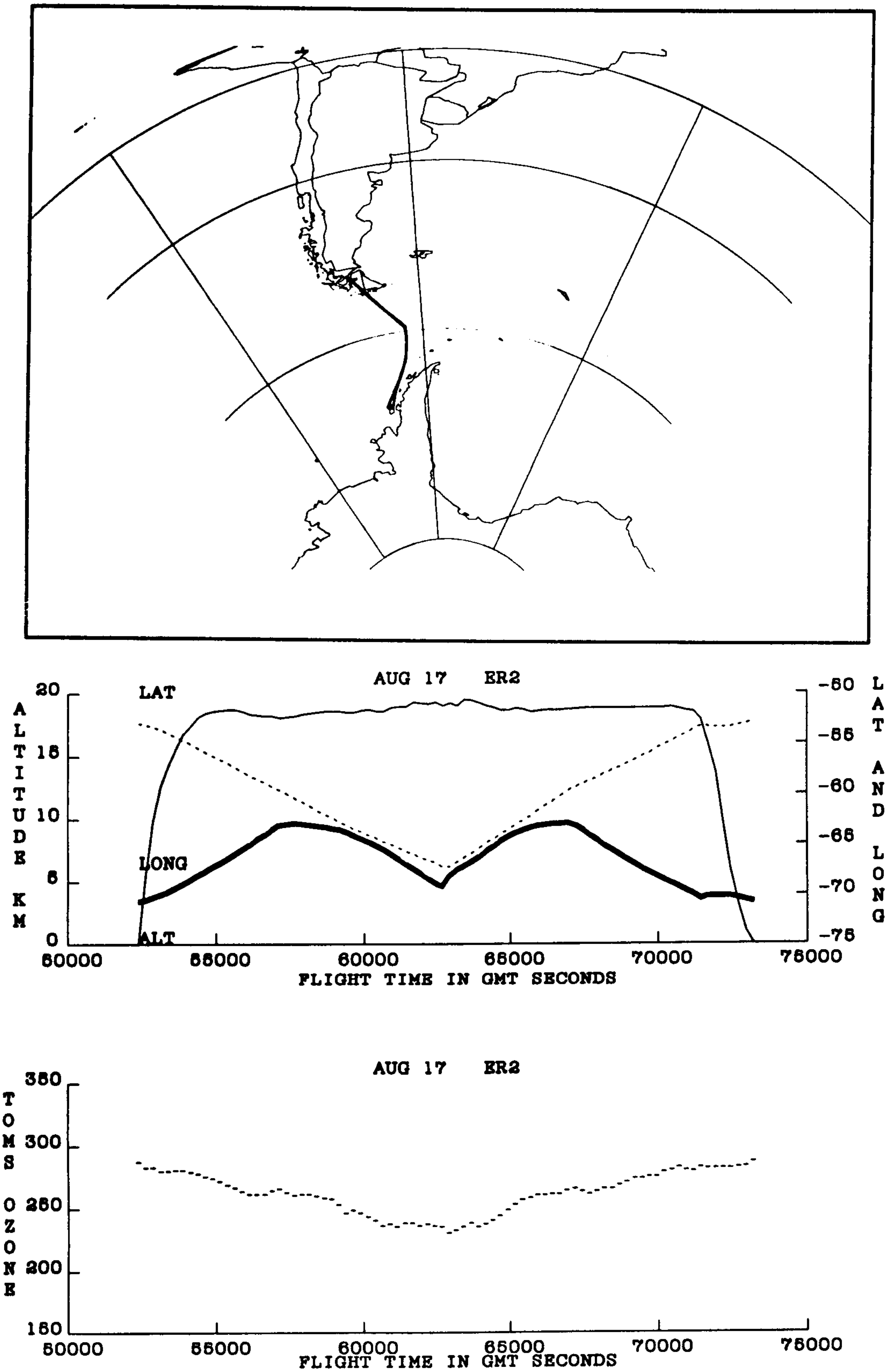


Figure 8a. Flight Path of the ER-2 mission for August 17 as mapped onto a polar projection (top) and as a time series of latitude, longitude, and altitude along with the corresponding TOMS total-ozone estimates along the flight path (bottom).

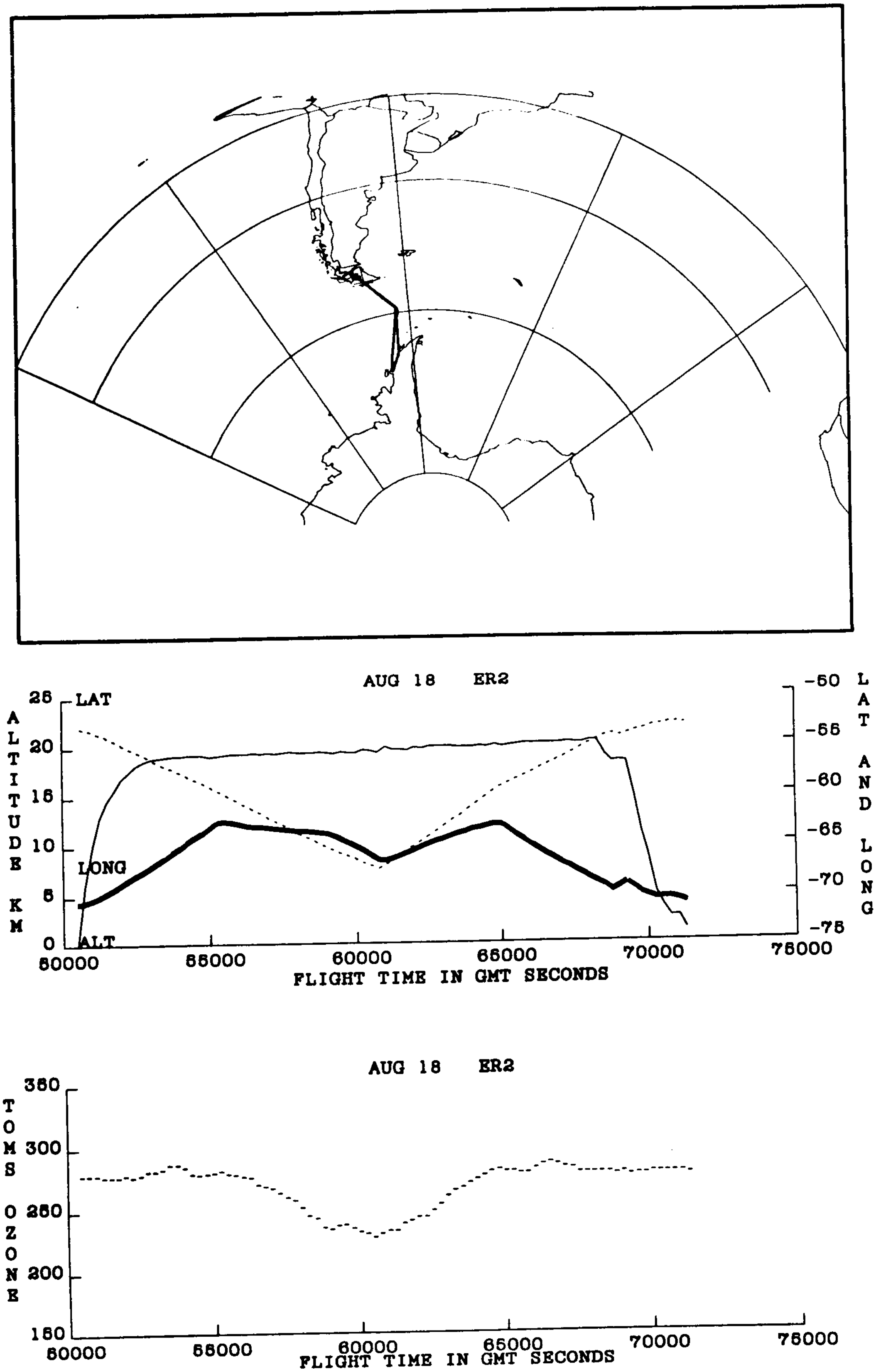


Figure 8b. Flight Path of the ER-2 mission for August 18 as mapped onto a polar projection (top) and as a time series of latitude, longitude, and altitude along with the corresponding TOMS total-ozone estimates along the flight path (bottom).

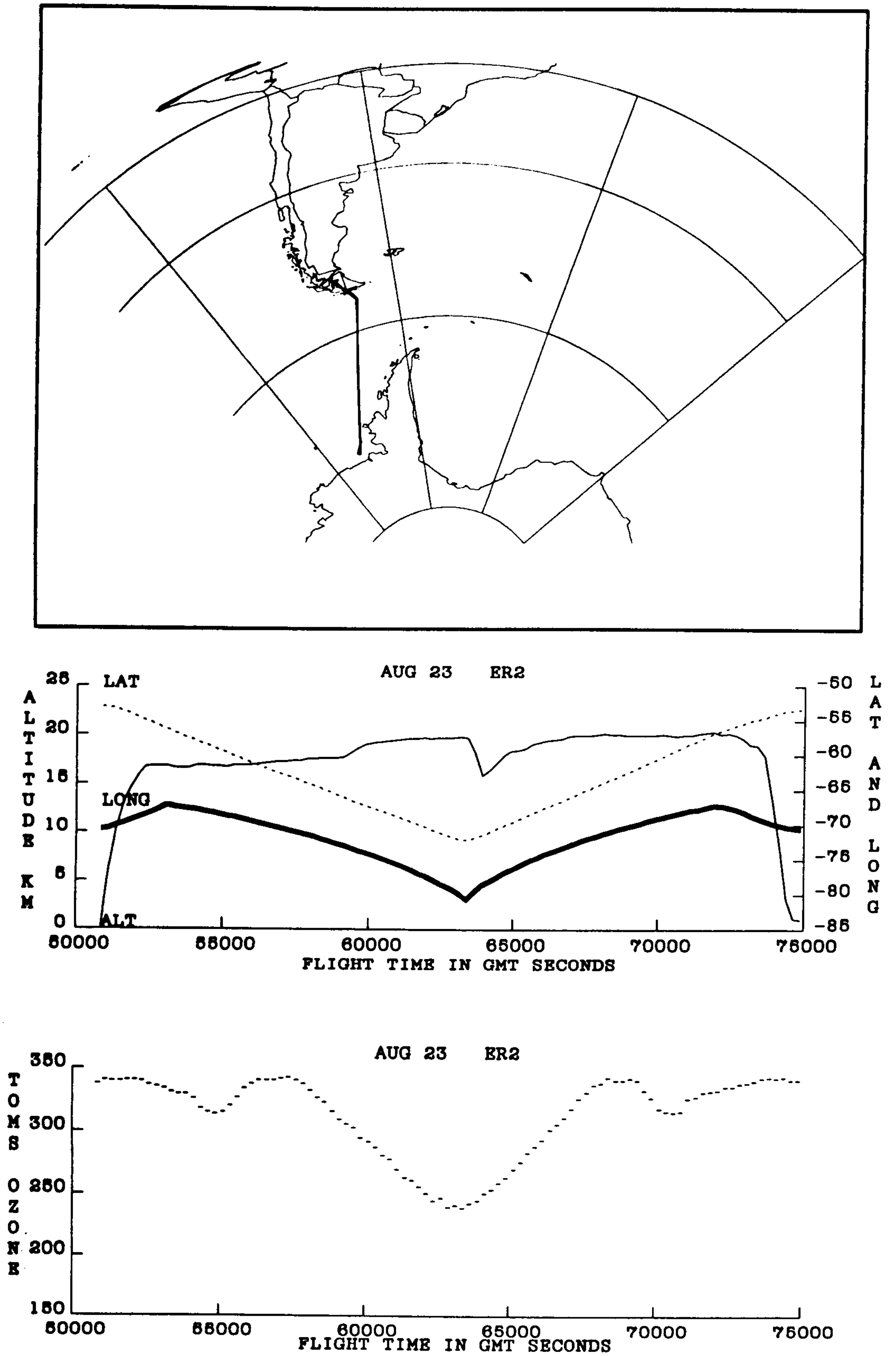


Figure 8c. Flight Path of the ER-2 mission for August 23 as mapped onto a polar projection (top) and as a time series of latitude, longitude, and altitude along with the corresponding TOMS total-ozone estimates along the flight path (bottom).

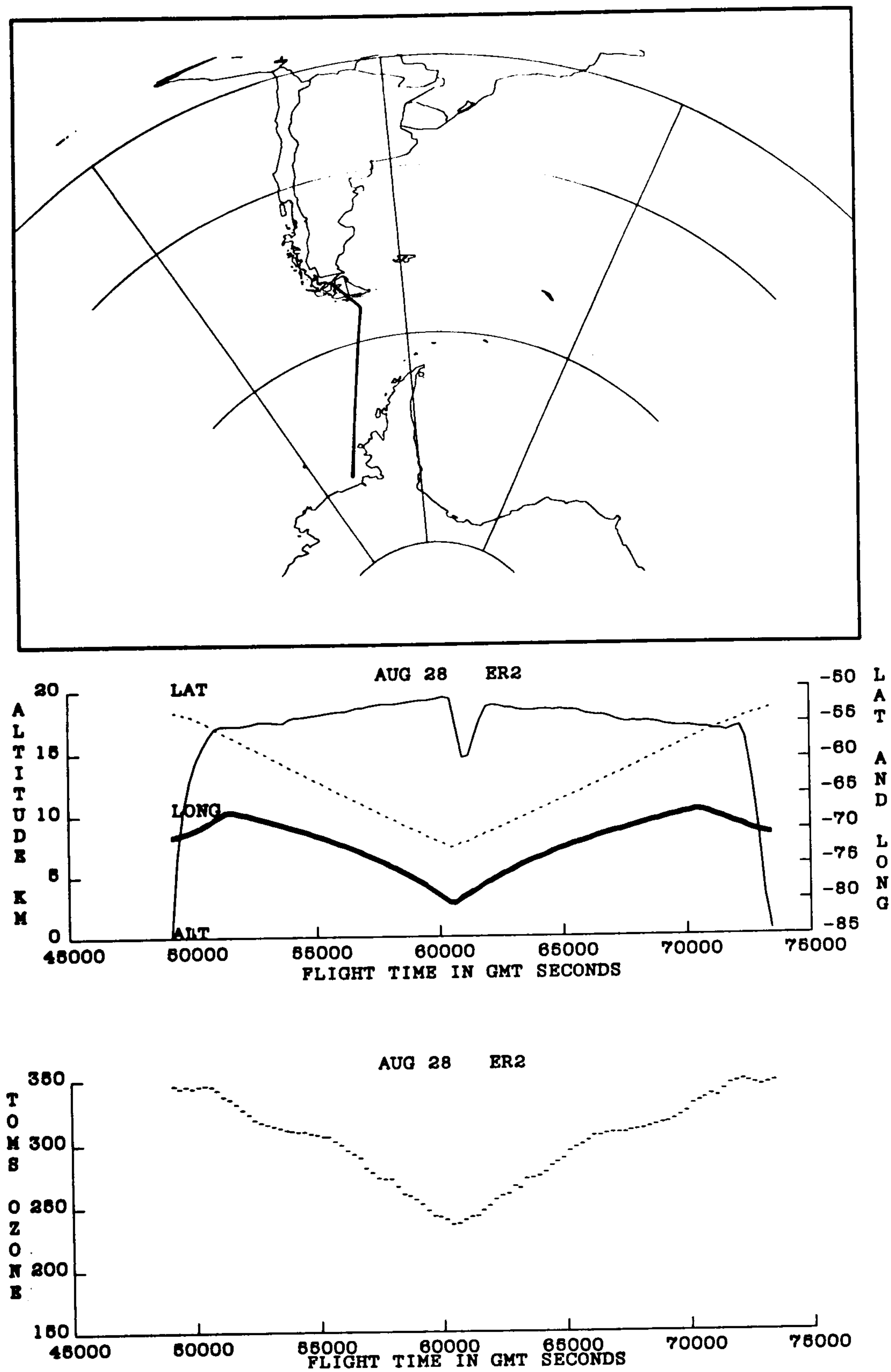


Figure 8d. Flight Path of the ER-2 mission for August 28 as mapped onto a polar projection (top) and as a time series of latitude, longitude, and altitude along with the corresponding TOMS total-ozone estimates along the flight path (bottom).

15 Front RP1201

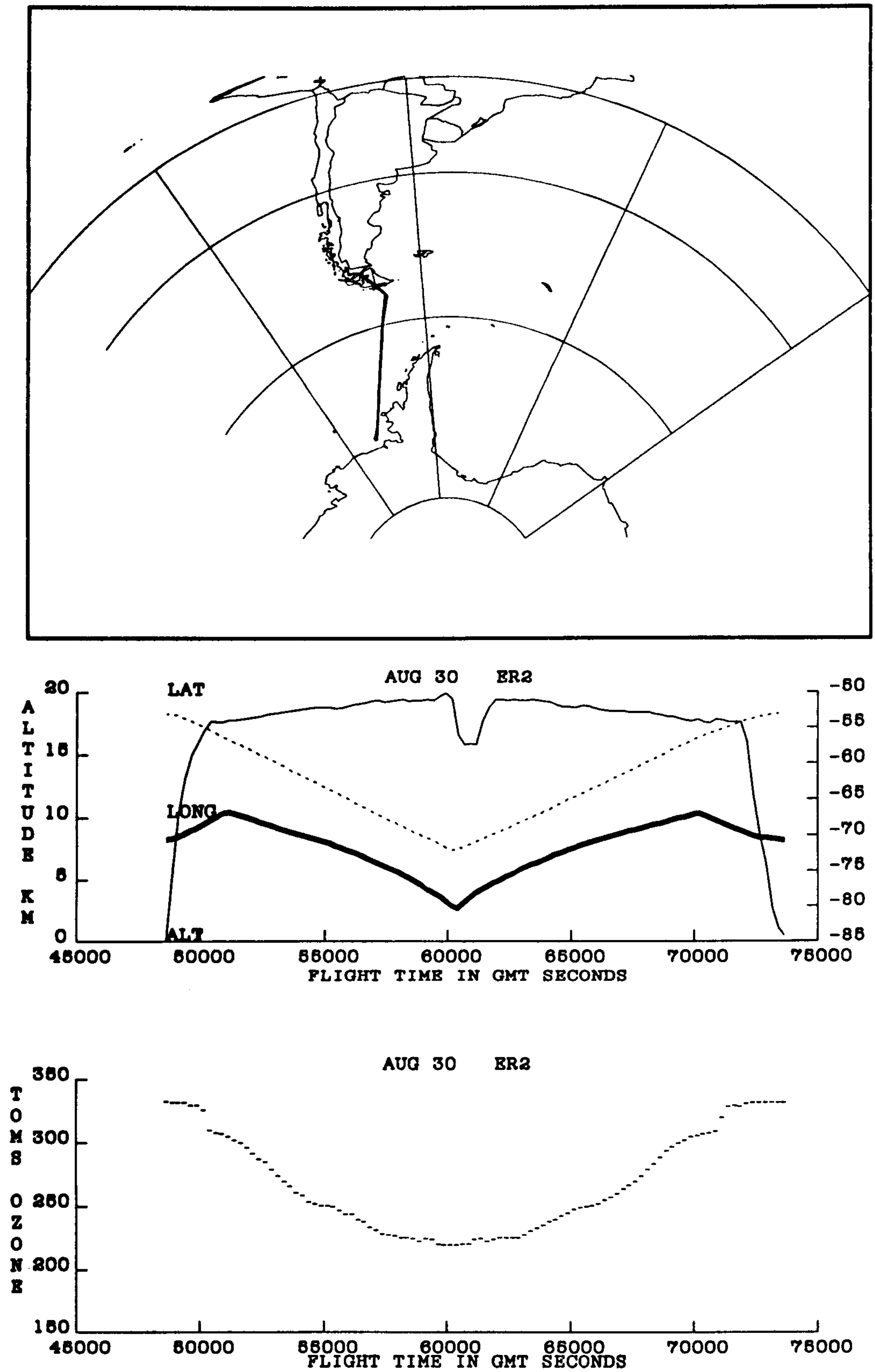


Figure 8e. Flight Path of the ER-2 mission for August 30 as mapped onto a polar projection (top) and as a time series of latitude, longitude, and altitude along with the corresponding TOMS total-ozone estimates along the flight path (bottom).

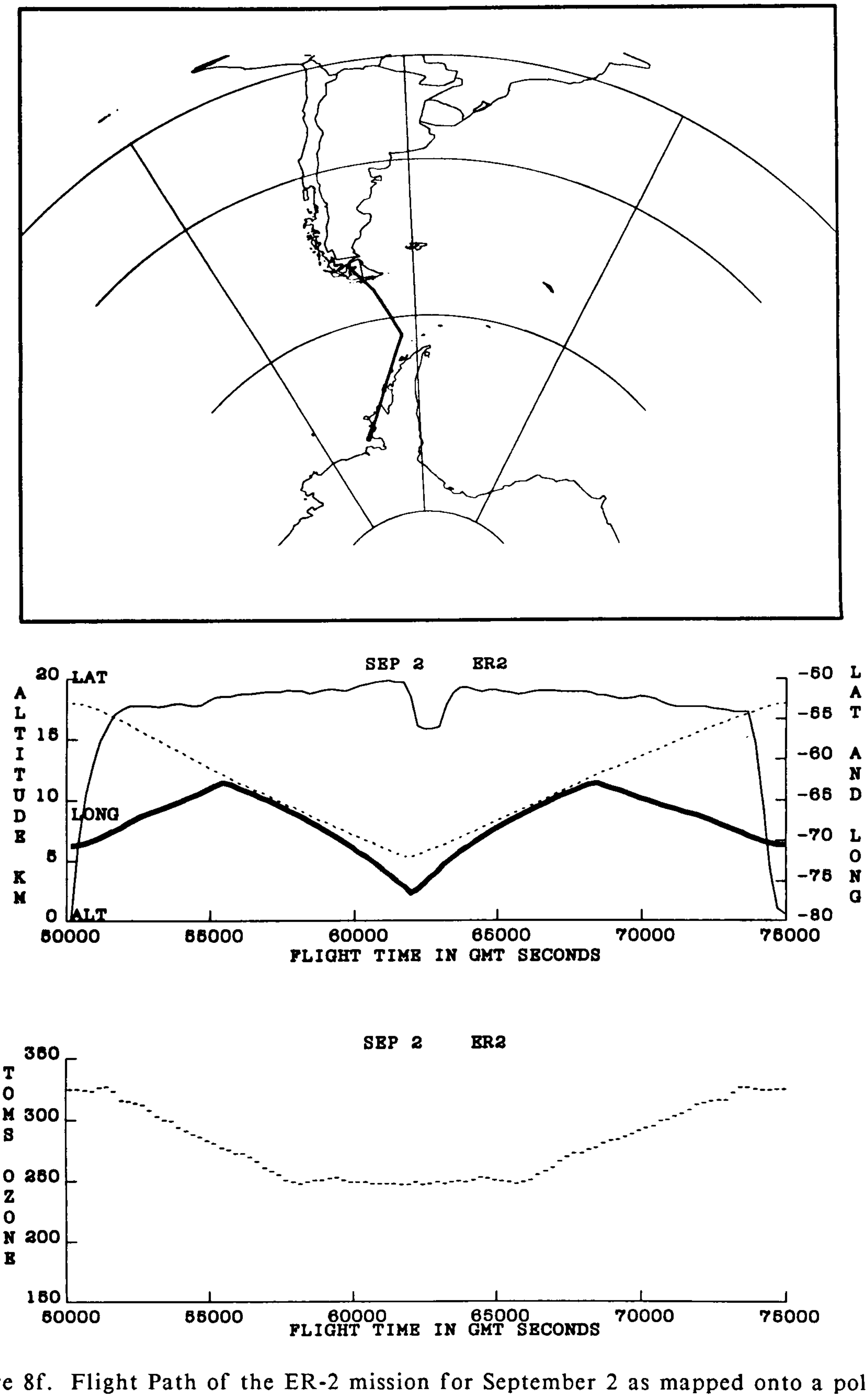


Figure 8f. Flight Path of the ER-2 mission for September 2 as mapped onto a polar projection (top) and as a time series of latitude, longitude, and altitude along with the corresponding TOMS total-ozone estimates along the flight path (bottom).

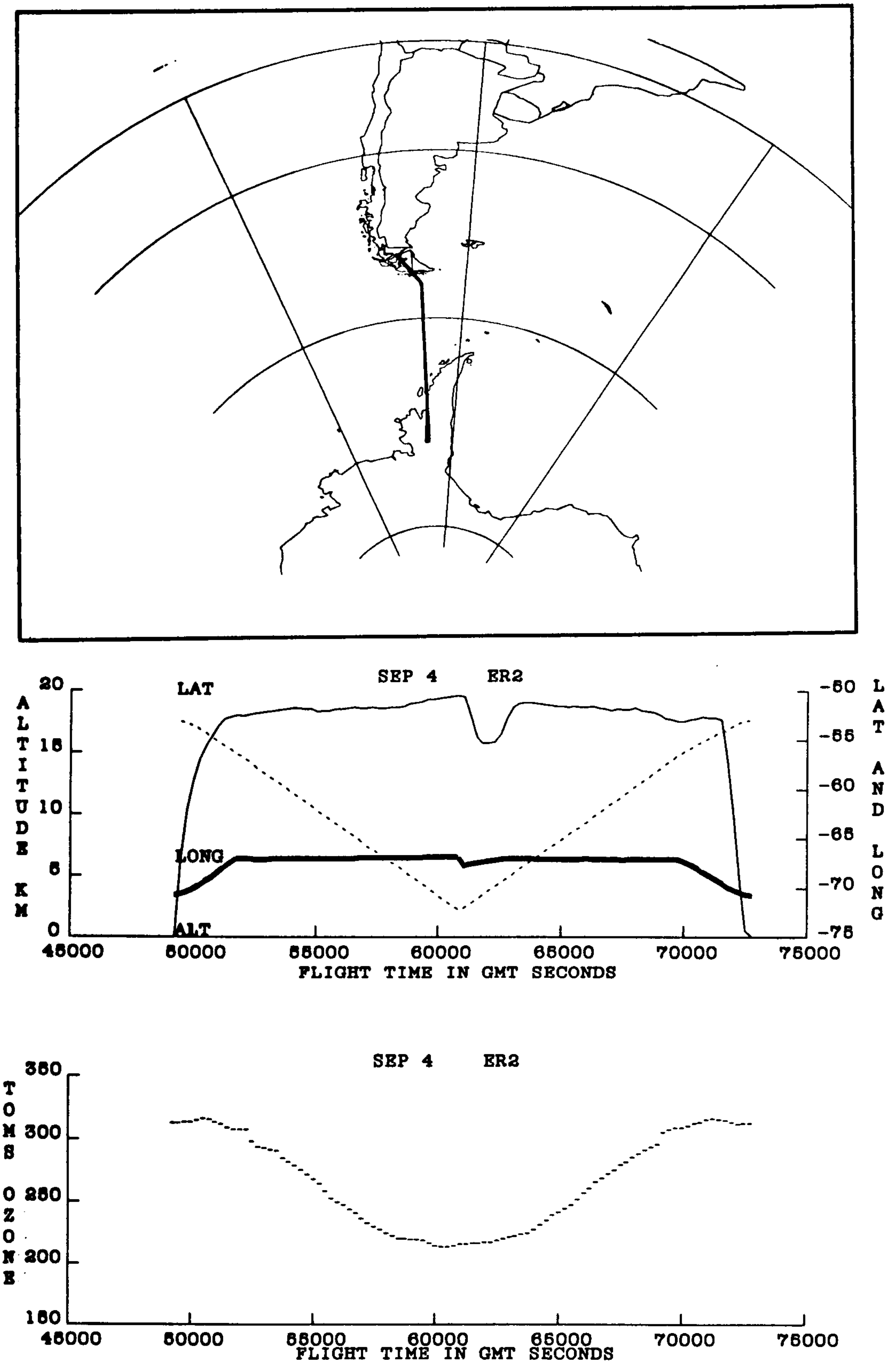


Figure 8g. Flight Path of the ER-2 mission for September 4 as mapped onto a polar projection (top) and as a time series of latitude, longitude, and altitude along with the corresponding TOMS total-ozone estimates along the flight path (bottom).

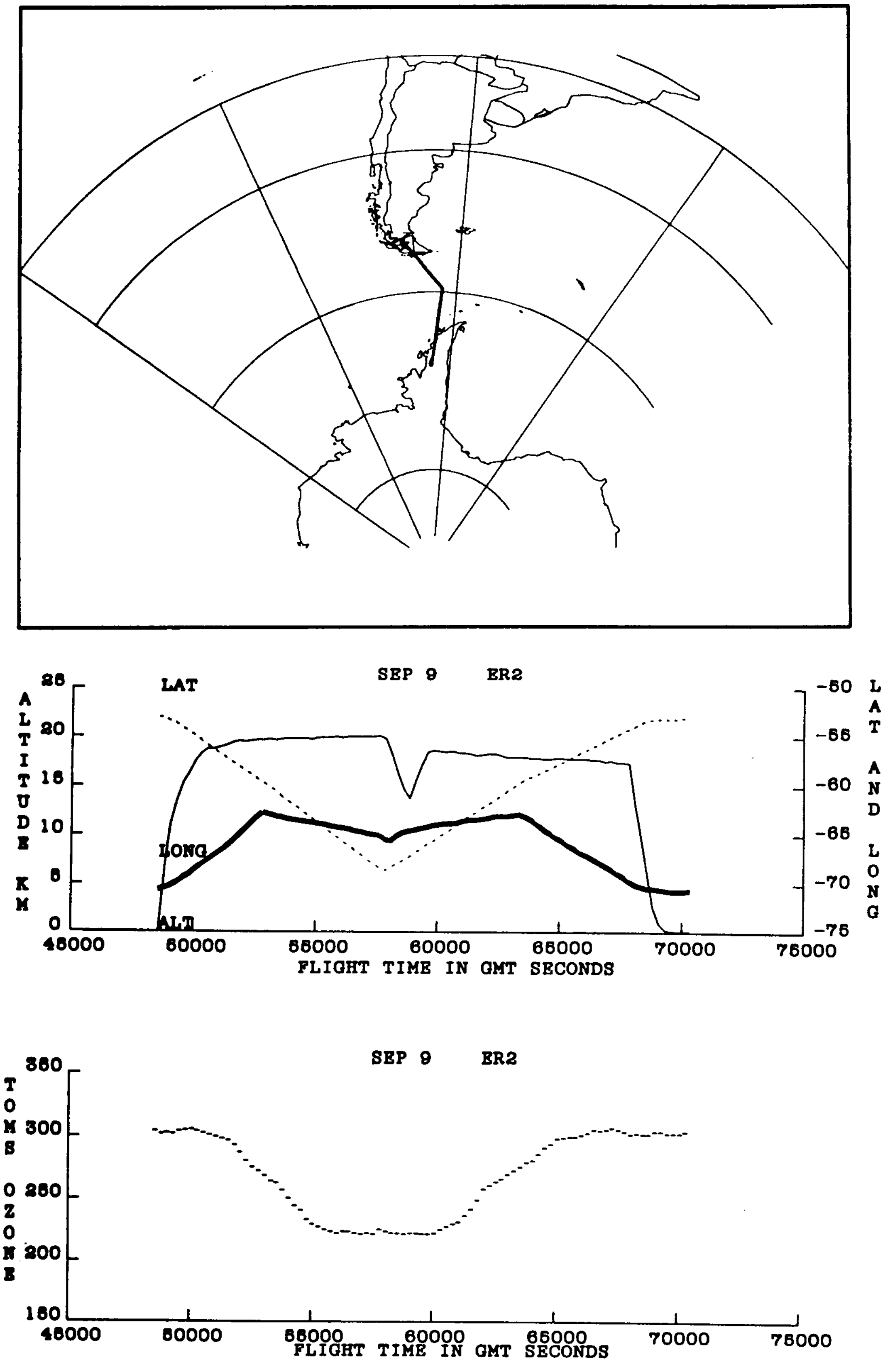


Figure 8h. Flight Path of the ER-2 mission for September 9 as mapped onto a polar projection (top) and as a time series of latitude, longitude, and altitude along with the corresponding TOMS total-ozone estimates along the flight path (bottom).

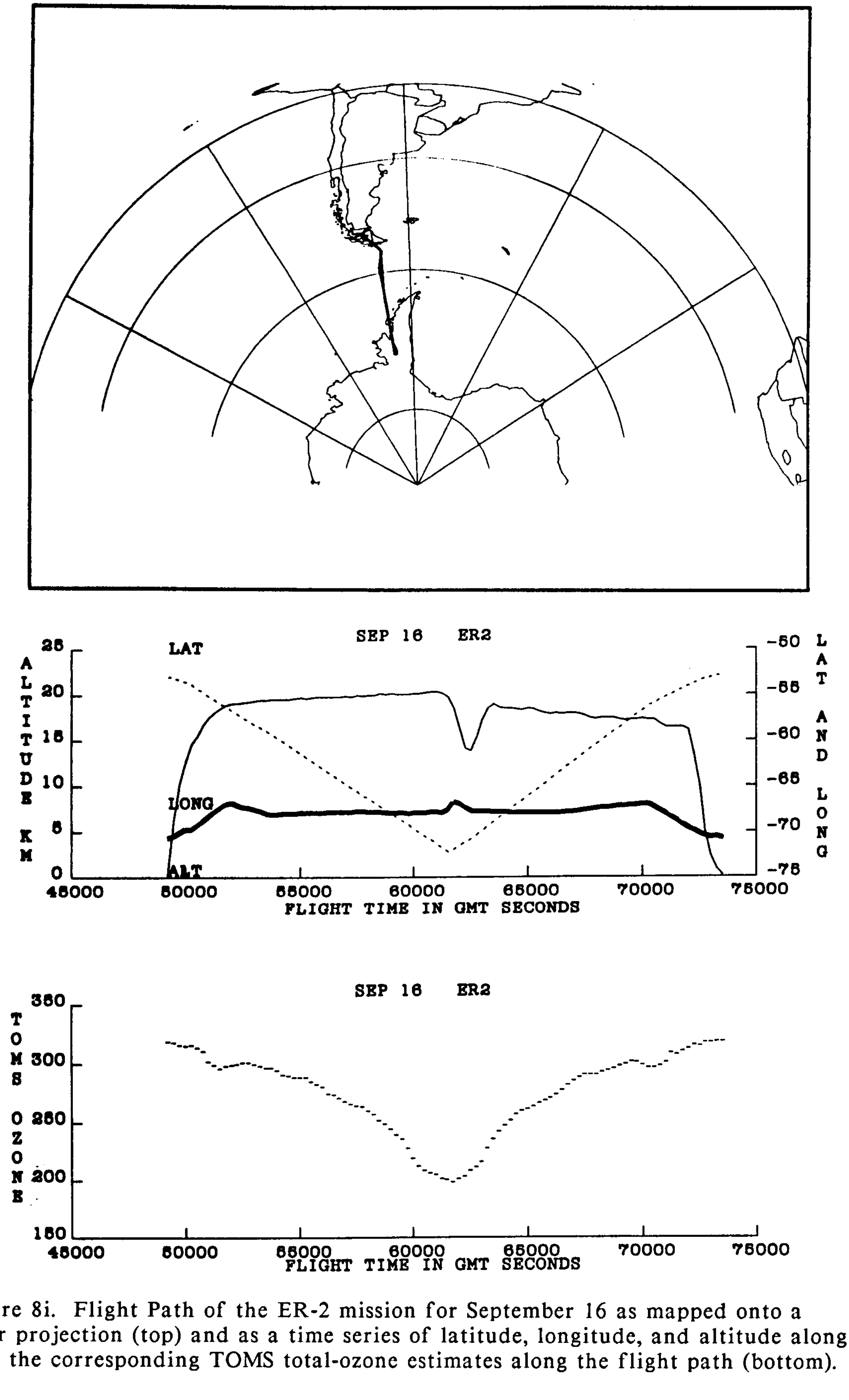


Figure 8i. Flight Path of the ER-2 mission for September 16 as mapped onto a polar projection (top) and as a time series of latitude, longitude, and altitude along with the corresponding TOMS total-ozone estimates along the flight path (bottom).

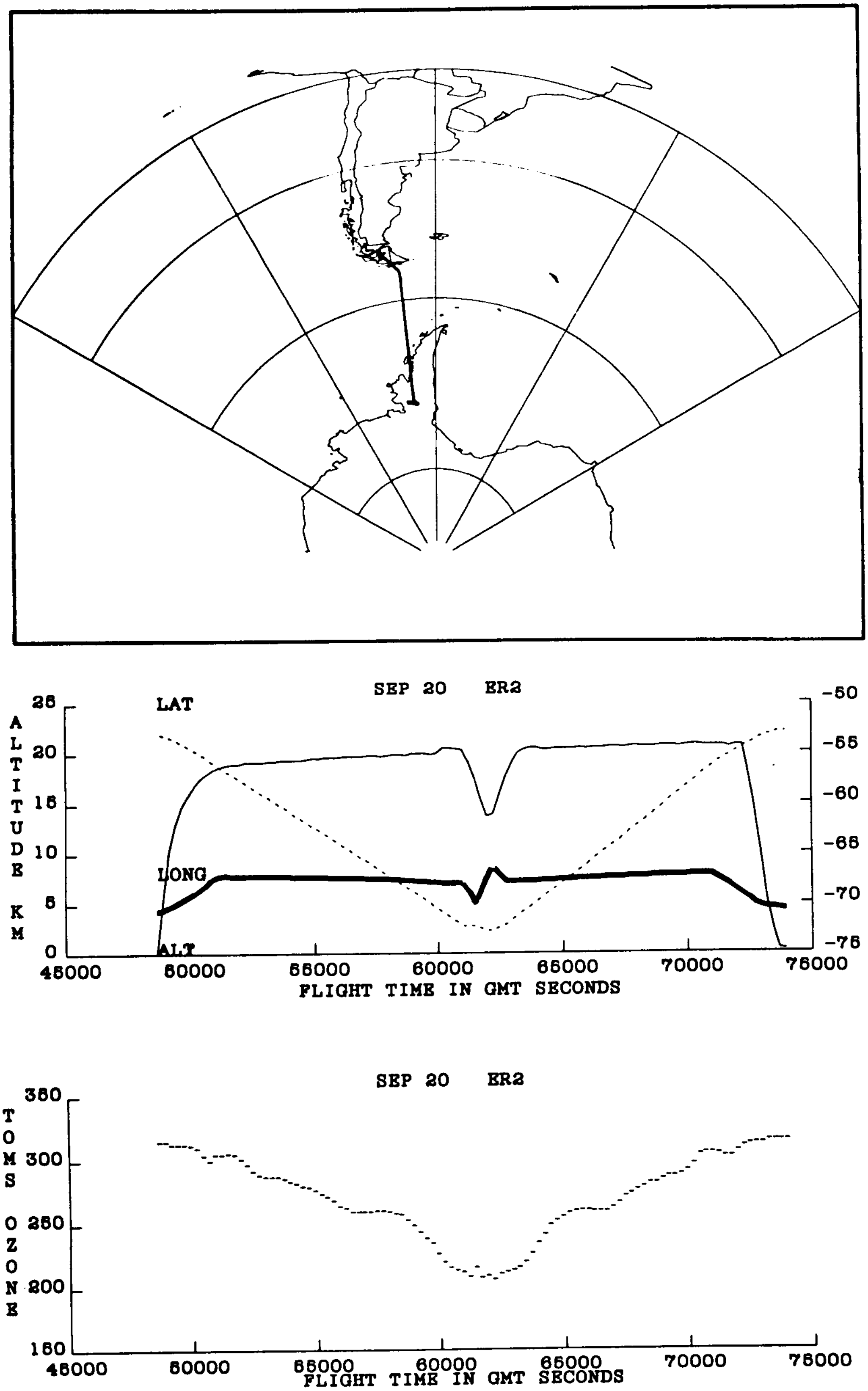


Figure 8j. Flight Path of the ER-2 mission for September 20 as mapped onto a polar projection (top) and as a time series of latitude, longitude, and altitude along with the corresponding TOMS total-ozone estimates along the flight path (bottom).

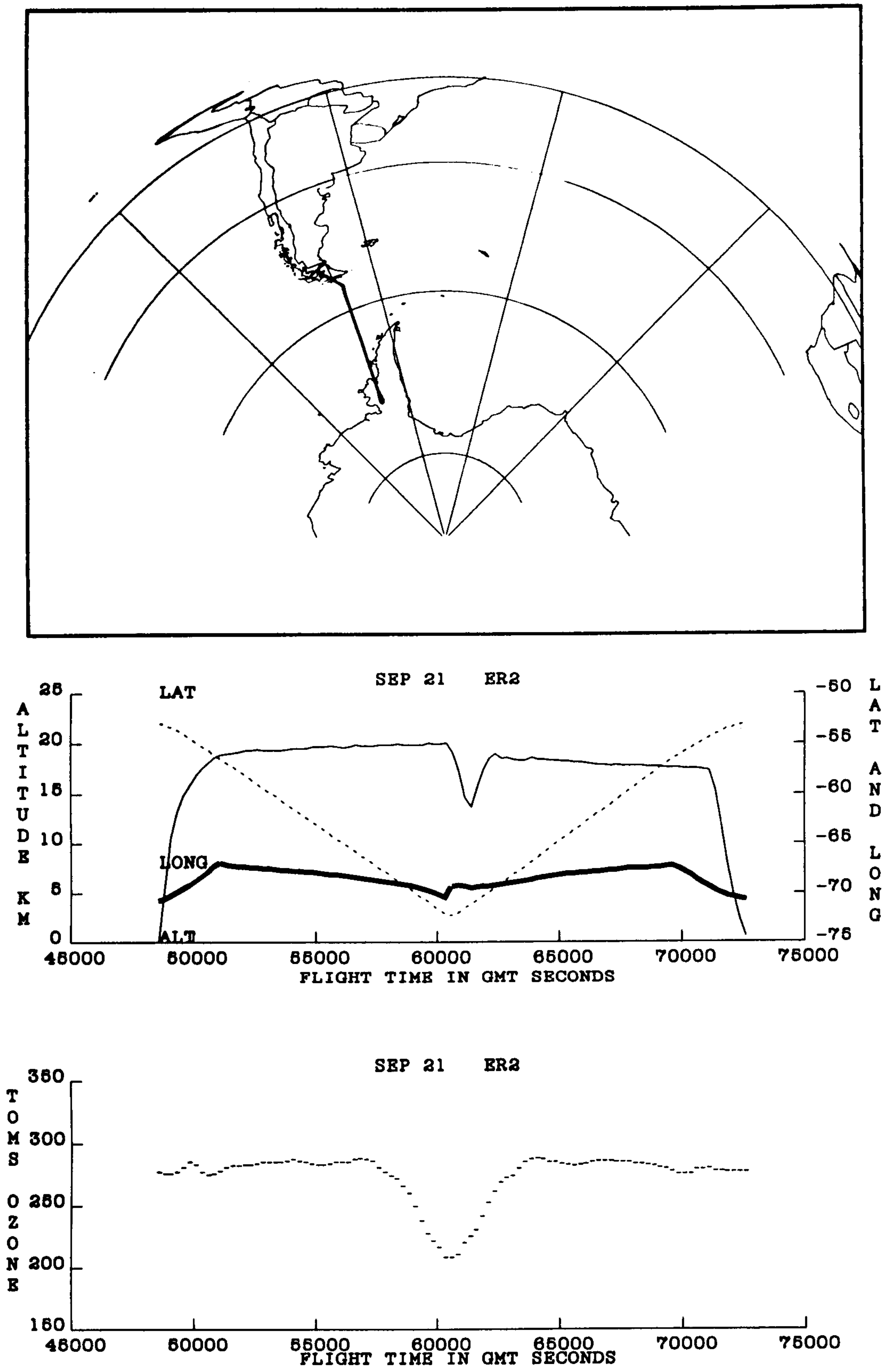


Figure 8k. Flight Path of the ER-2 mission for September 21 as mapped onto a polar projection (top) and as a time series of latitude, longitude, and altitude along with the corresponding TOMS total-ozone estimates along the flight path (bottom).

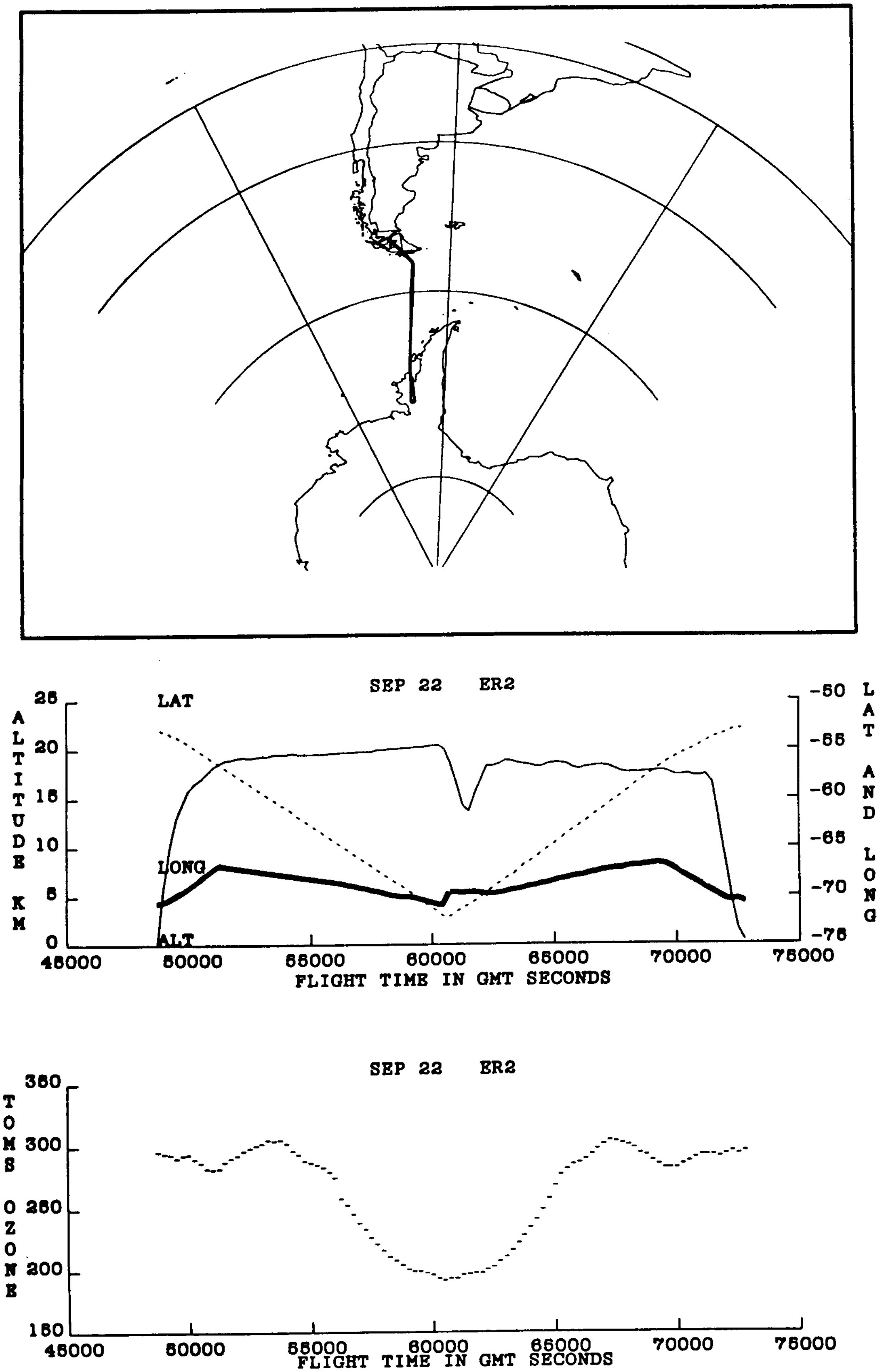


Figure 81. Flight Path of the ER-2 mission for September 22 as mapped onto a polar projection (top) and as a time series of latitude, longitude, and altitude along with the corresponding TOMS total-ozone estimates along the flight path (bottom).

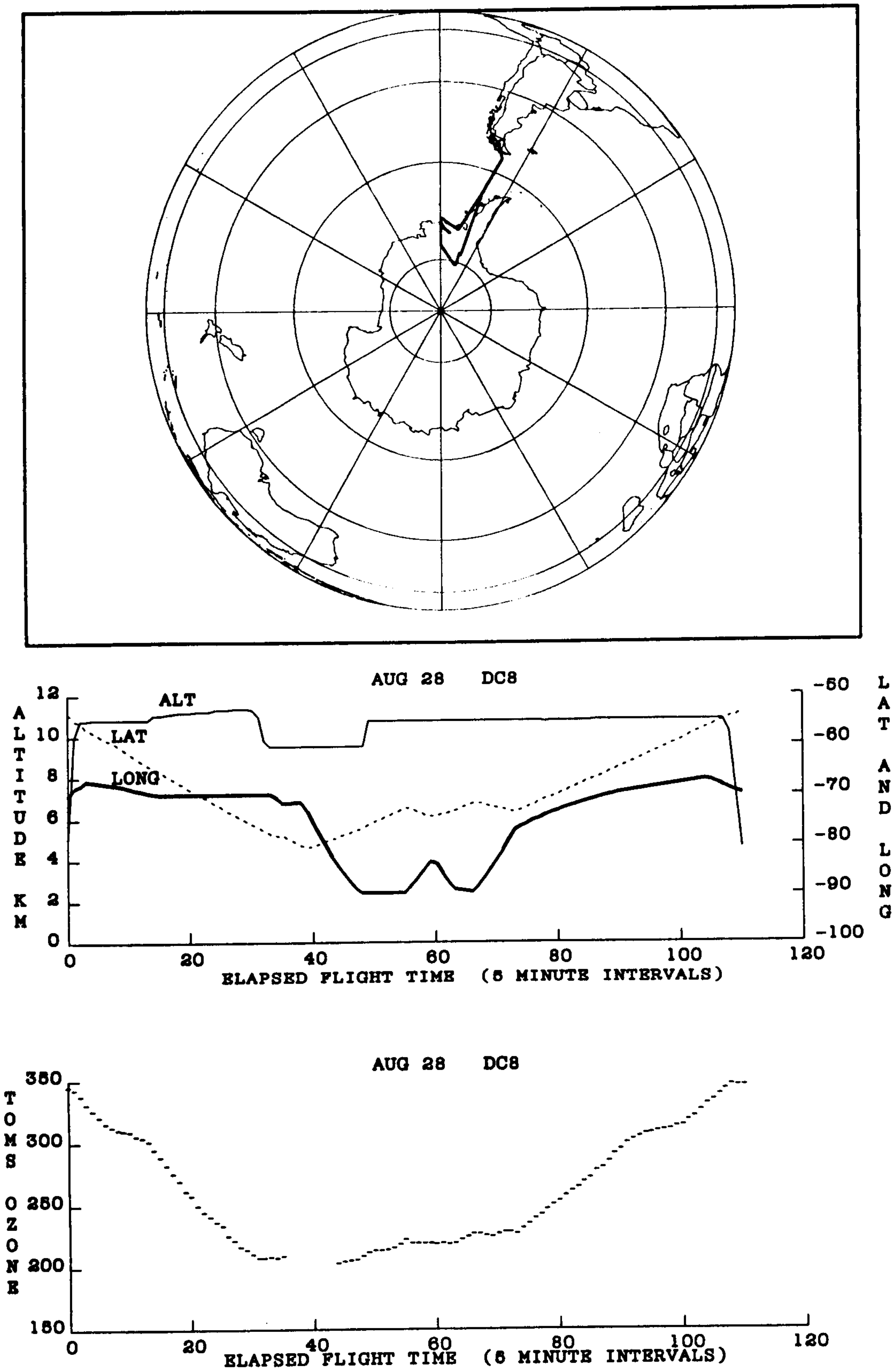


Figure 9a. Flight Path of the DC-8 mission for August 28 as mapped onto a polar projection (top) and as a time series of latitude, longitude, and altitude along with the corresponding TOMS total-ozone estimates along the flight path (bottom).

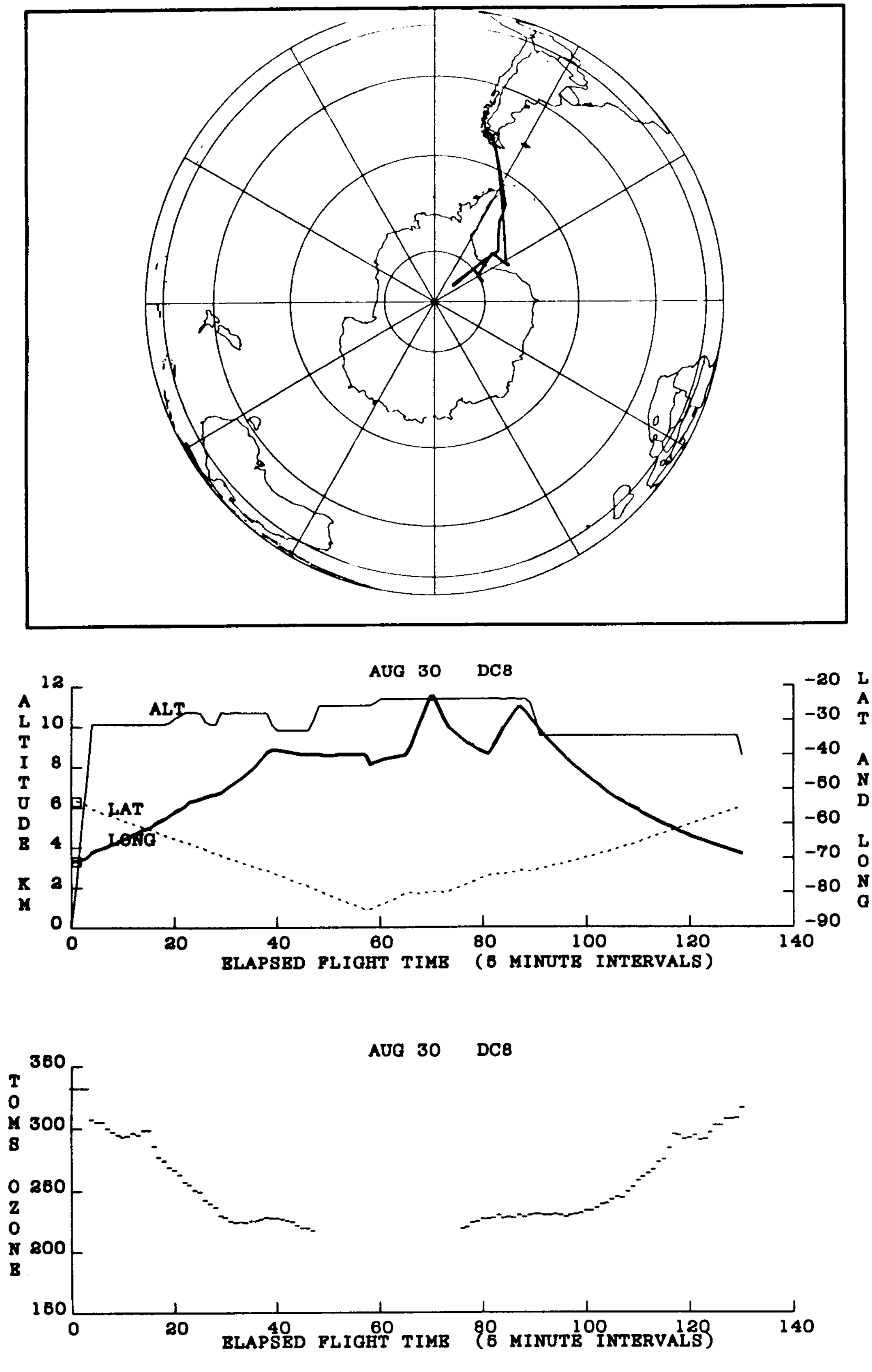


Figure 9b. Flight Path of the DC-8 mission for August 30 as mapped onto a polar projection (top) and as a time series of latitude, longitude, and altitude along with the corresponding TOMS total-ozone estimates along the flight path (bottom).

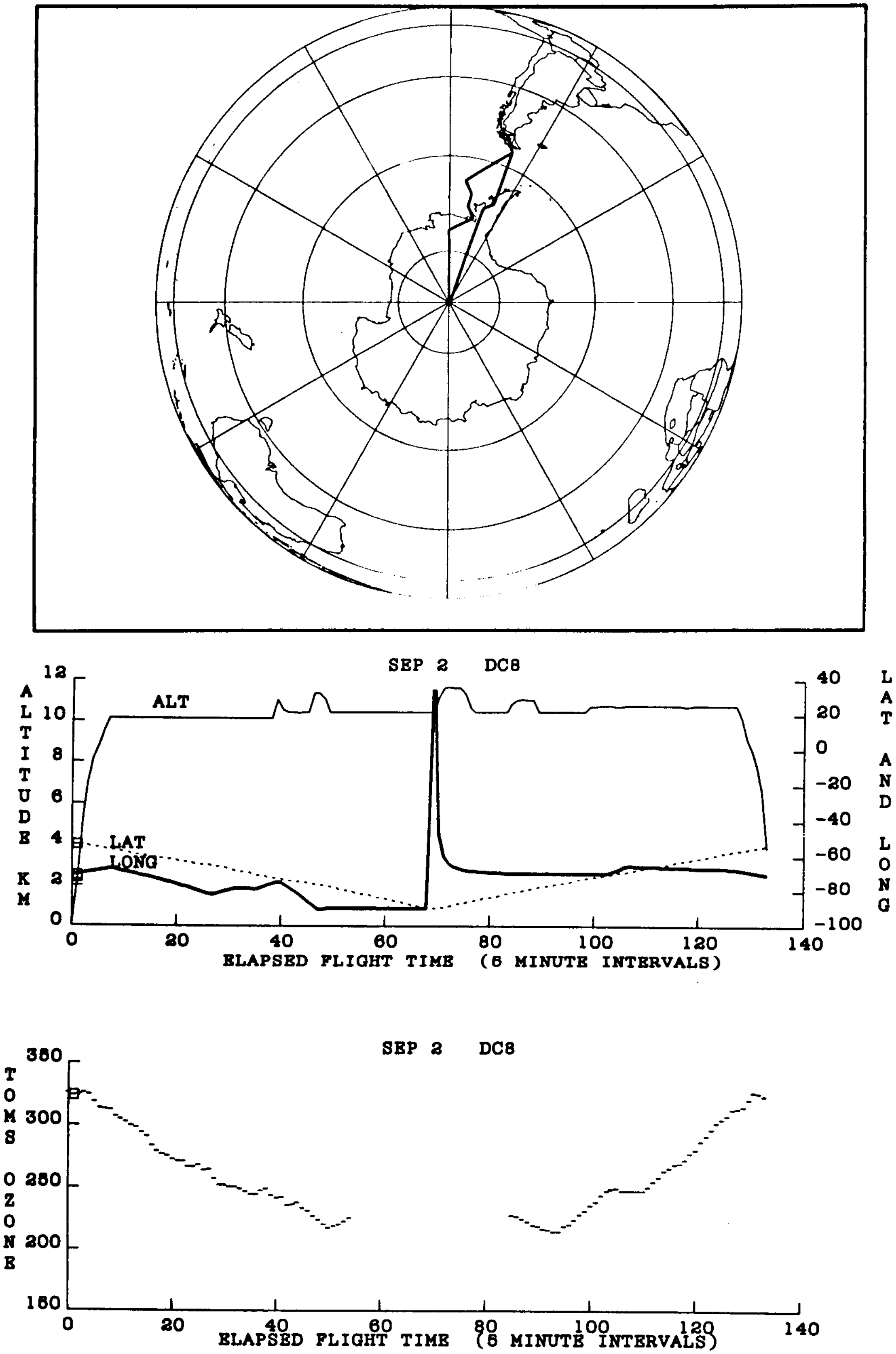


Figure 9c. Flight Path of the DC-8 mission for September 2 as mapped onto a polar projection (top) and as a time series of latitude, longitude, and altitude along with the corresponding TOMS total-ozone estimates along the flight path (bottom).

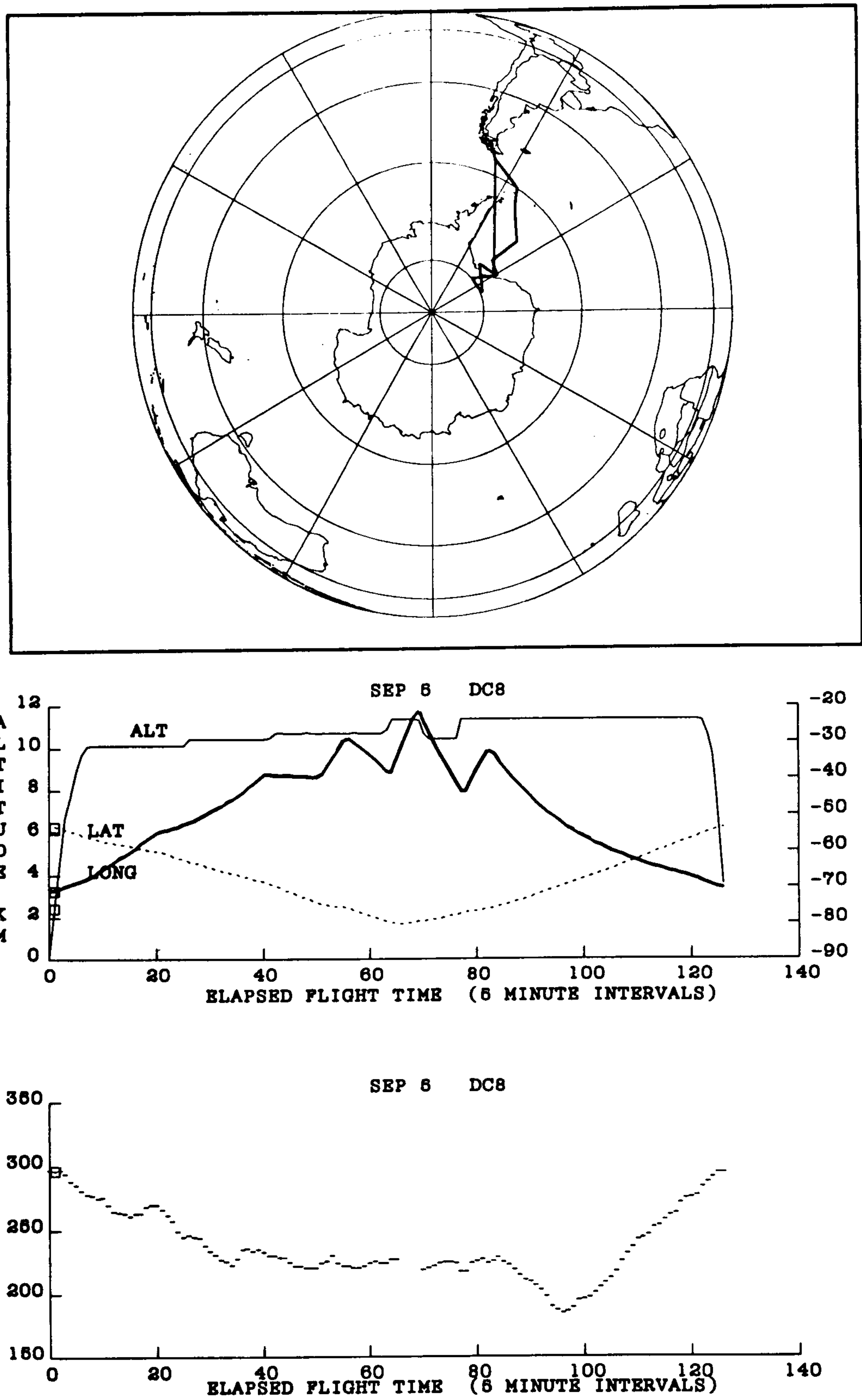


Figure 9d. Flight Path of the DC-8 mission for September 5 as mapped onto a polar projection (top) and as a time series of latitude, longitude, and altitude along with the corresponding TOMS total-ozone estimates along the flight path (bottom).

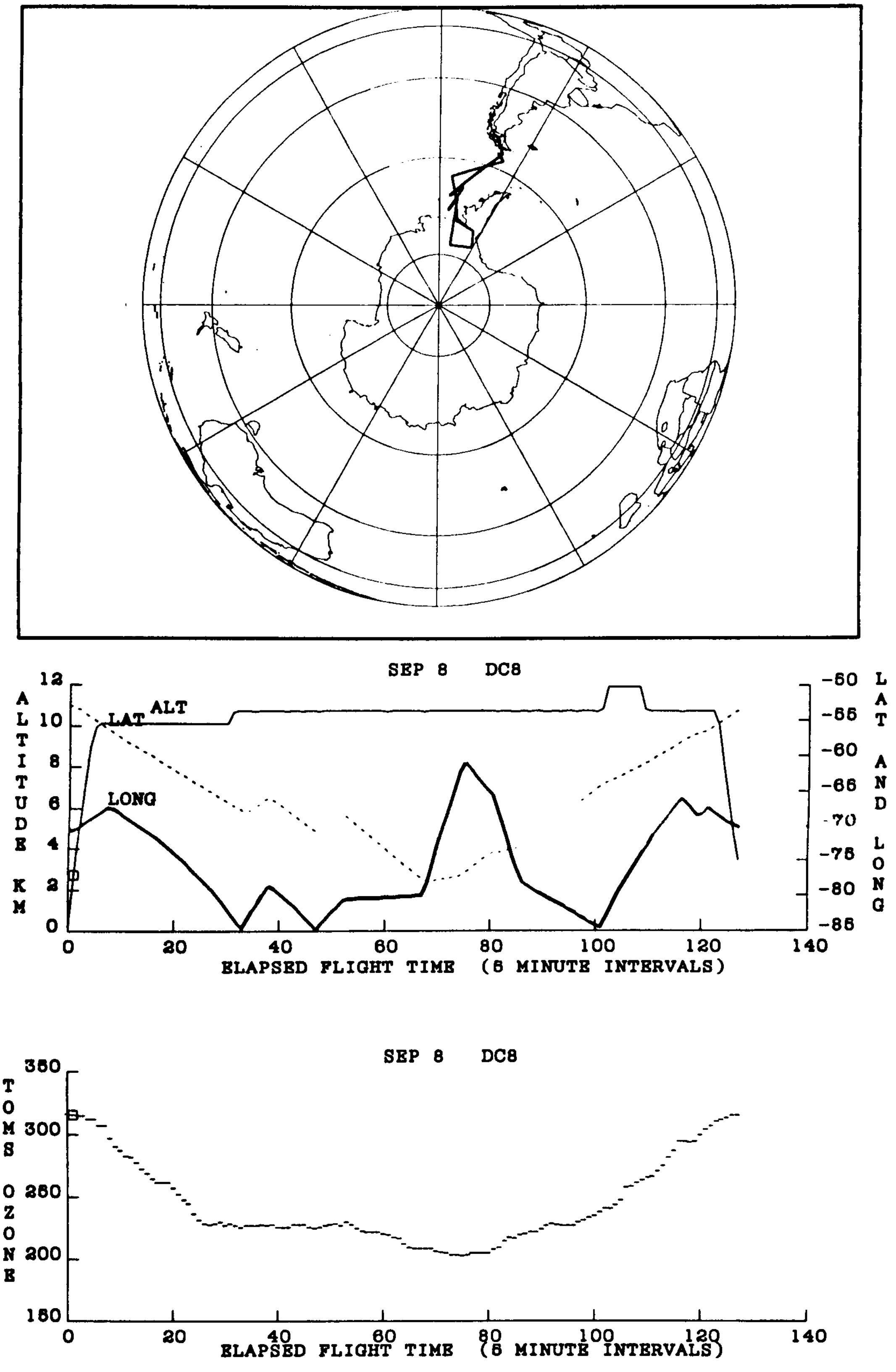


Figure 9e. Flight Path of the DC-8 mission for September 8 as mapped onto a polar projection (top) and as a time series of latitude, longitude, and altitude along with the corresponding TOMS total-ozone estimates along the flight path (bottom).

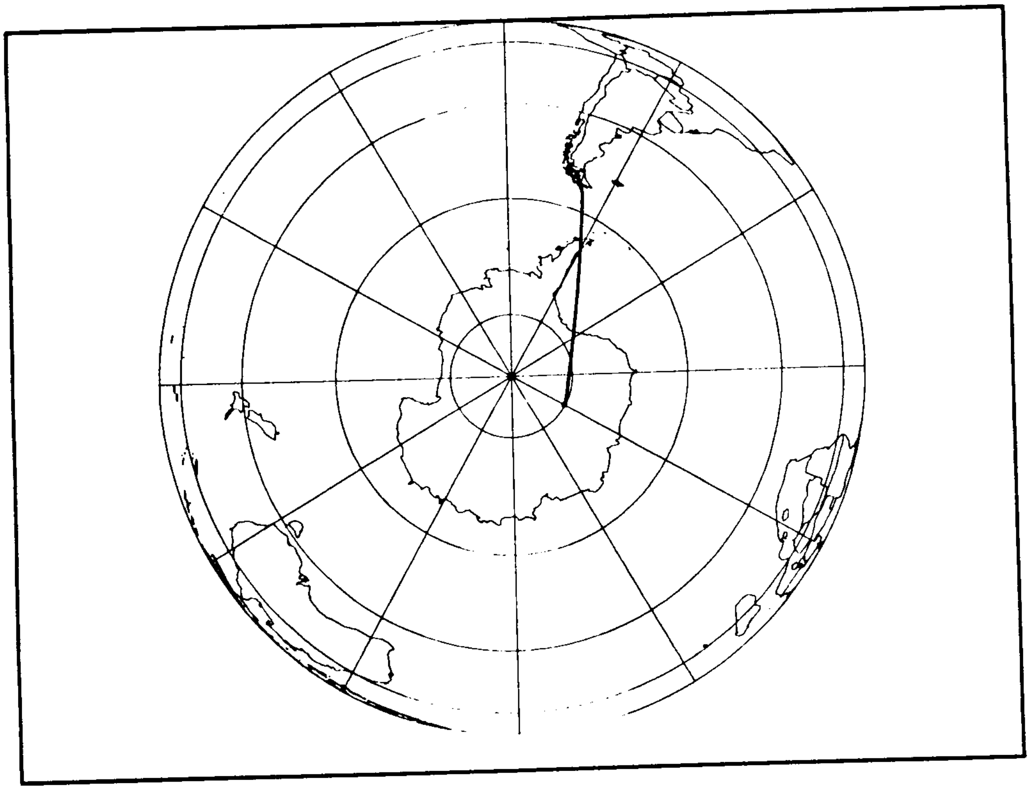

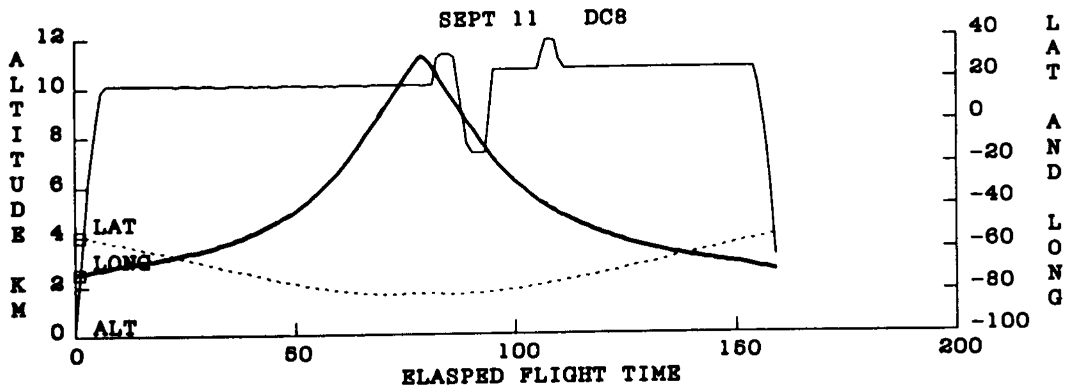


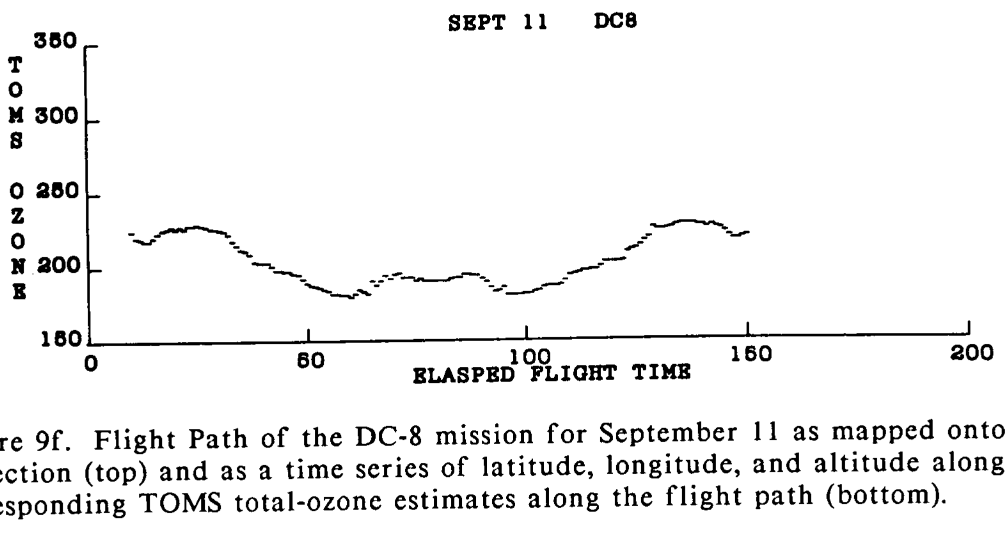


Figure 9f. Flight Path of the DC-8 mission for September 11 as mapped onto a polar projection (top) and as a time series of latitude, longitude, and altitude along with the corresponding TOMS total-ozone estimates along the flight path (bottom).

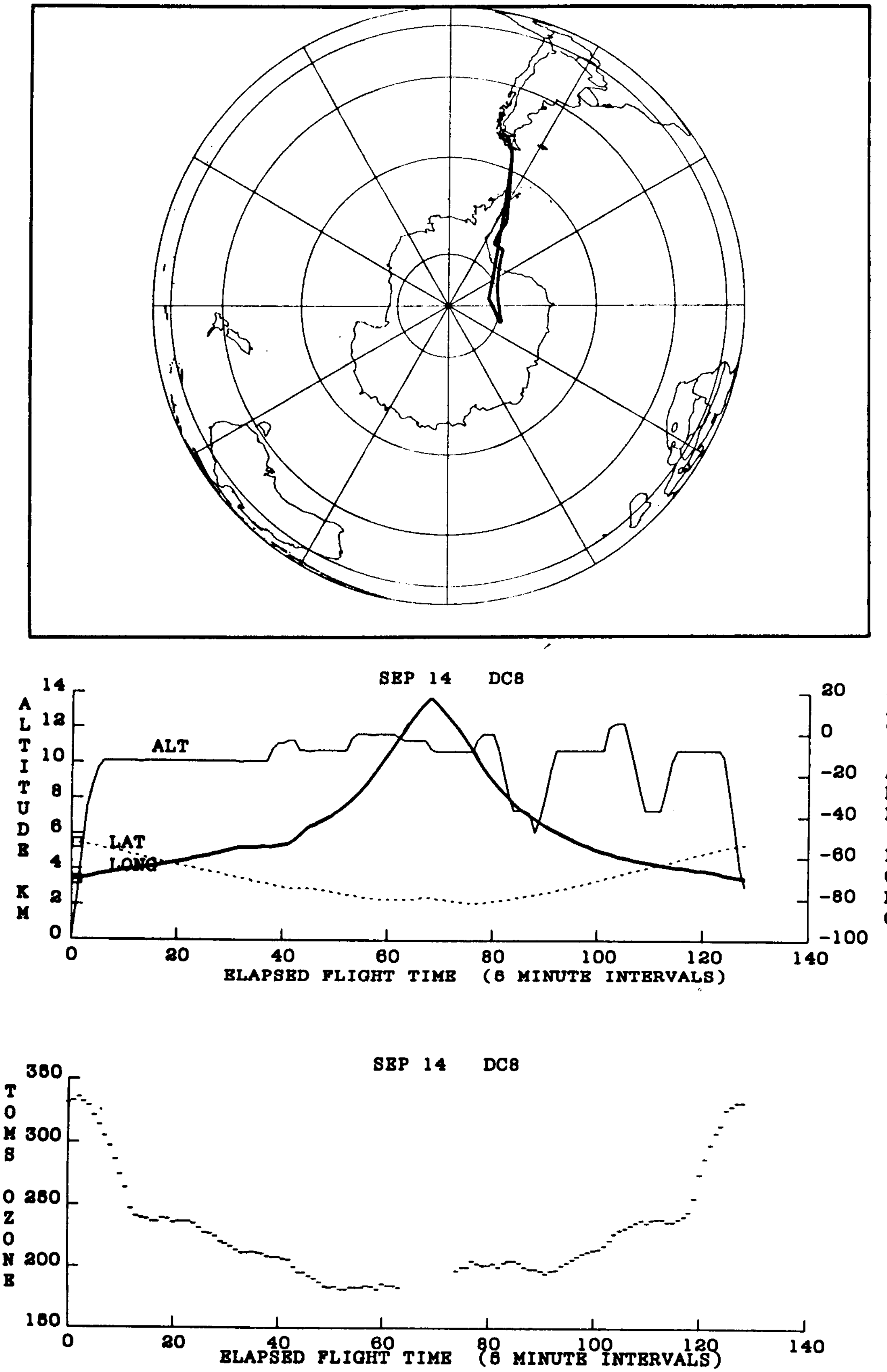


Figure 9g. Flight Path of the DC-8 mission for September 14 as mapped onto a polar projection (top) and as a time series of latitude, longitude, and altitude along with the corresponding TOMS total-ozone estimates along the flight path (bottom).

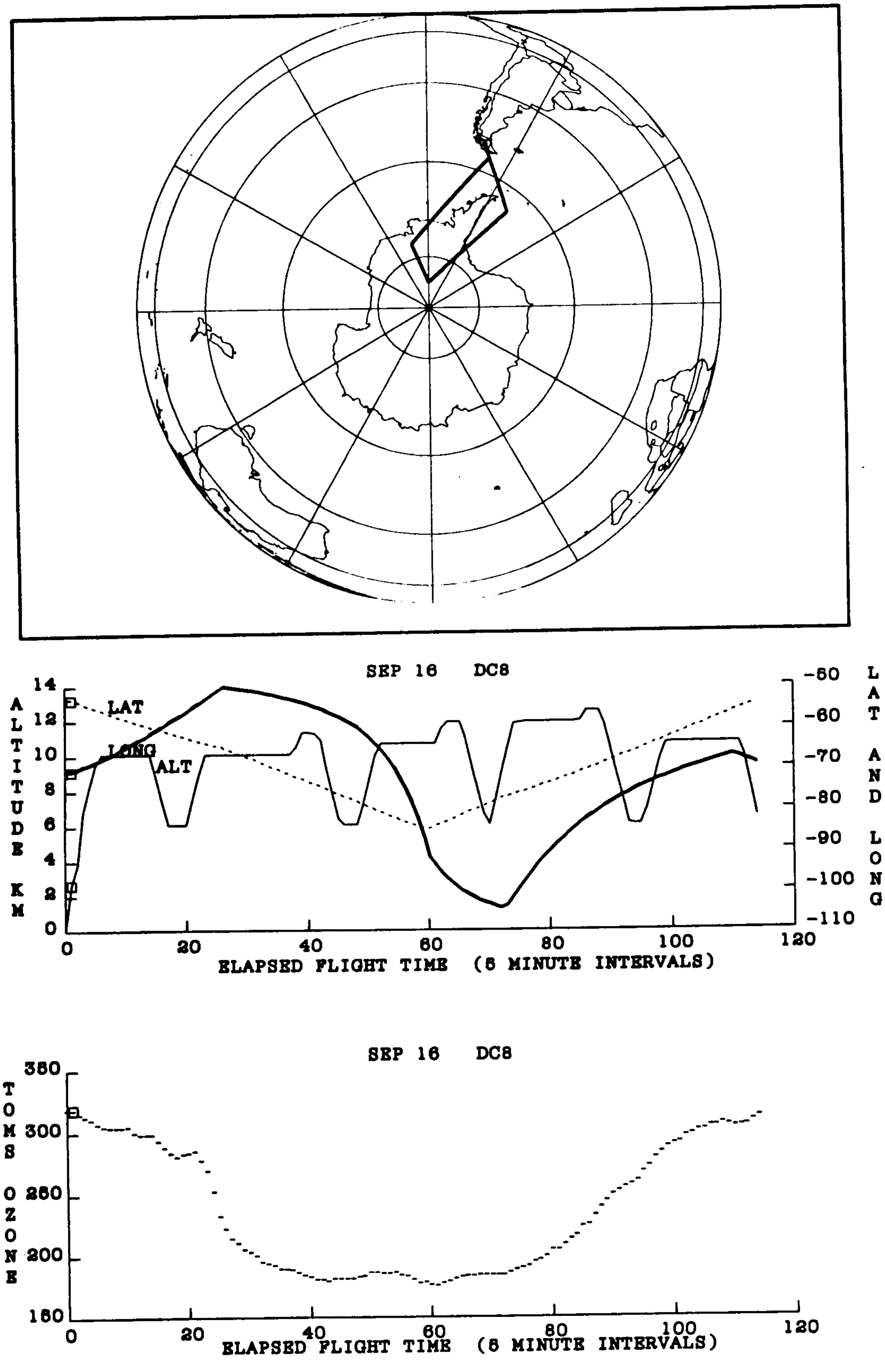


Figure 9h. Flight Path of the DC-8 mission for September 16 as mapped onto a polar projection (top) and as a time series of latitude, longitude, and altitude along with the corresponding TOMS total-ozone estimates along the flight path (bottom).

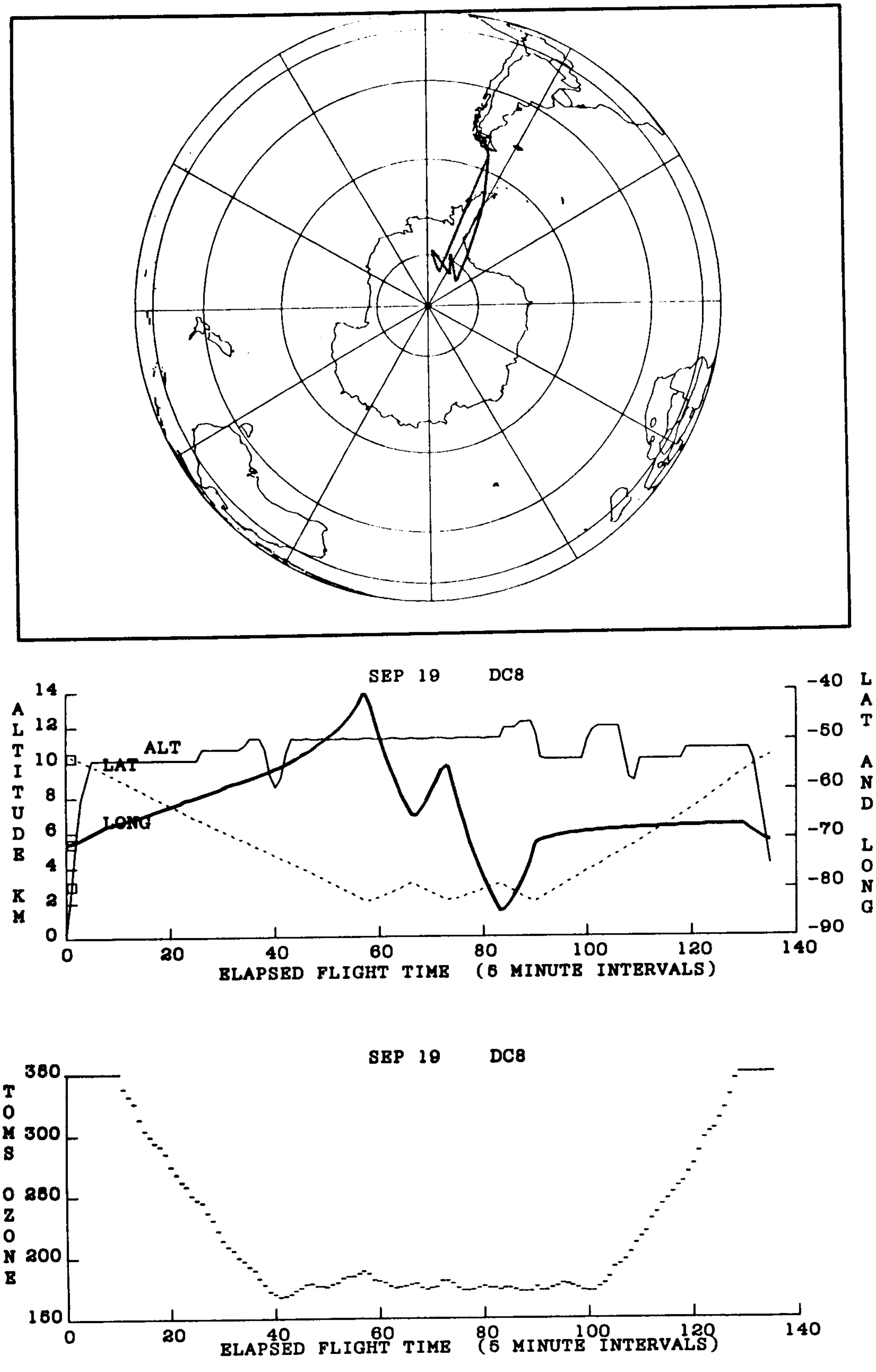


Figure 9i. Flight Path of the DC-8 mission for September 19 as mapped onto a polar projection (top) and as a time series of latitude, longitude, and altitude along with the corresponding TOMS total-ozone estimates along the flight path (bottom).

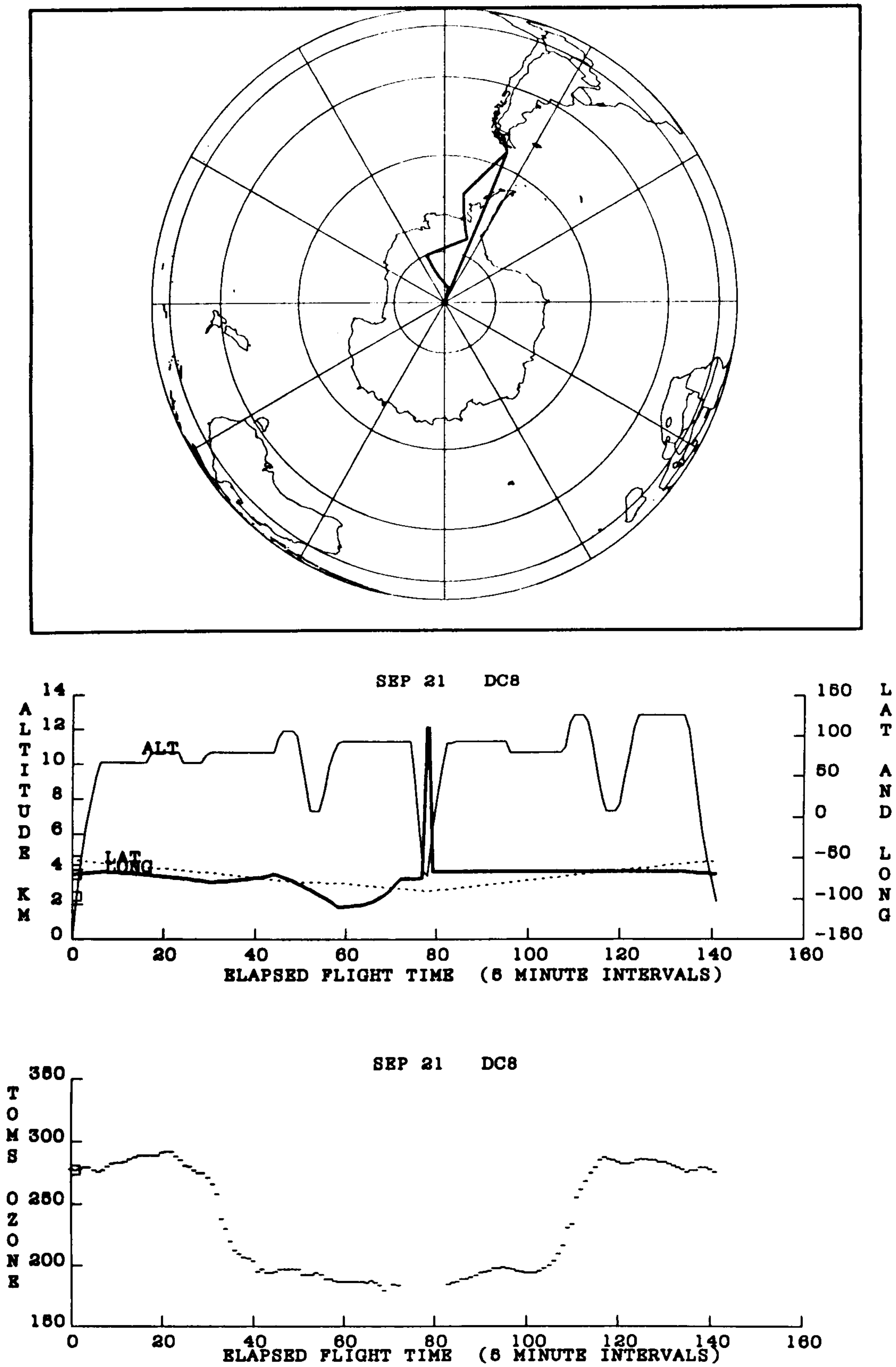


Figure 9j. Flight Path of the DC-8 mission for September 21 as mapped onto a polar projection (top) and as a time series of latitude, longitude, and altitude along with the corresponding TOMS total-ozone estimates along the flight path (bottom).

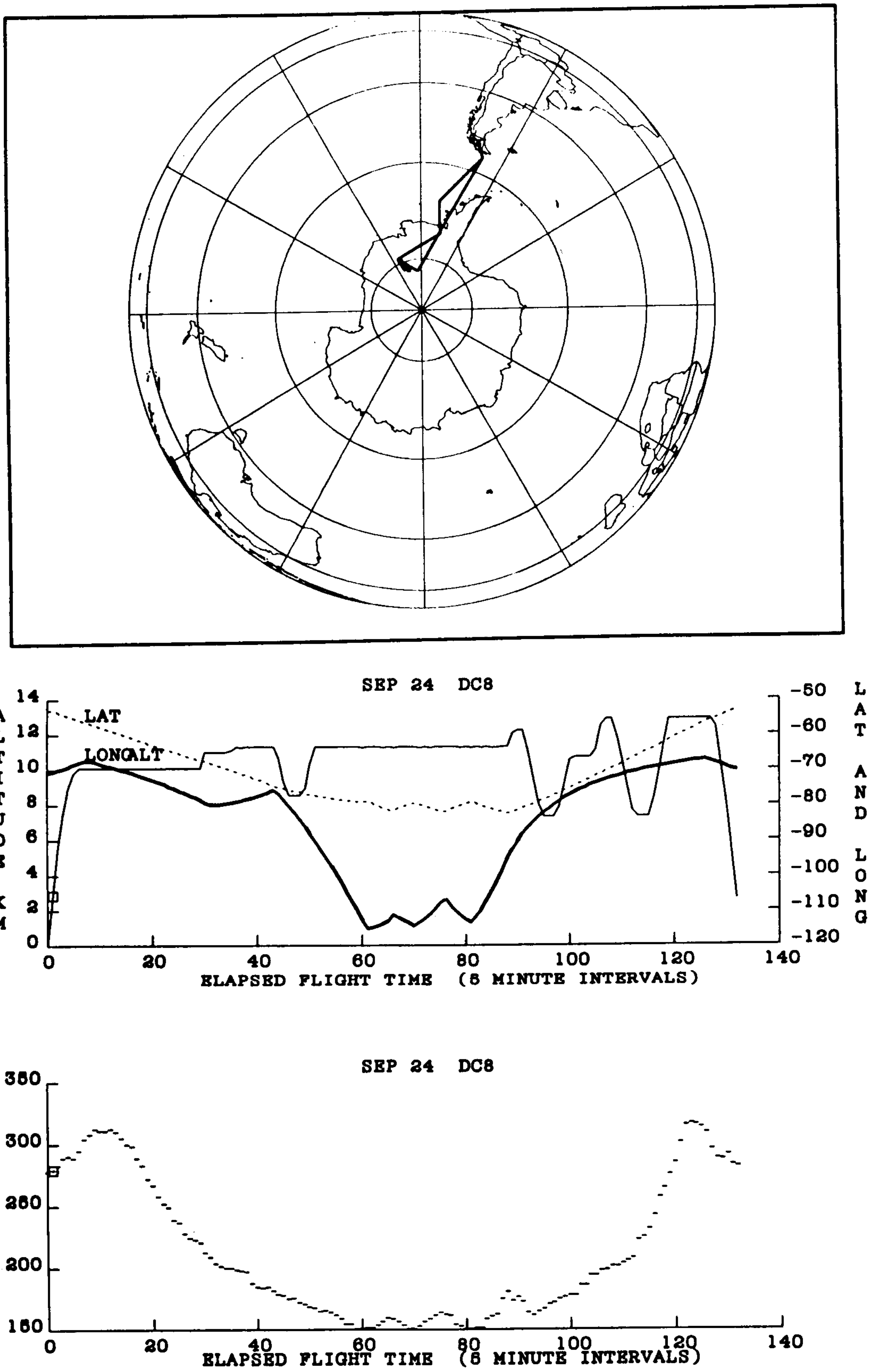


Figure 9k. Flight Path of the DC-8 mission for September 24 as mapped onto a polar projection (top) and as a time series of latitude, longitude, and altitude along with the corresponding TOMS total-ozone estimates along the flight path (bottom).

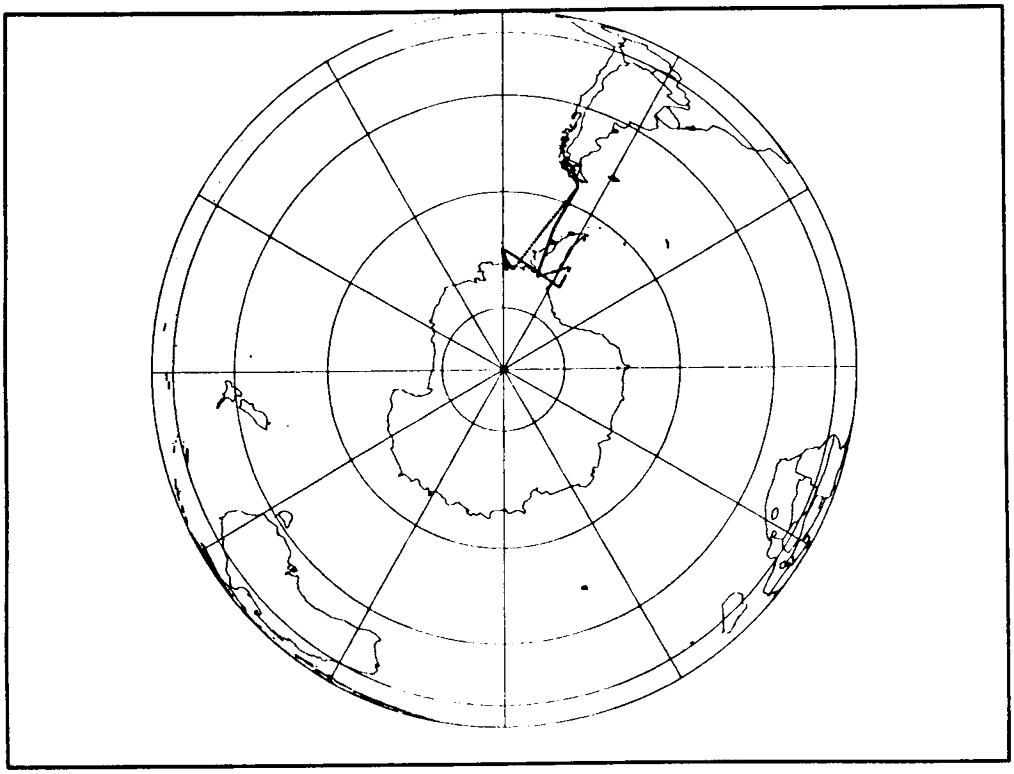

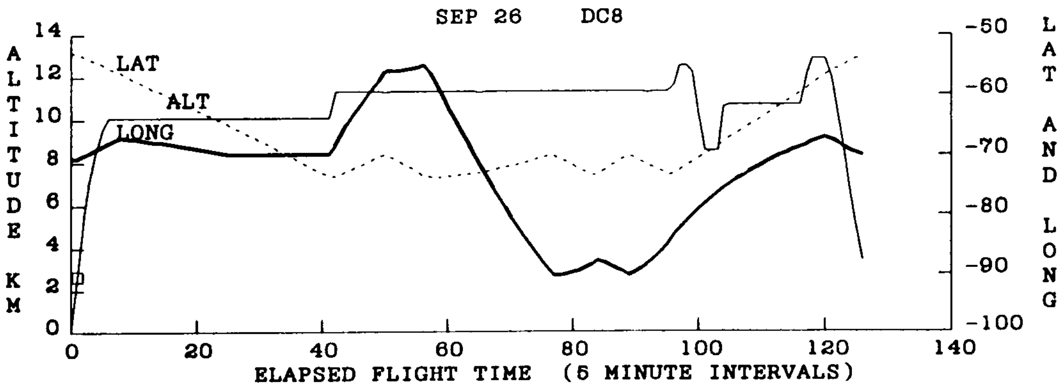


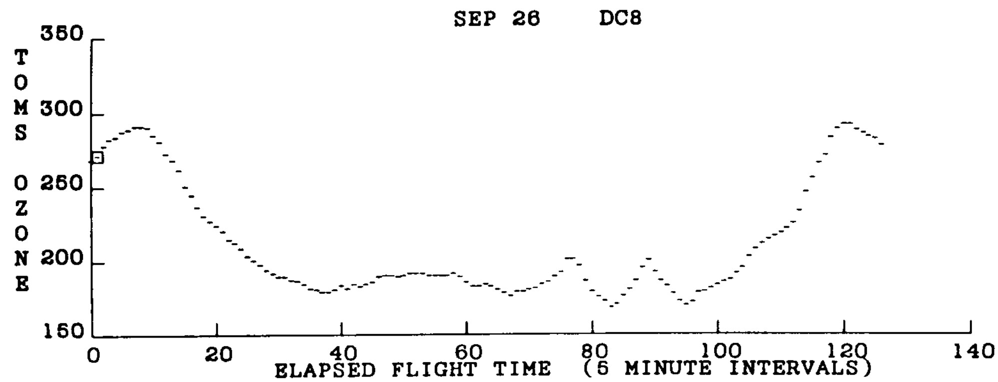


Figure 91. Flight Path of the DC-8 mission for September 26 as mapped onto a polar projection (top) and as a time series of latitude, longitude, and altitude along with the corresponding TOMS total-ozone estimates along the flight path (bottom).

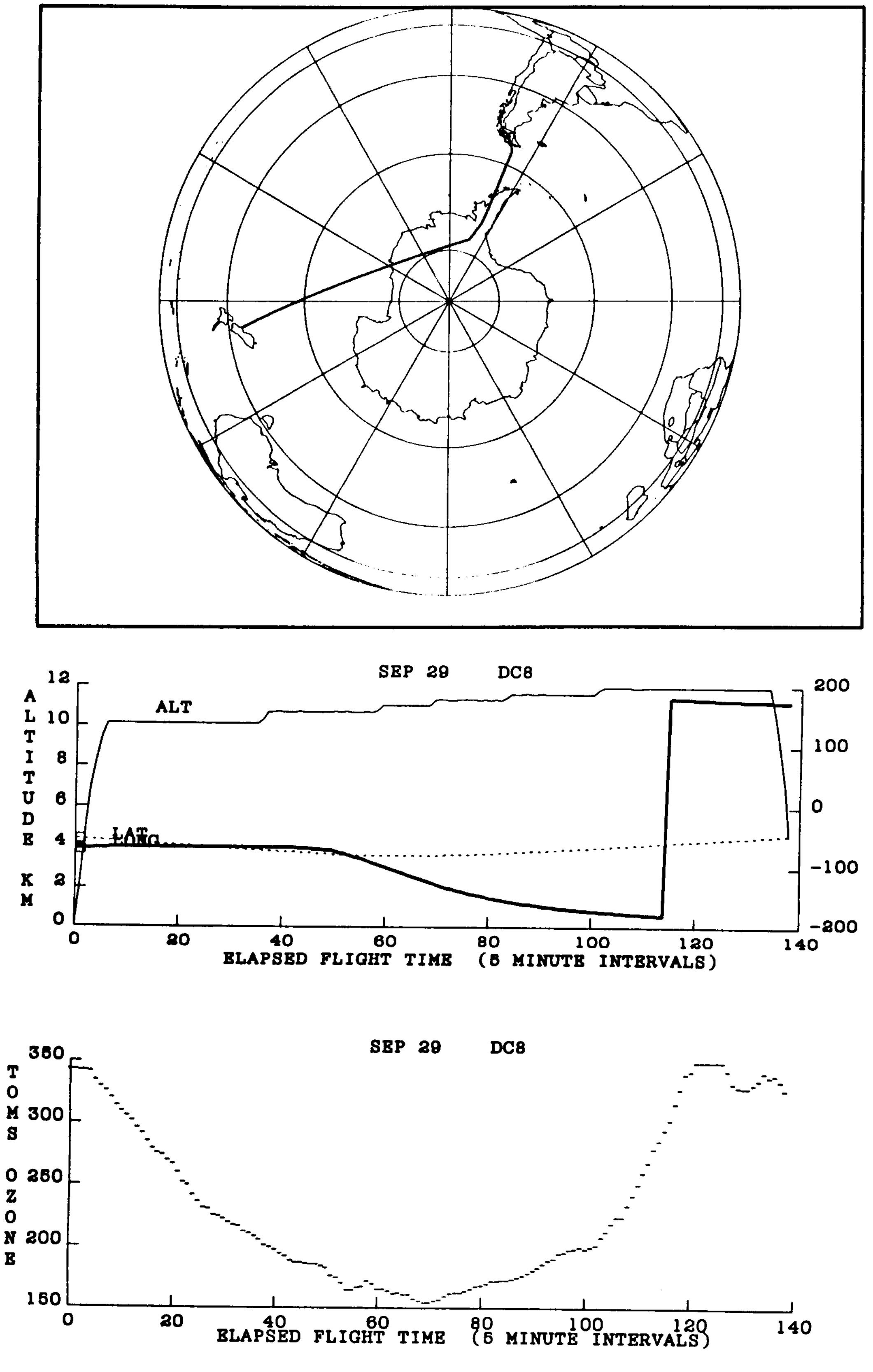


Figure 9m. Flight Path of the DC-8 mission for September 29 as mapped onto a polar projection (top) and as a time series of latitude, longitude, and altitude along with the corresponding TOMS total-ozone estimates along the flight path (bottom).

# 4. REFERENCES

Ardanuy, P., J. Victorine, F. Sechrist, A. Feiner, L. Penn, and the RDS Airborne Antarctic Ozone Experiment Team, 1987: Final report of the near-real-time TOMS, telecommunications, and meteorological support for the 1987 airborne Antarctic ozone experiment, NASA Contractor Report, in press.

Austin, J., E. E. Remsberg, R. L. Jones, and A. F. Tuck, 1986: Polar stratospheric clouds inferred from satellite data, Geophys. Res. Lett., 13, 1256-1259.

Callis, L. B., and M. Natarajan, 1986: The Antarctic ozone minimum: Relationship to odd nitrogen, odd chlorine, the final warming and the 11-year solar cycle, J. Geophys. Res., 91, 10771-10796.

Chandra, S., and R. D. McPeters, 1986: Some observations on the role of planetary waves in determining the spring time ozone distribution in the Antarctic, Geophys. Res. Lett., 13, 1224-1227.

Crutzen, P. J., and F. Arnold, 1986: Nitric acid cloud formation in the cold Antarctic stratosphere: A major cause for the springtime "ozone hole," Nature, 324, 651-655.

Dave, J. V., and C. L. Mateer, 1967: A preliminary study on the possibility of estimating total atmospheric ozone from satellite measurements, J. Atmos. Sci., 24, 414.

desJardins, M. L. and R. A. Petersen, 1985: GEMPAK: A meteorological system for research and education. Preprints, First AMS International Conference on Interactive Information and Processing Systems for Meteorology, Oceanography, and Hydrology. Los Angeles, CA, 313-319.

Farman, J. C., B. G. Gardiner, and J. D. Shanklin, 1985: Large losses of total ozone in Antarctica reveal seasonal $ClO_x/NO$ interaction, Nature, 315, 207-210.

Fleig, A. J., K. F. Klenk, P. K. Bhartia, and D. Gordon, 1982: User's guide for the Total-Ozone Mapping Spectrometer (TOMS) instrument first-year ozone-T data set, NASA Ref. Publ. 1096.

Heath, D., A. J. Krueger, and H. Park, 1978: The Solar Backscatter Ultraviolet (SBUV) and Total Ozone Mapping Spectrometer (TOMS) experiment, in The Nimbus-7 User's Guide, edited by C. R. Madrid, pp. 175-211, NASA Goddard Space Flight Center, Greenbelt, Md.

Klenk, K. F., P. K. Bhartia, A. J. Fleig, V. G. Kaveeshwar, R. D. McPeters, and P. M. Smith, 1982: Total ozone determination from the Backscattered Ultraviolet (BUV) experiment, J. Appl. Meteorol., 21, 1672-1684.

Koch, S. E., M. desJardins, and P. J. Kocin, 1983: An interactive Barnes objective map analysis scheme for use with satellite and conventional data, J. Clim. Appl. Meteor., 22, 1487-1503.

Krueger, A. J., M. R. Schoeberl, and R. S. Stolarski, 1987: TOMS observations of total ozone in the 1986 Antarctic spring, Geophys. Res. Letters, Vol. 14, No. 5, 527-530.

Mateer, C. L., D. F. Heath, and A. J. Krueger, 1971: Estimation of total ozone from satellite measurements of backscattered ultraviolet earth radiances, J. Atmos. Sci., 28, 1307-1311.

McCormick, M. P., and C. R. Trepte, 1986: SAM II measurements of Antarctic PSC's and aerosols, Geophys. Res. Lett., 13, 1276-1279.

Newman, P. A., and M. R. Schoeberl, 1986: October Antarctic temperature and total ozone trends from 1979-1985, Geophys. Res. Lett., 13, 1206-1209.

Nimbus Observation Processing System, 1986: Nimbus-7 Solar Backscattered Ultraviolet and Total Ozone Mapping Spectrometer (SBUV/TOMS), GRIDTOMS Tape Specification #T634436, 1-17.

Schoeberl, M. R., and A. J. Krueger, 1986: The morphology of Antarctic total ozone as seen by TOMS, Geophys. Res. Lett., 13, 1217-1220.

Stolarski, R., A. Krueger, M. Schoeberl, R. McPeters, P. Newman, and J. Alpert, 1986: Nimbus-7 SBUV/TOMS measurements of the spring time Antarctic ozone hole, Nature, 322, 808-811.

Toon, O. B., P. Hamill, R. P. Turco, and J. Pinto, 1986: Condensation of $HNO_3$ and HCl in the winter polar stratospheres, Geophys. Res. Lett., 13, 1284-1287.

PRECEDING PAGE BLANK NOT FILMED



PAGE 242 INTENTIONALLY BLANK

# 5. ACKNOWLEDGEMENTS

The Nimbus-7 TOMS total ozone data were reliably and regularly supplied to the Airborne Antarctic Ozone Experiment operations office in Punta Arenas. The quality, timeliness, and dependability of the near-real-time and delayed TOMS data sets permitted the TOMS total ozone observations to play a crucial role in the planning and successful completion of the aircraft flights. Without question, the reliable provision of the orbital and hemispheric TOMS observations played a central role in the outstanding success of the mission. The authors were provided assistance by many individuals during the course of the experiment. Without this help, the TOMS total ozone data could not have been delivered in a punctual manner, and indeed, the experiment may not have been possible. While it is not possible to name every individual who played a role, certain acknowledgements must be made.

The authors would like to express their appreciation to John Sissala, Mike Doline, and other members of the GE/RCA Service group for scheduling the data transfer from the Nimbus-7 satellite passes so as to obtain the telemetry in the quickest possible manner and for providing predictions of the Nimbus-7 orbital overpasses well in advance of the experiment. We also wish to thank Fred Shaffer, Hal Domchick, Herb Durbeck, and Scott Brittain of NASA/GSFC and the RMS Associates operations group for the smooth and continuous operations of the NSESCC during the experiment, and for adjusting the system maintenance schedule and job priorities to ensure the most rapid throughput of the TOMS data production on the IBM 3081. Also to be recognized are Robert Gray, Jerry Morrison, Damodar Goel, and Kirk Jones of STX who processed the raw TOMS data on the GSFC IBM 3081. The authors wish to thank the RDS telecommunications team, composed of James Victorine, Segun Park, Nasser Alizadeh, Susan Krupa, and Steven Gaines, who manned the communications center in Punta Arenas 24 hours a day, 7 days a week, and received the TOMS total ozone data. Recognition is due to Al Feiner and Woody Wheat of RDS who designed the real-time telecommunications network and monitored its installation and testing. We are also appreciative of Mary DesJardins of NASA/GSFC and Brian Doty and Ira Graffman of RDS for their timely modification of the GEMPAK software to permit its use in a southern hemisphere polar projection. We are also grateful to Brenda Vallette of RDS for the technical editing and assembly of this manuscript. Finally, we also wish to thank Arnie Oakes of NASA/GSFC, in his capacity as technical officer on the Nimbus Project, for helping to put together this uniquely qualified group of individuals that made the mission work.

# Report Documentation Page

National Aeronautics and Space Administration

| 1. Report No. | 2. Government Accession No. | 3. Recipient's Catalog No. |
|---|---|---|
| NASA RP-1201 | | |

| 4. Title and Subtitle | 5. Report Date |
|---|---|
| The 1987 Airborne Antarctic Ozone Experiment - The Nimbus-7 TOMS Data Atlas | March 1988 |
| | 6. Performing Organization Code<br>616 |
| 7. Author(s)<br>Arlin J. Krueger, Philip E. Ardanuy, Frank S. Sechrist, Lanning M. Penn, David E. Larko, Scott D. Doiron, and Reginald N. Galimore | 8. Performing Organization Report No.<br>88B0107 |
| | 10. Work Unit No. |
| 9. Performing Organization Name and Address<br>Goddard Space Flight Center<br>Greenbelt, MD 20771 | 11. Contract or Grant No. |
| | 13. Type of Report and Period Covered<br>Reference Publication |
| 12. Sponsoring Agency Name and Address<br>National Aeronautics and Space Administration<br>Washington, DC 20546-0001 | 14. Sponsoring Agency Code |

15. Supplementary Notes

Philip E. Ardanuy, Frank S. Sechrist, Lanning M. Penn, and David E. Larko are affiliated with Research and Data Systems Corporation, Lanham, MD, 20706; Scott D. Doiron and Reginald N. Galimore are affiliated with Science Applications Research Corporation, Lanham, MD, 20706; Arlin J. Krueger is with Goddard Space Flight Center.

16. Abstract Total ozone data taken by the Nimbus-7 Total Ozone Mapping Spectrometer (TOMS) played a central role in the successful outcome of the 1987 Airborne Antarctic Ozone Experiment. The near-real-time TOMS total ozone observations were supplied within hours of real time to the operations center in Punta Arenas, Chile, over a telecommunications network designed specifically for this purpose. The TOMS data preparation and method of transfer over the telecommunications links are reviewed. This atlas includes a complete set of the near-real-time TOMS orbital overpass data over regions around the Palmer Peninsula of Antarctica for the period of August 8 through September 29, 1987. Also provided in this atlas are daily polar orthographic projections of TOMS total ozone measurements over the southern hemisphere from August through November 1987. In addition, a chronology of the salient points of the experiment, along with some latitudinal cross-sections and time series at locations of interest of the TOMS total ozone observations are presented. The TOMS total ozone measurements are evaluated along the flight tracks of each of the ER-2 and DC-8 missions during the experiment. The ozone hole is shown here to develop in a monotonic progression throughout late August and September. We find that the minimum total ozone amount is obtained on October 5, when its all-time lowest value of 109 DU is recorded. The hole remains well defined, but fills gradually, from mid-October through mid-November. The hole's dissolution is observed here to begin in mid-November, when the hole elongates and begins to rotate. By the end of November, the south pole is no longer located within the ozone hole.

| 17. Key Words (Suggested by Author(s)) | 18. Distribution Statement |
|---|---|
| Antarctic ozone hole, TOMS, Nimbus-7, ozone hole, total ozone, airborne Antarctic ozone hole experiment, Total Ozone Mapping Spectrometer, field experiment | Unclassified-Unlimited<br>Subject Category 47 |

| 19. Security Classif. (of this report) | 20. Security Classif. (of this page) | 21. No. of pages | 22. Price |
|---|---|---|---|
| Unclassified | Unclassified | 252 | A12 |